DTIC FILE COPY

(2)

Army Corps of Engineers

AD-A216 450

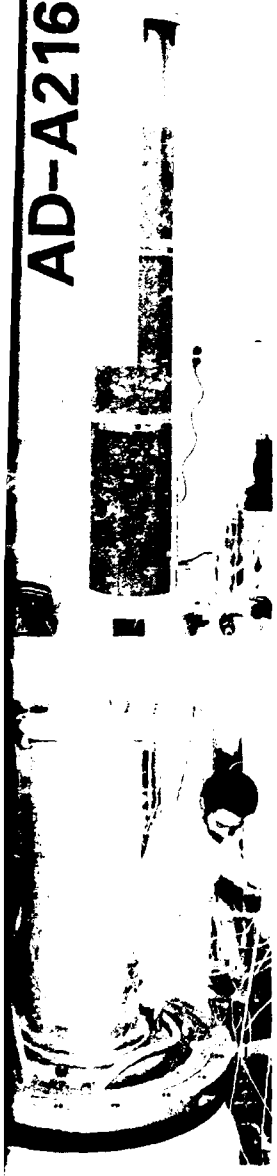

MISCELLANEOUS PAPER GL-89-27

DESIGN AND CONSTRUCTION OF MAT FOUNDATIONS

by

Lawrence D. Johnson

Geotechnical Laboratory

DEPARTMENT OF THE ARMY
Waterways Experiment Station, Corps of Engineers
3909 Halls Ferry Road, Vicksburg, Mississippi 39180-6199

DTIC
ELECTE
DEC 29 1989
S D
E

November 1989

Final Report

Approved For Public Release; Distribution Unlimited

Prepared for DEPARTMENT OF THE ARMY
US Army Corps of Engineers
Washington, DC 20314-1000

Under RDT&E Work Unit AT 22/A0/010

GEOTECHNICAL LABORATORY

89 12 28 096

Unclassified

SECURITY CLASSIFICATION OF THIS PAGE

REPORT DOCUMENTATION PAGE

Form Approved OMB No. 0704-0188

1a. REPORT SECURITY CLASSIFICATION Unclassified	1b. RESTRICTIVE MARKINGS
2a. SECURITY CLASSIFICATION AUTHORITY	3. DISTRIBUTION/AVAILABILITY OF REPORT
2b. DECLASSIFICATION/DOWNGRADING SCHEDULE	Approved for public release; distribution unlimited.
4. PERFORMING ORGANIZATION REPORT NUMBER(S) Miscellaneous Paper GL-89-27	5. MONITORING ORGANIZATION REPORT NUMBER(S)
6a. NAME OF PERFORMING ORGANIZATION USAEWES Geotechnical Laboratory 6b. OFFICE SYMBOL (If applicable)	7a. NAME OF MONITORING ORGANIZATION
6c. ADDRESS (City, State, and ZIP Code) 3909 Halls Ferry Road Vicksburg, MS 39180-6199	7b. ADDRESS (City, State, and ZIP Code)
8a. NAME OF FUNDING/SPONSORING ORGANIZATION US Army Corps of Engineers 8b. OFFICE SYMBOL (If applicable)	9. PROCUREMENT INSTRUMENT IDENTIFICATION NUMBER
8c. ADDRESS (City, State, and ZIP Code) Washington, DC 20314-1000	10. SOURCE OF FUNDING NUMBERS PROGRAM ELEMENT NO. / PROJECT NO. / TASK NO. / WORK UNIT ACCESSION NO. AT22/A0/010

11. TITLE (Include Security Classification)
Design and Construction of Mat Foundations

12. PERSONAL AUTHOR(S)
Johnson, Lawrence D.

13a. TYPE OF REPORT	13b. TIME COVERED	14. DATE OF REPORT (Year, Month, Day)	15. PAGE COUNT
Final report	FROM _____ TO _____	November 1989	354

16. SUPPLEMENTARY NOTATION This report is available from the National Technical Information Service, 5285 Port Royal Road, Springfield, VA 22161.

17. COSATI CODES			18. SUBJECT TERMS (Continue on reverse if necessary and identify by block number)
FIELD	GROUP	SUB-GROUP	Expansive soil, Mat foundation, Soil-structure interaction, Heave, Settlement

19. ABSTRACT (Continue on reverse if necessary and identify by block number)

Mat foundations commonly support all types of structures. Flat mats from 2 to 8 ft in thickness often containing two-way steel reinforcement top and bottom usually support multistory or heavy structures. Mats less than 1 ft thick often constructed with steel reinforced ribs or stiffening crossbeams usually support light one or two story structures. Many of these mats have been designed and constructed for supporting permanent military facilities, particularly in heaving/shrinking and compressible soil. Some of these mats have experienced significant differential movement leading to cracking in the structure and have required costly remedial work. Attempts to reduce such maintenance expenses of some structures have lead to substantially increased design and construction costs for mat foundations.

This report provides information on serviceability of structures, guidelines for evaluation of soil, and some structure input parameters for design analysis and guidelines for design and construction of ribbed mat foundations in expansive soils. Methods

(Continued)

20. DISTRIBUTION/AVAILABILITY OF ABSTRACT	21. ABSTRACT SECURITY CLASSIFICATION
☒ UNCLASSIFIED/UNLIMITED ☐ SAME AS RPT ☐ DTIC USERS	Unclassified
22a. NAME OF RESPONSIBLE INDIVIDUAL	22b. TELEPHONE (Include Area Code) / 22c. OFFICE SYMBOL

DD Form 1473, JUN 86 Previous editions are obsolete

SECURITY CLASSIFICATION OF THIS PAGE
Unclassified

20. ABSTRACT (Continued).

have been developed for evaluation of effective soil elastic moduli and stiffness of structures. New concepts are proposed for determining some soil input parameters for design in expansive soils such as the depth of the active zone for heave and edge moisture variation distance. Several case history studies of ribbed and flat mat foundations have been investigated to assist determination of suitable procedures for calculating deformation behavior of mat foundations.

Analysis of the performance of a large ribbed mat foundation supporting building 333, Red River Army Depot, proves the viability of selected instrumentation and methodology. The observed earth pressure distribution shows extremely large concentrations of soil pressure near the perimeter indicating rigid behavior on an elastic soil or soil shear at the perimeter. The extended distribution of earth pressures from column loads indicates the effectiveness of stiffening beams in spreading applied loads. Evidence is presented indicating that concrete shrinkage and foundation distortions during construction may sometimes let stiffening beams of ribbed mats hang in the trenches without soil support, which may contribute to mat fractures when superstructure loads are applied. Observed strains in the concrete mat were generally consistent with observed deformation patterns.

A preliminary systematic damage record system was developed to catalog most frequent damages, assist identification of causes of damage from foundation movements, and assist determination of requirements for maintenance and repair of military facilities. Recommendations are made for field surveys of detailed surface soil and foundation movement patterns and other work to investigate a new frequency spectrum approach and ground modification methods to improve understanding and performance of military facilities, improve design of foundations, and reduce maintenance and repair requirements.

Accession For
NTIS GRA&I ☒
DTIC TAB ☐
Unannounced ☐
Justification

By
Distribution/
Availability Codes

Dist	Avail and/or Special
A-1	

PREFACE

This report provides a comprehensive review and analysis of design and construction technology of mat foundations as of 1988 with guidelines for design and construction of ribbed mats in expansive soil. This report completes RDT&E Work Unit AT22/AO/010, "Mat Foundations for Intermediate and Heavy Military Structures," sponsored by the Office, Chief of Engineers (OCE), US Army. This work unit was begun in October 1982 and completed September 1988. Miscellaneous Papers GL-85-16, "BOSEF: Beam on Swelling Elastic Foundation", and Miscellaneous Paper GL-88-6, "Proceedings of the Workshop on Design, Construction, and Research for Ribbed Mat Foundations" were prepared to complete earlier phases of this study. Contract reports DACA39-87-M0835, "A Computer Program For Analysis of Transient Suction Potential in Clays," DACA39-87-M0557, "Study of Surface Deformations of Mat Foundations on Expansive Soils," and DACA39-87-M0754, "Selection of Design Parameters For Foundations on Expansive Soils," were also prepared to assist in completing this work unit. Mr. A. F. Muller, Mr. Richard F. Davidson and Mr. Wayne King were the OCE Technical Monitors.

This report was prepared by Dr. Lawrence D. Johnson, Research Group, Soil Mechanics Division (SMD), Geotechnical Laboratory (GL), US Army Engineer Waterways Experiment Station (WES). The Foundation and Materials Branch, Savannah District, South Atlantic Division (SAD), contributed data for analysis of the mat supporting Fort Gordon Hospital, Georgia. The Foundation and Materials Branch, Fort Worth District (FWD), Southwestern Division (SWD), contributed data for analysis of mats supporting military facilities in San Antonio, Texas. Messrs. R. L. James and B. H. James (SWD), Mr. W. R. Stroman (FWD), Messrs. G. B. Mitchell, C. L. McAnear, and Dr. L. D. Johnson (SMD), and Mr. A. F. Muller (OCE) participated in the field trip of May 1984 to San Antonio, TX, to assess visual performance of mat foundations.

Many helpful comments were provided by Dr. P. F. Hadala, Assistant Chief (GL), Mr. A. L. Branch, Jr. (FWD), Dr. G. Wayne Clough, Virginia Polytechnic Institute, Mr. J. P. Hartman (SWD), Dr. A. D. Kerr, University of Delaware, Mr. Wayne King (OCE), Mr. R. L. Mosher, Information Technology Laboratory (WES), and Mr. W. R. Stroman. In situ soil tests for analysis of the ribbed mat supporting Building 333, Red River Army Depot, were performed by the

following: pressuremeter tests by Briaud Engineers, College Station, TX, cone penetration tests by Fugro Inter, Inc., Houston, TX, and plate load tests by the Fort Worth District (SWD). Messrs. R. H. Floyd and T. Rosamond, Instrumentation Services Division (WES) installed earth pressure cells and strain gages in portions of the mat supporting building 333.

The work was performed under the direct supervision of Mr. C. L. McAnear, Chief, SMD, and general supervision of Dr. W. F. Marcuson III, Chief, GL. COL Larry B. Fulton, EN, was Commander and Director of WES during the preparation of this report. Dr. Robert W. Whalin was Technical Director.

CONTENTS

	Page
PREFACE	1
CONVERSION FACTORS, INCH-POUND TO METRIC (SI) UNITS OF MEASUREMENT	5
PART I: INTRODUCTION	6
Background	6
Description and Applications of Mats	6
Description of Foundation Movements	9
Serviceability	11
Philosophy of Design	14
Current Limitations of Design	16
Purpose and Scope	17
PART II: REVIEW OF METHODOLOGY	19
Introduction	19
General Design Procedure	19
Soil Profile	21
Total Displacements	24
Initial Mat Thickness	35
Minimum Depth of Foundation	41
Differential Soil Displacements	45
Final Design	52
PART III: CASE HISTORY STUDIES	61
Introduction	61
Soil Parameters	61
Structural Parameters	62
Ribbed Mat Foundations	64
Gymnasium, Brooks Air Force BAse	69
Data Processing Facility, Randolph Air Force Base	77
Maintenance Shop and Warehouse, US Army Reserve Center	85
Dental and Medical Clinics	93
Pest Management Training Facility	104
Summary and Conclusions	111
Flat Mat Foundations	112
Wilford Hall Hospital	113
Fort Gordon Hospital	123
Fort Polk Hospital	131
Summary and Conclusions	137
PART IV: APPLICATION OF FIELD PERFORMANCE	140
Introduction	140
Description of Soil	143
Classification Tests	143
Laboratory Strength Tests	143
Consolidometer Swell Tests	148
In Situ Soil Tests	149

Page

Field Instrumentation 154
Piezometers 154
Elevation Surveys 154
Earth Pressure Cells 163
Strain Gages 169
Analyses 182
Input Parameters 182
Plate on Elastic Foundation 193
Beam on Winkler Foundation 196
Frequency Spectrum Model 198
Summary and Conclusions 200

PART V: GUIDELINES FOR DESIGN AND CONSTRUCTION OF RIBBED MATS . . . 202

Applicability of Mat Foundations 202
Expansive Soil Behavior 202
Center Lift 203
Edge Lift 203
Soil Exploration 205
Site Characterization 205
Soil Characterization 206
Design of Ribbed Mats 213
Input Parameters 213
Foundation Plan 213
Rib Dimensions 220
Construction 220
Minimizing Problems 220
Preparation for Mat Construction 225
Site Finishing 234
Followup 235

PART V: RECOMMENDATIONS 238

REFERENCES 240

APPENDIX A: EQUIVALENT SOIL ELASTIC MODULUS A1

APPENDIX B: INFLUENCE OF SUPERSTRUCTURE RIGIDITY B1

APPENDIX C: USER'S MANUAL FOR COMPUTER PROGRAM SLAB2 . . . . . C1

APPENDIX D: PERFORMANCE ANALYSIS, CENTRALIZED TROOP CLINIC, FORT SAM HOUSTON, TEXAS D1

APPENDIX E: INFLUENCE OF SOIL MODEL ON MAT PERFORMANCE E1

APPENDIX F: LIGHT TRACK VEHICLE FOUNDATION DESIGN. F1

APPENDIX G: FIELD TESTS G1

CONVERSION FACTORS, NON-SI TO SI (METRIC) UNITS OF MEASUREMENT

Non-SI units of measurement used in this report can be converted to SI (metric) units as follows:

Multiply	By	To Obtain
cubic yards	0.7645549	cubic metres
Fahrenheit degrees	5/9	Celsius degrees or Kelvins*
feet	0.3048	metres
inches	2.54	centimetres
inch-poundss (force)	0.1129848	metre-newtons
kips (force)	4.448222	kilonewtons
miles (US statute)	1.609347	kilometres
pounds (force)	4.448222	newtons
pounds (force) per inch	175.1268	newtons per metre
pounds (force) per square foot	47.88026	pascals
pounds (force) per square inch	6.894757	pascals
pounds (mass) per cubic foot	16.01846	kilograms per cubic metre
pounds (mass) per cubic yard	0.593276	kilograms per cubic metre
square feet	0.09290304	square metres
square feet squared	0.0086309	square metres squared
square inches squared	416,231.4256	square millimetres squared
tons (2,000 pounds, mass)-feet	276.5098966	kilogram-metres
tons (2,000 pounds, mass)-square feet	84.280216	kilogram-square metres
tons (force)	8.896444	kilonewtons
tons (2000 pounds, mass)	907.1847	kilograms
tons (2000 pounds, mass) per cubic foot	32,036.92148	kilograms per cubic metre
tons (2000 pounds, mass) per foot	2,976.327756	kilograms per metre
tons (2000 pounds, mass) per square foot	9,764.856	kilograms per square metre

* To obtain Celsius (C) temperature readings from Fahrenheit (F) readings, use the following formula: $C = (5/9)(F - 32)$. To obtain Kelvin (K) readings, use $K = (5/9)(F - 32) + 273.15$.

DESIGN AND CONSTRUCTION OF MAT FOUNDATIONS

PART I: INTRODUCTION

Background

Description and Applications of mats

1. A mat foundation is a large concrete slab that supports column or line loads that are not all in the same straight line. The mat may be (1) thin (less than 1 ft thickness), Figure 1a, for supporting light structures on firm soil, (2) ribbed or reinforced with cross beams, Figure 1b, for supporting light structures on heaving/shrinking and compressible soil, or (3) thick (greater than 1 ft thickness), Figure 1c, for supporting heavy multistory structures. The stiffness of mat foundations may be designed to accommodate or inhibit differential soil movement. The mat foundation is usually preferred instead of spread footings to increase efficiency and economy of excavation and construction when the spread footings are large and closely spaced in one direction and require more than half of the construction area. By combining all individual footings into one mat, mat foundations reduce pressure on the supporting soil thereby reducing total and differential settlement and often increasing total bearing capacity.

2. Mats are especially useful in supporting structures on deep swelling or consolidating soil and fill that cannot be economically supported by pile or drilled shaft foundations. The weight of the superstructure on mats can balance hydrostatic uplift pressure. Mats can also be constructed to float, such as buoyancy or compensated mats, by excavating basement areas so that the weight of the excavated material balances the structural and normal live loads. Mats may be inverted with stiffening cross-beams on top, Figure 1d, if the soil is especially soft. Mats may also be placed on top of piles to reduce settlement in soft soil. Buoyancy rafts are occasionally designed with cellular spaces. Numerous permanent military facilities supported by mats have been designed and constructed by the Corps of Engineers.

3. Thick mats. The most common engineered mat foundations for multi-story "heavy" structures consist of flat 2 to 8 ft thick mats with continuous two-way reinforcement top and bottom. A thick mat usually supports structures

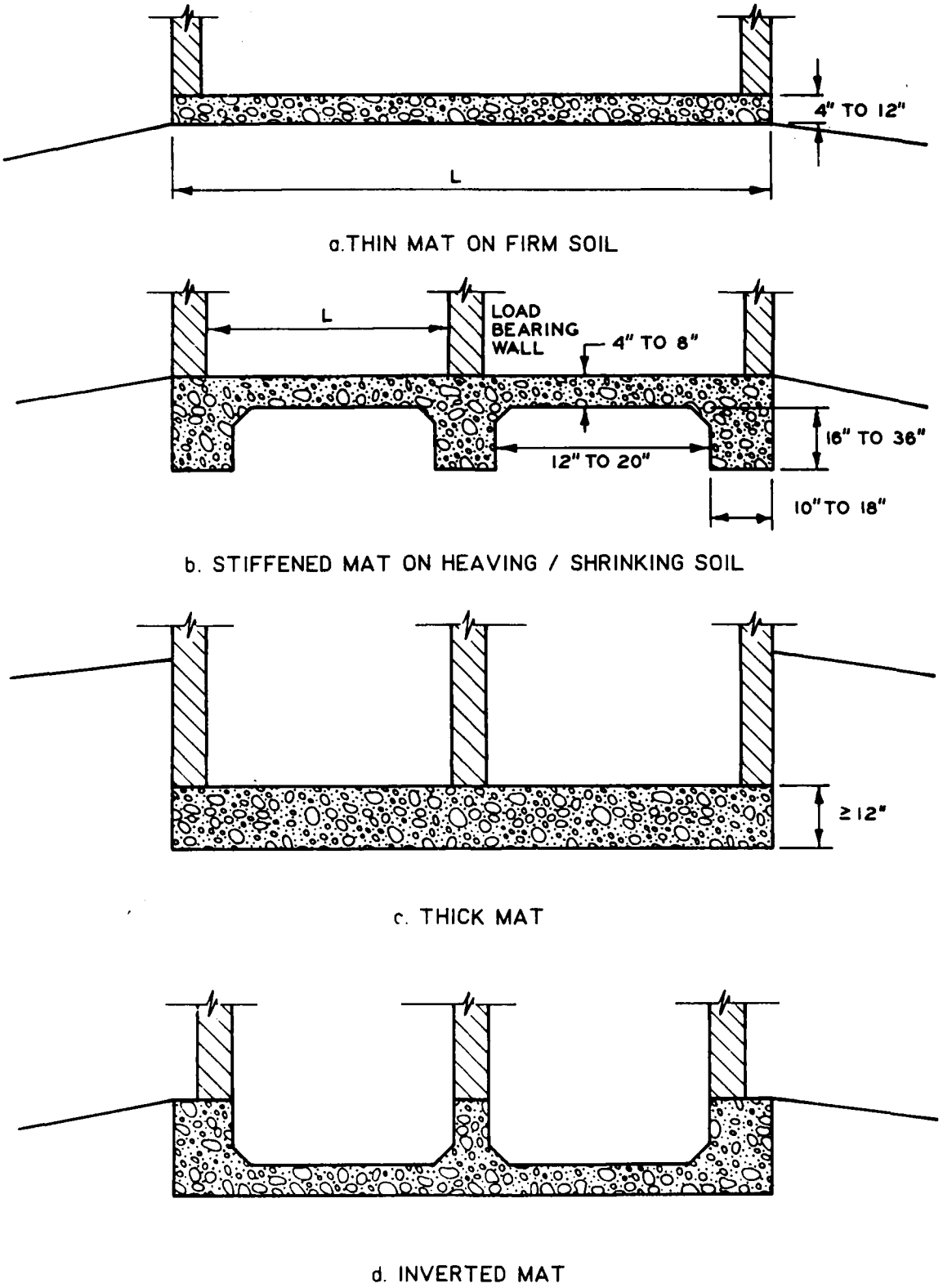

Figure 1. Types of mats

with more than 2 stories, but some 1 and 2 story structures could have large column loads causing these structures to be in the heavy category. Post-tensioned slabs of about 1-ft thickness may support light structures and reduce differential movement on soft or heaving soil. Mats may be square or rectangular shaped for supporting buildings or circular shaped for supporting chimneys, silos, and water tanks.

4. American practice tends to overdesign thick mats because of uncertainty involved with current analysis methodology. The extra cost of the additional unknown safety against a structural failure is considered relatively small for reasonable overdesign[1]. Problems with thick mats supporting storage tanks and silos, where foundation economy is essential, have occurred from excessive tilt and soil shear failures when supported by soft and weak soil[2].

5. Thin mats. Foundation costs of thin mats 4 to 8 inches thick are a greater proportion of the total cost of the structure than that for thick mats supporting multi-story structures. These foundations usually support light and intermediate structures on and near the ground surface in unstable soil areas such as expansive and collapsible soil. Thin mats are often reinforced with stiffening beams and placed on compacted nonexpansive low plasticity fill to reduce differential movements. These mats may be underdesigned because of inadequate knowledge of the soil profile, lack of design guidance, or to reduce construction costs. Underdesign leads to excessive total and differential movements that interfere with proper function of utilities, machinery, efficiency and comfort of occupants and damage to the superstructure. Overdesign leads to excessive construction time and cost. Ribbed and other mats also occasionally crack during and soon after construction.

6. Inadequate flatness from deficient design, construction or long-term distortion of foundation soils impairs performance of structures and it is costly to repair. Little guidance is available for specifying appropriate floor flatness for specific functional requirements. Long-term repair and maintenance expenses can be substantial exceeding the original cost of the foundation. The cost of repair of damage from heaving soil is typically

[1]Bowles 1976; refer to REFERENCES for complete listing
[2]Burland and Davidson 1976; Tomlinson 1980; Buttling and Wood 1982

greater than cost of repair of damage in settling soil because structures are generally less able to accommodate heaving. Heave tends to put the superstructure in tension, while settlement puts the superstructure in compression; structures are usually less able to resist tensile than compressive stress. Design guidelines for flexible (thin) mats are not well advanced beyond the relatively costly uniform pressure method applicable to rigid (thick) mats.

Description of Foundation Movements

7. Static and dynamic loads cause total and differential movements. Total movement is the magnitude of vertical heave or downward settlement. Vertical heave is caused by wetting and subsequent volume increase of expansive clay soils. Settlement is caused by elastic compression and consolidation of foundation soils under load and the collapse of meta-stable arrangements of particles in some unsaturated soils. Differential movement is the difference in vertical movement between various locations of the structure and distorts the structure. Ribbed mats with stiffening beams and mats subject to the stiffening action of a properly designed and connected superstructure increase stiffness and reduce differential movement caused by nonuniform heave and shrinkage of expansive soil or consolidation and collapse of other foundation soil.

8. Differential movements cause distortion and damage in structures. These are a function of soil moisture change and uniformity, stiffness of the structure and soil, and distribution of loads within the structure. Excessive differential movement may lead to tilting that can interfere with adjacent structures and disrupt the performance of machinery and people. Differential movement can cause cracking in the structure, distorted and jammed doors and windows, uneven floors and stairways, and other damage. Widespread cracking can impair structural integrity and lead to collapse of the structure, particularly during earthquakes. The height that a wall can be constructed on a foundation without cracking is related to the deflection/span length ratio Δ/L and angular distortion β of the foundation.

9. The deflection ratio Δ/L is a measure of the maximum differential movement Δ in the span length L, Figure 2. The span length may be between

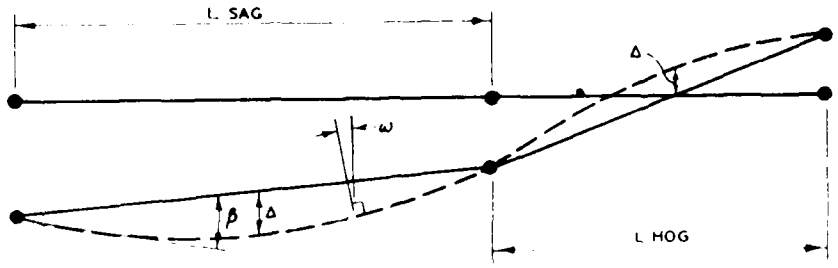

a. COMBINATION L SAG AND L HOG

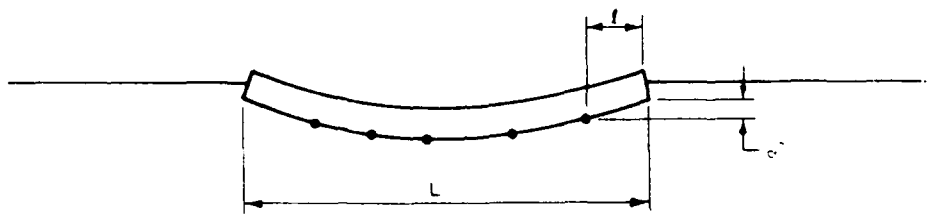

b. REGULAR SETTLEMENT

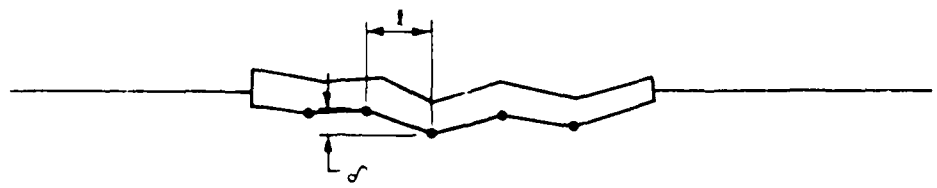

c. IRREGULAR SETTLEMENT

Figure 2. Schematic illustration of angular distortion ratio $\beta = \delta/\ell$ and deflection ratio Δ/L for settling (sagging) and heaving (hogging) profiles

two adjacent columns, L_{SAG} or L_{HOG}, Figure 2a. Angular distortion $\beta = \delta/\ell$ is a measure of differential movement δ between two adjacent points separated by the distance ℓ, Figure 2. Settlement (sagging) occurs from elastic compression, collapse, and consolidation of the foundation soil. Heave (hogging) occurs from swelling soil, shrinking or subsidence near the edges, downdrag from adjacent structures and movement from nearby excavations.

Serviceability

10. Serviceability is an obscure term, partly because it depends on the purpose of the structure, its response to movements, and the reaction of the owner and users of the structure to movement and cracking. Serviceability or performance of structures is especially related to limitations of total and differential movements to within acceptable values. Considerable judgment enters into evaluating whether a structure has performed "adequately" because the definition of adequate is subjective. A simple curtain wall for dividing space that cracks when subject to excessive differential movement can be easily repaired to full serviceability with a plastic joint filler, but the owner of that wall may not be satisfied with the appearance and may consider the wall a failure.

11. Functions of serviceability. Serviceability depends on the flexibility of structural members, joints, and other architectural details. Articulation by inclusion of joints in structures, steel frames, steel and wood studs, interior paneling and wallboard among other features increase structural flexibility. Expansion and crack control joints placed at regular intervals relieve stresses that would otherwise occur in walls and the mat foundation. Expansion joints are commonly placed at 150-ft intervals in ribbed mats, while construction joints in walls may be placed at approximately 25-ft intervals or less. Horizontal and vertical impervious membranes have been successfully used to reduce differential movement from soil moisture changes. Ground modification methods using chemicals or nonexpansive fills are useful for reducing total heaves to less than 1 inch.

12. Although superstructure stiffness tends to reduce differential movement of the foundation, modeling techniques are not yet able to simulate stiffness of the total structure so that calculated foundation movements agree

with field displacement measurements[3]. A contributing factor is that construction materials often display different stiffnesses than those used in design. External and internal loads on the superstructure can lead to distress and damage, even if the foundation performs within specifications, because of a trend toward longer spans between columns, higher permissible stresses, greater brittleness of wall and facing components, and larger structurally independent units.

13. Disturbance of the foundation soil during construction can influence serviceability by altering soil parameters used for design such as strength, elastic modulus and the modulus of subgrade reaction. Many things done to a site during construction such as soil disturbance during clearing, excavation, drainage or wetting of an adjacent area, and environmental effects can lead to greater differential movement. Care should be exercised by the contractor during construction to minimize differential movement by use of proper drainage, compaction control of fills, and grading.

14. Nonstructural damage occurs predominantly by long-term differential movement, while both immediate and long-term movement contribute to structural damage[4]. Structures on soil with relatively little long-term movement such as sands tend to show least superficial or cosmetic damage, although structural damage could occur during construction. This is probably related to the later placement of facing materials after most of the immediate settlement had occurred following construction of the structural members.

15. Limitations of total movement. Many structures can tolerate substantial total movement without cracking. Polshin and Tokar (1957) had indicated maximum total settlement of 3 inches for unreinforced masonry walls and 6 inches for reinforced brick and concrete walls; however, total settlement should not exceed 2 inches in practice for most facilities to help maintain differential movements within acceptable levels, minimize damage to connections with outside utilities, maintain adequate drainage, and maintain adequate serviceability of entry ways. A typical allowable total settlement for buildings is 1 inch. Total foundation heave, even without surcharge pressure from the mat foundation, should usually not exceed 1 to 1.5 inches.

[3]Focht Jr., Khan, and Gemeinhardt 1978; Bobe, Hertwig, and Seiffert 1981
[4]Skempton and McDonald 1956

16. Limitations of differential movements. Perimeter or center movements beneath mats exceeding 1 to 1.5 inches can be nearly impractical and not economical to accommodate in design. Larger differential movements may require innovative superstructure designs to increase flexibility such as vertical construction joints in walls, slip joints in interior walls and flexible, watertight utility connections[5]. Differential movements that can cause operation problems occur within some limited lateral distance; therefore these movements are better expressed in terms of angular distortion and deflection ratio. Chapter 2 of EM 1110-1-1904 provides guidelines of angular distortions and deflection ratios for different types of structures.

17. The maximum angular distortion from regular settlement, Figure 2b, occurs at the corner of a mat foundation. β_{max} is $4\Delta/L$ from geometrical relationships if settlement is in the shape of a circular arc. The deflection Δ between the center and corner of a mat is 0.75 of the center settlement if the Boussinesq stress distribution of a foundation on an elastic soil is applicable; therefore, the maximum angular distortion will be

$$\beta_{max} = \frac{3\,\rho_c}{L} \tag{1a}$$

where

ρ_c = center settlement, ft

L = the diagonal length $(N-1)\ell$, ft

ℓ = distance between columns along the diagonal, ft

N = number of columns on the diagonal

A safe limit of angular distortion for no cracking in buildings is 1/500[4,6]. Cracking should be anticipated when β exceeds 1/300. Considerable cracking in panels and brick walls and structural damage is expected when β is greater than 1/150. Equation 1a indicates that the differential displacement Δ should be less than 0.5 inch to maintain $\beta_{max} < 1/500$ for span lengths L of 60 to 80 ft. Allowable angular distortions in the superstructure should exceed the maximum angular distortion expected in the foundation to avoid structural distress. Tilting can be observed if $\beta > 1/250$ and must be

[5]Technical Manual 5-818-7, "Foundations in Expansive Soils"
[6]Feld 1965; Wahls 1981

limited to allow clearance between adjacent buildings, particularly in high winds. Underpinning may be necessary if tilt is excessive. The tilt angle ω is indicated in Figure 2.

18. Limiting Δ/L ratios for design is in the range of 1/240 to 1/600. This range is substantially greater than the 1/2500 limit required to avoid all cracking in masonry structures[7,8]; however, stiffness contributed by components in an assembled brick structure help maintain deflection ratios near 1/2500. The height that a wall can be constructed on a beam without a cracking failure is related to the deflection/span length Δ/L and the distortion β by[7]

$$\frac{\Delta}{L} = \frac{\beta_{max}}{3}\left[\frac{1 + 3.9\ (H_w/L)^2}{1 + 2.6\ (H_w/L)^2}\right] \tag{1b}$$

where

Δ = differential displacement, ft

L = span length, ft

H_w = wall height, ft

β_{max} = maximum angular distortion at support, $L = 0$

Equation 1b considers that cracking is initiated at a critical strain ϵ_{crit} = 0.075 percent. ϵ_{crit} was based on field observations of the onset of visible cracking in beams as a function of the wall height/span length ratio. If β_{max} = 1/500 for initiation of damage the corresponding deflection/span length ratio Δ/L is about 1/1333 or β_{max} is about 3 times greater than Δ/L.

Philosophy of Design

19. Mat foundations should be designed and constructed to be safe against a soil shear failure and with loads sufficiently less than the soil bearing capacity to maintain total and differential displacements that optimize the functional purpose and structural (shear and bending moment) capacity of the structure. The maximum pressure applied to foundation soil should be less than the maximum past pressure to avoid virgin consolidation settlements; therefore, heavy structures may be supported by compensated or

[7]Burland and Wroth 1978
[8]Polshin and Tokar 1957

floating mats placed in deep excavations. Thick mats are commonly designed by the uniform (rigid) pressure method described below assuming undrained soil conditions; however, the difference in material and construction expenses saved by using a flexible analysis may be significant. Many structures, especially 1 or 2 story buildings, are flexible or semi-flexible structures supported on stiffened ribbed mats.

20. Uniform pressure method. Mats designed by this method satisfy two criteria: the centroid of the area in contact with the soil should lie on the line of action of resultant loads applied to the soil, which promotes a uniform pressure distribution, and the mat dimensions are selected so that the allowable soil pressure is not exceeded. Mats should neither settle or tilt excessively if these two criteria are satisfied. The allowable pressure required to limit foundation settlement to within suitable values may be estimated by applying factors of safety (FS) to the ultimate bearing capacity. If the allowable pressure is less than the applied pressure or initial estimates of total settlement exceed allowable settlement, then a compensated mat or pile supported mat may be considered.

21. The structural design of mats by the American Concrete Institute Ultimate Strength Method (ACI 318-80) usually results in a nonuniform linear soil pressure distribution because column loads are multiplied by load factors and the mat size should be increased to accommodate the larger service loads specified by the building code[9]. The uniform pressure method with an illustrative example is described by Peck, Hanson, and Thornburn (1974).

22. Flexible method. Wray[10] documented 16 procedures applicable to design of flexible mats. Of these methods the Post-Tensioning Institute[11] and the US Army Engineer Southwestern Division[12] pocedures are more commonly used by designers. Flexible mat foundations may also be designed by soil-structure interaction analysis using finite difference or finite element numerical techniques. During the late 1970's, the Corps of Engineers designed and constructed several military hospital foundations with thick mats such as the Wilford Hall Hospital addition in Lackland Air Force Base, Texas, and the

[9]American Concrete Institute 318-80, Section 17.3
[10]Johnson 1988
[11]Post-Tensioning Institute 1980
[12]Hartman and James 1988

hospital in Fort Polk, Louisiana. The design of these mats used a finite element computer program[13] containing a hyperbolic stress-strain soil model to better define foundation movements. This model is applicable to soil for strains not exceeding the strain level at peak strengths. Program SLAB2[11] is a two-dimensional plate on elastic foundation finite element program modified to accommodate stiffening beams. Beam on Winkler foundation methods[14,15] have also been applied to design of flexible mats.

Current Limitations of Design

23. Soil input parameters. Advanced design methodology for mat foundations such as plate on elastic foundation, beam on Winkler foundation, and use of finite difference or finite element methods require thorough geotechnical investigations to assist evaluation of reasonable values for soil input parameters. These parameters include the elastic soil modulus and Poisson's ratio for the plate on elastic foundation, coefficient of subgrade reaction for a beam on a Winkler foundation, soil swell pressure, compression and swell indices, depth of the active zone of heaving soil, and edge moisture variation distance.

24. **Adequate guidelines for evaluation of elastic soil modulus E_s and coefficient of subgrade reaction for a foundation k_{sf} are not yet available.** Adequate estimates of k_{sf} required in the Winkler foundation is especially difficult to provide because proper modeling of soil behavior requires at least two parameters such as the elastic modulus and Poisson's ratio. Single parameter models cannot properly calculate both displacements and bending moments simultaneously[16,17]. For example, an appropriate k_{sf} for bending of ribbed mat T-sections (the stiffening beam or web with some width of the flat mat extending on each side of the stiffening beam, Figure 1b) may be different than that evaluated for settlement. The American Concrete Institute specifies that for bending an effective T-section width $S_e \leq L/4$ where L is the span length; the effective overhang distance on each side of the web shall be less than 1/2 the distance to the next web or stiffening beam and not exceed 8D

---

[13]Duncan amd Clough 1971
[14]Godden 1965
[15]Dawkins 1982
[16]Vesic 1961
[17]Vesic and Saxena 1968

where D is the thickness of the flat portion of the mat[18]. This implies that the effective support of the soil is provided within the width S_e. Actual support of ribbed mats by the underlying soil is not known.

25. Adequate guidelines for other soil parameters such as the active depth for heaving soil Z_a and the edge moisture variation distance e_m are especially incomplete. Z_a is defined as the depth below which vertical soil movements are insignificant. The amount of vertical soil strain that is considered insignificant at depth Z_a is unknown, consequently Z_a is poorly defined. e_m is the lateral distance beneath the mat from the mat perimeter subject to vertical movement from seasonal and long-term soil moisture changes.

26. Advanced facilities. Mat foundations are being used more frequently to support structures with functional requirements that limit the acceptable differential movement. For example, warehouses and service centers are becoming automated with robotic equipment that requires close tolerances on vertical alignment and "superflat" floor slabs. Experience is still limited concerning the toleration of this equipment to differential movement. Facilities containing specialized machinery establish requirements for limited differential movements. Technology does not yet exist that allows the reliable prediction of foundation movements under the given structural loads and soil conditions to the accuracy needed to assure "superflat" conditions. Adequate guidelines do not exist that allow economic design of foundations that can control deformations to within acceptable limits. The serviceability of these new facilities may therefore be restricted by the performance of the foundation.

Purpose and Scope

27. This report was prepared to provide guidelines for design and construction of mat foundations with emphasis on ribbed mats in expansive soil. A review of methodology, Part II, was initially completed as an aid in determining useful methodologies and current design limitations. Case histories of the performance of existing construction are discussed in Part III to provide documentation leading to appropriate procedures for design. A

[18]American Concrete Institute 318-80, Section 8.10.2

field study of a partially instrumented stiffened and ribbed mat described in Part IV documents the actual performance of a ribbed mat under service conditions. Guidelines for soil exploration, evaluation of soil input parameters for design of ribbed mat foundations, a procedure developed by the Southwestern Division of the Corps of Engineers for design of ribbed mat foundations in expansive soil using these input parameters[12], and construction methodology are described in Part V. Part VI concludes with recommendations for future work to improve serviceability of permanent military facilities, reduce requirements for design through ground modification or soil moisture stabilization methods, and to reduce maintenance and repair costs.

28. The scope of this report excludes the design of mats on piles. A study of methods for reducing foundation soil movements such as ground modification or soil moisture stabilization is also excluded.

PART II: REVIEW OF METHODOLOGY

Introduction

29. Design is a multi-discipline area that includes functional, aesthetic, geotechnical, structural, mechanical, and electrical considerations. Consequently, a satisfactory design for a structure is normally accomplished through cooperation between the owner, architect, geotechnical engineer, structural engineer, and others. This review is concerned only with those design functions necessary to analyze the performance of the foundation and supporting soil.

30. Serviceability of the structure is approached in terms of the expected total and differential foundation displacements and comparison with the allowable movements. Ultimate bearing capacities of the foundation soil normally do not control design because structural loads must be limited in order to maintain displacements within allowable total and differential movements. Allowable bearing capacities may be estimated from calculated ultimate bearing capacities using factors of safety that have been shown to maintain displacements within acceptable levels.

General Design Procedure

31. A general procedure for design of mat foundations is proposed in Table 1. An initial function of the geotechnical engineer is to evaluate different types of potentially applicable foundations and their relative economy and performance compatible with the soil profile, step 1, and structural requirements, step 2. Soil displacements, step 3, are estimated from given structural loads as an aid in selection of a suitable foundation. The most suitable foundation is subsequently determined in cooperation between the geotechnical engineer, structural engineer, architect, construction engineer, and the owner/operator. A mat may be selected if construction costs compare favorably with other foundation types, expected displacements are within structural limits, and expertise required for construction is locally available. Other items impacting the decision may include construction time, ease of construction, and ability to limit angular deformations or architectural distress.

Table 1

General Procedure for Design of Mat Foundations

Step	Evaluate	Remarks
1	Soil profile	Characterize the soil profile from in situ field tests, boring logs, and laboratory tests on soil samples; detailed tests performed on the probable foundation bearing stratum; soil parameters for design determined from results of field and laboratory tests.
2	Structural requirements	Determine preliminary distribution of loads, location and size of walls and columns based on initial structural design and functional requirements; determine maximum allowable total and differential movements; total settlements usually limited to 2 inches and total heave to 1.5 inches; differential movements depend on serviceability requirements and usually limited to 0.5 inch for normal design or 1 to 1.5 inches for stiffened ribbed mats.
3	Total soil displace-ments	Total displacements for the given structural loads are estimated from empirical relationships, elastic theory, Winkler concept, and consolidation/swell analysis; these movements are checked against allowable total movements.
4	Initial mat thickness	Determine minimum initial mat thickness by resistance of the mat to punching shear.
5	Minimum depth of mat base and bearing capacity	Base of mat should be below soil influenced by frost heave, soil erosion, and excessive soil moisture changes; design loads may require adjustments if the depth of mat base D_b is fixed within a limited range and the allowable bearing capacity exceeded; floating or compensated mats may be used if settlements would otherwise be excessive.
6	Differential soil dis-placements	Estimates of differential displacements may use elastic compression and consolidation or swell in soil-structure interaction analysis for given loads and soil profiles.
7	Final structural design	Final design checked for compliance with shear, bending moment, and deflection requirements; uniform pressure method and ACI 336-87, 318-80, 340-77), Strength Design Method usually applied; design of flexible mats may use a soil-structure interaction analysis.
8	Site development plan	Construction of additional nearby structures and changes in environment can affect performance of previous construction and must be considered in the site plan.

32. An initial estimate of mat thickness required to support the indicated loads is made when a mat foundation is considered, step 4. The minimum or most appropriate depth of the foundation base, step 5, is then selected based on the soil profile and functional requirements of the structure. Soil displacements should be analyzed in detail for the indicated structural loads and distribution of loads, step 6. If the allowable settlements or bearing capacity are exceeded, then adjustments to the design or foundation depth are indicated. The usual procedure for structural design of mat foundations, step 7, is the uniform pressure method assuming linear contact soil pressures. The last step should include a site development plan, step 8, because construction of additional adjacent structures and changes in soil conditions caused by the environment can influence the performance of previous construction. Excavation and loads of the proposed facility may also influence the performance of adjacent existing structures.

Soil Profile

33. Evaluation of soil parameters as a function of depth will permit estimation of potential movements and bearing capacities for selected mat dimensions and load distributions leading to an optimum foundation. A surface examination of the sites selected for possible construction of the structure should be conducted first followed by a subsurface soil sampling and testing program to obtain suitable soil parameters required for selection of the design and method of construction. Soil parameters should be plotted with results of visual boring logs as a function of depth to evaluate the soil profile.

34. Depth of exploration. The recommended depth of soil sampling is at least twice the minimum width B of the mat foundation or the depth to incompressible soil, whichever comes first. Greater exploration depths may not be necessary because stress intensities imposed by the structure on the foundation at these depths are about 10 percent or less of the loads applied at the foundation level[19]. Existence of soft layers beneath firm strata should be checked since soft layers can lead to excessive displacements under relatively small loads. In practice where primary geological formations, such as those of unweathered and unfissured rock and dense shale, are encountered

[19]Boussinesq 1885; Westergaard 1938

the depth of exploration is often not related to the size of the structure. It may be sufficient to limit exploration to a depth that includes the weathered and fissured materials and depths influenced by the effects of construction. Consideration should be given to obtaining samples near the proposed center, corner, and mid-edge of the structure. Details of surface and subsurface exploration programs are available in EM 1110-2-1804, "Geotechnical Investigations".

35. Field tests. In situ tests may be conducted to evaluate soil strength and deformation behavior. These tests are suitable as an aid to foundation design and construction, especially if undisturbed samples cannot be easily obtained during sampling such as in strata containing cohesionless soil. Field tests are often less costly than soil sampling and laboratory testing programs. An important limitation of field tests is that they are not a direct measure of soil parameters required for design, but are used to estimate soil parameters through correlation factors. Correlation factors vary substantially between types of soil; therefore, laboratory and different types of field tests should be performed whenever possible to verify soil parameters used for design. Some field tests appropriate for evaluation of soil parameters useful to mat foundation design are outlined in Table 2.

36. Laboratory tests. Laboratory tests such as Atterberg limits are initially performed on disturbed samples at relatively frequent depth intervals (within 5 ft) to identify soil suitable as a bearing stratum. Atterberg limits can be used to make a preliminary estimate of the relative potential for soil volume changes[5]. Unconfined compression (UC) and unconsolidated undrained (Q) tests will provide undrained parameters for analysis of bearing capacity and undrained soil elastic modulus for estimates of immediate displacements. UC tests may underestimate strengths because confining pressures are not applied. Confining pressures for Q tests should be on the order of in situ overburden pressures. Consolidated undrained tests with pore pressure measurements (R), although not commonly performed on cohesive soils, provide drained strength parameters for analysis of bearing capacity and drained soil elastic moduli for estimates of long-term displacements. One-dimensional (1D) consolidation and swell tests may be performed to evaluate long-term consolidation and heave. Results of 1D tests

Table 2

Field Soil Tests Useful for Analysis of Performance of Mat Foundations

Test	Application	Advantages	Disadvantages
Standard penetration SPT (ASTM D 1586)	Bearing capacity, elastic soil modulus, and settlement	Data easily obtained during exploration using standard split spoon sampler; useful in soils difficult to sample such as sands and silts; inexpensive when performed in association with sampling for laboratory classification tests	Numerous factors influence blowcount such as variation in drop height, interference with free fall, distorted sampler, and failure to seat sampler on undisturbed soil
Cone penetration CPT (ASTM D 3441)	Undrained shear strength friction angle elastic modulus and bearing capacity for clays and sands	Simulates shape of a pile so tip and side friction some function of same in pile foundations; soil parameters usually multiple of tip resistance	Substantial scatter in correlations between different soils; pore pressure buildup during driving may influence readings
Pressure-meter PMT (ASTM D 4719)	Most soil parameters for clays, silts, and sands	Readings theoretically related with soil stiffness useful in design of deep foundations	Requires carefully prepared borehole; careful calibration of device; more costly than SPT or CPT; inconsistencies in results common
Plate load PLT (ASTM D 1194)	Plate coefficient of subgrade reaction k_p for any soil	Direct measure of k_p within depth twice plate diameter; useful to estimate elastic soil modulus up to depths twice plate diameter	Costly; must extrapolate to mat dimensions; results not useful to depths below twice plate diameter
Dilatometer (Schmert-mann 1986)	Most soil parameters for clays, silts, and sands	Uses same pushing equipment as CPT; elastic modulus theoretically related with test data	Data depends on small 1.1 mm motion of membrane; soil disturbance from pushing probe may influence data

may be corrected to three-dimensional behavior by using the Skempton and Bjerrum procedure[20], but practical experience using one-dimensional analysis with normally consolidated soil indicates reasonable (± 50 percent) accuracy[7].

Total Displacements

37. Settlement of foundations cause by applied loads on underlying soil consists of elastic (immediate) and time dependent components

$$\rho_t = \left|\rho_i + U_t \cdot \rho_{con}\right| \leq \left|\rho_f\right| \tag{2a}$$

$$U_t = \frac{e_o - e_t}{e_o - e_f} \tag{2b}$$

where

ρ_t = total settlement at time t, ft

ρ_i = immediate settlement, ft

ρ_{con} = consolidation settlement, ft

ρ_f = long-term or final total settlement, ft

U_t = consolidation ratio at time t

e_o = initial void ratio

e_t = void ratio at time t

e_f = long-term or final void ratio

These settlements are negative values, while heave is denoted as positive. Immediate settlement occurs during placement of loads from elastic and inelastic soil deformation without change in water content. Consolidation settlement can be substantial in clays and occurs when pressures applied to the soil exceed the preconsolidation stress in the soil. Consolidation settlement is a result of volume reduction in the soil caused by expulsion of pore water from the soil and may be evaluated by standard consolidation analysis[21]. If the stresses beneath the base of the mat do not exceed the preconsolidation stress, then deformation will be limited to recompression settlement. Some heave may occur if stresses in soil beneath the base of the mat are significantly less than the actual swell pressure in the founding soil system and free water is made available to the founding system.

---

[20]Skempton and Bjerrum 1957

[21]Chapter 3, Engineer Manual 1110-1-1904, "Settlement Analysis"

38. Elastic settlement. Experimental data show that the immediate settlement of foundation soil resembles that of an elastic, isotropic solid[17,22] and may be calculated from Young's soil modulus E_s and Poisson's ratio μ_s. Poisson's ratio for soil usually varies from 0.25 to 0.49 with saturated soils approaching 0.49. Reasonable overall values of Poisson's ratio are 0.30 to 0.40. Calculation of elastic settlement is usually much more sensitive to in situ variations in elastic modulus rather than errors in estimating a value for μ_s.

39. Typical values of elastic modulus are shown in Table 3. An appropriate measure of E_s from laboratory consolidated-undrained triaxial strength tests is the initial tangent modulus $E_{ti} = 1/a$ of the hyperbolic model where a is the intercept of a plot of the ratio of strain/deviator stress versus strain, Figure 3[23]. The elastic modulus may also be taken as E_{sec}, the mean secant modulus at 1/2 of the undrained soil compression strength, Figure 3a[24]. Table 4 summarizes some methods of estimating the elastic modulus from in situ test resultrs. Initial elastic moduli such as E_{ti} or unload-reload moduli such as from the PMT, Table 4, often better simulate stiffness of su[illegible]ath mat foundations because earth pressures are usually small. Soil disturbance may also cause low estimates of elastic modulus from test data. E_s should be evaluated by several methods whenever possible such as those described in Table 4, particularly for important structures.

40. The average immediate settlement of a foundation on an elastic soil may be given by the improved Jambu approximation[25]

$$\rho_i = -\mu_o \cdot \mu_1 \cdot \frac{q_o \cdot B}{E_s^*} \tag{3}$$

where

μ_o = influence factor for depth D of foundation below ground surface, Figure 4

μ_1 = influence factor for foundation shape, Figure 4

---

[22]Pickett and Ray 1951
[23]Duncan and Chang 1970
[24]Skempton 1951
[25]Christian and Carrier 1978

Table 3

Typical Elastic Moduli

Soil	Relative Stiffness	Young's Soil Elastic Modulus, E_s, ksf
Clay	Very soft	10 - 100
	Soft	100 - 400
	Medium	400 - 1000
	Stiff, Silty	1000 - 2000
	Sandy	500 - 4000
	Shale	2000 - 4000
Sand	Loose	200 - 500
	Dense	500 - 2000
	Dense with gravel	2000 - 4000
	Silty	500 - 4000

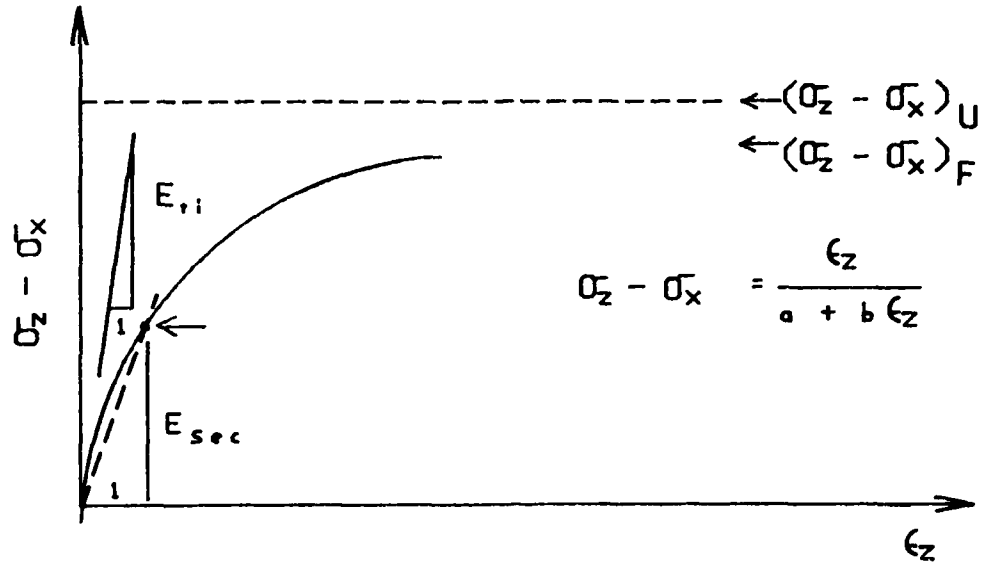

a. STRESS-STRAIN CURVE

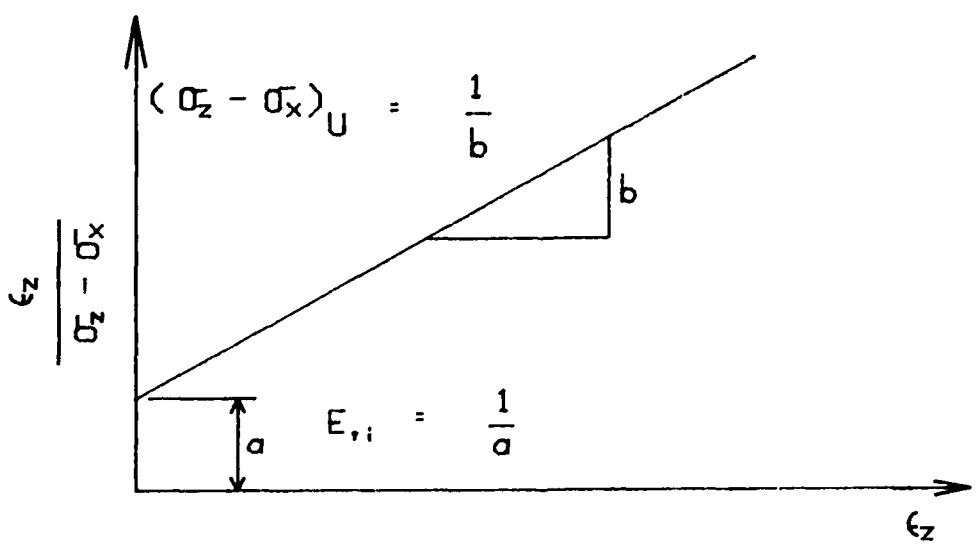

b. HYPERBOLIC PARAMETERS a, b

Figure 3. Elastic moduli from laboratory undrained strength tests

Table 4

Methods for Estimating Elastic Modulus From In Situ Soil Tests

Source	E_s, ksf	Definitions
	Standard Penetration Test	
Schultz and Sherif (1973)	$9.4N^{0.87}\sqrt{B}\cdot\left[1 + 0.4\frac{D}{B}\right]$	N = average blow count/ft B = width, ft D = embedment depth, ft
Bowles (1988) Normally consolidated sand: Overconsolidated sand: Saturated sand Clayey sand: Silty sand: Gravelly sand:	 10(N+15) 3600 + 15N 5(N+15) 6.4(N+6) 6(N+6) 24(N+6)	N based on actual input drive energy 55 percent of theoretical
	Cone Penetration Test	
Mitchell and Gardner (1975)	$\frac{(1 + \mu_s)(1 - 2\mu_s)}{(1 - \mu_s)}\cdot\alpha\cdot q_c$	α = correlation factor depending on soil, varies from 1 to 8 (see Table C-4, EM 1110-1-1904 for details on α) q_c = cone bearing resistance, ksf μ_s = Soil Poisson's ratio
	Pressuremeter Test	
Hughes (1982)	$(1 + \mu_s)\cdot E_p$	E_p = Unload-reload pressuremeter modulus, ksf
	Plate Load Test	
Bowles (1982)	$BI_w\cdot\frac{(1 - \mu_s^2)}{\Delta\rho/\Delta q_p}$	B = width or plate diameter, ft I_w = influence factor, $\pi/4$ for rigid circular plate 0.82 for rigid square $\Delta\rho$ = change in settlement, ft Δq_p = change in pressure on plate, ksf
	Dilatometer	
Schmertmann (1986)	$(1 - \mu_s^2)\cdot 34.7\cdot\Delta p$	Δp = change in pressure between inflated/deflated positions of the membrane

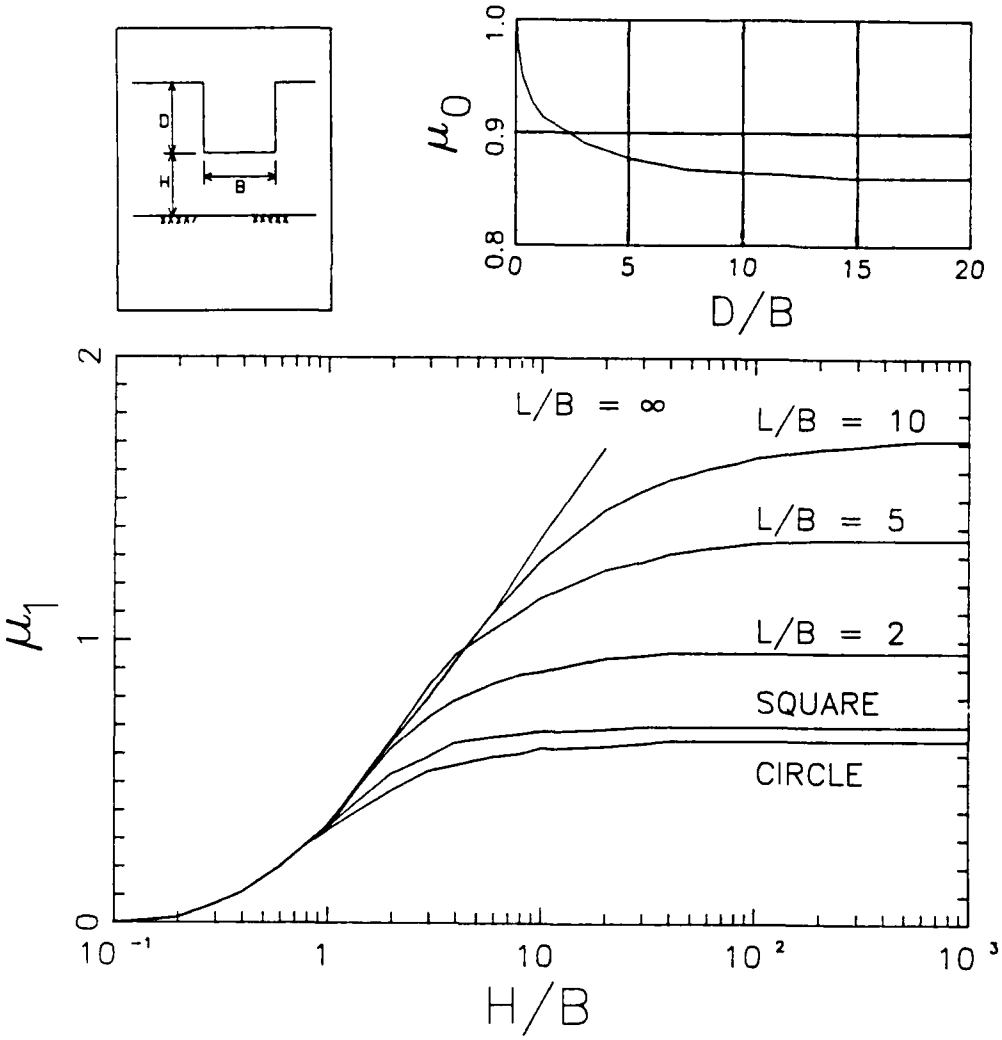

$$\rho_i = -\mu_0 \cdot \mu_1 \cdot \frac{q_o \cdot B}{E^*_s}$$

q_o = CONTACT PRESSURE, KIPS

L = LENGTH, FT

B = WIDTH, FT

E^*_s = YOUNG'S SOIL MODULUS, KSF

Figure 4. Chart for estimating immediate settlement in cohesive soil. Reprinted by permission of the National Research Council of Canada from the Canadian Geotechnical Jouirnal, Vol 15, 1978, "Janbu, Bjerrum, and Kjaernsli's Chart Reinterpreted", by J. T. Christian and W. D. Carrier III, p 127

q_o = bearing pressure, ksf

E_s = equivalent Young's modulus of the soil, ksf

Comparison of test calculations and results of finite element analysis have indicated errors from Equation 3 usually less than 10 percent and always less than 20 percent for H/B between 0.3 and 10, L/B between 1 and 5, and D/B between 0.3 and 3, Figure 4[25]. Reasonable results are given in most cases when μ_o is set equal to unity.

41. An equivalent elastic modulus E_s^* is required in many settlement analysis methods when stiffness varies with depth. The Briaud (1979) method

$$E_s^* = \frac{A}{\sum_{z=1}^{z=n} \frac{a_i}{E_{si}}} \tag{4a}$$

where

$A = \int_0^\infty I_z dz$, area under strain influence factor, Figure 5, for homogeneous soil and type of loading considered, ft

$a_i = \int_{z_i}^{z_i+1} I_z dz$, area under strain influence factor, Figure 5, for the ith soil layer and type of loading considered, ft

is applicable to a soil profile when stiffness varies with depth and considers edge or center types of loading, but evaluation of the integrals may be laborious. The equivalent radius $R = \sqrt{LB/\pi}$ where L = mat length, ft, B = mat width, ft, and $L \leq 2B$. The Kay and Cavagnaro (1983) method simplifies this analysis such that

$$E_s^* = \frac{2qR \bullet (1 - \mu_s^2)}{\rho_c} \tag{4b}$$

where

q = uniform pressure on soil, ksf

ρ_c = center settlement, ft

μ_s = soil Poisson's ratio

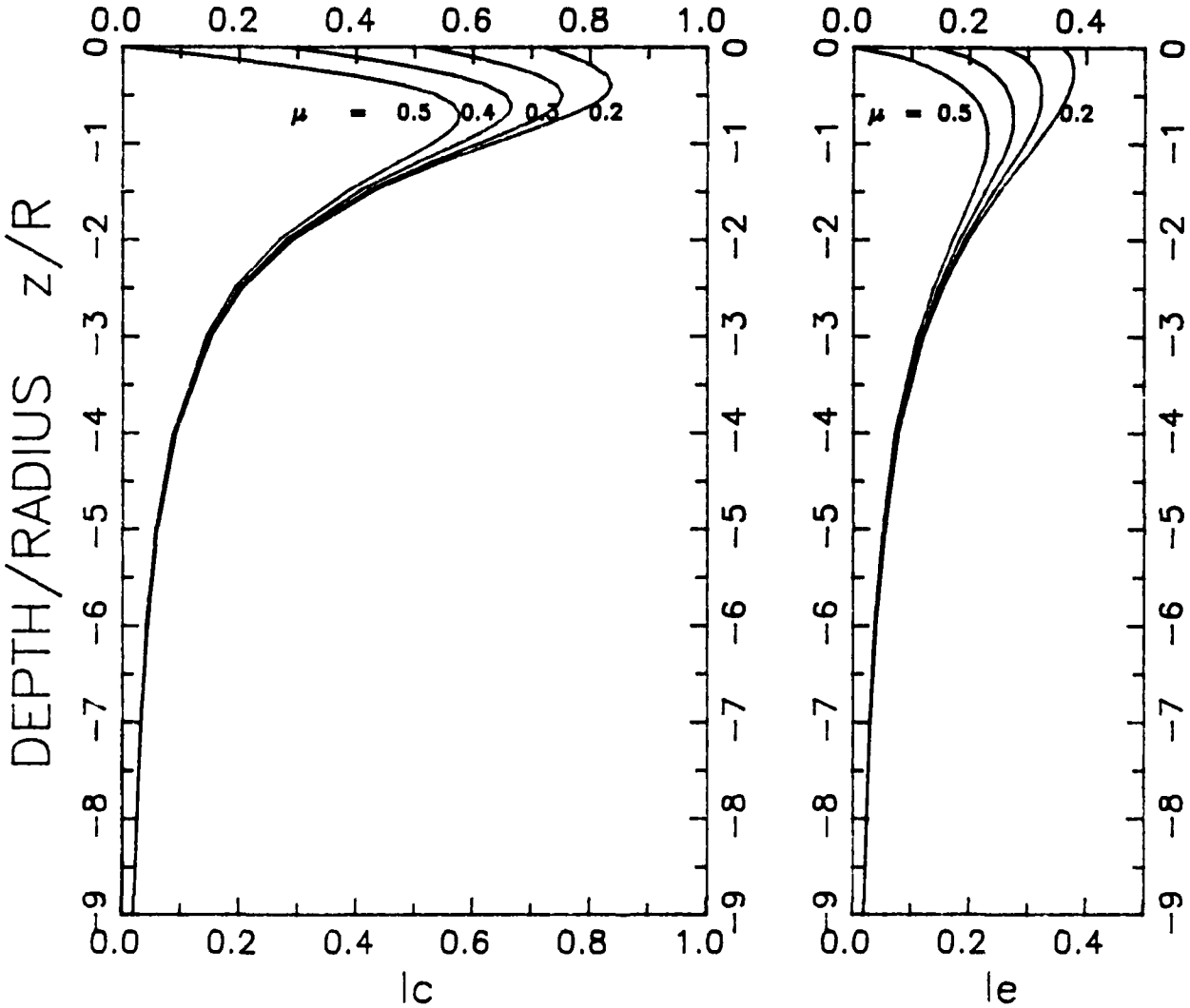

Figure 5. Influence factors I_c for center and I_e for edge settlement using data from Ahlvin and Ulery (1962). $R = \sqrt{LB/\pi}$ where L = length and B = width of the mat, μ_s = soil Poisson's ratio.

The center settlement may be calculated for a uniform pressure q as discussed later in paragraph 68. If the elastic modulus increases linearly with depth, then from Appendix A

$$E_s^* = \frac{2kR(1 - \mu_s^2)}{0.7 + (2.3-4\mu_s)\log n} \tag{4c}$$

where

k = constant relating E_s with depth z, ksf/ft

E_s = Young's elastic soil modulus, $E_o + kz$, ksf

E_o = initial elastic soil modulus at the ground surface, ksf

n = $kR/(E_o + kD_b)$

D_b = depth of mat below ground surface, ft

Equation 4c is applicable to a mat with base at depth D_b and the soil at depths greater than $2B$ is incompressible. The Gibson model (1967)

$$E_s^* = \frac{Bk}{2} \tag{4d}$$

is applicable for elastic moduli increasing linearly with depth from zero at the ground surface for the mat base at the ground surface,

42. Winkler settlement. The concept of subgrade reaction was introduced[26] for computation of displacements in soil beneath railroad tracks. This concept has been applied to the analysis of bending moments and deflections in footings, mats, grillage beams, and other foundations that can be represented by a beam resting on an elastic subgrade. A soil contact pressure q causes a deflection ρ related by a constant of proportionality

$$k_{sf} = \frac{q}{\rho} \tag{5}$$

where

k_{sf} = coefficient of subgrade reaction applicable to the foundation, kips/ft^3

q = contact pressure on soil, ksf

ρ = settlement, ft

[26]Winkler 1967

Each point behaves independently of any other as though the supporting soil is a fluid. Stress and strain computations are more easily and economically accomplished using the Winkler hypothesis than elastic theory. Displacements and bending moments in mats may be estimated from influence charts[22] for given loading pressure, mat characteristics, and the coefficient of subgrade reaction. Theoretical and experimental investigations have shown that the Winkler hypothesis is generally not satisfied except for beams of infinite length such as railroad ballast, roads, and embankments resting on a semi-infinite elastic subgrade. Appropriate values of k_{sf} are not easily determined because they are not unique depending on the location in the mat, mat size and depth of base, and whether bending moments or displacements are being determined[17]. Little is known on how k_{sf} varies across the mat.

43. Terzaghi's experience (1955) indicates that for long beams or continuous footings on the ground surface

$$\text{Sands:} \qquad k_{sfo} = k_{sp} \bullet \frac{(S+1)^2}{2S} \tag{6a}$$

$$\text{Clays:} \qquad k_{sfo} = k_{sp} \bullet \frac{1}{1.5S} \tag{6b}$$

where

k_{sfo} = coefficient of subgrade reaction at the ground surface beneath the footing, ksf/ft

k_{sp} = coefficient of subgrade reaction of 1-ft by 1-ft plate or beam 1-ft wide at the ground surface, ksf/ft

S = spacing of column or line loads on mat, ft

Table 5 provides some values of k_{sp} for sands and clays if plate load tests are not performed. If loads are applied to the mat by columns, then the influence of these loads becomes less with increasing distance from the columns. The maximum length of influence is about 7D where D is the mat thickness, ft[27]. S is therefore ≤ 7D for locally applied loads. If the footings are in sand with the base below the ground surface, then[28]

$$k_{sf} = k_{sfo}(1 + 2D_b/B)^{1/2} \tag{7a}$$

---

[27]Terzaghi 1955
[28]Ramasamy, Rao, and Prakash 1982

Table 5

Empirical Estimates of plate coefficient of Subgrade Reaction[27]

Sand			Clay		
Relative Density	k_{sp}, ksf/ft		Consistency	Undrained Shear Strength, ksf	k_{sp}, ksf/ft
	Dry/Moist	Submerged			
Loose	80	50	Stiff	1 - 2	150
Medium	260	160	Very Stiff	2 - 4	300
Dense	1000	600	Hard	> 4	600

$$k_{sf} = k_{sfz} \left[\frac{(1+K_o)(1+2D_b/B)}{(1+2K_o+4K_oD_z/B)} \right]^{1/2} \tag{7b}$$

where

k_{sfz} = coefficient of subgrade reaction at depth D_z, ksf/ft

D_b = embedment depth, ft

K_o = coefficient of earth pressure at rest

B = footing width, ft

44. k_{sf} may also be estimated from elasticity theory by substituting Equation 3 into Equation 5 to give

$$k_{sf} = \frac{E_s^*}{\mu_0 \mu_1 B} \tag{8a}$$

where μ_0 and μ_1 are found from Figure 4. Vesic and Saxena (1968) had performed parametric analysis that indicated good correlations with bending moments for

$$k_{sfm} = \sqrt[3]{\frac{E_s^*}{E_c}} \cdot \frac{E_s^*}{(1 - \mu_s^2)D} \tag{8b}$$

where

k_{sfm} = coefficient of subgrade reaction consistent with bending moments, ksf/ft

E_c = elastic modulus of concrete, ksf

D = mat thickness, ft

Equation 8b must be divided by 2.4 to obtain good correlation with displacements[17]. The Winkler foundation does not provide unique values of k_{sf} for both calculation of bending moments and displacements for mat foundations. If the coefficient of compressibility is known, then[29]

$$k_{sf} = \frac{1}{f m_v S} \tag{9}$$

where

f = factor from 0.5 to 1

m_v = coefficient of compressibility, ksf^{-1}

The coefficient of compressibility may be estimated from in situ dilatometer DMT tests or laboratory consolidation tests on undisturbed specimens.

45. A comparison of Equations 6b, 8a and 8b for a concrete mat of depth D = 1 ft on a medium stiff clay with E_s = 400 ksf, μ_s = 0.33, E_c = 432,000 ksf, B = spacing of loads = 25 ft is shown as follows:

Equation	Coefficient of Subgrade Reaction k_{sf}, ksf/ft
6b	14.3 ksf/ft
8a	16.7 ksf/ft
8b	43.8 ksf/ft

For Equation 6b, k_{sf} is assumed to be about 150 ksf/ft and S = 7D or 7 ft. For Equation 8a, the length to width ratio L/B is assumed 2 so that μ_1 = 0.96, Figure 4, and μ_o is assumed unity. The result of Equation 8b is valid for a comparison of bending moments. Dividing results of Equation 8b by 2.4 is 18.2 ksf/ft, which is consistent with results of Equations 6b and 8a.

Initial Mat Thickness

46. Thickness and reinforced steel requirements of mat foundations depend on applied loads and differential movements in the supporting

[29]Yong 1960

foundation soil. Applied loads should be arranged to cause a uniform pressure on the underlying foundation soil thereby reducing differential movement. A uniform distribution of pressure on the soil occurs when corner Q_c, edge Q_e, and interior Q_i column loads are in the ratio of 1 to 2 to 4; e.g., $Q_c = Q_i/4$ and $Q_e = Q_i/2$. Corners and edges of structures will nearly always have wall loads added to the floor loads, which can be accommodated to make a uniform pressure distribution, if necessary, by widening the mat beyond the limits of the superstructure. The total edge load Q_e at perimeter walls relative to the interior required to maintain uniform soil pressure also depends on the deck framing system. In order to avoid secondary moments in the mat, perimeter wall loads should be about 1/3 of the first interior column load and 3/8 of the next interior column load.

47. The initial mat thickness is evaluated to resist punching shear based on principles of statics. The force on the critical shear section of the concrete is equal to the force on the mat beyond the shear section caused by the soil pressure. The soil reaction pressure is assumed uniform. The critical shear section for diagonal tension failure is assumed to intersect at the base of the slab a distance $d/2$ from the face of a column support where d is the effective depth measured to the center of gravity of the reinforcement steel. This is the depth required to satisfy shear[30]. Perimeter and interior load bearing (shear) walls are checked for wide-beam shear at a distance d from the wall face[1].

48. The total mat thickness D required, after steel reinforcement is added to satisfy bending moments, is[1]

$$D = d + d_b + \text{Cover} \tag{10}$$

where

d = depth to satisfy shear, ft

d_b = distance from center of gravity of reinforcing steel to the bottom edge of the reinforcing steel (bar diameter/2), ft

Cover = 3 inches for reinforced concrete cast against and permanently in contact with ground; otherwise, 2 inches for No. 6 bars or larger and 1.5 inches for No. 5 bars and smaller[31]

---

[30]ACI Committee 340-77

[31]ACI Committee 318-80, Section 7.7.1

Reinforcement steel should not be added only to reduce mat thickness because the smaller thickness reduces rigidity. Reduced rigidity tends to localize column and wall loads instead of spreading them as assumed in rigid (conventional) design based on a linear soil pressure distribution. A good initial estimate of mat thickness may be found from Seelye (1956) which contains tables relating soil bearing pressures, column loads, concrete compressive strength, and 20 ksi reinforcement steel with the thickness of square column footings; however, yield strength of reinforcement steel currently used is often 60 ksi.

49. Column shear resistance. Equations 11 in Table 6 show the required thickness d to satisfy punching shear requirements for interior, edge, and corner column and floor loads that cause a uniform soil pressure q'. The shear strength v_c provided by concrete in diagonal tension for ultimate strength design USD is[32]

$$v_c = 4 \cdot \phi \sqrt{f'c} \cdot 0.144 \tag{12}$$

where

v_c = concrete shear strength, ksf

$f'c$ = concrete compressive strength, psi

ϕ = workmanship factor for shear, 0.85

The factor 0.144 converts from psi to ksf. v_c = 26.8 ksf for 3000 psi concrete. Steel will be required to satisfy bending in the longitudinal direction[33]

$$M_u = \phi \cdot A_s \cdot f_y \left[d - \frac{a'}{2} \right] \tag{13a}$$

$$a' = A_s f_y / (0.85 \cdot f'c \cdot b') \tag{13b}$$

where

M_u = bending moment per width of strip, in-lb

A_s = area steel per width of strip, in^2

d = effective mat thickness, inches

f_y = yield strength of steel reinforcement, psi

b' = width of strip, usually 12 inches

---

[32]ACI Committee 318-80, Section 11.10.3

[33]ACI Committee 318-80, Section 7.13

Table 6

Required Thickness to Resist Punching Shear

Location	Diagram: Plan	Diagram: Section	Equations
Interior	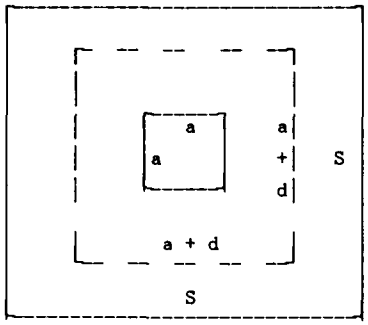	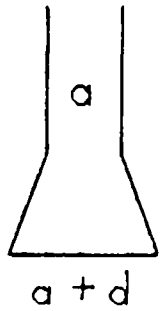	For equilibrium: $4v_c d(a + d) = q'S^2 - (a + d)^2$ $d = \dfrac{-ea + 2\sqrt{a^2 + \frac{q'}{v_c} \cdot \frac{S^2}{4} \cdot e^*}}{e^*}$ (11a)
Edge	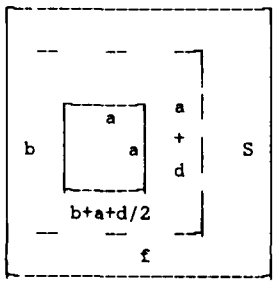	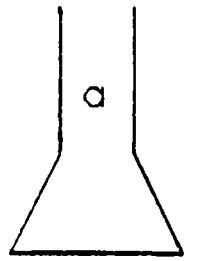	For equilibrium $(0 \le b \le d/2)$: $v_c\left[2(b+a+\frac{d}{2}) + (a+d)\right] \cdot d = q' \cdot \left[Sf - (a+d)(b+a+\frac{d}{2})\right]$ $d = \dfrac{-(b+\frac{3}{2})e + \sqrt{\left[(b+\frac{3}{2})e\right]^2 + \frac{2q'S}{v_c} e^* \left[Sf - a(a+b)\right]}}{e^*}$ (11b)
Corner	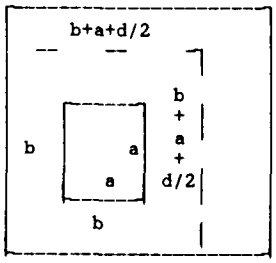		For equilibrium $(0 \le b \le d/2)$: $v_c\left[2(b+a+\frac{d}{2})\right] \cdot d = q' \cdot \left[f^2 - (b+a+\frac{d}{2})^2\right]$ $d = \dfrac{-2(a+b)e + 2 \cdot \sqrt{\left[(a+b)e\right]^2 + \frac{q'}{v_c} e^* \cdot \left[f^2 - (a+b)^2\right]}}{e^*}$ (11c)

Notation:

- a = column width, ft
- b = distance column from edge/corner, ft
- d = effective depth of mat, ft
- S = column spacing, ft
- v_c = concrete shear strength, ksf
- q' = soil pressure resisting punching shear, ksf
- e = $2 + q'/v_c$
- e^* = $4 + q'/v_c$
- f = $b + (a+S)/2$

Equations 11 for typical column widths a of 1 to 4 ft, column spacings of 10 to 30 ft, and distance b from the edge/corner of 1 ft indicate that the thickness of concrete mats may be 7 percent less at the edge and 20 percent less at the corner than in the interior of the mat.

50. Wall punching resistance. The mat thickness required to resist wide-beam shear for reinforced concrete walls and an applied uniform soil pressure q' is

$$d = \frac{\frac{q'}{2v_c}(S - a)}{1 + \frac{q'}{v_c}} \tag{14a}$$

where

v_c = $2 \cdot \sqrt{f'c} \cdot 0.144$ ksf[34]; note that this is 1/2 the resistance permitted for columns

d = effective depth, ft

a = wall thickness, ft

S = wall spacing, ft

ϕ = workmanship factor for shear, 0.85

For masonry walls,

$$d = \frac{\frac{q'}{2v_c}\left[S - \frac{a}{2}\right]}{1 + \frac{q'}{v_c}} \tag{14b}$$

The concrete shear strength v_c = 13.41 ksf for 3000 psi concrete. Equations 14 were developed similar to those in Table 6[35].

51. Figure 6 illustrates the trend in mat thickness d required to resist punching shear for interior 25-ft column spacings based on Equation 11b for applied uniform soil pressures qm' of 0.1, 0.2, and 0.4 ksf/story. qm' is the average pressure per story and equal to q'/Ns where Ns is the number of stories. Figure 6 also shows the distribution of mat thickness d

---

[34]Uniform Strength Design method ACI Committee 318-80, Section 11.10.1a
[35]after method of Bowles 1982

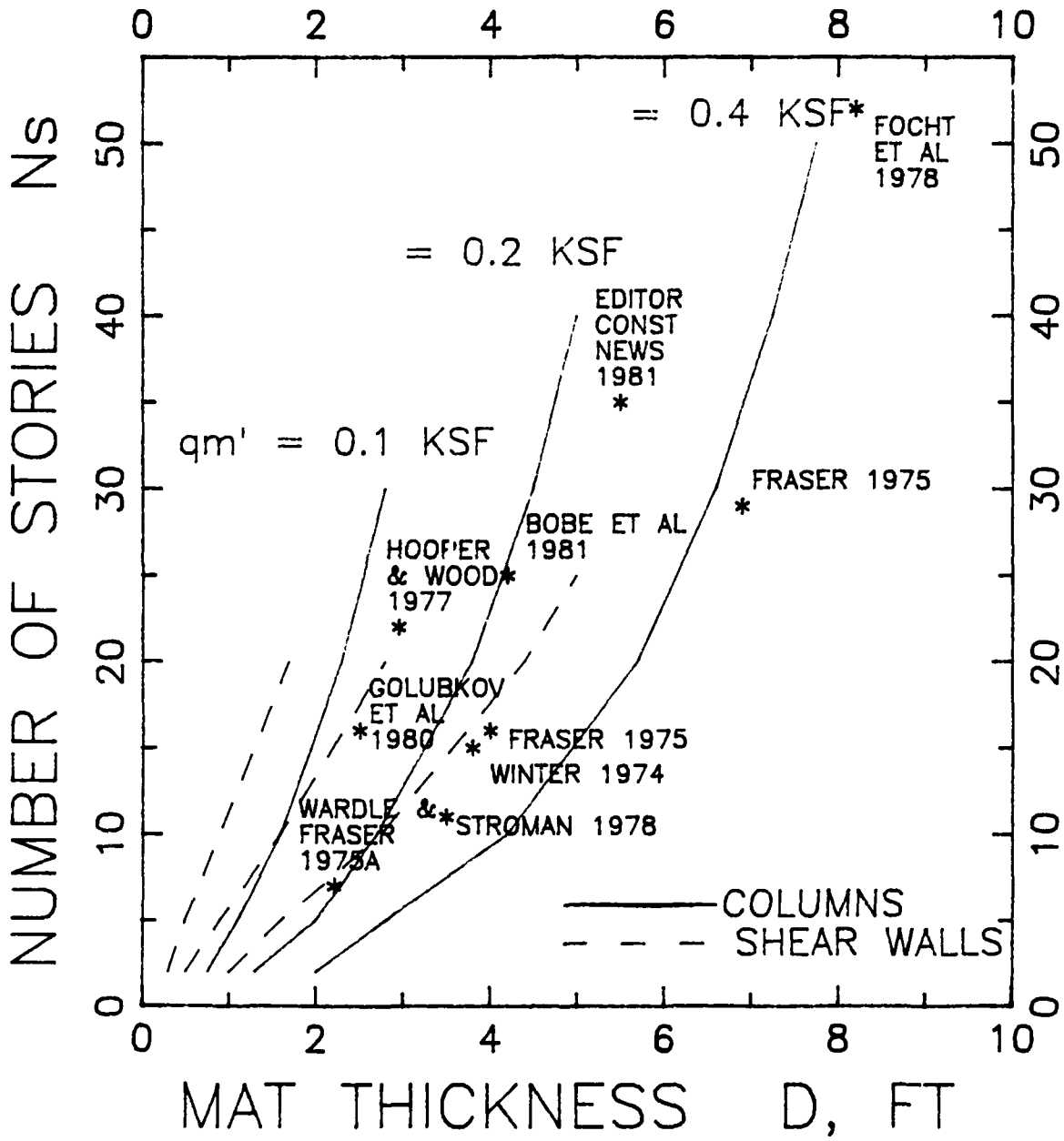

Figure 6. Number of stories for buildings versus thickness of mat

required to support shear walls as a function of the number of stories from Equation 14a assuming a 1-ft wall thickness, 25-ft wall spacing, and uniform soil pressure qm' of 0.1, 0.2, and 0.4 ksf/story using 3000 psi concrete. Thicker walls only slightly reduce the required mat thickness. About 0.3 ft should be added to the calculated required thickness d to obtain the total mat thickness D. The column width a was assumed to increase in proportion with the number of stories; i.e., $a = 1$, 2, and 4 ft for $Ns = 3$, 12, and 50 stories, respectively.

52. Figure 6 illustrates that the thickness of the 8.25-ft thick mat of the One Shell Plaza building with soil pressure of 0.4 ksf/story[36] is only 0.5-ft greater than that calculated for $qm' = 0.4$ ksf/story. A calculated soil pressure of 0.2 ksf/story is consistent with the observed 0.18 ksf/story given for the 7 story frame structure[37]. A calculated soil pressure of 0.3 ksf/story is also consistent with the observed 0.3 to 0.4 ksf/story for an 11 story hospital[38]. The 0.24 ksf/story pressure observed on the 3-ft mat of the 22 story residential building[39] is a little high for punching resistance only to column loads with a column spacing of 25 ft and indicates that some load may be carried through the walls or column spacing is less than 25 ft.

Minimum Depth of Foundation

53. A stratum selected to support the foundation and superstructure depends on functional requirements of the structure, locally existing practice for determining foundation depths necessary to avoid frost heave, soil erosion, soil moisture changes, and depths at which the soil bearing capacity is sufficiently large to support the structure. The depth of thin slabs for light structures is often above grade and on fill, unless a basement is required. Thin mats therefore often have distortion problems from soil foundations with 25-ft column spacing when punching shear controls design movements as a result of seasonal and long-term moisture changes in the soil beneath and near the perimeter of the mat. Mats constructed in excavations are subject to distortions caused by rebound of underlying soil, installation of utilities, and other construction effects. Thin mats subject to

---

[36]Focht, et al 1978
[37]Wardle and Fraser (1975a)
[38]Stroman 1978
[39]Hooper and Wood 1977

distortion $\beta > 1/500$ are often designed with ribs or crossbeams to provide the stiffness necessary to maintain differential displacements within functional requirements.

54. Stresses applied to supporting foundation soil should be limited to maintain settlements within levels tolerated by the structure and to optimize functional usefulness. Soil pressure should therefore be less than the precompression stress to avoid consolidation settlement and commonly limited to a value denoted as the allowable bearing capacity. The allowable bearing capacity is usually given so that settlement is about 1 inch. Evaluation of the allowable bearing capacity requires determination of the ultimate bearing capacity, increase in stress intensity in soil beneath the base of the foundation through any compressible soil layer subject to the applied loads, and guidelines for estimating appropriate factors of safety FS. Stress distributions in soil beneath foundations may be found by methodology in Appendix B, EM 1110-1-1904.

55. Ultimate bearing capacity. Mat foundations are required to be stable against a deep shear failure, which may cause rotation or a vertical punching failure. One of the first equations for estimating the vertical stress required to cause a shear failure is[40]

$$q_u = 1.3cN_c + 0.4\gamma' B N_\gamma + q_o N_q \tag{15a}$$

where

q_u = ultimate bearing capacity, ksf

c = cohesion or undrained shear strength C_u, ksf

N_c = dimensionless bearing capacity factor for cohesion

γ' = effective unit soil weight, kips/ft^3

B = mat width, ft

N_γ = dimensionless bearing capacity factor for surcharge

q_o = pressure applied to the soil at the mat base, ksf

N_q = dimensionless bearing capacity factor for friction

Improvements to determining ultimate bearing capacity accounting for foundation rigidity and shape, inclined and eccentric loading, base tilt and depth, and slope at the ground surface led to[41]

---

[40]Terzaghi 1943
[41]Hansen 1961, 1970

$$q_u = N_c \delta_c c + \tfrac{1}{2} B \gamma' N_\gamma \delta_\gamma + \gamma' D_b N_q \delta_q \tag{15b}$$

where

D_b = depth of mat base beneath the ground surface, ft

N_c, N_γ, N_q = dimensionless bearing capacity factors

δ_c, δ_γ, δ_q = dimensionless adjustment factors

Data from Milovic (1965) and Muhs (1959) indicate excellent agreement of bearing capacities with Equation 15b. For cases where bearing capacity may be critical such as in soft, cohesive soil, Equation 15a calculates an ultimate bearing capacity $q_u = 6.68c$, while Equation 15b with modifications to account for soil compressibility[42] calculates $q_u = 6.36c$. The ultimate bearing capacity appears to be at least $6C_u$ for practical applications where C_u is the average undrained shear strength in the bearing stratum.

56. Allowable capacity using factors of safety. Limiting soil pressures to the allowable bearing capacity is useful to limit settlements tolerated by the structure. Experience has shown that allowable bearing pressure q_a can often be evaluated using factors of safety applied to the ultimate capacity

$$q_a = \frac{q_u}{FS} \tag{16a}$$

where FS = 2 or 3 are usually used for limiting settlements to less than 2 inches in cohesionless and cohesive soils[1], respectively. Table 7 illustrates some methods of using results of field tests for estimating allowable bearing capacity and limiting settlement to 1 inch. These methods may be applied to estimating q_a of soil beneath stiffening beams of ribbed mats or footings supporting column loads. The plate load test is not included because extrapolation of results to mats is not reliable for $B > 3$ times the plate width.

57. Factors of safety applicable to applied uniform pressures on mats are variable and usually greater than 3 for limiting elastic settlements to less than 1 inch. If settlement ρ is to be limited to about 1 inch, then substituting Equation 16a into Equation 3 of the theory of elasticity and assuming $q_o = q_a$ and $q_u = 6C_u$ leads to

[42]Vesic 1975

Table 7

Allowable Bearing Capacity From Field Tests

Source	q_a, ksf		Definitions
	Standard Penetration Test		
Bowles (1988)	$\frac{N_{55}}{2.5} K_d$	$B \le 4$	$K_d = 1 + 0.33 \frac{D_b}{B} \le 1.33$
	$\frac{N_{55}}{4} \left[\frac{B+1}{B}\right]^2 K_d$	$B > 4$	D_b = depth of mat, ft B = width of mat, ft N_{55} = blow count, 55 percent efficiency
	$\frac{N_{70}}{2} K_d$	$B \le 4$	N_{70} = blow count, 70 percent efficiency
	$\frac{N_{70}}{3.2} \left[\frac{B+1}{B}\right]^2 K_d$	$B > 4$	
	Cone Penetration Test		
Schmertmann** (1978)	Sands:* $q_c \cdot \frac{B}{12.2} \cdot \left[1 + \frac{D_b}{B}\right]$		q_c = cone resistance, ksf N_c = cohesion bearing capacity factor
	Clays: $\frac{1}{FS} \cdot N_c \cdot 5 \left[\frac{q_c - \sigma_v}{N_k}\right] + \sigma_v$		σ_v = total overburden pressure, ksf N_k = cone factor
	Pressuremeter Test		
Briaud,** Tucker, & Coyle (1982)	$\frac{K_{PMT} p^* L_e + \sigma_v}{FS}$		K_{PMT} = pressuremeter bearing capacity factor $p^* L_e$ = equivalent pressuremeter limit pressure, ksf

* Factor of safety equals 3.3

** Factors of safety are intended to prevent bearing failure

$$FS \approx \frac{72C_u B}{E_s} \tag{16b}$$

The factors $\mu_0\mu_1$ in Equation 3 are taken as unity. For example, if $C_u = 1$ ksf, B = 50 ft, and $E_s = 200$ ksf, then FS ≈ 18. Factors of safety should not usually be used to estimate allowable bearing pressures for mat foundations on the basis of uniform applied pressures; instead, elastic settlements should be estimated for the given applied pressures on the mat to check that settlement will be less than 1 inch or within levels tolerated by the structure.

Differential Soil Displacements

58. Most procedures for analysis of soil displacements consider only the influence of loads applied on the soil as discussed in paragraph 37 on total soil displacements. Settlement analyses should also consider structural rigidity and distribution of loads. Foundations to be constructed on expansive or collapsible soil should also consider effects of differential soil movement caused by moisture changes on the long-term serviceability of the foundation and superstructure. Mat foundations that are rigid will not be subject to significant differential movement, although they may tilt. Designs often use a uniform load distribution as much as practical to minimize differential displacements and reduce moments and shears.

59. Differential displacements are used to estimate Δ/L ratios required for foundation and structural design. The ratio of the relative deflection Δ (maximum differential movement) to the total settlement varies from zero for rigid mats to as much as 50 percent for many flexible mats, which is directly related with the difference in center and edge settlement influence factors, Figure 5. Deformations in heterogeneous soil beneath rigid mats approach those similar to punching failure as illustrated in Figures 7a and 7c; hence, possible damage to adjacent structures is reduced. Differential movement can be greater in areas near localized changes in soil moisture for mats on swelling soil and can approach the total displacement. Differential movement can exceed the total settlement if portions of the foundation heave on swelling soil. Sophisticated analysis of differential displacements such as taking into consideration changes in structural stiffness and loading during construction are not yet worthwhile because of existing uncertainties in structural stiffness and soil parameters.

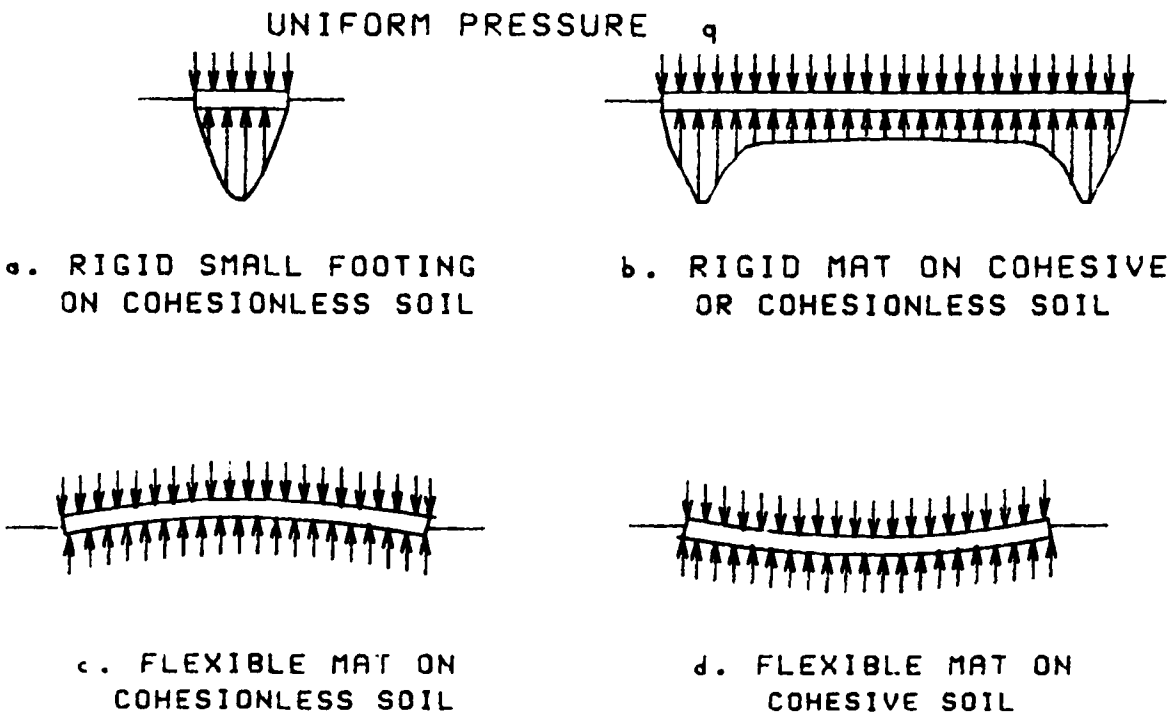

Figure 7. Relative distribution of soil contact pressures and displacements of rigid and flexible mats on cohesionless and cohesive soils

60. Deformation patterns. The shape of the deformation pattern beneath mats depends on the flexibility of the foundation and type of soil. The elastic modulus of homogeneous cohesionless soil or sand is a function of confining pressure, while the elastic modulus of homogeneous cohesive soil or clay is essentially constant and independent of confining pressure. Small rigid footings on cohesionless soil cause less soil contact pressure near the edge than near the center, Figure 7a, because this soil is pushed aside at the edges due to the reduced confining pressure. This leads to lower strength and lower elastic modulus near the edge than near the center. The saddle-shaped pressure distribution for large rigid footings and mats occurs because of soil shear at the perimeter[43], Figure 7b. The overburden pressure pressure under the edge may also confine a cohesionless soil increasing its strength[44]. A uniform pressure applied to a rigid foundation on cohesive soil will also cause a saddle shaped pressure distribution because of greater soil contact pressure near the edge than near the center. This is partly because soil behavior is influenced by stresses in adjacent soil and that additional contract pressure is necessary to provide the stress to shear the soil at the perimeter.

61. The distortion of a uniformly loaded flexible mat on cohesionless soil will be concave downward, Figure 7c, because the soil near the center is stressed under higher confining pressure such that the modulus is higher near the center. A uniform pressure applied to a flexible foundation on cohesive soil, Figure 7d, may cause greater settlement near the center than near the edge because the modulus of elasticity in the soil is constant laterally and cumulative stresses are greater near the center as a result of the pressure bulb stress distribution.

62. Structural rigidity. A measure of the relative structural rigidity ΩL is necessary to assist evaluation of differential displacements[45]

$$\Omega L = L \cdot \sqrt[4]{\frac{k_{sf} S}{4 E_c I}} \leq \frac{\pi}{4} \tag{17}$$

where

[43]Burmister 1963
[44]Kerr 1987
[45]Hetenyi 1946

Ω = relative rigidity per foot, ft^{-1}

L = length of member, ft

k_{sf} = coefficient of subgrade reaction, ksf/ft

S = width of member, ft

E_c = Young's modulus of concrete, ksf

I = moment of inertia, ft^4

When ΩL is less than or equal to $\pi/4$ or 0.785, the mat is considered rigid. The mat is divided into strips of width S equal to the spacing between column or shear walls. A mat is more likely to be rigid on soft soil or soil with a small coefficient k_{sf}. A mat may be considered flexible if $\Omega L \geq 1.75$ and semi-flexible for $1.75 > \Omega L > \pi/4$.

63. The soil pressure distribution under flexible mats depends on a variety of nonlinear factors that include (1) immediate settlement caused by loading increments during construction, (2) distribution of loads on the mat, (3) consolidation settlement or heave that overlaps immediate settlement even during construction, (4) increasing stiffness of the mat during construction, and (5) redistribution of loads and soil pressures on the mat from long-term differential movement. Optimum analysis requires sorting out each of these effects so that each contribution to the resultant soil pressure distribution can be individually analyzed.

64. Numerical analysis using finite element or finite difference computer programs is often used to assist computation of stress and strain because of the above complexity. The problem is simplified some by assuming that soil and structural components are linear elastic materials, which has been justified because of relatively low working loads and displacements usually observed in practice[46]. Even with this assumption, the analysis still requires programs and large capacity computers. A further simplification may be made by condensing the stiffness of the superstructure and foundation into an equivalent mat thickness. Differential displacements were reduced by about 1/2 when the stiffness of a 7 story open frame superstructure on a 2.2-ft thick mat was condensed into an equivalent mat of 3.1 ft thickness using Meyerhof's method[37]. This method described in Appendix B also considers

[46]Hooper 1978

additional stiffness from filling of the open frame structure so as to form continuous shear walls. A simple alternative method for estimating the influence of superstructure rigidity on deformation patterns is also proposed in Appendix B.

65. Methodology. Differential displacements may be estimated from the theory of elasticity using soil moduli from results of laboratory strength tests conducted on undisturbed samples from different locations and depths beneath the proposed foundation. Soil-structure interaction analyses that use the theory of elasticity in the solution of differential displacements include plate on elastic foundation programs such as SLAB2[11]. SLAB2 also evaluates bending moments and shears that are required for design. Soil displacements and reaction pressures may be analyzed with variable and nonlinear soil moduli using two-dimensional finite element computer programs such as AXIPLN[47]. The theory of elasticity generally indicates differential displacements from 0 to 50 percent of the total displacement for uniform applied pressures depending on the relative stiffness of the mat and thickness of compressible soil.

66. Mat foundations should be designed to accommodate the maximum angular distortion β_{max}. Unfortunately, many observed differential movements are irregular, Figure 2c, making nearly impossible estimation of the maximum angular distortion prior to construction. Moreover, estimation of β_{max} should consider and compare structural loads to heave, heave potential, and loading pressures. A rough estimate of β_{max} may be obtained from Equation 1a. A practical method for quickly estimating the maximum angular distortion when a potential for heave occurs is

$$\beta_{max} = \frac{S_{max} - \rho_i}{\ell/2} \tag{18}$$

where

ρ_i = immediate settlement, ft

S_{max} = maximum potential heave, ft

ℓ = distance between points of maximum and minimum settlement, ft

---

[47]Withiam and Kulhawy 1978

The maximum settlement may occur beneath the most heavily loaded part of the structure such as beneath columns and consist only of immediate elastic settlement; consolidation may not occur in a soil with potential for heave in situ. The maximum potential heave is a positive number (settlement is negative) and may occur beneath the most lightly loaded part of the foundation such as midpoint between diagonal columns. The total differential movement is the sum of S_{max} and $-\rho_i$. Nonuniform soil wetting may be caused by leaking water, sewer, and drain lines.

67. A simple method for estimating differential displacements that considers structural rigidity calculates elastic settlement at a particular location by[48]

$$\rho_i = q \sum_{i=1}^{n} \frac{I_i \cdot h_i}{E_{si}} \tag{19}$$

where

q = soil pressure applied by the foundation, ksf

I_i = influence factor for layer i

h_i = thickness of layer i, ft

E_{si} = Young's soil modulus of layer i, ksf

The influence factor I_i is given for center and edge settlement in Figure 5 and shown in Figure 8 for $\mu_s = 0.2$, 0.3, 0.4, and 0.5. The mat is converted to an equivalent circular raft of radius $R = \sqrt{LB/\pi}$ in which the length to diameter ratio L/B should be ≤ 2.

68. Figure 8 shows that the Kay and Cavagnaro (1983) method can be arranged to provide simple estimates of total and differential settlement relative to the center and edge of the mat. Edge settlement appears roughly 1/2 of the center settlement for a completely flexible mat. The differential settlement is found from

$$\rho = (\rho_c - \rho_e) R_s \tag{20}$$

where

ρ = differential settlement, ft

ρ_c = center settlement, ft

[48]Kay and Cavagnaro 1983

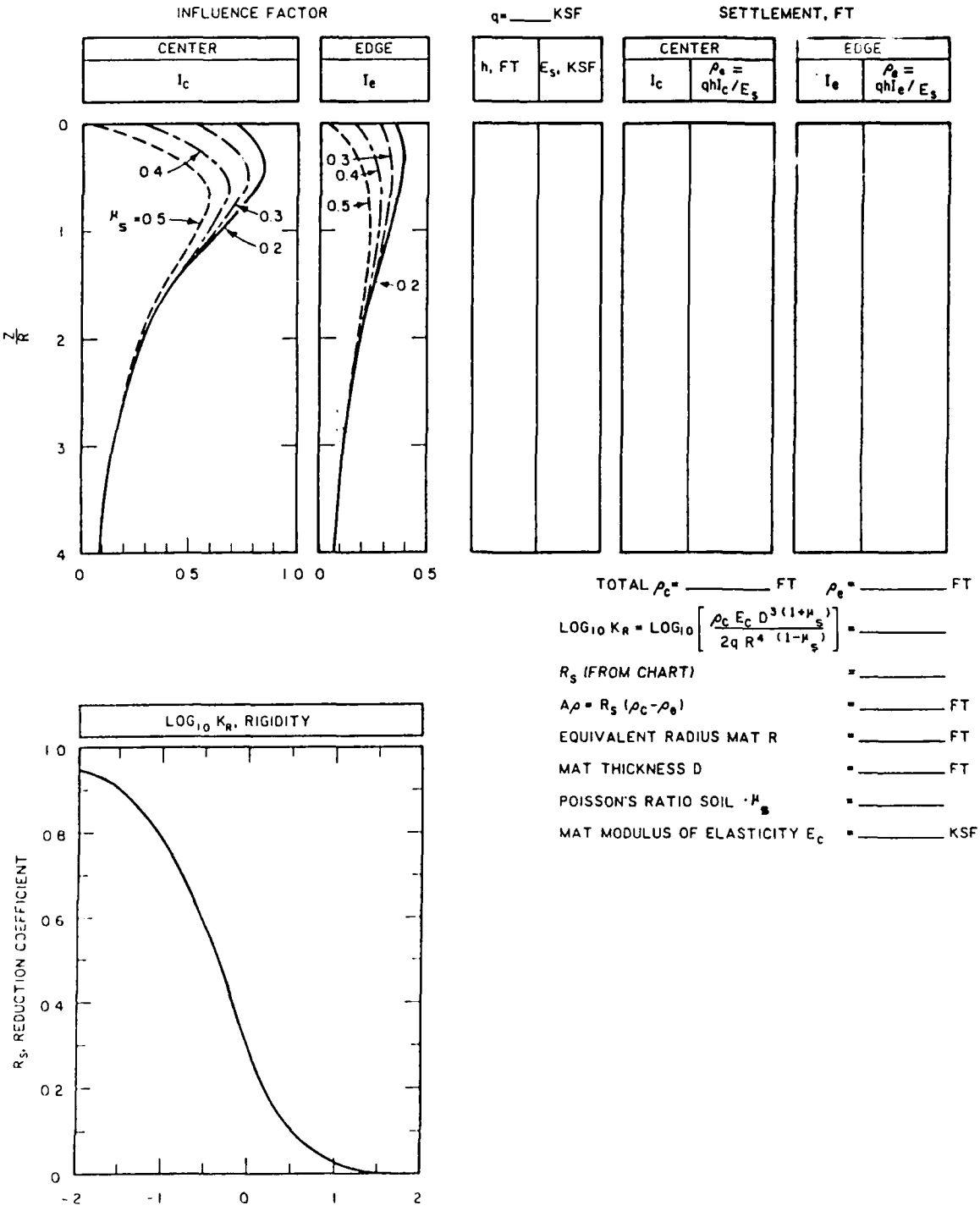

Figure 8. Settlement computation
(after Kay and Cavagnaro 1983)

ρ_e = edge settlement, ft

R_s = reduction coefficient, dimensionless

R_s shown in the chart, Figure 8, is related to the relative stiffness

$$K_R = \frac{\rho_c E_c D^3 (1 + \mu_s)}{2qR^4 (1 - \mu_s)} \tag{21}$$

where

E_c = Young's modulus of the mat concrete, ksf

q = uniform pressure applied on the mat, ksf

D = mat thickness, ft

R = equivalent mat radius $\sqrt{LB/\pi}$, ft

μ_s = Soil Poisson's ratio

The relative stiffness K_R is dimensionless. The mat thickness should be an equivalent thickness including superstructure rigidity as evaluated in Appendix B.

Final Design

69. Standard procedures for the structural design of mat foundations are documented by American Concrete Institute[49]. These procedures are grouped into the conventional or rigid uniform pressure and flexible or elastic design methods. The flexible method may provide a more economical design if the mat can be considered flexible by Equation 17 where $\Omega L > 1.75$ and L is the average of two adjacent load or column spacings that vary no more than 20 percent, paragraph 62. Except for unusual problems, the contact pressure q at the base of the mat may be assumed to follow a straight line distribution for the uniform pressure method or a distribution governed by the coefficient of subgrade reaction of the Winkler concept for the flexible method. Some mats are purposely designed with flexibility such as mats for silos or tanks when the primary purpose is containment and the mat should deform rather than crack with differential movement.

70. Uniform pressure method. This method applicable to rigid foundations assumes a uniform pressure or straight line distribution beneath the base of the mat. Eccentric loads with or without overturning moments can

[49]ACI Committees 318-1980, 336-1987 and 436-66

lead to trapezoidal (or nonuniform) pressure distributions and rotation of the foundation. The length of the foundation is made sufficiently large such that the resultant of overturning moments and axial loads from all columns in a line is located in the center of the length of the foundation and the resultant soil pressure distribution will be uniform provided the mat is rigid.

71. The general design procedure is as follows: (1) mat dimensions are selected such that the center of the mat and center of gravity coincide, (2) the mat may be divided into a series of equivalent beams centered on rows of columns, (3) a shear and moment diagram may be constructed assuming that the column loads are point loads, (4) the mat depth is selected to resist the maximum shear without reinforcement, and (5) the amount of reinforcement is subsequently selected to resist the maximum bending moment. Detailed criteria for design of rigid mats are provided in the literature[49,50,51]. Concrete floor slabs subject to heavy concentrated loads may be designed by procedures described in TM 5-809-12, "Concrete Floor Slabs on Grades Subjected to Heavy Loads". The uniform method may be recommended for mats on mud, soft clay, peat, organic soils, or even clays of medium stiffness.

72. Winkler foundation. The Winkler foundation may be applicable to mats subject to plane strain such as dry docks with long walls, pavements, or roads. The design of flexible mats commonly use the beam on Winkler foundation concept of k_{sf} to evaluate design parameters from charts[22] or computer programs[15,52,53]. Design parameters take the form[45]

Pressure intensity q': kips/ft/ft width

$$q' = E_c I \frac{d^4 \rho}{dx^4} \tag{22a}$$

Shear V: kips/ft width

$$V = E_c I \frac{d^3 \rho}{dx^3} \tag{22b}$$

---

[50]Teng 1975
[51]Bowles 1988
[52]Haliburton 1972
[53]Chou 1981

Bending moment M: kips-ft/ft width

$$M = E_c I \frac{d^2\rho}{dx^2} \tag{22c}$$

where

E_c = Young's elastic modulus of concrete, ksf

I = moment of inertia, ft^4

ρ = displacement, ft

x = horizontal distance along beam or mat strip of width S, ft

A simple solution to Equations 22 is accomplished by equating $q' = - k_{sf}S\rho$. The solution should be checked against allowable design parameters determined by criteria of the American Concrete Institute[49]. Deflections and bending moments determined by American Concrete Institute 318 and 336 should be consistent with calculated values from computer programs[51]. The solution depends on boundary conditions such as distribution of applied loads, beam length, and distribution of the soil reaction pressure. Soil response curves required for input are found by multiplying appropriate values of k_{sf} by width S. A major disadvantage of this approach is that reliable guidelines are not available for determining appropriate values of k_{sf} and how k_{sf} varies with horizontal locations.

73. The finite element method may be applied to relate forces and displacements of each element by[53]

$$[F] = [K]\cdot\{\delta_f\} + k_{sf}ab\cdot\{\delta_s\} \tag{23}$$

where

$[F]$ = matrix of 3 forces (vertical force, moment about x-axis, moment about y-axis for each node of the element)

$[K]$ = stiffness matrix of the foundation element (function of mat dimensions a and b of the element, Young's modulus and Poisson's ratio of the foundation), lb/ft

δ_f = displacement array for each node in the foundation element, ft

k_{sf} = coefficient of subgrade reaction of foundation soil, ksf/ft

δ_s = displacements array in the soil, ft

The finite element method for the Winkler concept was applied to develop program WESLIQID[53].

74. Elastic foundation. Flexible mats may also be analyzed using the plate on elastic semi-infinite foundation to evaluate design parameters[11,53,54]. Boussinesq's solution and Burmister's layered elastic solution are used to compute subgrade surface deflections for homogeneous and layered elastic foundations, respectively. The relationship between forces and displacements of each element can be written similar to Equation 23

$$\{F\} = ([K_f] + [K_s]) \cdot \{\delta\} \tag{24}$$

where

$\{F\}$ = externally applied nodal forces, lb

$[K_f]$ = stiffness matrix of the foundation (function of the finite element configuration and flexural rigidity of the mat), lb/ft

$[K_s]$ = stiffness matrix of the subgrade (function of nodal spacing, Young's modulus and Poisson's ratio of the soil), lb/ft

$\{\delta\}$ = nodal displacement array, consisting of a vertical deflection and two rotations, ft

The finite element method for the elastic foundation was applied in programs SLAB2[11], WESLAYER[53], FOCALS[55], SAP-5[56] and ANSYS[57].

75. The basic difference between Winkler and elastic foundations is that the Winkler deflections at a given node depend only on the forces at the node, while elastic deflections at a given node depends on the forces at the node and forces or deflections at other nodes.

76. Applications. Some specialized simple solutions of thin mats on swelling/shrinking soils are available and compared in Table 8. An improved design procedure for perimeter loads on ribbed thin mats up to 18 inches thick constructed in swelling soil have also been developed by the Post Tensioning Institute (1980) using program SLAB2 (Appendix C). Many of these simple methods assume some shape of the soil mound

$$y_m = C_m x^m \tag{25}$$

where

y_m = maximum soil heave without surcharge load, ft

x = horizontal distance, ft

---

[54]Huang 1974a, 1974b
[55]Wardle and Fraser 1975b
[56]Bathe, et al 1978
[57]DeSalvo and Swanson 1982

Table 8

Summary of Relevant Design Methods[58]

DESIGN METHOD	BRAB (1968)	LYTTON (1972)	WALSH (1978)	FRASER AND WARDLE (1975)
ASSUMED SLAB ACTION	Simplified Three Dimensional	Simplified Three Dimensional	Simplified Three Dimensional	Precise Three Dimensional
SLAB LOADING AND INITIAL MOUND SHAPE	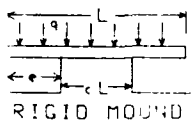	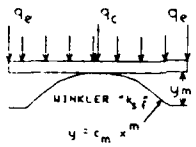	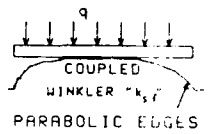	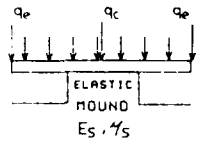
DETERMINATION OF SLAB SUPPORT AREA COEFFICIENT "c"	Empirically Related to Clay Type and Weather	$\frac{m+1}{m+2} \cdot \left[\frac{m+1}{m} \cdot \frac{q}{k \cdot y_m} \right]^{\frac{1}{m+1}}$ $\frac{2e}{L} = 1 - \left[\frac{0.05}{y_m} \right]^{\frac{1}{m}}$	Mathematically Related to e, y_m, k, q	$\frac{L - 2e}{L}$
CALCULATION OF "I"	Fully Cracked Section	Uncracked Section	Partially Cracked Section	Partially Cracked Section
CALCULATION OF LONG TERM "E"	$0.5E_c$	$0.5E_c$	Not Specified Use $0.75E_c$	Not Specified Use $0.75E_c$

LEGEND:

- c = support index
- e = edge distance, ft
- E = long-term modulus of concrete, ksf
- E_c = concrete modulus based on 28-day compressive strength, ksf
- I = moment of inertia, ft^4
- k_{sf} = coefficient of subgrade reaction of foundation soil, ksf/ft
- L = length of slab, ft
- m = mound exponent
- q_c = center pressure, ksf
- q_e = edge pressure, ksf
- q = average foundation pressure, ksf
- y_m = maximum differential heave across the mound before slab-soil interaction, inches
- C_m = constant characterizing mound shape
- E_s = soil elastic modulus, ksf
- μ_s = soil Poisson's ratio

[58] After Holland 1979

C_m, m = empirical constants

A reasonable value for m is 3[11,59]. A value of $m \leq 2$ provides a mound that rises too quickly, while $m \geq 4$ appears to flatten out the heave profile too much.

77. The Post Tensioning Institute design procedure is applicable to conventionally reinforced or post-tensioned ribbed mats for light, perimeter loads. Required soil input parameters include Atterberg limits, cation exchange capacity, percent clay less than 2 microns, unconfined compressive strength, elastic soil modulus and Poisson's ratio, edge moisture variation distance, and depth of active zone for soil heave. Required foundation parameters include the concrete compressive strength, elastic modulus and Poisson's ratio and yield strength of reinforcing steel. Development of the design equations used a parametric analysis that assumed the coefficient of subgrade reaction $k_{sf} \approx 7$ ksf/ft. This method should not be used for perimeter wall loads exceeding 2 kips/ft, stiffening beam depths exceeding 3 ft, beam spacing exceeding 20 ft, differential center lift movements exceeding 4 inches, differential edge movements exceeding 1.5 inches, and mat lengths and widths exceeding 300 ft, or for structures with significant concentrated loads on either the interior or perimeter. The procedure should tend to produce conservative designs because the analysis assumes simultaneous perimeter loads on all four edges, while many practical structures such as houses experience perimeter loads on only two edges. The procedure considers effect of climate on edge moisture variation distance and potential differential soil heave, but other effects such as unusual desiccated soil and rainfall, removal of pre-construction vegetation, and downhill creep are not considered.

78. A simple "untried" method of evaluating the required stiffness E_cI of a mat foundation to maintain differential movements within acceptable levels may be found from an application of the frequency spectrum approach, which was applied to the design of pavements on expansive soil[60]. This model assumes a beam on a Winkler foundation to evaluate EI from the relative rigidity ΩL, Equation 17. The relative rigidity per foot Ω times a model

---

[59]Lytton 1972
[60]McKeen and Lytton 1984

wavelength Γ may be found from the solution to the pavement model, Figure 9. The model wavelength Γ is an average length between bumps or depressions along the length of a pavement or mat section of width S. Aa is the acceptable differential movement of the pavement over a length of $\Gamma/2$ and Ae is the expected differential movement of the soil without the pavement on the soil over the same length. If the allowable deflection ratio Δ/L is 1/1333 such as for $\beta_{max} = 1/500$, a reasonable angular distortion for initiation of damage from paragraph 18, then $Aa = (\Gamma/2)/1333$ or $\Gamma/2666$. The rigidity of the pavement required to flatten or "squeeze the bumps" in the soil to the acceptable differential movement Aa is given by $\Omega\Gamma$ and the stiffness of the pavement $E_c I$ may then be found from Equation 17. The observed range of Γ for some pavements is 10 to 35 ft[60]. The analysis assumes complete contact of the soil with the pavement. Table 9 illustrates the differential movement y_m that can be flattened to within $\Delta/L = 1/1333$ for a ribbed mat of width B = 12.5 ft (spacing S = 12.5 ft between ribs), beam width w = 18 inches, and concrete modulus of elasticity $E_c = 432{,}000$ ksf. The mat thickness may vary from 4 to 8 inches. For example, if $k_{sf} = 7$ ksf/ft and $\Gamma = 20$ ft the ribbed mat with stiffening beam depth of 28 inches from the top of the mat will squeeze a soil heave of 5 inches sufficiently to result in a mat deflection ratio $\Delta/L = 1/1333$. This model is applicable to one-dimensional beams and not mat foundations.

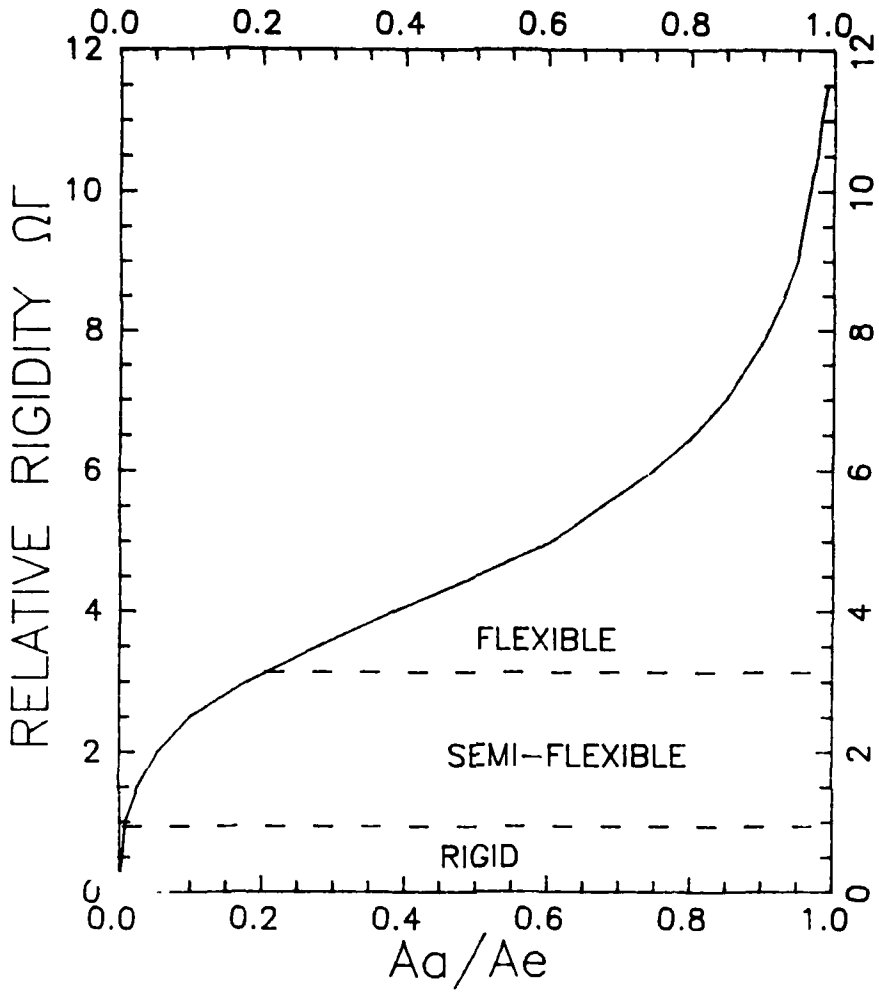

a. RELATIVE RIGIDITY VERSUS RELATIVE VERTICAL DISPLACEMENT

Ω = relative rigidity per foot, ft^{-1}
Γ = wavelength or average length between bumps/depressions, ft
Aa = acceptable differential movement over length $\Gamma/2$, ft
Ae = expected differential movement over length $\Gamma/2$, ft

b. NOMENCLATURE

Figure 9. Relative structural rigidity by the frequency spectrum model

Table 9

Examples of Maximum Soil Heave Squeezed to $\Delta/L = 1/1333$ By a Ribbed Mat 12.5 ft Wide With Beams 18 Inches Wide

Coefficient of Subgrade Reaction k_{sf}, ksf/ft	Wavelength Γ, ft	Maximum soil Heave y_m, inches		
		Beam Depth Below Top of Mat, inches		
		20	28	36
4	10	6.0	9.0	11.0
	20	4.0	7.5	10.0
	30	2.3	4.5	7.0
	50	0.8	1.7	3.0
7	10	5.0	7.5	9.0
	20	3.0	5.0	9.0
	30	1.5	2.9	4.9
	50	0.6	1.2	2.1
10	10	4.7	6.4	8.0
	20	3.0	5.0	9.0
	30	1.3	2.7	3.6
	50	0.5	0.9	1.4
14	10	4.0	6.0	7.5
	20	1.9	3.3	4.0
	30	0.8	2.1	2.9
	50	0.4	0.7	1.2

PART III: CASE HISTORY STUDIES

Introduction

79. Seven ribbed mats supporting moderate loads and three thick flat mats supporting heavy loads from multistory hospital buildings were analyzed to provide design information on soil parameters. These mats are located in San Antonio, TX, except for the thick mats supporting the hospital in Fort Gordon, GA, and Fort Polk, LA. Soil data available from field and laboratory investigations and elevation readings of the mats permit some analyses of the structural performance based on uniform pressure, Winkler, and plate on elastic foundation methods. Representatives of the Corps of Engineers from the Southwestern Division, Fort Worth District, Waterways Experiment Station, and Office, Chief of Engineers, visually examined these facilities in San Antonio in May 1984 to assist evaluation of performance. Results of these analyses are compared with design requirements given by the American Concrete Institute (ACI) and flexure theory. Application of the frequency spectrum method is made in Part IV.

Soil Parameters

80. Soil parameters were evaluated from results of laboratory tests performed on soil samples taken from the field before construction. Disturbed samples were obtained with an 8-inch auger. Relatively undisturbed samples were obtained with 6-inch Denison and core barrel samplers. Selected samples were sealed in airtight containers and shipped by truck to laboratories for testing. Boring holes were usually left open about 24 hr to detect perched water levels associated with gravel and other pervious strata, then backfilled with lean cement grout to inhibit seepage of perched water into underlying desiccated soil.

81. Shear strengths of the soil were evaluated from results of unconsolidated-undrained Q triaxial strength tests and occasionally from consolidated-undrained R tests. The elastic soil modulus E_s was evaluated from stress-strain data as a function of depth using the hyperbolic model, paragraph 39. Constrained modulus E_d was also evaluated from results of consolidometer tests by[61]

---

[61] Lambe and Whitman 1969

$$E_d = \frac{(1 + e_o)\sigma_v}{0.435C} \tag{26}$$

where

e_o = initial void ratio

σ_v = vertical overburden pressure on the in situ soil, ksf

C = compression C_c or swell C_s index

Both compression and swell indices were used to provide a range of E_d. The constrained modulus from Equation 26 includes the influence of consolidation or plastic strains and will usually be less than E_s evaluated from elastic strains of Q test results. Since E_d assumes negligible lateral deformation, while E_s includes lateral deformation, $E_d > E_s$. E_d should equal E_s when $\mu_s = 0.0$. An equivalent or uniform elastic modulus E_s^* and coefficient of subgrade reaction required for the analyzes were estimated from results of soil tests using methodology in PART II.

Structural Parameters

82. Bending moments and shears were evaluated from methods of the American Concrete Institute[62] and compared with values calculated from plate on elastic foundation program SLAB2[11] and beam on Winkler foundation program CBEAMC[15]. Observed displacements were compared with displacements calculated from SLAB2 and CBEAMC. Input parameters for SLAB2 include Young's elastic modulus of the mat concrete E_c normally assumed to be 432,000 ksf, Poisson's ratio of the mat concrete $\mu_c = 0.15$, an equivalent Young's elastic modulus of the soil E_s^*, and Poisson's ratio of the soil μ_s. Poisson's ratio of the soil was assumed 0.3. The total moment of inertia I of the entire mat cross-section in each of the long L and short S directions is also input to permit computation of the flexure stiffness E_cI in each of the two orientations. Tables B1 and B2 describe evaluation of I for each cross-sections of mat foundations, which may be added together to evaluate the total moment of inertia. Program SLAB2 can be made to simulate soil center heave patterns by imposing edge gaps and edge heave by imposing center gaps.

83. Program SLAB2 requires input of a uniform Young's elastic soil modulus that is applicable for the entire mat E_s^*. However, mats placed on

---

[62]Eshbach 1954

the ground surface and on expansive soil characteristic of this study are subject to soil deformation caused by moisture changes in the active zone of soil heave. This active zone of heave may include 20 or more feet of soil beneath the mat. The effective soil modulus representing heave beneath ribbed mats is therefore assumed in this study to be the average modulus within 50 ft beneath the ground surface. E_s^* may be evaluated from Equations 4.

84. Beam on Winkler foundation program CBEAMC[15] was also applied because beam programs are often used for design and they are simpler and more economical to operate than plate on elastic foundation programs. Input parameters of CBEAMC include the moment of inertia of the section (Tables B1 and B2). Program CBEAMC can simulate heave patterns by specifying displacements. Results of a CBEAMC analysis for uniform pressure applied on a soil of uniform stiffness will cause zero bending moments and shears in the mat section. The soil stiffness k' input into CBEAMC is in units of ksf and found from the coefficient of subgrade reaction of the mat k_{sf} by

$$k' = k_{sf} \cdot S \tag{27}$$

where S is assumed the spacing between columns or T-sections of ribbed mats. k_{sf} may be calculated from known soil pressure/settlement ratios, Equation 5 or estimated from Equations 6 to 9. The values of k_{sf} are consistent for displacements; therefore, bending moments calculated with these k_{sf} for the Winkler foundation may not be correct because k_{sf} are not unique for mat foundations. Winkler analysis is further handicapped because the extent of soil support under the flat portion of the ribbed mat is not known. Paragraph 24, PART I, describes the American Concrete Institute specification for bending of an effective T-section width that can be substantially less than the spacing S between ribs, which may partly compensate for the 2.4 times larger k_{sf} required to compute bending moments than that required for displacements described in paragraph 44. Because of these uncertain corrections for evaluating k_{sf}, the stiffness k' is calculated from Equation 27 with k_{sf} evaluated from given applied pressures and displacements calculated from SLAB2 analysis.

Ribbed Mat Foundations

85. Ribbed mats are composed of cross-beams supporting a flat floor slab, Figure 10. Mats selected for analysis and identified in Table 10 were constructed on about 4 ft of nonexpansive, low plasticity compacted fill overlying expansive soil strata. This fill is compacted to not less than 92 percent of maximum density after ASTM D1557. Trenches of about 3 ft in depth were excavated in the fill for placement of reinforcing steel and concrete for stiffening beams. Stiffness parameters of the compacted fill were not determined, but were assumed similar to those of the underlying soil. Six inches of granular material were placed on the prepared surface of the compacted fill between stiffening beams of all the mats. A polyethylene vapor barrier was placed on the granular fill beneath the flat portions of the mat prior to concrete placement and snugly fitted against the walls of the trenches for the stiffening beams.

86. Reliable benchmarks for level surveys were not available for any of these mat foundations. Reference benchmarks consisted of 2 or 3 manholes used for drainage located in the immediate vicinity of the ribbed mats. These benchmarks are identical to those used by the contractor during construction. Differences in displacements relative to the original elevations measured by the contractor therefore include both differences in elevation readings, elevation changes in these benchmarks, and contractor error. Consequently, only rough comparisons may be made between these measured displacements and those calculated from the analyses.

87. Table 10 illustrates the structural capacity of the T-beams of the selected ribbed mat foundations[62]. Letters A and B in the left column of Table 10 indicate T-sections described later in plan views of each mat. Numbers 1 to 6, U. S. Army Reserve Center Warehouse, indicate each of the six stiffening beams parallel with the short direction. All of these mats are flexible with $\Omega L \gg 1.75$ (see paragraph 62) as shown in Table 11a. Maximum differential displacement Δ between the center and edge of these mats will be at least 80 percent of the difference between center and edge settlement of a fully flexible mat as shown in Table 11b. Table 12 illustrates bending moments developed in these mats for the given maximum differential soil heave y_m using the Walsh (1978) method for a beam on a Winkler foundation, Table 8.

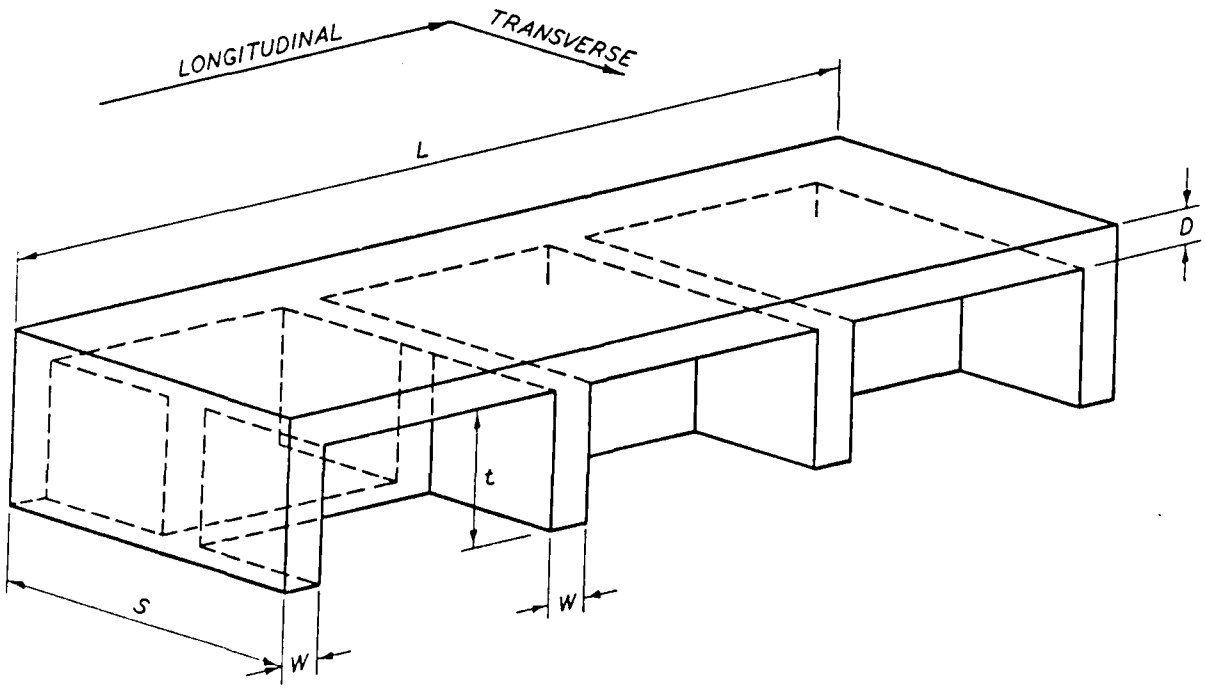

Figure 10. Schematic diagram of ribbed mat section of width S for soil-structure interaction analysis

Table 10

a. Structural Parameters for T-Beams

Mat	A_s, in.^{2}	W, in.	d, in.	j	M,* ft-kips	V, kips	Flexure Rigidity,** $E_c I_{oorm}$, kips-ft^2
Gymnasium ***							
Brooks - A	3.12	18	33	0.91	± 468	71	3,915,600
AFB - B	3.12	18	33	0.91	± 468	71	3,776,502
Data Processing Facility							
Randolph - A	3.27	12	33	0.91	- 490	47	3,062,108
AFB - B	4.00	12	33	0.91	+ 600	47	3,062,108
US Army Reserve Center Warehouse							
Fort Sam - 1	3.12	18	27	0.90	± 380	59	2,485,398
Houston - 2	3.12	18	36	0.91	± 513	76	4,940,494
- 3	3.12	18	44	0.92	± 631	92	8,541,116
- 4	3.12	18	53	0.93	± 765	108	13,453,350
- 5	3.12	18	61	0.93	± 885	126	21,649,488
- 6	3.12	18	69	0.93	±1005	142	30,037,626
Maintenance Building							
- A	1.20	18	33	0.94	± 186	71	3,951,668
- B	3.12	18	33	0.91	± 468	71	4,085,270
Dental Clinic							
Fort Sam - A	3.00	16	29	0.90	± 392	56	2,367,360
Houston - B	3.00	16	29	0.90	± 392	56	2,336,562
Medical Clinic							
Fort Sam - A	3.00	16	29	0.90	± 267	71	3,818,284
Houston - B	3.00	16	29	0.90	± 267	71	3,540,180
Pest Management Training Facility							
Fort Sam - A	2.00	12	27	0.90	± 243	39	1,567,097
Houston - B	2.00	12	27	0.90	± 243	39	1,600,245

* + indicates compression and - indicates tension in top fibers
** Includes steel
***Refers to the T-section analyzed in the mat described later

b. Nomenclature

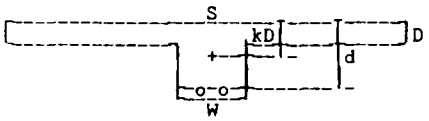

S = section spacing, in.

W = beam width, in.

D = slab thickness, in.

A = beam cross-section, W(3+d) in.^{2}

d = beam depth plus slab thickness minus 3 in.

A_s = area steel, in.^{2}

M = $A_s f_s jd$, maximum bending moment resisted by steel, lb-in.

V = $v_c A$, allowable vertical shear resisted by beam section, lb

f_s = steel tensile strength, 60,000 psi

j = 1 - k/3

k = $\left[2pn + (pn)^2\right]^{1/2} - pn$

p = A_s/Wd

n = E_{st}/E_c

v = allowable shearing stress resisted by concrete, $2\sqrt{f'c}$ 109.5 psi

f'c = ultimate concrete crushing strength after 28 days, 3000 psi

I_{oorm} = composite moment of inertia of ribbed mat T-section, in.^{4} (Equation B13)

Table 11

Relative Flexibility of Mats

a. Hetenyi (1946) Method

Mat	B, ft	k_{sf},* ksf/ft	S, ft	E_cI kips-ft^2	Ω,** ft^{-1}	L, ft	ΩL***
Gymnasium, Brooks AFB Section B1	85.3	5.2	17.3	3,776,502	0.050	85.3	4.20
Data Processing Facility, Randolph AFB, Section A	149.8	3.0	18.5	3,062,108	0.047	149.8	6.90
Maintenance Bldg, Section A	72.7	6.1	27.0	3,951,668	0.058	72.7	4.14
Troop Dental Clinic, Fort Sam Houston, Section A	109.7	4.0	13.8	2,367,360	0.050	109.7	5.38
Troop Medical Clinic, Fort Sam Houston, Section A	164.0	2.7	15.0	3,818,284	0.041	164.0	6.59
Pest Management Facility, Fort Sam Houston, Section A	58.7	7.5	15.0	1,567,097	0.066	98.7	6.42

* $k_{sf} = \dfrac{E_s}{(1 - \mu_s^2)BI_w}$ E_s = 400 ksf, μ_s = 0.3, I_w = 1.0

** $\Omega = \sqrt[4]{\dfrac{k_{sf}S}{4E_cI}}$

*** ΩL > 1.75 yields a flexible mat

b. Kay and Cavagnaro (1983) Method

Mat	S, ft	I, ft^4	E_cI, kips-ft^2	D,* ft	L, ft	B, ft	R,** ft	Log K_R***	R_s
Gymnasium, Brooks AFB Section B1	17.3	8.74	3,776,502	1.82	89.3	85.3	49.2	-1.03	0.80
Data Processing Facility, Randolph AFB, Section A	18.5	7.09	3,062,108	1.66	199.8	149.8	97.6	-2.05	0.95
Maintenance Bldg, Section A	27.0	9.15	3,951,668	1.60	204.0	72.7	68.7	-1.64	0.90
Troop Dental Clinic, Fort Sam Houston, Section A	13.7	5.48	2,367,360	1.68	143.3	109.7	70.7	-1.61	0.90
Troop Medical Clinic, Fort Sam Houston, Section A	15.0	8.84	3,818,284	1.92	190.0	164.0	99.6	-1.88	0.92
Pest Management Facility, Fort Sam Houston, Section A	15.0	3.63	1,567,097	1.43	98.7	58.7	42.9	-1.17	0.80

* $D = \sqrt[3]{\dfrac{12I}{S}}$

** $R = \sqrt{\dfrac{LB}{\pi}}$

*** $K_R = (1+\mu_s)^2 \left[\dfrac{D}{R}\right]^3 \dfrac{E_c}{E_s}$

μ_s = 0.3
E_c = 432,000 ksf
E_s = 400 ksf

Table 12

Maximum Bending Moments by Walsh (1978) Method

Mat	L, ft	e_m/L	w, kips/ft	Lift Mode	y_m, inches	Δ/y_m	$w/(k'y_m)$	C_1	M kips-ft
Gymnasium, Brooks AFB Section B1	85.33	0.2	2.3	Edge	0.25	0.25	0.5	0.98	42
					1.00	1.00	4.0	0.94	124
Data Processing Facility, Fort Sam Houston Section A	150.00	0.2	4.8	Center	0.60	0.40	2.0	0.98	270
Maintenance Building, Fort Sam Houston, Section A	72.67	0.4	4.6	Center	2.00	0.10	4.0	0.86	429
Dental Clinic, Fort Sam Houston, Section A	109.67	0.2	3.0	Center	1.00	0.20	1.0	0.96	180
Medical Clinic, Fort Sam Houston, Section A	164.00	0.4	2.7	Center	0.60	0.20	2.0	0.98	182
Pest Management Facility, Fort Sam Houston, Section B	58.67	0.4	2.5	Edge	2.00	0.10	2.0	0.79	226

Notation:

- L = length of section, ft
- e_m = edge moisture penetration distance, ft
- Δ = maximum tolerable differential movement, in.
- y_m = maximum differential heave, in.
- w = applied load/length of section, kips/ft
- k' = stiffness, $k_{sf}S$, kips/ft length/ft displacement
- C_1 = constant obtained from Table 1 of Walsh (1978)
- M = maximum bending moment, kip-ft, $(1 - C_1)wL^2/8$

The deflection requirement Δ/L is taken as 1/1333 from Equation 1b assuming $\beta_{max} = 1/500$ where L is the spacing S between adjacent beams. The Walsh method can calculate large changes in bending moments for small change in the constant C_1 when C_1 approaches 1.0, Table 12.

Gymnasium, Brooks Air Force Base

88. The gymnasium is an L-shaped building located in the south portion of Brooks Air Force Base near San Antonio, Texas, at the intersection of West Gate and Inner Circle Roads. Construction was initiated in the fall of 1981. Superstructure framing consists of a steel roof deck on open web steel joists supported by steel trusses and concrete columns in the gym area and load bearing masonry walls and steel beams in the locker room areas. Stiffening beams, Figure 11, are 18 inches wide by 3 ft depth below the mat top. Beam spacing S is variable from 8 to 34 ft. Mat thickness D between stiffening beams is 5 inches. The building was equipped with downspouts and 2-ft long splash blocks directing rainfall away from the mat foundation. The grade was nearly flat around the building.

89. Soil parameters. Soil parameters from results of laboratory tests on soil samples from five borings taken in June 1977 are shown in Figure 12. Overburden soil consists of lean clay, sands, and silts of generally alluvial origin down to a depth of about 15 ft. A perched water table was found about 8 ft below ground surface in the gravel GC stratum. Below the overburden soil is 4 to 7 ft of yellow-brown medium plastic CH-CL clay with caliche weathered from the underlying primary formation. The primary stratum consists of about 75 ft of noncalcareous, bentonitic clay shales of the Midway formation of Tertiary age.

90. The results of Q triaxial strength tests on specimens from relatively undisturbed boring samples indicated an undrained shear strength C_u of about 1.6 ksf that increases at a rate of about 0.04 ksf/ft of depth, Figure 12. The ultimate bearing capacity of this soil is at least 10 ksf providing an allowable bearing capacity for pressures on the stiffening beams of more than 3 ksf assuming a factor of safety of 3. The elastic soil modulus E_s appears to be about 400 ksf, while the constrained modulus E_d is much less at about 80 ksf based on swell indices. Swell pressure tests (Method C,

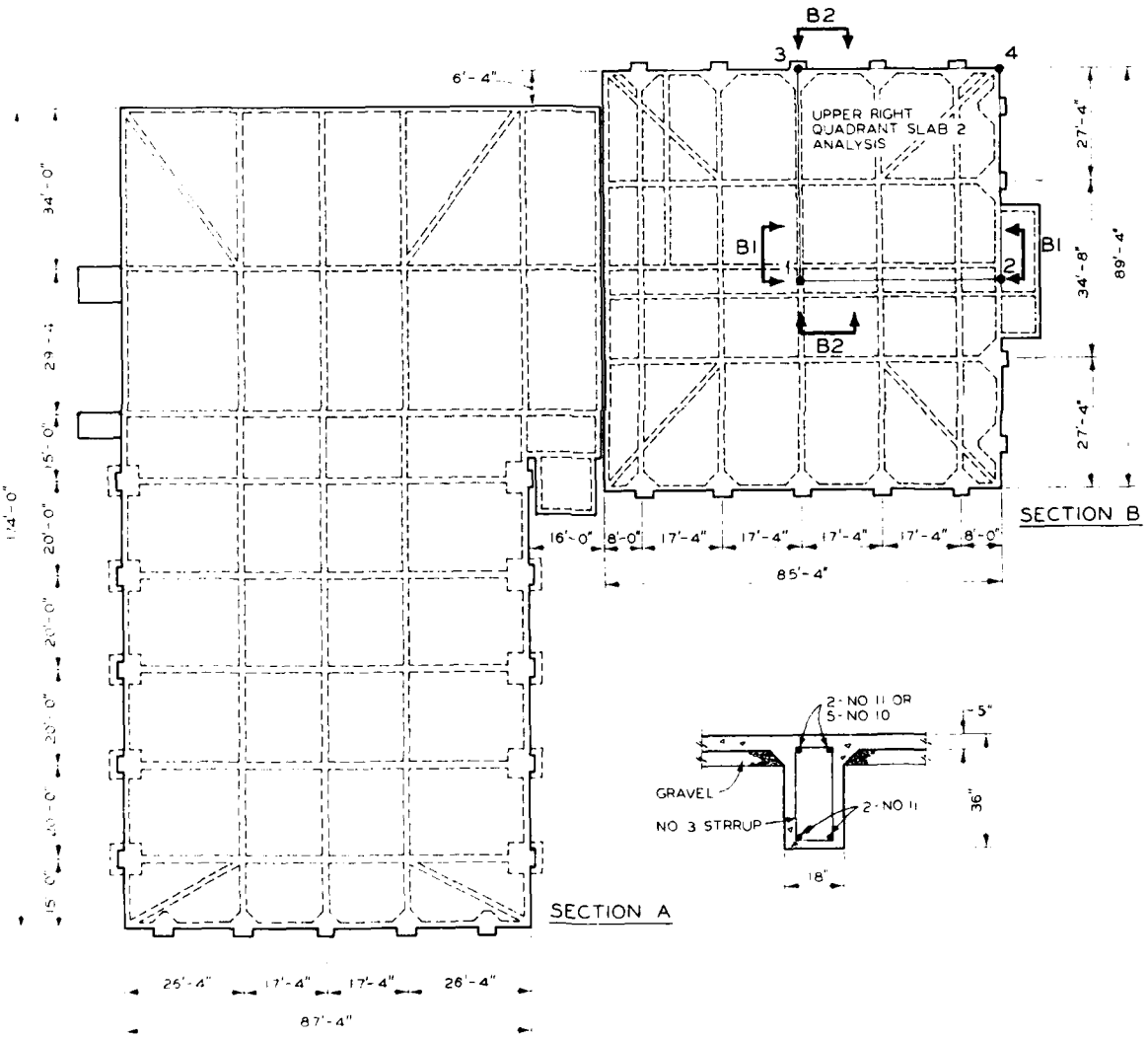

Figure 11. Foundation plan Brooks Air Force Base Gymnasium

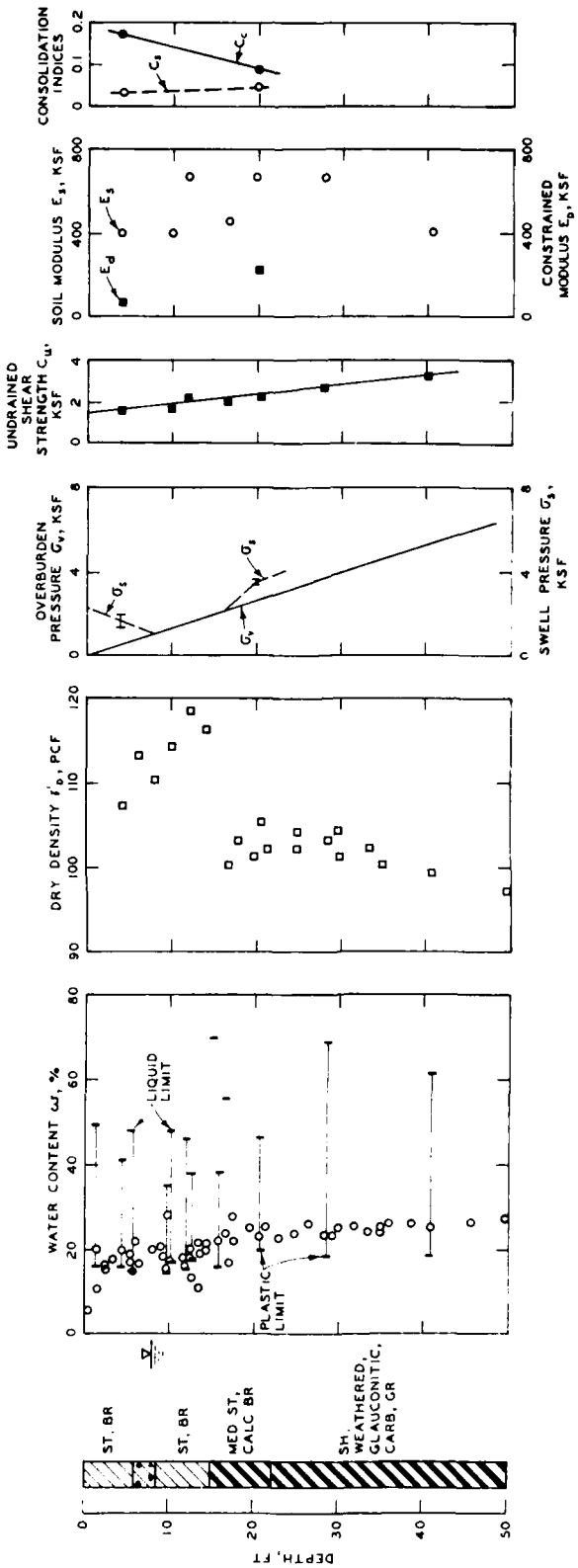

Figure 12. Soil parameters Brooks Air Force Base gymnasium

ASTM D 4546) indicate a desiccated zone with potential for swell above and below the perched water table.

91. Level survey. A level survey of the gymnasium taken November 1983, Figure 13, relative to the original contractor survey shows small and uniform settlements up to 0.3 inch in the gymnasium area and up to 0.8 inch in the adjacent locker room and administrative facilities. Slight heave or apparent center lift was observed near point 5 of the gymnasium. A level survey repeated in April 1985 indicated a slight (0.05 inch) decrease in heave near point 5 and slight (0.05 inch) increase in heave near points 25, 31, and 32 relative to the November 1983 survey. The maximum observed Δ/L ratio is on the order of 1/900 near points 1-2 and 4-5 in the gymnasium (section A) near the exterior beam and points 24-30 and 24-25 in the locker room area (section B). A 1/8-inch diagonal crack was observed during the May 1984 field trip in the concrete masonry units in the locker room area on the second floor inside the stairwell on the northwest side near point 25. Vertical control joints were not observed in the superstructure except between the two distinct parts of the building. Water was observed to be leaking out beneath the south wall of the gymnasium over the exterior stiffening beam near points 2 and 3. Heave measured at point 5 could be a direct consequence of this leaking water.

92. Analysis. Program SLAB2 was used to analyze the soil-structure interaction behavior of the locker room for uniform beam loads of 2 ksf and 1 ksf, Figure 14, assuming $E_s^* = 400$ ksf. A uniform pressure $q = 1$ ksf on the stiffening beams appears to cause displacements reasonably representative of the observed displacements in the locker room. Negative displacements refer to settlement and positive displacements heave. Calculated bending moments and shears for no soil heave ($y_m = 0.0$) for sections B_1 and B_2 are well within structural capacities of the mats. The calculated Δ/L ratio for no heave is about 1/3000 for points 1-2, 4-5, 24-25, and 24-30. An induced edge lift $y_m = 0.25$ inch penetrating 10 ft beneath the perimeter of the mat is representative of the maximum observed Δ/L ratio of about 1/900 and displacement pattern, Figures 13 and 14. This edge lift increases the maximum calculated bending moments to about 100 kips-ft and maximum shears to about 10 kips, Figure 14. A maximum induced edge lift of 1 inch, much greater than currently impressed on the building, would begin to mobilize the full

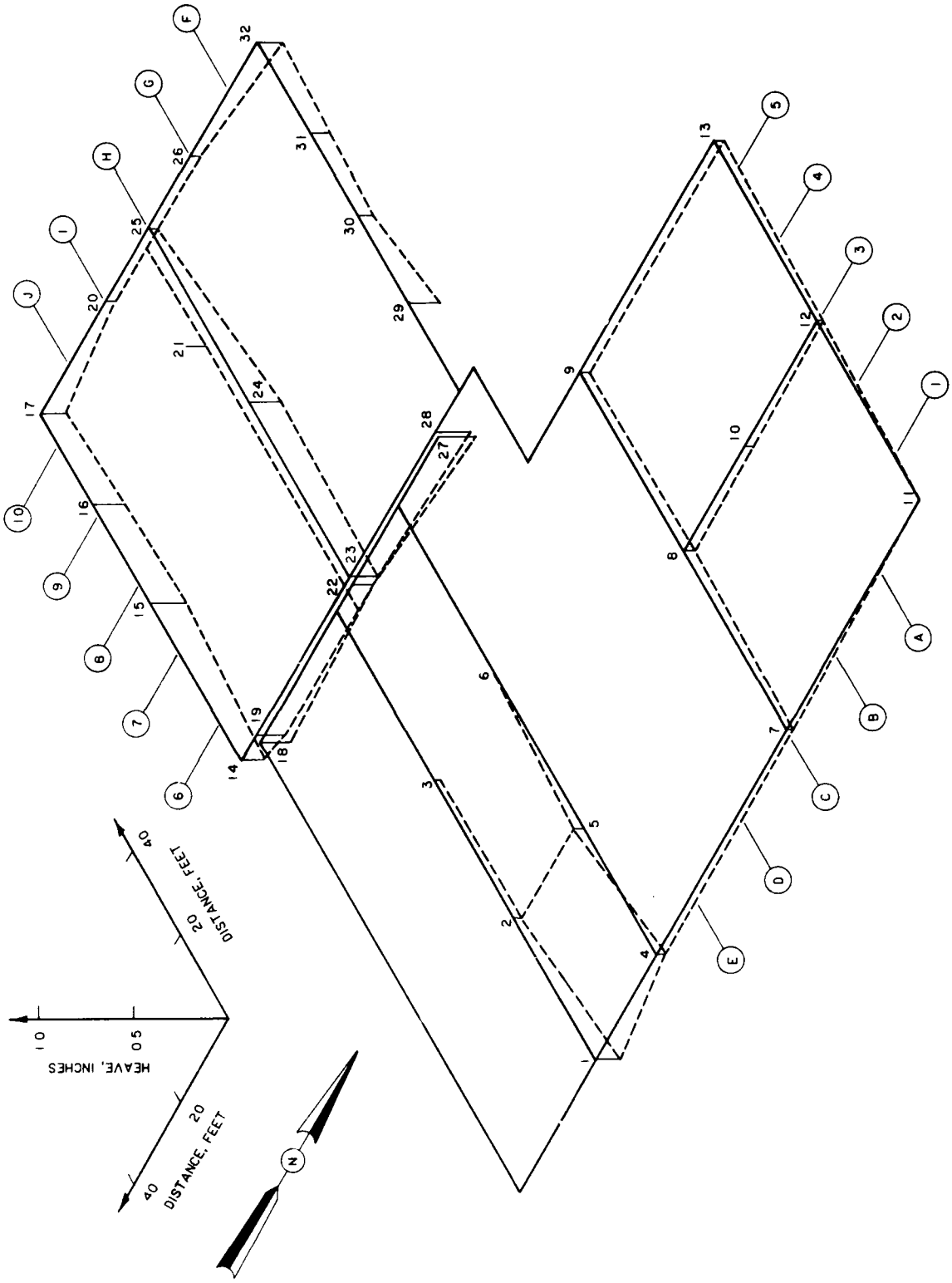

Figure 13. November 1983 level survey, Brooks Air Force Base gymnasium

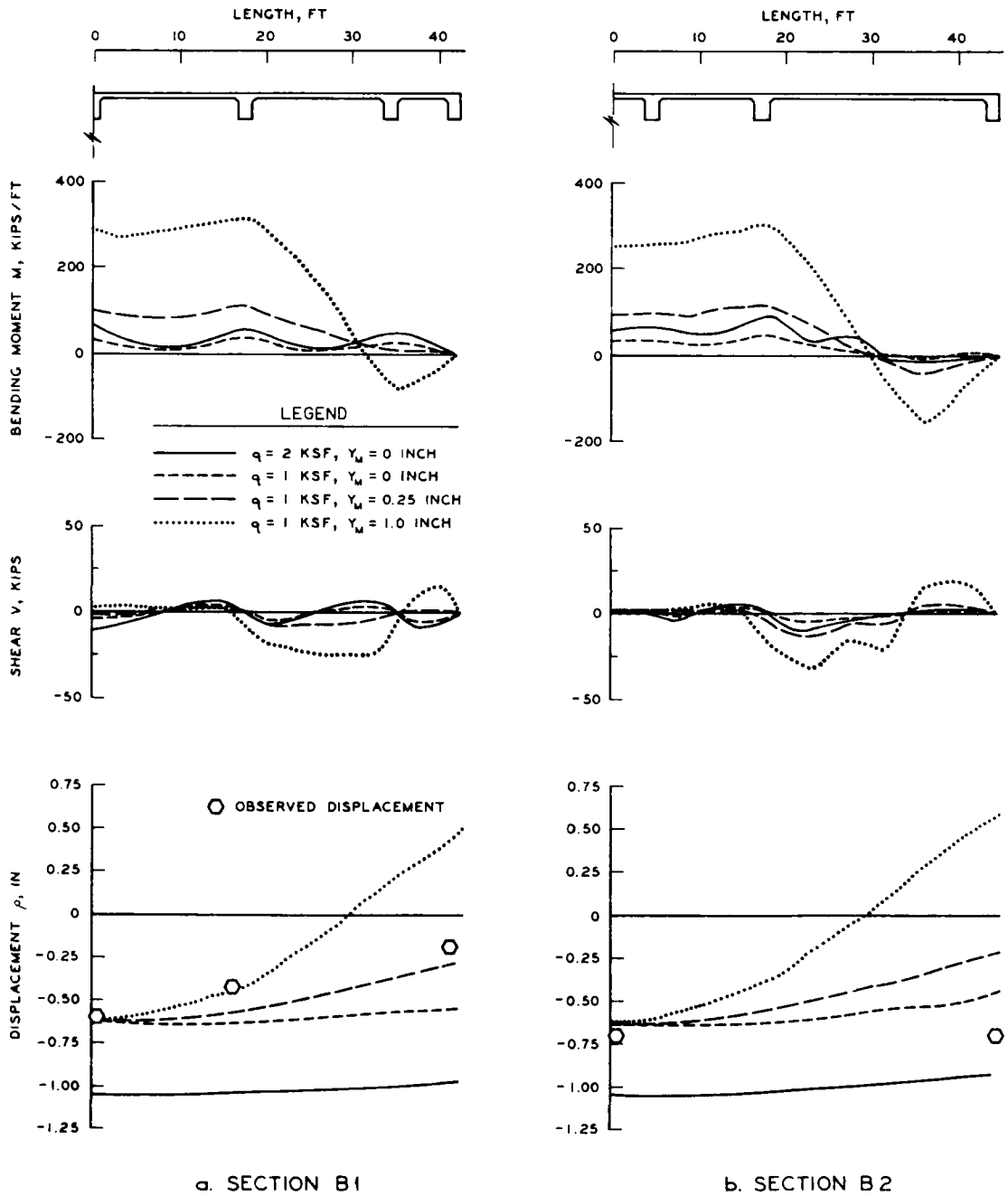

Figure 14. Soil-structure interaction analysis of section B, Brooks Air Force Base gymnasium, using SLAB2

structural capacity. The effective concrete modulus is probably less than the assumed E_c = 432,000 ksf, which would decrease moments and shears. The Walsh (1978) method predicts maximum bending moments less than results of SLAB2 for similar edge lift conditions, Table 12.

93. The displacements ρ_i calculated by SLAB2 in the center (point 1), edges (points 2 and 3), and corner (point 4), Figure 11, are 0.636, 0.541, 0.490, and 0.408 inch, respectively, indicating a dishing action characteristic of a flexible, uniformly loaded mat on a deep elastic, compressible cohesive soil, Figure 7d. A beam on a Winkler foundation analysis that simulates the SLAB2 displacements requires that the coefficient of subgrade reaction k_{sf} should vary across the mat as follows for an average pressure on the mat q = 0.21 ksf (or 1 ksf only on stiffening beams)

Point	Location	ρ, inch	k_{sf}, ksf/ft	$\mu_0\mu_1$
1	Center	0.636	3.96	1.18
2	Middle lomg	0.541	4.66	1.01
3	Middle short	0.490	5.14	0.91
4	Corner	0.408	6.18	0.76

The above table also shows how the influence factor $\mu_0\mu_1$ calculated from Equation 8a (paragraph 44) required to vary in order to match displacements for E_s^* = 400 ksf and S = 85.33 ft. This shows that k_{sf} is not unique for mat foundations. This trend in k_{sf} determined as a function of location are used as described below to calculate influence factors $\mu_0\mu_1$ that may be applied in Equation 8a to evaluate appropriate k_{sf} depending on location in mat foundations.

94. A CPEAMC analysis was performed for section B_1, Figure 11, using a linear distribution of k_{sf} between points 1 and 2 bounded by the above coefficients and q = 1 ksf on the stiffening beams of the T-section or q = 0.21 ksf over the full T-section with width equal to beam spacing. The soil stiffness k′ required for input into CBEAMC was found from Equation 27. These results from CBEAMC provide displacements on the order of those using SLAB2, Figure 15. Three cases were performed using CBEAMC to compare SLAB2 results:

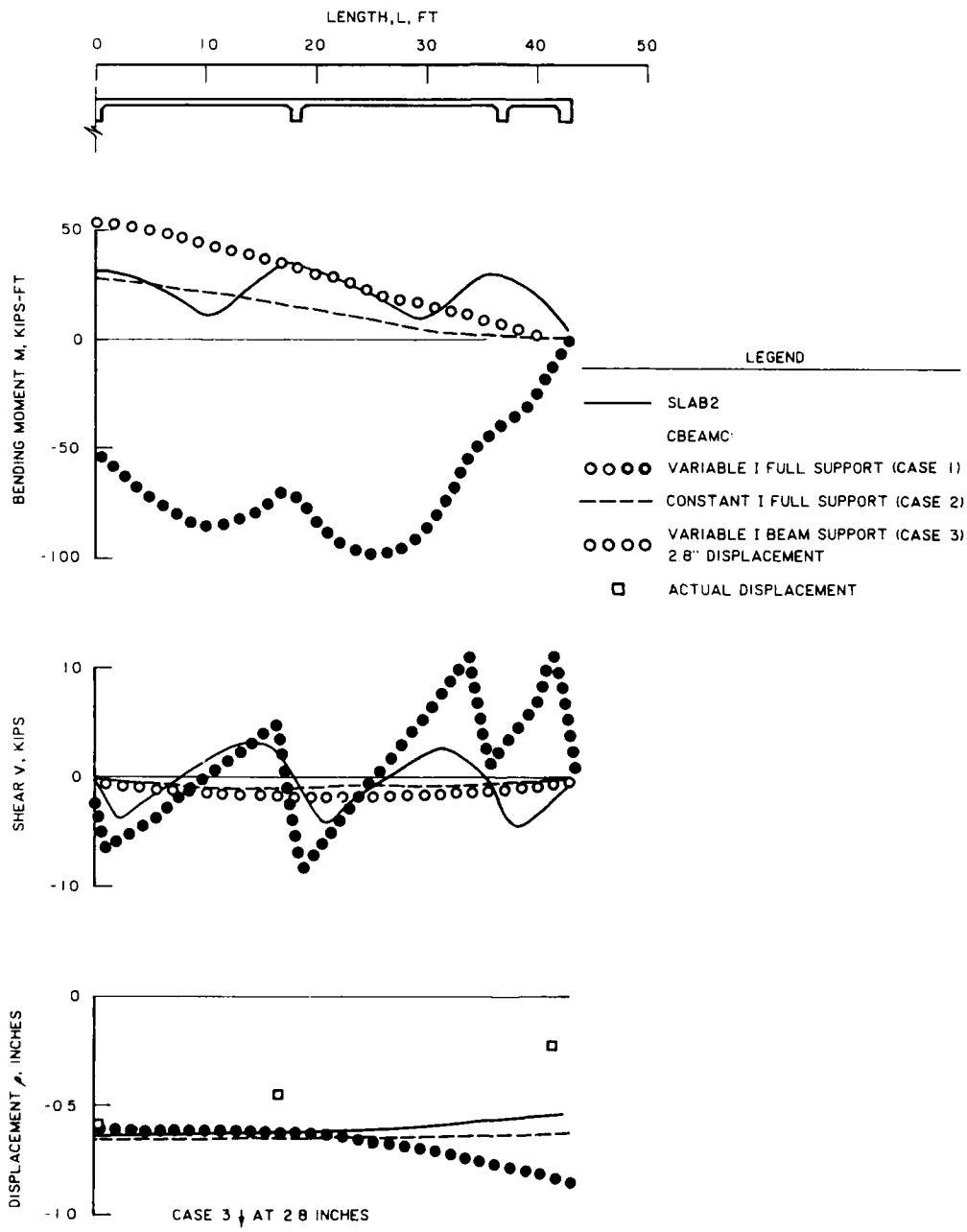

Figure 15. Comparison of results between SLAB2 and CBEAMC for section B_1, Brooks Air Force Base gymnasium

Case	Description
1. Variable I, full support	The moment of inertia is that of the T-beam section indicated in Table 10b between cross-beams, but equal to $$I = \frac{S(t + D)^3}{12}$$ at each cross-beam, Figure 10. Soil support was used under the entire T-beam section. All stiffening beams loaded q = 1 ksf.
2. Constant I, full support	Moment of inertia represented only by the T-beam section, Table 10b. Cross-beam I excluded. Soil support provided under the full T-section
3. Variable I, beam support	Moment of inertia same as case 1, but soil supports only the stiffening beams.

Case 2 simulates SLAB2 results best, but moments at each cross-beam are not simulated because loads were not applied on the cross-beams. Case 1 where loads were applied on the portion of the mat supported by stiffening beams caused large edge settlements and negative bending moments (tension in the top fibers) that contrasted with the positive moments from SLAB2 (compression in top fibers). Results of case 3 show that the flat portion of the mat contributes substantial support since actual displacements are much less than 2.8 inches.

Data Processing Facility, Randolph Air Force Base

95. The data processing facility, located on Randolph Air Force Base near San Antonio, Texas, between First Street East and First Street West adjacent to J street, was completed in 1975. The facility is a rectangular 200 by 150-ft single story masonry building constructed on a ribbed mat with fairly regular beam spacings from 13 to 19 ft, Figure 16. Beam width is normally 12 inches and beam depth below the mat top is 36 inches. Mat thickness between stiffening beams is 6 inches.

96. Soil parameters. Soil parameters from results of laboratory tests on soil samples from five borngs taken in May 1972 are shown in Figure 17.

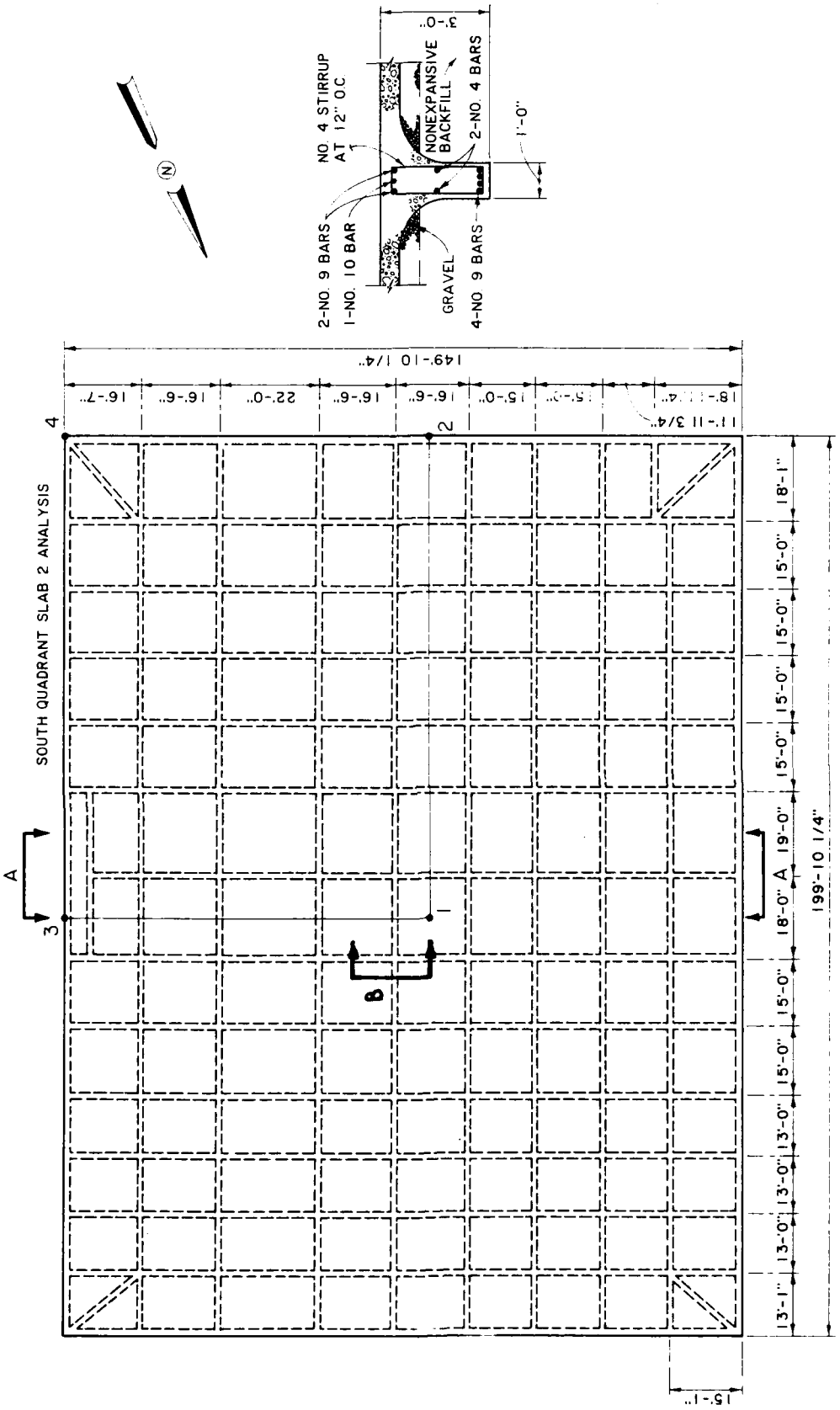

Figure 16. Foundation plan for the Data Processing Facility, Randolph Air Force Base

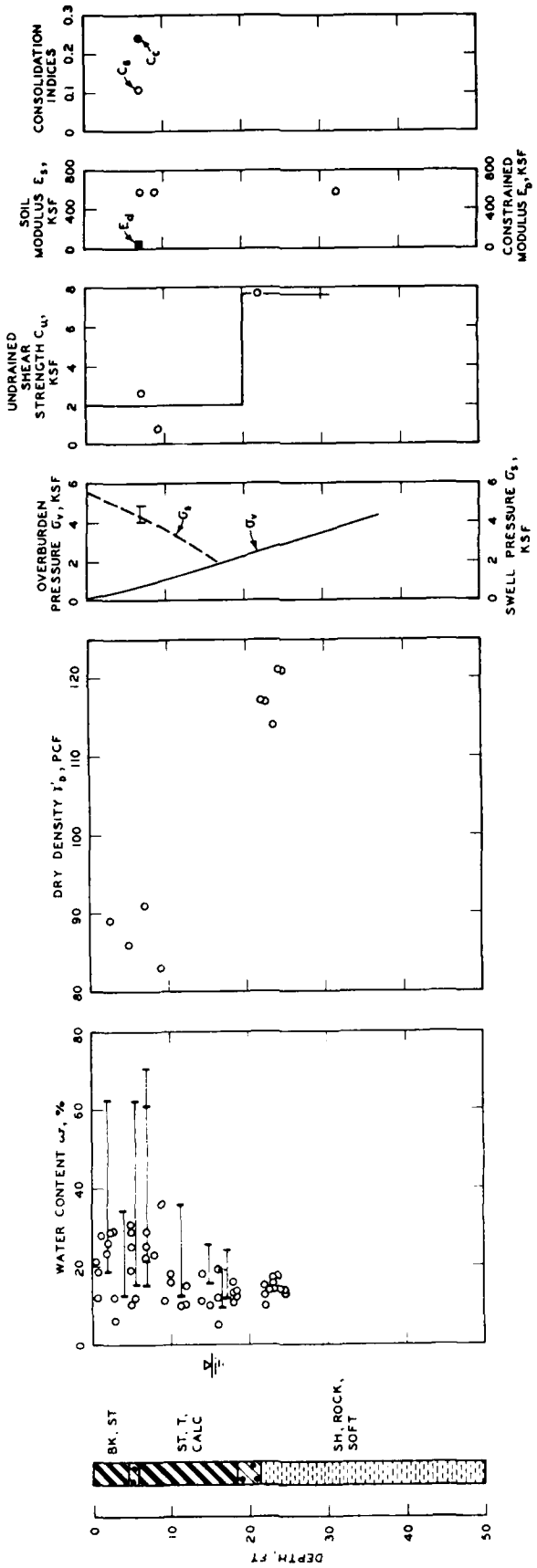

Figure 17. Soil parameters for the Data Processing Facility, Randolph Air Force Base

The overburden soil consists of about 8 to 10 ft of plastic CH dark gray to black, noncalcareous, stiff clay containing some scattered, discontinuous zones of clayey gravel. About 7 to 9 ft of tan to light gray, low to medium plastic CL clay containing calcareous particles up to cobble size was encountered beneath the surface overburden soil. Two to 3 ft of clayey and silty gravel overlying the primary formation was encountered about 18 ft below the ground surface. A perched water table was observed 12 to 15 ft below ground surface, which probably collected in the permeable gravel layer overlying the relatively impervious tan to gray clay shale of the primary formation. The primary formation is Taylor marl of Cretaceous age.

97. Results of several undrained triaxial Q tests shown in Figure 17 indicate that the allowable bearing capacity should be at least 2 ksf assuming a safety factor of about 3. Young's soil modulus evaluated from results of Q tests is about 600 ksf, while the constrained modulus E_d is only about 60 ksf based on swell indices and Equation 26. Swell pressure from a consolidometer/swell test (Method C, ASTM D 4546) on an undisturbed specimen taken 7 ft below ground surface in the overburden soil was 4 ksf indicating desiccation.

98. Level survey. A level survey conducted in November 1983 indicated center lift up to 0.5 inch toward the southwest portion of the mat, Figure 18. Settlement is about 0.3 inch in the West corner increasing to about 0.6 inch at the south and north corners. The east corner shows substantial settlement of about 1.1 inches. A 20-ft addition had been added to the northeast side and east corner during 1979. This addition was secured with dowels into the existing building. A level survey conducted in April 1985 indicated a general heave increasing to 0.25 inch at the east corner relative to the November 1983 survey.

99. Distress was not observed prior to 1979 before the addition. A long fracture was observed in the mat in May 1984, Figure 18, inside the building near the east corner. The ceiling and floor tiles were showing several inches of lateral distortion near the center of the original building. Excessive settlement caused by the addition appears to be contributing to the interior distress in the superstructure; therefore, consideration should be given to

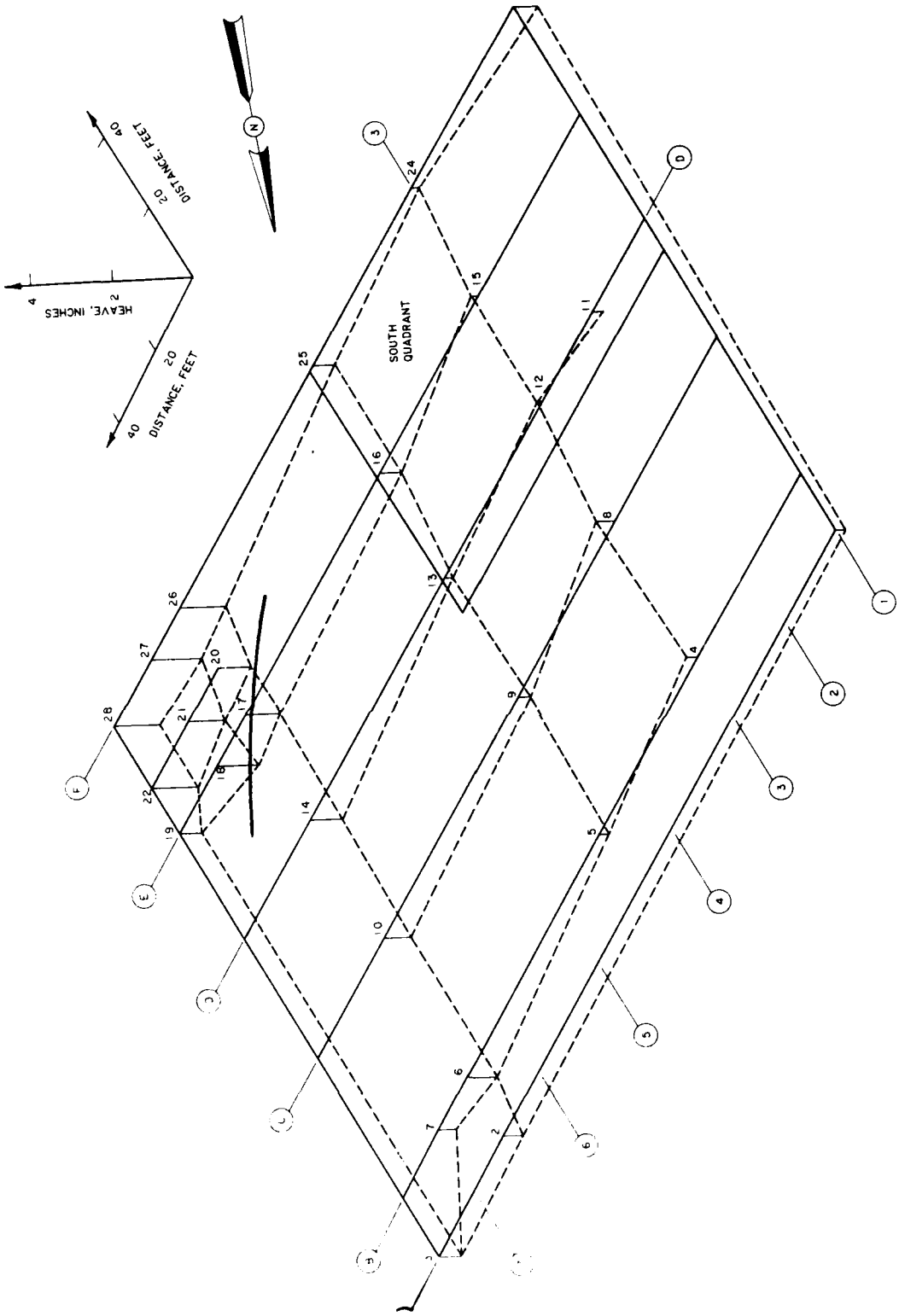

Figure 18. Lev· ' survey for the Data Processing Facility, Randolph Air Force Base

providing flexible connections with new additions. The grade around the perimeter was about 1 percent or more. The maximum observed Δ/L ratio was 1/400 near points 19-22.

100. Analysis. Soil-structure interaction analyses were performed for sections A and B shown in Figure 16 using program CBEAMC and for the south quadrant using program SLAB2. Option NSYM = 4 in SLAB2, Table C3, requires analysis of only 1/4 of the mat with symmetry about the X and Y axes. The soil elastic modulus was taken as 600 ksf. Loading pressure on the stiffening beams was assumed 2 ksf. For section A, the beam width is 18.5 ft with length 150 ft and for section B, the beam width is 16.5 ft with half length of 100 ft. The mat coefficient k_{sf} for the CBEAMC analysis is 3.1 ksf/ft leading to a soil stiffness $k' = 56.4$ ksf for section A and 50.3 ksf for section B. The finite element mesh for program SLAB2 is illustrated in Figure 19.

101. Results of program SLAB2 for the south quadrant sections A and B, Figure 16, are shown in Figure 20. Calculated moments and shears for no imposed heave are small with a maximum center settlement of 1.1 inches. Settlement calculated by CBEAMC for sections A and B for loads consistent with the SLAB2 analysis are 0.92 and 1.0 inches, respectively. While settlements calculated by CBEAMC are flat, SLAB2 settlements resemble a shallow bowl. The distribution of k_{sf} required to duplicate SLAB2 displacements using program CBEAMC for points 1 to 4, Figure 18, for an average pressure $q = 0.264$ ksf, $E_s^* = 600$ ksf, and $B = 149.8$ ft is

Point	Location	ρ, inch	k_{sf}, ksf/ft	$\mu_0\mu_1$
1	Center	1.073	2.82	1.42
2	Middle short	0.789	3.96	1.01
3	Middle long	0.814	3.76	1.07
4	Corner	0.610	5.13	0.78

The above table also shows the distribution for the influence factor $\mu_0\mu_1$, Equation 8a. The Δ/L ratio between center and edge is a maximum of 1/1800 such that cracking is not expected if heave is not imposed on the foundation.

102. Figure 20 shows that the locations of the maximum (+) and minimum (-) moments and shears for no imposed heave are located near the midedge and

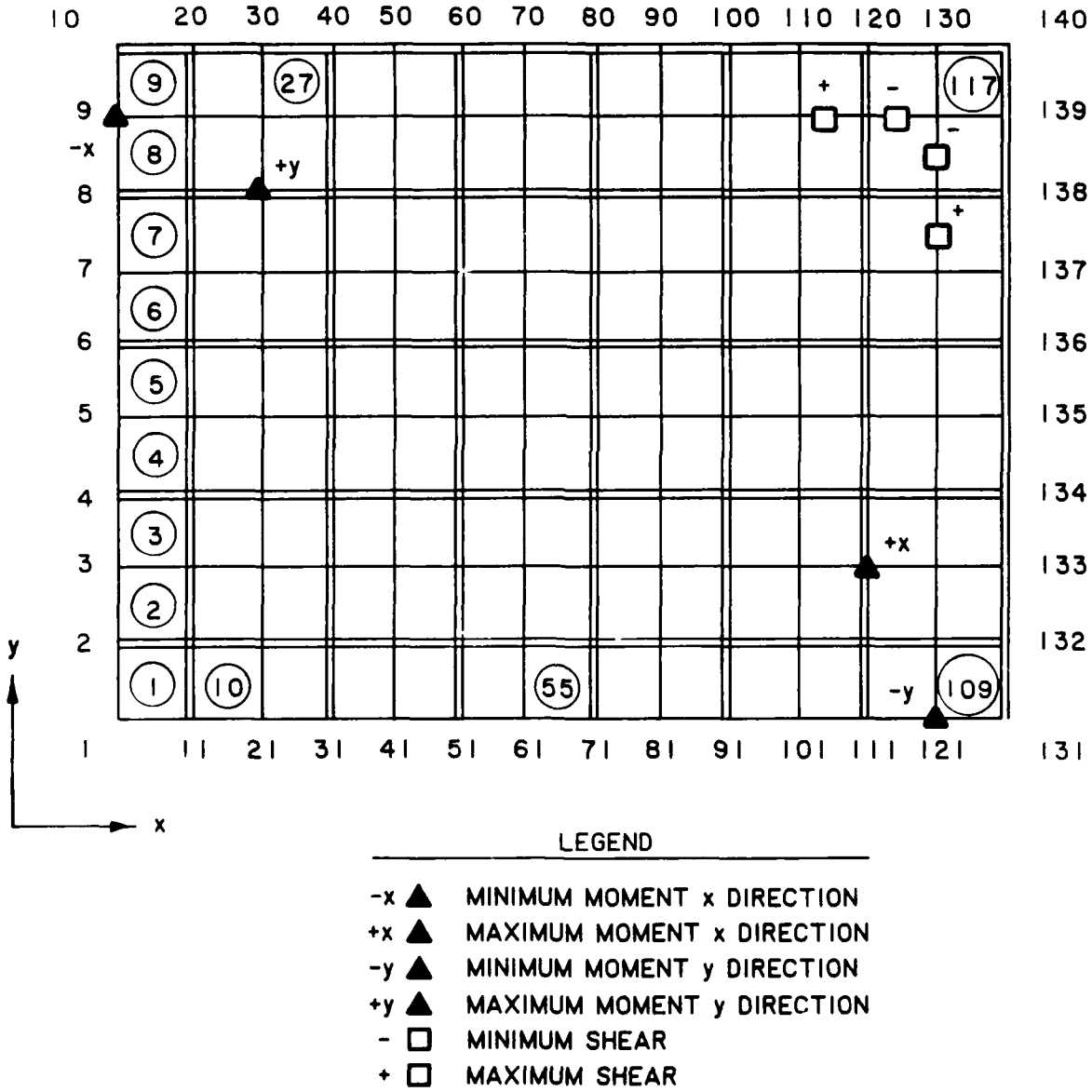

Figure 19. Finite element mesh for SLAB2 analysis, Data Processing Facility, Randolph Air Force Base

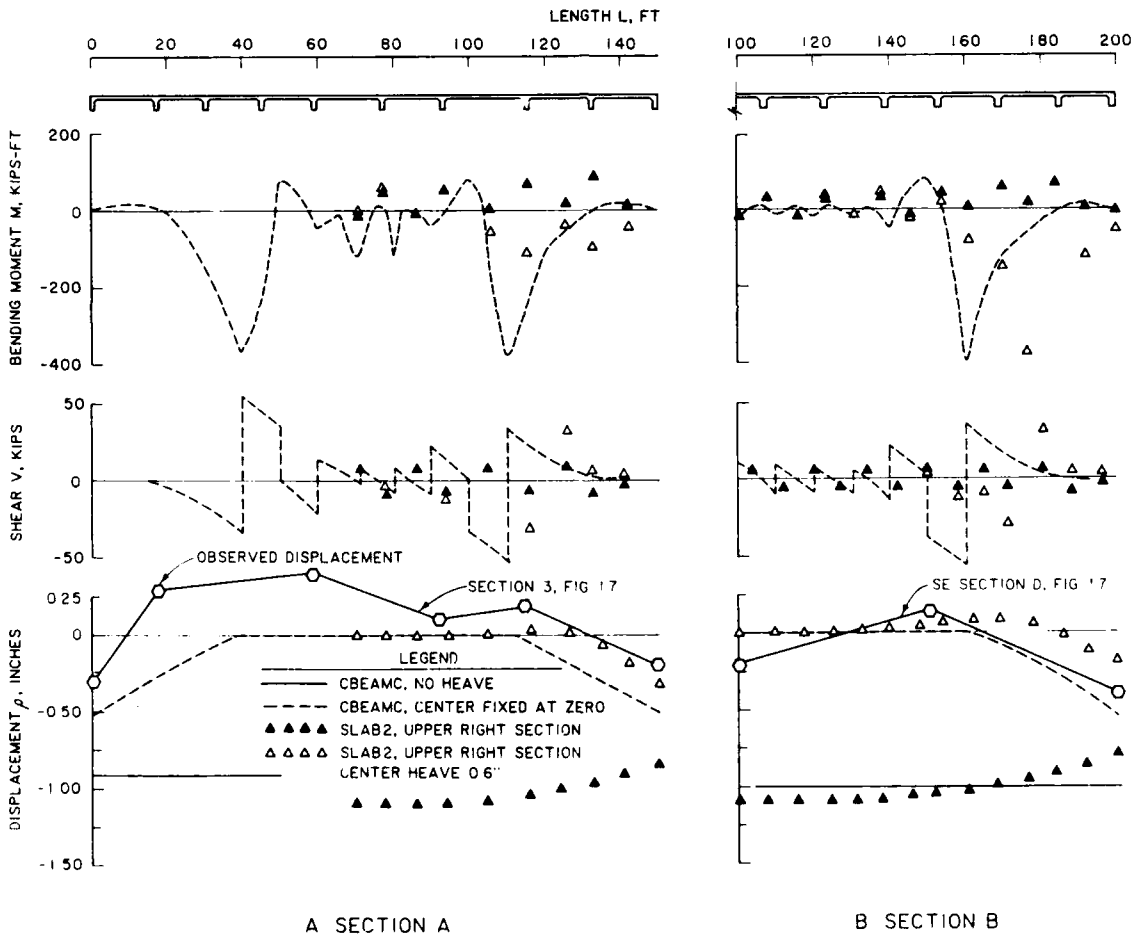

Figure 20. Soil-structure interaction analysis, Data Processing Facility, Randolph Air Force Base. q = 2 ksf

corner, respectively. Distances from the edge and corner are approximately the same or less than the relative stiffness length[11]

$$\beta' = \sqrt[4]{\frac{E_c I}{E_s}} \tag{28}$$

where

β' = relative stiffness length, ft

E_c = Young's concrete modulus, 432,000 ksf

E_s = Young's soil modulus, 600 ksf

I = moment of inertia of the mat cross-section, ft^4

103. Imposing zero center displacement for sections A and B using CBEAMC and edge-down gaps in the south quadrant using SLAB2 roughly simulated the observed displacements, Figure 20. Displacements calculated by SLAB2 were realigned to simulate zero displacement near the mat center. Calculated moments and shears from both programs CBEAMC and SLAB2 appear to be similar and approach the capacity of the T-beams, Table 10 The maximum and minimum moments and shears calculated by SLAB2 were located near the mat corners within distance β', Equation 28, and approximated the mat capacity. The Walsh method, Table 12 predicts high bending moments of 270 kip-ft, but still within the mat capacity.

Maintenance Shop and Warehouse
US Army Reserve Center

104 The maintenance shop and warehouse of the US Army Reserve Center were constructed in 1980 and are located between Sultan and Winans Road near Harry Wurzback Road in Fort Sam Houston, Texas. They are steel frame rectangular buildings with metal siding and concrete masonry unit walls. The layout and size of the foundations are illustrated in Figure 21. Beam spacings vary from 17 to 27 ft. Beam depth for the maintenance shop is 3 ft including the 5 inch thickness of the flat portion of the mat between stiffening beams. The depth of each of the six beams for the warehouse mat from left to right varies from 2.5 to 6 ft (numbers 1 to 6, Table 10) including the 5-inch thick flat slab between stiffening beams. Beam width varies from 1 ft at the bottom to 2.5 ft near the top; analyses assumed an average width of 1.5 ft. Steel reinforcement consists of two number 11 bars

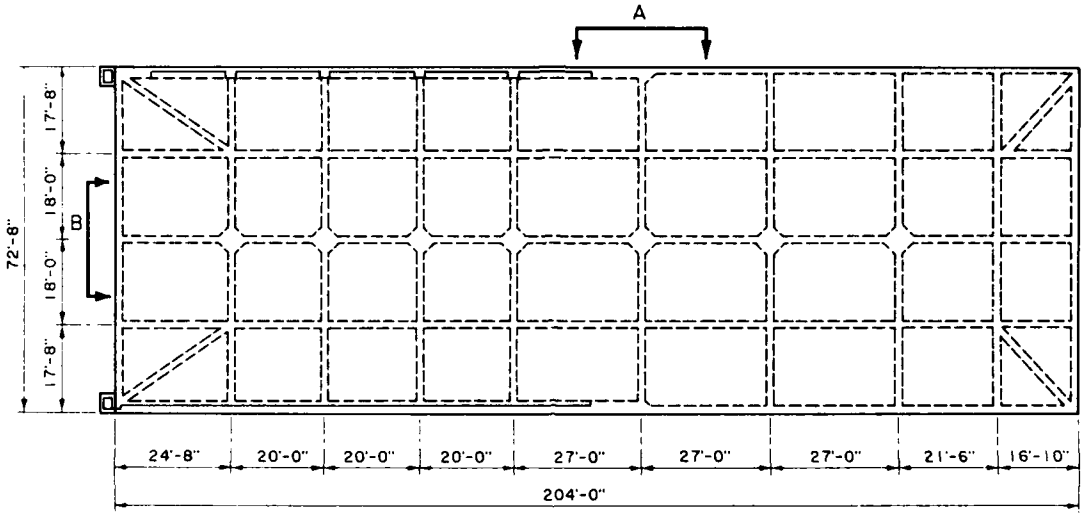

MAINTENANCE BUILDING

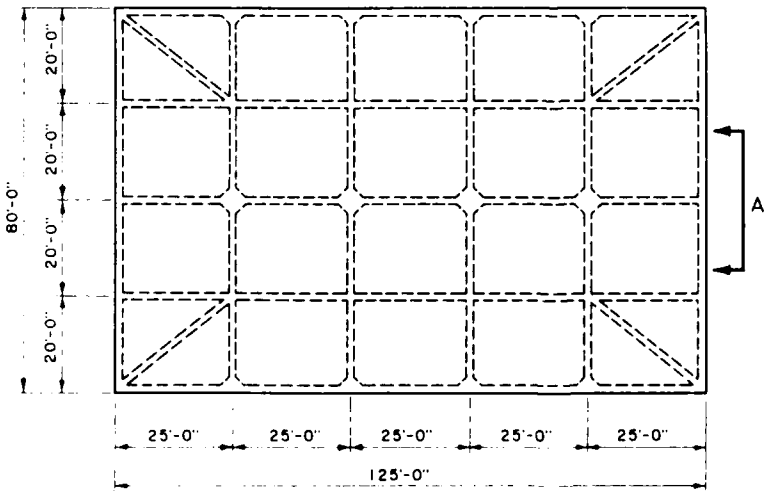

WAREHOUSE

Figure 21. Foundation plan Maintenance Shop and Warehouse, US Army Reserve Center, Fort Sam Houston

top and bottom in each beam, except beams in the short direction of the maintenance shop contain two number 7 bars top and bottom.

105. Soil parameters. Soil parameters evaluated from results of laboratory tests on soil samples of 34 core borings obtained October and November 1978 are shown in Figure 22. Overburden materials consist of about 2 ft of medium plasticity (CL) black clay, 3 or 4 ft of high plasticity (CH) brown clay, about 7 ft of white, calcareous medium plastic (CL) clay, and about 3 ft of clayey gravel. The gravel contains a perched water table with water level beginning about 14 ft below ground surface. The primary material underlying the overburden is a tan to gray, weathered and jointed clay shale of the Anacacho formation of Cretaceous age. This material is about 200 ft thick and consists predominantly of moderately hard calcareous shale with occasional hard limestone interbeds up to 20 ft thick. Weathered shale is found down to about 49 ft below ground surface and the unweathered, hard, blue shale is found below this depth.

106. Results of triaxial undrained strength Q tests indicate that the soil has an undrained shear strength of 2 ksf near the ground surface increasing linearly with depth at the rate of 2 ksf/15 ft of depth. The allowable bearing capacity of soil beneath the stiffening beams is at least 4 ksf. The elastic Young's soil modulus is about 400 ksf down to 30 ft and 800 ksf or more below this depth. The constrained modulus is about 200 ksf or less down to 30 ft and more than 400 ksf below this depth. Consolidometer/swell test results indicate swell pressures of about 2 ksf and significant swell potential above 14 ft of depth.

107. Level survey. A survey conducted on the mat surface of the maintenance building in November 1983, Figure 23, shows a general settlement increasing toward the north from 0.5 to 1.2 inches. An unusual, symmetrical dual-shaped differential heave in the northern part of the mat appears, which could be a construction error in the mat elevation. The northern half of the mat was designed with a slope that caused the east and west perimeters to be 4 inches lower than the center to permit drainage of runoff water from washing operations. A 1-inch error in the slope at points 19-13-9 and 17-11-7 will account for this unusual displacement pattern. Visual observations in May 1984 indicate no distress, except for a small crack in the concrete masonry

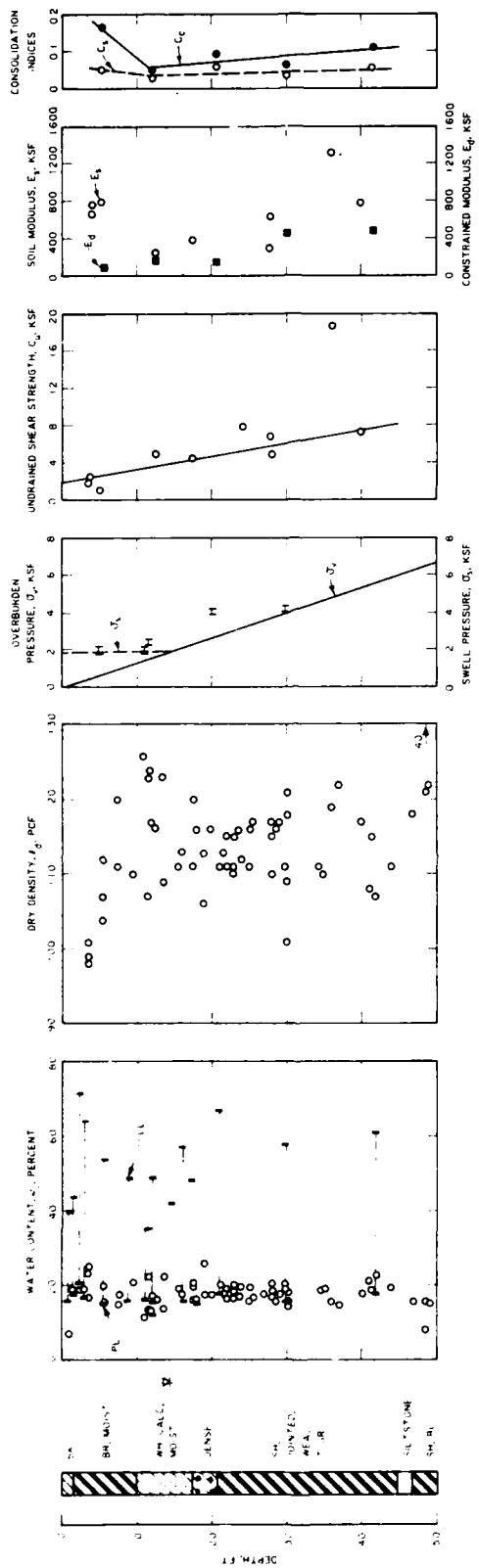

Figure 22. Soil parameters Maintenance Shop and Warehouse, US Army Reserve Center, Fort Sam Houston

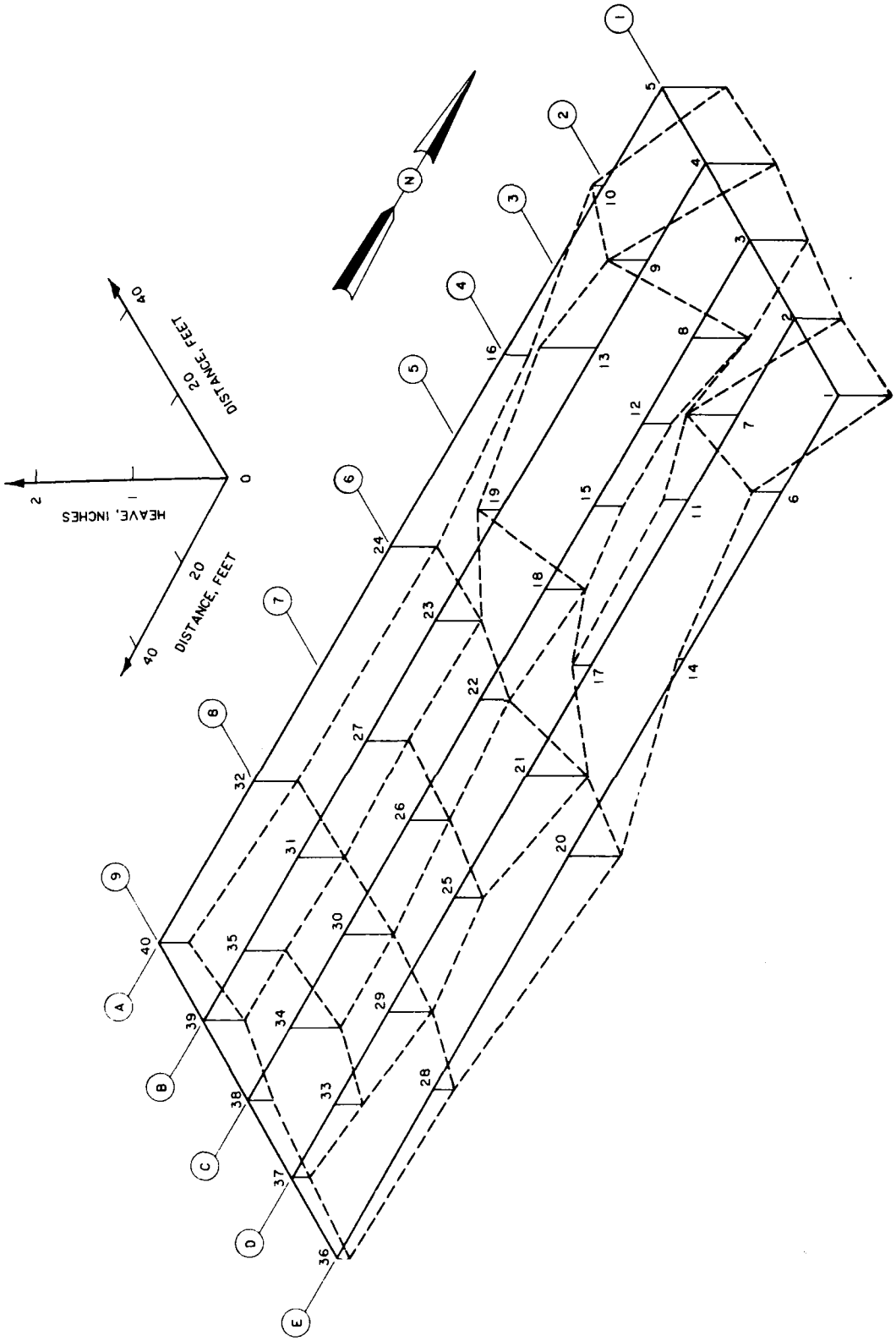

Figure 23. November 1983 level survey Maintenance Shop, US Army Reserve Center, Fort Sam Houston

units of the wall near point 10 at ground level, Figure 23. If mat distortion recorded in Figure 23 is correct, the maximum observed Δ/L ratio is 1/200 near points 8-9; otherwise, the maximum observed Δ/L ratio will probably be about 1/400 near points 12-8. Level readings taken in April 1985 are not significantly different than those of November 1983.

108. Analyses. Results of the soil-structure interaction analysis using program SLAB2 for E_s = 400 ksf and q = 1 ksf, Figure 24, indicate relatively low bending moments and shears for no soil heave. The maximum calculated Δ/L ratio is about 1/2000 so that distress is not expected in the mat or superstructure. The SLAB2 analysis indicates bending moments and shears that are larger in the short direction than in the long direction; specifications indicate less steel in the short direction.

109. The finite element mesh for the maintenance shop shown in Figure 25, assuming mat symmetry about the X or long axis, shows the location of maximum moments and shears near the northwest corner and mat center. Calculated settlements near the center are greater than near the edge, in contrast to flat displacements from Winkler solutions. The observed dish-shaped pattern of displacements appears consistent with the SLAB2 elastic foundation analysis, Figure 23.

110. Displacements input into SLAB2 in an attempt to simulate the distortion pattern observed in Figure 23 led to excessive bending moments and shears that would fracture the mat, but such damage was not observed. The mat stiffness is too large to simulate this distortion pattern in the north part of the mat indicating gaps should appear beneath the mat. Results of the Walsh method, Table 12 predict bending moments exceeding the structural capacity, Table 10. A construction error therefore appears to cause the slope to be about an inch less than intended. The distribution of k_{sf} and $\mu_0\mu_1$ required to simulate SLAB2 displacements for points shown in Figure 22 using the Winkler foundation with no heave and a uniform pressure q = 0.17 ksf, E_s^* = 400 ksf, and B = 72.7 ft is

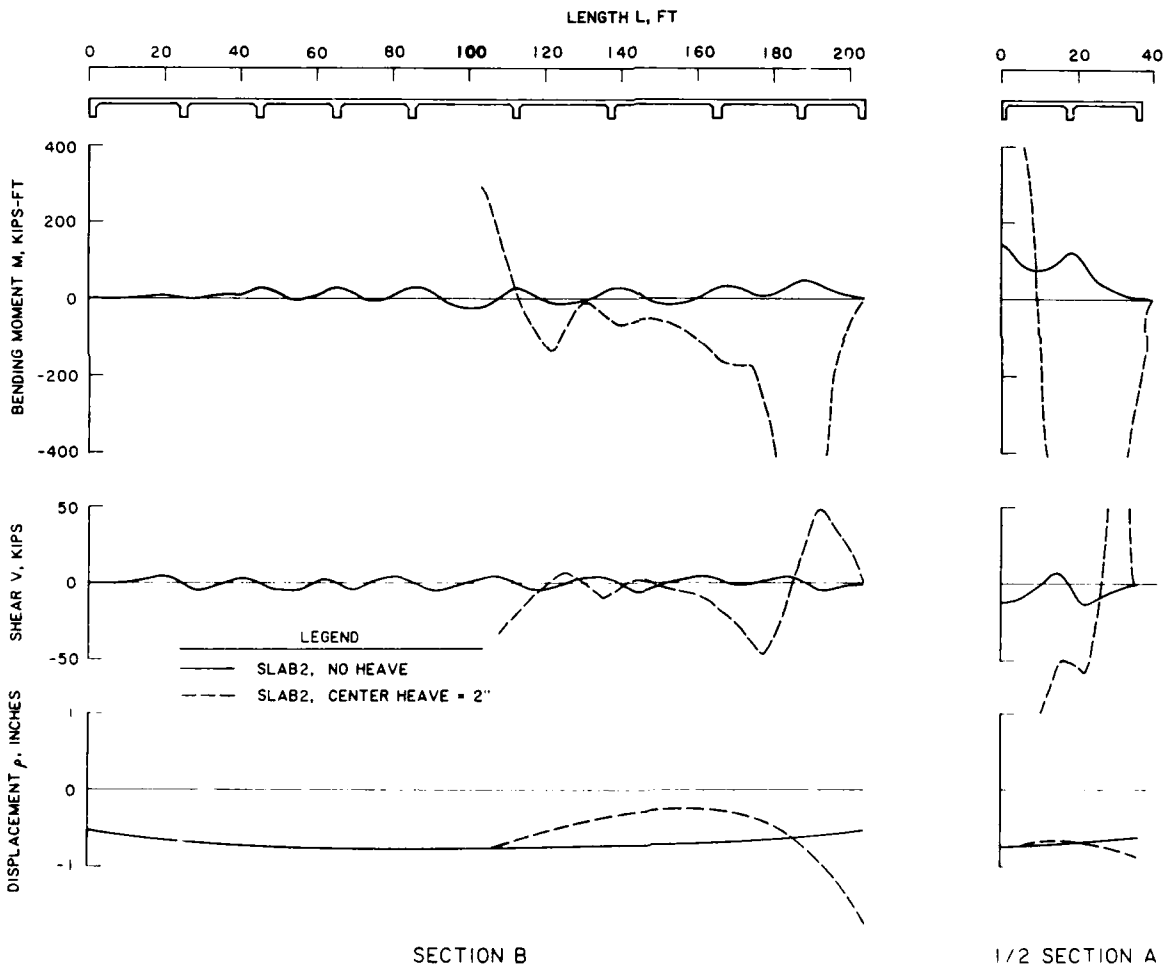

Figure 24. Soil-structure interaction analysis Maintenance Shop, US Army Reserve Center, Fort Sam Houston using SLAB2

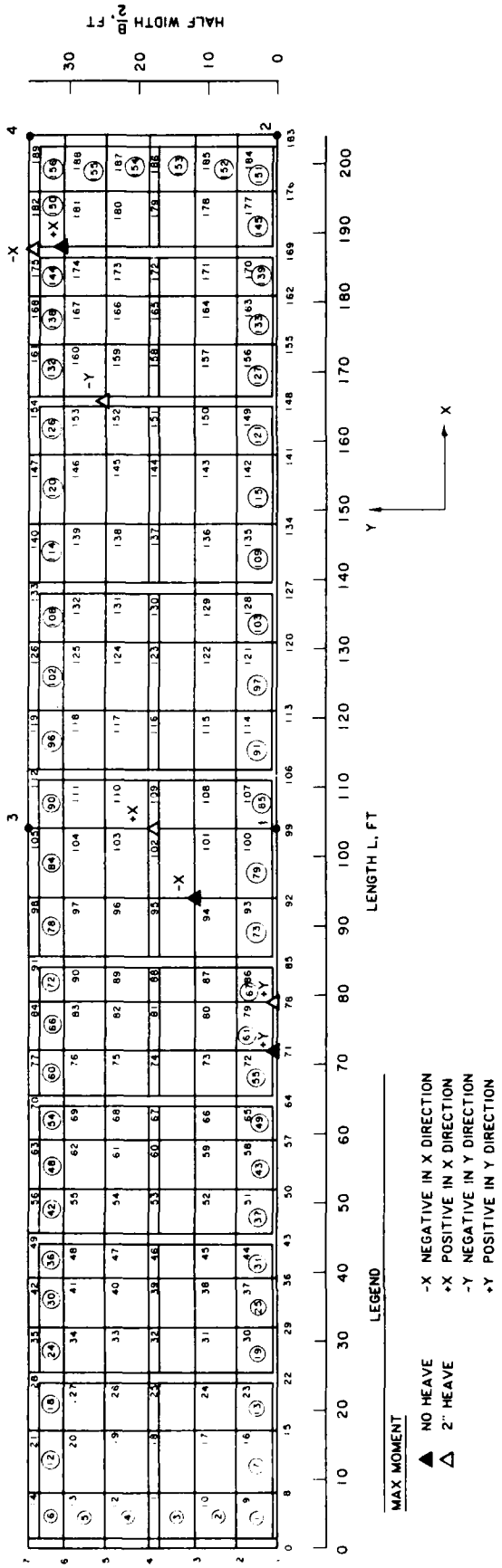

Figure 25. Finite element mesh of the mat supporting the Maintenance Shop, US Army Reserve Center

Point	Location	ρ, inch	k_{sf}, ksf/ft	$\mu_0\mu_1$
1	Center	0.737	2.77	1.99
2	Middle short	0.541	3.77	1.46
3	Middle long	0.628	3.25	1.69
4	Corner	0.450	4.53	1.21

Dental and Medical Clinics

111. The dental and medical clinics, located in northeastern Fort Sam Houston near Garden Avenue and Harvey Road, were constructed in 1980 and 1981. The clinics are single story, rectangular brick and concrete masonry structures supported on ribbed mats, Figure 26. Vertical construction joints were closely placed in the superstructure at approximately 4-ft intervals to increase flexibility. The site slopes downward from northwest to southeast at a slope of about 3 percent leading to a grade differential close to 8 ft across the diagonal of both structures. Beam spacings vary from 10 to 15 ft in the dental clinic and 11 to 30 ft in the medical clinic. Beam depth of the dental clinic mat is 2 ft 8 inches from the mat top with beam width of 1 ft 4 inches. Beam depth of the medical clinic is 3 ft from the mat top with beam width of 1 ft 6 inches. Thickness of the flat part of the mat is 6 inches. Reinforcement steel consists of three number 9 bars placed both top and bottom in the stiffening beams supporting the medical clinic.

112. Soil parameters. Results of laboratory tests on soil samples from borings taken at the dental clinic site in December 1977 and January 1978 are shown in Figure 27a. Results of laboratory tests on soil samples from five additional borings obtained at the medical clinic site in January 1979 are shown in Figure 27b. Overburden material varies from 6 to 16 ft thick and consists of dark brown to black, gravelly, medium CL to high CH plasticity clay and clayey gravel GC. Figure 27a shows about 10 ft of black CH clay overlying about 6 ft of clayey gravel beneath the dental clinic site. Figure 27b shows about 6 ft of black CL to CH gravelly clay overlying about 2 ft of sandy gravel beneath the medical clinic site. The clayey gravel contains a perched water table with water level 7 to 12 ft below ground surface. The primary material below the overburden is the Taylor formation of upper Cretaceous age. This material is yellow-brown, calcareous, slightly silty,

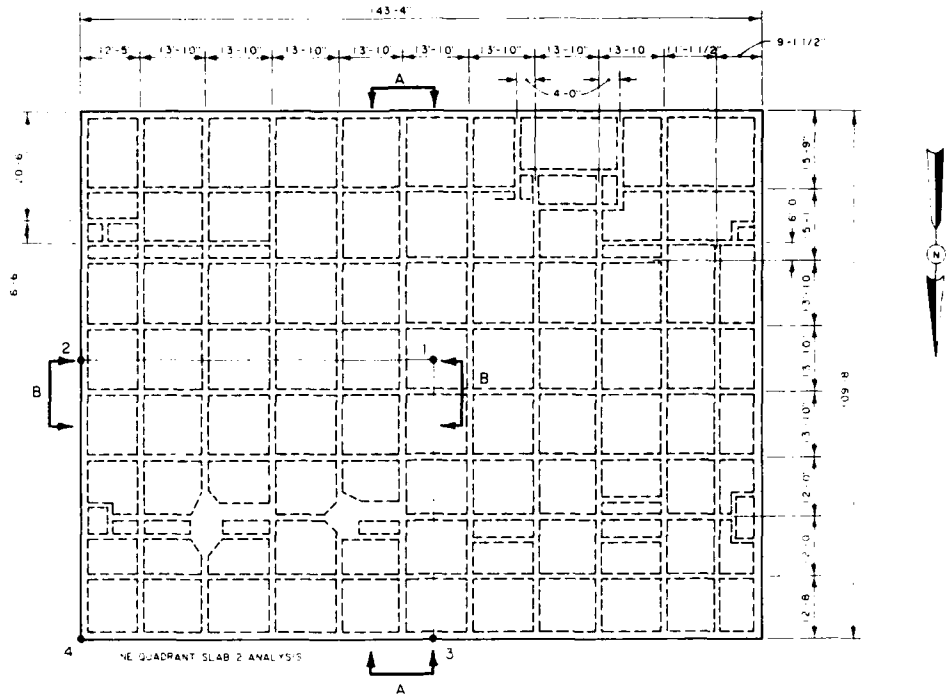

A TROOP DENTAL CLINIC

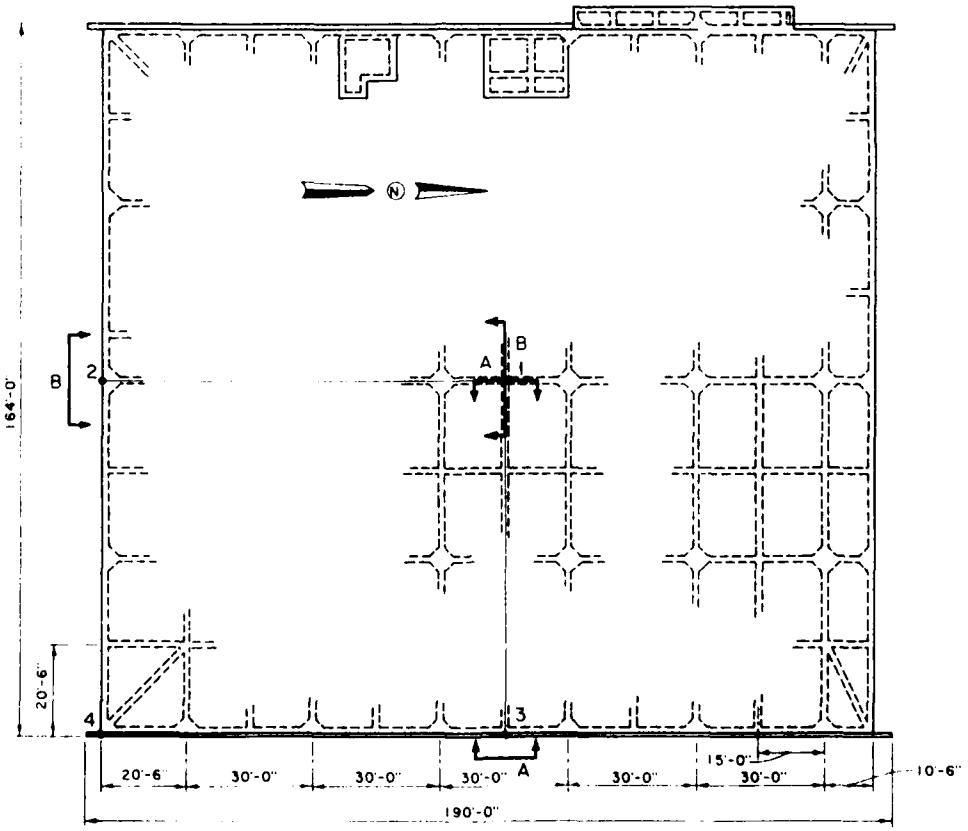

B TROOP MEDICAL CLINIC

Figure 26. Foundation plan Troop and Medical Clinics, Fort Sam Houston

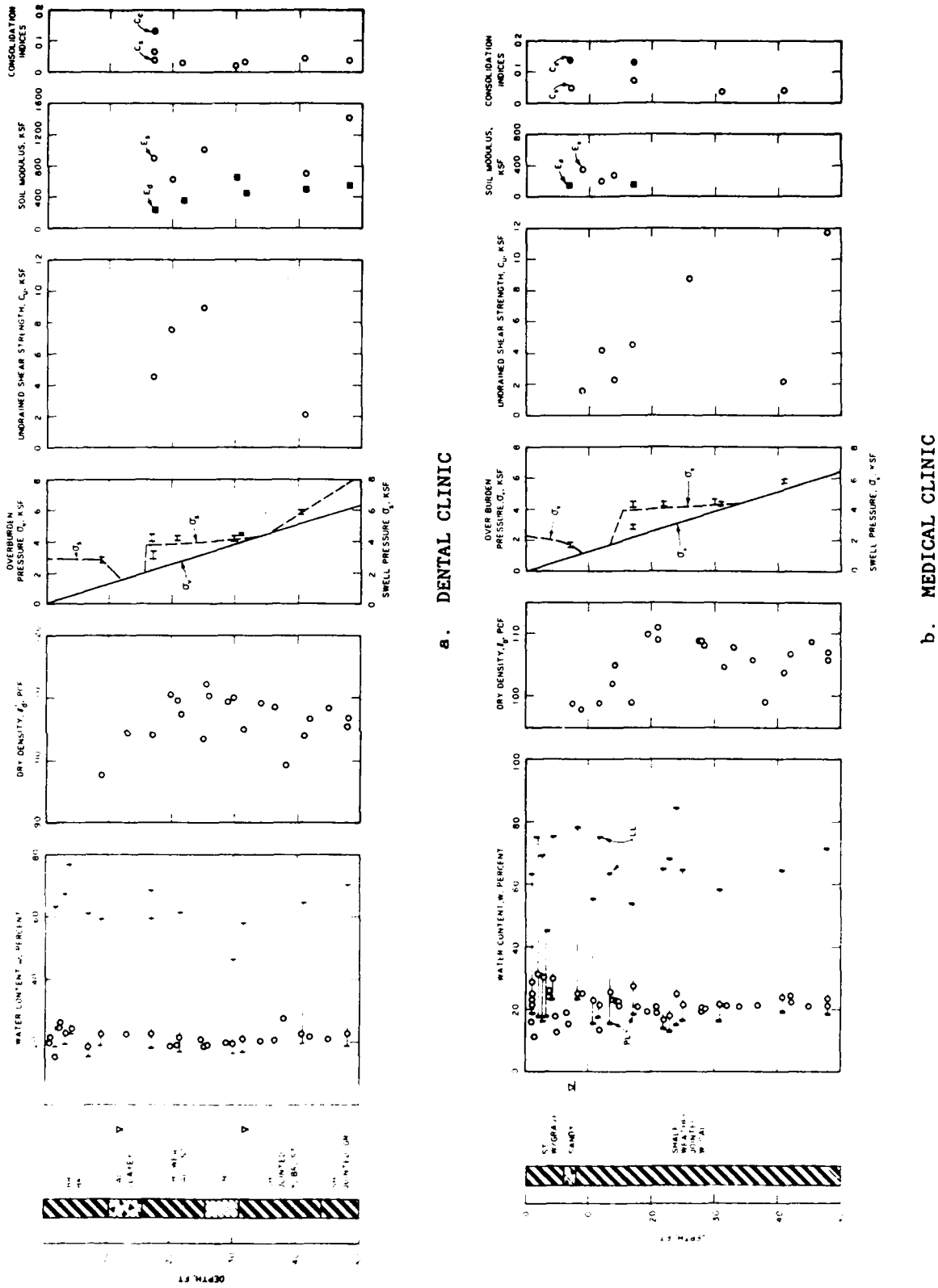

Figure 27. Soil parameters Troop and Medical Clinics, Fort Sam Houston

soft to moderately hard (Rock classification) clay shale containing occasional hard marl up to 3 ft thick. The shale is expansive CH jointed and weathered clay up to 50 or 60 ft below ground surface.

113. Results of triaxial undrained Q strength tests indicated an undrained shear strength of 1.6 ksf about 9 ft below ground surface with substantially greater strengths below this depth. The allowable bearing capacity is at least 3 ksf. The soil elastic modulus E_s varies from 200 to 400 ksf within the top 15 ft of soil and 600 to 1000 ksf below 15 ft from the ground surface. Results of consolidometer/swell tests indicate a potential for swell and swell pressures exceeding calculated vertical overburden pressures above 7 ft and below 17 ft, Figure 27.

114. Level survey, dental clinic. A level survey of the dental clinic conducted in November 1983, Figure 28, indicates a tendency toward center heave up to about 1 inch. Settlement of about 0.5 inch was measured near the east edge. The April 1985 survey indicated about 0.3 inch reduction in settlement (or heave) near the east edge relative to the November 1983 survey and about 0.1 inch more heave near the mat center. Visual observations of the building in May 1984 indicated no cracks in the exterior brick panels; these panels include vertical construction joints at 4-ft intervals. Cracks were observed in the exterior stiffening beams on both east and west sides of the dental clinic mat. The maximum observed Δ/L ratio was about 1/250 near points 6-16, 9-20, and 27-28, Figure 28, running east to west.

115. Analysis, dental clinic. Results of soil-structure interaction analysis of the dental clinic mat, Figure 29, were completed for sections A and B in Figure 26a using CBEAMC and for the northeast quadrant of Figure 28 using SLAB2. The soil modulus E_s^* was taken as 400 ksf. Mat settlement for a uniform pressure of 1 ksf on the stiffening beams of section A was 0.83 inch using CBEAMC. SLAB2 calculated about 1.0 inch of center settlement and 0.8 inch edge settlement. The distribution of k_{sf} for points 1 to 4, Figure 26a required to simulate SLAB2 displacements using the Winkler foundation, q = 0.22 ksf uniform pressure, E_s^* = 400 ksf and B = 109.7 ft is

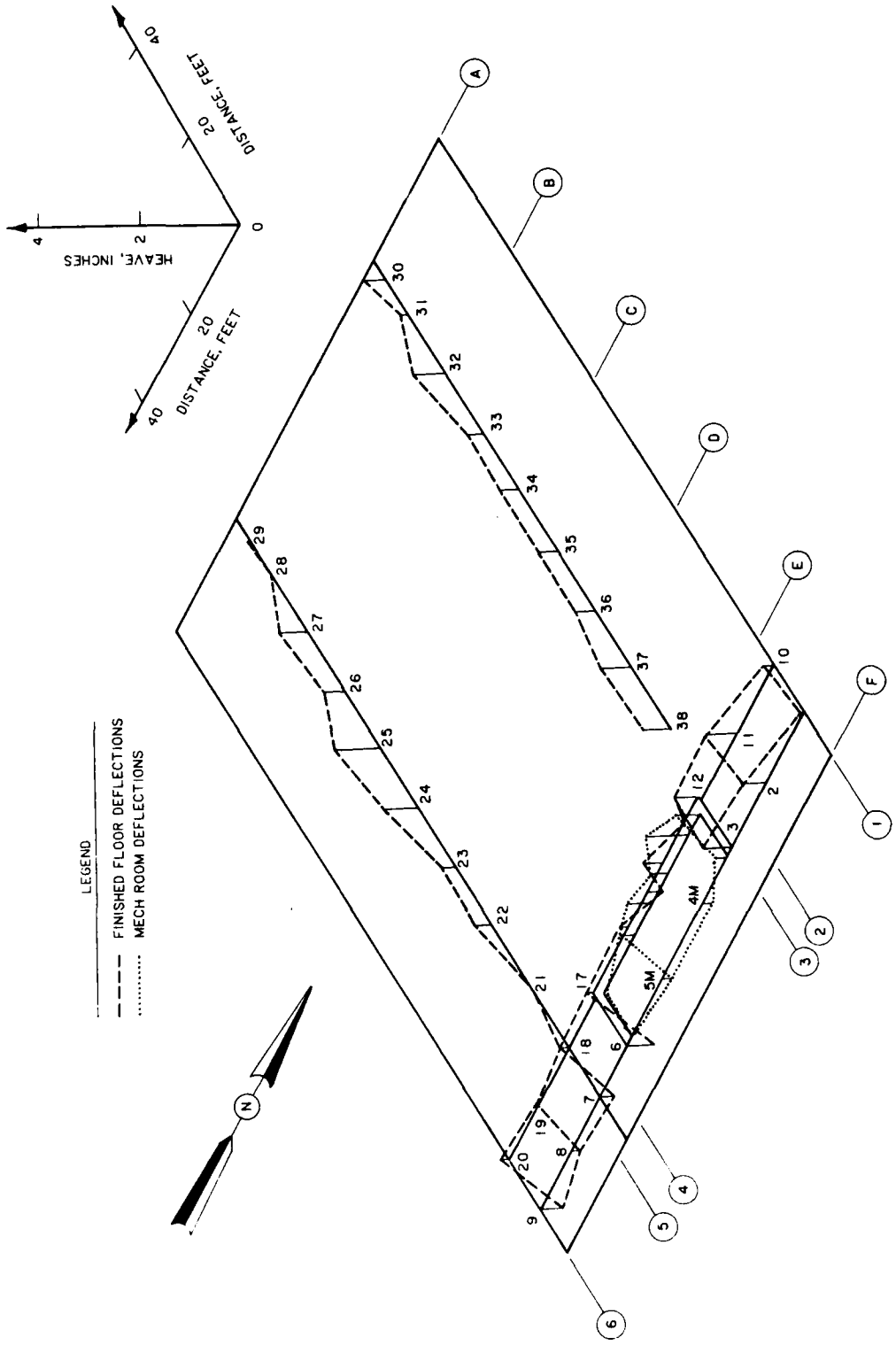

Figure 28. November 1983 level survey Dental Clinic, Fort Sam Houston

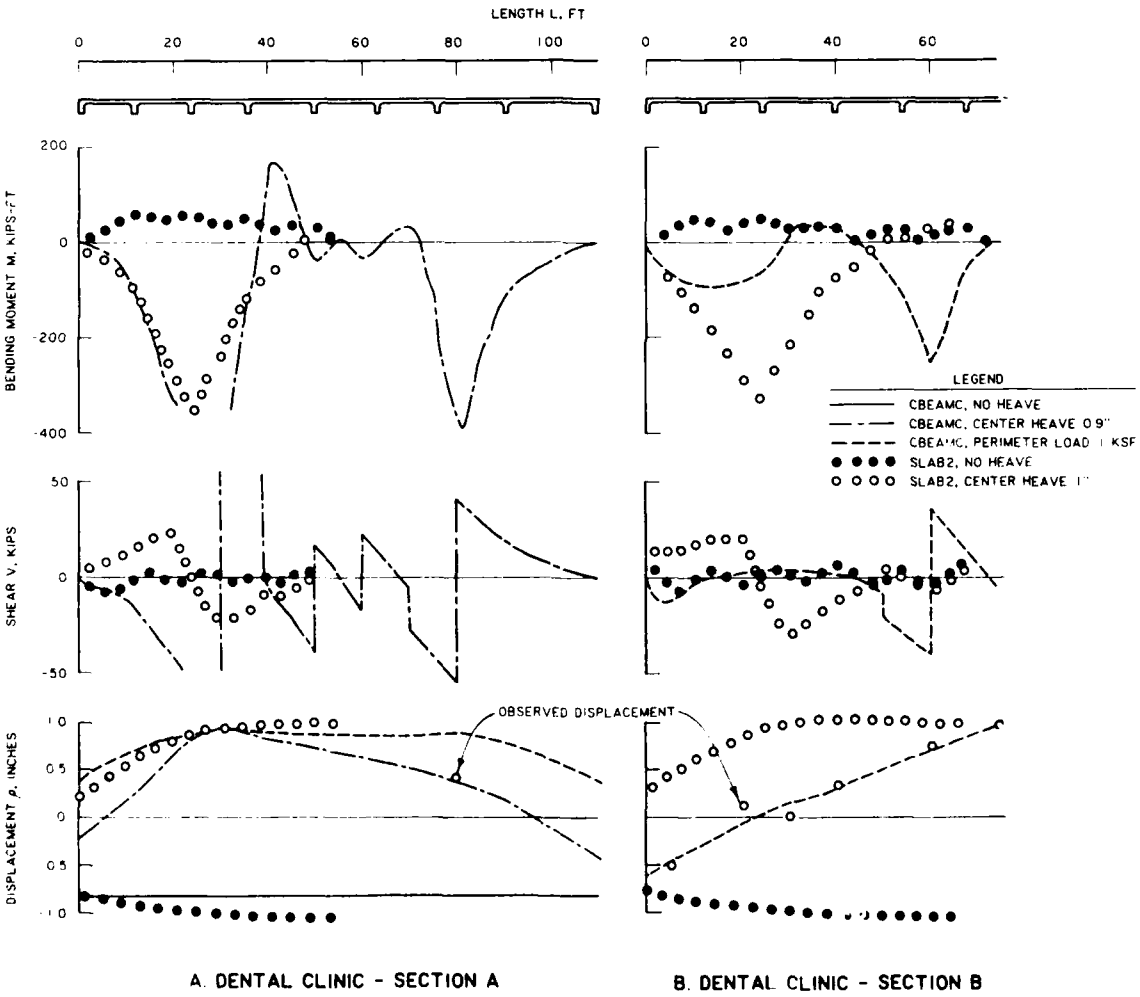

Figure 29. Soil-structure interaction analysis Dental Clinic, Fort Sam Houston

Point	Location	ρ, inch	k_{sf}, ksf/ft	$\mu_0\mu_1$
1	Center	1.073	2.45	1.49
2	Middle short	0.789	3.33	1.09
3	Middle long	0.814	3.23	1.13
4	Corner	0.610	4.31	0.85

116. Imposing center heave and perimeter loads increased moments and shears toward the structural capacity of the mat, Table 10. This was particularly evident from results of CBEAMC for center heave which caused moments to exceed the structural capacity. The corresponding calculated displacements shown in Figure 29 imposing a 1 ksf perimeter load for the CBEAMC analysis and edge gaps for the SLAB2 analysis to simulate heave illustrates the center doming pattern that can be obtained. Gaps imposed for SLAB2 analysis to simulate displacements of section B appear to compare better along lines 2 and 3, Figure 28, than along lines 4 and 5. CBEAMC calculated displacements simulate those along lines 4 and 5 well. The gap procedure required to simulate soil heave using SLAB2 is restrictive and cannot be used if areas affected by soil heave are relatively small. A three-dimensional view of displacements calculated by SLAB2 in the northeast quadrant for center heave, Figure 30, shows a ripple near the corner causing unusually large moments and shears that may exceed maximum permissible limits in this area. Since some fractures were observed in the exterior stiffening beams on east and west sides parallel with section A, results calculated by CBEAMC and SLAB2 appear realistic. Shears calculated by CBEAMC show spikes caused by fixing vertical input displacements. Maximum bending moments predicted by the Walsh method, Table 12, are about 180 kips-ft and within mat capacity, Table 10.

117. Level survey, medical clinic. The November 1983 level survey of the medical clinic, Figure 31, indicates a cylindrical center heave pattern of about 1 inch toward the south with settlement up to 0.5 inch toward the northwest corner of the mat. The April 1985 survey indicates up to an additional 0.3 inch heave toward the south end and slight settlement up to 0.1 inch along the east and north perimeters relative to November 1983. The soil appears to be wetting toward the south. Visual observation of the medical clinic in May 1984 indicated a diagonal crack in the east half of the south

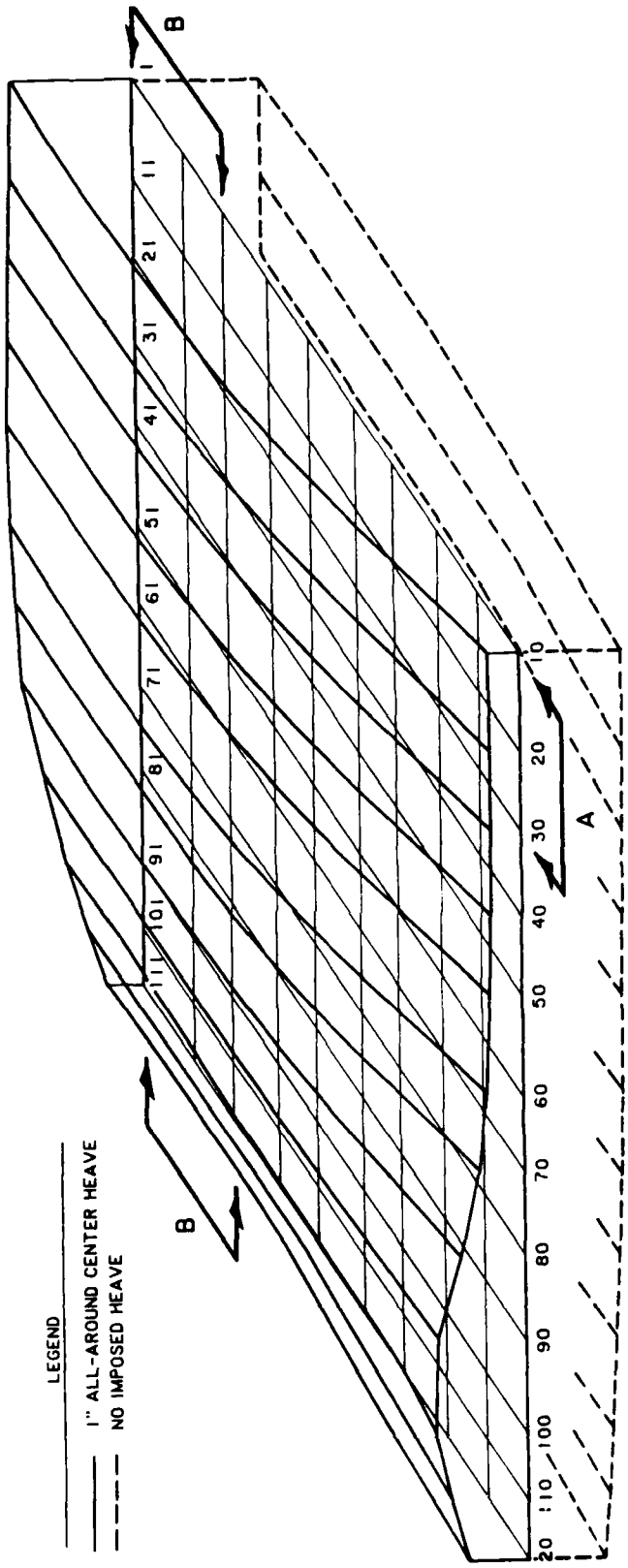

Figure 30. Displacement pattern of the Dental Clinic for $E_s^* = 400$ ksf and $q = 1$ ksf on stiffening beams

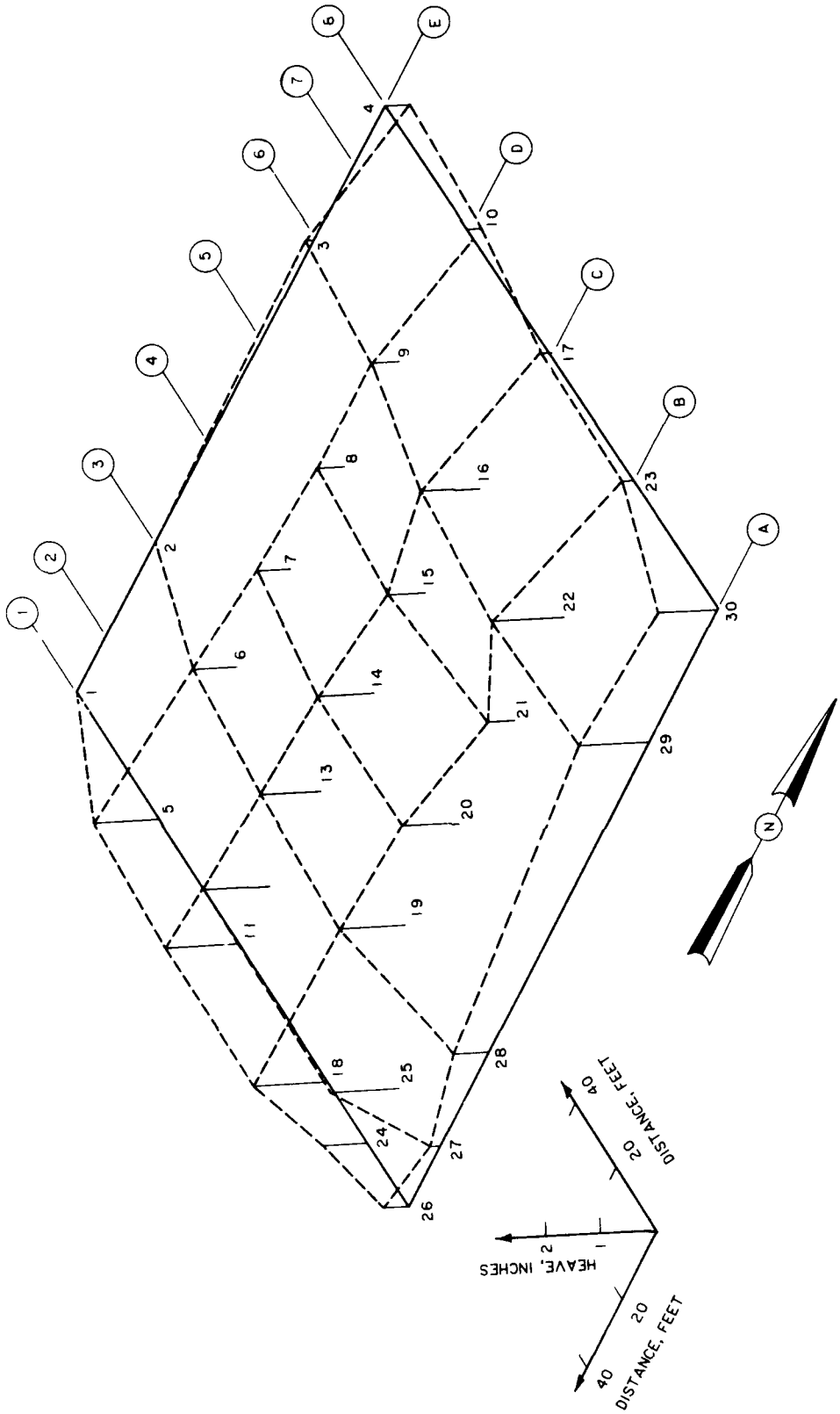

Figure 31. November 1983 level survey Troop Medical Clinic, Fort Sam Houston

exterior wall. A vertical crack over the door of the main entrance in the east wall existed since construction. Cracks were observed on the inside wall partitions near the south wall directly opposite the exterior diagonal crack. Vertical control joints had not been placed in the brick exterior wall. The maximum observed Δ/L ratio is 1/250 near points 27-25 of Figure 31 in the area of the observed cracks near the south walls of the medical clinic.

118. Analysis, medical clinic. Settlement of section A calculated by CBEAMC for loads on the stiffening beam of 1 ksf is 1.1 inches, Figure 32, which compares well with settlements calculated by SLAB2. The distribution of k_{sf} to simulate SLAB2 displacements using a Winkler foundation, average pressure on the mat $q = 0.18$ ksf, $E_s^* = 400$ ksf, and $B = 164$ ft for points 1 to 4, Figure 26b, is

Point	Location	ρ, inch	k_{sf}, ksf/ft	$\mu_0\mu_1$
1	Center	1.301	1.67	1.46
2	Middle short	0.944	2.30	1.06
3	Middle long	0.957	2.27	1.07
4	Corner	0.715	3.04	0.80

119. Observed displacements were reasonably simulated by imposing center heave (i.e., perimeter gaps) using SLAB2 or perimeter loading using CBEAMC and translating calculated displacements as shown in Figure 32. Moments and shears calculated for these displacements approach the maximum capacity, Table 10. A rough estimate of maximum bending moment by the Walsh method, Table 12, is about 2/3 of the maximum capacity. The maximum calculated and observed Δ/L ratios are about 1/500 which should not cause damage in the mat, but some superstructure damage is possible. Fractures were observed in May 1984 in the south brick exterior wall. The exterior walls of the medical clinic did not have vertical control joints. Upper portions of a nearby interior wall made of concrete masonry units parallel with the south exterior wall also exhibited cracking. Appendix D describes results of a movement study of the medical clinic completed by the Fort Worth District, which is in general agreement with this analysis.

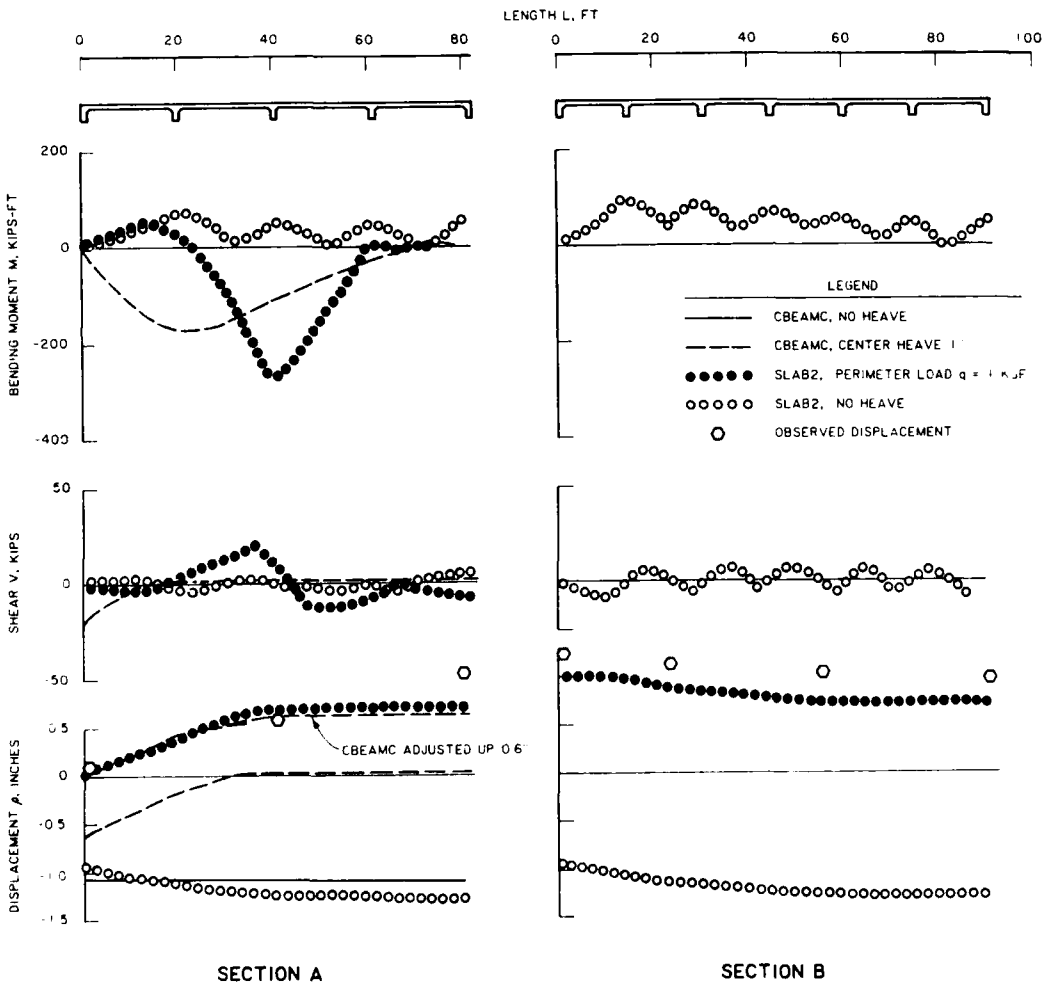

Figure 32. Soil-structure interaction analysis Medical Clinic, Fort Sam Houston, for $E_s^* = 400$ ksf and q = 1 ksf on stiffening beams

Pest Management Training Facility

120. This facility was constructed from 1978 to 1979 and it is located off W. W. White Road on the east edge of Fort Sam Houston, Texas. The foundation, Figure 33, supports a single story structure of load bearing concrete masonry units with a metal roof deck. The load distribution shown in Figure 33 simulates the actual force/ft applied by the load bearing walls. Beam spacing varies from 7 to 23 ft, beam depth is 30 inches from the mat top, beam width is 12 inches and mat thickness between stiffening beams is 5 inches. Steel reinforcement in the stiffening beams consists of two number 9 bars placed both top and bottom. The top 18 inches of natural soil was replaced with compacted low plasticity fill.

121. Soil parameters. The soil at this site consists of about 9 ft of CH clay overburden overlying a thin layer of clayey gravel deposited on the primary formation, Figure 34. The primary formation is Taylor marl of upper Cretaceous age. Strength parameters of this soil are considered similar to those of the US Army Reserve Center and the dental and medical clinics. Additional soils data are not available. The allowable bearing capacity of this soil is estimated at 2 ksf beneth stiffening beams and the soil Young's modulus is considered to be about 400 ksf.

122. Level survey. Level observations of the Pest Management facility soon after construction indicated differential movement had increased through November 1983, Figure 35. Heave approached 4 inches on the east side and settlement of 0.5 inch near the south side and southwest corner by November 1983. Heave had decreased some on the east side and settlement slightly increased toward the west side by April 1985. Water has been observed to seep from fractures in portions of the exterior stiffening beams on the north and east bearing walls.

123. Analysis. Sewer and water lines are located out from the east wall where most heave has been observed. Figure 36 illustrates the water content and soil suction profiles (refer to TM 5-818-7 for the measurement procedure) near point 7, Figure 33, inside the walkway and outside the east wall. Suctions were almost zero about 5-ft below ground surface outside the east perimeter where most structural distress and water lines are located. Extensive fractures were observed in the exterior concrete masonry walls of

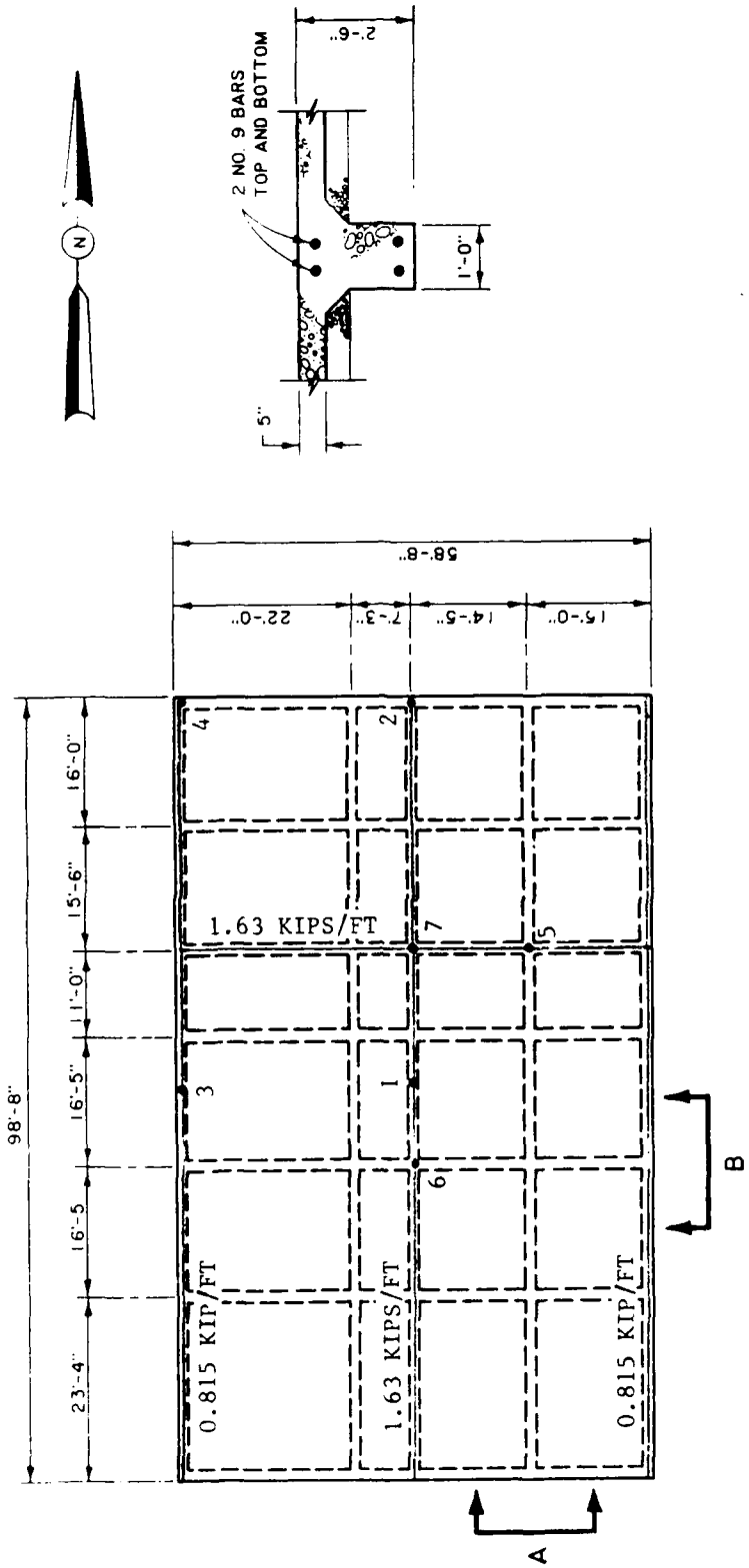

Figure 33. Foundation plan Pest Management Training Facility, Fort Sam Houston

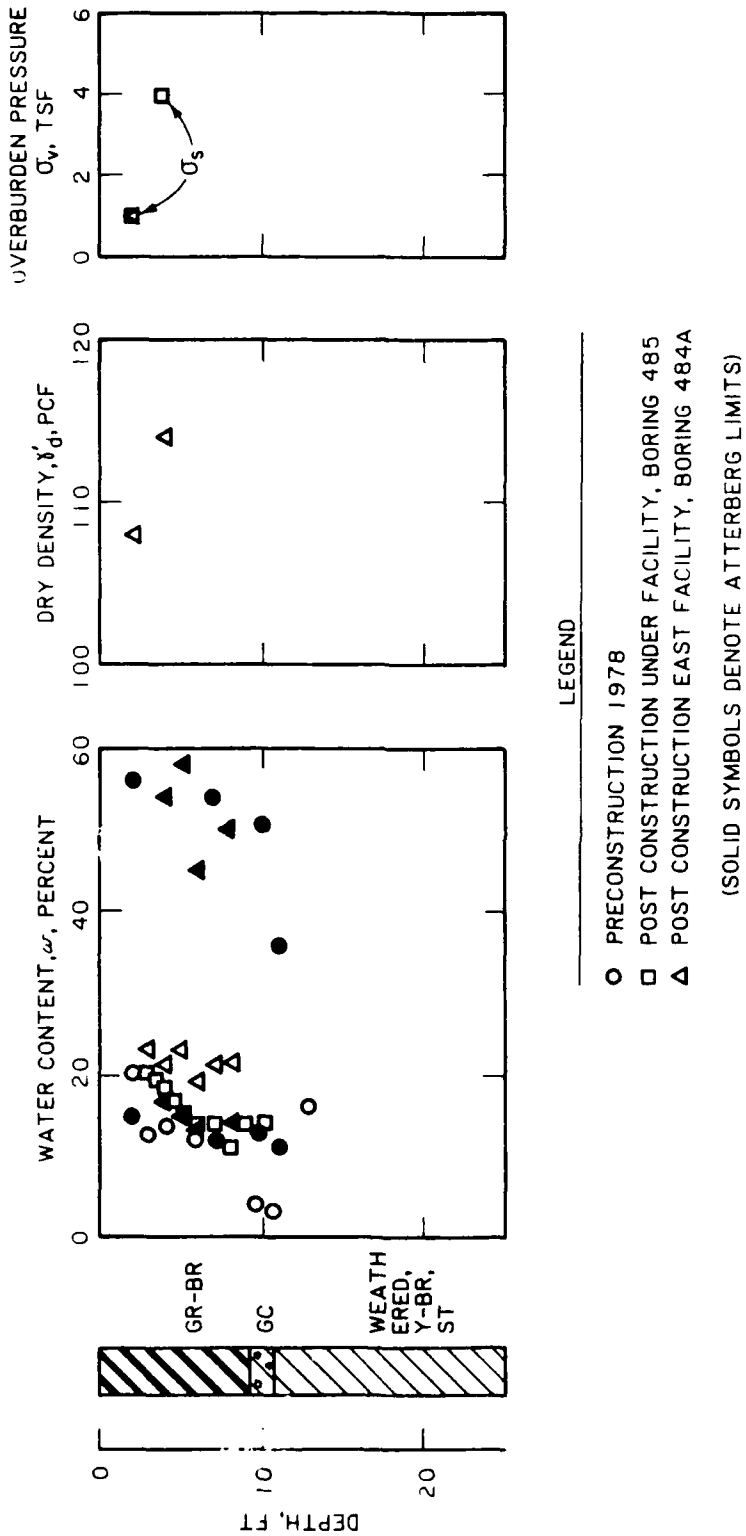

Figure 34. Soil parameters Pest Management Training Facility, Fort Sam Houston

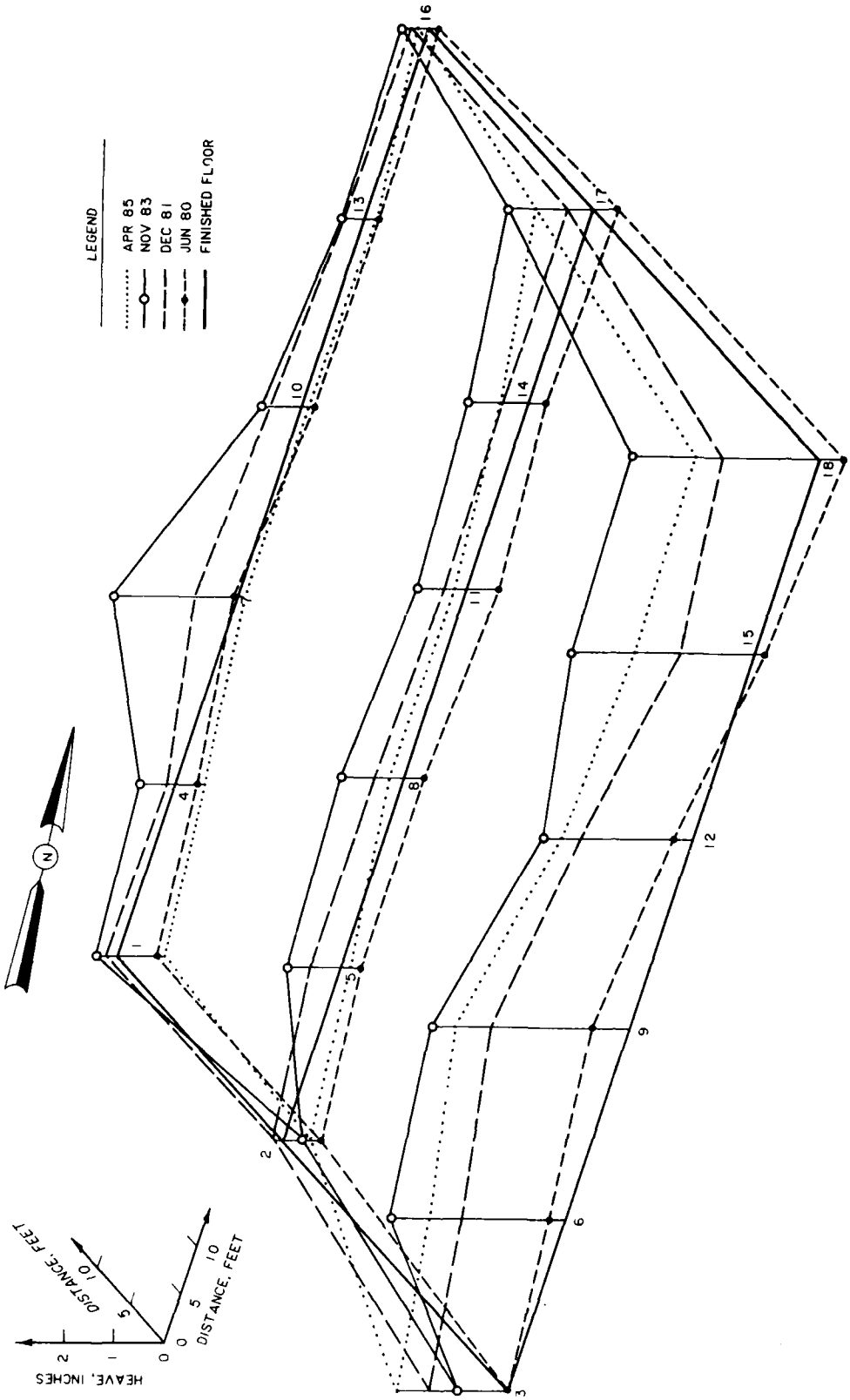

Figure 35. Level surveys Pest Management Training Facility, Fort Sam Houston

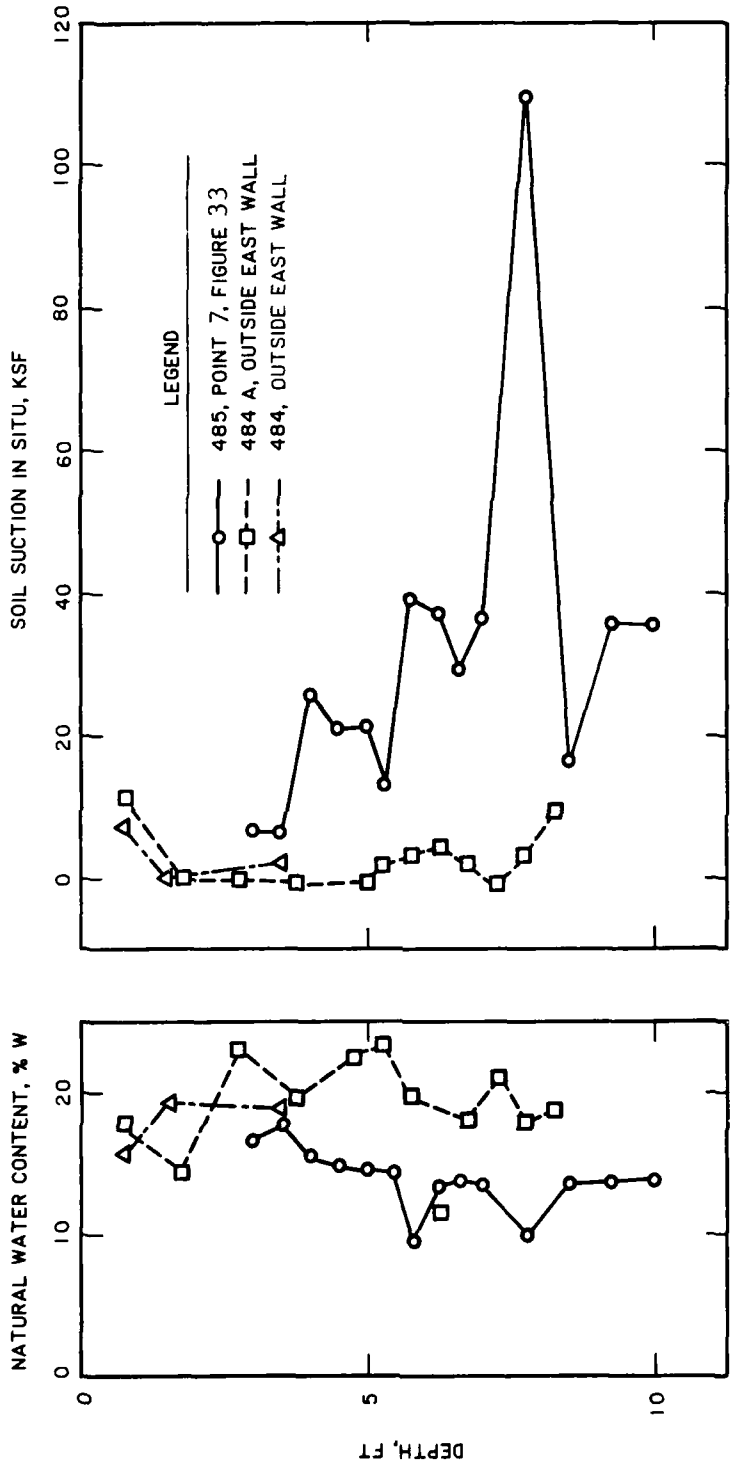

Figure 36. Water content and soil suction profiles in February 1982, Pest Management Training Facility, Fort Sam Houston

this facility with cracks up to an inch in width. The maximum Δ/L ratio is about 1/120, which should lead to structural damage in single story buildings. Vertical control joints were not used in this structure, which contributed to the observed superstructure damage. Parts of the mat that could be observed inside the facility did not indicate unusual distress and the interior floor tile was found in a satisfactory condition. The grade around the facility provided positive drainage.

124. Results of the soil-structure interaction analysis for uniform pressure on the stiffening beams of $q = 1$ ksf and $E_s^* = 400$ ksf are shown in Figure 37. Settlement of section B calculated by CBEAMC was 0.4 inch and in close agreement with results of SLAB2. The distribution of k_{sf} required to simulate the settlements of an elastic foundation using the Winkler foundation based on an average pressure $q = 0.15$ ksf, $E_s^* = 400$ ksf, and $B = 58.7$ ft for points 1 to 4, Figure 33, is

Point	Location	ρ, inch	k_{sf}, ksf/ft	$\mu_0\mu_1$
1	Center	0.465	3.87	1.76
2	Middle short	0.338	5.33	1.28
3	Middle long	0.358	5.03	1.35
4	Corner	0.263	6.85	0.99

An additional analysis performed using SLAB2 for the more realistic load distribution of 1.63 kips/ft on internal beams and 0.815 kip/ft on exterior beams indicate maximum moments of 48 kips-ft located near point 5 on section A and 72 kips-ft near point 6 on section B, Figure 33. Maximum settlement was 0.3 inch at point 7 and minimum settlement was 0.15 inch at the southeast corner.

125. A 2-inch center heave was simulated using SLAB2 and 2-inch gaps around the edges. This gap simulation for heave approximated movement along section A, but not along section B. A 2-inch edge heave was simulated in CBEAMC for section B and the calculated settlement translated up 1.7 inches. Calculated moments from both programs CBEAMC and SLAB2 greatly exceeded structural capacity, Table 10. The Walsh method, Table 12, indicates maximum moments near the structural capacity of the mat. Structural distress is therefore expected from these calculations.

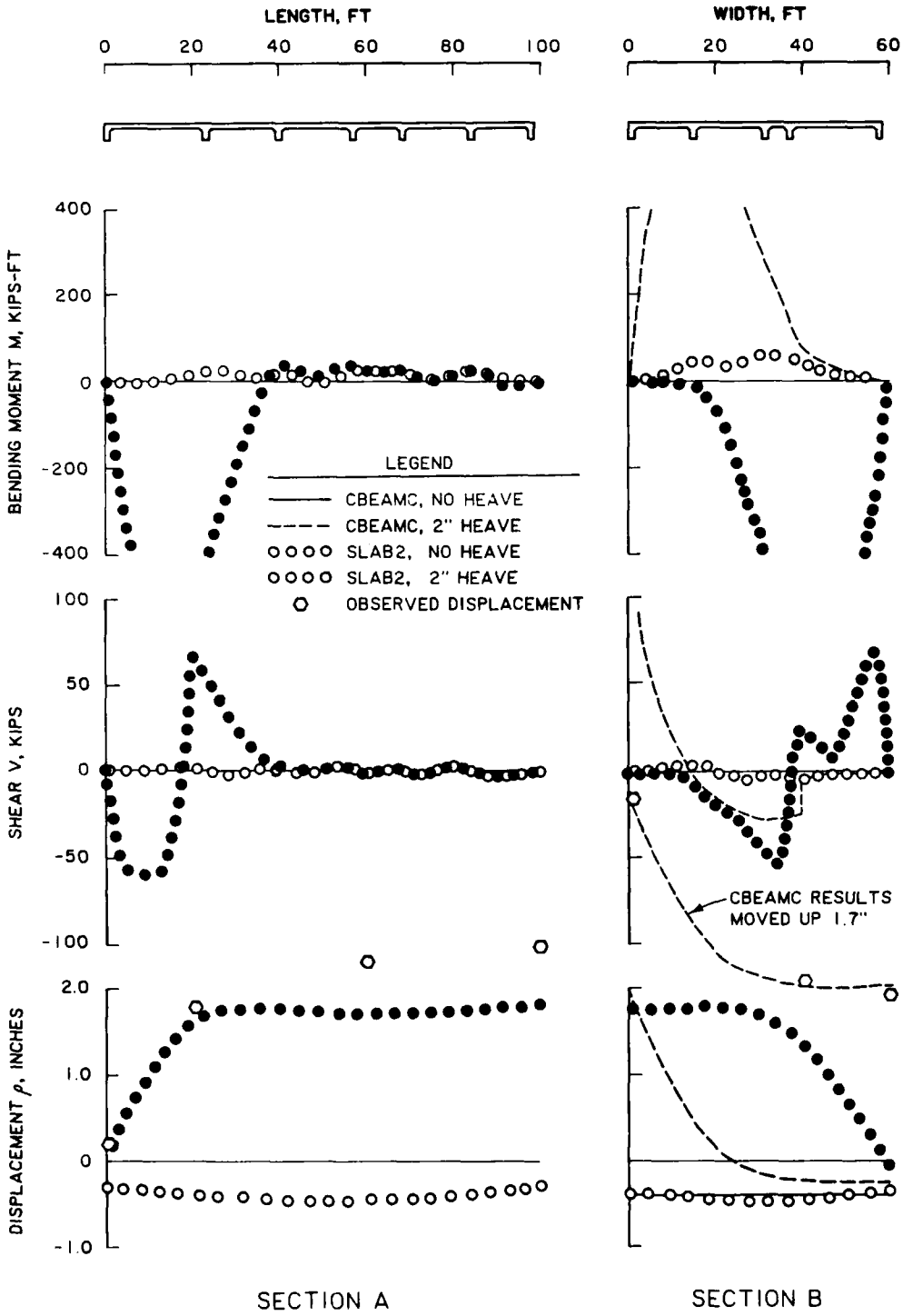

Figure 37. Soil-structure interaction analysis Pest Management Facility, Fort Sam Houston, for $E_s^* = 400$ ksf and $q = 1$ ksf

Summary and Conclusions

126. Observed long-term displacement patterns of these mats are influenced by heave in addition to settlement and cannot be readily predicted from the available data. Reliable predictions of displacements require reasonable estimates of soil moisture changes and distribution of applied loads. Some moisture changes that caused heaves such as those observed in the Gymnasium, Brooks Air Force Base and Pest Management Training Facility are attributed to leaks in plumbing and poor drainage that cannot be readily predicted. Observed distress is in general agreement with calculated deflection ratios Δ/L.

127. All of these ribbed mats are flexible and require consideration of soil-structure interaction effects for proper analysis of mat performance. Programs SLAB2 and CBEAMC appear to provide comparable and realistic bending moments for similar given displacement patterns. Plate program SLAB2 considers two-dimensional lateral restraint of ribbed mats, which strongly influences mat performance. One-dimensional Winkler foundation program CBEAMC will calculate bending moments and shears similar to SLAB2 if soil movements can be anticipated and input into CBEAMC. Larger bending moments were observed in the short direction than the long direction of the Maintenance Shop, US Army Reserve Center.

128. The Winkler foundation requires evaluation of a coefficient of subgrade reaction k_{sf} that varies with location beneath the mat in order to simulate displacements of an elastic foundation. k_{sf} may be evaluated from Equation 8a where the influence factor $\mu_0\mu_1$ as a function of the length/width ratio L/B is

	$\mu_0\mu_1$			
L/B	Center	Short Edge (B/2 from center)	Long Edge (L/2 from center)	Corner
1.0	1.3	1.0	0.9	0.7
1.5	1.6	1.3	1.1	0.9
2.0	1.8	1.5	1.3	1.1
2.5	1.9	1.6	1.4	1.2
3.0	2.0	1.8	1.6	1.3

The above factors illustrate the dishing action of mats on the surface of compressible, cohesive soils with a variation of about 30 percent settlement between the center and edge and about 45 percent between the center and corner.

129. Soil stiffness and movements within the top 50 ft of soil beneath the mat appeared to determine the effective soil modulus. The effective soil modulus for SLAB2 analysis is approximately 400 ksf and may be given by the initial tangent modulus of soil from UU test results on undisturbed soil samples.

130. The flat portion of the mat provides some support. The American Concrete Institute considers this by recommending a standard effective T-section width (ACI 318, art. 8.10.2). Additional analyses of ribbed mats instrumented to allow estimates of bending moments from strains and measurements of soil pressures exerted by the mat are necessary to provide data to improve guidelines for estimating effective T-section widths. Plate load tests may provide reasonable values of the coefficient of subgrade reaction k_{sf} that simulate loading pressures on stiffening beams.

Flat Mat Foundations

131. Thick mats of uniform thickness supporting three hospitals were analyzed using a rigid beam with Godden's (1965) Winkler foundation method, plate on elastic foundation program SLAB2[11], beam on Winkler foundation program CBEAMC[15], and plate on Winkler foundation program WESLIQID[53]. Godden's method using a rigid beam is similar to the uniform pressure method and designated below as the uniform pressure method. WESLIQID was modified to calculate bending moments and shears in addition to displacements. Hand methods of calculating soil-structure interaction behavior of a plate on a Winkler foundation based on results of parametric analyses[50] are beyond practical application for this size of problem. The results of a single series of correct hand calculations should provide results similar to WESLIQID for a single point on the mat.

132. The three mats support Wilford Hall hospital, Lackland Air Force Base, Texas; Fort Gordon hospital, Georgia; and Fort Polk hospital, Louisiana. Level elevations were referenced to the elevations of permanent deep

benchmarks near these hospitals. Displacements are elastic, recompression settlements because applied loads are compensated by construction of the mats in excavations.

133. These mats excluding the stiffness of the superstructure are flexible after Equation 17. The superstructure, however, increases the effective flexural stiffness of the mat by an unknown amount. Increases in stiffness from the superstructures of these hospitals were estimated using Equation B6 to calculate a composite moment of inertia of the combined mat and superstructure I_{oofm}. The equivalent thickness of each mat was subsequently determined using Equation B11.

Wilford Hall Hospital

134. The mat addition to the hospital complex supports an 11 story tower located in the northwest sector of Lackland Air Force Base near San Antonio, Texas. The mat, constructed in 1977, is 3.5 ft thick by 108.33 ft wide by 209.83 ft long and it was placed in an excavation 27 ft below the existing ground surface. This mat is adjacent to and east of the existing hospital complex supported on drilled shafts. Steel reinforcement in the mat constitutes 5 percent of the cross-section and it is located in both top and bottom parts of the mat. The superstructure is built of a structural steel frame supporting a masonry facing.

135. Load pattern. The dead and live column load distribution, Figure 38, leads to a weight of about 55,000 kips plus 12,000 kips contributed by the mat weight or a total building weight of about 67,000 kips. The applied uniform pressure excluding weight of the mat concrete $q = 2.415$ ksf. Weight of soil displaced by the building is about 74,000 kips so that there may be a small net loss of weight on the foundation soil beneath the mat.

136. The mat is designed for bending moments of 36,000 kips-ft per 26-ft wide section from Equation 13a. The required thickness for the maximum applied column loads is about 2.5 ft from Equation 11a, which is about 1 ft less than the actual thickness. The effective structural stiffness that includes stiffness contributed by the tower for an average ceiling height of 10 ft leads to an equivalent mat thickess of 36.8 ft from Equation B11, excluding stiffness from steel reinforcement. Significant stiffness is also contributed by the reinforced concrete walls of the basement.

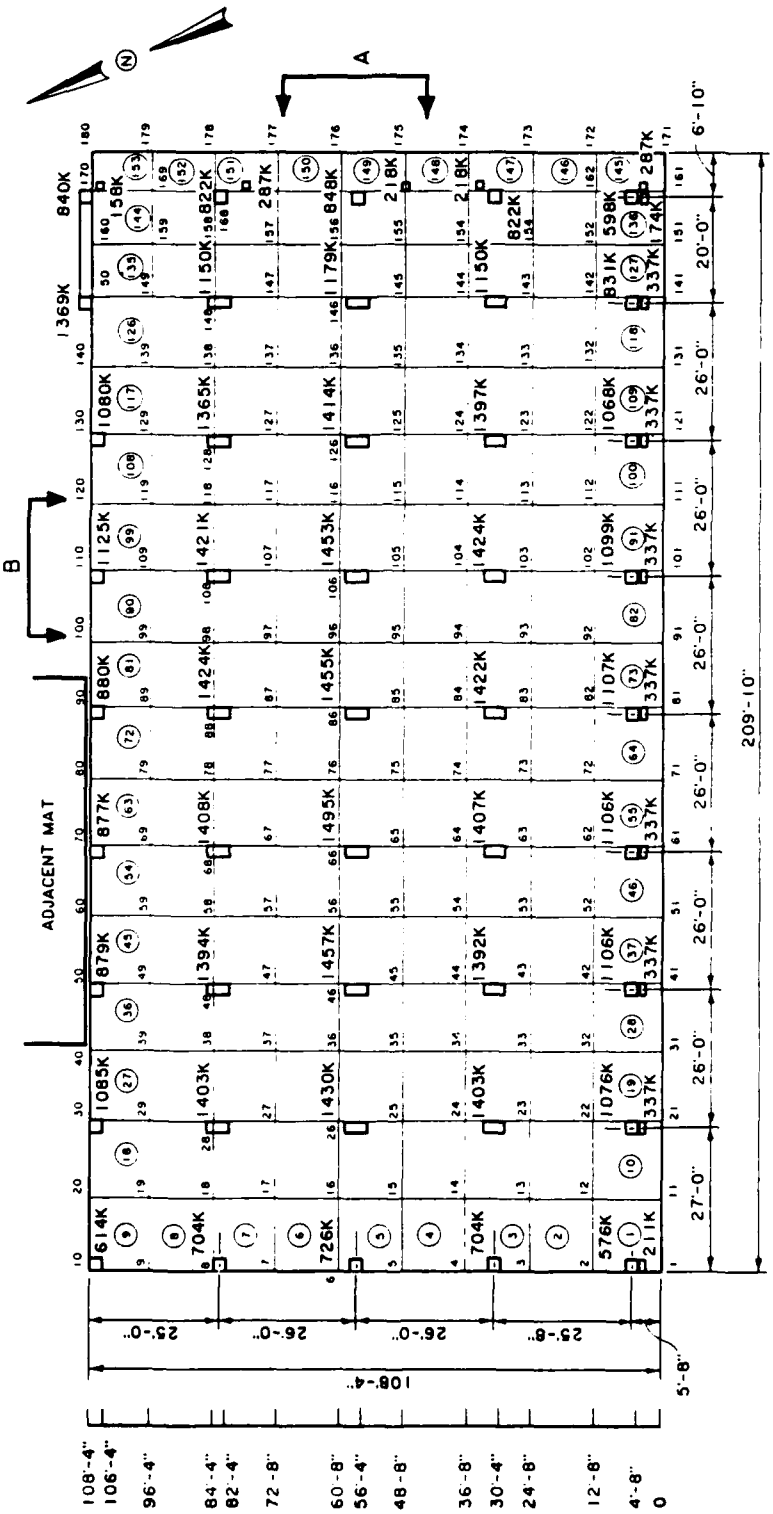

Figure 38. Foundation plan Wilford Hall Hospital, Lackland Air Force Base, with column loads in kips

137. Soil parameters. Soil parameters, Figure 39, indicate an expansive plastic CH clay overburden and shale with a perched water table about 23 ft below ground surface. The soil profile consists of overburden, Lower Midway, and Navarro formations with an occasional stratum of clayey gravel in the vicinity of the perched water table. Consolidometer/swell tests indicate potential for swell in the overburden down to about 17 ft below ground surface and within a 10-ft thickness of soil immediately beneath the mat.

138. Results of undrained triaxial shear strength tests indicate relatively large shear strengths and adequate bearing capacity. The soil elastic modulus can be approximated as increasing linearly with depth

$$E_s = kz = 25z \tag{29}$$

where E_s is in units of ksf and depth z is in feet. The elastic modulus at the ground surface E_o is taken as zero. An upper range is also shown in Figure 40 where $k = 32$ ksf/ft.

139. The equivalent soil modulus E_s^* and coefficient of subgrade reaction k_{sf} must be evaluated to complete the soil-structure interaction analysis. Figure 8 was used to obtain a center settlement $\rho_c = 0.127$ ft for a loading pressure of $q = 2.415$ excluding the mat weight as shown in Figure 40. From Equation 4b, the equivalent soil modulus is

$$E_s^* = \frac{2 \cdot 2.415 \cdot 85.06 \cdot (1 - 0.3^2)}{0.127} = 2943 \text{ ksf}$$

The compressible soil depth beneath the mat was taken as 320 ft or nearly 4 times the equivalent mat radius $R = 85.06$ ft. Poisson's ratio was assumed 0.3. $E_s^* = 3100$ ksf from Equation 4c assuming an infinite depth of elastic soil beneath the mat and using $k = 25$ ksf/ft from Equation 29. Equation 4a should provide similar results to Equations 4b and 4c.

140. Assuming $E_s^* = 2943$ ksf is reasonable, the settlement from Equation 3 is

$$\rho = 0.96 \cdot \frac{2.415 \cdot 108.33}{2943} = 0.085 \text{ ft}$$

or 1 inch, where $\mu_1 = 0.96$ (L/B = 2) and $\mu_0 = 1.0$. The effective coefficient of subgrade reaction from Equation 5 should be approximately

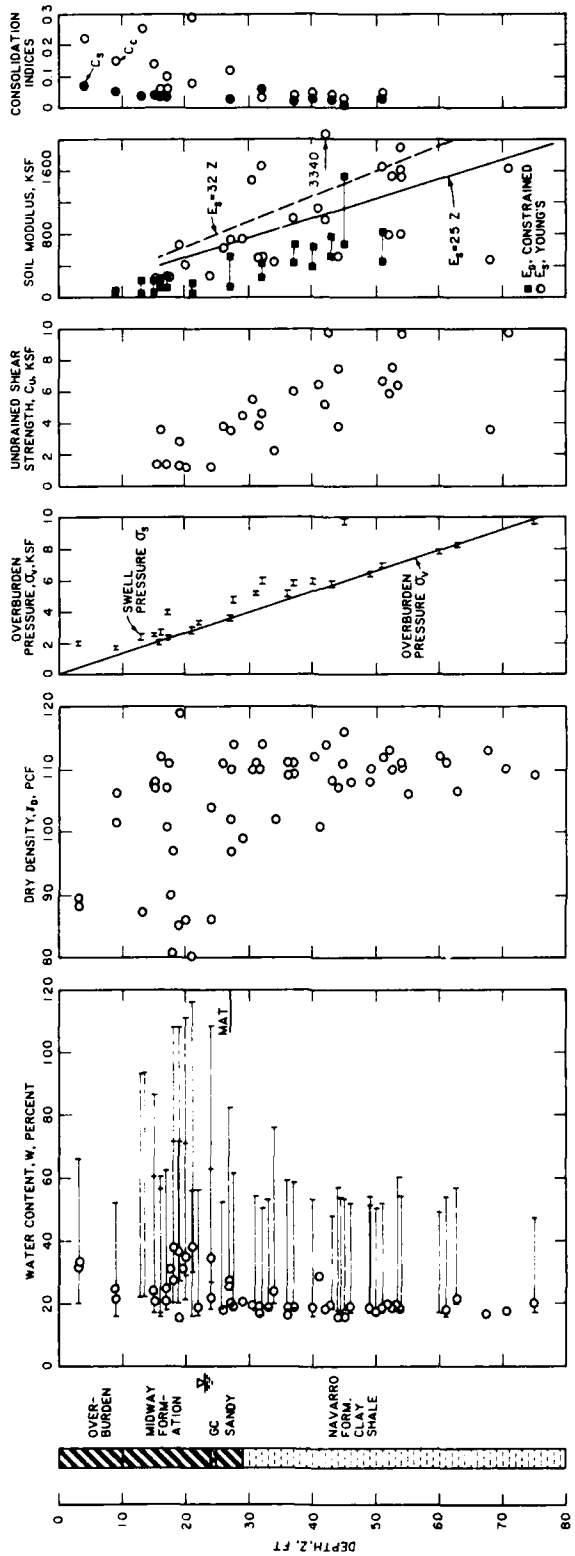

Figure 39. Soil parameters, Wilford Hall Hospital, Lackland Air Force Base, Texas

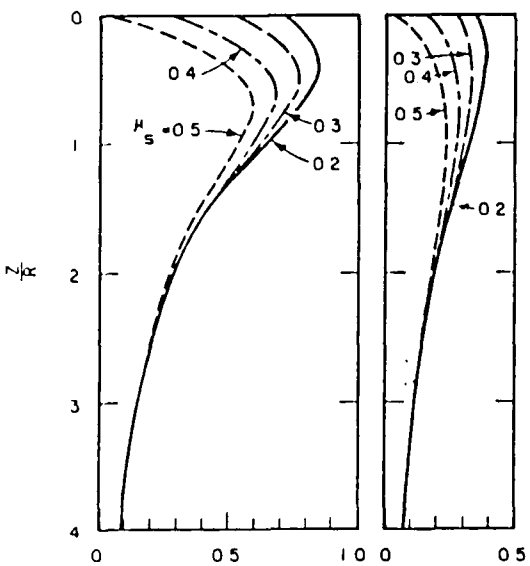

q = 2.4 KSF

h, FT	E_s, KSF	SETTLEMENT, FT CENTER I_c	CENTER $\rho_c = qhI_c/E_s$	EDGE I_e	EDGE $\rho_e = qhI_e/E_s$
20	875	.55	.03036	.26	.01435
20	1375	.68	.02389	.30	.01054
20	1875	.75	.01932	.31	.00799
20	2375	.70	.01424	.30	.00610
20	2875	.60	.01008	.29	.00487
20	3125	.52	.00804	.27	.00417
20	3875	.44	.00548	.25	.00312
20	4375	.36	.00397	.22	.00243
20	4875	.30	.00297	.20	.00198
20	5375	.25	.00225	.18	.00162
20	5875	.20	.00164	.16	.00132
20	6375	.17	.00129	.14	.00106
20	6875	.15	.00105	.12	.00084
20	7375	.13	.00085	.11	.00072
20	7875	.11	.00067	.10	.00061
20	8375	.10	.00058	.10	.00058

TOTAL ρ_c = 0.127 FT ρ_e = 0.062 FT

$\text{LOG}_{10} K_R = \text{LOG}_{10}\left[\frac{\rho_c E_c D^3 (1+\mu_s)}{2q R^4 (1-\mu_s)}\right]$ = -1.76

R_s (FROM CHART) = 0.92

$\Delta\rho = R_s(\rho_c - \rho_e)$ = 0.06 FT

EQUIVALENT RADIUS MAT R = 85.06 FT

MAT THICKNESS D = 3.5 FT

POISSON'S RATIO SOIL μ_s = 0.3

MAT MODULUS OF ELASTICITY E_c = 432,000 KSF

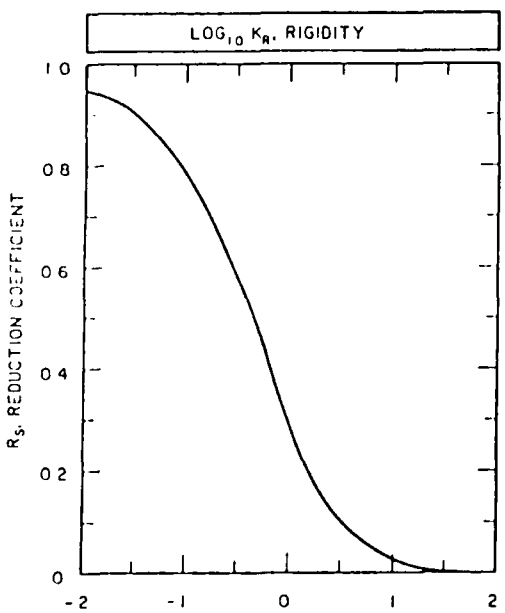

Figure 40. Settlement computation for Wilford Hall Hospital, Lackland Air Force Base, after Figure 8

$$k_{sf} = \frac{q}{\rho} = \frac{2.415}{0.085} = 28 \text{ ksf/ft.}$$

k_{sf} from the Kay and Cavagnaro method. Figure 40, for center and edge settlement is 19 and 36 ksf/ft, respectively, for $q = 2.415$ ksf. A uniform conservative value $k_{sf} = 24$ ksf/ft was selected for the Winkler foundation analysis and $E_s^* = 2943$ ksf was selected for the elastic foundation analysis. As a point of interest, k_{sf} of 24 to 28 ksf/ft is similar to $k = 25$ ksf/ft from Equation 29. k_{sf} should be approximately k from Equations A6 and A7.

141. Level survey. Level surveys were performed on the mat surface relative to the initial survey taken in December 1977, Figure 41, following mat construction; thus, this initial survey excludes settlement from the mat weight. The August 1978 survey indicated most settlement of about 1 inch in the center decreasing to about 0.8 inch along the east and west edges in the long direction. The mat was relatively flat from north to south, except along the eastern edge, indicating relatively large rigidity along the short direction. The general deformation pattern is consistent with a semi-flexible mat on a semi-infinite elastic soil.

142. The November 1983 survey indicates about 0.2 inch heave toward the western edge since August 1978. The older hospital complex is adjacent to this western edge of the mat where soil had been observed to heave into the void space beneath grade beams supported on drilled shafts. The May 1985 survey indicates a continuation of about 0.2 inch settlement uniformly distributed beneath the mat since November 1983.

143. Visual observation of the building in May 1984 indicated minimal distress in the mat and superstructure. The Δ/L ratio was about 1/1000 in August 1978 between points Q-35 and S-35, Figure 41, in the northeast corner. Some hairline to 1/16 inch cracks were observed May 1984 in the exterior stiffening beams on the northeast side of the adjacent ribbed mat supporting a cafeteria. These crack widths had increased to 1/8 to 1/4 inch in May 1985. An underground tunnel is located in this area below the north side of the ribbed mat. Distress observed in this mat is above the tunnel area that is placed over compacted, low plasticity fill without an impervious moisture barrier. Further west, distress was not observed in the mat where

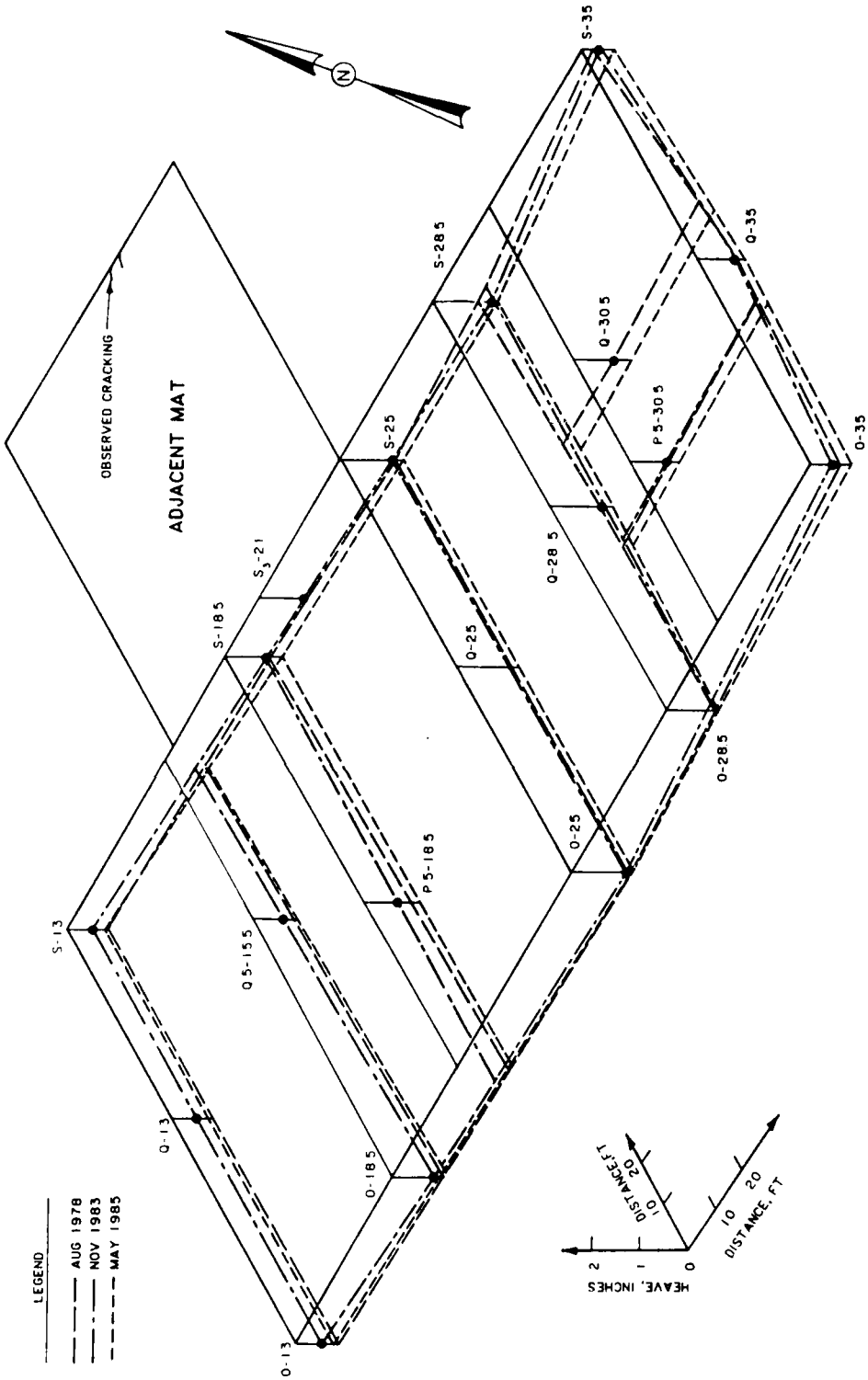

Figure 41. Level surveys, Wilford Hall Hospital, Lackland Air Force Base

the tunnel was constructed over a chlorinated polyethylene impervious moisture barrier placed directly on the natural expansive soil.

144. Analysis. Results of soil-structure interaction analyses of sections A and B of Figure 38 are shown in Figure 42. Winkler soil programs CBEAMC and WESLIQID using high mat stiffness (an effective concrete modulus of 500,000,000 ksf or mat thickness 36.8 ft to include superstructure stiffness) and the uniform pressure method (Godden's procedure for a rigid beam[14]) all provide similar results for section A, Figure 42a. The magnitudes of negative bending moments are greatest for the plate on the Winkler foundation calculated by WESLIQID. These bending moments are well within the mat structural capacity of 36,000 kips-ft from Equation 13a. Negative bending moments indicate tension in the mat top or an edge down displacement pattern.

145. Bending moments calculated by SLAB2 for the 35-ft thick mat are relatively small, Figure 42b, and well within mat bending resistance calculated by Equation 13a. Bending moments calculated by SLAB2 for the complete structure using an equivalent mat thickness D_e of 36.8 ft (from Equation B11) were positive and substantially larger than those calculated for the mat on a Winkler soil. The bending resistance of the composite structure including stiffness of the superstructure is about 8 times that calculated by Equation 11a using Equation B15; therefore, calculated bending moments of the structure are still well within capacity.

146. Observed displacements shown in Figure 41 for May 1985 are generally consistent with the dish-shaped or center down displacement pattern calculated from SLAB2. The flexible mat of 3.5-ft thickness ignoring rigidity contributed by the superstructure is generally consistent with the observed displacement pattern. Observed displacements in May 1985 tend to be slightly less than those calculated, but observed displacements do not include the unmeasured settlement caused by the mat weight. Overall, the assumed soil modulus and coefficient of subgrade reaction are reasonable.

147. A finite element soil-structure plane strain analysis performed in 1977 on the Wilford Hall 3.5-ft thick mat used similar loads[38]. The analysis was made using the hyperbolic soil model[23]. Calculated settlements of about 0.7 inch were determined using a representative soil modulus of about 1600 ksf and 80 ft of foundation soil beneath the mat underlain by an incompressible

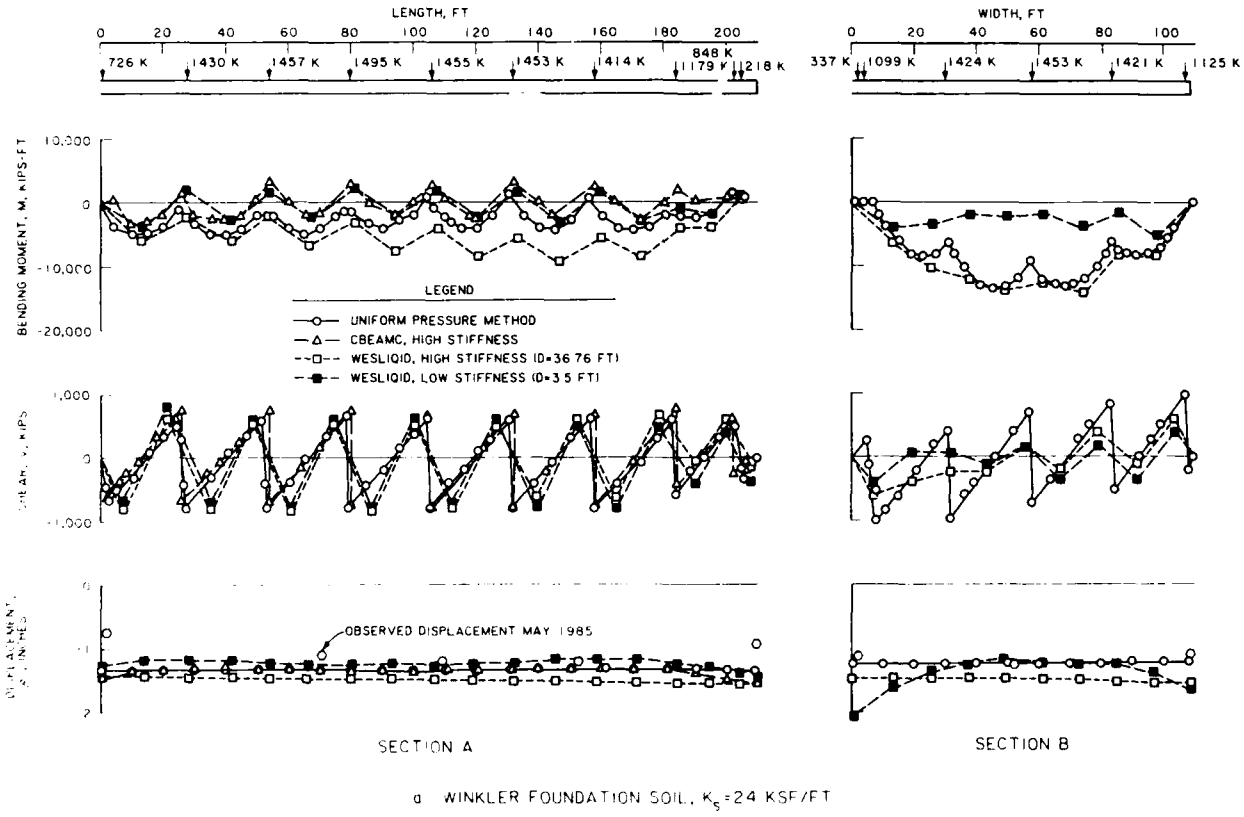

a. Winkler foundation, k_{sf} = 24 ksf/ft

Figure 42. Soil-structure interaction analysis of Wilford Hall Hospital, Lackland Air Force Base

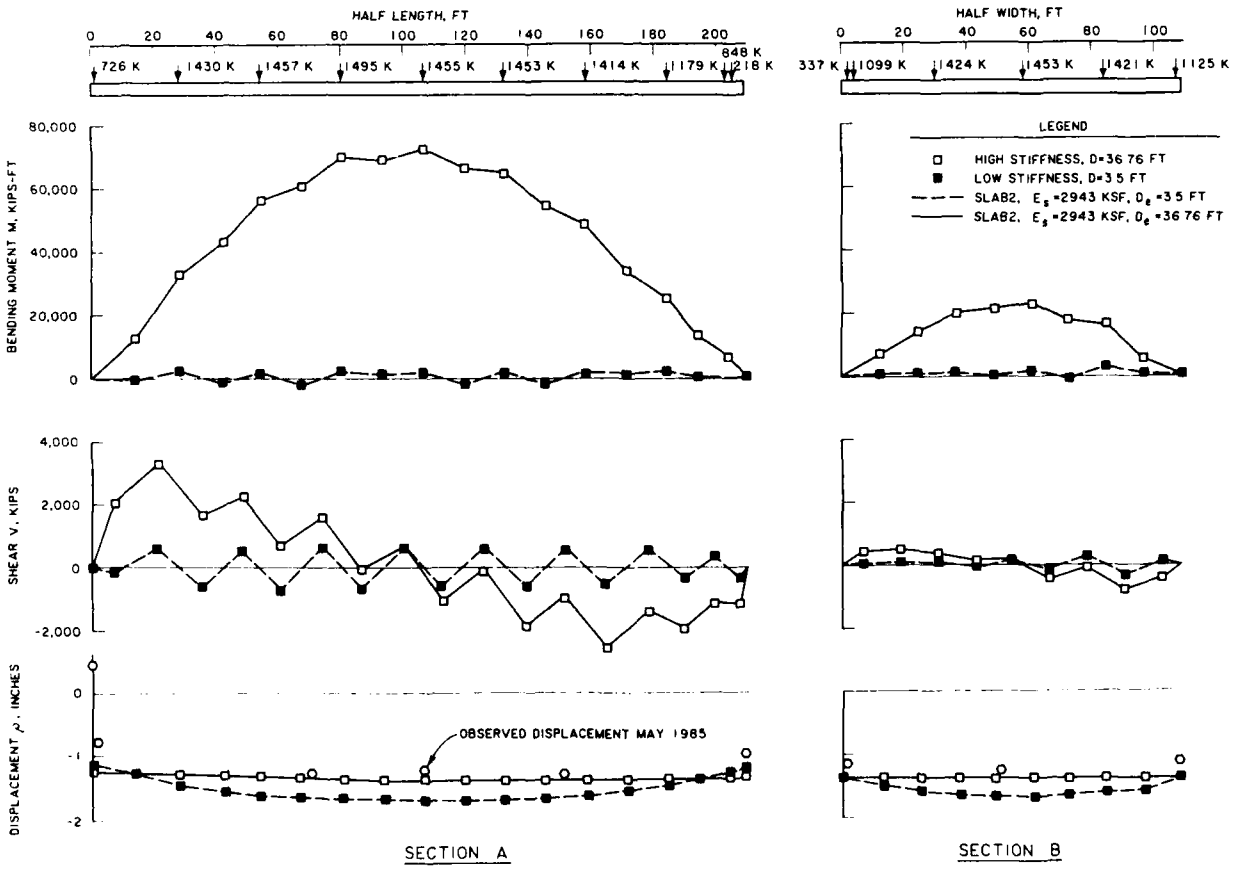

b SEMI-INFINITE ELASTIC SOIL, E_s =2943 KSF

b. Semi-infinite elastic soil, $E_s^* = 2943$ ksf

Figure 42. (Concluded)

base. These results indicate a more stiff soil profile than the results of the analysis described in Figure 42. The settlement of large mats is influenced by the stiffness of the soil profile for considerable distances beneath the mat.

Fort Gordon Hospital

148. The 11-story tower of Fort Gordon Hospital in Georgia, constructed in 1971, is supported by a 5-ft thick flat mat 331 ft long by 106 ft wide. This mat is placed in an excavation approximately 35 ft deep. Much of the steel reinforcement is composed of number 11 bars placed top and bottom providing about 0.3 percent of the cross-section area. Steel is preferentially placed, either top or bottom of the mat, to take the positive and negative bending moments that may occur. The column load distribution is symmetrical, Figure 43, leading to 119,110 kips or bearing pressure of 3.4 ksf excluding the mat weight. Total bearing pressure on the supporting soil is 4.1 ksf

149. Soil parameters. Soil parameters, Figure 44, indicate silty and clayey sands with some plastic CH clay layers. At the bottom of the mat the soil overburden pressure had been approximately 4 ksf, which fully compensates for the weight of the hospital. All observed displacements should be elastic, recompression settlements with insignificant long-term consolidation of the clays. Bearing capacity of this soil is adequate. Groundwater elevations were not determined, but results of consolidometer/swell tests indicate swell pressures consistent with overburden pressures and any potential for heave should not exist.

150. Shear strength data from R triaxial tests of the sands above the mat elevation, Figure 44, indicate soil elastic moduli of at least 3200 ksf. The soil modulus should be substantially greater at deeper depths because the blow count increases substantially with increasing depth, Figure 44. Settlement from Equation 3 is

$$\rho = 1.1 \cdot \frac{4.1 \cdot 106}{3200} = 0.149 \text{ ft}$$

where $\mu_1 = 1.1$ for L/B = 3 and $\mu_0 = 1.0$. The coefficient of subgrade reaction k_{sf} from Equation 5 is 4.1/0.149 = 27 ksf/ft. The maximum bending resistance of the mat for a 24-ft wide section is on the order of 6000 kips-ft

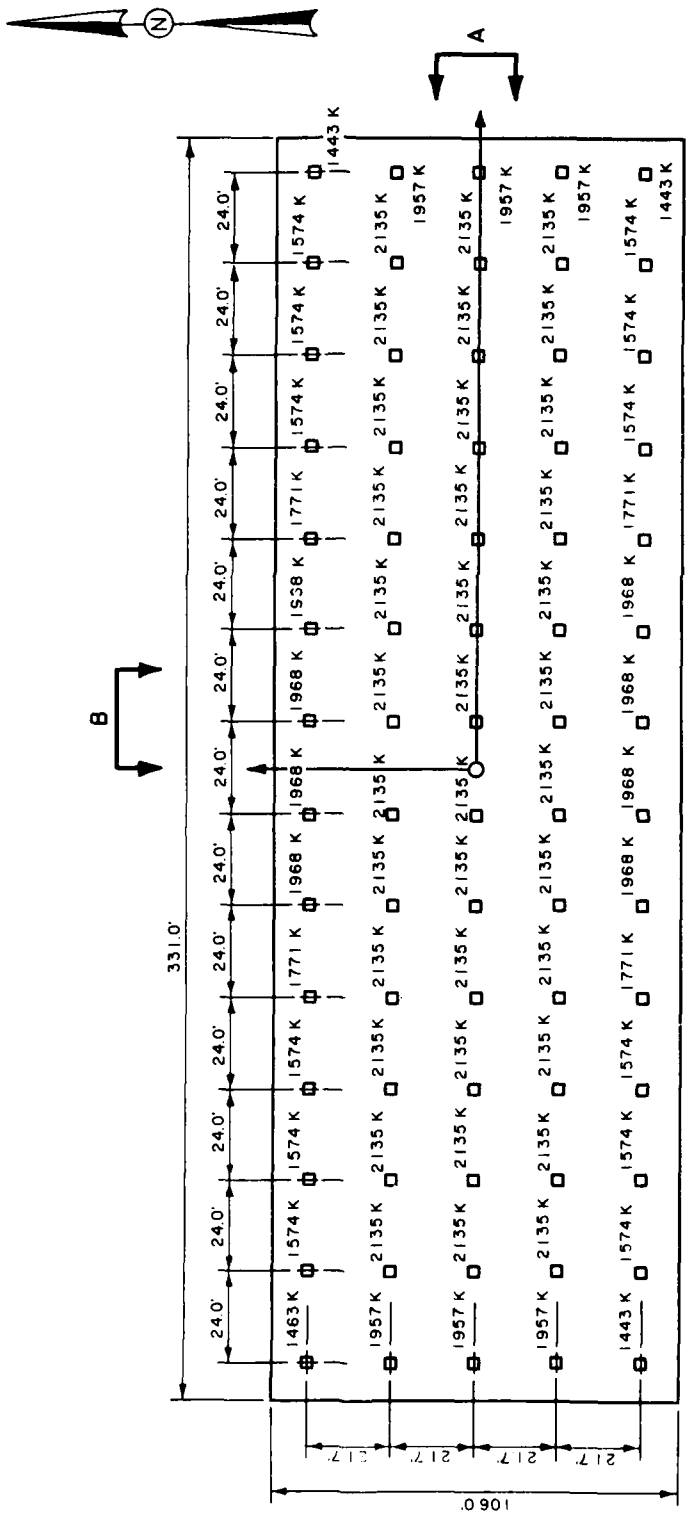

Figure 43. Foundation plan and load distribution, Fort Gordon Hospital

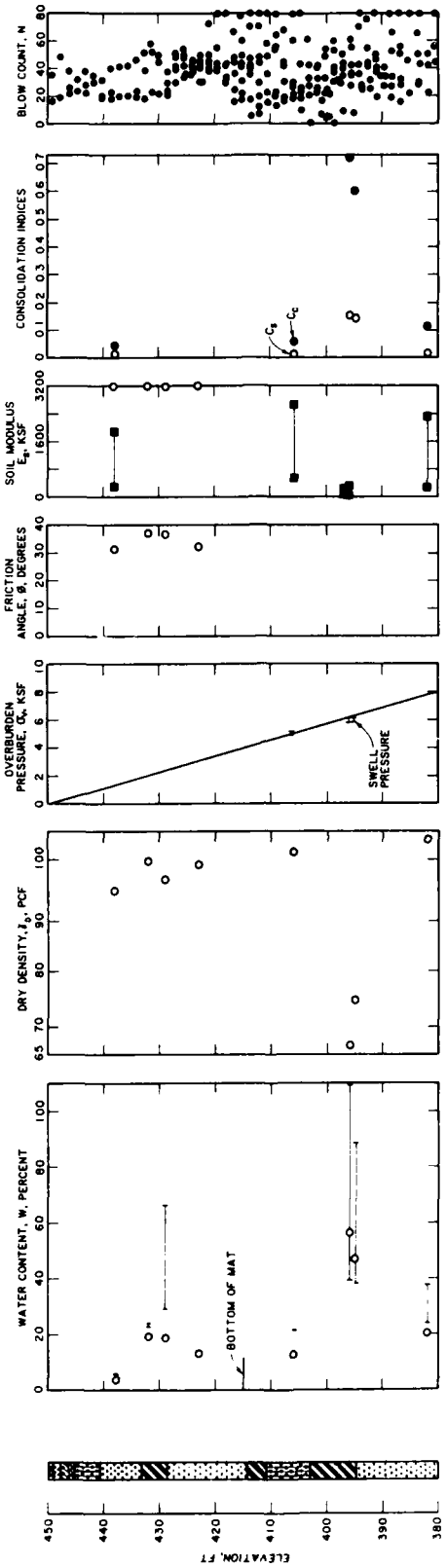

Figure 44. Soil parameters, Fort Gordon Hospital

from Equation 13a and the required mat thickness to satisfy punching shear is 3.3 ft, Equation 11a. The stiffness that may be contributed by the 11 story tower may lead to an effective mat thickness of about 36 ft from Equation B6.

151. Level survey. Displacements of the mat observed in February 1974, 3 years after construction, are fairly uniform at about 0.5 inch settlement, Figure 45. The southwest corner indicates no settlement in 1974. These observed displacements of about 0.3 inch exclude settlement due to mat weight. The maximum Δ/L ratio in 1974 was less than 1/1300. New surveys conducted in 1984 indicate increased settlement in the northwest to 0.5 inch, but the eastern half of the mat appears to have moved up for a net heave of 0.2 inch at the east end. The maximum Δ/L ratio is still less than 1/1300 in 1984. Differential movement is less in the short direction than in the long direction.

152. The soil profile, Figure 46, does not indicate any greater presence of clay soils near the west end compared to the east, or any significant unsyummetrical slope of the original ground surface. Loads applied on and in the mat vicinity are symmetrical. Soil swell pressures exceeding applied pressures were not observed. The soil, particularly clay beneath the west end, appears to be compressing more than the soil beneath the east end. The entire mat is slightly tilting toward the west. The blow counts of some of the soils immediately beneath the west end are relatively low compared to those beneath the east end and indicates a greater potential for compression.

153. Analysis. Soil-structure interaction analyses performed using the Winkler foundation program WESLIQID and elastic program SLAB2 excluding mat weight, Figure 47, calculated settlements substantially greater than those observed for $k_{sf} = 27$ ksf/ft and $E_s^* = 3600$ ksf. The actual effective k_{sf} and E_s^* may be up to 4 times greater than those indicated in the soil above the mat elevation, Figure 44, based on the record of larger blow counts observed at deeper depths beneath the mat. The relatively flat displacement observed in 1974 and apparent uniform tilt toward the west observed in 1984 indicate that the Winkler foundation using a constant $k_{sf} = 100$ ksf/ft appears appropriate for these sandy friction soils. Calculated bending moments for the 5-ft thick mat excluding superstructure stiffness from results of both programs WESLIQID and SLAB2 are well within the bending moment

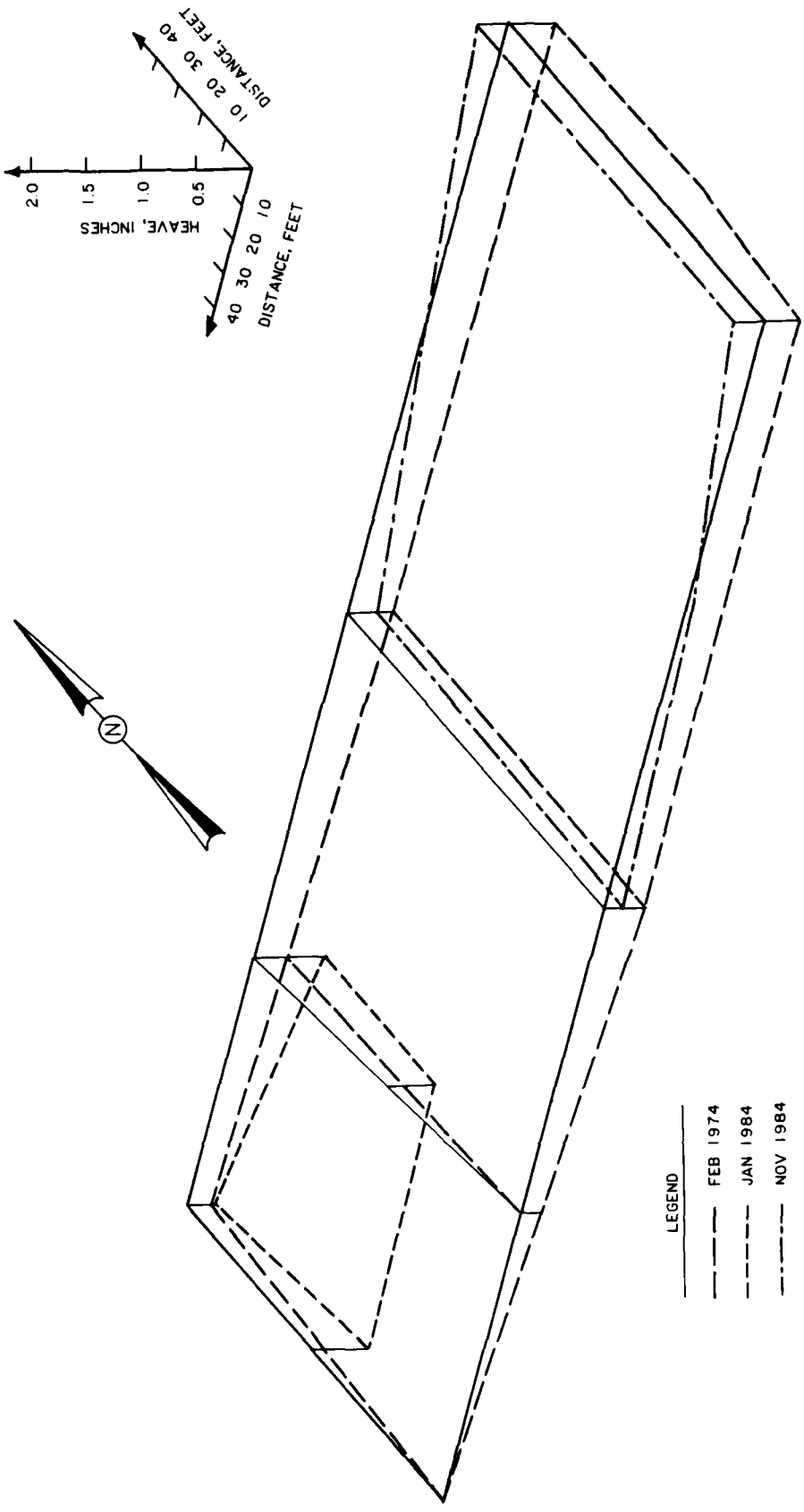

Figure 45. Level surveys, Fort Gordon Hospital

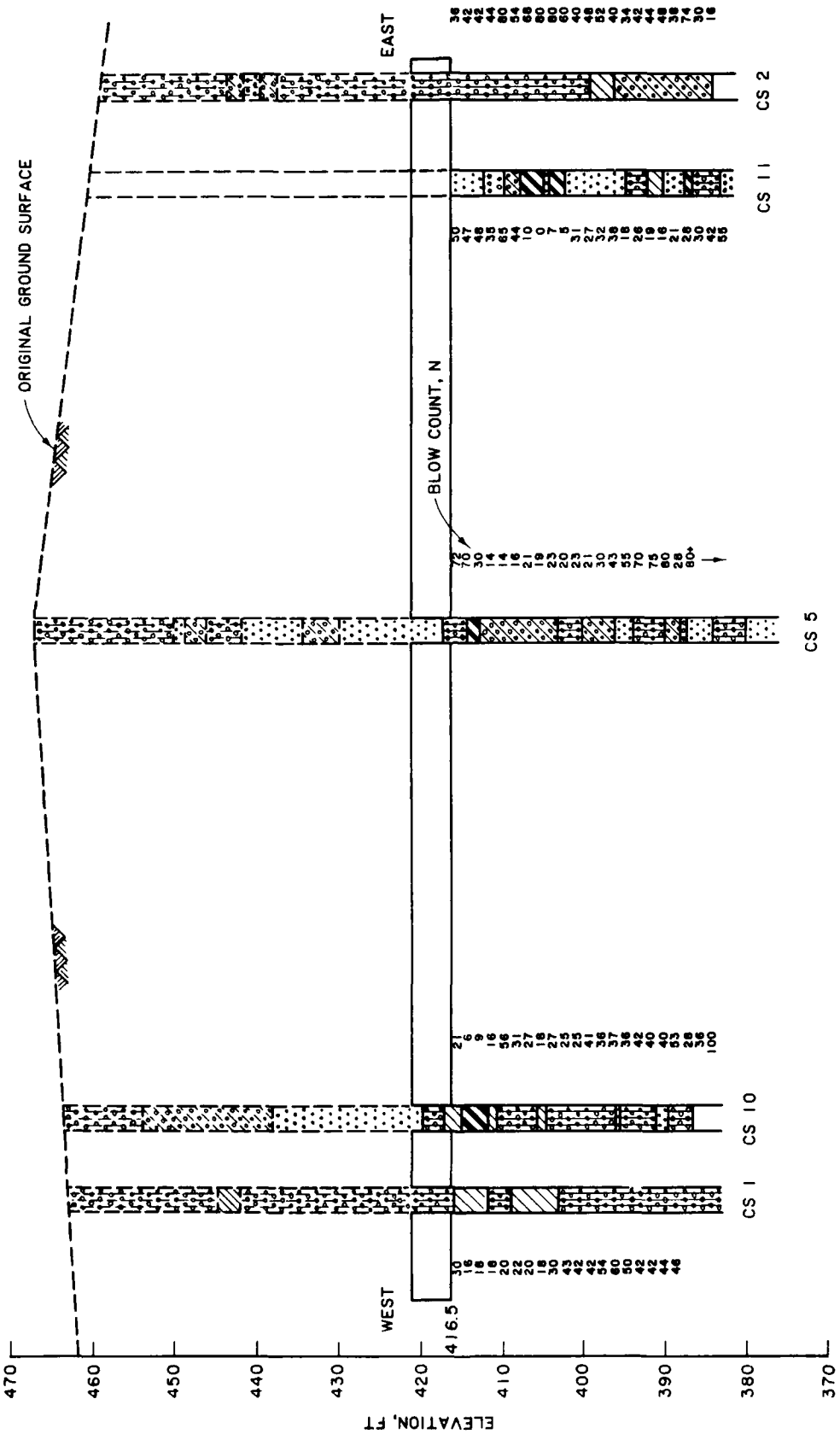

Figure 46. Soil profile, Fort Gordon Hospital

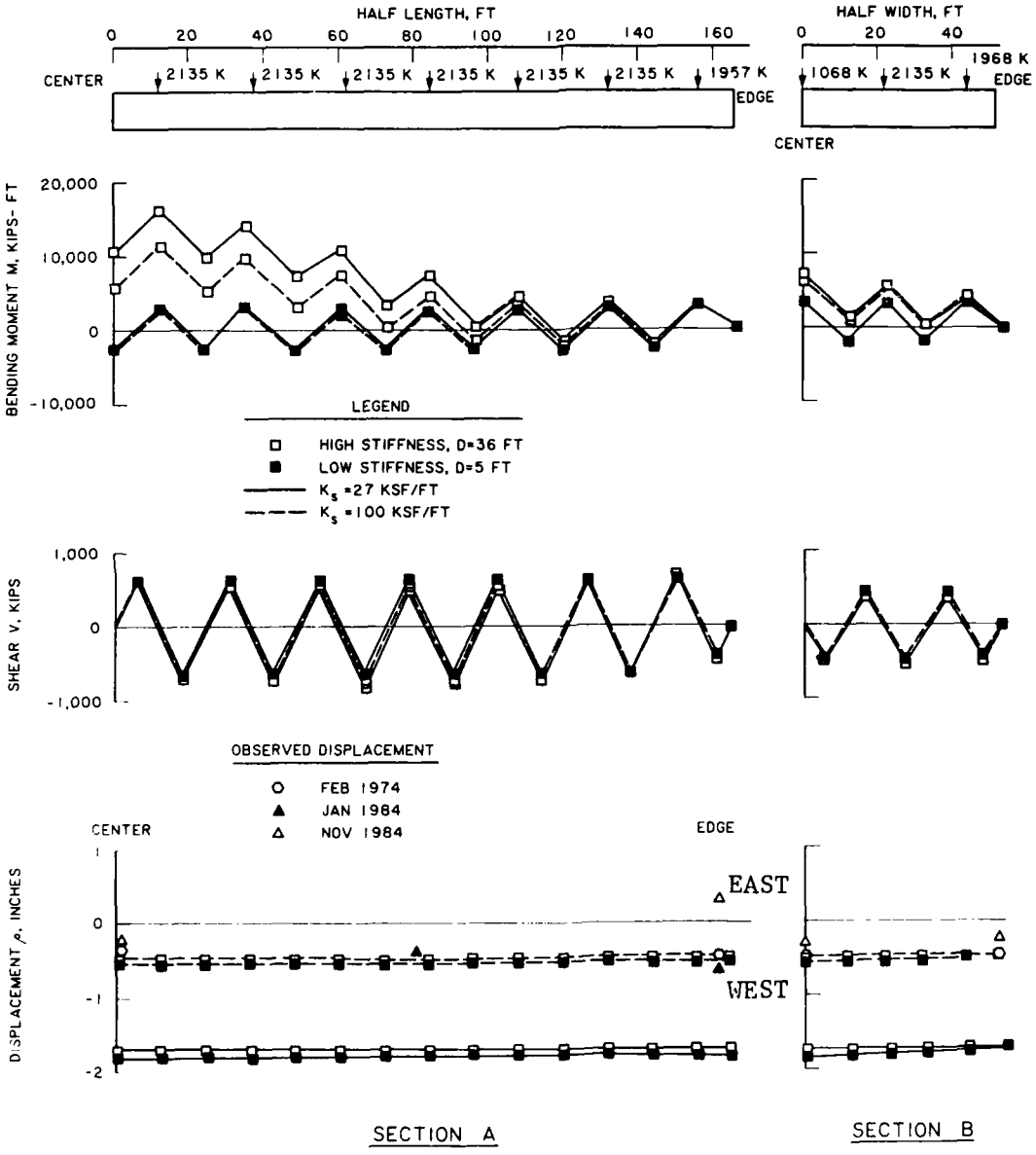

a. Winkler soil, WESLIQID

Figure 47. Soil-structure interaction analysis, Fort Gordon Hospital

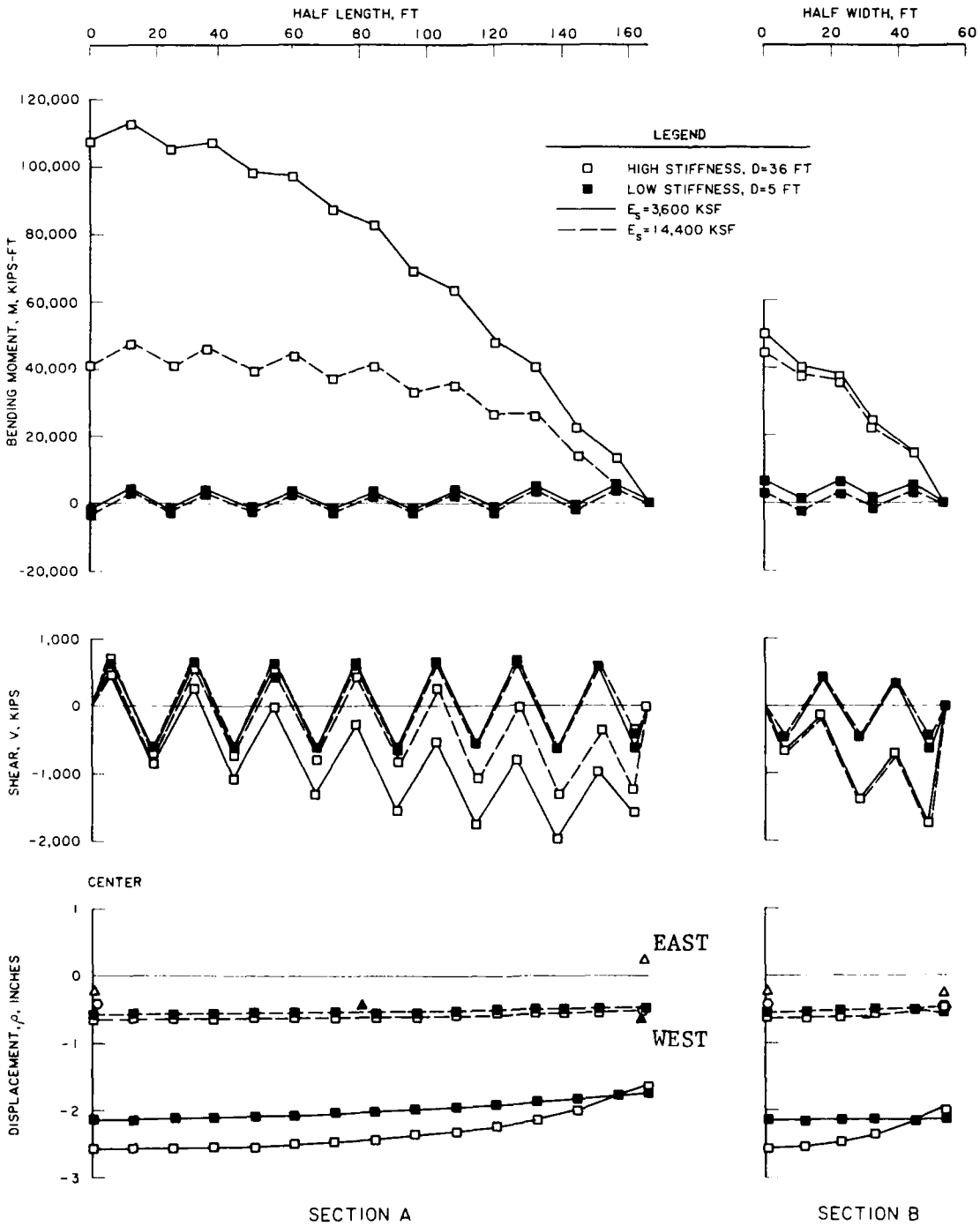

b. Elastic soil, SLAB2

Figure 47. (Concluded)

resistance of 6000 kips-ft. The structure is performing in a satisfactory manner.

Fort Polk Hospital

154. This hospital, constructed in 1978-1979, is located south of 3rd street, west of Mississippi Avenue on South Fort Polk, Louisiana. The topography is hilly and slopes down to the south and southwest at approximately an 8 percent grade. The 242.5-ft by 259-ft rectangular multistory structure consists of a 7 story central tower section with adjacent 2 story elements. The mat supporting the hospital is 3 ft thick beneath the tower section and 2 ft thick beneath the low rise sections as illustrated in the west half of the foundation plan, Figure 48. Minimum bottom reinforcement in the 3-ft thick portion of the mat consists of number 10 bars at 12-inch centers each way, whlich contributes a positive (tension in bottom fibers) bending moment resistance of 171.4 kips-ft/ft width of mat from Equation 11a. The superstructure is relatively flexible consisting of precast concrete panels on a structural steel frame. Column loads, Figure 48, lead to an average pressure of 1.4 ksf. The mat weight contributes an additional 0.5 ksf for a total average applied pressure $q = 1.9$ ksf.

155. Soil parameters. Thirty-two borings were made from December 1976 through March 1977 for the purpose of obtaining information for foundation design and to select the optimum site. Surface soil consists of loose, silty sands (SM, SC) from a few inches to about 2 ft in thickness underlain by beds of high CH to medium CL plasticity clays of the Blount Creek member of the Fisk formation, Figure 49. Water content of the clays is approximately 20 percent. A perched water table is indicated within 10 ft beneath the mat base.

156. Consolidometer/swell tests indicate swell pressures in excess of the overburden pressure with possible potential for soil swell at depths exceeding 10 ft beneath the mat. The pressure exerted by the structure and overlying soil is less than the swell pressure so that the soil can heave on wetting and some uplift of the structure may occur. The soil elastic modulus within 30 ft beneath the mat base appears highly variable and may be as large as 3300 ksf.

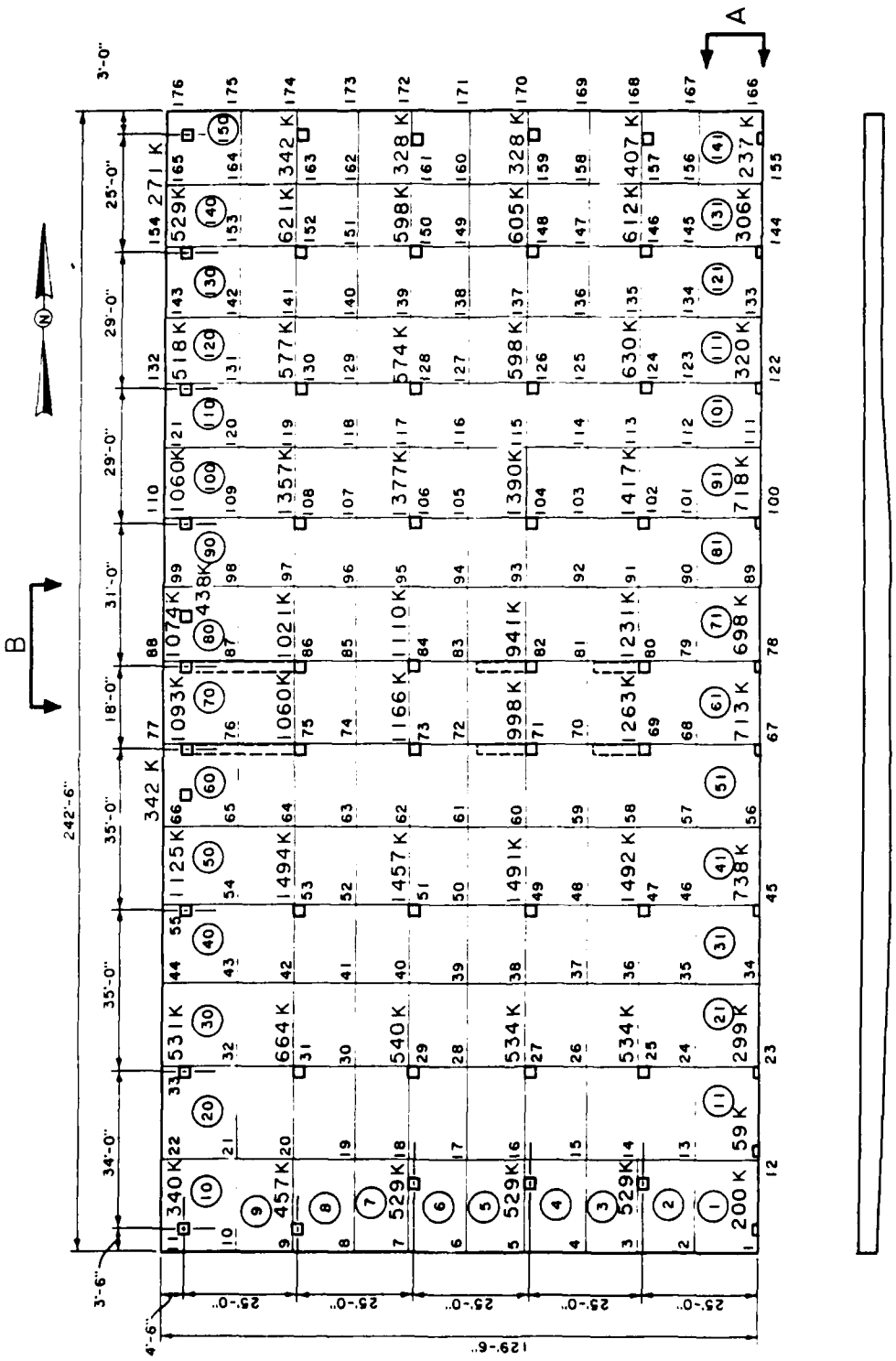

Figure 48. West half of foundation plan, Fort Polk Hospital, Louisiana

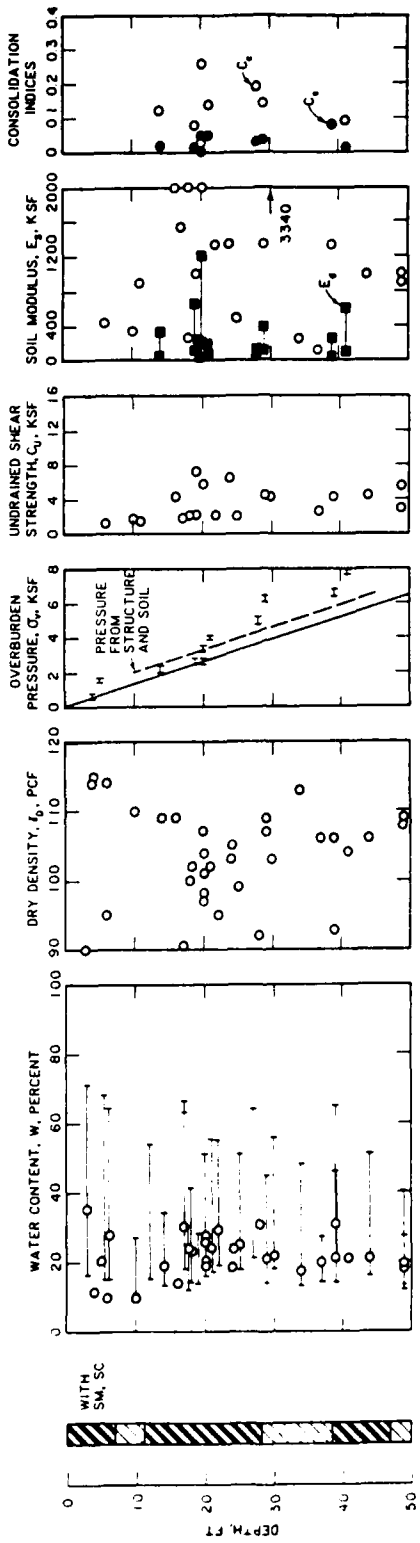

Figure 49. Soil parameters, Fort Polk Hospital

157. Level survey. Level surveys conducted following construction of the mat in September 1979, Figure 50, indicate an initial slight rebound in November 1979 to a maximum of 0.35 inch near the northeast corner where the depth of excavation of about 15 ft is greatest. At that time the center west edge appeared to experience the greatest differential movement of about 1/500 and settlement of about 0.4 inch. During further construction and placement of the superstructure to April 1980, the entire mat settled and reached a maximum settlement near the north perimeter. Average settlement was about 0.3 inch. 0.5 inch was taken as the actual settlement to compensate for some swell. The effective modulus E_s^* is 11,000 ksf from Equation 3 assuming ρ = 0.5 inch, q = 1.9 ksf, μ_1 = 0.7 and μ_0 = 1.0. This modulus is substantially larger than those from soil tests.

158. A level survey conducted in February 1981, about 1.5 years following completion of construction, indicated a small heave of about 0.5 inch relative to April 1980 distributed fairly evenly over the mat except in the southeast corner. The basis for this heave is presumably the potential for swell, Figure 49. Level readings taken in March 1982 indicate a fairly uniform settlement relative to February 1981. The overall displacement by March 1982 relative to the initial readings in September 1979 was only about 0.1 inch of settlement. The maximum recorded settlement in March 1982 was 0.4 inch near the southeast corner and maximum recorded heave of about 0.5 inch was near the northeast corner. Structural distress had not been observed in the hospital. The dishing action characteristic of uniformly loaded flexible mats on deep, compressible, cohesive soil is not readily apparent.

159. Analysis. Results of soil-structure interaction analyses performed using programs WESLIQID, CBEAMC, and SLAB2 are shown in Figure 51. Analysis denoted as Run 1 used a constant mat thickness D = 3 ft, constant coefficient of subgrade reaction k_{sf} = 27.6 ksf/ft, and E_c = 432,000 ksf. k_{sf} = 27.6 ksf/ft is approximately equivalent to E_s^* = 5500 ksf for an elastic analyis when simulating displacements. Analysis denoted as Run 2 used a variable k_{sf} calculated from Equation 8a using E_s^* = 11,000 ksf and influence factor $\mu_0\mu_1$ derived from the ribbed mat analyses. These influence factors are in part justified by noting that the stiffness of this mat should approximately be the same stiffness as the ribbed mats. Results show that bending moments and

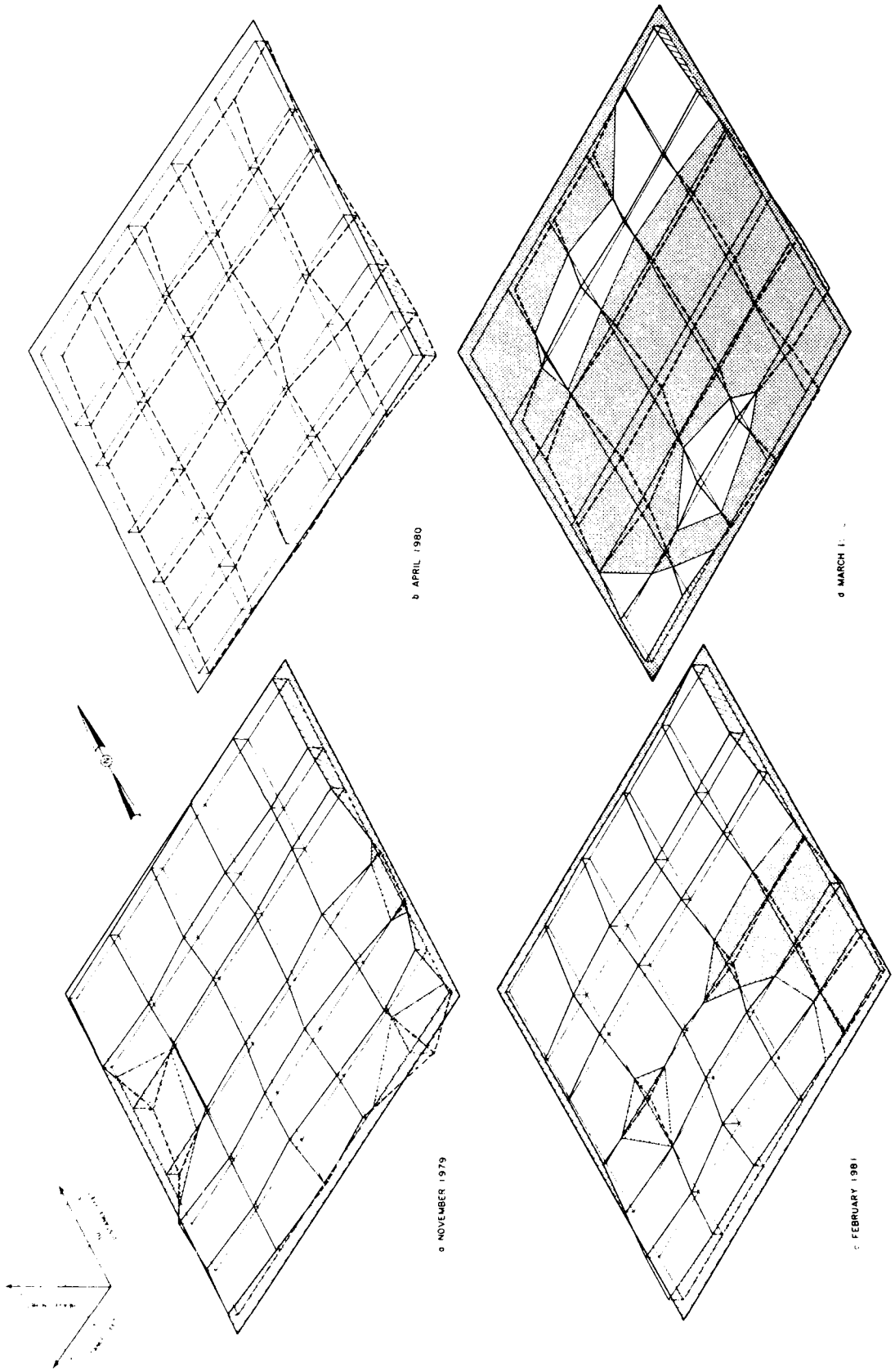

Figure 50. Level surveys, Fort Polk Hospital

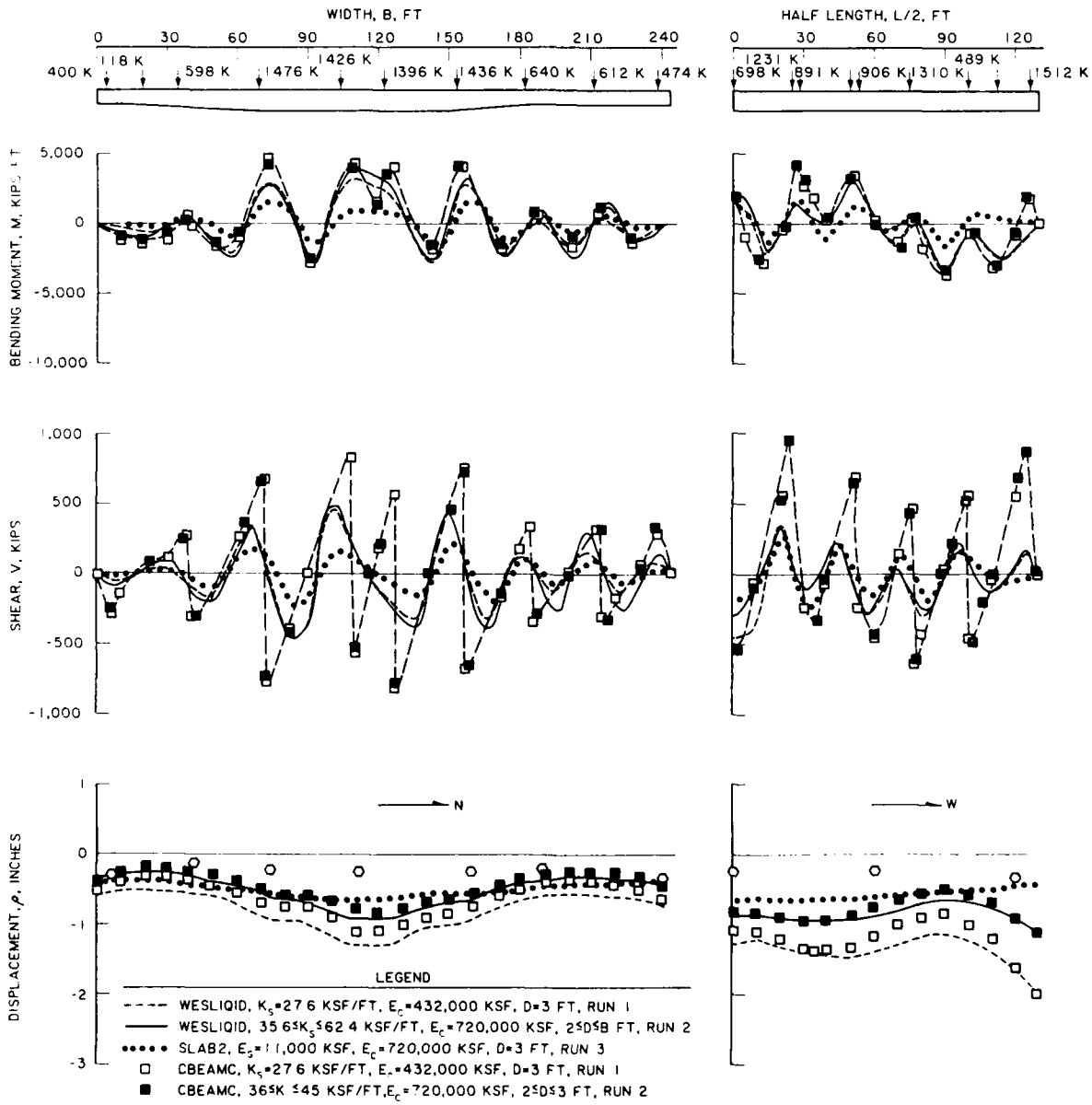

Figure 51. Soil-structure interaction analysis, Fort Polk Hospital

shears from SLAB2 are least, while those from CBEAMC are greatest. All bending resistances are within capacity.

160. Calculated displacements for the Winkler foundation indicate maximum settlement near the center section A with edge down behavior. Calculated displacements at the edge of section B had substantial edge down movement. CBEAMC results indicated slightly smaller settlements than W#ESLIQID results from Runs 1 and 2. Results from SLAB2 indicate center down displacements relative to the edges and appear most representative of the observed mat performance. A comparison of WESLIQID and SLAB2 displacements is better given in Figure 52. Modeling the variations in mat thickness and varying k_{sf} across the mat dimensions appear to have limited influence on the calculated performance. Actual displacements are less than calculated because the soil stiffness may be greater than that assumed and some soil heave had occurred. The SLAB2 analysis indicates less differential movement in the short direction than in the long direction.

161. A two-dimensional finite element plane strain program using the hyperbolic model soil model was performed in 1977 (data furnished by the Fort Worth District) that simulated excavation and construction loading increments. The soil elastic modulus was similar to $E_s^* = 5500$ ksf. The maximum depth of the finite element mesh was about 60 ft beneath the mat base. Calculated mat displacements for section A was a maximum of 1 inch settlement in the center with a net heave of about 0.4 inch near the north end. Actual movements observed in 1982, Figure 50d, indicate heave in the north corner of about 0.4 inch and maximum settlement of about 0.5 inch in the center.

Summary and Conclusions

162. Settlement of these multistory structures is primarily from recompression of the soil. The influence of environmental changes such as moisture flow and heave could be observed on differential movements, but these differential movements did not significantly reduce performance. Differential movement in the short direction was less than in the long direction.

163. The stiffness of these complete structures on flat mats is semi-flexible. Plate on elastic foundation computer program SLAB2 appeared to provide an adequate correlation of calculated deformation of flat mats in cohesive soil, while the Winkler foundation using a constant k_{sf} appeared

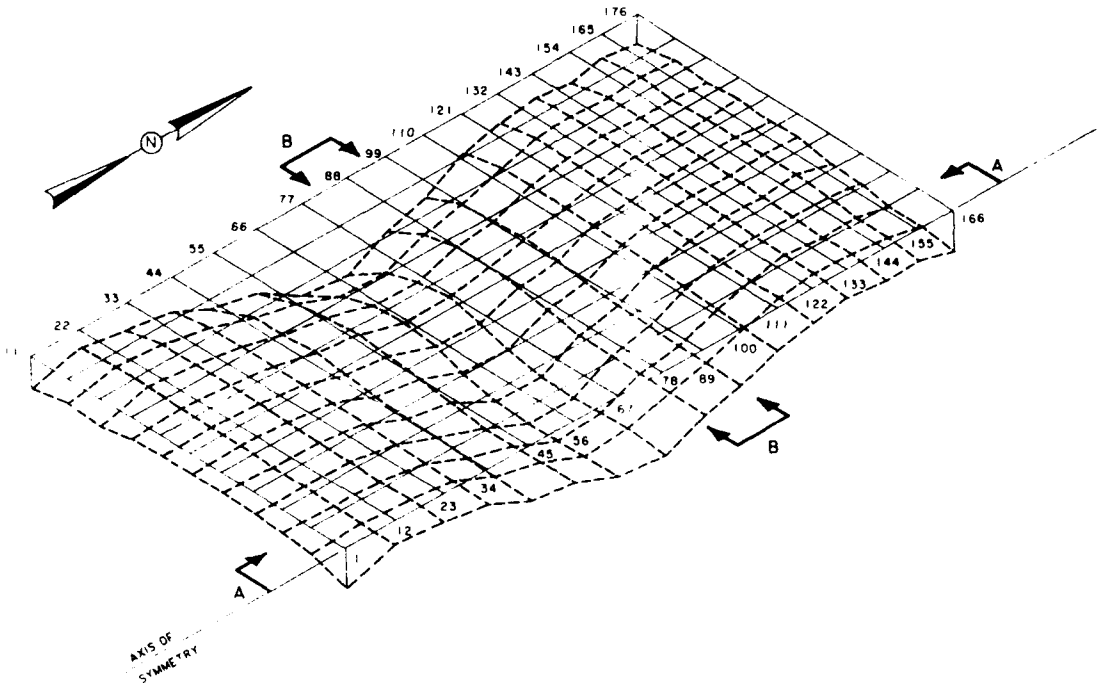

a WINKLER FOUNDATION, $35.6 \leq K_s \leq 62.4$ KSF/FT, $2 \leq D \leq 3$ FT

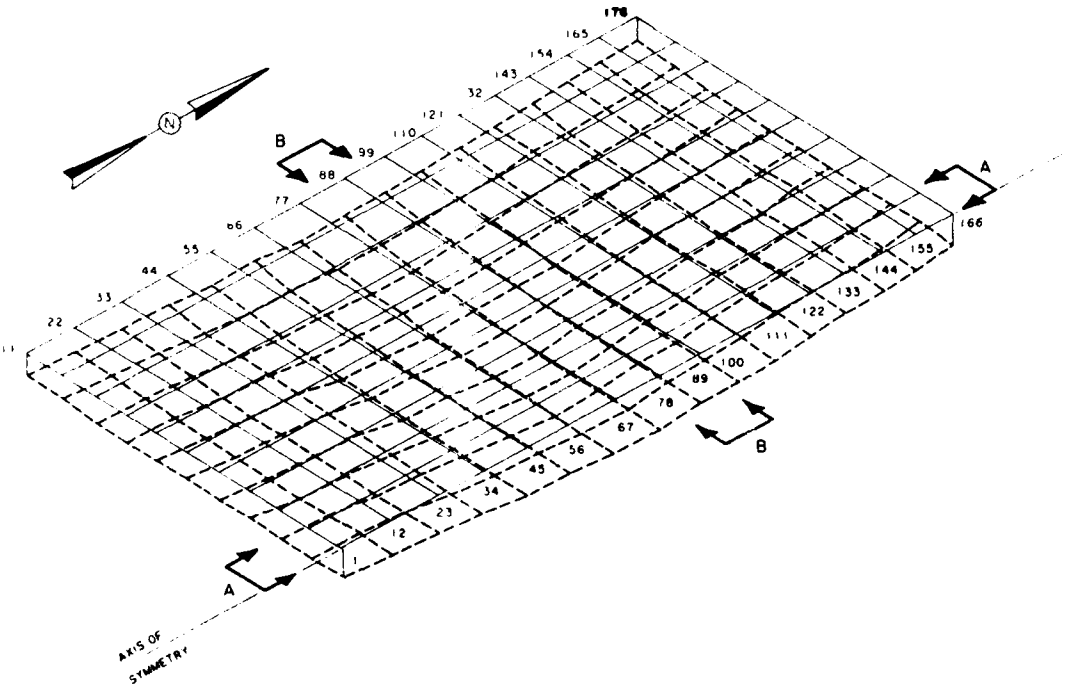

b SEMI-INFINITE ELASTIC FOUNDATION,
$E_s = 11{,}000$ KSF, $\mu_s = 0.3$, $D = 3$ FT

Figure 52. Displacement patterns of Fort Polk Hospital mat, $E_c = 720{,}000$ ksf

superior in cohesionless soil. k_{sf} may be evaluated from elasticity theory using Equation 8a when simulating displacements. k_{sf} is also similar to the constant k relating the Young's soil modulus with depth z, Equation 29. This observation is consistent with the correlation between k_{sf} and k given in Appendix A. Young's soil modulus is taken as the initial tangent modulus evaluated by the hyperbolic soil model from results of triaxial strength Q tests. A representative elastic modulus may be calculated from Equations 4 for nonuniform soil and depends on the soil stiffness for substantial depths beneath the mat. The depth of soil testing should be about twice the minimum width of uniformly loaded flat mats.

164. Stresses in mat foundations developed by heaving soil as a result of changes in soil moisture are often significantly more severe than stresses caused by normal displacements under structural loads. Appendix E shows that bending moments substantially increase in mats supported by soil of greater stiffness for given soil heave patterns. The soil heave pattern is typically random for these studies and not easily predictable for any of these structures. If differential movements caused by changes in soil volume do not occur, increasing soil stiffness decreases bending moments because of imnproved soil support, reduced settlement and distortion.

PART IV: APPLICATION OF FIELD PERFORMANCE

Introduction

165. A field study of building 333 at the Red River Army Depot (RRAD), "Light Track Vehicle Shop" of the Maintenance modernization Project was initiated to provide improved understanding of the performance of ribbed mats constructed in cohesive/expansive soil. The site is located on the eastern edge of the RRAD west of Texarkana, TX, bounded by Texas Avenue on the north, K avenue on the east, 8th street on the south, and G Avenue on the west.

166. Building 333, under construction from 1983 to 1985, is a flexible, steel framed structure on a ribbed mat spanning 678 ft by 304 ft and includes two expansion joints dividing the mat into three monolithic units, Figure 53a. Stiffening beams are placed on 12.5-ft centers near the perimeter with interior beams on 25-ft centers as indicated by an enlarged view of the Southeast corner of the mat plan, Figure 53b. All stiffening beams are 1.5-ft wide by 3-ft in depth below the top surface of the mat. Column loads are placed on enlarged sections of the stiffening beams up to 10.5 ft on a side as illustrated in Figure 53b by the squares for interior columns and triangles for the perimeter or corner columns. Reinforcement steel consists of two No. 11 bars placed top and bottom with 4 inches of concrete cover below the top surface of the mat and above the bottom of each stiffening beam. Steel was not continuous between each monolithic unit at the expansion joints.

167. Excavation of from 5 to 8 ft of overburden and placement of compacted cohesive, nonexpansive, low plasticity fill was initiated on the north end of the site during 1983 and completed on the south end by August 1984. A 6-inch gravel layer and a plastic polyethylene vapor barrier were placed on the fill. A vapor barrier was also placed in the bottom of the stiffening beam excavation trenches and seated snugly against the walls of the trenches. The limits of the fill extend 5 ft outside of the ribbed mat perimeter. The construction site also includes an old drainage ditch aligned along the east-west direction near line 23 (shown later in Figure 55a). Appendix F provides the foundation design by the Facilities System Engineering Corporation using the Post-Tensioning Institute method[11] and foundation design analysis by the US Army Engineer District, Fort Worth.

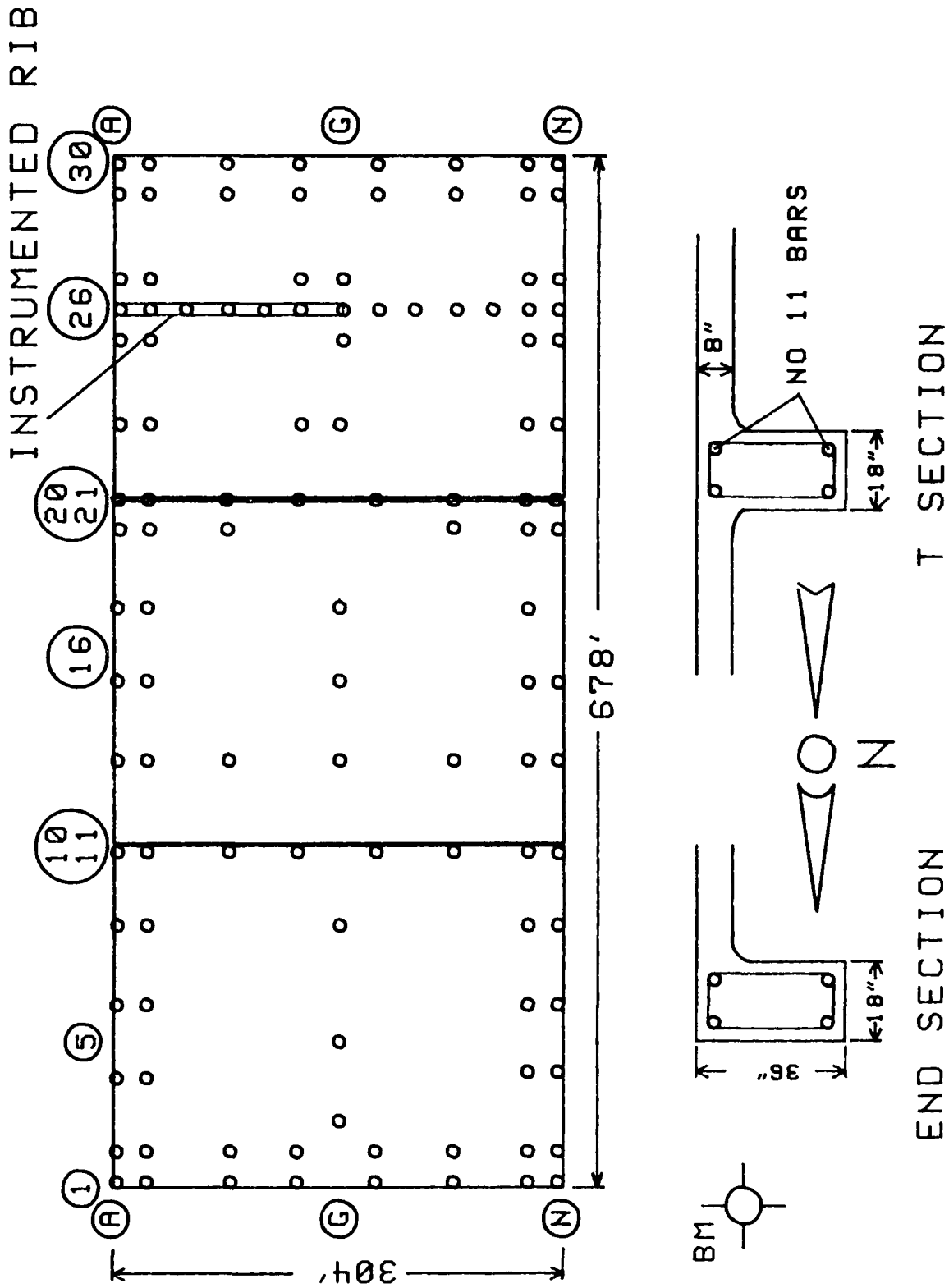

Figure 53a. Plan view of mat for building 333

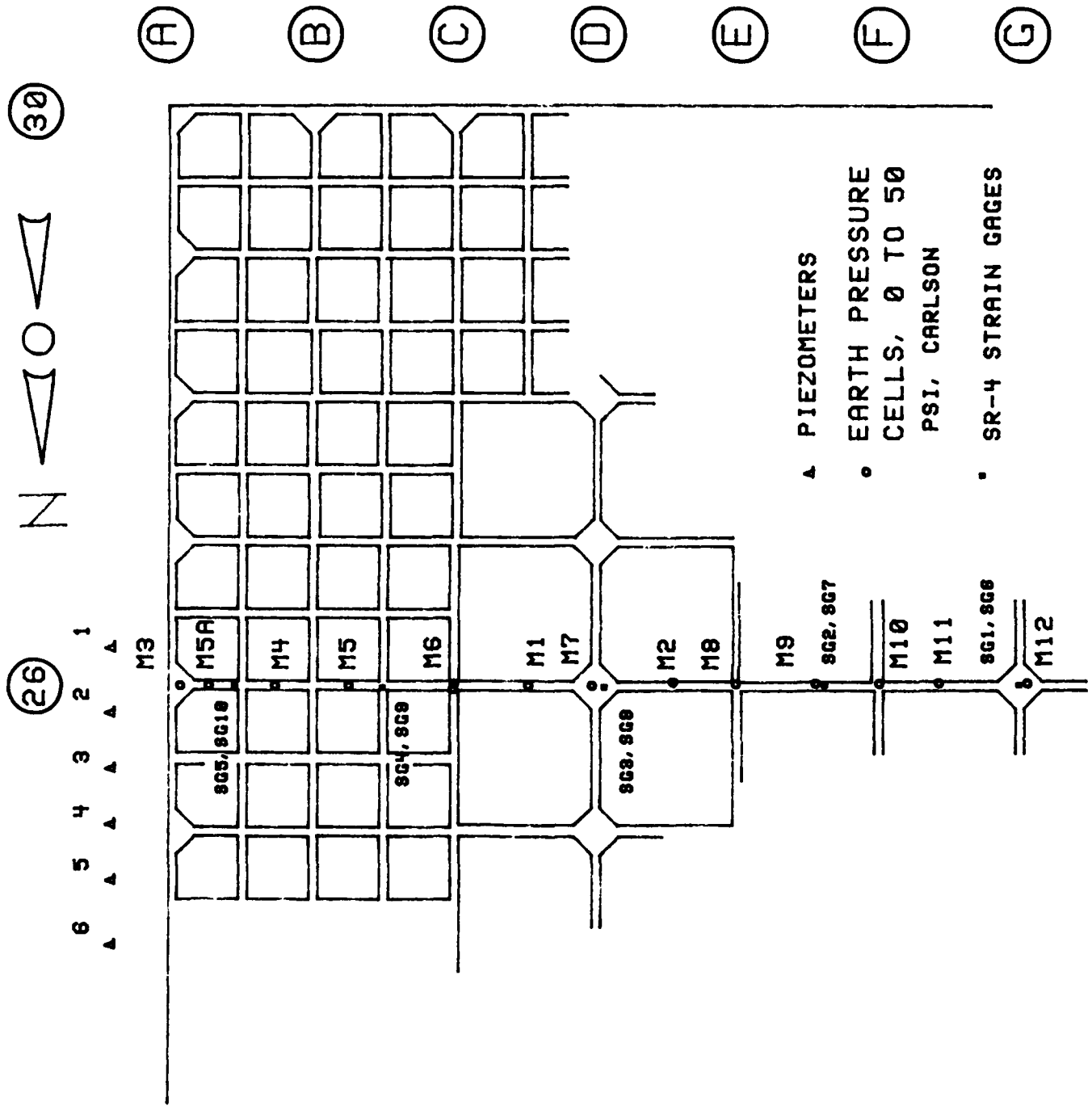

Figure 53b. Southeast corner of the mat plan

Description of Soil

168. Twenty-two borings were made during April and May 1979 to determine subsurface soil conditions and to obtain samples for laboratory testing. Undisturbed boring samples were obtained by 6-inch diameter Denison and core barrel samplers and disturbed samples were obtained by an 8-inch auger. Boring holes left open for various time periods indicated a possible perched water table about 9 ft below ground surface. An additional 6-inch diameter undisturbed boring sample was obtained in June 1985, 15 ft east of column A-23 at the location of piezometer 1 with tip elevation 80 ft below ground surface.

Classification Tests

169. Classification of soil from the boring samples indicated that much of the area had been covered with a variable earth fill up to 8 ft thick consisting of medium CL to high plasticity CH clays, clayey SC sands, clayey sandy GC gravel, sandy silty ML-CL clays and silty SM sands with some organic material. Much of this existing fill was excavated and replaced with nonexpansive red and brown cohesive granular material of adequate bearing capacity to support the mat foundation. This fill of low plasticity index <12, was compacted by sheeps foot and rubber tired rollers to exceed 92 percent of optimum density determined by ASTM D1557.

170. Material underlying the fill consists of a high plastic CH clay shale identified as the Midway group of Tertiary age, Figure 54a. The natural water content in the clay shale is highly variable 8 to 12 ft below ground surface from a low of 20 to over 40 percent. Additional classification data from soil of boring 6DC-425 taken June 1985, Figure 55a, is consistent with these results from soil of the 1979 boring samples.

Laboratory Strength Tests

171. Soil strength parameters were evaluated from triaxial undrained strength Q tests performed on 1.4-inch diameter undisturbed specimens at a confining pressure similar to the total vertical overburden pressure on the in situ soil. The results of undrained Q tests performed on specimens from the earlier boring samples taken in 1979, solid circles in Figure 54b, indicate least soil strength 5 to 12 ft below ground surface. The ground surface coincides with the elevation of the bottom surface of the flat portion of the

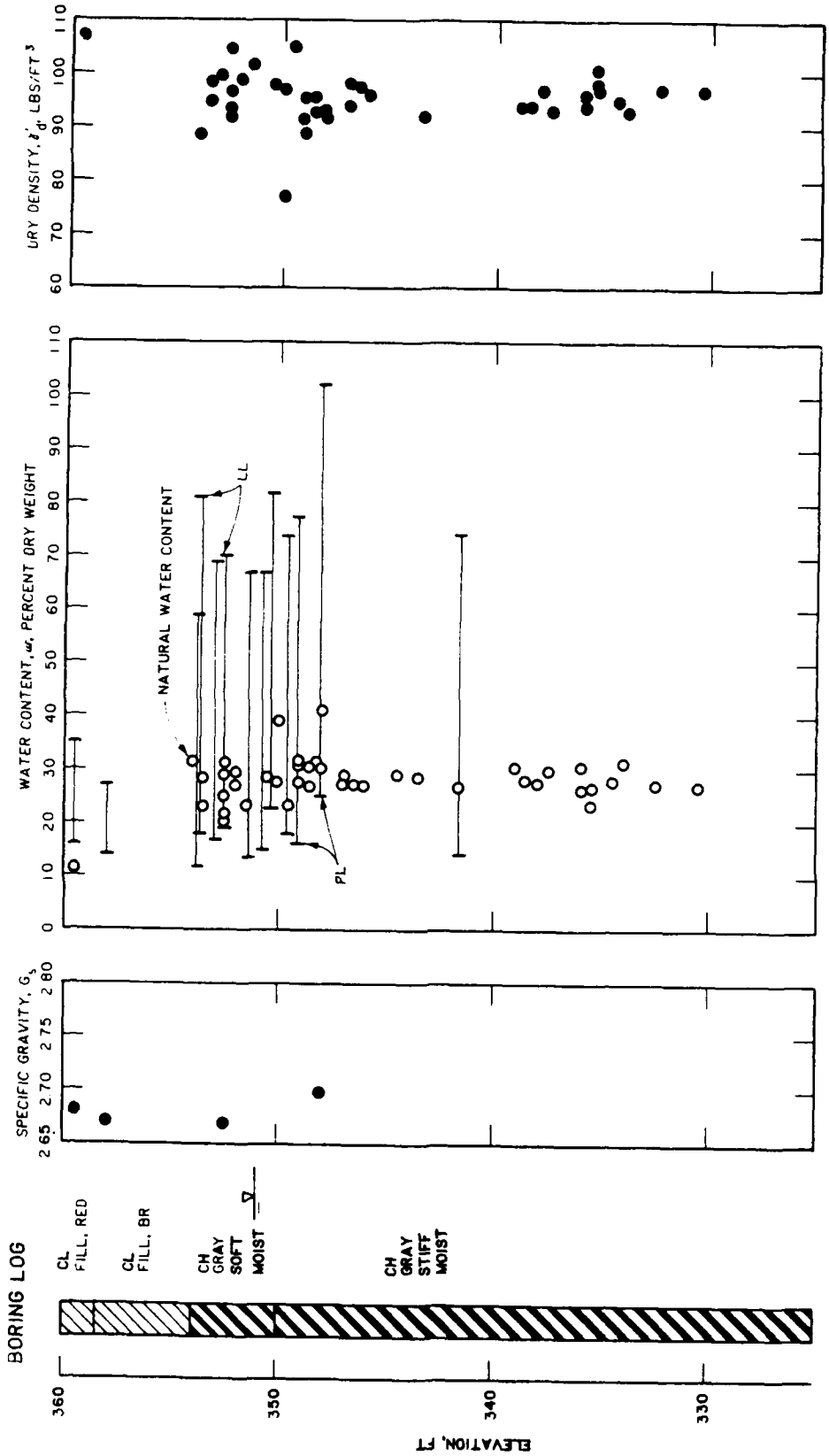

a. CLASSIFICATION DATA

Figure 54. Soil parameters from 1979 boring samples

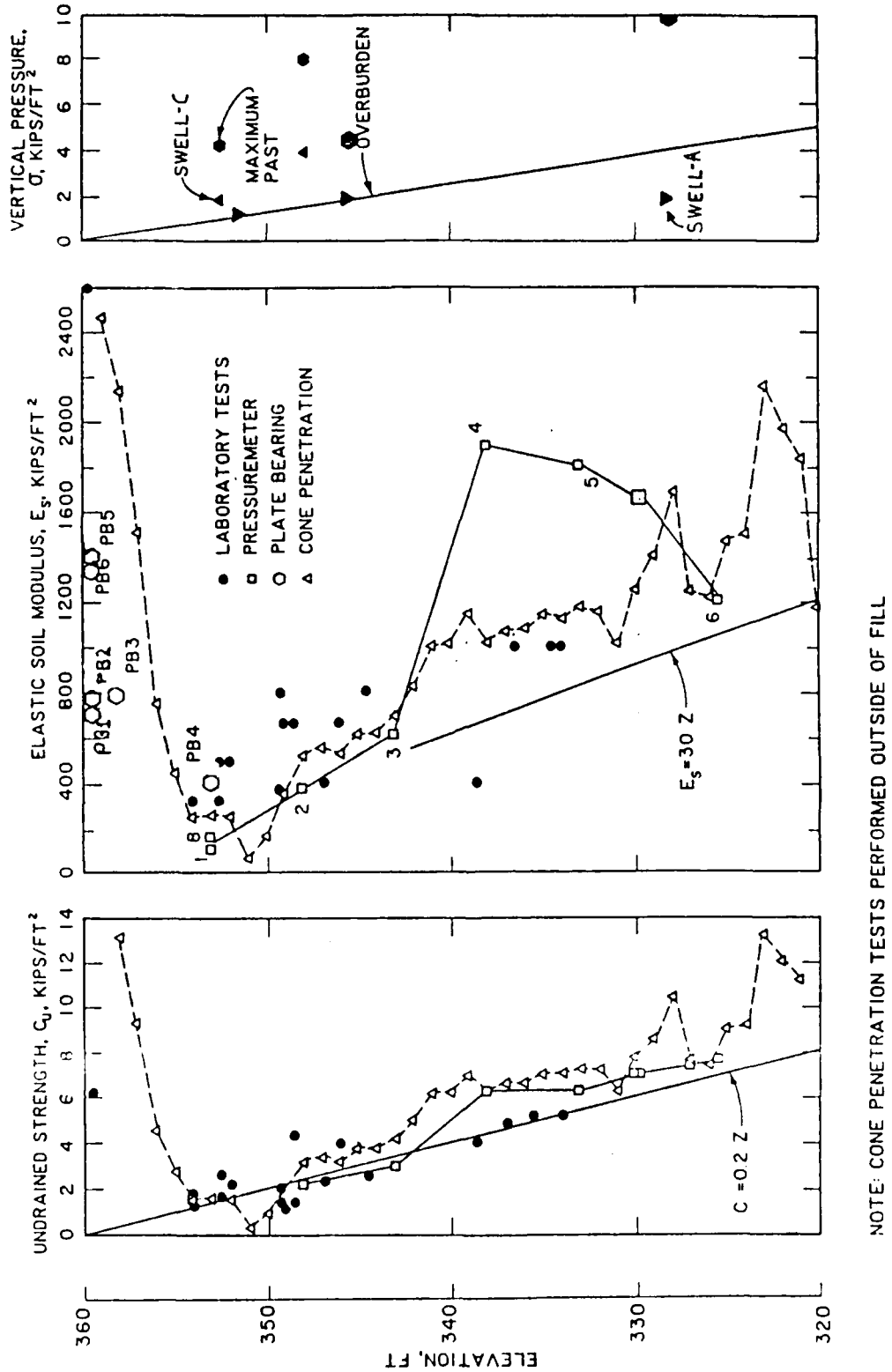

b. MECHANICAL PARAMETERS

Figure 54. (Concluded)

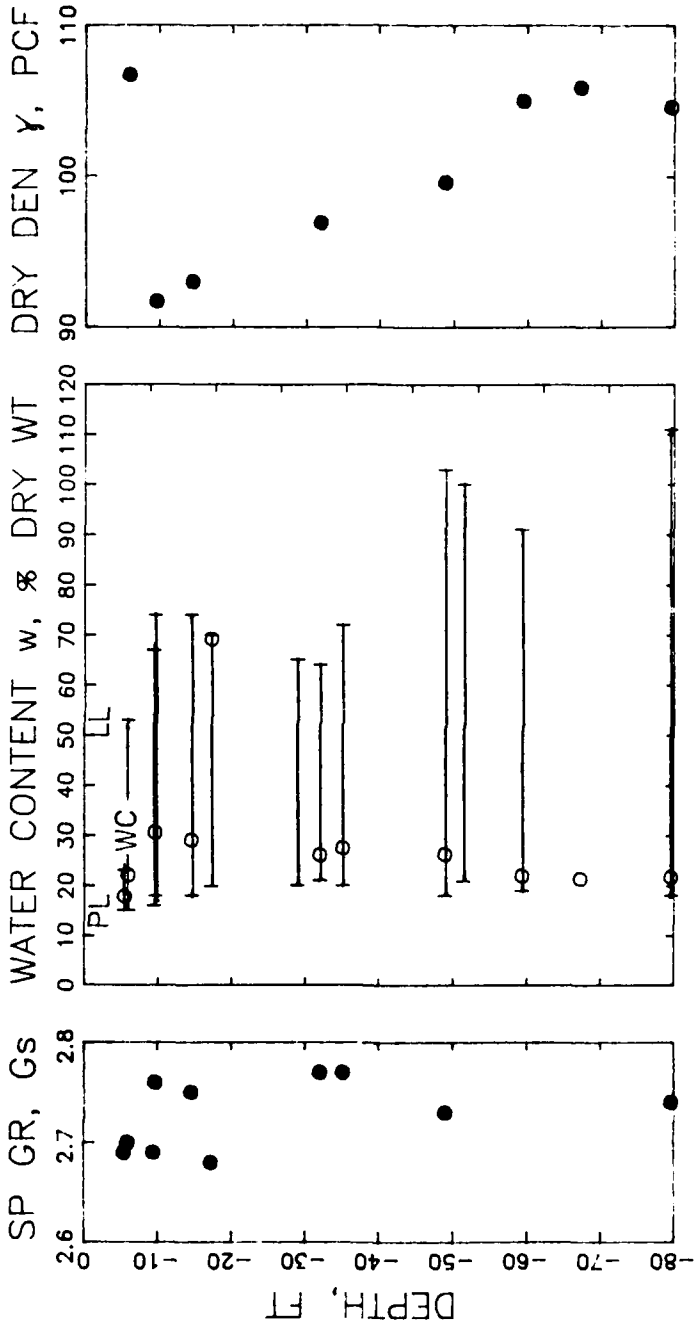

a. CLASSIFICATION DATA

Figure 55. Soil parameters from boring 6DC-425, June 1985

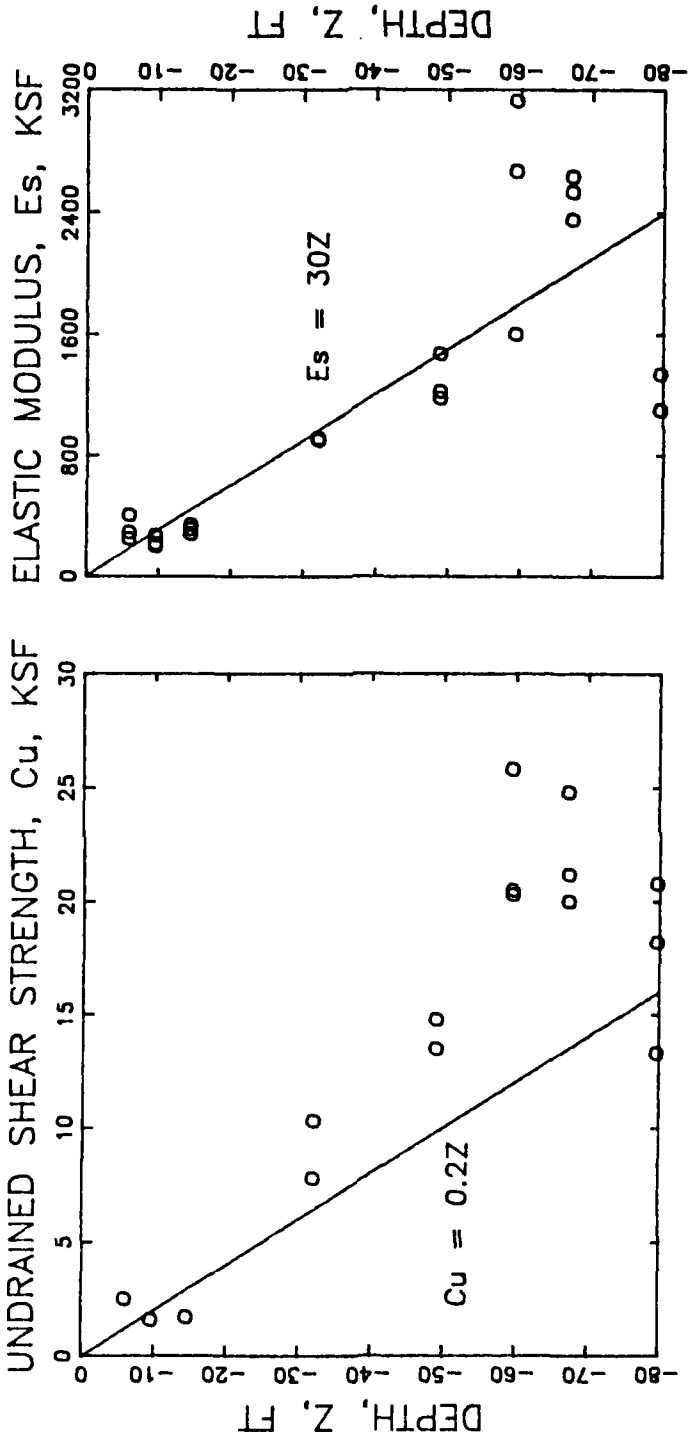

b. MECHANICAL PARAMETERS

Figure 55. (Concluded)

mat, elevation 365.33 ft above sea level. The nominal elevation of the finish floor surface is 366.00 ft. The undrained strength may increase linearly with depth below 5 ft of depth by

$$C_u = 0.2z, \quad z > 5 \text{ ft} \tag{30}$$

where

C_u = undrained strength, ksf

z = depth, ft

Additional strength tests performed on specimens from boring sample 6DC-425 taken June 1985 confirm earlier results, Figure 55b.

172. The elastic soil moduli E_s determined from laboratory tests, solid symbols in Figures 54b and 55b, are the initial moduli calculated by the hyperbolic model[23]. The elastic modulus approaches a minimum of 200 ksf from 6 to 10 ft below the ground surface and appears to increase with depth below 10 ft approximately by

$$E_s = 30z, \quad z > 5 \text{ ft} \tag{31}$$

where E_s is the soil elastic Young's modulus, ksf. Combining equations 30 and 31 indicate that E_s *is about 150 times* C_u.

Consolidometer Swell Tests

173. Two consolidometer swell tests were performed on undisturbed specimens from soil samples obtained in 1979 after ASTM D4546 method C (labeled SWELL-C in Figure 54b) and an additional three tests were performed on undisturbed specimens from boring sample 6DC-425 after ASTM D 4546 method A (labeled SWELL-A in Figure 54b). The results of method C on the 1979 soil specimens indicate that swell pressures σ_s exceed the vertical overburden pressure above 20 ft of depth. Results of method A on the 1985 soil specimens indicate σ_s on the order of the vertical overburden pressure above 20 ft and σ_s = 1.95 tsf or about 1/2 of the total vertical overburden pressure at 32 ft of depth. The soil is overconsolidated with an overconsolidation ratio (OCR) of about 4 above 20 ft and an OCR of 10 at 32 ft of depth. The compression index C_c is 0.20 ± 0.05 and the swell index C_s is about 0.07 ± 0.1.

174. A shallow water table may exist at this site based on comparison of the overburden pressures with swell pressure results from the 1985 soil

specimens using method A. Removal of these specimens from the field had relieved the vertical and lateral confining pressures and caused the pore pressures in these specimens to decrease by approximately the mean normal confining pressure

$$\sigma_m = \frac{\sigma_v (1 + 2K_o)}{3} \tag{32}$$

where

σ_m = mean normal confining pressure, ksf

σ_v = total vertical overburden pressure, ksf

K_o = coefficient of earth pressure at rest

For OCR of 4 to 10, K_o is about 1.2 to 1.5[63]. At 32 ft σ_m is about 5.2 ksf where σ_v is about 3.8 ksf and K_o is about 1.5. Assuming the effective stress remains constant following removal of the soil samples from the field, the in situ positive pore water pressure $u_w = \sigma_m - \sigma_s$ or $5.2 - 3.8 = 1.4$ ksf. This translates to a pressure head of 23 ft at 32 ft of depth. The groundwater level should be about 9 ft below ground surface assuming that the pore water pressure is hydrostatic. This is consistent with the actual observed groundwater level of 9 ft below ground surface in open boreholes during soil sampling. Piezometric data described later as part of the field instrumentation program show that a shallow perched water table exists following construction above 50 ft of depth with groundwater level approximately 5 ft below ground surface.

In Situ Soil Tests

175. Pressuremeter, cone penetration, and plate bearing tests were performed to complement results of the laboratory tests. Figure 56 illustrates the relative location of these field tests. Details of these tests are provided in Appendix G.

176. Pressuremeter. Eight tests, besides calibration tests to compensate for volume losses and membrane resistances, were performed 26 November 1983 in two hand augered holes. One test was conducted in a borehole 10 ft west of column A on line 26 of the planned location of building 333, Figure 56, in the bottom of the open excavation prior to placement of the

[63]Brooker and Ireland 1965

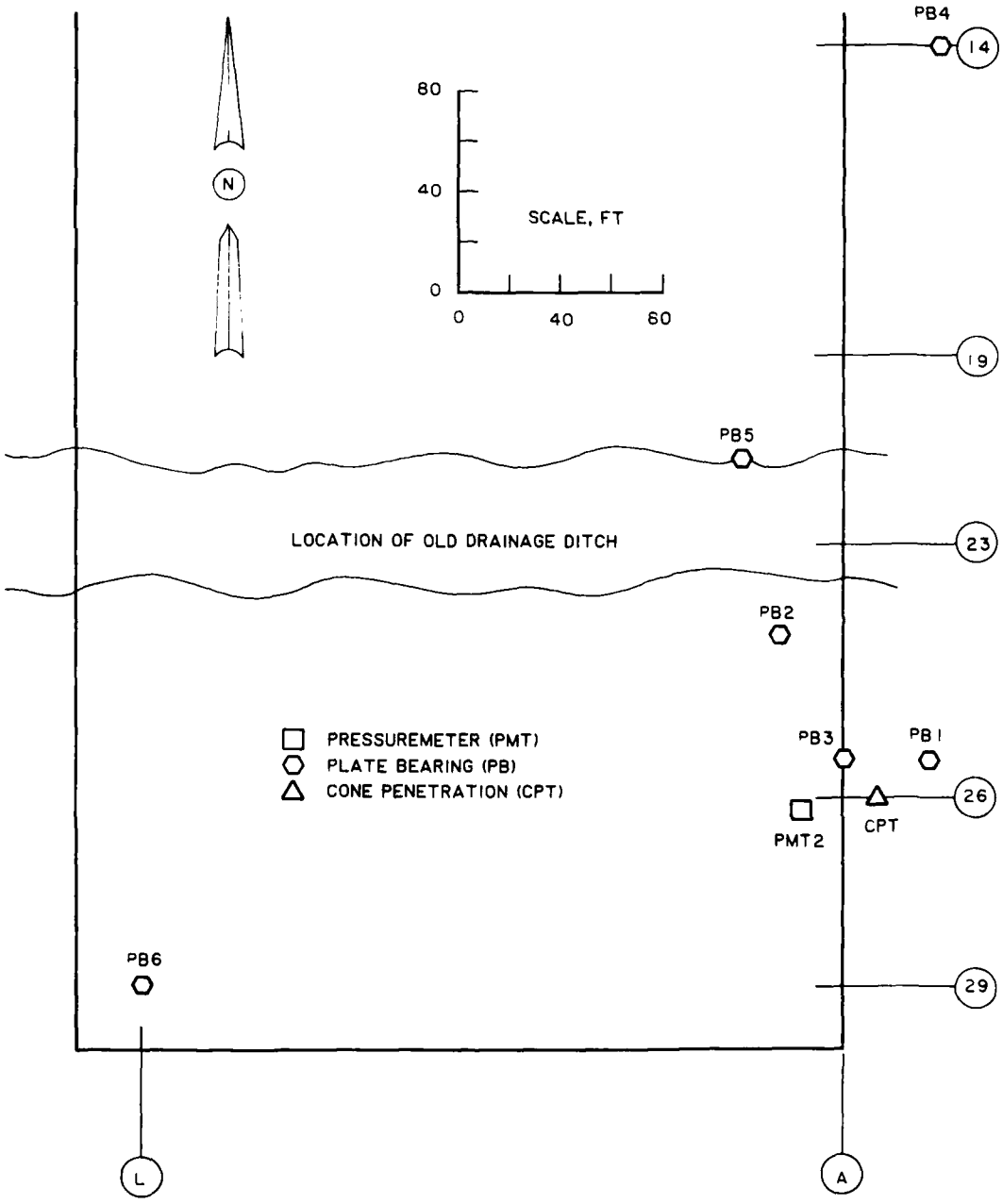

Figure 56. Location of field tests

compacted fill. The remaining tests were conducted 16 ft west and 6 ft south of location A-26, at the bottom of the excavation. Results of the pressuremeter tests were used to estimate the undrained shear strength and Young's elastic soil modulus.

177. The undrained shear strength evaluated from the pressuremeter limit pressure by

$$C_u = \frac{P_L^*}{10} + 0.5 \tag{33}$$

where

C_u = undrained shear strength, ksf

P_L^* = limit pressure, ksf

compares well with results of the laboratory undrained strength data, except between 330 to 345 ft, Figure 54b. An anomaly such as this may be due to local variations in soil stiffness. Equation 33 provides estimates of soil shear strength that are least among several methods[64].

178. The pressuremeter modulus may be evaluated by

$$E_p = \frac{(1 + \mu_s)\ \Delta P\ (R_o + \Delta R_m)}{\Delta R} \tag{34}$$

where

μ_s = Poisson's ratio of soil, 0.33

ΔP = change in pressure measured by the pressuremeter, ksf

R_o = probe radius, 2.28 inches

ΔR_m = change in radius from R_o at midpoint of straight portion of pressuremeter curve, inches

ΔR = change in radius between selected straight portions of pressuremeter curve, inches

The first load pressuremeter modulus calculated from Equation 34 was evaluated from the slope of the straight portion of the pressuremeter curves on loading. This pressuremeter modulus, Figure 54b, is consistent with the initial soil modulus evaluated from the undrained triaxial strength test results for soil above 20 ft of depth, but substantially greater than laboratory data between

---

[64]Baguelin, Jezequel, and Shields 1978

20 and 30 ft. Table 4 indicates that the elastic modulus is $(1 + \mu_s) \cdot E_p$; this is consistent with the initial soil modulus from laboratory strength tests.

179. Cone penetration. The cone penetration test (CPT) was conducted 15 ft east of location A-26, Figure 56, on 17 August 1984 in accordance with ASTM D3441 with the exception of the rate of penetration. This test was conducted outside the limits of the compacted fill, Figure 56. The cone is a Fugro electronic friction sleeve type hydraulically pushed into the ground at a constant rate of 4.72 inches/sec. The CPT sounding was conducted to a depth of 40 ft before the test was terminated due to friction buildup on the cone rods that exceeded the 20-ton capacity of the truck.

180. The CPT data indicated a soil classification consistent with that observed from laboratory classification tests on soil specimens, Figure 54a. Estimates of the undrained shear strength may be made from the tip resistance by

$$C_u = \frac{q_c - \sigma_v}{N_k} \tag{35}$$

where

q_c = tip resistance, ksf

σ_v = vertical overburden pressure, ksf

N_k = tip cone factor

Figure 54b shows estimates of C_u determined from q_c at 1-ft increments for N_k equal to 20. These cone derived strengths are initially high exceeding 12 ksf in the natural subgrade and decreasing rapidly to about 1.5 ksf in the Midway clay. An exceptionally low value of 0.4 ksf was observed in the Midway clay 9 ft below grade indicating a soft material. Results from other tests were not available to check the cone strength at 9 ft. The CPT is able to provide a continuous log of soil parameters in the profile and can detect the existence of thin strata that might otherwise be missed. Undrained strengths below 9 ft increase at approximately a constant rate slightly greater than 0.2 ksf/ft as the depth increases.

181. The constrained soil moduli may be roughly estimated from q_c by

$$E_d = \alpha \cdot q_c \tag{36}$$

where α is an empirical constant that often varies from 3 to 8 for lean

clays when q_c is less than 14 ksf. E_d estimated from Equation 36 for $\alpha = 8$ is shown in Figure 54b. Young's soil elastic modulus will be roughly 30 percent of the constrained modulus for $\mu_s = 0.4$; these moduli are reasonably consistent with results of the other tests.

182. Plate bearing. A series of plate bearing tests was performed 16 to 20 July 1984 in general accordance with ASTM Standard Test Method D1194 at six different locations on prepared surfaces, Figure 56. The soil surface at each location was initially leveled by scraping away loose material within a 3-ft diameter. Clean, fine sand was subsequently sprinkled on the prepared soil surface to assist leveling of the plates. Three circular steel bearing plates at least 1 inch thick each with diameters of 12, 18, and 30 inches were concentrically positioned at each location with the 30-inch plate on the bottom. The maximum pressure applied through the 12 and 18-inch plates to the 30 inch plate by the truck and water tank loading system was 30 psi.

183. The plate coefficient of subgrade reaction k_{sp} measured from these tests was converted to an elastic soil modulus by the elastic equation 8a

$$E_s = \mu_0 \mu_1 k_{sp} \cdot B_p \tag{37}$$

where

μ_0 = depth influence factor, Figure 3

μ_1 = shape influence factor, 0.62 (Figure 3)

k_{sp} = plate coefficient of subgrade reaction, ksf/ft

B_p = plate diameter, 2.5 ft

The depth influence factor μ_o was normally 1.0 for tests conducted at the ground surface except for test PB-4 where μ_o was taken as 0.9 because the test was conducted 6.7 ft below ground surface. The elastic soil modulus surface. The elastic soil modulus evaluated by Equation 37 from results of the plate bearing test, Appendix G, shows values from 700 to 1300 ksf in the compacted fill or natural grade.

184. After plate bearing test PB-2, a 6-inch diameter mold was pushed into the compacted red fill by the hydraulic jack reacting against the truck weight at this same location, Figure 56, to obtain a soil sample for laboratory tests. Results of an unconsolidated-undrained triaxial test of a

specimen cut from this soil sample indicated an elastic modulus of 2600 ksf. The elastic moduli evaluated from results of the plate bearing test are influenced by the soil stiffness down to about twice the plate diameter or about 5 ft below the plate. Therefore, the average elastic soil modulus in the fill may be substantially less than the 2600 ksf that was measured within the fill near the ground surface. Result of plate bearing test PB-4 conducted 6.7 ft below grade is consistent with results of E_s evaluated from laboratory strength tests, but more than twice E_p evaluated from Equation 34 for the pressuremeter first load modulus, Figure 54b.

Field Instrumentation

Piezometers

185. Six Casagrande type porous stone piezometers 1 through 6 were installed with tips at depths of 80, 50, 40, 26, 8, and 5 ft, respectively, below ground surface in front of building 333 in June 1985 near column A-26, Figure 53b. Detail of the tip installation is shown in Figure 57. Tip locations of piezometers 5 (8 ft) and 6 (5 ft) were selected to determine the ground water level just below the base of the fill and within the fill. Piezometers 2 (50 ft), 3 (40 ft) and 4 (26 ft) were selected to evaluate the hydraulic head in the clay shale. The piezometer tip at 80 ft is used to detect any deep water level within 80 ft of the ground surface.

186. Piezometric readings from August 1985 through June 1988 indicate a shallow permanent perched water table with water level about 5 ft below ground surface, Figure 58. The piezometric head from this shallow water table decreases below 40 ft; however, pore pressures are increasing 50 ft below ground surface. Falling head tests in these piezometers indicated permeability of about 10^{-8} cm/sec, while permeability of the shallow clay is about 10^{-5} cm/sec. The piezometer at 50 ft may not yet have reached equilibrium. The dry piezometer at 80 ft indicates no deep water table within 80 ft of the ground surface.

Elevation Surveys

187. Elevation surveys were periodically performed on at least 114 locations on the mat surface, Figure 53a. These locations are fixed with brass boltheads set in the concrete floor during mat construction in August

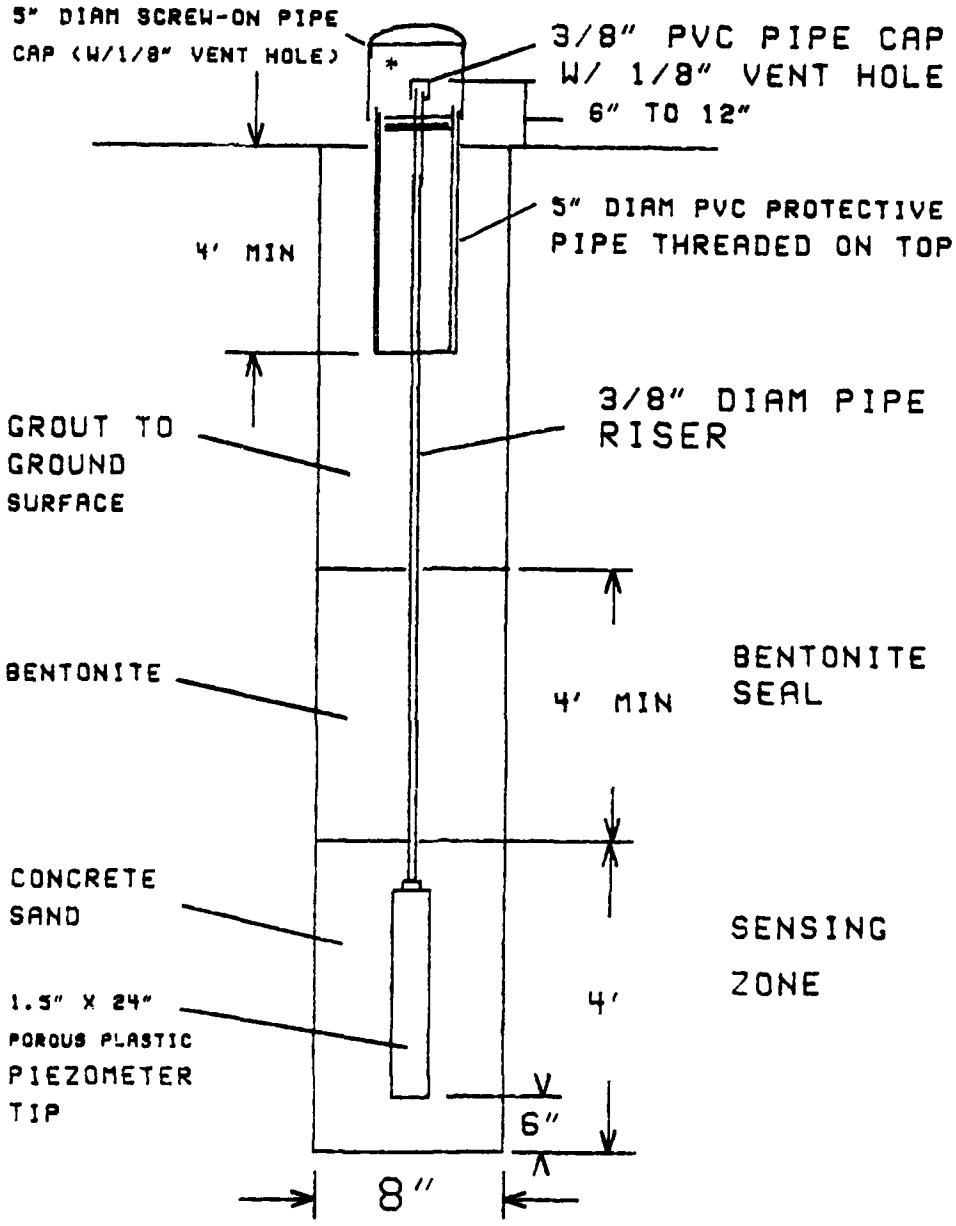

* RISER SHOULD EXTEND 1" TO 2" ABOVE PROTECTIVE PIPE WHEN PROTECTIVE PIPE CAP IS REMOVED

Figure 57. Piezometer installation detail

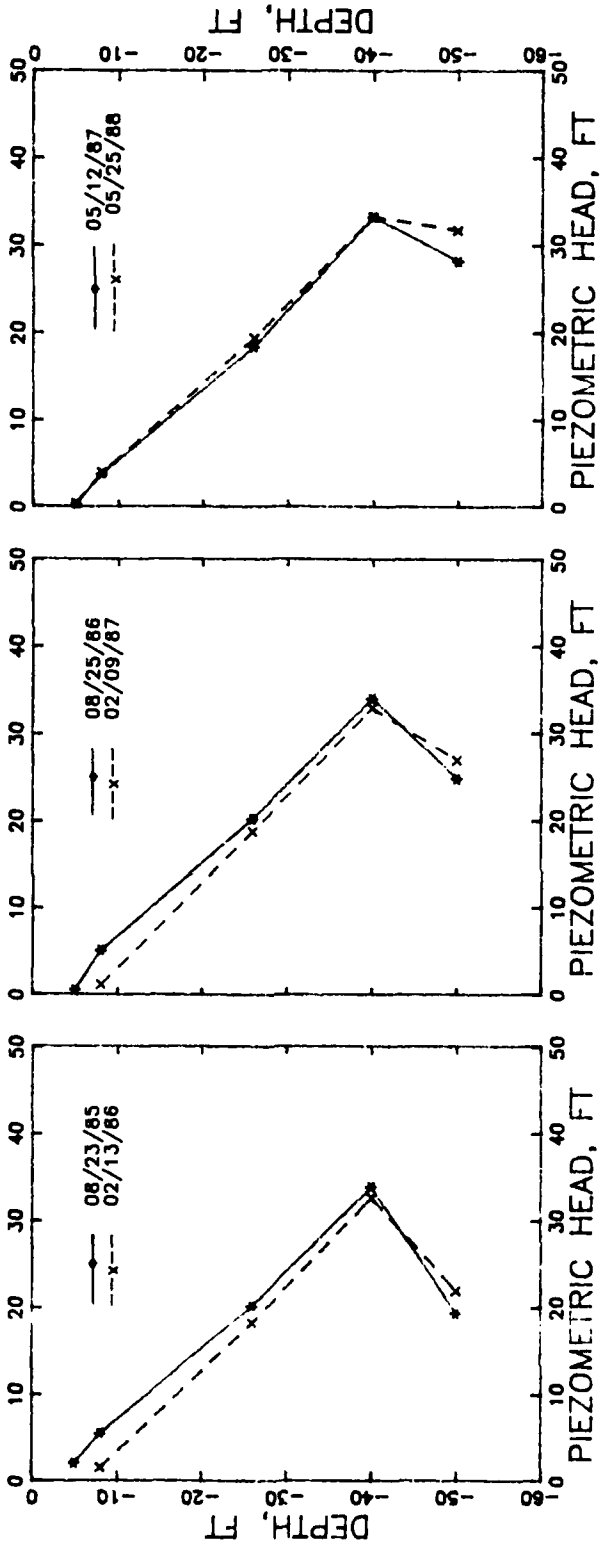

Figure 58. Piezometric heads

1984. Additional elevations were determined along line 26 at 12.5-ft increments from Column A to Column N.

188. Temporary benchmarks were established at six different locations by the contractor during construction. These temporary benchmarks include rims of two concrete manholes for sewer lines, a concrete foundation for a pump station adjacent to a sludge pond, concrete docks of buildings 345 and 315, and a railroad rail. The initial elevation survey made 6 September 1984, 31 October 1984 survey and the 28 Jan 1985 survey used these temporary benchmarks. A permanent deep benchmark with tip elevation 80 ft below ground surface was installed about 100 ft NW of the NW corner of building 333 in June 1985 with details shown in Figure 59. Tabulated elevations from all surveys are provided in Appendix G.

189. Figure 60 illustrates three dimensional views of the displacement of this mat from results of the surveys relative to 6 September 1984. Settlement through May 1987 is approximately 0.1 to 0.3 inch with most settlement near the center. A slight heave was observed in the south end along line 26. One distinctive feature observed from these plots is the unusual V-shaped settlement approximately 1/3 of the way from the south end of the mat. This settlement, which exceeded 1 inch after August 1985, coincides with an old drainage ditch that passed through the construction site, Figure 56. Softening of the subsoil below this drainage ditch from long-term wetting, possible reduction of compaction efficiency above this soft soil, deeper fill depth at this location, and the expansion joint at this location may have contributed to this settlement. This settlement has not hindered operations. A second feature is the appearance of the dish-shaped pattern characteristic of flexible plates on a semi-infinite elastic foundation. The mat appears stiffer in the east-west or short direction consistent with results of plate on elastic foundation analysis in the short direction in Part III. The mat appeared to have reduced edge-down distortion in the south end after August 1985 to June 1986. This correlates well with the removal of heavy equipment temporarily stored on the south end prior to installation.

190. Two-dimensional views of the deformation patterns in the long (line G) and short (line 26) directions of the mat are shown in Figure 61. The length is taken from line 1 to line 30 (0 to 678 ft) and the width is

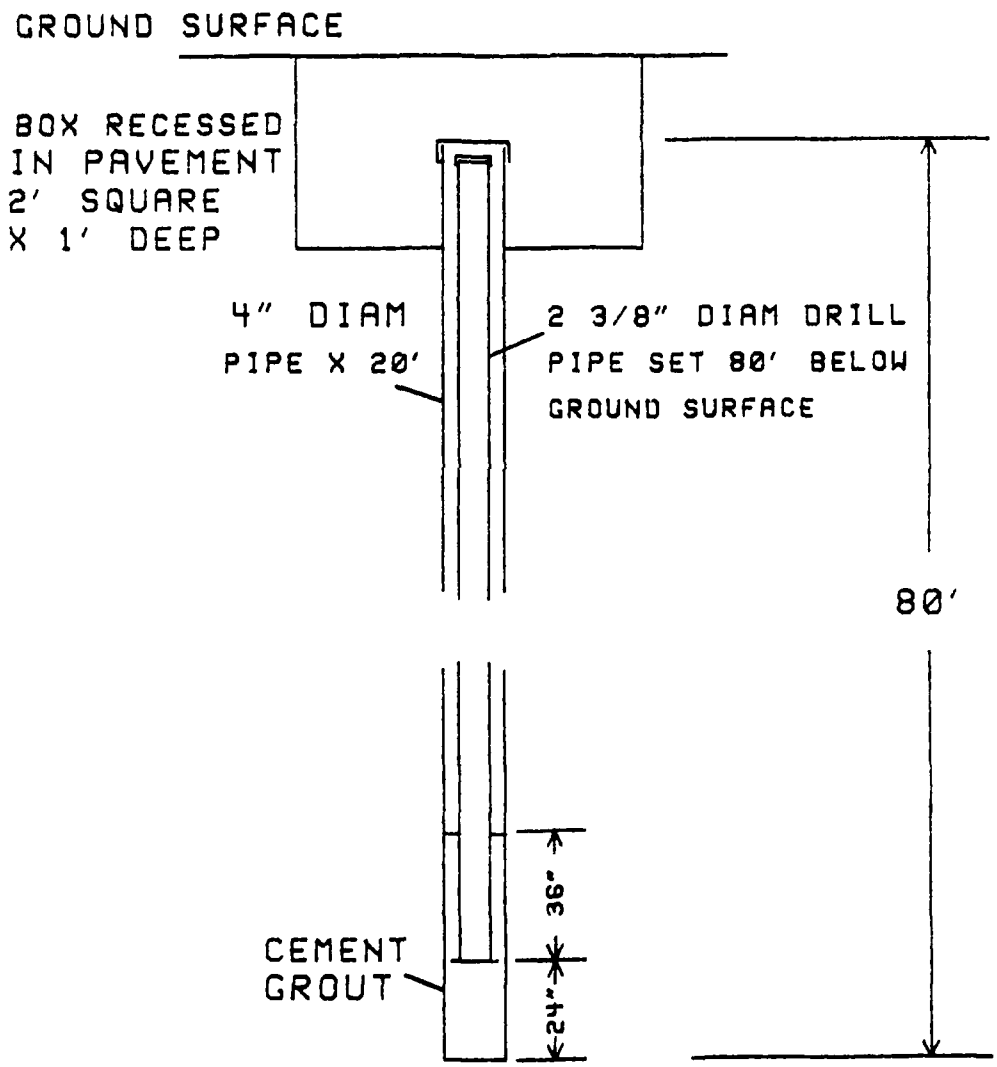

Figure 59. Deep benchmark detail

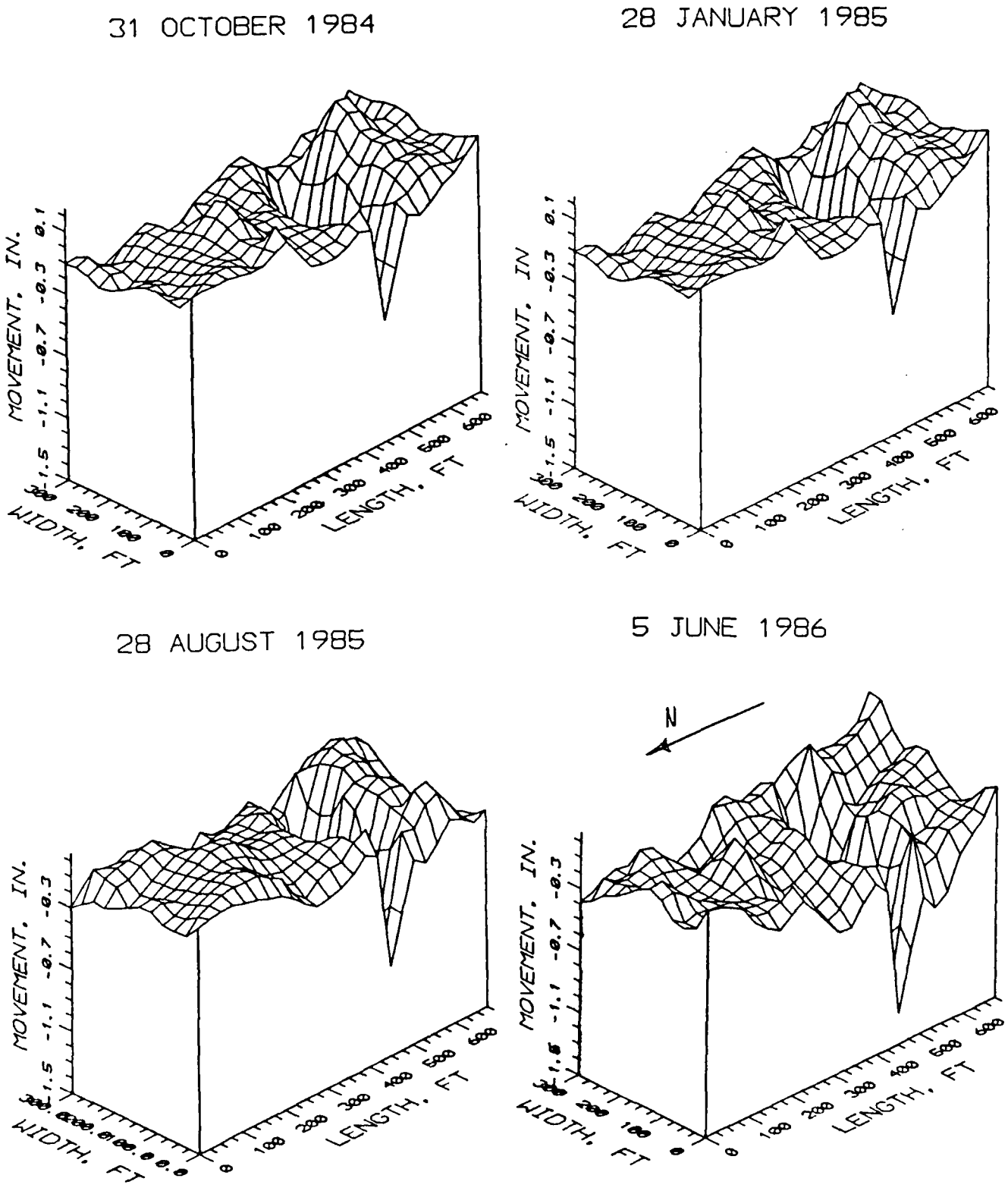

Figure 60. Three-dimensional view of mat movement

12 MAY 1987

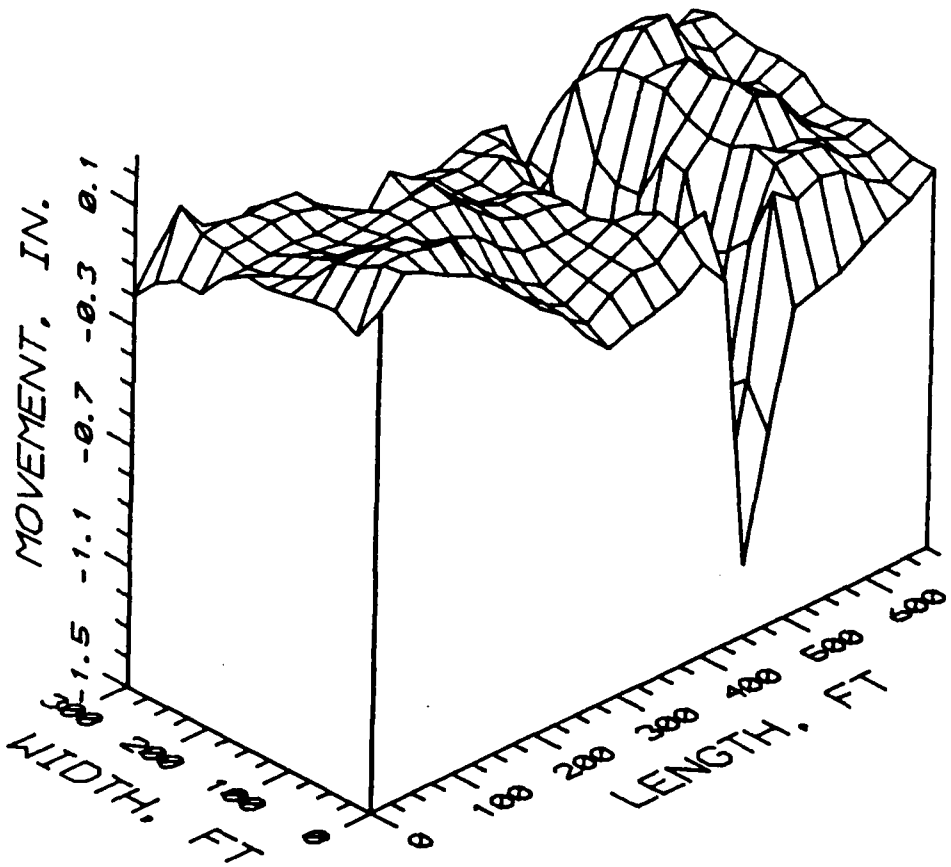

Figure 60. (Concluded)

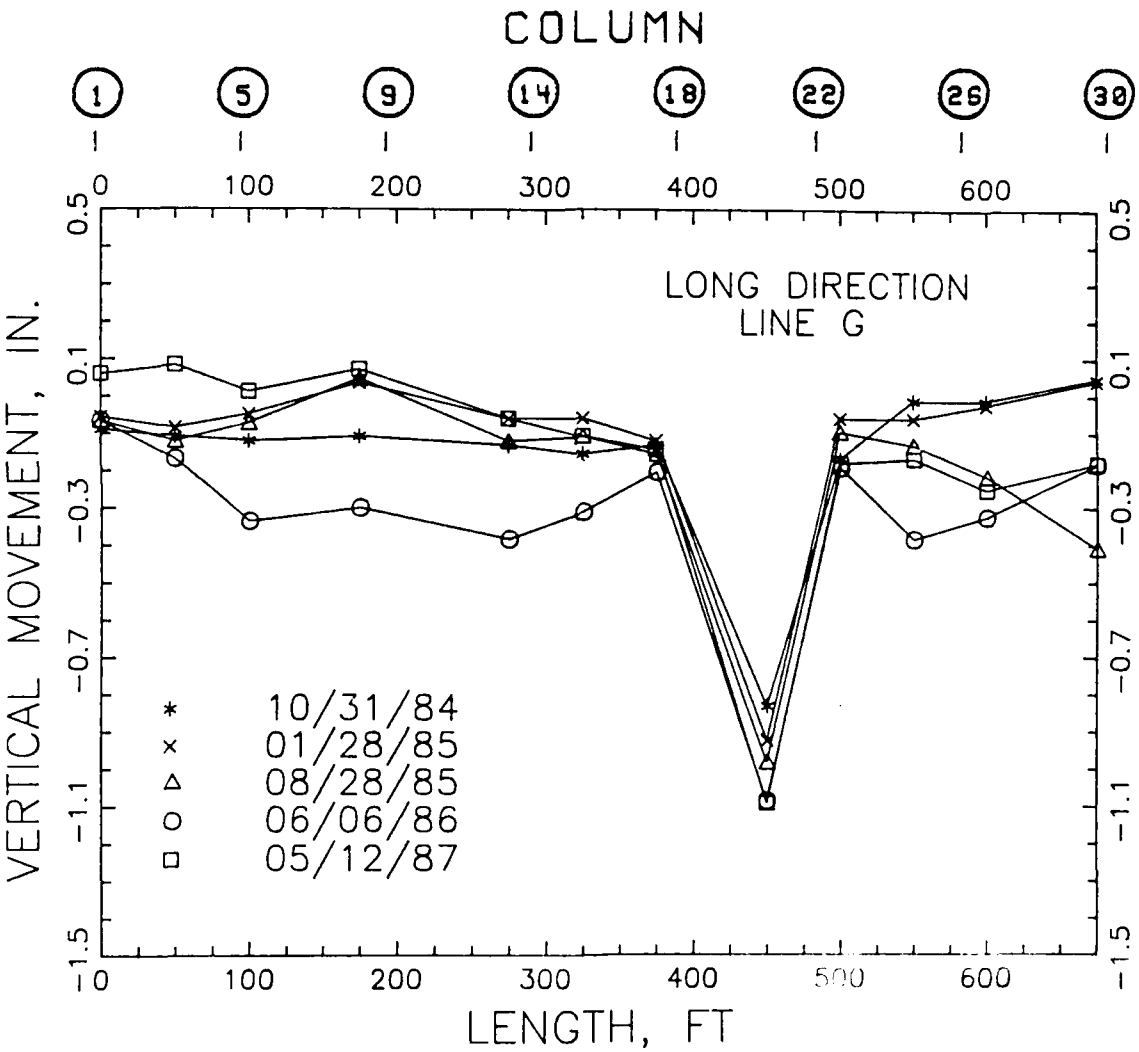

a. LONG DIRECTION LINE G

Figure 61. Two-dimension deformation patterns

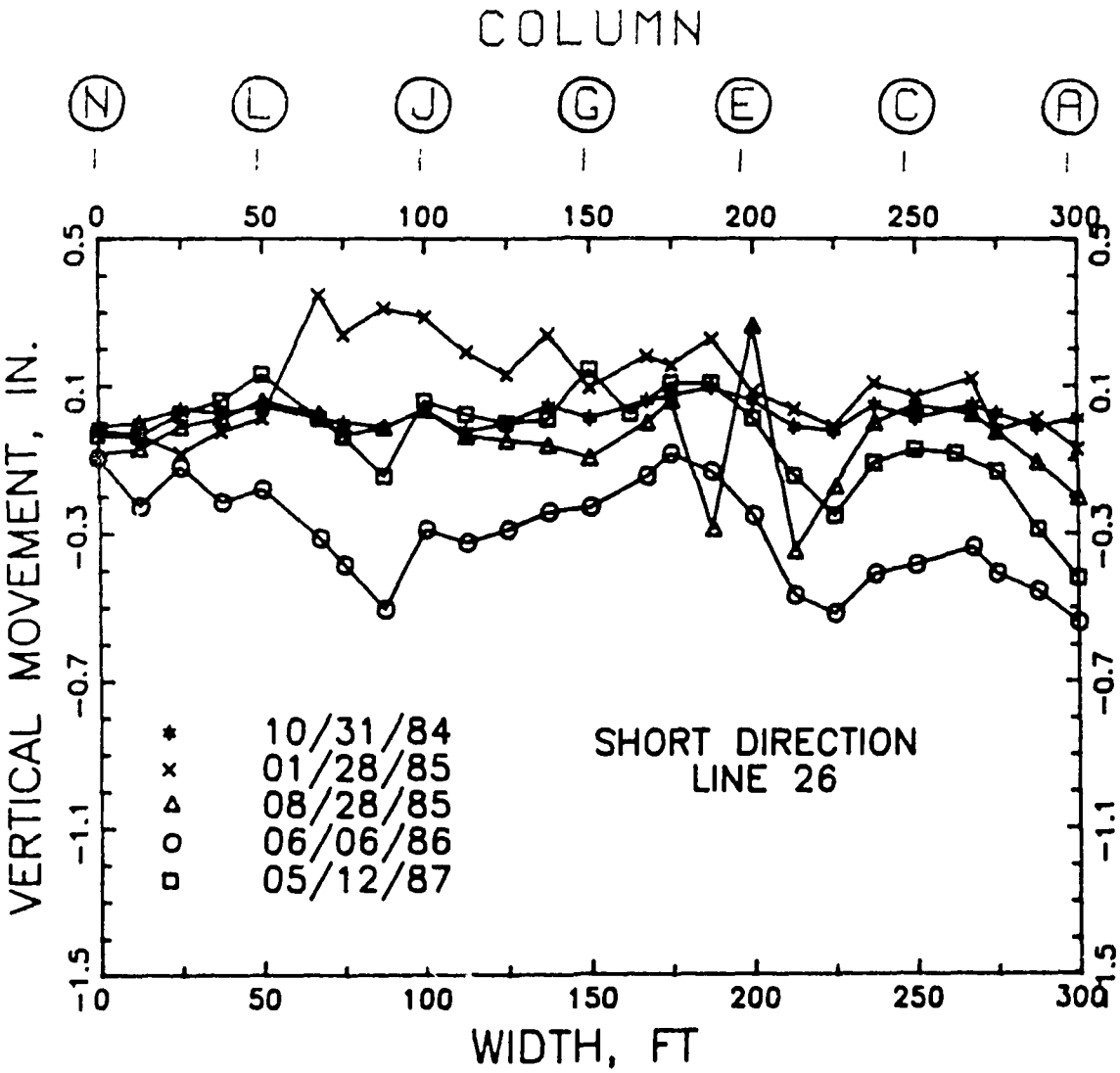

b. SHORT DIRECTION LINE 26

Figure 61. (Concluded)

taken from line A to line N (0 to 304 ft), Figure 53. The deformation in the long direction, Figure 61a, tends to show a dishing shape characteristic of a flexible plate on an elastic foundation, particularly by June 1986. The deformation in the short direction, Figure 61b, tends to show a rigid pattern. Differential moment Δ/L is about 1/600 and greatest in the short direction near column A at lines 20/21 where settlement into the old drainage ditch is significant. Settlement increases toward column N or the west.

Earth Pressure Cells

191. Installation. Thirteen Carlson soil earth pressure cells labeled M-1 to M-12 were placed on the bottom of the trench for the stiffening beam located along line 26 from Column A to Column G, Figure 53b, on 24 July 1984. These cells are 7.25 inches in diameter with a stem 4.35 inches high by 1 inch in diameter, Figure 62, and have a maximum pressure range of 50 psi. Details of the installation procedure are described in Instruction Report 3[65].

192. The moisture barrier was cut away at the bottom of the stiffening beam trench in each area where a pressure cell was to be placed and the subgrade surface scraped smooth. A thin layer of masonry sand was placed on the prepared subgrade surface to level each earth pressure cell. Each cell was held in place by a 2-inch layer of masonry sand/cement (3:1 ratio) mortar and allowed to set 24 hr prior to placement of concrete for the beam. Several shovels of concrete were manually placed around and on each cell immediately before concrete was placed in the grade beam trench on 25 July 1984. The minimum compressive strength of the concrete was 3000 psi.

193. Readings. Initial readings 20 hours (07/26/84) after placement of concrete in the stiffening beam trench indicates initial earth pressures of about 3 psi, Figure 63, consistent with the weight of the concrete in the beam trench. Earth pressures were larger near Column F consistent with the weight of a concrete pump truck providing concrete for placement of the flat portion of the mat south of line 26. The 40 hour readings appear erratic with greatest pressure near column G and zero pressure near Column E. Readings 1 day (08/03/84) after placement of the flat portion of the mat indicate some redistribution of earth pressures with maximum near column B.

---

[65]Sherman 1957

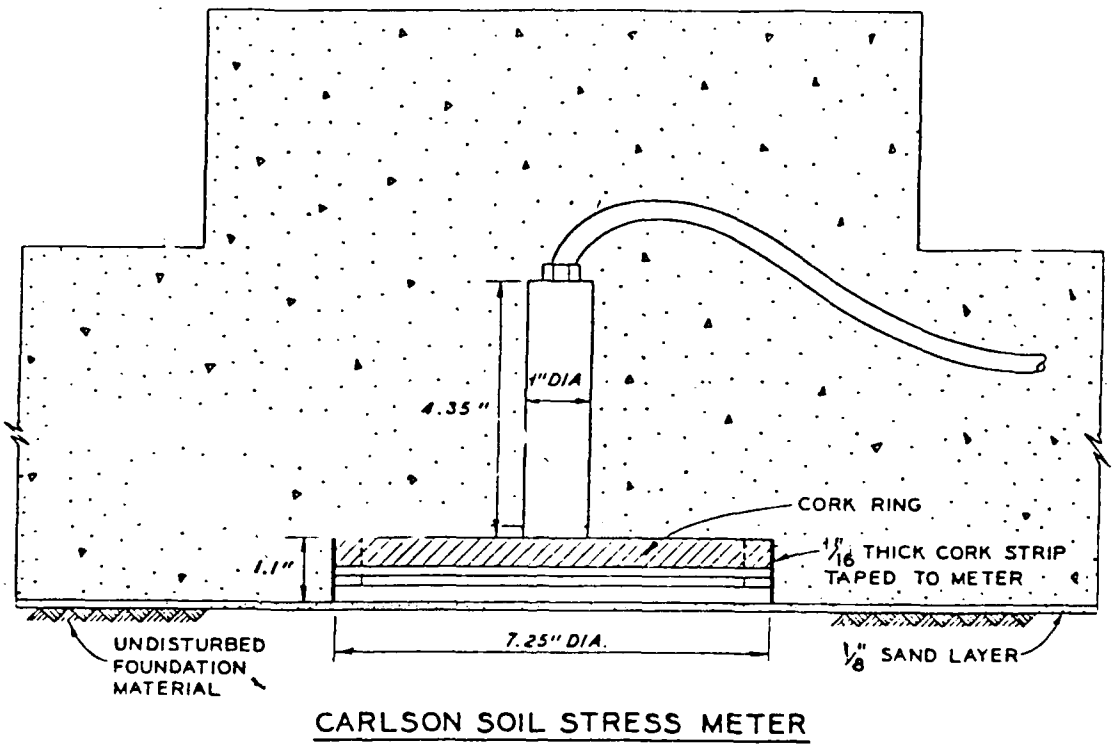

Figure 62. Diagram of earth pressure cell installation
(after Figure 16, Sherman and Trahan 1968)

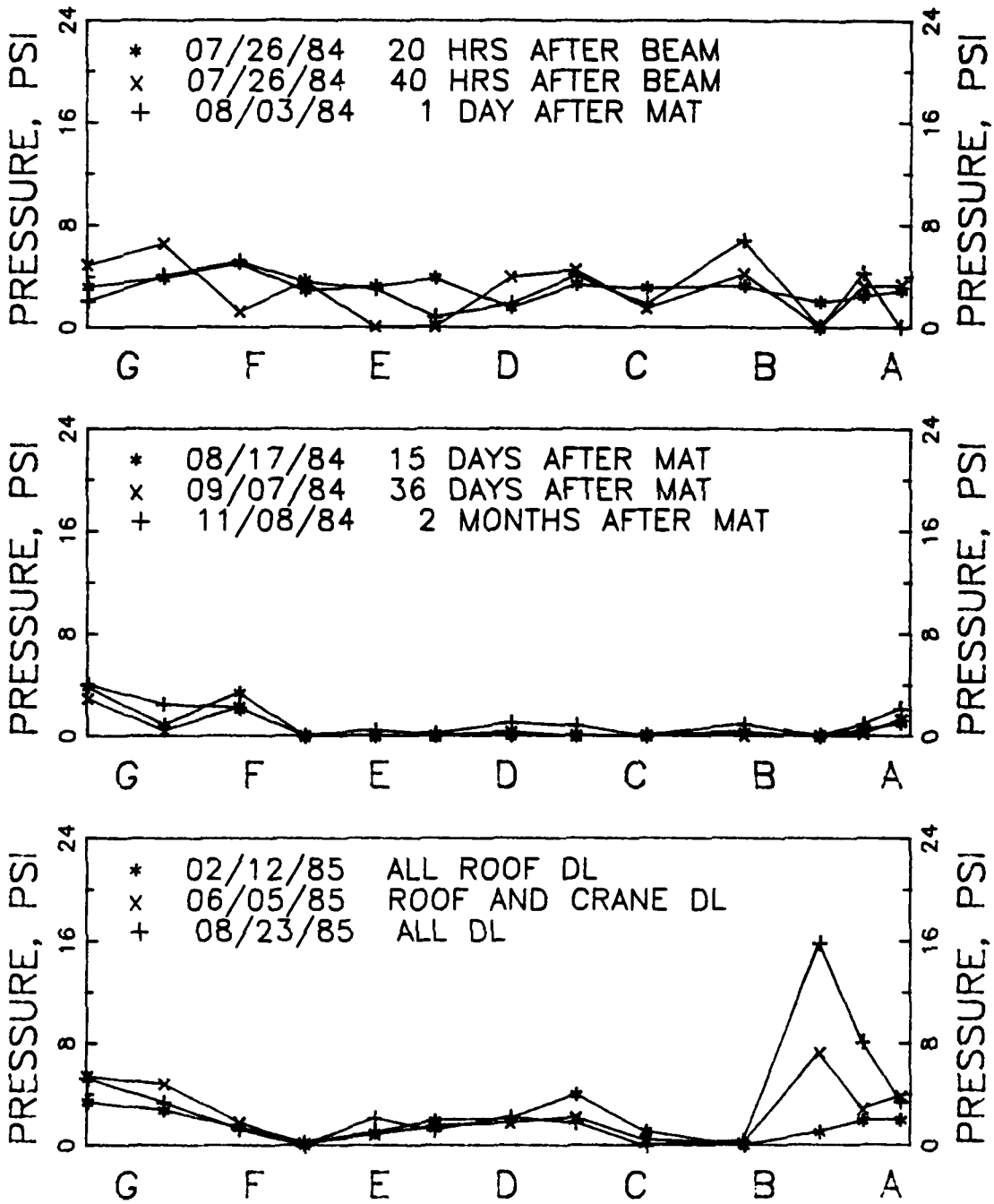

Figure 63. Earth pressures during construction

194. Readings taken 15 days (08/17/84) to 2 months (11/08/84) after mat placement, Figure 63, indicate earth pressures had decreased to zero or near zero between Columns F and A. Concrete shrinkage during cure appears to be transferring weight of the overlying beam and mat from the soil beneath the beam to adjacent soil beneath the flat portion of the mat to let the beam "hang" in the trench. This may increase the probability of cracking in the mat as loads are applied to the stiffening beams during construction until the stiffening beams are firmly seated on the underlying soil.

195. Permanent loads such as the roof dead load, roof live load, crane dead load, and wall loads for building 333 lead to axial loads of approximately 32, 64, and 128 kips for corners, edges, and interior columns (see paragraph 216). These loads are placed on widened beam sections of side 10.5 ft beneath each column, Figure 53b: squares for interior columns and triangles for perimeter or corner columns. The pressure applied on these widened sections assuming that all of the column load is concentrated only on these sections is about 8 psi. This pressure drops to about 4 psi assuming loads are actually distributed to a soil area twice the area of the widened beams. Maximum pressure on the foundation soil is designed to be less than 2 ksf or 14 psi.

196. Permanent dead loads from construction of the superstructure were in place by 23 August 1985. Earth pressures in 1985, Figure 63, vary from 4 to 6 psi near columns G and D. Earth pressures near the perimeter column A appear to be increasing substantially to at least 16 psi by 23 August 1985. Pressures between the column loads such as FE and CB are negligible.

197. Installation of equipment within the building continued from August 1985 through 1987. Earth pressures increased to about 9 psi at column G, remained stable at about 4 psi near column D and had increased substantially near column A exceeding 40 psi by 23 February 1987, Figure 64. Earth pressures at column G during operations of 25 May 1988, Figure 65, decreased to about 8 psi.

198. The extremely large perimeter earth pressure is consistent with the behavior in the short direction of a rigid mat on a semi-infinite elastic foundation cohesive (or cohesionless) soil and attributed to shear[43]. The relative displacement diagrams in Figures 60 and 61 tend to show rigidity in

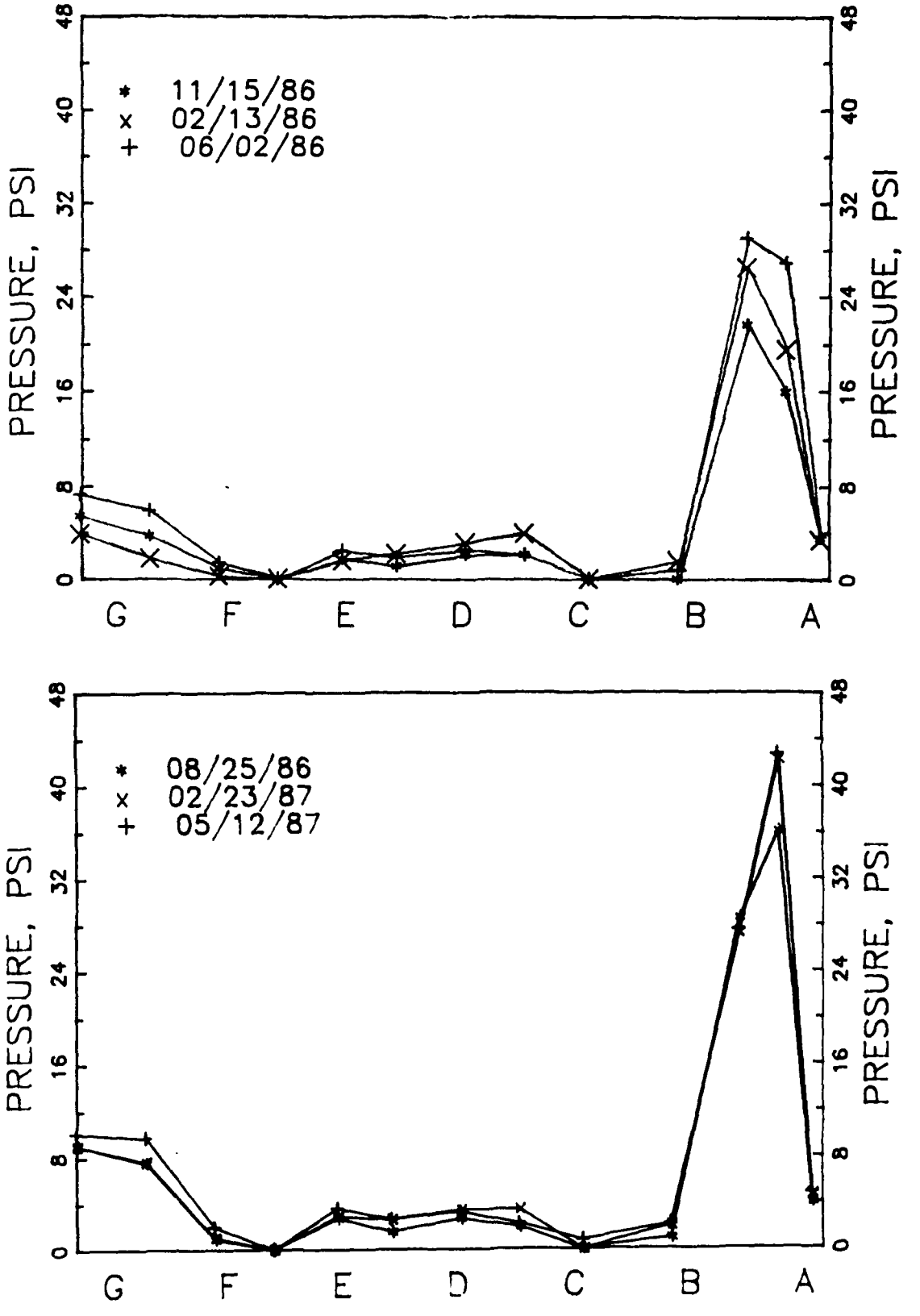

Figure 64. Earth pressures during equipment installation

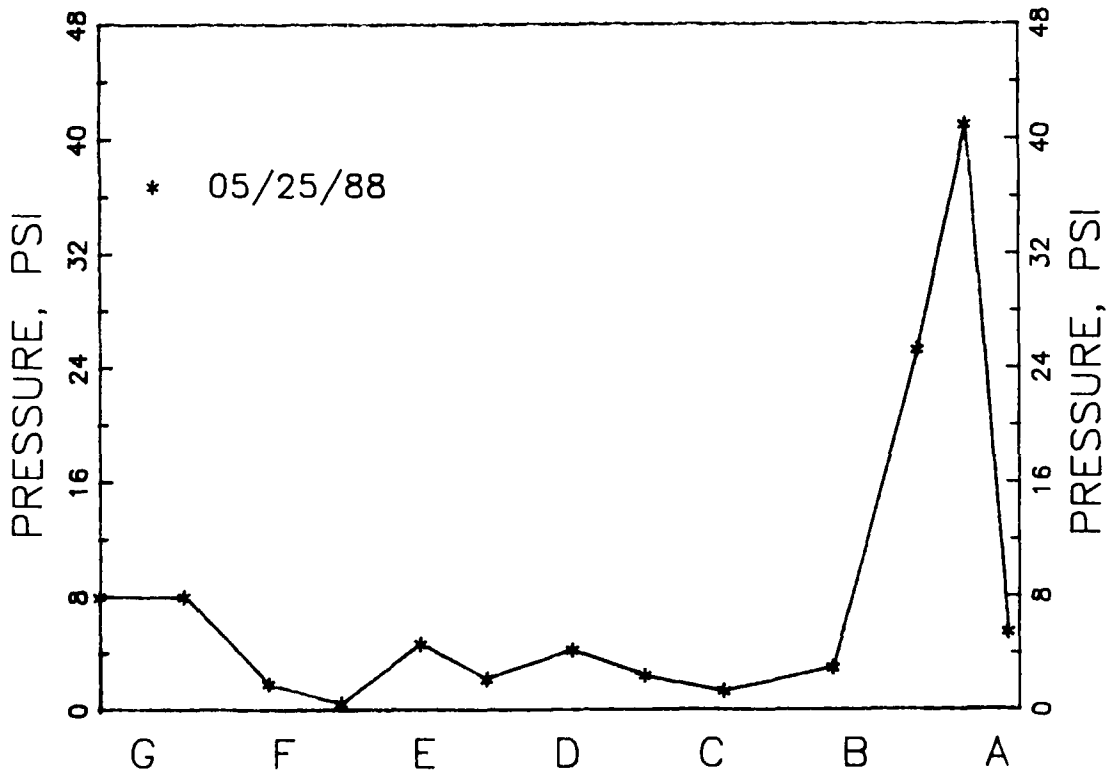

Figure 65. Earth pressures during operation

the short direction parallel with line 26 of the instrumented beam and the characteristic dish-shaped flexible behavior in the long direction. The distribution of earth pressures on both sides of column D shows the effect of beam stiffness on spreading the column loads to the underlying soil. Higher earth pressures at column G than at D may indicate less distribution of pressures from the footing to the soil beneath column G and possible fracture in the stiffening beam of the mat near column G. Visual observations indicate cracks in the mat betweem columns G and F. These observed earth pressures along line 26 appear consistent with observed deformation of the mat.

Strain Gages

199. Installation. Ten SR-4 type temperature compensated strain gages labeled SG-1 to SG-10 were mounted with epoxy cement to 3-ft lengths of No. 4 reinforcement bars at the Waterways Experiment Station by the Instrumentatiom Services Division. Strain gage assemblies SG-6 to SG-10 were tied to the inside of the bottom left No. 11 reinforcement bars looking west from Column A-26, Figure 53b. Strain gage assemblies SG-1 to SG-5 were tied to one of the two top No. 11 reinforcement bars. SG-1 and SG-2 were tied beneath the top left No. 11 bar (looking west from Column A-26) and SG-3, SG-4, and SG-5 were placed on the right side of the top left No. 11 bar. The top No. 11 bars are separated by 28 inches from the bottom reinforcement bars. Locations of these strain gages are illustrated in Figure 53b.

200. Cables from both earth pressure cells and strain gages were threaded through 2-inch diameter plastic electrical conduit placed on the existing ground surface 20 inches above the bottom of the stiffening beam adjacent to the stiffening beam on line 26. The electrical conduit and cables at Column A-26 were conducted ouside the mat perimeter through a 6-inch diameter opening made in the exterior stiffening beam. This opening is located about 18 inches above the bottom of the beam and 5 ft left of the center of Column A-26 viewing toward the west. The cable ends were coiled and placed in two concrete street light ground boxes located adjacent to the mat perimeter and level with the surface of the concrete ramp used by robot operated cargo containers.

201. Readings. Twenty hours (07/26/84) after the concrete was placed in the beam trench the initial readings of the five bottom gages indicated

about 90 microinches/inch of tension, Figure 66a. This tension is attributed to natural drying shrinkage of concrete[66]. Forty hours (07/27/84) after concrete placement the readings of the bottom gages indicated over 100 microinches/inch of compression beneath Column G. The stiffening beam near column G appears to be curling down consistent with the increased earth pressure observed near column G at this same time, Figure 63 (07/26/84). The compression continues to increase in the bottom strain gage beneath column G at 1 day (08/03/84) and 15 days (08/17/84) following placement of the concrete for the mat, Figure 66a. All of the bottom strain gages indicate some reduction in the initial tensile strains by 15 days after the mat concrete was placed indicative of an edge-down (or center heave) behavior. The top strain gages at this time are covered with concrete of the flat portion of the mat and indicate about 100 microinches/inch of tensile strain again attributed to natural drying shrinkage of concrete. Except for strains beneath and near column G, strains appear fairly uniform. The mat may be heaving slightly on line 26, which appears confirmed by the level survey along line 26 conducted 31 October 1984, Figure 60. This apparent heave may be attributed to arching from settlement exceeding 1 inch observed near lines 20/21 and settlement of about 0.2 inch observed at the perimeter on line 30, Figure 60. Heavy equipment stored in the south end of the building prior to installation may have contributed to settlement near the perimeter, Figure 60.

202. Continued construction of the superstructure with increased column loads cause substantial increases in compressive strains in the bottom strain gages beneath and near column G, Figure 66b. Some tensile strain still remains in the bottom gage beneath column G and near column A. The top strain gages indicate about -100 microinches/inch of tensile strain except beneath column G where compression is building up 2 months (11/08/84) after placement of the mat. By 12 February 1985, Figure 66b, compressive strain in the bottom gage beneath column G had peaked at about 800 microinches/inch and dropped back to about 400 microinches/inch by 5 June 1985. Tensile strains seem to be increasing in the top strain gages to about -150 microinches/inch by 5 June 1985, except beneath column G where compression had increased to about 250

[66]Ytterberg 1987

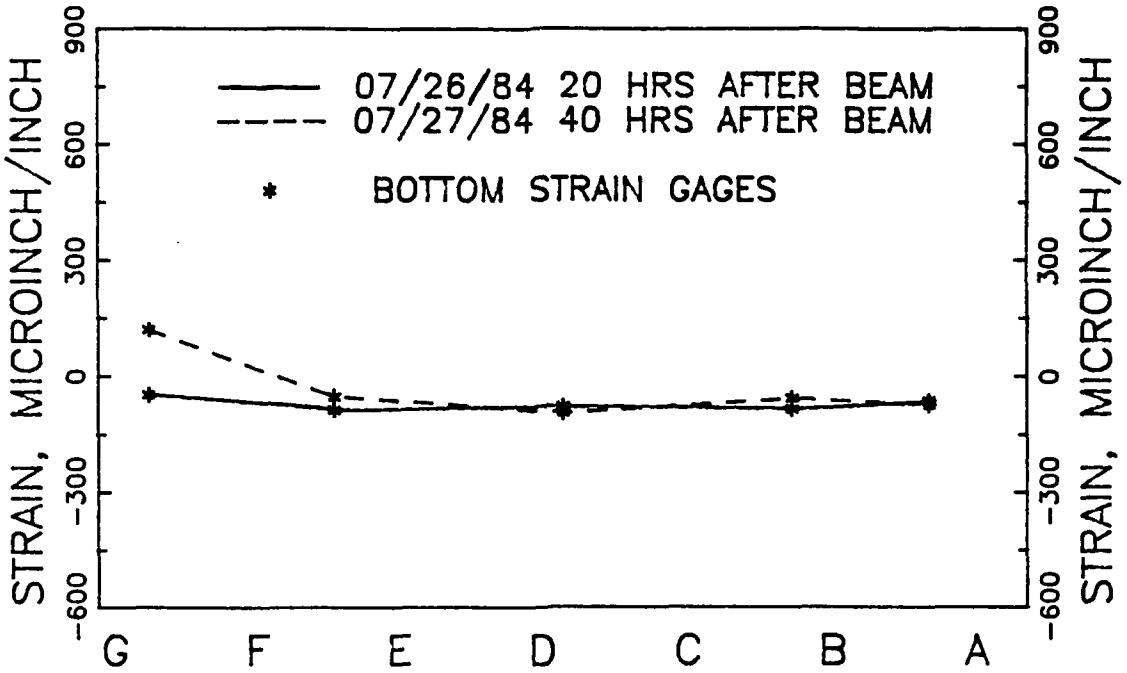

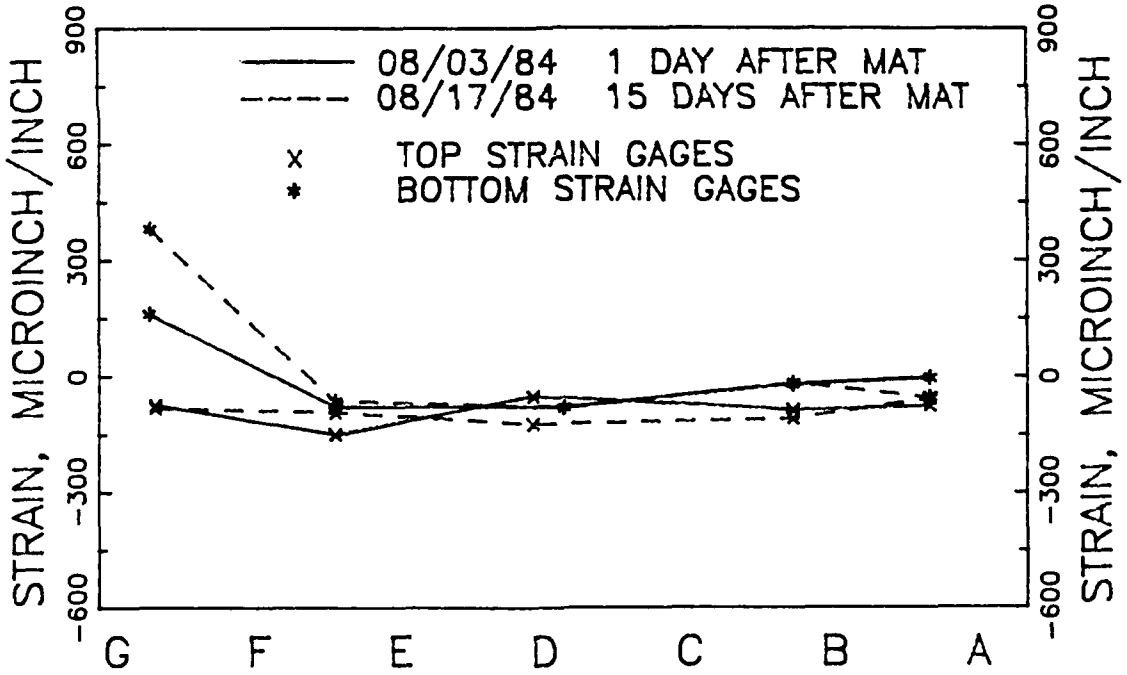

a. BEFORE SUPERSTRUCTURE CONSTRUCTION

Figure 66. Strains during construction

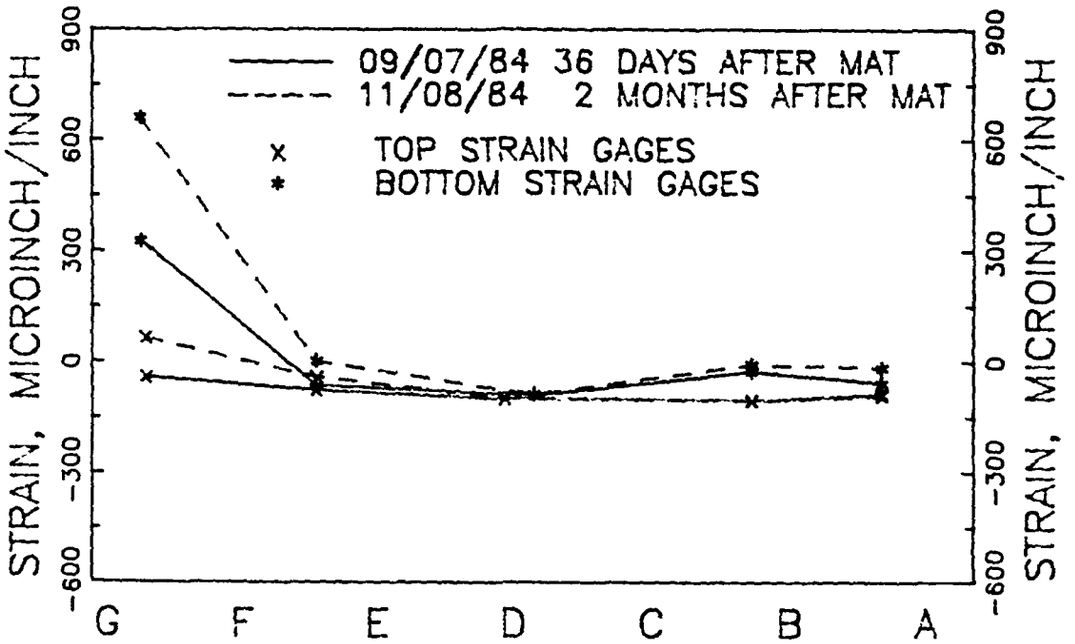

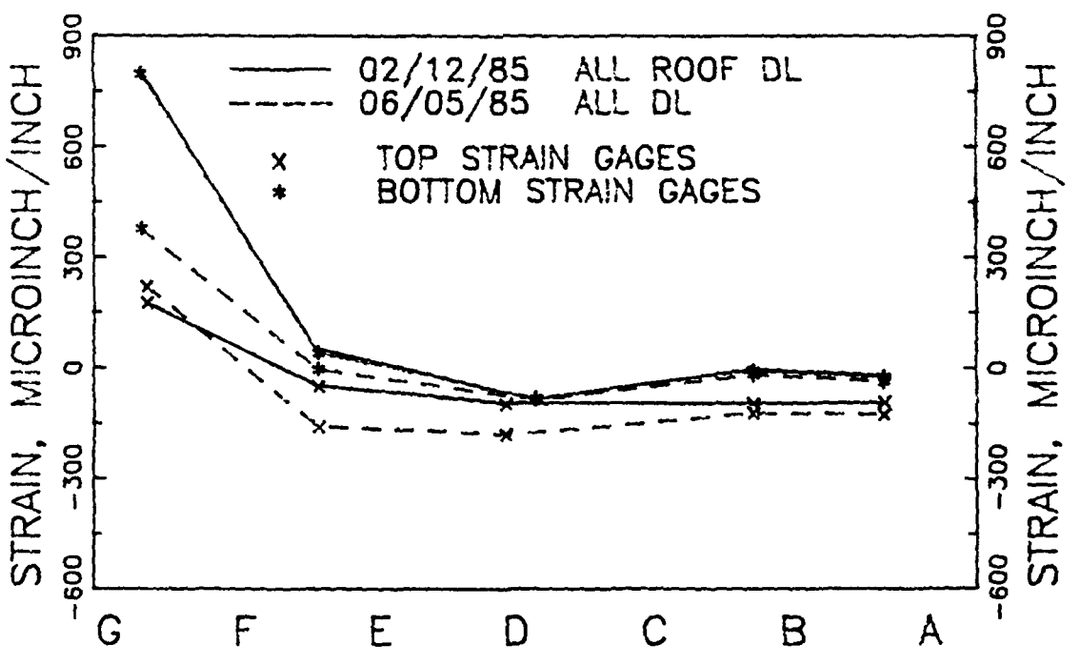

b. DURING SUPERSTRUCTURE CONSTRUCTION

Figure 66. (Concluded)

microinches/inch in the top strain gage. Continued drying shrinkage may have contributed to the greater tensile strains in the top gages. These strains indicate a concentration of strains (and stress) in the footing of column G. The level survey conducted 28 January 1985 indicate an increased center hump that diminished by 28 August 1985, Figure 60. Upward curling near edges or the perimeter attributed to moisture loss from the upper surface of the mat and drying shrinkage does not appear significant. Earth pressure cells indicate increased soil pressures beneath the columns, Figure 63, during superstructure construction.

203. The top strain gages are generally subject to more tensile strain than the bottom gages during equipment installation from 23 August 1985 to 2 June 1986, Figure 67. The plastic vapor barrier beneath the stiffening beams appears to have restricted evaporation of moisture from near the bottom of the stiffening beams, while evaporation and drying shrinkage continued from the mat surface. The level surveys of 28 August 1985 and 28 January 1986 confirm a humped distortion pattern along line 26, Figure 60. Compressive strains were increasing in the bottom strain gage beneath column G from 23 August 1985 through 13 February 1986, then dropped substantially indicating a large tensile strain of about 300 microinches/inch by 2 June 1986.

204. By 25 August 1986 tensile strain in the bottom strain gage near column G had increased in tension much further to -3000 microinches/inch suggesting a possible fracture in the bottom of the beam beneath or near column G, Figure 67. The compressive strain in the bottom gage near column F dropped nearly to zero by 25 August 1986. From 25 August 1986 through 23 February 1987 the strains in the two bottom gages near columns G and F appear to have rebounded and become positive; strains in the bottom gages indicate increasing tension near columns G, F, and A by 25 May 1988. Tensile strains in the top gages appear fairly steady from 23 February 1987 through 25 May 1988. Additional drying shrinkage appears insignificant since August 1986. The level survey conducted 6 June 1986, Figure 61b, shows a reversal of curvature near column G compared to the earlier level survey of 28 August 1985. Column G appears to have risen some from 6 June 1986 to 12 May 1987 consistent with increased compression in the bottom gages near G and F from 25 August 1986 to 23 February 1987, Figure 67.

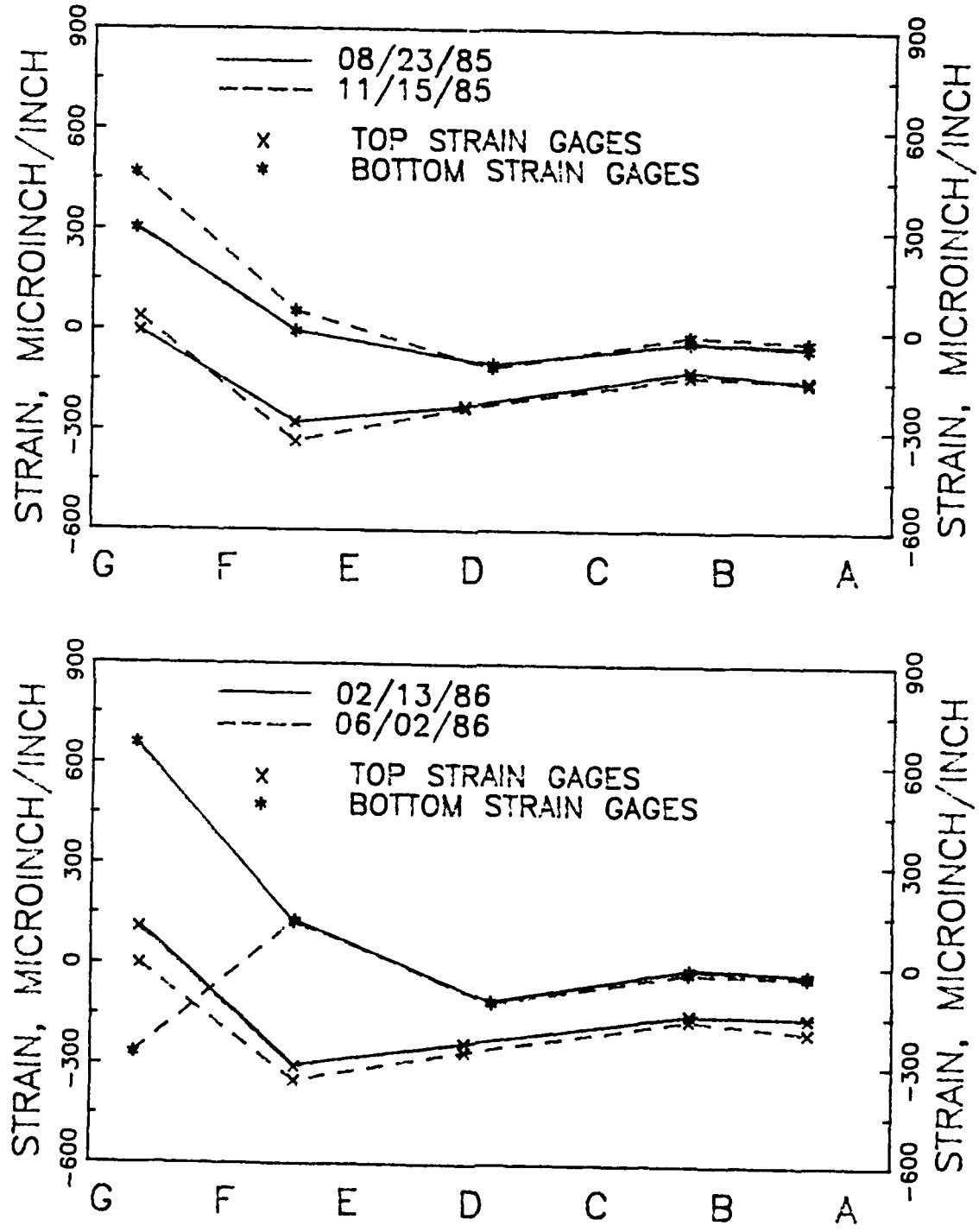

Figure 67. Strains during installation of equipment

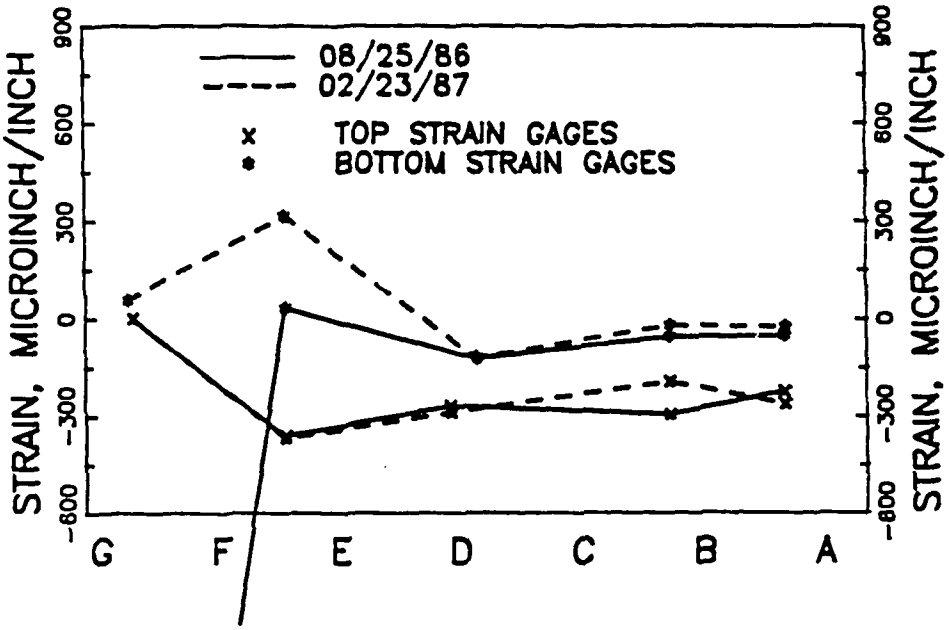

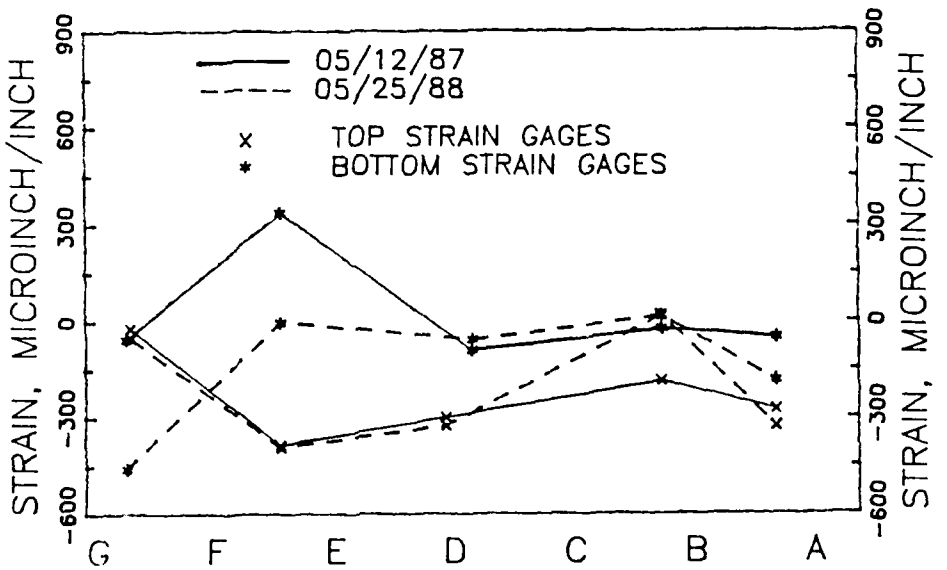

Figure 67. (Concluded)

205. Stress and bending moments. The strain data may be sorted into axial and bending strains and then converted to stresses and bending moments by compound stress theory[67]. This analysis ignores tensile strains from drying shrinkage and assumes no slip between the re-bar steel and the concrete. For the assumption of a rectangular section consisting of a typical stiffening beam, strains at the top ϵ_t and bottom ϵ_b of the beam, Figure 68, may be found from

$$\epsilon_t = \frac{d \cdot \epsilon_{tmeas} - D_{cov} \cdot \epsilon_{bmeas}}{d - D_{cov}} \tag{38a}$$

$$\epsilon_b = \frac{d \cdot \epsilon_{bmeas} - D_{cov} \cdot \epsilon_{tmeas}}{d - D_{cov}} \tag{38b}$$

where

ϵ_t = total strain top of section, μin./in.

ϵ_b = total strain bottom of section, μin./in.

ϵ_{tmeas} = strain measured in a gage mounted on the top reinforcement steel, μin./in.

ϵ_{bmeas} = strain measured in a gage mounted on the bottom reinforcement steel, μin./in.

d = $H_b - D_{cov}$, 31.33 in.

H_b = height of beam, 36 in.

D_{cov} = distance from beam surface to center of reinforcement steel, 4.67 in.

For the stiffening beam of building 333 where $d = 31.33$ inches and $D_{cov} = 4.67$ inches, top and bottom total strains are

$$\epsilon_t = 1.175\epsilon_{tmeas} - 0.175\epsilon_{bmeas} \tag{39a}$$

$$\epsilon_b = 1.175\epsilon_{bmeas} - 0.175\epsilon_{tmeas} \tag{39b}$$

206. Axial ϵ_a and bending strains top ϵ_{mt} and bottom ϵ_{mb} may be found from ϵ_t and ϵ_b by

$$\epsilon_a = \frac{\epsilon_b C_t - \epsilon_t C_b}{C_t + C_b} \tag{40a}$$

[67]Popov 1968

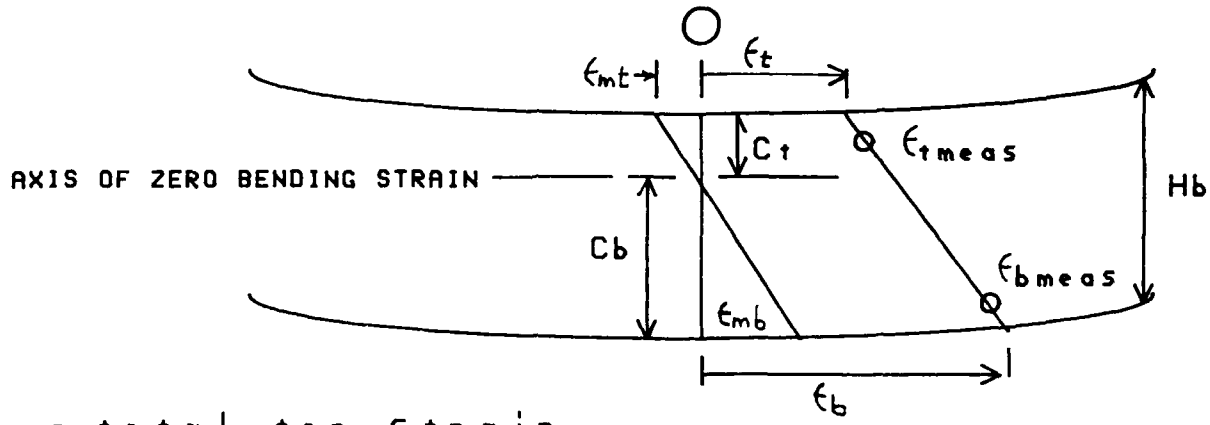

ϵ_t = total top strain
ϵ_b = total bottom strain
ϵ_{tmeas} = measured strain on top reinforcement bar
ϵ_{bmeas} = measured strain on bottom reinforcement bar
Hb = height of beam
Ct = distance above axis of zero bending strain
Cb = distance below axis of zero bending strain

+M

a. DIAGRAM OF STRAIN

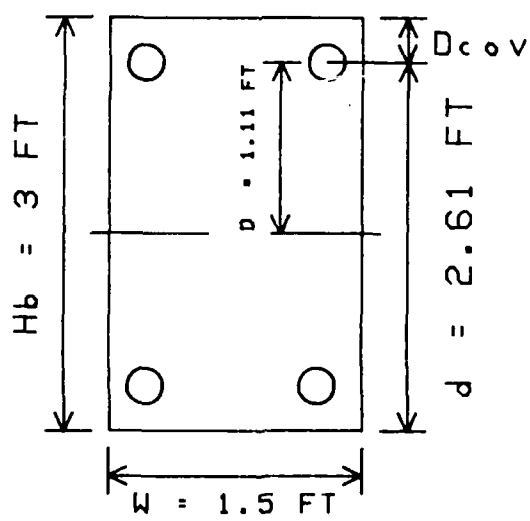

b. BEAM DIMENSIONS

Figure 68. Schematic of strain distribution in beam

$$\epsilon_{mt} = (\epsilon_t - \epsilon_b) \frac{C_t}{C_t + C_b} \tag{40b}$$

$$\epsilon_{mb} = (\epsilon_b - \epsilon_t) \frac{C_b}{C_t + C_b} \tag{40c}$$

where

ϵ_a = axial strain, μin./in.

ϵ_{mt} = top bending strain, μin./in.

ϵ_{mb} = bottom bending strain, μin./in.

C_t = distance from top to axis of zero bending strain, in.

C_b = distance from bottom to axis of zero bending strain, in.

The neutral axis is the axis of zero bending strain and has been taken as the distance kd below the top of the mat where kd is defined in Table 10. The actual depth of the neutral axis in the T-section will probably be in the upper half of the beam below the bottom of the slab or the T-section flange.

207. The axis of zero bending in the rectangular section of interest in this analysis is assumed for simplicity to be in the centroid. Then, $C_t = C_b$ and

$$\epsilon_a = \frac{\epsilon_t + \epsilon_b}{2} \tag{41a}$$

$$\epsilon_{mt} = \frac{\epsilon_t - \epsilon_b}{2} \tag{41b}$$

$$\epsilon_{mb} = \frac{\epsilon_b - \epsilon_t}{2} \tag{41c}$$

208. Axial stress σ_a may be evaluated from

$$\sigma_a = E_{eff} \cdot \epsilon_a \tag{42}$$

where

σ_a = axial stress, ksf

E_{eff} = effective modulus of elasticity of the section, ksf

The effective modulus of the rectangle section may be found from

$$E_{eff} = \frac{E_s I_s + E_c (I_c - I_s)}{I_c} \tag{43a}$$

$$I_c = \frac{W H_b^3}{12} \tag{43b}$$

$$I_s = 4 I_{so} + 4 A_s d_1^2 \tag{43c}$$

where

E_s = modulus of elasticity of steel, 4,320,000 ksf

E_c = modulus of elaticity of concrete, 432,000 ksf

I_s = steel moment of iertia, .054 ft^4

I_c = concrete moment of iertia, 3.375 ft^4

W = width of beam, 1.5 ft

H_b = height of beam, 3 ft

I_{so} = $(\pi/4) r^4$, ft^4

r = radius of reinforcement steel, .059 ft

A_s = cross-section area of steel bar, .0108 ft^2

d_1 = distance from center of beam to center of reinforcement steel, 1.1108 ft

Substituting the above values into Equation 43a leads to E_{eff} = 489,600 ksf.

209. Figure 69a shows the distribution of axial stress on line 26 including drying shrinkage from A to G calculated using Equation 42 from the strain measurements for 12 May 1987 and 25 May 1988 assuming E_{eff} = 489,600 ksf. Figure 69b shows the axial stress distribution with the initial tensile strain of at least -90 μin./in. subtracted from the measured strains. The stiffening beam is still in tension except near B where level measurements indicate a slight hump, Figure 60. The initial tensile strains may be associated with the drying shrinkage.

210. The bending moment M may be evaluated from

$$M = -\epsilon_{mb} \frac{E_{eff} I_c}{C_b} \tag{44}$$

where

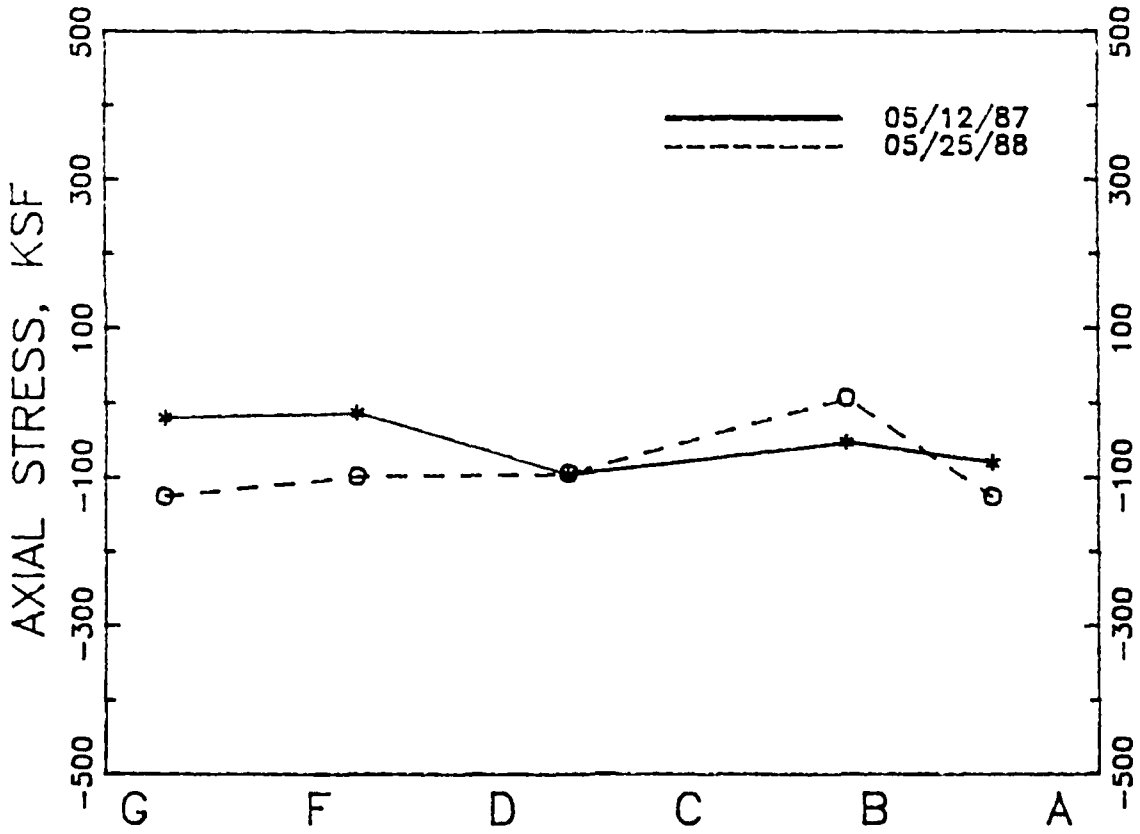

a. WITH DRYING SHRINKAGE STRAINS

Figure 69. Axial stresses from strain data

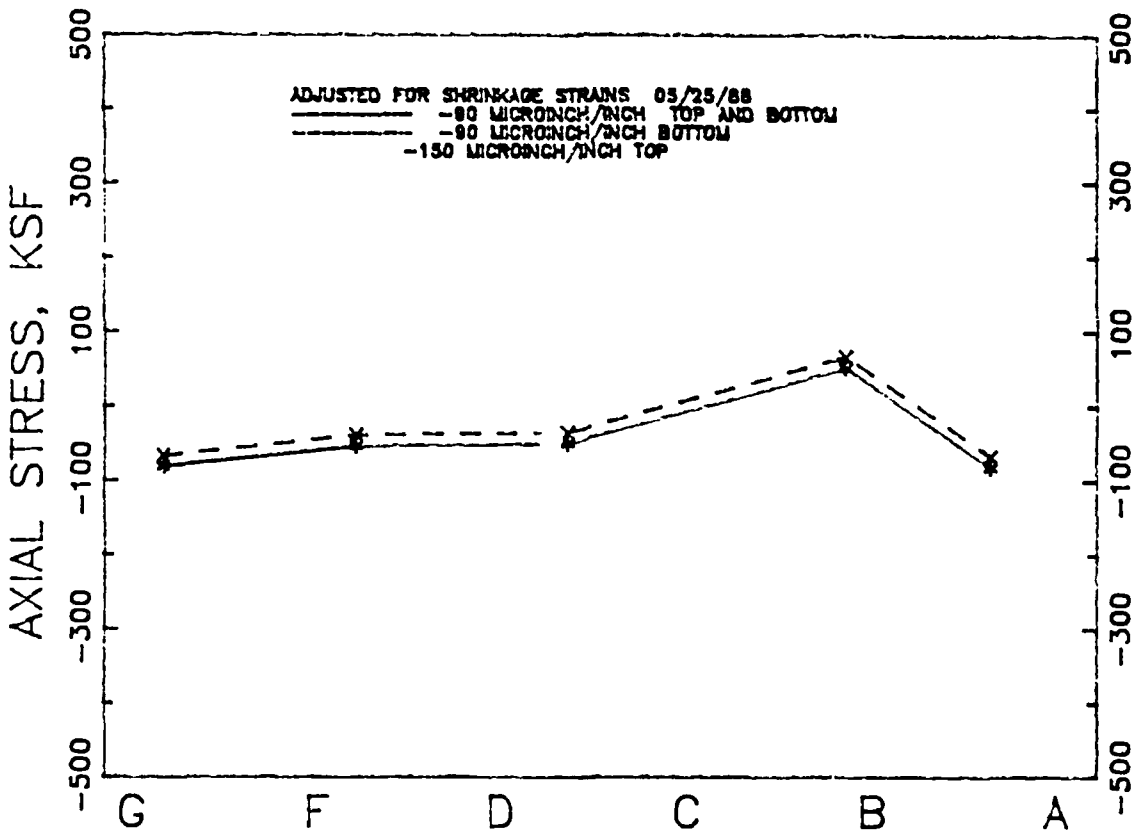

b. WITHOUT DRYING SHRINKAGE STRAINS

Figure 69. (Concluded)

M = bending moment, kip-ft/ft

$E_{eff}I_c$ = stiffness of composite section, ksf-ft^2

C_b = 1.5 ft

Figure 70a shows the distribution of bending moments in the instrumented beam on line 26 for 12 May 1987 and 25 May 1988 including drying shrinkage. Figure 70b shows the bending moment distribution when excluding drying shrinkage. A positive bending moment indicates a depression and a negative bending moment indicates a hump in the surface, Figure 68a. Bending moments tend to be negative indicating an edge down pattern or hump, which is consistent with displacements on line 26 in Figure 61b. Bending moments near G are positive indicating a dish-shaped (center down) pattern consistent with Figure 61b at this location (150 ft on line 26). A large negative bending moment of about -30 kip-ft/ft existed near F, 12 May 1987. The resisting bending moment for the steel reinforcement of two No. 11 bars top and bottom is 435 kip-ft or 35 kip-ft/ft assuming a 12.5-ft spacing between stiffening beams after the calculation for moments given in Table 10. Observations of fractures near columns F and G indicate some distress in the mat. The distortion pattern on line 26, Figure 61b, for 12 May 1987 is consistent with these bending moment signs: a depression near G and a hump near F (150 to 200 ft).

Analyses

211. Analyses selected to determine the performance of the mat foundation supporting building 333 include plate on elastic foundation using program SLAB2, beam on Winkler foundation using CBEAMC, and the frequency spectrum model. The distortion pattern observed through May 1987 indicates primarily elastic compression. Accomplishment of the proposed analyses requires that (1) pertinent soil input parameters simulating the in situ environment should be determined, (2) the size, depth, and stiffness of the mat foundation should be characterized, and (3) a reasonable magnitude and distribution of structural loads should be estimated.

Input Parameters

212. Soil. Input parameters of these soils required for analyses of mat performance includes values for the soil Poisson's ratio, effective soil elastic modulus, and the effective coefficient of subgrade reaction.

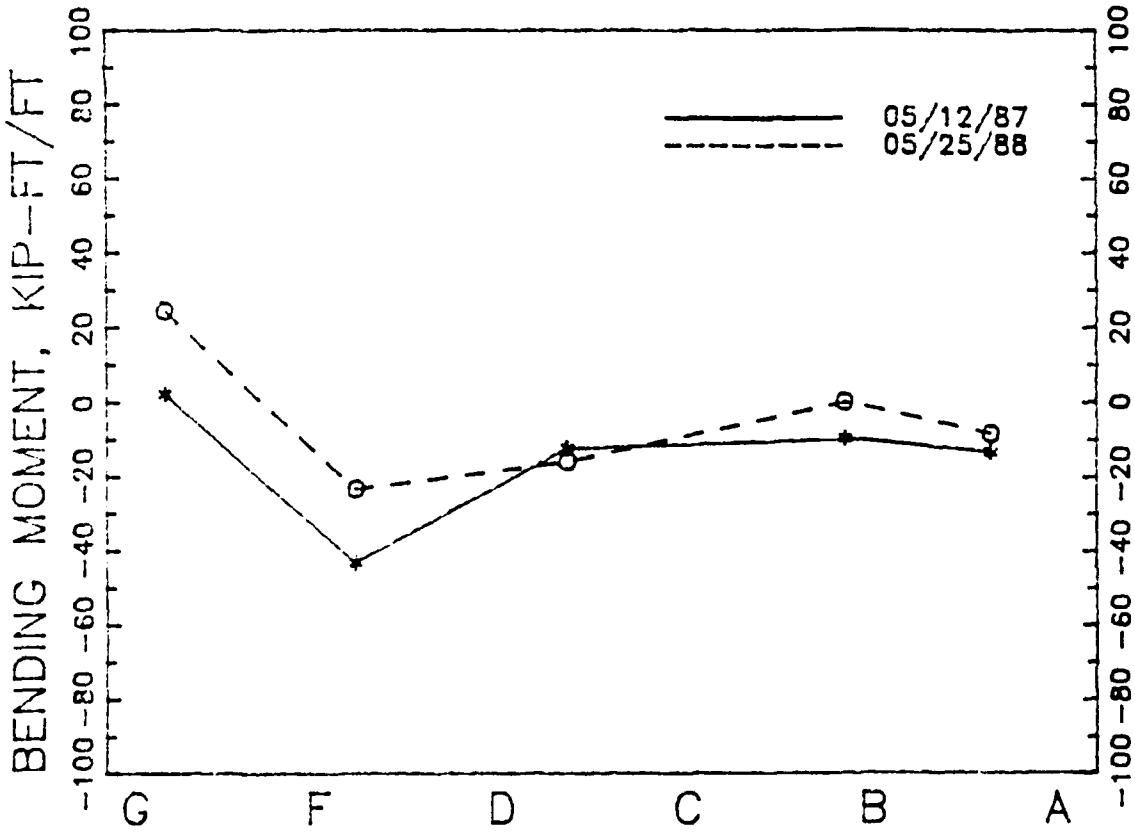

a. WITH DRYING SHRINKAGE STRAIN

Figure 70. Bending moments from strain data

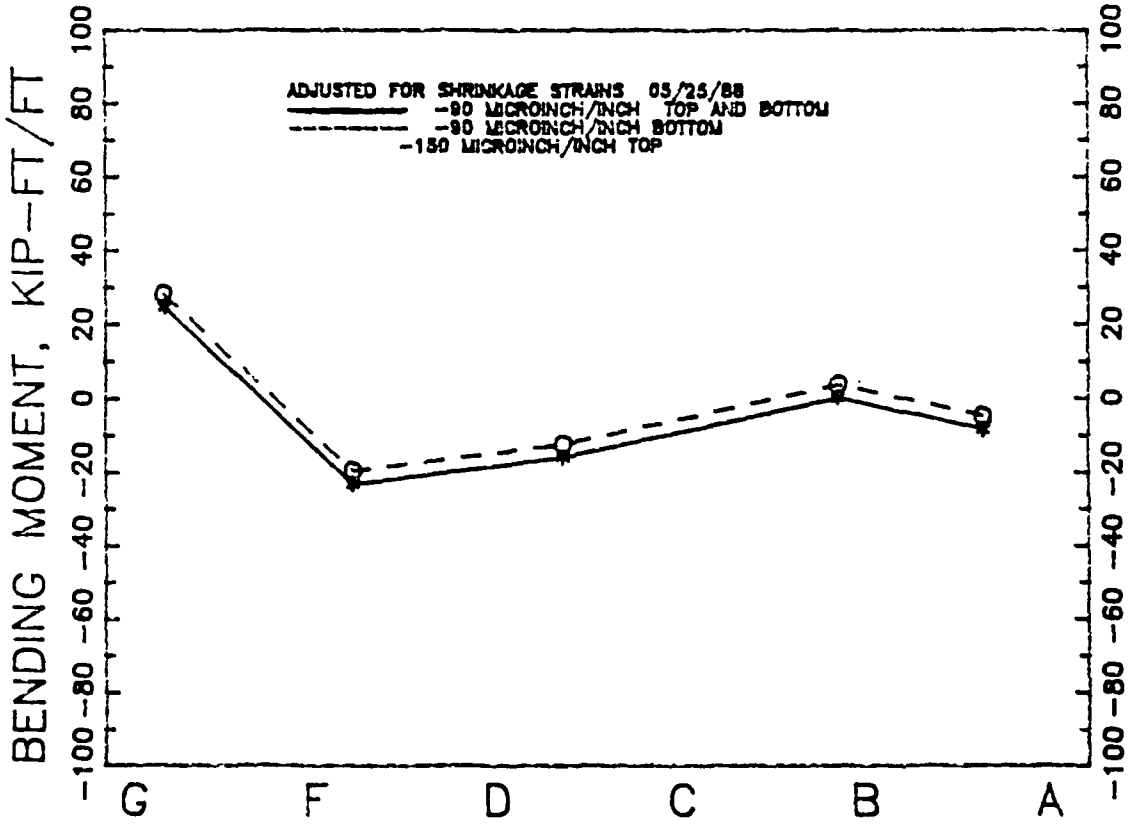

b. WITHOUT DRYING SHRINKAGE STRAINS

Figure 70. (Concluded)

Piezometric data indicate that a perched water table exists at this site near the bottom of the nonexpansive fill. Variations of the groundwater level of this water table are assumed to have negligible effect on soil volume changes. The overall Poisson's ratio of the soil at this site is assumed 0.4.

213. The strength and stiffness of the soil may be approximated as increasing linearly with depth, Figures 54b and 55b. The effective elastic soil modulus may therefore be estimated from Equation 4c for a soil with an elastic modulus that increases linearly with depth down to an essentially infinite depth

$$E_s^* = \frac{2kR(1 - \mu_s)}{0.7 + (2.3 - 4\mu_s)\log_{10} n} \tag{4c}$$

$$E_s^* = \frac{2 \cdot 30 \cdot 255.93 \cdot (1 - 0.16)}{0.7 + (2.3 - 1.2)\log 85.31}$$

$$E_s^* = 4{,}567 \text{ ksf} \quad (31{,}718 \text{ psi})$$

where

k = constant relating elastic soil modulus with depth, 30 ksf/ft from Equation 31

R = equivalent mat radius, $\sqrt{LB/\pi}$, 255.93 ft

L = mat length, 677.8 ft

B = mat width, 303.6 ft

μ_s = Poisson's ratio of soil, 0.4

n = R/D_b, 85.31

D_b = depth of mat below ground surface, 3 ft

The soil elastic modulus at the ground surface E_o is taken as zero. An effective modulus of 4,567 ksf or 31,718 psi is substantially larger than that evaluated from any of the soil samples above 80 ft of depth below ground surface. The Gibson model, Equation 4d, calculates a nearly identical modulus $E_s^* = 304 \bullet 30/2 = 4560$ ksf.

214. A coefficient of subgrade reaction k_{sf} applicable to this mat may be estimated after Equation 8a

$$k_{sf} = \frac{E_s^*}{\mu_0\mu_1 B} \tag{8a}$$

$$k_{sf} = \frac{4567}{\mu_0\mu_1 \cdot 303.6}$$

$$k_{sf} = \frac{15}{\mu_0\mu_1} \text{ ksf/ft or } \frac{8.7}{\mu_0\mu_1} \text{ psi/in}$$

where $\mu_0\mu_1$ is the influence factor. For L/B = 2 similar to this mat supporting building 333 (L/B = 677.8/303.6 = 2.23), $\mu_0\mu_1$ = 1.8, 1.5, 1.3, and 1.10 at the center, at the edge along the short direction B/2 from center, at the edge along the long direction L/2 from center, and at the corner, respectively, based on the case history analyses for ribbed mats given in paragraph 128, Part III. k_{sf} is therefore 8.3, 10.0, 11.5, and 13.6 ksf/ft (4.8, 5.8, 6.7, and 7.9 psi/in) from center to corner. At line 26 from Column A to G, $\mu_0\mu_1$ varies from 1.20 to 1.50; therefore, k_{sf} varies from 12.5 to 10.5 ksf/ft (7.3 to 5.8 psi/in.), respectively. Note that these values of k_{sf} are less than half of the constant k = 30 ksf/ft of Equation 31, paragraph 171. k_{sf} will be less than half of k when n > 100, Equation A7 which is consistent with the observed soil stiffness and location of this mat on the ground surface. The modulus of subgrade reaction k' input into program CBEAMC is found by multiplying k_{sf} by S, the width of the beam section.

215. Mat. The ribbed mat is 678 ft long by 304 ft wide with a cross grid of internal stiffening beams at a spacing of 12.5 ft within 50 ft of the perimeter and expansion joints located at lines 10-11 and 20-21, Figure 53. Each stiffening beam has dimensions indicated in Figure 71.

216. A computer program MOM.BAS was developed, Table 13, to evaluate the center of gravity and moments of inertia (M.O.I.) after Table B2. This program calculates T-section M.O.I. for uncracked, top cracked (cracked above the center of gravity) and bottom cracked (cracked below the center of gravity) T-sections. A description of input parameters is provided in the comment (REM) statements of the program in Table 13. Table 14 provides the center of gravity and M.O.I. in the long and short directions for the mat supporting building 333. For example, the total uncracked moment of inertia

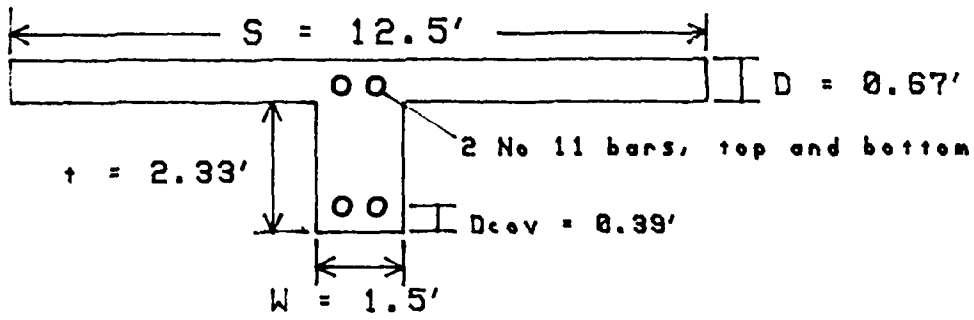

a. INTERIOR T-SECTION 1

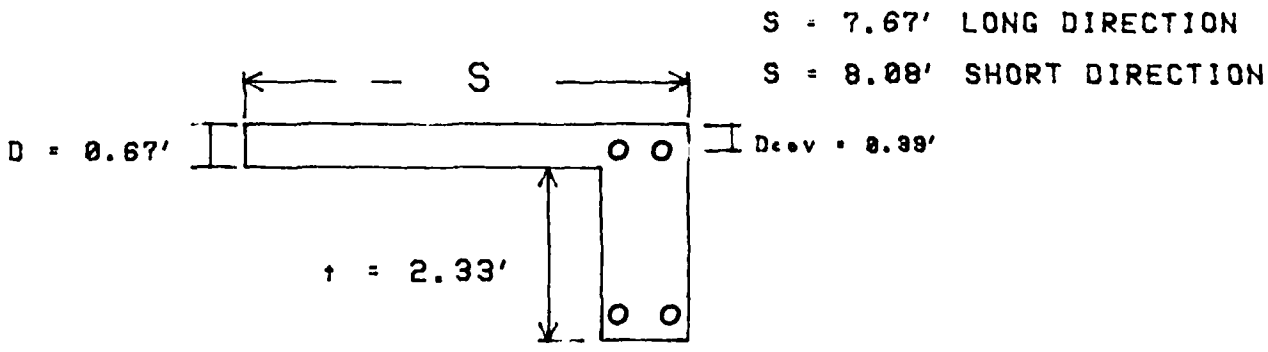

b. END SECTION 2

Figure 71. T- and End-section dimensions for stiffening beams supporting building 3??

Table 13

Listing of Computer Program MOM.BAS

```
100  REM PROGRAM MOM.BAS FOR MOMENT OF CROSS-SECTION INERTIA
110  REM NCR=1 IF UNCRACKED; =2 IF TOP CRACKED; =3 IF BOTTOM CRACKED
120  REM A$ = "DESCRIPTION OF CROSS-SECTION"
130  REM NISEC = NUMBER OF T-SECTIONS OF DIFFERENT DESIGN IN THE SECTION
140  REM EC = CONCRETE ELASTIC MODULUS, PSI; EST = STEEL ELASTIC MODULUS
150  REM W = BEAM WIDTH, INCHES; T = BEAM HEIGHT EXCLUDING MAT THICKNESS, INCHES
160  REM S = FLANGE WIDTH ON T-SECTION, INCHES
170  REM D = THICKNESS OF FLAT PORTION OF MAT, INCHES
180  REM DIAMS = DIAMETER STEEL, INCHES
190  REM NB = NUMBER OF BARS IN BEAM BOTTOM; NT = NUMBER OF BARS IN BEAM TOP
200  REM COV = CONCRETE COVER OVER STEEL PLUS DIAMS/2, INCHES
210  REM M = NUMBER OF T-SECTIONS OF IDENTICAL DESIGN
220  PI=3.14159265
225  FOR NCR=1 TO 3
230  OPEN "C:RIB.DAT" FOR INPUT AS #1
240  INPUT #1,A$,NISEC,EC,ES
245  LPRINT A$
250  XMOI=0.0
260  FOR I=1 TO NISEC
270  INPUT #1,W,T,S,D,DIAMS,NB,NT,COV,M
280  AREAST = PI*(DIAMS/2.)^2.
290  XOST = PI*(DIAMS/2.)^4./4.
300  HC=(W*T^2. + S*D^2. + 2.*S*D*T)/(2.*(W*T + S*D))
310  LPRINT
320  LPRINT "CENTER OF GRAVITY =  ";HC;"  INCHES";"  FOR T-SECTION =    ";I
330  LPRINT
340  IF NCR=1 THEN GOTO 510
350  IF NCR=2 THEN GOTO 610
360  HCB=(W*(T+D-HC)*(D+T+HC)/2. + (S-W)*D*(T+D/2.) + NB*AREAST*COV)/(W*(T+D-HC) + (S-W)*D + NB*AREAST)
370  LPRINT "     CRACKED BOTTOM CENTER OF GRAVITY = ";HCB;"  INCHES^4"
380  XOORMCB=(S*D^3. + W*(T-HC)^3.)/12. + S*D*(D/2. + T - HCB)^2. + W*(T-HC)*(HCB-(HC+T)/2.)^2.
390  LPRINT "     CRACKED BOTTOM T-SECTION M.O.I. EXCLUDING STEEL = ";XOORMCB;"  INCHES^4"
400  XIOSTB=NB*(XOST + AREAST*(HCB-COV)^2.)
410  XIOSTT=NT*(XOST + AREAST*(T+D-COV-HCB)^2.)
420  LPRINT "     BOTTOM STEEL M.O.I. = ";XIOSTB;"  INCHES^4"
430  LPRINT "     TOP    STEEL M.O.I. = ";XIOSTT;"  INCHES^4"
440  EI=EC*(XOORMCB - XIOSTT) + ES*(XIOSTB + XIOSTT)
450  XI=EI/EC
460  LPRINT "     EFFECTIVE BOTTOM CRACKED M.O.I. = ";XI;"  INCHES^4"
462  LPRINT
464  IF I=NISEC THEN LPRINT "          BOTTOM CRACKED"
470  GOTO 900
510  XOORM=(W*T^3. + S*D^3.)/12. + W*T*(HC - T/2.)^2. + S*D*(HC - T - D/2.)^2.
520  LPRINT "     UNCRACKED T-SECTION M.O.I. EXCLUDING STEEL =  ";XOORM;"  INCHES^4"
530  XST = NB*(XOST+AREAST*(HC-COV)^2.) + NT*(XOST+AREAST*(D+T-HC-COV)^2.)
540  LPRINT "     STEEL M.O.I. =  ";XST;"  INCHES^4"
550  EI=EC*(XOORM - XST) + ES*XST
560  XI=EI/EC
570  LPRINT "     EFFECTIVE M.O.I. = ";XI;"  INCHES^4"
572  LPRINT
574  IF I =NISEC THEN LPRINT "          UNCRACKED"
580  GOTO 900
610  HCT=(W*HC*HC/2. + NT*AREAST*(T+D-COV))/(W*HC + NT*AREAST)
620  LPRINT "     CRACKED TOP CENTER OF GRAVITY =";HCT;"  INCHES"
630  XOORMCT=W*HC^3./12. + W*HC*(HCT-HC/2.)^2.
640  LPRINT "     CRACKED TOP T-SECTION M.O.I. EXCLUDING STEEL = ";XOORMCT;"  INCHES^4"
650  XIOSTB=NB*(XOST + AREAST*(HCT-COV)^2.)
660  XIOSTT=NT*(XOST + AREAST*(T+D-COV-HCT)^2.)
```

Table 13 (Concluded)

```
670  LPRINT "     BOTTOM STEEL M.O.I. =";XIOSTB;"  INCHES^4"
680  LPRINT "     TOP    STEEL M.O.I. =";XIOSTT;"  INCHES^4"
690  EI=EC*(XOORMCT-XIOSTB) + ES*(XIOSTB + XIOSTT)
700  XI=EI/EC
710  LPRINT "     EFFECTIVE TOP CRACKED M.O.I. = ";XI;"  INCHES^4"
720  LPRINT
730  IF I =NISEC THEN LPRINT "          TOP CRACKED"
900  XMOI=XMOI + M*XI
910  NEXT I
930  B$ = "          TOTAL MOMENT OF INERTIA OF CROSS-SECTION =  "
940  LPRINT B$;
950  LPRINT USING "##########.##";XMOI;
960  LPRINT "  INCHES^4"
962  LPRINT
964  LPRINT
965  CLOSE #1
966  NEXT NCR
999  END
```

Table 14

Calculations of Moments of Inertia for building 333

a. Long Direction

```
LONG DIMENSION BUILDING 333

CENTER OF GRAVITY =   26.67606   INCHES  FOR T-SECTION =     1

     UNCRACKED T-SECTION M.O.I. EXCLUDING STEEL =   154325.2   INCHES^4
     STEEL M.O.I. =   1695.099   INCHES^4
     EFFECTIVE M.O.I. =  169016.1   INCHES^4


CENTER OF GRAVITY =   24.68387   INCHES  FOR T-SECTION =     2

     UNCRACKED T-SECTION M.O.I. EXCLUDING STEEL =   133777.4   INCHES^4
     STEEL M.O.I. =   1503.979   INCHES^4
     EFFECTIVE M.O.I. =  146811.9   INCHES^4

         UNCRACKED
         TOTAL MOMENT OF INERTIA OF CROSS-SECTION =    9251474.00  INCHES^4


LONG DIMENSION BUILDING 333

CENTER OF GRAVITY =   26.67606   INCHES  FOR T-SECTION =     1

     CRACKED TOP CENTER OF GRAVITY = 13.45862   INCHES
     CRACKED TOP T-SECTION M.O.I. EXCLUDING STEEL =  28481.48   INCHES^4
     BOTTOM STEEL M.O.I. = 279.7796   INCHES^4
     TOP    STEEL M.O.I. = 1073.988   INCHES^4
     EFFECTIVE TOP CRACKED M.O.I. =  41288.12   INCHES^4


CENTER OF GRAVITY =   24.68387   INCHES  FOR T-SECTION =     2

     CRACKED TOP CENTER OF GRAVITY = 12.47914   INCHES
     CRACKED TOP T-SECTION M.O.I. EXCLUDING STEEL =  22567.94   INCHES^4
     BOTTOM STEEL M.O.I. = 224.9115   INCHES^4
     TOP    STEEL M.O.I. = 1190.413   INCHES^4
     EFFECTIVE TOP CRACKED M.O.I. =  36024.5   INCHES^4

         TOP CRACKED
         TOTAL MOMENT OF INERTIA OF CROSS-SECTION =    2260320.00  INCHES^4


LONG DIMENSION BUILDING 333

CENTER OF GRAVITY =   26.67606   INCHES  FOR T-SECTION =     1

     CRACKED BOTTOM CENTER OF GRAVITY =  31.83818   INCHES^4
     CRACKED BOTTOM T-SECTION M.O.I. EXCLUDING STEEL =  6917.514
     BOTTOM STEEL M.O.I. =  2420.525   INCHES^4
     TOP    STEEL M.O.I. =  .4696128   INCHES^4
     EFFECTIVE BOTTOM CRACKED M.O.I. =  30319.99   INCHES^4
```

Table 14 (Continued)

```
CENTER OF GRAVITY =   24.68387   INCHES  FOR T-SECTION =     2

     CRACKED BOTTOM CENTER OF GRAVITY =  31.46775   INCHES^4
     CRACKED BOTTOM T-SECTION M.O.I. EXCLUDING STEEL =  5756.839
     BOTTOM STEEL M.O.I. =  2356.544   INCHES^4
     TOP    STEEL M.O.I. =  1.272744   INCHES^4
     EFFECTIVE BOTTOM CRACKED M.O.I. =  28547.8   INCHES^4

          BOTTOM CRACKED
          TOTAL MOMENT OF INERTIA OF CROSS-SECTION =    1664055.00  INCHES^4
```

DATA FOR LONG DIRECTION

```
"LONG DIMENSION BUILDING 333",2,3.0E06,29.0E06
18.,28.,150.0,8.,1.410,2,2,4.0,53
18.,28.,92.0,8.,1.410,2,2,4.0,2
```

b. Short Direction

```
SHORT DIMENSION BUILDING 333

CENTER OF GRAVITY =   26.67606   INCHES  FOR T-SECTION =     1

     UNCRACKED T-SECTION M.O.I. EXCLUDING STEEL =   154325.2   INCHES^4
     STEEL M.O.I. =   1695.099   INCHES^4
     EFFECTIVE M.O.I. =  169016.1   INCHES^4

CENTER OF GRAVITY =   24.9125   INCHES  FOR T-SECTION =     2

     UNCRACKED T-SECTION M.O.I. EXCLUDING STEEL =   136064.9   INCHES^4
     STEEL M.O.I. =   1523.394   INCHES^4
     EFFECTIVE M.O.I. =  149267.6   INCHES^4

          UNCRACKED
          TOTAL MOMENT OF INERTIA OF CROSS-SECTION =    4185904.00  INCHES^4

SHORT DIMENSION BUILDING 333

CENTER OF GRAVITY =   26.67606   INCHES  FOR T-SECTION =     1

     CRACKED TOP CENTER OF GRAVITY = 13.45862   INCHES
     CRACKED TOP T-SECTION M.O.I. EXCLUDING STEEL =  28481.48   INCHES^4
     BOTTOM STEEL M.O.I. = 279.7796   INCHES^4
     TOP    STEEL M.O.I. = 1073.988   INCHES^4
     EFFECTIVE TOP CRACKED M.O.I. =  41288.12   INCHES^4
```

Table 14 (Concluded)

```
CENTER OF GRAVITY =   24.9125   INCHES  FOR T-SECTION =     2

     CRACKED TOP CENTER OF GRAVITY = 12.59142   INCHES
     CRACKED TOP T-SECTION M.O.I. EXCLUDING STEEL =  23200.46   INCHES^4
     BOTTOM STEEL M.O.I. = 230.8968   INCHES^4
     TOP    STEEL M.O.I. = 1176.763   INCHES^4
     EFFECTIVE TOP CRACKED M.O.I. =  36576.95   INCHES^4

         TOP CRACKED
         TOTAL MOMENT OF INERTIA OF CROSS-SECTION =    1022781.00  INCHES^4


SHORT DIMENSION BUILDING 333

CENTER OF GRAVITY =   26.67606   INCHES  FOR T-SECTION =     1

     CRACKED BOTTOM CENTER OF GRAVITY =  31.83818   INCHES^4
     CRACKED BOTTOM T-SECTION M.O.I. EXCLUDING STEEL =  6917.514
     BOTTOM STEEL M.O.I. =  2420.525   INCHES^4
     TOP    STEEL M.O.I. =  .4698128   INCHES^4
     EFFECTIVE BOTTOM CRACKED M.O.I. =  30319.99   INCHES^4


CENTER OF GRAVITY =   24.9125   INCHES  FOR T-SECTION =     2

     CRACKED BOTTOM CENTER OF GRAVITY =  31.52613   INCHES^4
     CRACKED BOTTOM T-SECTION M.O.I. EXCLUDING STEEL =  5785.551
     BOTTOM STEEL M.O.I. =  2366.572   INCHES^4
     TOP    STEEL M.O.I. =  1.089294   INCHES^4
     EFFECTIVE BOTTOM CRACKED M.O.I. =  28671.85   INCHES^4

         BOTTOM CRACKED
         TOTAL MOMENT OF INERTIA OF CROSS-SECTION =     754703.50  INCHES^4
```

DATA FOR SHORT DIRECTION

```
"SHORT DIMENSION BUILDING 333",2,3.0E06,29.0E06
18.,28.,150.0,8.,1.410,2,2,4.0,23
18.,28.,97.0,8.,1.410,2,2,4.0,2
```

of the mat cross-section parallel with the long direction is 9,251,474 $inches^4$ and the total mat uncracked M.O.I. parallel with the short direction is 4,185,904 $inches^4$. This calculation assumes T-section dimensions indicated in Figure 71 with stiffening beams uniformly placed with spacing at 12.5-ft centers. Table 14 also shows the input data listing for program MOM.BAS. A simplified arrangement of vertical loads applied only at the columns is assumed for these analyses. A reasonable assumption of structural dead loads excluding wind and snow loads is approximately 32, 64, and 128 kips on the corner, edge, and interior columns. A 32, 64, and 128 kip load distribution will cause approximately 8 psi pressure on the widened beams or footings beneath each column.

Plate on Elastic Foundation

217. A finite element mesh, Figure 72, describes the dimensions and load distribution. Loads were assumed to be uniformly distributed within the rectangle at each column area indicated in Figure 72. The area of these rectangles is about twice the actual footing size beneath each column leading to an applied pressure of 4 psi consistent with the earth pressures measured near column D. The total load applied at each column is assumed to spill on to some of the soil adjacent to that beneath each column.

218. Soil input parameters include an equivalent soil elastic modulus $E_s^* = 30{,}000$ psi (4320 ksf) and soil Poisson's ratio $\mu_s = 0.4$. Mat input parameters include an elastic modulus of concrete $E_c = 1{,}500{,}000$ psi (216,000 ksf) with a concrete Poisson's ratio $\mu_c = 0.15$. A partial gap beneath line 20-21 at the expansion joint was also input to simulate the loss of support in the softened soil in this area. The computer analyses also assumed a joint at line 20-21 to simulate the expansion joint, Figure 53a. Analyses were performed with and without the weight of the mat.

219. Analysis for the southeast quadrant, Figure 73, indicate displacements of 0.05 ft without the mat weight and 0.15 ft with the mat weight. These displacements bound the 0.1 ft measured in the southeast quadrant 12 May 1987, Figure 74. The calculated V-shaped settlement, Figure 73, also reasonably matches the measured settlement, Figure 74. The results of additional computer analyses performed without the expansion joint were similar to those in Figure 73.

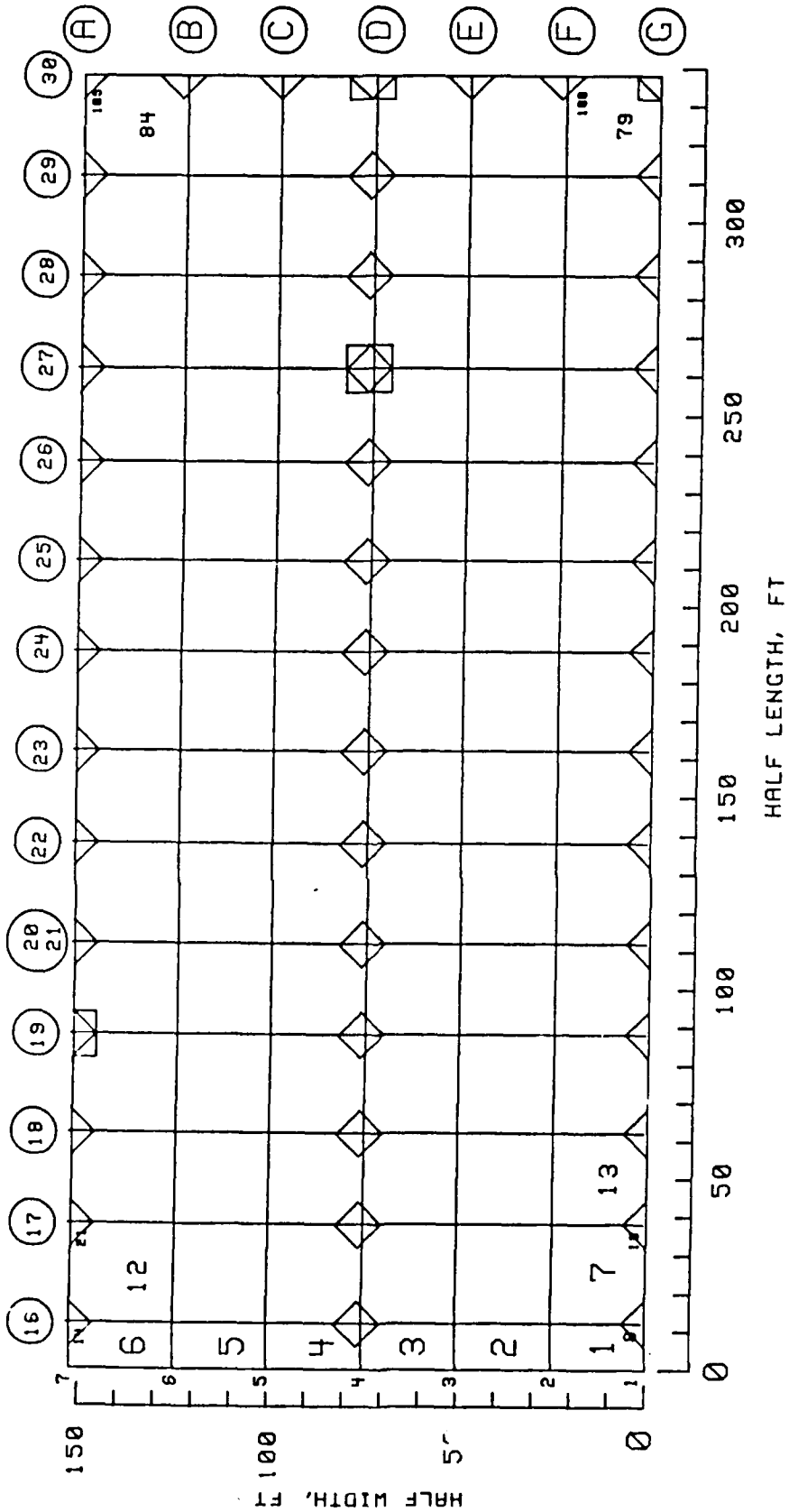

Figure 72. Finite element mesh for building 333

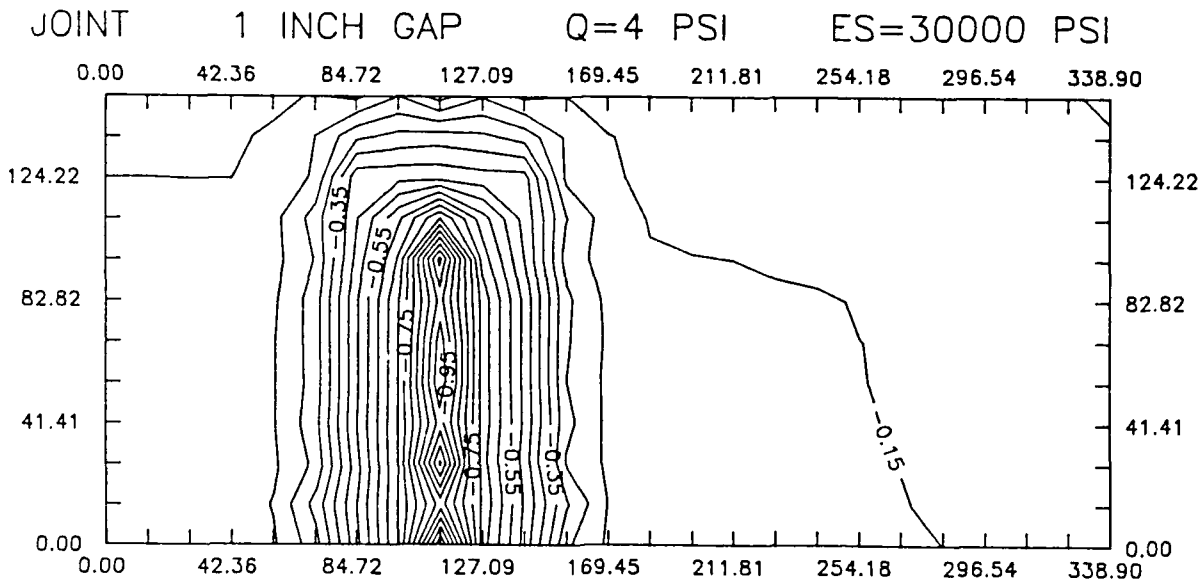

a. 0.7 PSI UNIFORM PRESSURE FROM MAT WEIGHT

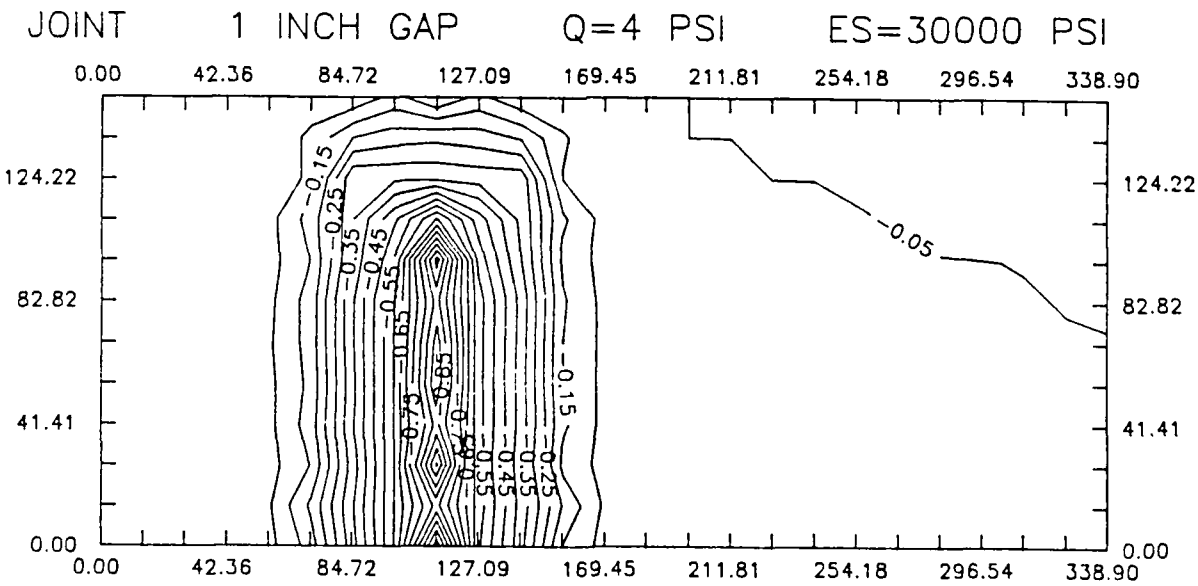

b. WITHOUT PRESSURE FROM MAT WEIGHT

Figure 73. Deformation pattern calculated for building 333 using program SLAB2

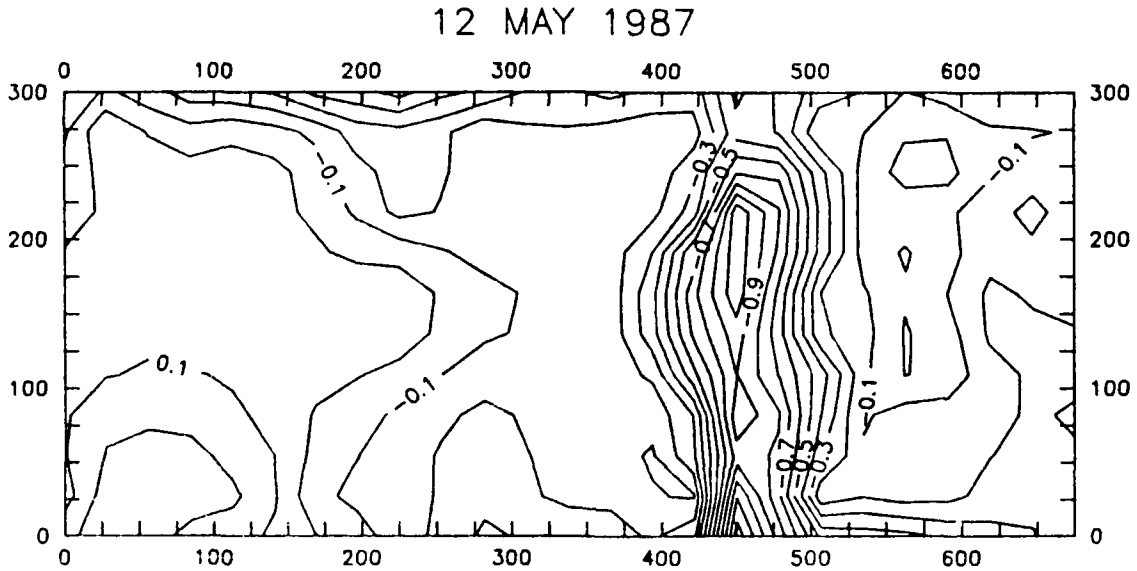

Figure 74. Measured displacement pattern in the southeast quadrant

Beam on Winkler Foundation

220. A beam on Winkler foundation analysis was completed for line 26 from Column A to Column G using k_{sf} from 7.3 to 5.6 psi/in., respectively. The modulus of subgrade reaction k' input into program CBEAMC is $k_{sf} \cdot S$ where S is the width of the section in inches. If S is assumed 240 inches (20 ft), then k' varies from 1710 to 1365 psi. Spacing S = 20 ft is a little less than the interior beam spacing of 25 ft.

221. A plot of the deformation pattern using program CBEAMC for an applied pressure of 4 psi or loads of 64 kips at the perimeter Column A and 128 kips at the interior columns D and G indicate maximum settlements of nearly 0.2 inch at the perimeter and about 0.1 inch at the interior columns, Figure 75. Doubling these loads will approximately simulate the maximum observed settlements by 6 June 1986 along line 26, Figure 61b (about 1/3 of the distance from the south perimeter). Negative bending moments in Figure 75 denote compression in the top and tension in the bottom fibers.

222. Beam programs similar to CBEAMC do not consider stiffness contributed by adjacent portions of the stiffened mat (two-dimensional stiffness) and they do not consider the cohesive or interactive particulate

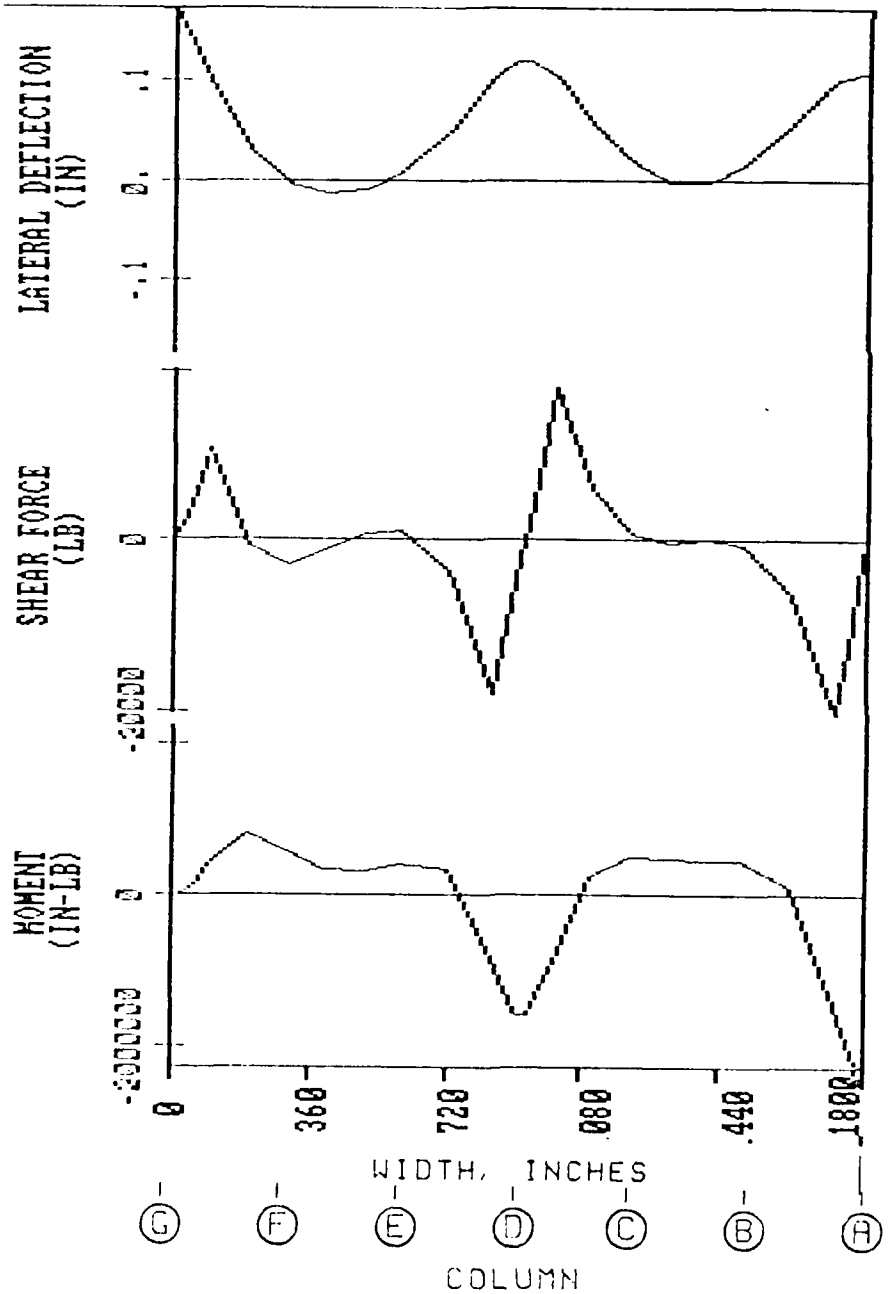

Figure 75. Calculated performance of mat supporting building 333 using program CBEAMC on line 26 from column G to A. (Note that the lateral deflection of this section is the vertical movement on line 26)

nature of soil; that is, soil does not behave as an independent bed of springs simulated by the Winkler foundation. Calculated perimeter settlements are therefore greater than interior settlements for this type of loading pattern. Vertical deformations predicted by an independent method must be input into beam on Winkler foundation models to calculate proper stresses and bending moments. The Winkler procedure for design of ribbed mats developed by the Southwestern Division of the US Army Corps of Engineers[12] uses movement data.

Frequency Spectrum Model

223. An application of the pavement frequency spectrum model described in paragraph 78 to this mat foundation is provided in Table 15. This model ignores the two-dimensional stiffness of the mat. The relative rigidity/ft Ω is evaluated from Equation 17, paragraph 62, for the given stiffness E_cI of the mat. Minimum and maximum values for the foundation coefficients of subgrade reaction k_{sf} are assumed 4 and 14 ksf/ft. The Ω evaluated for this range is multiplied by the wavelength Γ of 10, 20, and 30 ft to obtain the relative rigidity. Figure 9 is subsequently used to evaluate the ratio of the acceptable to the expected amplitude Aa/Ae. The accepted amplitude or deflection Δ of the mat is $\Gamma/2666$ from paragraph 84 for an allowable deflection ratio $\beta_{max} = 1/500$. The maximum amplitude or displacement of the soil without the mat in feet for the given mat stiffness E_cI is shown in the last column on the right, Table 15.

224. Table 15 shows that the uncracked T-section with spacing S = 12.5 ft can squeeze soil with $k_{sf} = 4$ ksf/ft down to $\Delta/L < 1/1333$ for heaves without the mat > 8 inches and soil wavelengths of 10 to 30 ft. If the section is cracked, then the maximum heave is reduced to about 3 inches. If the section contains only steel, then the maximum heave is reduced further. The maximum heave tolerated for harder soil, $k_{sf} = 14$ ksf/ft, is substantially less than for the softer soil. The observed deformation of the mat at the expansion joint (line 20/21) lying over the old drainage area appears consistent with this model. Although these computations only indicate trends in performance because loads are not considered, the model is limited to one dimension and soil wavelengths and amplitudes beneath facilities are not known, this application illustrates the simplicity and potential power of frequency spectrum models when developed for mat applications.

Table 15

Frequency Spectrum Application of Interior T-section, Figure 71a

1	2	3	4	5	6	7	8	9
Case	Moment of Inertia I, ft^4	E_cI, $kip\text{-}ft^2$	k_{sf}, ksf/ft	Ω, ft^{-1}	Γ, ft	$\Omega\Gamma$	Aa/Ae	Ae, ft
Uncracked	8.15	3,521,200	4	0.0434	10	0.434	0.004	0.95
					20	0.868	0.009	0.83
					30	1.302	0.017	0.67
			14	0.0594	10	0.594	0.006	0.63
					20	1.188	0.014	0.54
					30	1.782	0.038	0.30
Top Cracked	1.99	859,750	4	0.0617	10	0.617	0.006	0.63
					20	1.234	0.015	0.50
					30	1.851	0.042	0.27
			14	0.0850	10	0.850	0.009	0.42
					20	1.700	0.035	0.21
					30	2.550	0.109	0.10
Bottom Cracked	1.46	631,666	4	0.0667	10	0.667	0.007	0.54
					20	1.334	0.018	0.42
					30	2.001	0.048	0.24
			14	0.0912	10	0.912	0.009	0.42
					20	1.824	0.041	0.18
					30	2.736	0.140	0.08
Only Steel	0.57	246,500	4	0.0844	10	0.844	0.008	0.48
					20	1.688	0.034	0.22
					30	2.532	0.106	0.11
			14	0.1154	10	1.154	0.013	0.29
					20	2.308	0.075	0.10
					30	3.462	0.270	0.04

Column 2: Moment of Inertia from Table 14

Column 3: E_c = 432,000 ksf

Column 5: Ω calculated from Equation 17, $\sqrt[4]{\frac{k_{sf}S}{4E_cI}}$

Column 8: From Figure 9

Column 9: Expected soil movement without mat section Ae = (Γ/2666)/Column 8

Summary and Conclusions

225. The soil supporting building 333 is of an expansive nature, but the placement of an engineered nonexpansive fill to depths of 5 to 8 ft and the existence of a perched water table with groundwater level about 5 ft below ground surface have essentially eliminated any potential for swell or shrinkage at this site. Soil swell may have been realized if a perched water table had not existed prior to construction, but developed later in the life of the project. This site was cleared of trees and vegetation and supported earlier facilities. Construction in a previously forested site may not contain a perched water table because trees take moisture out of the soil.

226. Data from field instruments show that the mat performance is similar to a plate on an elastic foundation. Elevation surveys show that loads applied through August 1987 have led to relatively small settlements from 0.1 to 0.3 inch, except where a drainage ditch had previously existed. Settlement in this area exceeds 1 inch perhaps because of settlement of an increased fill thickness and softening of the subsurface soil; less efficient compaction of fill is possible above softened soil. Observed distortions are consistent with data from earth pressure cells and strain gages. The distortion pattern shows rigid behavior in the short direction consistent with the exceptionally large earth pressures observed near the perimeter simulating a plate on an elastic soil. The observed tensile and compressive strains are consistent with the depression and hump observed on line 26. The hump may have developed because of arching in the mat from (1) temporary heavy loads placed near line 30 from A to N leading to additional settlement and (2) settlement approaching 1.5 inch near line 20-21. The stiffening beam on line 26 near column G appears to have fractured based on the unusually large strains measured near G; fractures were observed on the mat during construction between columns G and F near line 26. Stiffening beams hanging in the trenches without soil support following shrinkage from concrete cure or arching of the mat may aggravate fracture in the mat following beam loading during construction of the superstructure. Axial stress and bending moments calculated from the strain gages assuming a rectangular beam are generally reasonable.

227. Analyses show that an equivalent elastic modulus may be evaluated leading to good comparisons of calculated with measured settlement using plate on eastic program SLAB2. Beam on Winkler foundation program CBEAMC did not provide realistic results. One-dimension, single parameter models such as the Winkler concept will not calculate reliable stresses and bending moments unless displacements can be accurately predicted and input into the analysis such as observed in Part III. The frequency spectrum model indicates consistent distortions for the given mat stiffness. The mat may be overdesigned, except where the old drainage ditch was located, because the design was based on a potential heave y_m of 1.5 inches (Appendix F), while the actual heave potential may be negligible. Field measurements of wavelengths and amplitudes of soil movements beneath and adjacent to facilities and correlations with distress of facilities are recommended to calibrate the frequency spectrum model to foundations.

PART V: GUIDELINES FOR DESIGN AND CONSTRUCTION

Applicability of Mat Foundations

228. Mats are an appropriate, economical foundation system, particularly where a stable bearing stratum not subject to significant volume change is more than 30 ft below the ground surface. Ribbed mats useful for supporting light (family housing) and intermediate (warehouses, operational and maintenance facilities) consist of a thin slab on grade monolithic with a grid of stiffening beams beneath the slab. The stiffening beams or ribs may be cast into trenches excavated in the foundation soil. Flat mats useful for supporting heavy multi-story structures such as hospitals are usually 3 to 5 ft thick and often constructed 25 to 30 ft below grade such that the net increase in pressure on the bearing stratum is insignificant. Settlement of such floating foundations is limited to elastic recompression. Mats supporting heavy structures designed by conventional techniques[49,50,51] have performed adequately. Mats supporting light and intermediate structures in expansive soil have been subject to distress and therefore design of these mats is the subject of this part.

Expansive Soil Behavior

229. Expansive soil exhibits volume changes caused by changes in soil moisture that occur predominantly in the vertical direction. The plastic CH cohesive soils containing montmorillonitic clay minerals are most susceptible to volume changes, although lean CL clays can also lead to structural damage if soil water content changes are sufficiently large. These soils when exposed to the natural environment swell and shrink during wet and dry seasons. The natural fissure system inherent in these soils influences the amount of volume change that occurs within a given time frame or season. Numerous fissures, for example, promotes flow of free water from surface runoff through the soil into deeper, possibly desiccated zones increasing the depth of active soil volume change Z_a, while fewer fissures restrict the flow of free water limiting the depth of penetration and volume change that can occur within a single season. Soil movement for analysis of foundation performance is characterized by center and edge lift deformation modes.

Center Lift

230. Center lift is upward movement of the mat relative to the edge, Figure 76, caused by increases in soil water content and heave toward the center relative to the perimeter or decreases in water content and shrinkage toward the perimeter relative to the center. Placement of the foundation on the ground surface inhibits evaporation of moisture from the ground surface and eliminates transpiration of moisture from previously existing vegetation. The soil therefore tends to increase in water content, particularly toward the center of the mat where environmental conditions at the perimeter have least influence. Soil outside the perimeter may also dry out during drought causing the perimeter to settle relative to the center. Figure 76a illustrates the center lift deformation assumed for design where the mat acts as a cantilever.

231. Two important input parameters required for design are y_m and e_m, Figure 78. y_m is the maximum soil surface heave relative to the edge under no foundation load and depends on the type of soil and water content change within the depth of the active zone for heave Z_a. e_m is the maximum edge moisture variation distance or lateral distance into the interior from the perimeter where seasonal moisture changes cause the mat to lift off of the soil. The maximum deflection Δ, bending moment M, and shear stress V will be determined by the design analysis.

Edge Lift

232. Edge lift is upward movement of the edge relative to the center, Figure 78b, caused by increases in soil water content and heave near the perimeter or decreases in soil water content and shrinkage toward the center. Seasonal rainfall or summer irrigation in arid and semi-arid climates commonly cause edge lift. Edge lift may also occur from drying out of soil beneath interior portions of the mat when moisture flows away from heated areas. Figure 76b illustrates edge lift assumed for design where the mat is supported at the edge and at some interior location. Interior loads cause the mat to sag and contact the soil as shown. The mat acts as a beam simply supported by soil at the edge and at some interior point.

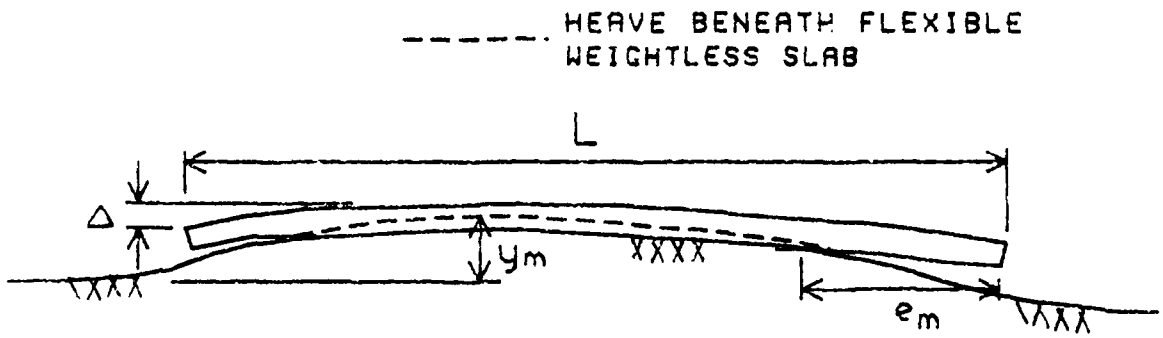

a. CENTER LIFT OR DOWNWARPING

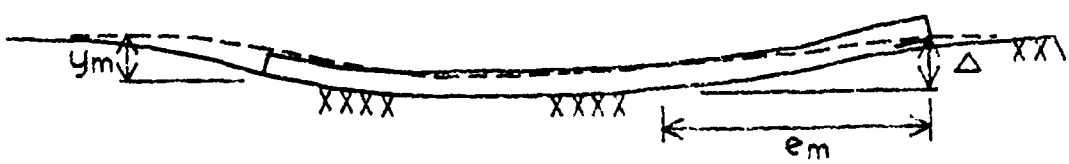

b. EDGE UPLIFT

Figure 76. Soil-slab displacements on heaving soil

Soil Exploration

233. A thorough field investigation must be conducted of the proposed construction site to determine site characteristics for construction and soil input parameters to accomplish the design.

Site Characterization

234. Foundation soil and groundwater characteristics should be determined early in the design process to avoid unexpected obstacles to construction such as underground streams, sink holes, boulders, poor site trafficability, poor drainage, unstable excavation slopes, excessive heave of excavation bottoms, and loss of ground adjacent to excavations.

235. Surface soil. Surface soils within and near the potential construction site should be identified to determine trafficability of construction equipment and suitability of the soil to support the structure or use as fill. Plastic soils can reduce site trafficability and may be potentially expansive. Expansive and plastic surface soils are easily identified following dry periods by a polygon network of fissures appearing on the ground surface; otherwise, they may be identified by their slick and sticky texture when wet. Expansive soil often contains montmorillonite and it is associated with high plasticity CH cohesive clay with plasticity index PI > 40 and liquid limit > 50. Lean CL soil with PI ≥ 15 can cause structural damage to the foundation and superstructure if water content changes and subsequent differential movements are sufficiently large.

236. Collapsible soil is also an undesirable foundation material. It has a loose structure often associated with mudflows and partly saturated windblown colluvial, cohesive silty sands found in arid and semi-arid climates. Cohesion is often imparted by precipitation of soluble compounds such as calcium carbonates, gypsum, or ferrous iron that dissolve when wet leading to rapid volume decreases and substantial nonuniform settlement.

237. Topography. Topography of the site should be checked for adequate drainage of surface water away from the site and a suitable level location for the foundation. Cuts or excavations to level sites are undesirable, especially in low permeable, cohesive soil because long-term rebound can cause substantial heave. Combination cut and fill earth work to level sites aggravate differential movement from settlement of the fill and rebound of the

cut. Sites requiring cuts should be overcut and a minimum depth of 2 ft of fill placed beneath the full area of the proposed foundation.

Soil Characterization

238. Soil strength and stiffness parameters such as the allowable bearing pressure q_a, elastic soil Modulus E_s, and the coefficient of subgrade reaction k_{sf} are required for design of mats on stable (nonexpansive) soil. Additional parameters such as the depth of the active zone for heave Z_a, edge moisture variation distance e_m, swell pressure σ_s and maximum potential swell y_m are required for design in expansive soil. Soil parameters are evaluated from a combination of in situ and laboratory soil tests. Results of in situ tests will be a primary source of data for soil that cannot be easily sampled such as cohesionless sands. In situ tests and soil sampling should be conducted on each strata down to depths of twice the least width of the proposed foundation or to the depth of incompressible strata, whichever comes first. A minimum of three cone penetration tests, for example, may be conducted initially for economically significant structures to determine a preliminary classification of the soil and to provide a basis for judging lateral variations in soil parameters. These tests should be located at the center, corner and middle edge of the longest dimension of the proposed structure. Other types of field tests such as standard penetration, pressuremeter, and dilatometer tests may also assist the reasonable estimation of soil parameters.

239. Several disturbed and undisturbed boring samples should be obtained from each strata at locations of potential soil weakness such as softened, loose, expansive, or collapsible soil depending on results of field tests. Disturbed boring samples should be used to classify the soil in each stratum. At least one consolidometer swell test described in EM 1110-2-1906 or ASTM D 4546 should be performed on soil from each strata with plasticity indices PI greater than 15 and Liquid Limits greater than 35 to determine the potential swell. Soil sampling should be conducted near the end of dry periods to provide maximum estimates of swell pressure and potential heave.

240. Strength and stiffness. Field tests illustrated in Appendix G may be used to estimate the soil shear strength, elastic modulus, and coefficient

of subgrade reaction for a plate. Refer to Part II for further details on estimating the soil stiffness and strength required for design.

241. Depth of active zone for heave. The depth of the active zone (Z_a) for heave is defined as the least soil depth above which soil heave may occur because of change in environmental conditions or climate following construction. The water content distribution should not change with time below Z_a. Past experience indicates Z_a may be approximated by guidelines in Table 16. Climate is defined in terms of the maximum amplitude of surface suction range 2Uo and the cycles/year n that this maximum amplitude occurs. For example, severe extreme may be an arid or desert climate subject to a heavy rainfall every other year. Piezometers should be placed in construction sites to determine groundwater levels, which assist in determining reasonable estimates of Z_a.

242. Preliminary criteria for Z_a based on soil suction principles are shown in Table 17 as a function of the severity of the climate. Z_a may be derived from maximum and minimum suction envelopes for cyclic surface suction changes[68] such as illustrated in Figure 77

$$Z_a = \frac{\ln \frac{\Delta u}{2Uo}}{\sqrt{\frac{n\pi}{\alpha}}} \tag{45}$$

where

Δu = maximum acceptible change in suction at depth Z_a, 0.4 pF; Suction in pF units is the logarithm to the base 10 of suction in units of centimeters of water or ≈ 3 + logarithm to the base 10 of suction in tons/square foot (tsf)

Uo = 1/2 of the maximum range in suction at the ground surface from the climate, pF

n = number of cycles per year that the climate oscillates from peak to peak range

α = diffusion coefficient, ft^2/year

Δu = 0.4 pF is recommended at this time because calculated Z_a using this value is comparable with past experience[5], Table 16. The diffusion

[68]McKeen and Eliassi 1988

Table 16

Guidelines For Estimating Depth of the Active Zone Z_a

Relative To	Guideline
Water table	Z_a will extend to depths of shallow groundwater levels ≤ 20 ft (see Figure 77)
Swell pressure	Z_a will be located within depths where $\sigma_{sj} - \sigma_{fj} \geq 0$ where σ_{sj} = average swell pressure of stratum j and σ_{fj} = total average vertical overburden pressure prior to construction in stratum j
Fissures	Z_a will be within the depth of the natural fissure system caused by seasonal swell/shrinkage
Climate	

	TMI	Z_a, ft
humid	> 20	10
semi-arid	-20 to 20	15
arid	< -20	20

TMI = Thornthwaite Moisture Index[69]

[69]Thornthwaite 1948

Table 17

Preliminary Criteria for Depth of Seasonal Active Zone

Climate	Maximum Suction Range 2Uo, pF	Cycles/year, n	Depth of Seasonal Active Zone Z_a, ft
Severe Extreme	5	0.5	15 - 22
Severe Moderate	4	1.0	10 - 14
Normal	3	1.5	7 - 10
Moderate	2	2.0	5 - 7
Mild	1	2.5	< 5

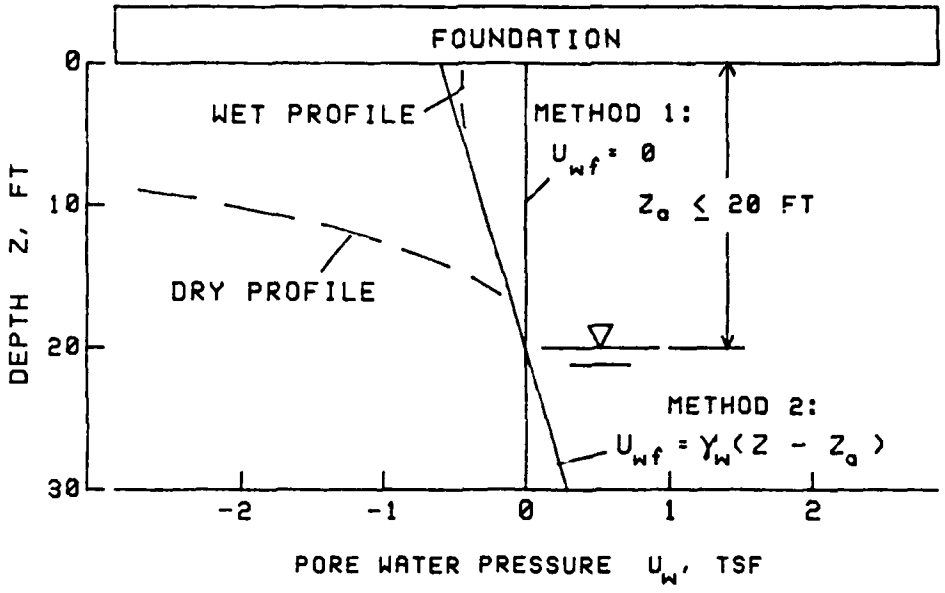

a. SHALLOW GROUNDWATER LEVEL

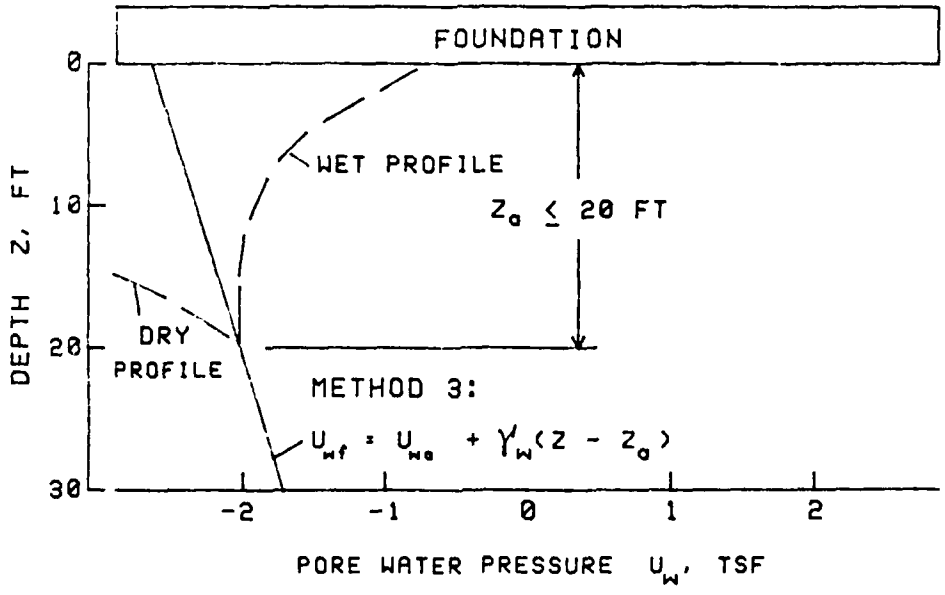

b. DEEP GROUNDWATER LEVEL

Figure 77. Anticipated equilibrium pore water pressure profiles

coefficient α is a measure of the rate of moisture flow through soil and related with the permeability by

$$\alpha = k \frac{\partial u}{\partial \theta} \tag{46a}$$

where

∂u = rate of change of suction head in feet with respect to θ, the fraction of volumetric water content, $wG_s/(100(1+e)$

$\partial \theta$ = rate of change of volumetric water content

w = water content, percent

G_s = specific gravity

e = void ratio

A selected range of α from 60 to 120 ft^2/year is consistent with observation[68]. The results of Table 17 are plotted in Figure 78a to show how the seasonal active zone fluctuates with the severity of the range in suction. In situ diffusion coefficients $\alpha < 60$ ft^2/year will reduce Z_a and be above the solid line in Figure 78a and $\alpha > 120$ ft^2/year will increase Z_a and be below the dotted line. Table 17 must be confirmed from results of field tests; this does not consider long-term wetting or drying of the soil profile.

243. Edge moisture variation distance. The edge moisture variation distance e_m is the distance inside the mat from the perimeter that soil is subject to variations in moisture. This parameter is not well known, but experience appears to show that it may vary from 2 to 8 ft[11] and become larger with more severe climates. A more severe climate is associated with a dryer environment that occurs over longer periods of time before a heavy rainfall. Larger fissures caused by greater drying (droughts) reduce the diffusion coefficient α and increase the active zone depth Z_a. Parametric analysis of two-dimensional moisture flow beneath a ribbed mat[70] shows that the edge moisture variation distance is a function of Z_a and the depth of the perimeter stiffening beam D, Figure 78b, and approximately

$$e_m = \frac{Z_a}{2} - D \tag{46b}$$

Figure 78b must be confirmed from results of field tests.

---

[70]Vallabhan and Sathiyakumar

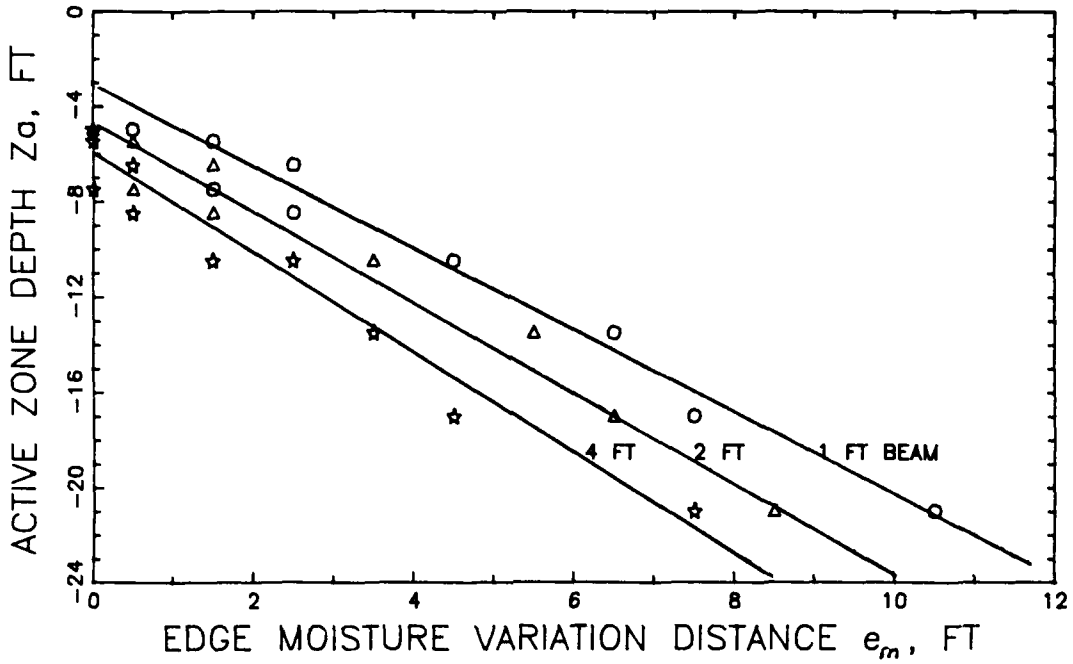

b. EDGE MOISTURE VARIATION DISTANCE

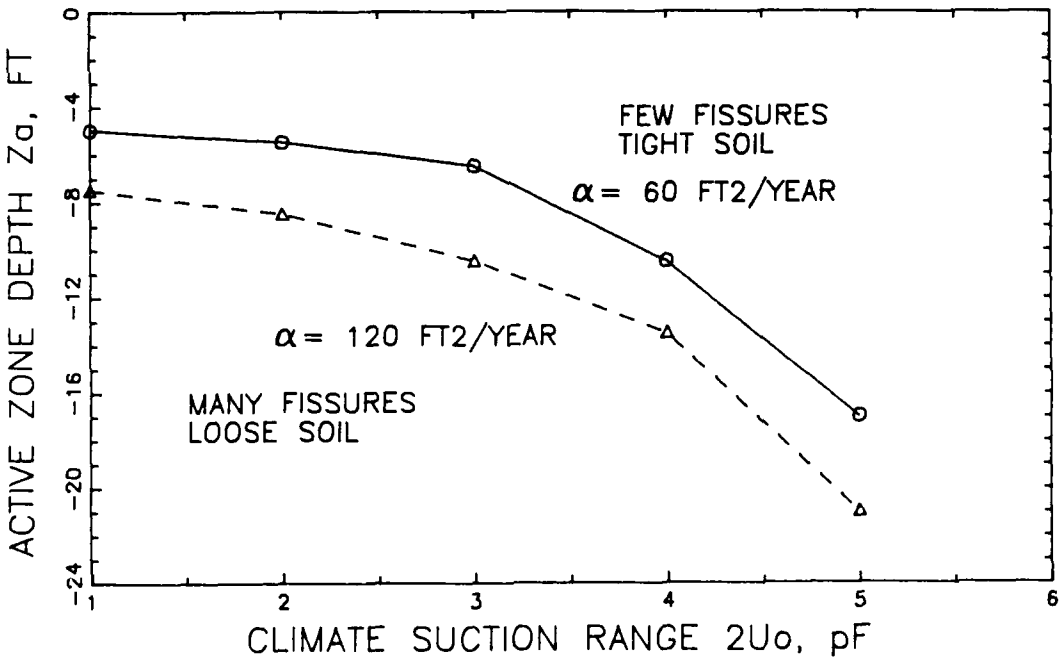

a. ACTIVE ZONE DEPTH
(Data from Table 17)

Figure 78. Preliminary relationships for active zone depth and edge moisture variation distance

244. Swell Pressure. Swell pressure σ_s, evaluated from results of consolidometer swell tests[71,72], should be determined down to the depth of the active zone for heave Z_a.

245. Potential Swell. Useful estimates of the anticipated heave y_m based on results from consolidometer swell tests can often be made. Computer program HEAVE[73] is useful for calculating potential heave beneath mat foundations in multi-layered expansive soil. The anticipated heave is

$$y_m = \sum_{j=1}^{n} \frac{e_{fj} - e_{oj}}{1 + e_{oj}} \cdot h_j \tag{47a}$$

where

y_m = maximum potential vertical heave, ft

h_j = thickness of stratum j, ft

e_{fj} = final void ratio of stratum j

e_{oj} = initial void ratio of stratum j

n = number of strata within the depth of heaving soil Z_a

The initial void ratio, which depends on a number of factors such as the maximum past pressure, type of soil, and environmental conditions, may be measured by standard consolidometer test procedures.

246. The final void ratio depends on changes in soil confinement pressure and water content following construction of the structure; it may be anticipated from reasonable estimates of the equilibrium pore water pressure u_{wf}, depth of active zone Z_a, and edge effects by rewriting Equation 47a in terms of swell pressure

$$y_m = \sum_{j=1}^{n} \frac{C_{sj}}{1 + e_{oj}} \cdot \log_{10} \frac{\sigma_{sj}}{\sigma'_{fj}} \cdot h_j \tag{47b}$$

where

C_{sj} = swell index of stratum j

σ_{sj} = swell pressure of stratum j, tsf

---

[71]Engineer Manual 1110-2-1906, "Laboratory Soils Testing"
[72]ASTM D4546
[73]Johnson 1982

σ'_{fj} = final or equilibrium average effective vertical pressure of stratum j, $\sigma_{fj} - u_{wfj}$, tsf

σ_{fj} = final average total vertical pressure of stratum j, tsf

u_{wfj} = equilibrium pore water pressure in stratum j, tsf

The swell index and swell pressure of the soil in each stratum may be determined from results of consolidometer swell tests. Table 18 illustrates the evaluation of the equilibrium pore water pressure. The equilibrium pore water pressure is independent of the type of strata in the soil profile. An application of the heave prediction method is provided in Chapter 5, EM 1110-1-1904.

Design of Ribbed Mats

247. A useful procedure for design of stiffened ribbed mats in expansive soil areas[12] adopted in this report, Table 19, is a conservative and simple methodology applicable to the beam on Winkler foundation concept. This procedure inputs displacement values based on estimates of maximum differential heave y_m, and can provide useful calculations of bending moments and shears based on reasonable input data. A computer program RIBMAT is available from the Southwestern Division to assist analysis. The Post Tensioning Institute method[11] illustrated in Appendix F for building 333 is recommended when conditions are satisfied, paragraph 77.

Input Parameters

248. Step 1 to determine input parameters may be accomplished using Table 20 and results of laboratory and field soils tests with consideration of past experience.

Foundation Plan

249. Step 2 to determine foundation plan dimensions and loads is initially accomplished by knowledge of structural functional requirements and minimum requirements described in Table 21. Some rules of thumb for line and column loads described in Table 22 are based on a survey of engineering firms. Tall multistory structures may have column loads exceeding 1000 tons. Column spacings are often 20 to 25 ft or more. The average pressure per story of a building often varies from 0.2 to 0.4 ksf.

Table 18

Equilibrium Pore Water Pressure (Figure 77)

Profile	Equation	Remarks
Saturated (Method 1)	$u_{wf} = 0$	Realistic for most practical cases: houses or buildings exposed to watering of perimeter vegetation and possible leaking of underground water and sewer lines. Water may also condense or collect in permeable soil beneath slabs and penetrate into underlying expansive soil unless drained away or protected by a moisture barrier. This profile should be used if other information on the equilibrium pore water pressure profile is not available.
Hydrostatic with shallow water table (Method 2)	$u_{wf} = \gamma_w(z - Z_a)$	Realistic beneath highways and pavements where surface water is drained from the pavement and where underground sources of water such as leaking pipes or drains do not exist. This assumption leads to smaller anticipated heave than Method 1.
Hydrostatic without shallow water table (Method 3)	$u_{wf} = u_{wa} + \gamma_w(z - Z_a)$	Similar as Method 2 but without shallow water table.

Note: γ_w = unit weight of water, 0.031 tsf

z = depth below the foundation, ft

Z_a = depth of active zone for heave, ft

u_{wa} = value of negative pore water pressure at depth Z_a; evaluated by methodology described in TM 5-818-7.

Table 19

Southwestern Division Structural Design of Ribbed Mats

Step	Description

1. Determine input parameters for design from Table 20.

2. Determine foundation plan dimensions and initial geometry and spacing of ribs S from functional and minimum requirements, Table 21.

3. Calculate interior P_i and perimeter P_p loads, lb/ft. Interior or perimeter column loads may be converted to P_i or P_p by dividing by spacing S_s or S_l in feet. Calculate uniform pressure q in psf on the T-section being analyzed. Loads should consist of full dead (DL) and live (LL) loads including DL of slab and ribs. L equals S_s or S_l.

4. Estimate rib width w in inches from applied loads and allowable bearing capacity

$$w \geq 12 \cdot \frac{P_i}{q_a} \quad \text{or} \quad 12 \cdot \frac{P_p}{q_a}$$

where q_a = allowable bearing capacity (Table 20), psf.

5. Estimate effective T-section width S_e in inches after ACI 318, Section 8.10.2 by $S_e \leq 1/4$ beam span length L and the effective overhang (OH) distance on each side of the web shall not exceed

$OH \leq 8D$
$OH \leq 1/2$ clear distance to next web

Span Length L:

L initially S_s or S_l

Center Lift: $L = 4L_c$ (step 8)

Edge Lift: $L = L_e$ (step 10)

6. Estimate effective moment of inertia of mat cross-section I_e, in.^{4}, after ACI 318, Section 9.5.2.3 for center and edge lift

$$I_e = \left[\frac{M_{cr}}{M_r}\right]^3 I_g + \left[1 - \left[\frac{M_{cr}}{M_r}\right]^3\right] I_{cr}$$

Since M_r is initially unknown use

$$M_r = 0.005 A_g \cdot f_y \cdot j \cdot d$$
$$= 240 A_g \cdot d \text{ for ASTM60 grade steel}$$

OR

Estimate I_e as:

CENTER LIFT: $I_e = 0.7 I_g$

EDGE LIFT: $I_e = 0.4 I_g$

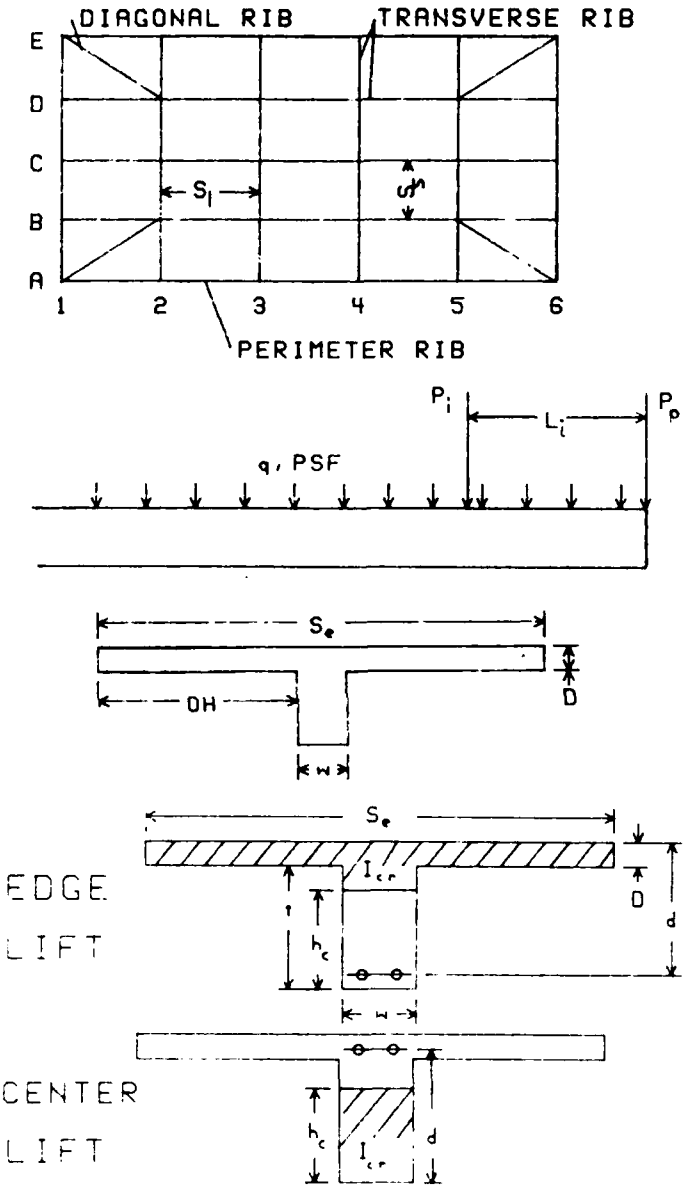

M_r = calculated maximum moment, in.-lb
A_g = gross beam area $w(t + D)$, in.^{2}
f_y = tensile yield strength of reinforcement steel, psi
Initially estimate $20 \leq t \leq 36$ in.
$d = D + t - 3$ in. (3 in. = concrete cover)
I_g = gross moment of inertia, in.

$$I_g = \frac{wt^3 + BD^3}{12} + \left[h_c - \frac{t}{2}\right]^2 wt + S_e D\left[t + \frac{D}{2} - h_c\right]^2$$

$$h_c = \frac{wt^2 + 2DtS_e + S_e D^2}{2(wt + S_e D)}$$

Table 19 (Concluded)

Step	Description
7. Calculate moment of inertia I in $in.^4/ft$ by $I = I_e/S$ $S = S_1$ or S_e in feet	I_{cr} = cracked moment of inertia, $in.^4$ M_{cr} = cracked moment, in.-lb CENTER LIFT: $I^*_{cr} = \frac{wh_c^3}{12} + wh_c\left[h_c - \frac{t}{2}\right]^2$ $\quad M_{cr} = \frac{7.5\sqrt{f'c}}{h_c}\cdot I_g$ EDGE LIFT: $I^*_{cr} = \frac{w}{3}(t - h)^3 + \frac{S_e D^3}{12} + S_e D\left[t - h_c + \frac{D}{2}\right]^2$ $M_{cr} = \frac{7.5\sqrt{f'c}}{t + D - h_c}\cdot I_g$ f'c = concrete compressive strength, 3000 psi *Neglects steel reinforcement
8. Calculate maximum M_r from Table 23b for transverse rib subject to center lift. Recalculate S_e (step 5), I_e (step 6), and I (step 7), using M_r. Then calculate maximum shear V_r, maximum deflection at perimeter Δ_p, and maximum angular distortion β_{max}. Check β_{max} ≤ limits of Table 24.	
9. Calculate minimum top reinforcement steel area A_s in transverse rib to accommodate maximum moment M_r for center lift. Select size and number of reinforcement bars with total area ≥ A_s. Calculate required area of stirrups A_r to accommodate maximum shear V_r and determine size of stirrups for spacing s.	A_s = area of reinforcement steel, $in.^2$ $A_s = \frac{M_r}{\phi\cdot f_y\cdot j\cdot(d - \frac{D}{2})} = \frac{M_r}{50{,}700(d - \frac{D}{2})}$ for ASTM Grade 60 steel ϕ = 0.90 f_y = 60,000 psi j = 0.939
10. Calculate maximum deflection at perimeter Δ_p, angular distortion β_{max}, moment M_r, and shear V_r for transverse rib subject to edge lift, Table 23c. Check β_{max} ≤ limits of Table 24.	A_r = area of stirrup, $in.^2$ $A_r = \frac{(V_r - v_c\cdot w\cdot j\cdot d)\cdot s}{f_y\cdot s\cdot j\cdot d}$ $v_c = 2\sqrt{f'c}$ s = stirrup spacing, ≤ 24 in.
11. Calculate minimum bottom reinforcement steel to accommodate maximum moment in transverse rib for edge lift similar to step 9. Check required area of stirrups to resist maximum shear.	
12. Calculate maximum moment and shear of perimeter ribs by conventional methods: center lift, ribs support perimeter P_p and span between transverse ribs assuming no soil support; edge lift, perimeter ribs span between transverse ribs and subject to net uplift $R - R_p$ where R is soil reaction from step 10.	
13. Calculate moment and shear capacity of diagonal ribs as larger of two adjacent transverse ribs. Diagonal ribs support corners for center lift if soil support lost beneath both perimeter ribs.	
14. Calculate maximum moment, shear, deflection interior ribs (not subject to soil heave) by conventional beam on Winkler foundation methods. Interior ribs and rib intersections should be located at wall and column loads. Design should be consistent with minimum requirements, Table 21.	

Table 20

Input Parameters For Design

Parameter	Equation	Description
Allowable soil bearing pressure q_a, psf	See Table 7 From Q Test: $2C_u$	Factor of safety should be at least 3 or settlement limited to less than 1 inch C_u = average undrained shear strength of undisturbed soil sampled from base of rib; determined from undrained triaxial Q test with confining pressure at σ_o, psf σ_o = soil overburden pressure prior to construction, psf
Coefficient of subgrade reaction k_s, pci	$\frac{E_s}{S_e}$ $\frac{k_{sp}B_p}{1.5S_e}$	E_s = soil modulus of elasticity, psi; initial tangent or hyperbolic modulus determined from triaxial Q test with confining pressure at σ_o. S_e = equivalent width of T-section, in., from step 5, Table 19. k_{sp} = coefficient of subgrade reaction from plate load test, pci (see Appendix G) B_p = diameter of plate, in. Clay: Soft E_s 700-3500, k_s 40-90; Medium 2000-7000, 90-170; Hard 7000-14000, > 170 Sand: Silty 1000-3000, 90-170; Loose 1400-3500, 20-60; Medium, 35-290; Dense 7000-12000, 230-460; Clayey, 110-290 Permissible range: $50 \le k_s \le 200$ pci
Edge Moisture Variation Distance e_m, ft		Climate / e_m, ft: Arid 8; Semi-arid 6; Humid 4 The permissible range of the edge moisture variation distance is 2 to 8 ft; see Figure 78b for further guidance on evaluating e_m
Soil swell pressure P_{sw}, psf	$\sigma_s - \sigma_o$	σ_s = average soil swell pressure from results of consolidometer swell test determined at the initial void ratio by ASTM D4546 on soil within the active zone Z_a beneath the mat, psf σ_o = soil overburden pressure prior to construction, psf Permissible range of P_{sw}: 1000 to 8000 psf
Soil heave y_m, in.	$\sum_{0}^{Z_a} \Delta h$	Δh = heave of 1 ft thickness of soil at depth z beneath mat down to active depth Z_a, in.; soil subject to σ_o prior to construction; Equations 47 may be used to calculate y_m; Z_a may be estimated from Table 16 and Figure 78a; refer to ASTM D4546 or EM1110-2-1906 to estimate Δh from results of consolidometer swell tests; assume saturated active zone (Method 1, Table 17 and Figure 77) where long term pore water pressure is zero; refer to MP GL-82-7 for calculation by program HEAVE; y_m may differ for center and edge lift conditions; permissible range is 0.5 to 3.0 inches

Table 21

Minimum Requirements

Item	Component	Description
Subgrade preparation	Vapor barrier	6 mil (preferably 10 mil) PVC membrane
	Capillary water barrier	6 inches gravel beneath membrane
	Fill	18 inches cohesive, granular, nonexpansive
Slab	4 inches thick	Family housing; small, lightly loaded buildings
	5 inches thick	Other buildings
	Reinforcing	0.2 percent
	Vehicular loading	Design for maximum wheel load similar to paving; use 650 psi flexural strength concrete
Grid geometry of ribs in mat	Grid	Continuous
	Spacing	≤ 20 ft in expansive soil; ≤ 25 ft in nonexpansive soil
	Location	Support wall, column loads; resist thrust from rigid reactions; adjacent large openings in slab
	Expansion joints	250 ft intervals; break irregular shapes into rectangular elements except not required for family housing
Rib dimensions	Depth, t	≥ 20 inches; ≤ 3 ft
	Width, w	≥ 12 inches; ≥ 10 inches family housing; allowable soil bearing capacity q_a may not be exceeded based on total width = w + 2D where D = slab thickness or provide fillets at rib intersections acting as spot footings to support column loads
Rib capacity	Concrete	Compressive strength f'c = 3000 psi at 28 days
	Steel	ASTM Grade 60; use No. 3 ties Grade 40 at 24 in.
	Area ratio	Cross-section area steel/concrete = 0.005 top and bottom
Construction joint detail	Conventional	Spacing ≤ 50 ft either direction; horizontal joint may be provided in ribs at base elevation of the capillary water barrier where unstable trench walls may cause construction problems
	Post-tensioned	Spacing ≤ 75 ft either direction; tendons within each placement shall be stressed to 15% final post-tensioned stress ≤ 24 hr after concrete has attained sufficient strength to withstand partial post-tensioning

Table 22

Some Typical Loads on Foundations*

Structure	Line Load, kips/ft	Column Load, kips
Apartments	1 to 2	60
Individual housing	1 to 2	< 10
Warehouses	2 to 4	100
Retail Spaces	2 to 4	80
Two-story buildings	2 to 4	80
Multistory buildings	4 to 10	200
Schools	2 to 6	100
Administration buildings	2 to 6	100
Industrial facilities		100

*Uniform total pressures are about 0.2 to 0.4 ksf/story, except housing and apartments where pressures may be less.

Rib Dimensions

250. Rib dimensions are determined by steps 3 to 5 with the assistance of Table 23. Reinforcement steel required to resist the calculated moments and shears may be determined by steps 6 to 11. The calculated maximum deflection should be checked to maintain angular distortions acceptable to the functional requirements and compatible with the flexibility of the superstructure, Table 24. Additional information on allowable deflections is provided by ACI Committee 435 (1980). Perimeter, diagonal, and interior ribs may be designed last, steps 12 to 14. An example application is provided in Technical Report ITL-88-1.

Construction

251. A properly designed foundation can be expected to perform as intended if the construction methodology avoids significant disturbance of the foundation soil, the soil is of adequate bearing capacity, soil heave potential is either reduced to tolerable levels or the effects are accounted for in the structural/architectural details, and the foundation exceeds flexural rigidity and strength requirements. The foundation soil and groundwater characteristics should be adequately investigated to avoid unexpected obstacles to construction such as underground streams, sinkholes, boulders, poor site trafficability and drainage, unstable excavation slopes, excessive heave of excavation bottoms, and loss of ground adjacent to excavations. Unforeseen problems caused by lack of prior subsurface investigations of soil and groundwater conditions will increase the cost of construction and may reduce quality of the foundation. Construction should be located where the foundation is supported by a uniform soil of adequate bearing capacity and resistant to differential movement on change in soil water content. Foundation soils that are not laterally uniform aggravate differential movement.

Minimizing Problems

252. Many problems with foundations of structures can be avoided by using proper construction practice and adequate quality control of materials and workmanship. Adequate field records are essential to confirm that contract specifications are met. Specifications must be explicit and concise

Table 23

Analysis of Transverse Ribs

a. Nomenclature

Term	Units	Definition
e_m	ft	Edge moisture variation distance, Table 20
I	$in.^4/ft$	Moment of inertia per foot, I_r/S
I_r	$in.^4$	Moment of inertia of rib
k_s	$lbs/in.^3$ (pci)	Coefficient of subgrade reaction, Table 20
L_b	ft	Width of bearing soil at perimeter, edge lift
L_c	ft	Equivalent length of cantilever, center lift
L_e	ft	Equivalent length of simple beam, edge lift
L_i	ft	Distance from perimeter to location of interior load
L	ft	Basic length of cantilever
L_*	ft	Location of maximum moment from perimeter, edge lift
l	in.	Length between maximum difference in deflection Δ; $48L_c$ for center lift; $12L_e$ for edge lift
M	ft-lb/ft	Bending moment per foot
M_r	ft-lb	Maximum moment for a given rib, $M_{max}S$
M_{max}	ft-lb/ft	Maximum bending moment per foot
P_i	lb/ft	Interior load per foot
P_p	lb/ft	Perimeter load per foot
P_{sw}	lb/ft^2 (psf)	Soil swell pressure, Table 20
q	lb/ft^2 (psf)	Uniform applied pressure
R	lb	End reaction at perimeter for equivalent simple beam
S	ft	Rib spacing; $= S_s$ short direction; $= S_l$ long direction
V	lb/ft	Shear per foot
V_{max}	lb/ft	Maximum shear per foot
V_r	lb	Maximum shear for a given rib, $V_{max}S$
y_m	in.	Soil heave without foundation load, Table 20
Δ	in.	Deflection
Δ_p	in.	Deflection at perimeter
θ	radians	Rotation of support of equivalent cantilever
β_{max}	in./in.	Maximum angular distortion

b. Center Lift Beneath Transverse Rib

Calculation	Equation	Comment	Diagram
Maximum moment for a given rib M_r, ft-lbs	$L_c = L_oC$ $M_{max} = P_pL_c + \frac{qL_c^2}{2}$ $M_r = M_{max}S$	$C = 0.8y_m^{0.12} \cdot I^{0.16}/P_p^{0.12}$ $L_o = 2.3 + 0.4e_m$ M_{max} located distance L_c from perimeter and assumed to vary linearly from M_r to zero at the perimeter and $5L_c$ from the perimeter	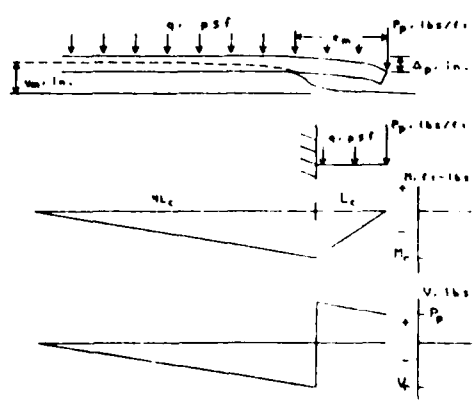
Maximum shear for a given rib V_r, lbs	$V_{max} = P_p + wL_c$ $V_r = V_{max}S$	V_{max} located distance L_c from the perimetr and assumed to vary linearly to P_p at the perimeter and and approach zero $5L_c$ from the perimeter	

Table 23 (Concluded)

Calculation	Equation	Comment	Diagram
Maximum deflection at perimeter Δ_p, in.	$\Delta_p = 0.11 + 12L_c\theta$ $\theta = \dfrac{M_{max}^{1.4}}{9800I \cdot k_s^{0.5}}$	0.11 in. is an approximation for support translation plus cantilever bending and 12 converts L_c to inches	
Maximum angular distortion β_{max}	$\beta_{max} = \Delta_p/l$ $l = 4(12L_c)$	$\beta_{max} \leq$ allowable angular distortion (Table 24)	

c. Edge Lift Beneath Transverse Rib

Calculation	Equation	Comment	Diagram
Maximum deflection Δ_p, in.	$L_e = \dfrac{7.5I^{0.17}L_i^{0.37}\Delta_p^{0.12}}{q^{0.07}P_i^{0.11}}$ $R = P_p + \dfrac{qL_e}{2} + \dfrac{P_i(L_e - L_i)}{L_e}$ $L_b = \dfrac{1.1R}{P_{sw}}$ $\Delta_p = y_m(e_m - L_b)e_m^2$	An iteration scheme is required to calculate L_e because Δ_p is unknown. Initially assume $\Delta_p < y_m$ then calculate L_e, R, L_b, and Δ_p. Repeat calculation until last Δ_p is within 0.01 inch of previous Δ_p. If $P_i = 0$ or $L_i > L_e$, then $L_e = 10.51^{0.17}\Delta_p^{0.12}/q^{0.07}$	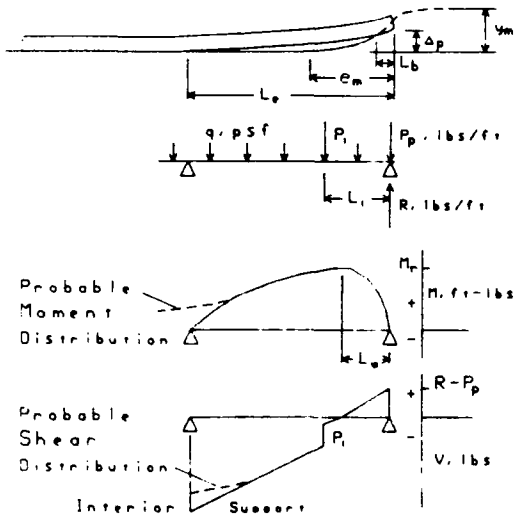
Maximum angular distortion β_{max}	$\beta_{max} = \Delta_p/L_e$	$\beta_{max} \leq$ allowable angular distortion (see Table 24)	
Maximum moment for given rib M, ft-lb	$M^* = L(R-P_p) - \dfrac{qL^2}{2}$ $M = M^*$ $M = M^* - P_i(L-L_i)$ $M_{max} = \dfrac{(R-P_p)^2}{2q}$ $M_r = M_{max}S$	Moment calculated by statics. Location M_{max}, $L_* = \dfrac{R-P_p}{q}$ If $L \leq L_i$ If $L \geq L_i$	
Maximum shear for given rib V_r, lb	$V_{max} = q(L_i - L_e) - P_i$ $V_r = V_{max}S$	Distributed support from soil reduces shear calculated near interior support; hence, limit V_{max} as given	

Table 24

Limiting Angular Distortions to Avoid Potential Damages[6,8,74]

Limits to Avoid Damage	Length / Height	Allowable Angular Distortion, $\beta = \delta/\ell$
Hogging of unreinforced load-bearing walls		1/2000
Load bearing brick, tile, or concrete block walls	≥ 5 ≤ 3	1/1250 1/2500
Sagging of unreinforced load-bearing walls		1/1000
Machinery sensitive to settlement		1/750
Frames with diagonals		1/600
No cracking in buildings; tilt of bridge abutments; tall slender structures such as stacks, silos, and water tanks on a rigid mat		1/500
Steel or reinforced concrete frame with brick, block, plaster or stucco finish	≥ 5 ≤ 3	1/500 1/1000
Circular steel tanks on flexible base with floating top; steel or reinforced concrete frames with insensitive finish such as dry wall, glass, panels		1/300 - 1/500
Cracking in panel walls; problems with overhead cranes		1/300
Tilting of high rigid buildings observed		1/250
Structural damage in buildings;, flexible brick walls with length/height ratio > 4		1/150
Circular steel tanks on flexible base with fixed top; steel framing with flexible siding;		1/125

[74]Technical Manual 5-818-1, "Procedures for Foundation Design of Buildings and Other Structures (Except Hydraulic Structures)

spelling out exactly what the contractor or construction engineer is expected to accomplish. Records will also be an important source of factual data in case lawsuits are filed seeking compensation for losses incurred by contractors or by owners of the construction. Lack of explicit specifications reduces quality and may leave the owner open to claims. Records will also be useful if the structure becomes damaged at some future time to assist determination of the cause of damages and appropriate remedial measures.

253. Preparation of foundation soil, engineered fill placement and mat construction should be closely monitored by a responsible inspector, geotechnical engineer, and/or representative of the owner/operator to confirm that assumptions used by the designers actually occur in the field. Parameters of the load bearing soils should be checked to be sure they are similar to those used in the design, have sufficient bearing capacity, and located at the expected depth. The unexpected detection of unstable soils such as expansive, collapsible and soft materials should be brought to the attention of the designers and owners of the project so proper adjustments may be made to the structure. Construction materials should meet or exceed design specifications such as use of proper fill plasticity and density, reinforcing steel of proper size and strength, and concrete of adequate strength and workability.

254. Identification of soil. Foundation soils encountered during construction should be identified, particularly if the soils are expansive or collapsible, paragraphs 235 and 236. Observations of soils actually encountered during construction will be used to confirm the assumptions made by the designers and to check that the intent of the foundation design will be accomplished during construction. Actual soil conditions that do not match design assumptions will require modifications to the design to assure that the foundation will perform adequately on the supporting soil over the projected life of the facility. Examination of the condition and types of structures adjacent to the construction site can provide additional information on the foundation soils.

255. Maintenance of constant water content. Every practical procedure should be taken to promote constant soil moisture and therefore maintain adequate soil strength and bearing capacity. Deformation that occurs will

therefore be limited to the normal elastic recompression settlement. Changes in water content can be minimized by promoting drainage, dewatering, and construction efficiency. Adequate drainage will eliminate ponding of surface water and reduce percolation of runoff into the foundation soil.

256. Rapid construction reduces time available for rainfall to occur and collect in the foundation soil and reduces evaporation from prepared soil bearing surfaces before the foundation can be placed. Construction efficiency may be improved by having equipment and materials required for a particular task at a convenient location adjacent to the site. All unnecessary items should be removed from the construction site to reduce clutter and increase mobility. Materials required for a particular construction sequence should be ordered sufficiently in advance to be available on site prior to the time of construction. Quality control and quality assurance must be maintained while rapid construction is facilitated. Construction errors should be corrected as soon as possible after they are made to reduce delay and cost. Delays can be minimized by careful management including frequent checking for adequate quality and frequent communication with subcontractors, construction workers, and suppliers of equipment and material. Delays early in construction should especially be avoided to prevent soil preparation work from "slipping" into wet or adverse weather seasons.

Preparation for Mat Construction

257. The site should always be provided with adequate drainage to promote runoff of rainfall and minimize change in soil moisture and subsequent differential movement. Site drainage should provide dry working conditions on firm soil surfaces. Trafficability should be adequate to promote mobility of mechanized equipment. A granular fill layer up to 1 ft thick provides temporary roads for rapid movement of equipment and materials into and out of the site. This fill can also improve the grade to promote drainage and can also exert a surcharge pressure on underlying foundation soil that can help suppress swell pressures in the soil that develop on long-term wetting. Lime and/or cement mixed into surface soil of low trafficability often increases bearing capacity and site mobility. Site preparation work should be completed prior to the wet season, without delay and with adequate quality control to

optimize performance of the foundation soil. Soil preparation work should occur continuously until protected by the foundation of the structure to reduce detrimental effects of rainfall and drying on the foundation soil.

258. Clearing the site. Existing trees and other vegetation removed from the site may leave depressions. Depressions, holes, and trenches may often be filled with the natural soil compacted at the natural water content and density of the in situ soil to initially level the ground surface. Soil removed in cuts should be minimized because cut areas reduce the overburden pressure on underlying foundation soil, which also reduces the pore water pressure in the soil. If the soil is relatively impervious such as for cohesive materials, considerable time is required for these pore pressures to increase to an equilibrium consistent with the surrounding area. Rebound and a long-term time dependent heave may occur that will aggravate differential movement over many years, particularly if the soil is expansive. A perched water table may even develop, if not already present, because previously existing vegetation may have desiccated the soil. Trees can desiccate soil to depths exceeding 50 or 60 ft.[75]

259. Excavation. Prior to initiation of any excavation work, maps of subsurface utilities should be investigated to determine the location and types of utilities that will be encountered so accommodations may be made to continue service and prevent damage to the utilities. During excavation work unexpected as well as expected problems must be identified and dealt with such as loss of slope stability, loss of ground, bottom heave, and groundwater. Excavations should be completed to the design depth as rapidly as possible and exposed soil protected from both wetting and drying. Equipment should be selected to optimize removal of overburden soil depending on the size and depth of the final excavation. Transportation equipment to remove overburden to appropriate disposal areas should be selected depending on the rate of excavation and haul distance. Table 25 provides an example of excavation specifications.

260. The bearing soil at the design depth should be checked prior to excavating to the design depth to be sure that this soil is satisfactory and will support the foundation within allowable displacements. If this soil is

---

[75]Blight 1987

Table 25

Example Excavation Requirements

Excavations conformed to the dimensions and elevation of each structure.

Excavations include trenching for utility and foundation drainage systems to a point 5 ft beyond the building line.

Excavations extend sufficient distance from walls and footings to allow for placing and removing forms.

Excavation below indicated depths are not permitted except to remove unsatisfactory material. Satisfactory material removed below depths indicated shall be replaced with satisfactory material at no additional cost to the government. The thickness of concrete footings shall be increased in thickness to the bottom of the overdepth excavations and overbreak in rock excavations.

Excavation shall be performed so that the area will be continually and effectively dewatered* and surface drained**. Water from any source shall not be permitted to accumulate in crawl space areas and in the excavation. The excavation shall be drained by pumping or other satisfactory methods to prevent softening of the foundation bottom, undercutting of footings, or other actions detrimental to proper construction.

Shoring including sheet piling shall be furnished and installed as necessary to protect workmen, banks, adjacent paving, structures, and utilities.

---

*dewater refers to the elimination of any ground water in the excavation

**surface drained refers to the elimination of any surface water

not satisfactory, then this weak or soft soil must be excavated to a sufficient depth beneath the proposed foundation depth and replaced with fill compacted to a satisfactory density and bearing capacity. The depth of overexcavation depends on the extent of unsatisfactory material and economics of this situation. Some redesign of the foundation may be required if unsuitable bearing soils are found and some delay and additional cost may occur. A thorough soil investigation prior to construction should minimize encountering this kind of problem.

261. After the final layer of soil to be excavated is removed, the exposed surface of the load bearing soil should be immediately protected from disturbance such as wetting or drying. This is especially critical with clays and shales that may flake, spall, shrink, swell or otherwise deteriorate from exposure to the atmosphere. A layer of concrete called a "mudslab" or a permanent membrane may be placed on the exposed bottom of the excavation to protect the soil. A chlorinated polyethylene membrane of about 10-mil thickness may also adequately protect the soil surface. Asphalt coatings may also be applied to protect the excavation bottom, but these may be sticky and difficult to use.

262. The foundation and superstructure should be constructed as soon as possible on the prepared surface of the excavation bottom to replace the loss in pressure applied to the underlying soil from the excavated overburden. Rapid construction and placement of the structural loads replace the original soil weight and therefore reduce heave from rebound and subsequent settlement and differential movement caused by recompression of the underlying soil.

263. Surface runoff from rainfall, groundwater seeping into the excavation, and other sources of water must be drained from the site and excavation. Ponded water must not be permitted to collect in open excavations because this water will seep into the underlying soil and reduce its shear strength. The soil may also expand with some or most expansion taking place following construction of the foundation. Pumping equipment may be required to dewater the excavation.

264. The excavation perimeter must be stable against a slope failure. An open excavation in normally consolidated clay will stand vertically without support for heights up to 4 times the undrained shear strength divided by the

wet density of the soil until drying and/or pore pressure recovery reduces the mass strength. Loess and stiff glacial tills will stand vertically over long periods. Moist sands and sandy gravels can stand vertically from cohesion caused by negative pore water pressure. Dry sands and gravels will stand at slopes equal to their angle of repose. Removal of lateral pressure, however, may open fissures and exposure to the environment will cause deterioration and may increase pore water pressure near the surface of the perimeter soil of the excavation; slides may subsequently occur. Consideration should be given to placement of a temporary impervious membrane or sprayed bituminous coating on the exposed perimeter soil.

265. Pavements, facilities and other property near the excavation must be protected. Property must be checked and their condition recorded prior to any excavation. Periodic level readings of temporary benchmarks or stakes placed around the perimeter and near existing structures and pavements should be recorded to monitor loss of ground. Loss of ground or vertical settlement on the ground surface outside the perimeter of an excavation exceeding 1/4 inch may indicate lateral deformation and creep of the perimeter into the excavation, seepage of groundwater into the excavation, or heave of the excavation bottom. Loss of ground should not exceed 1/2 inch or lateral creep should not exceed 2 inches to avoid any damage to adjacent facilities.

266. Excavation slopes may be supported by inclined or horizontal braces against vertical piles and sheet walls, closely-spaced cast-in-place concrete drilled shafts, sheet pile walls with ground anchors, or reinforcing the earth with steel rods driven through a facing material such as wood planks or metal sheets. Excessive rebound of the excavation bottom may be reduced by limiting the size of the excavation and constructing the foundation and superstructure in several sections.

267. Fill placement. Cohesive, low plasticity fills compacted to a density with adequate bearing capacity are commonly used to replace unsatisfactory soil of low bearing capacity or soil of a swelling/collapsible nature to depths of about 4 to 8 ft beneath the mat, raise the existing ground surface to the final grade elevation, and place around the perimeter of structures constructed in excavations. Materials selected for fills should be sands and gravels containing a less than Number 40 mesh fraction of fines with

plasticity index less than 12 and liquid limit less than 35. Peats, organic materials, silty sands and silts of high plasticity are not acceptable fill materials.

268. The fill should have cohesion to allow construction of trenches for ribs and utility lines with minimal form work. The cohesion also reduces permeability of the fill and minimizes seepage of surface water down into the natural stratum beneath the fill. Seepage into a pervious fill overlying a relatively impervious natural stratum can contribute to a perched water table in the fill and may lead to long-term differential movement if the underlying stratum is desiccated expansive or collapsible soil. Table 26 provides an example fill specification.

269. Sufficient laboratory classification and compaction tests should be performed during the site and soil exploration program to identify potential fill materials, to assure adequate quantities and to determine compaction characteristics of the various materials available in the borrow areas. Accurate identification by Atterberg limit and gradation tests assist selection of appropriate fill material and water content limits required to achieve adequate density and bearing capacity of a particular fill. The fill should be uniform in the horizontal direction to minimize differential movement of the mat foundation. Compaction effort normally required for cohesive fill is at least 90 percent of optimum density determined by the compactive effort described in ASTM D 1557. This high compactive effort is comparable with modified AASHTO. For the low plasticity fills of plasticity index < 12 often recommended beneath structures compaction should be at least 92 percent of optimum density. Laboratory tests should be performed prior to construction on the proposed fill material to be sure that the plasticity, stiffness and strength of the compacted fill will provide optimum performance of the foundation.

270. The first fill layer following compaction should be checked to meet density and material specifications such as those in Table 26. Substantial delays can and will occur if unsatisfactory compacted material must be removed and replaced with satisfactory material. In situ density tests such as ASTM D 1556 should be performed to check the density and used to calibrate surface moisture nuclear gages. Numerous surface moisture gage

Table 26

Example Fill Requirements

Type of materials permitted in fill include GW, GM, GC, GP, SW, SP, SM, SC, and CL of the Unified Soil Classification System. The plasticity index should be less than 12 and the liquid limit less than 35. Such material may be cohesive and should be compacted to not less than 92 percent of optimum density.

Unsatisfactory materials include PT, OH, OL, ML, MH, and CH of the Unified Soil Classification System.

When subgrade surfaces are less than the specified density, the surface shall be broken up to a minimum depth of 6 inches, pulvrized and compacted to the specified density.

The excavated surface shall be scarified to a depth of 6 inches before fill placement is begun.

Satisfactory unfrozen material shall be placed in horizontal layers not exceeding 8 inches in loose depth and then compacted.

Materials shall not be placed on surfaces that are muddy, frozen, or contain frost.

Compaction shall be accomplished by sheepsfoot rollers, pneumatic-tired rollers, steel-wheeled rollers, or other approved equipment well suited to the soil being prepared.

Materials shall be moistened or aerated as necessary to provide proper water content that will readily facilitate obtaining the specified compaction with equipment used.

Fill materials shall be compacted to densities after ASTM Standard D 1557:

	Cohesive	Cohesionless
Under structures	92	95
Under sidewalks and grassed areas	85	90

readings can subsequently be made following compaction of additional layers of fill. Nuclear gages should be periodically checked with results of ASTM D 1556 or other appropriate density measurement method performed on compacted fill. If inclement weather stops the fill operation, then upon resuming work the top layer of compacted fill affected by rainfall should be scarified until the correct range of water content is achieved before recompacting and continuing with fill placement.

271. Construction of stiffening beams. Trenches for construction of stiffening beams and utilities may be excavated in the cohesive granular fill using a trenching machine capable of a minimum width of 12 inches and depths up to at least 3 ft below grade. Widths of 18 inches or more are usually required to accommodate placement of steel reinforcement in the beams.

272. Vapor barriers. Vapor barriers such as plastic films may be placed in trenches and beneath slabs. These barriers prohibit accumulation of moisture into the concrete with possible sweating of this moisture up through the concrete to the surface of the floor. This is especially important where compacted fills of relatively high permeability have been placed over relatively impervious natural soil. Groundwater tends to accumulate in these fills. Plastic films should be checked to be free of punctures, holes, and other leaks before placing the concrete.

273. Plastic films also prevent loss of moisture into underlying soil from the concrete mix; therefore, the concrete mix should not contain excess water to minimize drying shrinkage. Drying shrinkage occurs at the surface of the mat and may cause some upward curling at the edges or joints. Stiffening beams at the perimeter and expansion joints of the mat foundation can effectively reduce curling. Vapor barriers should be placed snugly against trench walls to avoid any gaps between the trench walls and the membrane; the concrete stiffening beams otherwise will not have the correct shape and dimensions required to resist bending moments. Incorrectly placed vapor barriers must be removed or corrected to allow stiffening beams to form with the correct dimensions.

274. Reinforcement steel. Steel reinforcement should be placed in the proper location to provide adequate concrete cover and optimum bending moment resistance. Reinforcement steel should be ASTM Grade 60, except Grade 40 may

be used for ties. Refer to Chapter 4.7, ACI 302 (1980) for further details on reinforcement steel. Steel tendons and anchors for post-tensioned concrete must be properly supported and means provided for holding post-tensioning anchorage assemblies in place. Concrete near anchors should be reinforced with additional steel. The post-tensioning stress should be applied as soon as the concrete reaches its design strength. Columns should have sufficient freedom to move laterally when the post-tensioning stress is applied. Proper post-tensioning requires careful control of construction under expert supervision.

275. Concrete. Concrete should be of the correct composition to provide the design strength, which is usually 3000 psi after 28 days. The slump should be 4 to 6 inches and no water should be added to the mix after leaving the batch plant. Further details on concrete for building construction are in the literature[76].

276. Excess water cannot drain out of concrete placed on impervious membranes. Water reducing admixtures (ASTM C494) may be added to increase workability, reduce water required to obtain the desired slump, and thereby increase strength of the finished concrete. Concrete shrinkage may be reduced by using cement with lower water demand such as Type I and coarse aggregates that do not shrink when dried[66]. High range water reducers or superplasticizers are prohibited in guide specification CEGS 03300. Mats supporting large structures are commonly constructed in sections where concrete is placed on portions of the foundation area, while excavation and preparation of the bearing soil surface proceeds in other areas. Concrete should be adequately cured before removal of forms and before permitting traffic on the mat. Refer to TM 5-818-7 for further construction details on expansive soil.

277. Concrete for large ribbed mats may be placed in one or two stages. If placed in two stages, the first stage is to place concrete for the stiffening beams followed a few days later with concrete for the remaining mat. The exposed concrete surface on the stiffening beams must be kept clean to allow the fresh concrete to adhere to concrete placed earlier. The

---

[76]Corps of Engineers Guide Specification (CEGS) 03300, ACI 302 (1980), Technical Manuals 5-809-2 and 5-809-12

finishing of concrete is important in obtaining sufficient levelness and flatness of the floor to optimize operational efficiency. Guidelines for the degree of floor flatness/levelness required to achieve adequate operational efficiency, however, are not complete. A standard recommended for specifying floor flatness/levelness is the F-number system[77].

Site Finishing

278. Site finishing involves connection of utility lines, backfill of open excavations, installation of drainage systems, and landscaping. Utility connections to outside lines should be flexible and watertight. Backfill materials should be nonexpansive with low permeability to inhibit migration of surface moisture down to soil with potential for volume change.

279. The site should be graded to provide at least a 1 percent slope from the perimeter of the structure for positive drainage. A 5 percent slope should be provided for at least 10 ft from the perimeter of the structure for foundations on potentially expansive soil to promote rapid runoff of surface water. Fill placed to raise structures above the original ground surface contributes to a positive grade for drainage and reduces differential movements from volume changes in nonuniform foundation soils. The structure should be provided with gutters and downspouts to collect rainfall. Runoff from downspouts should be directed on to splash blocks at least 5 ft long and sloped for positive drainage from the structure. Impervious horizontal moisture barriers or membranes about 10 ft wide placed around the perimeter and protected by 6 inches of fill helps to promote uniform changes beneath the mat and moves the edge moisture variation distance out from beneath the foundation. These should be placed at the end of the wet season. Underground perforated drain lines adjacent to mats placed in excavations to collect seepage should be constructed with a 1 percent slope to avoid water ponding in the line. The drain must be connected to an outlet to drain seepage collected around the foundation. An impervious membrane placed beneath the drain will minimize seepage into desiccated subsoil. Underground drains, however, are usually not recommended because they have been a source of moisture into expansive/collapsible subsoils aggravating differential foundation movements.

---

[77]Face 1987, ASTM E 1155

Followup

280. The foundation and superstructure should be observed periodically to evaluate performance of the structure. Table 27 illustrates a preliminary systematic record system for rating performance of foundations. Table 27a defines the type of movement, whether center mound (center heave) or center dish (edge heave or center settlement) expected depending on the type of observed cracks. Table 27b allows the observer to evaluate the angular distortion ß from the measured crack dimensions and to rate the distress. Cracks, distortions, and other structural deterioration should be recorded similar to that illustrated in Table 27c. The type of movement, ß estimate, and level of distress may also be entered in Table 27c. A floor and wall plan of the facility should also be attached to Table 27 to complete the damage record. The grade around the perimeter should be checked for adequate slope and control of erosion. The grade may become impaired with time around the perimeter from settlement of backfill or heave of in situ expansive soil. An expansive soil is not restrained from heave outside the perimeter and may destroy the grade. Eventually, rainfall may be directed toward the foundation until positive drainage is restored.

Table 29

Preliminary

SYSTEMATIC DAMAGE RECORD SYSTEM

For Record of Differential Movement in Foundation Soils

a. Type of Movement

Component	Distress		Center Mound	Center Dish
Exterior Walls	Horizontal Cracks	- near top (roof restraint)	X	
		- wall bulging out	X	
		- wall bulging in		X
	Vertical Cracks	- larger near top, more frequent near top	X	
		- larger near bottom, start near bottom		X
	Diagonal Cracks	- up toward corner from bottom of wall	X	
		- up toward corner from top of window	X	
		- down away from window	X	
		- up from corner		X
		- radiate up toward interior		X
Slabs	Tilting up toward center of facility		X	
	Tilting up toward perimeter			X
	Cracks parallel with wall, larger at top surface		X	
Deep Foundation	Fractured Plinths	- near center of facility	X	
		- near edge of facility		X

b. Damage Rating

Hand Level Readings		Crack Widths	
ß, Vertical Change / Level Length	Distress	Width, in.	Degree of Damage
		< 1/8	Slight
		1/8 - 1/4	Minor
> 1/150	Structural damage	1/4 - 1/2	Mild
> 1/250	Inconvenience to occupants	1/2 - 3/4	Moderate
		> 3/4	Severe
> 1/500	Cracking		

c. Site Assessment

Inspector_____ Date_____ Facility_____

Age (yrs)_____

Location_____

Check
Climate: Humid___ Semi-arid___ Arid___

Check Foundation:
- Ribbed mat_____
- Flat mat_____
- Drilled shaft_____
- Driven pile_____
- Shallow footings___
- Strip footings_____

Depth of Foundation Base Below Ground Surface, ft_____

Check Drainage:
- Downspouts_____
- Splash blocks_____
- Gutters_____

Slope from perimeter:_____

Soil Description: _____

Utility Water Loss:_____

Level Record

Location	Vertical Change, in.	ß

Level length, in. _____

Crack Distress Record

Location	Orientation	Length, in.	Maximum Width, in.

Visible Moisture Source to Soil _____

_____

_____

Performance Rating

Maximum Crack Width, in._____

Shape of Movement: Mound_____ Dish_____

Check probable Movement: Heave_____ Settlement_____

Maximum ß _____

Distress _____

Degree of Damage_____

Occupant Comments:_____

_____

_____

_____

_____

_____

Inspector Comments:_____

_____

_____

_____

_____

_____

PART VI. RECOMMENDATIONS

281. A systematic damage record system to document foundation distortion, distress in facilities, and maintenance requirements should be fully developed in preparation of field surveys of constructed facilities to catalog damages to structures and therefore make possible progress in identifying the cause of damage, requirements for repair and efficiency of operations, particularly the impact of foundation movement on machinery and robotic equipment. Field surveys should subsequently be performed to measure surface displacements inside and outside of existing structures and to rate the performance of structures using the frequency spectrum method with the systematic performance record system. The specific floor flatness/levelness requirements to provide optimum performance of facilities should be determined. Guidelines may then be implemented to minimize these damages and their effects on short and long-term structural performance and aid in reducing repair and long-term maintenance.

282. Research is recommended to determine methods for reducing soil movement by ground modification or soil moisture stabilization and therefore, to reduce requirements of designing foundations to resist soil movements. Research and development efforts are necessary to verify the effectiveness of soil moisture stabilization, establish criteria for stabilization, establish structural criteria for mats on moisture-stabilized soils, and develop construction details for perimeter moisture barriers.

283. Research is recommended to investigate the problem of cracking during construction of ribbed mats. Drying shrinkage in stiffening beams, which may let the ribs hang in the trenches, may be a factor in cracking. Research may be useful to recommend spacing of construction joints, acceptability of joints between stiffening beam ribs and slabs, location of the membrane vapor barrier, concrete strength and mix design, percent and location of reinforcement, and curing methods.

284. Research is recommended to determine proper specifications for preparation and compaction of low plasticity, nonexpansive, cohesive fills commonly placed to support ribbed mats and other shallow foundation systems. Current specifications for compaction of cohesive clays and cohesionless sands may not be appropriate for these engineered fills.

285. A field survey of Corps of Engineers division and district offices, real estate developers, contractor organizations, casualty insurance writers, private consultants, and educational institutions is recommended to collect a detailed list of all design/construction procedures and local practices for ground modification and soil moisture stabilization in unstable (expansive/collapsible,soft) soil areas. These practices should be rated to determine their relative usefulness in providing economical and adequate guidelines for design and construction of foundations in unstable soils.

286. Centrifuge and/or field tests should be performed with unstable soil to confirm and improve appropriate soil input parameters for design such as the active depth of heave, edge moisture variation distance, potential soil heave and to obtain information on a fundamental new parameter, the maximum acceptable change in suction at the lower boundary of the depth of soil subject to heave. The centrifuge can simulate a full scale field test by subjecting a small model to acceleration such that the field situation is simulated. A sequence of events such as placement of loads and diffusion of moisture of a full scale test can be simulated rapidly in the centrifuge so that the distribution of volume changes and vertical displacements from applied loads and moisture changes can be observed in just a few days rather than months or years required in the field. Costs can be substantially reduced by eliminating many full scale field test sections with associated instrumentation and monitoring and analysis of data over a long period of time. Field test sections in different climates will validate design guidelines for general applications. These tests may be used to analyze the effectiveness of ground modification techniques and the ability of design methodology to predict behavior of the foundation in the soil. Guidelines for ground modification techniques that reduce potential volume changes leading to the design and construction of more economical foundation systems may subsequently be developed.

287. Two- or three-dimensional soil-structure interaction models such as the plate on elastic foundation, frequency spectrum model for mats or other model shown to reasonably simnulate field behavior may be improved to aid the analysis and design of mat foundations in unstable soil. Boundary elements, which are particularly appropriate for moisture diffusion problems, as well as the finite element method may be considered in analyses.

REFERENCES

ACI Committee 302. 1980. "Guide for Concrete Floor and Slab Construction", Construction Practice and Inspection Pavements, Part 2, ACI Manual of Concrete Practice, American Concrete Institute, Detroit, MI

ACI Committee 318. 1980. "Part 4-General Requirements", Use of Concrete in Buildings: Design, Specifications, and Related Topics, Part 3, ACI Manual of Concrete Practice, American Concrete Institute, Detroit, MI

ACI Committee 336. 1987. "Suggested Design Procedures for Combined Footings and Mats", American Concrete Institute Committee 336, American Concrete Institute, Detroit, MI

ACI Committee 340. 1977. "Slab Design In Accordance With ACI 318-77", Supplement To Design Handbook In Accordance With The Strength Design Method, ACI Publication SP-17 (73)(S), American Concrete Institute, Detroit, MI

ACI Committee 435. 1980. "Allowable Deflections," Use of Concrete in Buildings: Design, Specifications, and Related Topics, Part 3, ACI Manual of Concrete Practice, American Concrete Institute, Detroit, MI

ACI Committee 436. 1966. "Suggested Design Procedures for Combined Footings and Mats," Journal of the American Concrete Institute, Reported by S. V. DeSimone, Vol 63, Detroit, MI, pp 1041-1056

Ahlvin, R. G. and Ulery, H. H. 1962. "Tabulated Values for Determining the Complete Pattern of Stresses, Strains, and Deflections Beneath a Uniform Circular Load on a Homogeneous Half Space," Stress Distribution in Earth Masses, Highway Research Board Bulletin 342, NAS-NRC, Washington, D. C., pp 1-13

Annual Book of ASTM Standards. 1988. "Chemical Admixtures For Concrete," ASTM Standard Specification C494-86, Concrete and Aggregates, Part 04.02, American Society for Testing and Materials, Philadelphia, PA

_____. 1988. "Bearing Capacity of Soil for Static Load on Spread Footings," ASTM Standard D1194-72, Soil and Rock; Building Stones; Geotextiles, Volume 04.08, American Society for Testing and Materials, Philadelphia, PA

_____. 1988. "Density of Soil in Place by the Sand-Cone Method," ASTM Standard Test Method D1556-82, Soil and Rock; Building Stones; Geotextiles, Volume 04.08, American Society for Testing and Materials, Philadelphia, PA

_____. 1988. "Moisture-Density Relations of Soils and Soil-Aggregate Mixtures Using 10-lb (4.54-kg) Rammer and 18-in. (457-mm) Drop." ASTM Standard D1557-78, Soil and Rock; Building Stones; Geotextiles, Volume 04.08, American Society for Testing and Materials, Philadelphia, PA

_____. 1988. "Penetration Test and Split-Barrel Sampling of Soils," ASTM Standard D1586-84, Soil and Rock; Building Stones; Geotextiles, Volume 04.08, American Society for Testing and Materials, Philadelphia, PA

_____. 1988. "Deep, Quasi-Static, Cone and Friction-Cone Penetration Tests of Soil," ASTM Standard D3441-79, Soil and Rock; Building Stones; Geotextiles, Vol 04.08, American Society for Testing and Materials, Philadelphia, PA

_____. 1988. "One-Dimensional Swell or Settlement Potential of Cohesive Soils," ASTM Standard D4546-85, Soil and Rock; Building Stones; Geotextiles, Vol 04.08, American Society for Testing Materials, Philadelphia, PA

_____. 1988. "Pressuremeter Testing of Soils," ASTM Standard D4719-87, Soil and Rock: Building Stones; Geotextiles, Vol 04.08, American Society for Testing Materials, Philadelphia, PA

_____. 1988. "Standard Test Method for Determining Floor Flatness and Levelness Using the F-number System", E1155-87, Building Seals and Sealants; Fire Standards; Building Constsructions, Vol 04.07, American Society for Testing and Materials, Philadelphia, PA

Baquelin, F., Jezaquel, J.-F., and Shields, D. H. 1978. The Pressuremeter and Foundation Engineering, Trans-Tech Publications, Rockport, MA

Bathe, K., Peterson, F., and Wilson, E. 1978. "SAP5-WES Structural Analysis Program," Program No. 713-F3-R0012, U. S. Army Engineer Waterways Experiment Station, Vicksburg, MS

Blight, G. E. 1987. "Lowering of the Groundwater Table by Deep-Rooted Vegetation - The Geotechnical Effect of Water Table Recovery", Groundwater Effects in Geotechnical Engineering, Proceedings Ninth European Conference on Soil Mechanics and Foundation Engineering, Dublin, pp 285-288

Bobe, R., Hertwig, G., and Seiffert, H. 1981. "Computing Foundation Slabs With Building Rigidity," Proceedings of the 10th International Conference on Soil Mechanics and Foundation Engineering, Vol 2, Stockholm, Sweden, pp 53-56

Boussinesq, J. 1885. Application of Potential to the Study of the Equilibrium and Movements in Elastic Soils, Gauthia-Villard, Paris

_____. 1976. "Mat Foundations," Analysis and Design of Building Foundations, Chapter 8, editor H. Y. Fang, Envo Publishing Company, Lehigh Valley, Pa, pp 209-231

_____. 1982. Foundation Analysis and Design, 3rd Edition, McGraw-Hill Book Company, New York, NY, pp 187-188, 240-258

_____. 1988. Foundation Analysis and Design 4th Edition, McGraw-Hill Book Company, pp 219-222, 266

Briaud, Jean-Louis. 1979. "The Pressuremeter: Application to Pavement Design," Ph.D. Thesis, Department of Civil Engineering, School of Graduate Studies, University of Ottawa, Ottawa, Canada, pg 184-188.

Briaud, J.-L., Tucker, L., and Coyle, H. M. 1982. "Pressuremeter, Cone Penetrometer, and Foundation Design," Civil Engineering Department, Texas A&M University, College Station, TX

Brooker, E. W. and Ireland, H. O. 1965. "Earth Pressures at Rest Related to Stress History", Canadian Geotechnical Journal, Vol 11, pp 1-15

Building Research Advisory Board (BRAB). 1968. "Criteria for Selection and Design of Residential Slabs-on-Ground," Publication No. 1571, National Academy of Sciences-National Research Council, Washington, D. C.

Burland, J. B. and Davidson, W. 1976. "A Case Study of Cracking of Columns Supporting A Silo Due to Differential Foundation Settlement," No. CP42/76, Building Research Station, Building Research Establishment, London, England

Burland, J. B. and Wroth, C. P. 1978. "Settlement of Buildings and Associated Damage," Foundations and Soil Technology, The Construction Press, Lancaster, England, pp 287-329

Burmister, D. M. 1963. "Prototype Load-Bearing tests for Foundations of Structures and Pavements", Field Testing of Soils, American Society for Testing and Materials Standard Technical PublicationNo. 322, pp 98-119, Philadelphia, PA

Buttling, S. and Wood, L. A. 1982. "A Failed Raft Foundation on Soft Clays," Ground Engineering, Vol 15, No 5, pp 40-44

Chou, Y. T. 1981. "Structural Analysis Computer Programs for Rigid Multicomponent Pavement Structures With Discontinuities - WESLIQUID and WESLAYER," Technical Report GL-81-6 (3 Reports), U. S. Army Engineer Waterways Experiment Station, Vicksburg, MS

Christian, J. T. and Carrier III, W. D. 1978. "Janbu, Bjerrum, and Kjaernsli's Chart Reinterpreted," Canadian Geotechnical Journal, Vol 15, pp 123-128

Dawkins, W. P. 1982. "User's Guide: Computer Program for Analysis of Beam-Column Structures With Nonlinear Supports (CBEAMC),' Instruction Report K-82-6, U. S. Army Engineer Waterways Experiment Station, Vicksburg, MS

Department of the Army. Corps of Engineers, Office of the Chief of Engineers, 1984. "Geotechnical Investigations," Engineer Manual EM 1110-2-1804, Washington, D. C.

_____. (To Be Published). "Settlement Analysis," Engineer Manual EM 1110-1-1904, Washington, D. C.

_____. 1970. "Laboratory Soils Testing," Engineer Manual EM 1110-2-1906, Washington, D. C.

_____. 1972. "Soil Sampling," Engineer Manual EM 1110-2-1907, Washington, D. C.

_____. 1987. "Concrete for Building Construction", Corps of Engineers Guide Specification 03300, Washington, D. C.

Desai, C. S., Johnson, L. D., and Hargett, C. M. 1974. "Analysis of Pile-Supported Gravity Lock", Journal of the Geotechnical Engineering Division, Proceedings of the American Society of Civil Engineers, Vol 100, pp 1009-1029

DeSalvo, G. J. and Swanson, J. A. 1982. ANSYS Engineering Analysis System User's Manual, Swanson Analysis System, Inc. Houston, PA

Duncan, J. M. and Chang, C. Y. 1970. "Nonlinear Analysis of Stress and Strain in Soils," Journal of the Soil Mechanics and Foundations Division, Proceedings of the American Society of Civil LEngineers, Vol 97, pp 1629-1653

Duncan, J. M. and Clough, G. W. 1971. "Finite Element Analysis of Port Allen Lock," Journal of the Soil Mechanics and Foundations Division, Proceedings of the American Society of Civil Engineers, Vol 97, pp 1053-1068

Editor, 1982. "Structural Foundations," Construction News, June 11, pp 18-19, 21-22

Eshbach, O. V. 1954. Handbook of Engineering Fundamentals, 2nd Edition, John Wiley & Sons, pp 5-64 to 5-68

Face, A. 1987. "Specifying Floor Flatness and Levelness: The F-Number System", The Constrsuction Specifier, Alexandria, VA

Feld, J. 1965. "Tolerance of Structures to Settlement," Journal of the Soil Mechanics and Foundations Division, American Society of Civil Engineers, Vol 91, No SM3, pp 63-77

Focht, Jr., J. A., Khan, F. R., and Gemeinhardt, J. P. 1978. "Performance of One Shell Plaza Deep Mat Foundation," Journal of the Geotechnical Engineering Division, American Society of Civil Engineers, Vol 104, No GT5, pp 593-608

Fraser, R. A. 1975. "Review of Investigation on Raft Foundations for Major Buildings on Deep Soils, Perth Area," Paper III, Proceedings of Symposium on Raft Foundations, Perth, Western Australia, pp 23-40

Fraser, R. A. and Wardle, L. J. 1975. "The Analysis of Stiffened Raft Foundations on Expansive Soils," Symposium on Recent Developments in the Analysis of Soil Behavior and Their Application to Geotechnical Structures, Vol 2, Department of Civil Engineering Materials, University of New South Wales,m Kensington, N.S.W., Australia, pp 89-98

Gibson, R. E. 1967. "Some Results Concerning Displacements and Stresses in a Nonhomogeneous Elastic Half-Space," Geotechnique, Vol 17, pp 58-67

Godden, W. G. 1965. Numerical Analysis of Beam and Column Structures, Prentice-Hall, Inc., Englewood Cliffs, NJ

Golubkov, V. N., Tugaenko, Y. F., Matus, Y. V., Sinyavskii, S. D., and Varenik, P. F. 1980. "Investigation of Deformations in Soil Beneath Foundation Mat of 16-Story Residential Building," Translated from Osnovaniya, Fundamenty i Mekhanika Gruntov, No. 6, Odessa Civil Engineering Institute, Russia, pp 232-235

Haliburton, T. A. 1972. "Soil Structure Interaction: Numerical Analysis of Beams and Beam-Columns," Technical Publication No. 14, School of Civil Engineering, Iklahoma State University, Stillwater, OK

Hansen, J. B. 1961. "A General Formula For Bearing Capacity," Bulletin No. 11, Danish Geotechnical Institute, Copenhagen, pp 38-46

_____. 1970. "A Revised and Extended Formula For Bearing Capacity," Bulletin No. 28, Danish Geotechnical Institute, Copenhagen, pp 5-11

Hartman, J. P. and James, B. H. 1988. "Development of Design Formulas for Ribbed Mat Foundations on Expansive Soils," Technical Report ITL-88-1, U. S. Army Engineer Waterways Experiment Station, Vicksburg, MS

Headquarters, Department of the Army. 1984. "Concrete Structural Design for Buildings", Technical Manual 5-809-2, Washington, D. C.

_____. 1979. "Concrete Floor Slabs On Grades Subjected to Heavy Loads," Technical Manual 5-809-12, Washington, D. C.

_____. 1983. "Soils and Geology Procedures for Foundation Design of Buildings and Other Structures (Except Hydraulic Structures)", Technical Manual 5-818-1, Washington, D. C.

_____. 1983. "Foundations in Expansive Soils," Technical Manual 5-818-7, Washington, D. C.

Hetenyi, M. 1946. Beams on Elastic Foundation, The University of Michigan Press, Ann Arbor, MI, p 46

Holland, J. E. 1979. "Behavior of Experimental Housing Slabs on Expansive Clays," 7th Asian Regional Conference on Soil Mechanics and Foundation Engineering, Singapore

Hooper, J. A. 1978. "Foundation Interaction Analysis," Chapter 5, Developments in Soil SMechanics-1, C. R. Scott, editor, Applied Science Publishers LTD, London, England, pp 149-211

Hooper, J. A. and Wood, L. A. 1977. "Comparative Behavior of Raft and Piled Foundations," Proceedings of the Ninth International Conference on Soil Mechanics and Foundation Engineering, Vol 1, Tokyo, pp 545-549

Huang, H. H. 1974a. "Analysis of Symmetrically Loaded Slab on Elastic Solid," Technical Note, Journal of Transportation Engineering, American Society of Civil Engineers, Vol 100, No TE2

Huang, Y. H. 1974b. "Finite Element Analysis of Concrete Pavements With Partial Subgrade Contact," Transportation Research Record 483, Transportation Research Board, Washington, D. C.

Hughes, J. M. O. 1982. "Interpretation of Pressuremeter Tests for the Determination of Elastic Shear Modulus," Proceerdings of Engineering Foundation Conference on Updating Subsurface Sampling of Soils and Rocks and Their In Situ Tests, Santa Barbara, CA

Johnson, L. D. 1982. "Users Guide for Computer Program Heave", Miscellaneous Paper GL-82-7, U. S. Army Engineer Waterways Experiment Station, Vicksburg, MS

Johnson, L. D. 1988. "Proceedings of the Workshop on Design, Construction, and Research for Ribbed Mat Foundations," Miscellaneous Paper GL-88-6, U. S. Army Engineer Waterways Experiment Station, Vicksburg, MS

Kay, J. N. and Cavagnaro, R. L. 1983. "Settlement of Raft Foundations," Journal of Geotechnical Engineering, American Society of Civil Engineers, Vol 109, No 11, pp 1367-1382

Kerr, A. D. 1987. "Analysis of Footings on a Sand Base", Interim Progress Report for Contract CE DACW39-86-M-1358, Submitted to U. S. Army Engineer Waterways Experiment Station, Vicksburg, MS

Lambe, T. W. and Whitman, R. V. 1969. Soil Mechanics, John Wiley & Sons, New York, NY, p 153, 202

Lytton, R. L. 1972. "Design Methods for Concrete Mats on Unstable Soils," Proceedings of the 3rd Inter-American Conference on Materials Technology, Rio-de-Janeiro, Brazil, pp 171-177

McKeen, R. G. and Eliassi, M. 1988. "Selection of Design Parameters For Foundations on Expansive Soils," Prepared for U. S. Army Engineer Waterways Experiment Station, Vicksburg, MS, under Contract DACA39-87-M-0754

McKeen, R. G. and Lytton, R. L. 1984. "Expansive Soil Pavement Design Using Case Studies," International Conference on CAse Histories in Geotechnical Engineering, editor Shamsher Prakash, Vol III, St. Louis, MO, pp 1421-1427

Meyerhof, G. G. 1953. "Some Recent Foundation Research and Its Application to Design," Structural Engineer, London, England, Vol 31, pp 151-167

Milovic', D. M. 1959. "Comparison Between the Calculated and Experimental Values of the Ultimate Bearing Capacity," Proceedings of the 6th International Conference on Soil Mechanics and Foundation Engineering, Vol 2, Montreal, Canada, pp 142-144

Mitchell, J. K. and Gardner, W. S. 1975. "In Situ Measurement of Volume Change Characteristics," SOA Report, Proceedings of the American Society of Civil Engineers Special Conference on the In Sitsu Measurement of Soil Properties, Raleigh, N. C.

Mitchell, P. W. 1980. "The Structural Analysis of Footings on Expansive Soils," Kenneth W. G. Smith & Associaters Research Report No. 1, Webb & Son, 16 Fenn Place, Adelaide, Australia

Muhs, H. J. 1959. "Neuere Entwicklung der Untersuchung in Berechnung von Flachfundationer," Schweiz. Bauzeitung, Germany, Vol 19, p 11

Peck, R. B., Hanson, W. E., and Thornburn, T. H. 1974. Foundation Engineering, 2nd Edition, John Wiley & Sons, New York, NY

Pickett, G. and Ray, G. K. 1951. "Influence Charts for Concrete Pavements," Transactions, American Society of Civil Engineers, Vol 116, pp 49-73

Polshin, D. E. and Tokar, R. A. 1957. "Maximum Allowable Non-uniform Settlement of Structures," Proceedings of the 4th International Conference on Soil Mechanics and Foundation Engineering, Vol 1, London, England, pp 402-406

Popov, E. P. 1968. Introduction to Mechanics of Solids, Prentice-Hall, Inc. Englewood, CA, pp 378-389

Post-Tensioning Institute (PTI). 1980. Design and Construction of Post-Tensioned Slabs on Ground, 1st Edition, Post-Tensioning Institute, Phoenix, AZ

Ramasamy, G., Rao, A. S. R., and Prakash, C. 1982. "Effect of Embedment on Settlement of Footings on Sand," Indian Geotechnical Journal, Vol 12, No 2, pp 112-131

Schmertmann, J. H. 1978. "Guidelines for Cone Penetration Test Performance and Design," Report No. FHWA-TS-78-209, U. S. Department of Transportation, Federal Highway Administration, Office of Research and Development, Washington, D. C.

Schmertmann, J. H. 1986. "Dilatometer to Compute Foundation Settlement," Use of Insitu Tests in Geotechnical Engineering, Geotechnical Special Publication No. 6, American Society of Civil Engineers, New YOrk, NY 10017, pp 303-321

Schultze, E. and Sherif, G. 1973. "Prediction of Settlements From Evaluated Settlement Observations for Sand," Proceedings 8th International Conference on Soil Mechanics and Foundation Engineering, Moscow, Vol 1.3, pp 225-230

Seelye, E. E. 1956. Foundations Design and Practice, John Wiley and Sons, Inc., New York, NY, pp 2-2 to 2-5

Sherman, W. C. 1957. "Instructions for Installation and Observations of Engineering Measurement Devices; Port Allen Lock, Gulf Intracoastal Waterway, Plaquemine-Morgan City Route", Instruction Report 3, U. S. Army Engineer Waterways Experiment Station, Vicksburg, MS

Sherman, W. C. and Trahan, C. C. 1968. "Analysis of Data From Instrumentation Program, Port Allen Lock", Technical Report S-68-7, U. S. Army Engineer Waterways Experiment Station, Vicksburg, MS

Skempton, A. W. 1951. "The Bearing Capacity of Clays," Proceedings of the Building Research Congress, Division I, Part III, London, England, pp 180-189

Skempton, A. W. and Bjerrum, L. 1957. "A Contribution to the Settlement Analysis of Foundations on Clay," Geotechnique, Vol 7, No 4, pp 168-178

Skempton, A. W. and MacDonald, D. H. 1956. "Allowable Settlement of Buildings," Proceedings of the Institute of Civil Engineers, Part III, Vol 5, pp 727-768

Sowers, G. B. and Sowers, G. F. 1972. Introductory Soil Mechanics and Foundations, 3rd Edition, The MacMillan Company, New York, NY

Stroman, W. R. 1978. "Design and Performance of a Mat Slab Foundation in Expansive Soils," Preprint 3317, American Society of Civil Engineers Convention and Exposition, Chicago, IL

Teng, W. C. 1975. "Mat Foundations," Foundation Engineering Handbook, editors, Winterkorn and Fang, Van Nostrand-Reinhold, New York, NY, pp 528-536

Terzaghi, K. 1943. Theoretical Soil Mechanics, Chapter 8, John Wiley & Sons, New York, NY

Terzaghi, K. 1955. "Evaluation of Coefficient of Subgrade Reaction," Geotechnique, Vol 5, pp 297-326

Thornthwaite, C. W. 1948. "An Approach Toward a Rational Classification of Climate", Geographical Review, Vol 38, pp 55-94

Tomlinson, M. J. 1980. Foundation Design and Construction, 4th Edition, Pitman Publishing Limited, London, England

Vallabhan, C. V. and Sathiyakumar, N. 1987. "A Computer Program For Analysis of Transient Suction Potential in Clays," Prepared for U. S. Army Engineer Waterways Experiment Station, Vicksburg, MS, under Contract DACA39-87-M-0835

Vesic, A. S. 1961. "Bending of Beams Resting on Isotropic Elastic Solid," Journal of the Engineering Mechanics Division, American Society of Civil Engineers, Vol 87, No EM2, pp 35-51

Vesic, A. S. 1975. "Bearing Capacity of Shallow Foundations," Foundation Engineering Handbook, Chapter 3, editors, H. F. Winterkorn and H. Y. Fang, Van Nostrand-Reinhold Company, New York, NY, pp 121-147

Vesic, A. S. and Saxena, S. K. 1968. "Analysis of Structural Behavior of Road Test Rigid Pavements," Soil Mechanics Series No. 13, School of Engineering, Duke University, Durham, NC

Wahls, H. E. 1981. "Tolerable Settlement of Buildings," Journal of the Geotechnical Engineering Division, American Society of Civil Engineers, Vol 107, No GT11, pp 1489-1504

Walsh, P. F. 1978. "The Analysis of Stiffened Rafts on Expansive Clays," Technical Paper No. 23 (2nd Series), Division of Building Research, Commonwealth Scientific and Industrial Research Organization, Australia

Wardle, L. J. and Fraser, R. A. 1975a. "Methods for Raft Foundation Design Including Soil Structure Interaction," Paper I. Proceedings of the Symposium on Raft Foundations, Perth, Western Australia, pp 1-12

_____. 1975b. "Program FOCALS-Foundation on Cross Anisotropic Layered System: User's Manual," Geomechanics Computer Program No 4, Commonwealth Scientific and Industrial Research Organization, Division of Applied Geomechanics, Australia

Westergaard, H. M. 1938. "A Problem of Elasticity Suggested by a Problem in Soil Mechanics: Soft Material Reinforced by Numerous Strong Horizontal Sheets," Contributions to the Mechanics of Solids, Stephen Timoshenko 60th Anniversary Volume, The Macmillan Company, New York, NY, pp 268-277

Winkler, E. 1867. Die Lehre von Elastizitat und Festigkeit (On Elasticity and Fixity), Prague, p. 182

Winter, E. 1974. "Calculated and Measured Settlements of a Mat Foundation in Arlington, Virginia, USA," Settlement of Structures, British Technical Society, John Wiley & Sons, New York, NY, pp 451-459

Withiam, J. L. and Kulhawy, F. H. 1978. "Analytical Modeling of the Uplift Behavior of Drilled Shaft Foundations," Geotechnical Engineering Report 78-1, School of Civil and Environmental Engineering, Cornell University, Ithaca, NY

Woodburn, J. A. 1979. Footings and Foundations for Small Buildings in Arid Climates, Institute of Engineers, Australia

Yong, R. N. Y. 1960. "A Study of Settlement Characteristics of Model Footings on Silt," Proceedings of the 1st Pan-American Conference on Soil Mechanics and Foundation Engineering, Mexico, D. F., pp 492-513

Ytterberg, R. F. 1987. "Shrinkage and Curling of Slabs on Grade, Part I-Drying Shrinkage," Concrete International Design and Construction, American Concrete Institute, Vol 9, pp 22-31

APPENDIX A: EQUIVALENT ELASTIC SOIL MODULUS

Modulus Increasing Linearly With Depth

1. The Kay and Cavagnaro (1983) model may be used to derive an equivalent soil modulus E_s^* from elastic soil moduli E_s that increase linearly with depth z

$$E_s = E_o + kz \tag{A1}$$

where

E_o = Young's soil modulus at the ground surface, ksf

k = constant relating E_s with z in units of ksf/ft.

The influence factor I_c in Figure 5 may be approximated as shown in Table A1. The functions of I_c with depth z in Table A1 and Equation A1 may be integrated to evaluate the center displacement in units of feet

$$\rho_c = q \int \frac{I_c}{E_s} dz \tag{A2}$$

where q is the pressure applied on the soil in units of ksf.

2. Integration of Equation A2 leads to the following settlement function for $z^* = 0.0$ to 4.0

$$\rho_c = \frac{q}{k}\left[(a-b/n)\ln(1+0.5n)+(c+d/n)\ln\left[\frac{1+2n}{1+0.5n}\right] + (e+f/n)\ln\left[\frac{1+4n}{1+2n}\right] - g\right] \tag{A3}$$

where

$z^* = (z - D_b)/R$

$n = kR/(E_o + kD_b)$

$R = \sqrt{LB/\pi}$

D_b = depth of mat base below ground surface, ft

If the elastic soil modulus at the ground surface $E_o = 0$, then $n = R/D_b$. If $D_b = 0$ for the base of the mat on the ground surface, then $n = kR/E_o$. The constants in the above equation are given in Table A2. The solution of Equation A3 as a function of n results in the parametric equations for ρ_c shown in Table A3. ρ_c may therefore be given for $z^* = (z - D_b)/R = 0.0$ to $z^* = 4.0$ or soil of approximately infinite depth by

Table A1

Variation of Influence Factor I_c With Depth

Soil Poisson's Ratio, μ_s	Range of Depth, z* $z^* = (z-D_b)/R$	Influence Factor I_c
	0.0 - 0.5	0.700 + 0.300z*
0.2	0.5 - 2.0	1.050 - 0.400z*
	2.0 - 4.0	0.400 - 0.075z*
	0.0 - 0.5	0.500 + 0.500z*
0.3	0.5 - 2.0	0.917 - 0.333z*
	2.0 - 4.0	0.400 - 0.075z*
	0.0 - 0.5	0.250 + 0.900z*
0.4	0.5 - 2.0	0.850 - 0.300z*
	2.0 - 4.0	0.400 - 0.075z*
	0.0 - 0.5	1.200z*
0.5	0.5 - 2.0	0.717 - 0.233z*
	2.0 - 4.0	0.400 - 0.075z*

z = depth below ground surface, ft
D_b = depth of mat base below ground surface, ft
R = equivalent mat radius, $\sqrt{LB/\pi}$, ft where $L \leq 2B$
L = length of mat, ft
B = width of mat, ft

Table A2

Constants for Equation A3

Constant	Poisson's Ratio μ_s			
	0.2	0.3	0.4	0.5
a	0.700	0.500	0.250	0.000
b	0.300	0.500	0.900	1.200
c	1.050	0.917	0.850	0.717
d	0.400	0.333	0.300	0.233
e	0.400	0.400	0.400	0.400
f	0.075	0.075	0.075	0.075
g	0.600	0.400	0.150	-0.100

Table A3

Settlement as a Function of Poisson's Ratio

Soil Poisson's Ratio, μ_s	Dimensionless Settlement, $\rho_c \cdot (k/q)$
0.2	$0.70 + 1.56\log_{10}n$
0.3	$0.70 + 1.18\log_{10}n$
0.4	$0.70 + 0.73\log_{10}n$
0.5	$0.65 + 0.30\log_{10}n$

$n = kR/E_o + kD_b)$

k = constant relating E_s with depth z, ksf/ft

q = pressure applied on soil, ksf

Table A4

Relationship of n with k/k_{sf}, Equation A7

n	$\frac{k}{k_{sf}}$
1	0.70
2	0.90
3	1.03
5	1.19
10	1.40
100	2.10
1000	2.80

Note: $n = kR/(E_o + kD_b)$

$$\rho_c = (q/k)\left[0.7 + (2.3 - 4.0\mu_s)\log_{10}n\right] \tag{A4a}$$

Below $z^* = 4.0$ the soil is assumed incompressible. For more shallow soil settlement is given from $z^* = 0.0$ by

$$z^* = 2 \qquad \rho_c = (q/k)\left[0.55 + (2.507 - 4.533\mu_s)\log_{10}n\right] \tag{A4b}$$

$$z^* = 0.5 \qquad \rho_c = (q/k)\left[-0.46 + 1.44\mu_s + (2.42 - 4.6\mu_s\log_{10}n\right] \tag{A4c}$$

Settlement is especially sensitive to soil stiffness for $z^* = 0.5$.

3. The equivalent soil modulus E_s^* may be found by substituting Equation A4a for $z^* = 4.0$ into Equation 4b to obtain Equation 4c. Equation 4c shows that increasing μ_s toward the undrained state of 0.5 and decreasing the ratio n increases E_s^*.

4. Substituting Equation A4a into

$$\rho_c = q/k_{sf} \tag{A5}$$

where k_{sf} is the coefficient of subgrade reaction of the foundation, leads to

$$k_{sf} = \frac{k}{0.7 + (2.3 - 4\mu_s)\log_{10}n} \tag{A6}$$

If $\mu_s = 0.4$, a reasonable value for many clays,

$$\frac{k}{k_{sf}} = 0.7 + 0.7\log_{10} n \tag{A7}$$

5. Table A4 illustrates values of k/k_{sf} for given values of n. k_{sf} is approximately k when n is from 2 to 3. The flat thick mats described in Part III have n values (R/D_b ratios when $E_o = 0$) approximately in this range. Therefore, k_{sf} should approximately equal k for these thick mats. k_{sf} will be less than half of k when $n > 100$. n can be greater than 100, for example, if the mat is placed on the ground surface ($D_b = 0$) and $kR > 100E_o$. This was observed for the large mat on the ground surface described in Part IV.

Constant Elastic Modulus

6. Graphical integration of the influence factor I_c for center settlement, Figure 5, for a constant elastic soil modulus $E_s = E_o$ indicates center settlements as a function of soil Poisson's ratio μ_s, Table A5. Solution of Equation A2 when $E_s = E_o$ for some depth ranges of compressible soil z^* is given in Table A6. Settlements are only slightly influenced by soils greater than $z^* = 4.0$.

Table A5

Center Settlement for Constant Elastic Modulus

μ_s	$\rho_c \cdot E_o/qR$
0.2	$0.81 + 1.31 \cdot \log_{10} z^*$
0.3	$0.71 + 1.28 \cdot \log_{10} z^*$
0.4	$0.62 + 1.26 \cdot \log_{10} z^*$
0.5	$0.50 + 1.16 \cdot \log_{10} z^*$

Note: $z^* = (z - D_b)/R$

Table A6

Center Settlement for Various Depth Ranges z^*

z^*	$\rho \cdot E_o/qR$
0.5	$0.55 - 0.8\mu_s$
2.0	$1.50 - 1.4\mu_s$
4.0	$1.85 - 1.4\mu_s$

APPENDIX B: INFLUENCE OF SUPERSTRUCTURE RIGIDITY

Meyerhof's Method

1. Meyerhof (1953) developed a simple analysis to compensate for superstructure rigidity

$$(EI)_{su} = \sum_{i=1}^{N_s} \left[E_b I'_{bi} + \frac{E_p I_{pi} L^2}{2h_i^2} \right] \tag{B1}$$

$$I'_{bi} = I_{bi} \left[1 + \frac{\dfrac{I_{Li}}{h_i} + \dfrac{I_{ui}}{h_i}}{\dfrac{I_{bi}}{l} + \dfrac{I_{Li}}{h_i} + \dfrac{I_{ui}}{h_i}} \right] \tag{B2}$$

where

$(EI)_{su}$ = superstructure stiffness, kips-ft^2
E_b = elastic modulus of beam, ksf
E_p = elastic modulus of wall panels, ksf
L = length of building, ft
h_i = height of story i, ft
l = span length between columns or beam length, ft
I_{pi} = panel moment of inertia, ft^4
I_{bi} = beam moment of inertia, ft^4
I_{Li} = lower half of column moment of inertia, ft^4
I_{ui} = upper half of column moment of inertia, ft^4
N_s = number of stories

The rigidity from Equation B1 should be added to the foundation rigidity to obtain the composite structure rigidity or stiffness. Meyerhof assumed that the rigidity contributed by the foundation is much less than that of the superstructure and may often be ignored in practice.

Proposed Method

2. The following method calculates a composite moment of inertia for the structure that includes the effect of a simple framed building or shear wall on the mat foundation. The moment of inertia with respect to the centroid of a composite structure I_{oo} may be given by the parallel axis theory[67]

$$I_{oo} = \sum_{i=1}^{N_s} (I_{oi} + A_i h_{cci}^2) \tag{B3}$$

where

I_{oi} = moment of inertia of the axis passing through the centroid axis of story i, ft^4

A_i = area of cross-section of story i, ft^2

h_{cci} = distance between center of story i and centroid axis, ft

The centroid axis h_c is found from

$$h_c = \sum_{i=1}^{N_s} \frac{A_i h_{ci}}{A_i} \tag{B4}$$

where h_{ci} is the centroid of each section or story from the bottom of the mat.

Flat Mats

3. The centroid for a structure on a flat mat with a simple shear wall as schematically shown in Table B1 is

$$h_c = \frac{a_w h^2 N_s^2 + 2a_w hDN_s + BD^2}{2(BD + a_w hN_s)} \tag{B5}$$

where

a_w = wall thickness, ft

D = thickness of mat foundation, ft

h = height of each story, ft

N_s = number of stories

B = width of foundation or spacing S, ft

Each story is assumed to be equal in height.

Table B1

Centroid and Moment of Inertia of Composite Structure With a Flat Mat

<u>Centroid</u> h_c

If $h_1 = h_2 = \ldots = h_{Ns} = h$,

Then

$$h_c = \frac{\sum_{i=1}^{N_s} \left(a_w h_i \frac{2i-1}{2} h_i\right) + a_w h N_s D + \frac{BD^2}{2}}{BD + \sum_{i=1}^{N_s} a_w h_i}$$

Since $\sum_{i=1}^{N_s} (2i-1) = N_s^2$,

Then

$$h_c = \frac{a_w h^2 N_s^2 + 2 a_w h N_s D + BD^2}{2(BD + a_w h N_s)}$$

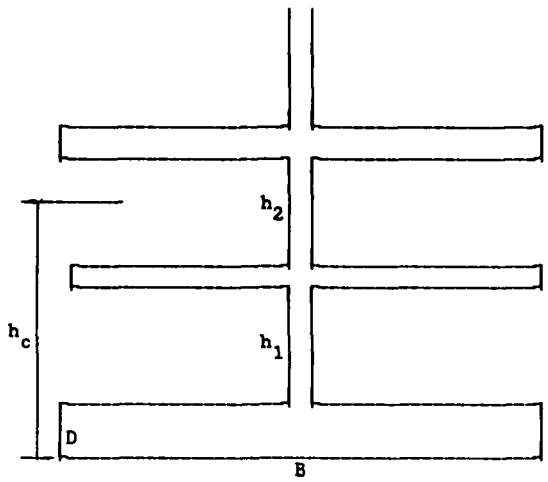

<u>Moment of Inertia</u> I_{oofm}

$$I_{oofm} = \frac{BD^3}{12} + BD\left[h_c - \frac{D}{2}\right]^2 + \sum_{i=1}^{N_s} \left(I_{oi} + A_i h_{cci}^2\right)$$

i	I_{oi}	$A_i h_{cci}^2$
1	$\frac{a_w h_i^3}{12}$	$a_w h_1 \left[h_c - \left[\frac{h_1}{2} + D\right]\right]^2$
2	$\frac{a_w h_2^3}{12}$	$a_w h_2 \left[h_c - \left[\frac{3h_2}{2} + D\right]\right]^2$
i	$\frac{a_w h_i^3}{12}$	$a_w h_i \left[h_c - \left[\frac{2i-1}{2} D\right]\right]^2$
Sum	$\frac{N_s a_w h^3}{12}$	$I^* = a_w h\left[N_s h_c^2 - N_s^2 h\, h_c - 2h_c N_s D + \frac{N_s(4N_s^2 - 1)h^2}{12} + N_s^2 Dh + ND_s^2\right]$

$$I_{oofm} = \frac{BD^3 + N_s a_w h^3}{12} + BD\left[h_c - \frac{D}{2}\right]^2 + I^*$$

4. The composite moment of inertia for a flat mat from Table B1 is

$$I_{oofm} = \frac{BD^3 + N_s a_w h^3}{12} + BD\left[h_c - \frac{D}{2}\right]^2 + I^* \tag{B6a}$$

$$I^* = a_w h\left[N_s h_c^2 - N_s^2 h_c h + \frac{N_s(4N_s^2 - 1)h^2}{12} - 2h_c N_s D + N_s^2 Dh + N_s D^2\right] \tag{B6b}$$

5. A parametric analysis was performed to calculate the composite moment of inertia I_{oofm} for a flat mat from Equation B6 with h_c evaluated from Equation B5 and mat thickness D evaluated from Equation 11a plus 0.3 ft. The wall thickness a_w was evaluated as an equivalent thickness for columns of width a and spacing S by[78]

$$a_w = \frac{a^2}{S} \tag{B7}$$

If a is assumed to vary in proportion with the number of stories N_s; i.e., $a = 1$, 2, and 4 ft for $N_s = 3$, 12, and 50 stories, respectively, then the composite moment of inertia is approximately

$$I_{oofm} = (17.3 - 0.4S)\cdot N_s^{(3.42 + 0.011S)} \tag{B8}$$

The height of each story h was assumed 10 ft.

6. The moment of inertia of a continuous shear wall I_{sw} excluding the mat foundation is

$$I_{sw} = \frac{a_w(N_s h)^3}{12} \tag{B9a}$$

If $h = 10$ ft and a_w is found from Equation B7 with a varying with N_s as above, then

$$I_{sw} = \frac{27.77N_s^4}{S} \tag{B9b}$$

where $3 \le N_s \le 50$ stories and $15 \le S \le 30$ ft. Comparison of Equations B8

[78]Desai, Johnson, and Hargett 1974

and B9b shows that the composite I_{oofm} is significantly greater than I_{sw} for the same number of stories without the mat, especially for fewer stories when the mat is less thick; therefore, the mat rigidity should be included in the overall stiffness of the structure if this analysis is a realistic interpretation of structural stiffness.

7. The effect of superstructure rigidity on a mat foundation was estimated for a wall spacing $S = 25$ ft, story height $h = 10$ ft, and soil pressure $q'_m = 0.2$ ksf/story is

(1) N_s	(2) a, ft	(3) D, ft	(4) I_{oofm}, ft	(5) I_{oofm}/I_{mat}	(6) D_e, ft	(7) L_{max}, ft
3	1.0	1.8	412	34	5.8	25
12	2.0	3.3	69,663	930	32.2	91
50	4.0	5.6	13,684,290	37,402	187.2	341

The mat thickness D was estimated from Equation 11a plus 0.3 ft. I_{oofm} in column 4 was estimated from Equation B8. The ratio of the structure moment of inertia to that of the mat shown in column 5 is

$$\frac{I_{oofm}}{I_{mat}} = 12 \cdot \frac{I_{oofm}}{BD^3} \tag{B10}$$

Column 6 shows the equivalent mat thickness D_e if the stiffness of the entire structure is collapsed into the mat

$$D_e = \sqrt[3]{\frac{12 \cdot I_{oofm}}{S}} \tag{B11}$$

D_e shown above, although large, may not be unreasonable because Hooper and Wood (1977) calculated an equivalent thickness of at least 6 times that of the actual mat thickness in order to calculate differential displacements in agreement with observed displacements. The superstructure exerts a large influence on the mat rigidity consistent with previous observations of soil-structure interaction analysis[79]. The concrete elastic modulus E_c may also be increased to give the same equivalent rigidity ΩL that would be calculated using D_e or I_{oofm} substituted for I in Equation 17.

---

[79]Wardle and Fraser 1975a; Focht, et al 1978; Stroman 1978; Bobe, et al 1981

8. Column 7 above illustrates the maximum mat length L_{max} such that the mat appears rigid from the criterion of Equation 17. The coefficient of subgrade reaction k_{sf} was calculated from Equation 6b as 27 ksf/ft assuming $S = 25$ ft and $k_{sp} = 1000$ ksf/ft, an upperbound value simulating hard clay[27]. The PTI (1980) used $k_{sf} = 7$ ksf/ft for a long-term coefficient to determine the PTI design equations, which leads to L_{max} 1.4 times those shown in column 7. If $k_{sp} = 150$ ksf/ft simulating a stiff clay, then L_{max} will be twice those shown in column 7. E_c was assumed 432,000 ksf. A multi-story structure with 11 or more stories may therefore appear rigid as had been observed from records of uniform displacements[80]. Superstructure stiffness may be neglected for cases such as steel storage tanks or low-rise buildings with open floor plans and large areas[46].

Ribbed Mats

9. The centroid for a structure on a ribbed mat with a simple shear wall schematically shown in Table B2 is

$$h_c = \frac{wt^2 + BD^2 + 2BDt + 2a_w h(t+D)N_s + a_w h^2 N_s^2}{2(wt + BD + N_s a_w h)} \tag{B12}$$

where

a_w = wall thickness, ft

w = thickness of stiffening beam, ft

t = depth of stiffening beam, ft

B = width of foundation or spacing S, ft

D = mat thickness, ft

h = height of each story, ft

N_s = number of stories

10. The composite moment of inertia is given from Table B2

$$I_{oorm} = \frac{wt^3 + BD^3 + N_s a_w h^3}{12} + wt\left[h_c - \frac{t}{2}\right]^2 + BD\left[h_c - t - \frac{D}{2}\right]^2 + I^{**} \tag{B13a}$$

---

[80]Hooper and Wood 1977, Stroman 1978, Focht, et al 1978

Table B2

Centroid and Moment of Inertia of Composite Structure With a Ribbed Mat

Centroid h_c

If $h_1 = h_2 = \ldots = h_{N_s} = h$,

Then

$$h_c = \frac{\sum_{i=1}^{N_s} a_w h \frac{2i-1}{2} h + N_s a_w h(t+D) + BDt + \frac{wt^2 + BD^2}{2}}{\sum_{i=1}^{N_s} a_w h_i + BD + wt}$$

Therefore,

$$h_c = \frac{wt^2 + BD^2 + 2BDt + 2a_w h N_s (t+D) + a_w h^2 N_s^2}{2(wt + BD + N_s a_w h)}$$

Moment of Inertia I_{oorm}

$$I_{oorm} = wt\left[h_c - \frac{t}{2}\right]^2 + BD\left[h_c - t - \frac{D}{2}\right]^2 + \sum_{i=1}^{N_s}(I_{oi} + A_i h_i'^2)$$

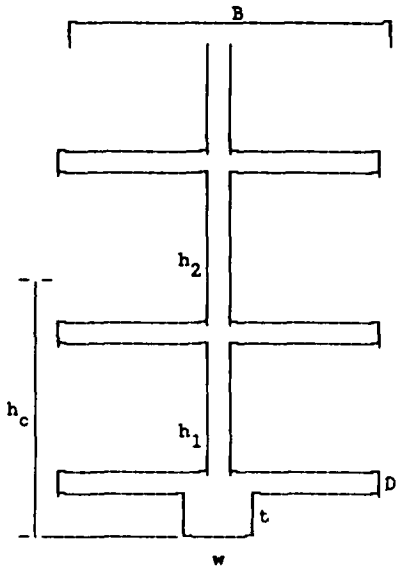

i	I_{oi}	$A_i h_i'^2$
1	$\frac{a_w h_1^3}{12}$	$a_w h_1\left[h_c - \left[t + D + \frac{h_1}{2}\right]^2\right]$
2	$\frac{a_w h_2^3}{12}$	$a_w h^2\left[h_c - \left[t + D + \frac{3h_2}{2}\right]^2\right]$
3	$\frac{a_w h_1^3}{12}$	$a_w h_1\left[h_c - t + D + \frac{2i-1}{2} h_i\right]^2\Big]$
Sum	$\frac{N_s a_w h^3}{12}$	$I^{**} = a_w h\left[N_s h_c^2 - 2(t+D)N_s h_c - h h_c N_s^2 + N_s(t+D)^2 + (t+D)hN_s^2 + \frac{N_s(4N_s^2-1)h^2}{12}\right]$

$$I_{oorm} = \frac{wt^3 + BD^3 + N_s a_w h^3}{12} + wt\left[h_c - \frac{t}{2}\right]^2 + BD\left[h_c - t - \frac{D}{2}\right]^2 + I^{**}$$

$$I^{**} = a_w h\left[N_s h_c^2 - 2(t+D)N_s h_c - hh_c N_s^2 + N_s(t+D)^2 + (t+D)hN_s^2 + \frac{N_s(4N_s^2-1)h^2}{12}\right] \quad \text{(B13b)}$$

A parametric analysis was performed to calculate I_{oorm} of ribbed mats from Equations B13 for column width $a = 1$ ft where a_w was found from Equation B7, $h = 10$ ft, and stiffening beam width $w = 1$ ft

$$I_{oorm} = (28 + 5t - 0.72S)N_s^{(3 - 0.13t)} \quad \text{(B14)}$$

where

N_s = number of stories, ≤ 3

t = thickness of stiffening beam, ≤ 3 ft

S = column or wall spacing, ft

The mat thickness was 0.5, 0.75, and 1.0 ft for $N_s = 1$, 2, and 3 stories, respectively. A comparison of I_{oorm} from Equation B14 for a ribbed mat and I_{oofm} from Equation B8 for a flat mat with $N_s = 3$ stories indicates similar moments of inertia for each case. Comparison of I_{oofm} from Equation B6 for a flat mat and I_{oorm} from Equation B13 for a ribbed mat shows that the stiffening beam increases I_{oo} about 2, 7, and 14 percent with $t = 1$, 2, and 3 ft, respectively, when $N_s = 2$. I_{oo} is similarly increased 6, 23, and 56 percent with $t = 1$, 2, and 3 ft, respectively, when $N_s = 1$. The additional stiffness from a stiffening beam in a ribbed mat becomes increasingly significant as the number of stories in the superstructure decreases.

Resisting Bending Moment

11. The resisting moment after the flexure formula (Popov 1968) is

$$M = A_s f_s (h_c - 3.0) \quad \text{(B15)}$$

where

M = resisting moment of steel, lbs-in

A_s = area of reinforcement steel, in^2

f_s = steel tensile strength, psi

h_c = centroid of structure, in.

If the steel is placed in the bottom of the mat with 3.0 inches of cover, the bending moment resistance will be increased about 4 and 10 times for 3 and 5-

ft thick mats, respectively, supporting 11 stories using the parameters in paragraph 5 above. The increase in bending moment resistance from the superstructure can be substantial.

Limitations of Model

12. Although this framed building or shear wall model appears similar to that illustrated in Figure 3.1 of ACI 435 (1980), "Allowable Deflections", the above model requires confirmation. For example, the effective width B or spacing S is not known and may be less than the actual width or spacing such that the composite moment of inertia of the structure may be less than that calculated by this model. Moreover, only a portion of the structure may be constructed with a shear wall further complicating selection of an appropriate value for B. Cross-frames, struts, and other structural components also complicates calculation of the composite moment of inertia of the structure.

APPENDIX C: USER'S MANUAL FOR COMPUTER PROGRAM SLAB2

Introduction

1. SLAB2 is a fortran finite element program originally developed by Huang[54] and modified by W. K. Wray and R. L. Lytton for ribbed mats in expansive soil[11]. This program is available from the Soil Mechanics Branch, Soil and Rock Mechanics Division, Geotechnical Laboratory of the US Army Engineer Waterways Experiment Station. The stiffness of the ribs is considered by calculating the total stiffness of the sum of the ribs in each of the X and Y orientations. SLAB2 provides solutions in the X and Y orientations for stresses, deflections, bending moments, and shear forces due to loading and/or warping in a single rectangular mat, or two mats connected by dowel bars at the joint, resting on a foundation of the elastic solid type. The program was written on a permanent file SLAB2.FOR for IBM PC compatible microcomputers and it is available from the Soil Mechanics Division, Geotechnical Laboratory of the US Army Engineer Waterways Experiment Station. The program requires 640K of memory to execute. Input data is saved on a file DASLAB.TXT. Output data is sent to a file SLAOUT.TXT. In addition, deflection, X-direction and y-direction bending moments are sent to plot files CAL.DEF, CALX.MOM, and CALY.MOM.

2. The program is composed of the main routine and eight subroutines. Subroutine SOLID calculates stresses for mats of constant thickness. Subroutine TEE calculates stresses for mats with stiffening beams. Subroutine MFSD is the algorithm to factor a symmetrical positive definite matrix. Subroutine TRIG applies the Gauss elimination method to form an upper triangle banded matrix for a given contact condition which can be used repeatedly. Subroutine LOADM uses the triangularized matrix from Subroutine TRIG to compute mat deflections. Subroutine SINV inverts a symmetrical positive matrix. Subroutine QSF computes the vector of integral values for a given equidistant table of function values. Subroutine SHEAR calculates the shear force in units of lbs/in.

3. The mat foundation is divided into rectangular finite elements of various sizes. The elements and nodes are numbered consecutively from bottom to top along the Y axis and from left to right along the X axis. If two slabs are connected by dowel bars at the joint, each node at the doweled joint

must be numbered twice, one for the left and the other for the right mat. The dowels are assumed 100 percent efficient, so that the deflections at the joint are the same for both mats. Loads may be applied to either or both mats, and the stresses at any node in either mat may be computed. The program can determine the stresses and deflections due to dead load, temperature warping, or live load, either combined or separately. Options are as follows:

Option 1: Mat and subgrade are in full contact: Set NOTCON = 0, NWT = 0, and NCYCLE = 1

Option 2: Mat and subgrade are in full contact at some points but completely out of contact at the remaining points because of large gaps between the mat and subgrade. Set NOTCON = number of points not in contact, NGAP = 0, NWT = 0, and NCYCLE = 1

Option 3: Mat and subgrade may or may not be in contact because of warping of the slab. When the slab is removed, the subgrade will form a smooth surface with no depressions or initial gaps. Set NOTCON = 0, NGAP = 0, NCYCLE = maximum number of cycles for checking contact

Option 4: When mat is removed, the subgrade will not form a smooth surface, but shows irregular deformation. Set NOTCON = 0, NGAP = number of nodes with initial gaps, NCYCLE = maximum number of cycles for checking contact

Application

4. Table C1 illustrates the organization of the input parameters for program SLAB2, while Table C2 defines the input parameters. Input data is normally consistent with units of pounds and inches. Mat width and length and their respective nodal distances are input in units of feet. Input lines are omitted if the option is not selected. Data must be placed in the correct format shown in Table C2 for proper operation of the program. An example of input data is shown in Table C3 for analysis of the ribbed mat described in PART IV. Output data for this problem is shown in Table C4. Deflections are in inches, moments in lbs-in./in. of width, and shears are in lbs/in. of width.

Table C1

Organization of Input Data

Line	Input Parameters	Format Statement
1	NPROB	I5
2	XXL XXS XEC XYMX MMM ISOTRY LIFT	4F10.4,3I5
3	BEAMLW BEAMSW BEAMLL BEAMSL ASPACE BSPACE (Line 3 omitted if ISOTRY = 0)	9F8.3
4	MOIX MOIY (Line 4 omitted if ISOTRY = 0)	2E13.6
5	NSLAB PR T YM YMS PRS NSYM NOTCON NREAD NPUNCH NB	I5,2F8.4,2E10.3, F8.4,5I5
6	NX1 NX2 NY NCYCLE NPRINT NP(1)...NP(I)	14I5
7	X(1)...X(I) Y(1)...Y(I)	9F8.3
8	NZ(1)...NZ(I) (Line 8 omitted if NOTCON = 0)	14I5
9	NGAP NTEMP NLOAD ICL NCK NWT TEMP Q DEL DELF RFJ ICLF	6I5,2F8.3, 2F8.5,F5.2,I5
10	NODCK(1)...NODCK(I) (Line 10 omitted if NCK = 0)	14I5
11	CURL(1)...CURL(I) (Line 11 omitted if NREAD = 0 or 2)	6E13.6
12	NG(1)...NG(I) (Line 12 omitted if NREAD = 1 or 2, NGAP not used)	14I5
13	CURL(NG(1))...CURL(NG(I)) (Line 13 omitted if NREAD = 1 or 2, NGAP not used)	9F8.4
14	QSLAB (Line 14 omitted if NREAD = 1 or NWT = 0)	F7.3
15	NL(I) XDA(I,1) XDA(I,2) YDA(I,1) YDA(I,2) (Line 15 repeated for each I = 1,NLOAD)	I5,4F10.5

Table C2

Definition of Input Parameters

Line	Parameter	Definition
1	NPROB	Number of problems to be solved; new input data for each problem
2	XXL	Length of mat, ft
	XXS	Width of mat, ft
	XEC	Edge penetration distance, ft
	XYMX	Amount of differential shrink or swell y_m, inches
	MMM	Exponent "m" of Equation 25
	ISOTRY	= 0 for flat mat; = 1 for stiffened mat
	LIFT	= 0 for no swell; = 1 for center lift; = 2 for edge lift
3		Beam dimensions - omitted if ISOTRY = 0
	BEAMLW	Depth below flat portion of mat in short direction, inches
	BEAMSW	Width in short direction, inches
	BEAMLL	Depth below flat portion of mat in long direction, inches
	BEAMSL	Width in long direction, inches
	ASPACE	Beam spacing in long direction, inches
	BSPACE	Beam spacing in short direction, inches
4		Moment of inertia - omitted if ISOTRY = 0; MOIX MOIY
	MOIX	Total moment of inertia of mat section along length, $inches^4$
	MOIY	Total moment of inertia of mat section along width, $inches^4$
5	NSLAB	Number of mats in problem, either 1 or 2
	PR	Poisson's ratio of concrete in mat
	T	Thickness of flat portion of mat, inches
	YM	Young's modulus of concrete, psi
	YMS	Young's modulus of soil, psi
	PRS	Poisson's ratio of soil
	NSYM	=1 for no symetry; = 2 for symmetry with respect to Y (vertical) axis; = 3 for symmetry with respect to X (horizontal) axis; = 4 for symmetry with respect to Y and X axis; = 5 for four mats symmetrically loaded
	NOTCON	Total number of nodes with reactive pressure = 0; if NCYCLE = 1, these nodes will never be in contact; if NCYCLE > 1, these nodes may or may not be in contact depending on calculated results
	NREAD	Gaps or precompression to be read in = 0 for line 11 omitted, CURL(I) = 0.0, I = 1,NX NY = 1 for lines 12, 13, and 14 omitted, CURL(I) read in for I = 1,NX NY, NGAP not used = 2 for lines 11, 12, and 13 omitted; use gaps and precompressions from previous problem, NGAP not used

Table C2 (Continued)

Line	Parameter	Definition
	NPUNCH	Not used. Put 0
	NB	Half band width, (NY + 2) 3
6	NX1	Number of nodes in X-direction (left to right) for mat 1
	NX2	Number of nodes in X-direction for mat 2
	NY	Number of nodes in Y-direction (bottom to top); nodes numbered from bottom to top and toward the right
	NCYCLE	Maximum number of cycles for checking subgrade contact; use 10
	NPRINT	Number of nodes at which stresses are to be printed; if = 0 stresses at all nodes are printed
	NP(I)	Node number I to be printed; leave blank if NPRINT = 0; continue until I = 1, NPRINT
7	X(I)	X coordinate starting from zero and increasing from left to right, ft; read X twice at joint if NSLAB = 2; continue until I = NX = NX1 + NX2
	Y(I)	Y coordinate starting from zero and increasing to top, ft; continue until I = NY; follows immediately after the last X coordinate
8	NZ(I)	Number of node at which reactive pressure is initially zero; continue until I = NOTCON; omitted if NOTCON = 0
9	NGAP	Total number of nodes at which a gap exists between mat and subgrade; = 0 if no gap or very large gap
	NTEMP	Warping condition; = 0 no temperature gradient; = 1 for temperature gradient
	NLOAD	Number of loads applied to mat
	ICL	Maximum number of permitted iterations for coarse control; use 10
	NCK	Number of nodal points for checking convergence
	NWT	Consideration of mat weight; = 0 weight not considered; = 1 weight considered for non-constant cross-section; = -1 weight considered for flat rectangular cross-section
	TEMP	Difference in temperature between top and bottom of mat, °C
	Q	Pressure from loads on mat, psi
	DEL	Coarse tolerance to control convergence; use 0.001
	DELF	Fine tolerance to control convergence; use 0.0001
	RFJ	Joint relaxation factor; use 0.5
	ICLF	Maximum number of iterations for fine control; use 30
10	NODCK(I)	Number of nodal point for checking convergence; continue until I = NCK; omitted if NCK = 0

Table C2 (Concluded)

Line	Parameter	Definition
11	CURL(I)	Amount of gap between mat and subgrade for each nodal point I if NREAD = 1; continue on additional lines until I = NX NY omitted if NREAD = 0 or 2
12	NG(I)	Number of node at which gap is specified between mat and subgrade; continue on additional lines until I = NGAP; omitted if NREAD = 1 or 2, NGAP = 0
13	CURL(NG(I))	Amount of gap between mat and subgrade for nodal point NG(I), inches; continue on additional lines until I = NGAP; omitted if NGAP = 0, NREAD = 1 or 2
14	QSLAB	Pressure from weight of mat as uniformly distributed load, psi; omitted if NREAD = 1 or NWT = 0 or -1
15		Placement of loading pressure Q of line 9 on portions of element I; use -1 for lower bound of element and +1 for upper bound of element; continue until I = NLOAD; an element may be loaded more than once
	NL(I)	Number of element subject to loading q; elements numbered bottom to top, left to right
	XDA(I,1)	Left limit of loaded area in X-direction
	XDA(I,2)	Right limit of loaded area in X-direction
	YDA(I,1)	Lower limit of loaded area in Y-direction
	YDA(I,2)	Upper limit of loaded area in Y-direction

Table C3

Input Parameters for Ribbed Mat, PART IV

```
  1
677.8     303.67      0.0       0.0       1    1    0
28.     18.     23.     18.    150.    150.
9.251474E 06 4.185904E 06
  1   .15    8.     1.500E 06 3.000E 04  0.4       4   21    0    0   27
 15    0    7   10    0    0
 0.0    12.5    37.5    62.5    87.5   112.5   137.5   162.5   187.5
212.5   237.5   262.5   287.5   312.5   338.9      .0    25.0    50.0
 75.0   100.0   125.0   151.83
 29   30   31   32   33   34   35   36   37   38   39   40   41   42
 43   44   45   46   47   48   49
 21    0  116   10    8    1   0.0     4.0   0.001    .0001  0.5    30
 15   27   45   56   65   75   93  104
 29   30   31   32   33   34   35   36   37   38   39   40   41   42
 43   44   45   46   47   48   49
0.5     0.5     0.5     0.5     0.0     0.0     0.      1.      1.
1.      1.      1.      0.      0.      0.5     0.5     0.5     0.5
0.      0.      0.
1.0
  1   -.08      1.      -1.       -.46
  3   -.08      1.        .46      1.
  4   -.08      1.      -1.       -.46
  6   -.08      1.        .442     1.
  7  -1.       -.46     -1.       -.46
  7    .46      1.      -1.       -.46
  9  -1.       -.46       .46      1.
  9    .46      1.        .46      1.
 10  -1.       -.46     -1.       -.46
 10    .46      1.      -1.       -.46
 12  -1.       -.46       .442     1.
 12    .46      1.        .442     1.
 13  -1.       -.46     -1.       -.46
 13   .46      1.      -1.       -.46
 15  -1.       -.46       .46      1.
 15    .46      1.        .46      1.
 16  -1.       -.46     -1.       -.46
 16    .46      1.      -1.       -.46
 18  -1.       -.46       .442     1.
 18    .46      1.        .442     1.
 19  -1.       -.46     -1.       -.46
 19    .46      1.      -1.       -.46
 21  -1.       -.46       .46      1.
 21    .46      1.        .46      1.
 22  -1.       -.46     -1.       -.46
 22    .46      1.      -1.       -.46
 24  -1.       -.46       .442     1.
 24    .46      1         .442     1.
 25  -1.       -.46     -1.       -.46
 25    .46      1.      -1.       -.46
 27  -1.       -.46       .46      1.
 27    .46      1.        .46      1.
 28  -1.       -.46     -1.       -.46
 28    .46      1.      -1.       -.46
 30  -1.       -.46       .442     1.
 30    .46      1.        .442     1.
 31  -1.       -.46     -1.       -.46
 31    .46      1.      -1.       -.46
```

Table C3 (Continued)

33	-1.	-.46	.46	1.
33	.46	1.	.46	1.
34	-1.	-.46	-1.	-.46
34	.46	1.	-1.	-.46
36	-1.	-.46	.442	1.
36	.46	1.	.442	1.
37	-1.	-.46	-1.	-.46
37	.46	1.	-1.	-.46
39	-1.	-.46	.46	1.
39	.46	1.	.46	1.
40	-1.	-.46	-1.	-.46
40	.46	1.	-1.	-.46
42	-1.	-.46	.442	1.
42	.46	1.	.442	1.
43	-1.	-.46	-1.	-.46
43	.46	1.	-1.	-.46
45	-1.	-.46	.46	1.
45	.46	1.	.46	1.
46	-1.	-.46	-1.	-.46
46	.46	1.	-1.	-.46
48	-1.	-.46	.442	1.
48	.46	1.	.442	1.
49	-1.	-.46	-1.	-.46
49	.46	1.	-1.	-.46
51	-1.	-.46	.46	1.
51	.46	1.	.46	1.
52	-1.	-.46	-1.	-.46
52	.46	1.	-1.	-.46
54	-1.	-.46	.442	1.
54	.46	1.	.442	1.
55	-1.	-.46	-1.	-.46
55	.46	1.	-1.	-.46
57	-1.	-.46	.46	1.
57	.46	1.	.46	1.
58	-1.	-.46	-1.	-.46
58	.46	1.	-1.	-.46
60	-1.	-.46	.442	1.
60	.46	1.	.442	1.
61	-1.	-.46	-1.	-.46
61	.46	1.	-1.	-.46
63	-1.	-.46	.46	1.
63	.46	1.	.46	1.
64	-1.	-.46	-1.	-.46
64	.46	1.	-1.	-.46
66	-1.	-.46	.442	1.
66	.46	1.	.442	1.
67	-1.	-.46	-1.	-.46
67	.46	1.	-1.	-.46
69	-1.	-.46	.46	1.
69	.46	1.	.46	1.
70	-1.	-.46	-1.	-.46
70	.46	1.	-1.	-.46
72	-1.	-.46	.442	1.
72	.46	1.	.442	1.
73	-1.	-.46	-1.	-.46
73	.46	1.	-1.	-.46
75	-1.	-.46	.46	1.
75	.46	1.	.46	1.
76	-1.	-.46	-1.	-.46
76	.46	1.	-1.	-.46

Table C3 (Concluded)

78	-1.	-.46	.442	1.
78	.46	1.	.442	1.
79	-1.	-.488	-1.	-.46
79	.433	1.	-1.	-.46
79	.433	1.	.46	1.
80	.433	1.	-1.	-.46
80	.433	1.	.46	1.
81	.433	1.	-1.	-.46
81	-1.	-.488	.46	1.
81	.433	1.	.46	1.
82	-1.	-.488	-1.	-.46
82	.433	1.	-1.	-.46
82	.433	1.	.46	1.
83	.433	1.	-1.	-.46
83	.433	1.	.46	1.
84	.433	1.	-1.	-.46
84	-1.	-.488	.442	1.
84	.433	1.	.442	1.

Table C4

Output Data for Ribbed Mat, PART IV

```
-INITE ELEMENT ANALYSIS OF CONCRETE SLABS

        NO. OF SLABS =          1  POISSON RATIO OF CONCRETE=    0.1500      THICKNESS OF CONCRETE=     6.0000
   MODULUS OF CONCRETE= 0.150E+07        MODULUS OF SUBGRADE= 0.300E+05  POISSON RATIO OF SUBGRADE=    0.4000

 NSYM=         4     NFROB=         1     NPEAD=         0     NPUNCH=         0


SUMMARY OF VARIABLES:
  SLAB LENGTH = 677.80 FT    EDGE EFFECT =   0.00 FT    YM = 0.00 IN
  SLAB WIDTH = 303.67 FT    BEAM DEPTH =   6.00 IN
  PARABOLIC EQUATION EXPONENT "M" =   1


MOMENT OF INERTIA:   0.925147E+07   0.418540E+07

  DIMENSIONS OF GRADE BEAMS

                                LONG DIMENSION        SHORT DIMENSION        SPACING
                                --------------        ---------------        -------

      TRANSVERSE GRADE BEAM          28.00000              18.00000          150.00000

      LONGITUDINAL GRADE BEAM        28.00000              18.00000          150.00000

   NX1=        15       NX2=         0       NY=         7     NCYLE=        10     NOTCON=        21     NB=        27
 VALUES OF X ARE:
   0.000     12.500     37.500     62.500     87.500    112.500    137.500    162.500    187.500    212.500
 237.500    262.500    287.500    312.500    338.900

 VALUES OF Y ARE:
   0.000     25.000     50.000     75.000    100.000    125.000    151.830

 REACTIONS AT THE FOLLOWING NODES ARE ASSUMED INITIALLY ZERO:
     29        30        31        32        33        34        35        36        37        38
     39        40        41        42        43        44        45        46        47        48
     49
       IER=         0


  NGAP=   21      NTEMP=    0       NLOAD=  116          ICL=   '0          NCK=    8          NWT=    1
  TEMP=   0.00000     Q=   4.00000     RFJ=   0.50000     DEL=   0.00100    DELF=   0.00010    ICLF=   30

  THE FOLLOWING NODES ARE USED TO CHECK CONVERGENCE:
     15        27        45        56        65        75        93       104

 NODAL NUMBERS AND INITIAL GAPS ARE TABULATED AS FOLLOWS:
 29   0.50000   30   0.50000   31   0.50000   32   0.50000   33   0.00000   34   0.00000   35   0.00000
 36   1.00000   37   1.00000   38   1.00000   39   1.00000   40   1.00000   41   0.00000   42   0.00000
 43   0.50000   44   0.50000   45   0.50000   46   0.50000   47   0.00000   48   0.00000   49   0.00000
```

Table C4 (Continued)

NODE	DEFLECTION	NODE	DEFLECTION	NODE	DEFLECTION	NODE	DEFLECTION
1	0.232646E+00	2	0.224480E+00	3	0.220939E+00	4	0.221860E+00
5	0.205883E+00	6	0.191427E+00	7	0.172275E+00	8	0.233566E+00
9	0.224288E+00	10	0.220759E+00	11	0.222583E+00	12	0.204624E+00
13	0.190456E+00	14	0.172267E+00	15	0.228773E+00	16	0.220621E+00
17	0.217054E+00	18	0.218212E+00	19	0.203453E+00	20	0.188757E+00
21	0.170236E+00	22	0.232695E+00	23	0.224429E+00	24	0.221221E+00
25	0.219361E+00	26	0.200683E+00	27	0.186645E+00	28	0.168323E+00
29	0.729930E+00	30	0.721414E+00	31	0.719416E+00	32	0.718660E+00
33	0.211426E+00	34	0.188873E+00	35	0.165460E+00	36	0.121978E+01
37	0.121167E+01	38	0.120824E+01	39	0.120730E+01	40	0.118109E+01
41	0.185905E+00	42	0.165385E+00	43	0.725792E+00	44	0.717308E+00
45	0.715410E+00	46	0.714838E+00	47	0.207963E+00	48	0.186462E+00
49	0.165448E+00	50	0.224305E+00	51	0.216095E+00	52	0.213082E+00
53	0.211569E+00	54	0.193436E+00	55	0.180355E+00	56	0.163485E+00
57	0.215945E+00	58	0.207860E+00	59	0.204584E+00	60	0.206250E+00
61	0.192112E+00	62	0.178263E+00	63	0.160637E+00	64	0.212937E+00
65	0.204891E+00	66	0.201763E+00	67	0.203205E+00	68	0.187436E+00
69	0.174275E+00	70	0.157205E+00	71	0.206874E+00	72	0.198878E+00
73	0.195895E+00	74	0.197673E+00	75	0.182593E+00	76	0.169687E+00
77	0.153023E+00	78	0.199742E+00	79	0.191812E+00	80	0.189015E+00
81	0.191064E+00	82	0.176312E+00	[illegible]	0.163964E+00	84	0.147947E+00
85	0.190473E+00	86	0.182682E+00	87	0.180117E+00	88	0.182515E+00
89	0.168451E+00	90	0.156883E+00	91	0.141701E+00	92	0.177466E+00
93	0.170711E+00	94	0.168428E+00	95	0.170395E+00	96	0.158105E+00
97	0.147862E+00	98	0.133401E+00	99	0.152905E+00	100	0.151450E+00
101	0.149504E+00	102	0.146918E+00	103	0.140925E+00	104	0.132955E+00
105	0.118995E+00						

NODE	MOMENT X	MOMENT Y	MOMENT XY
1	0.267014E+03	0.579237E+03	0.137648E+01
2	0.628269E+03	-0.222229E+03	-0.694103E+00
3	0.632731E+03	-0.221233E+03	0.959937E+00
4	0.336957E+03	0.598303E+03	-0.422608E+00
5	-0.264970E+03	-0.231990E+03	-0.453696E+00
6	0.237069E+03	0.150908E+03	0.766288E+00
7	-0.372923E+02	0.000000E+00	0.000000E+00
8	-0.953425E+03	0.664536E+03	-0.843615E+00
9	-0.116901E+04	-0.263268E+03	-0.671487E+00
10	-0.118032E+04	-0.267947E+03	0.592383E+00
11	-0.101473E+04	0.714358E+03	-0.560937E+01
12	0.111778E+04	-0.322336E+03	-0.364091E+01
13	-0.435783E+02	0.152874E+03	0.315458E+01
14	0.810163E+02	0.000000E+00	0.000000E+00
15	0.348078E+04	0.593849E+03	0.636689E+00
16	0.357015E+04	-0.227749E+03	0.409615E+00
17	0.358497E+04	-0.215655E+03	-0.311846E+00
18	0.361459E+04	0.562672E+03	0.320029E+02
19	-0.347464E+04	-0.183617E+03	0.175150E+02
20	0.342914E+02	0.120656E+03	-0.152247E+02
21	-0.190126E+02	0.000000E+00	0.000000E+00
22	-0.139568E+05	0.588582E+03	-0.458258E+00
23	-0.139693E+05	-0.243304E+03	-0.563206E+01
24	-0.140274E+05	-0.131575E+03	0.242961E+02
25	-0.141804E+05	0.557783E+03	-0.148744E+03
26	0.131507E+05	-0.260926E+03	-0.884176E+02
27	-0.177759E+03	0.125803E+03	0.879175E+02
28	0.463872E+02	0.000000E+00	0.000000E+00

Table C4 (Continued)

29	-0.376670E+04	-0.943036E+02	0.242328E+00
30	-0.378636E+04	0.119795E+04	0.275227E+01
31	-0.367519E+04	-0.557449E+04	-0.116257E+02
32	-0.352445E+04	0.211125E+05	0.789095E+02
33	-0.507924E+05	-0.205613E+05	-0.247480E+03
34	0.316206E+03	0.502320E+04	-0.302022E+03
35	-0.123713E+03	0.000000E+00	0.000000E+00
36	0.298597E+05	0.935447E+03	-0.148986E-01
37	0.298882E+05	-0.975576E+03	0.125136E-01
38	0.297635E+05	0.258146E+04	0.517062E-01
39	0.296114E+05	-0.985564E+04	0.880373E-01
40	0.807442E+05	0.396229E+05	0.232014E+00
41	-0.357807E+03	-0.367319E+05	0.690979E+00
42	0.634840E+02	0.000000E+00	0.000000E+00
43	-0.375963E+04	-0.955767E+02	-0.178870E+00
44	-0.378515E+04	0.119577E+04	-0.268276E+01
45	-0.367395E+04	-0.557623E+04	0.116802E+02
46	-0.351696E+04	0.211109E+05	-0.788235E+02
47	-0.507775E+05	-0.205739E+05	0.247706E+03
48	0.360527E+03	0.499331E+04	0.302355E+03
49	0.264649E+02	0.000000E+00	0.000000E+00
50	-0.139725E+05	0.586579E+03	0.231400E+00
51	-0.139601E+05	-0.245974E+03	0.554814E+01
52	-0.140178E+05	-0.134600E+03	-0.241072E+02
53	-0.141937E+05	0.555131E+03	0.149003E+03
54	0.131273E+05	-0.269992E+03	0.883726E+02
55	-0.188259E+03	0.117095E+03	-0.884242E+02
56	-0.579048E+01	0.000000E+00	0.000000E+00
57	0.355819E+04	0.582739E+03	-0.133991E+00
58	0.355437E+04	-0.232705E+03	0.232692E+00
59	0.356768E+04	-0.220809E+03	-0.184676E+00
60	0.368238E+04	0.562560E+03	-0.325051E+02
61	-0.335946E+04	-0.190411E+03	-0.172305E+02
62	0.679328E+02	0.122490E+03	0.153405E+02
63	0.327674E+02	0.000000E+00	0.000000E+00
64	-0.865682E+03	0.574950E+03	0.439408E-01
65	-0.863275E+03	-0.226646E+03	-0.359753E-01
66	-0.872221E+03	-0.229249E+03	0.235943E+00
67	-0.898383E+03	0.615192E+03	0.831220E+01
68	0.872943E+03	-0.260382E+03	0.444551E+01
69	0.538637E+01	0.137540E+03	-0.358793E+01
70	0.302426E+01	0.000000E+00	0.000000E+00
71	0.249985E+03	0.574613E+03	-0.211262E-01
72	0.249069E+03	-0.230441E+03	0.941750E-01
73	0.251994E+03	-0.229802E+03	0.108028E+00
74	0.255591E+03	0.603733E+03	-0.188498E+01
75	-0.194761E+03	-0.247194E+03	-0.844684E+00
76	0.205512E+02	0.132559E+03	0.126513E+01
77	0.290010E+02	0.000000E+00	0.000000E+00
78	-0.120873E+02	0.571493E+03	0.103412E-01
79	-0.143591E+02	-0.232165E+03	0.997958E-01
80	-0.145780E+02	-0.232132E+03	0.154263E+00
81	-0.[illegible]877E+02	0.603685E+03	0.788741E+00
82	0.903839E+02	-0.252872E+03	0.654236E+00
83	0.309476E+02	0.132266E+03	0.172420E+00
84	0.237819E+02	0.000000E+00	0.000000E+00
85	0.407974E+02	0.563746E+03	-0.290000E+00
86	0.437177E+02	-0.232738E+03	0.280745E+00
87	0.431340E+02	-0.232876E+03	0.406971E-01
88	0.378400E+02	0.594267E+03	0.225941E+00
89	0.802973E+01	-0.253394E+03	0.601616E+00

Table C4 (Concluded)

90	0.127694E+02	0.132555E+03	0.566208E+00
91	0.166444E+02	0.000000E+00	0.000000E+00
92	0.274027E+03	0.488931E+03	-0.375000E-01
93	0.162580E+03	-0.200647E+03	0.190581E+01
94	0.161690E+03	-0.201281E+03	-0.153205E+01
95	0.270946E+03	0.516256E+03	0.536267E+00
96	0.161567E+03	-0.223823E+03	0.238808E+01
97	0.137890E+03	0.143332E+03	0.382425E+00
98	0.143694E+03	0.000000E+00	0.000000E+00
99	0.000000E+00	0.850791E+02	0.000000E+00
100	0.000000E+00	-0.543437E+01	0.000000E+00
101	0.000000E+00	-0.439218E+01	0.000000E+00
102	0.000000E+00	0.986481E+02	0.000000E+00
103	0.000000E+00	-0.280563E+01	0.000000E+00
104	0.000000E+00	0.140605E+03	0.000000E+00
105	0.000000E+00	0.000000E+00	0.000000E+00

CALCULATED SHEAR IN LONG DIRECTION (LBS/IN)

INCR	SHEAR X	INCR	SHEAR X	INCR	SHEAR X	INCR	SHEAR X	INCR	SHEAR X	INCR	SHEAR X
1	-0.453581E+00	2	-0.435260E+00	3	-0.509997E+00	4	-0.855259E+00	5	-0.510385E+00	6	-0.513193E+00
7	-0.864986E+00	8	0.402230E+00	9	0.401638E+00	10	0.478478E+00	11	0.728920E+00	12	0.385689E+00
13	0.368718E+00	14	0.729729E+00	15	-0.207716E-01	16	-0.572629E-01	17	-0.261209E+00	18	0.173397E+00
19	0.189285E+00	20	0.181421E+00	21	0.165032E+00	22	0.124702E-01	23	0.344232E-01	24	0.900527E+00
25	-0.863475E+00	26	-0.847947E+00	27	-0.831826E+00	28	-0.827548E+00	29	0.575178E-01	30	0.408360E-01
31	-0.337375E+01	32	0.364924E+01	33	0.354861E+01	34	0.351081E+01	35	0.352129E+01	36	-0.105030E+00
37	-0.170654E+00	38	0.133728E+02	39	-0.144864E+02	40	-0.140158E+02	41	-0.139443E+02	42	-0.139640E+02
43	0.169358E+00	44	0.700118E+00	45	-0.520926E+02	46	0.565347E+02	47	0.555112E+02	48	0.552844E+02
49	0.553355E+02	50	-0.376460E+00	51	-0.114296E+01	52	0.201922E+03	53	-0.342788E+02	54	-0.325522E+02
55	-0.321357E+02	56	-0.322552E+02	57	0.822255E+00	58	0.208530E+01	59	-0.416246E+03	60	-0.104270E+03
61	-0.105596E+03	62	-0.106284E+03	63	-0.106113E+03	64	0.593045E+00	65	-0.212910E+01	66	0.415204E+03
67	0.104595E+03	68	0.105551E+03	69	0.106296E+03	70	0.106144E+03	71	-0.147501E+01	72	0.174104E+01
73	-0.200753E+03	74	0.333345E+02	75	0.327255E+02	76	0.321349E+02	77	0.321574E+02	78	0.479515E+00
79	-0.125714E+01	80	0.522780E+02	81	-0.555944E+02	82	-0.556945E+02	83	-0.553474E+02	84	-0.550257E+02
85	-0.363036E+00	86	0.354933E+00	87	-0.144480E+02	88	0.145050E+02	89	0.150444E+02	90	0.149602E+02
91	0.139976E+02	92	0.383247E+00	93	-0.914847E+00	94	0.435818E+01	95	-0.424602E+01	96	-0.572724E+01
97	-0.567381E+01	98	-0.385297E+01								

CALCULATED SHEAR IN SHORT DIRECTION (LBS/IN)

INCR	SHEAR Y	INCR	SHEAR Y	INCR	SHEAR Y	INCR	SHEAR Y	INCR	SHEAR Y	INCR	SHEAR Y
1	-0.436716E+00	2	0.479243E+00	3	-0.330641E+00	4	0.345160E+00	5	-0.136206E-02	6	-0.295696E+00
7	-0.445184E+00	8	0.122443E+01	9	-0.247257E+01	10	0.239081E+01	11	0.265155E-02	12	-0.230372E+01
13	-0.411713E+00	14	0.128525E+01	15	-0.282537E+01	16	0.275892E+01	17	-0.102082E-03	18	-0.265552E+01
19	-0.410316E+00	20	0.128724E+01	21	-0.285992E+01	22	0.277762E+01	23	-0.339440E-04	24	-0.267888E+01
25	-0.411724E+00	26	0.125052E+01	27	-0.281973E+01	28	0.281064E+01	29	0.253253E-02	30	-0.268392E+01
31	-0.427175E+00	32	0.138616E+01	33	-0.298700E+01	34	0.268596E+01	35	-0.100013E-01	36	-0.267114E+01
37	-0.380450E+00	38	0.715462E+00	39	-0.217655E+01	40	0.318417E+01	41	-0.358593E-01	42	-0.270137E+01
43	-0.363695E+00	44	0.252381E+01	45	-0.224747E+01	46	0.157995E+01	47	0.484215E+00	48	-0.280116E+01
49	-0.155971E+02	50	0.842718E+02	51	-0.139731E+03	52	0.892064E+02	53	-0.226134E+02	54	0.431634E+01
55	0.114089E+03	56	-0.255472E+03	57	0.164146E+03	58	-0.412082E+02	59	0.118199E+02	60	-0.636143E+01
61	-0.156019E+02	62	0.865142E+02	63	-0.138412E+03	64	0.822380E+02	65	-0.224614E+02	66	0.428104E+01
67	-0.330742E+00	68	0.963521E+00	69	-0.239464E+01	70	0.266840E+01	71	0.294756E+00	72	-0.275328E+01
73	-0.374754E+00	74	0.107226E+01	75	-0.255441E+01	76	0.247570E+01	77	0.431675E-01	78	-0.270874E+01
79	-0.474822E+00	80	0.157649E+01	81	-0.344516E+01	82	0.329072E+01	83	-0.144380E-01	84	-0.309275E+01
85	-0.459716E+00	86	0.126873E+01	87	-0.275815E+01	88	0.274816E+01	89	0.448042E-02	90	-0.267162E+01

APPENDIX D: PERFORMANCE ANALYSIS, CENTRALIZED TROOP CLINIC, FORT SAM HOUSTON, TEXAS

Purpose

1. On 4 November 1983 it was reported that the subject structure was apparently moving. This assessment was based on cracking of interior plaster board and exterior brick walls. The structure was inspected on 10 November 1983 by geotechnical and structural personnel. In conjunction with a cooperative research project being conducted by Fort Worth District and the Waterways Experiment Station, a vertical survey of the structure was conducted on 14 November 1983. This report presents a summary of foundation design and construction, results of the visual inspection and the vertical survey. Recommendations for monitoring the structure and potential remedial procedures is also made.

Design

2. The structure was designed by Harwood K. Smith and Partners, Dallas, Texas, under contract to the Fort Worth District. The structure consists of precast concrete exterior panels with face-brick fillers. The roof is supported on steel frames with interior pipe columns. Column bays are generally 30 by 41 feet. The structural foundation consists of a reinforced concrete ribbed mat slab. The ribs are placed on 15 by 20.5-ft centers and coincide with the superstructure framing system. Beams are widened at column locations so that the resultant soil pressure does not exceed 2.0 ksf. The foundation materials consist principally of 5 to 10 ft of CH clays overlying clay shale. From 2.0 to 5.5 ft of the CH materials were removed and replaced with nonexpansive fill compacted to at least 92 percent maximum density. Typical profiles through the structure are shown on Figure D1. During design it was predicted that the subgrade materials would move to the point that the perimeter of the foundation would cantilever 7.5 ft. Based on this, the exterior beams were reinforced with four No. 11 T&B.

Construction

3. Construction of the building, accomplished by Fortec Construction Co., San Antonio, Texas, proceeded from February 1981 to September 1982.

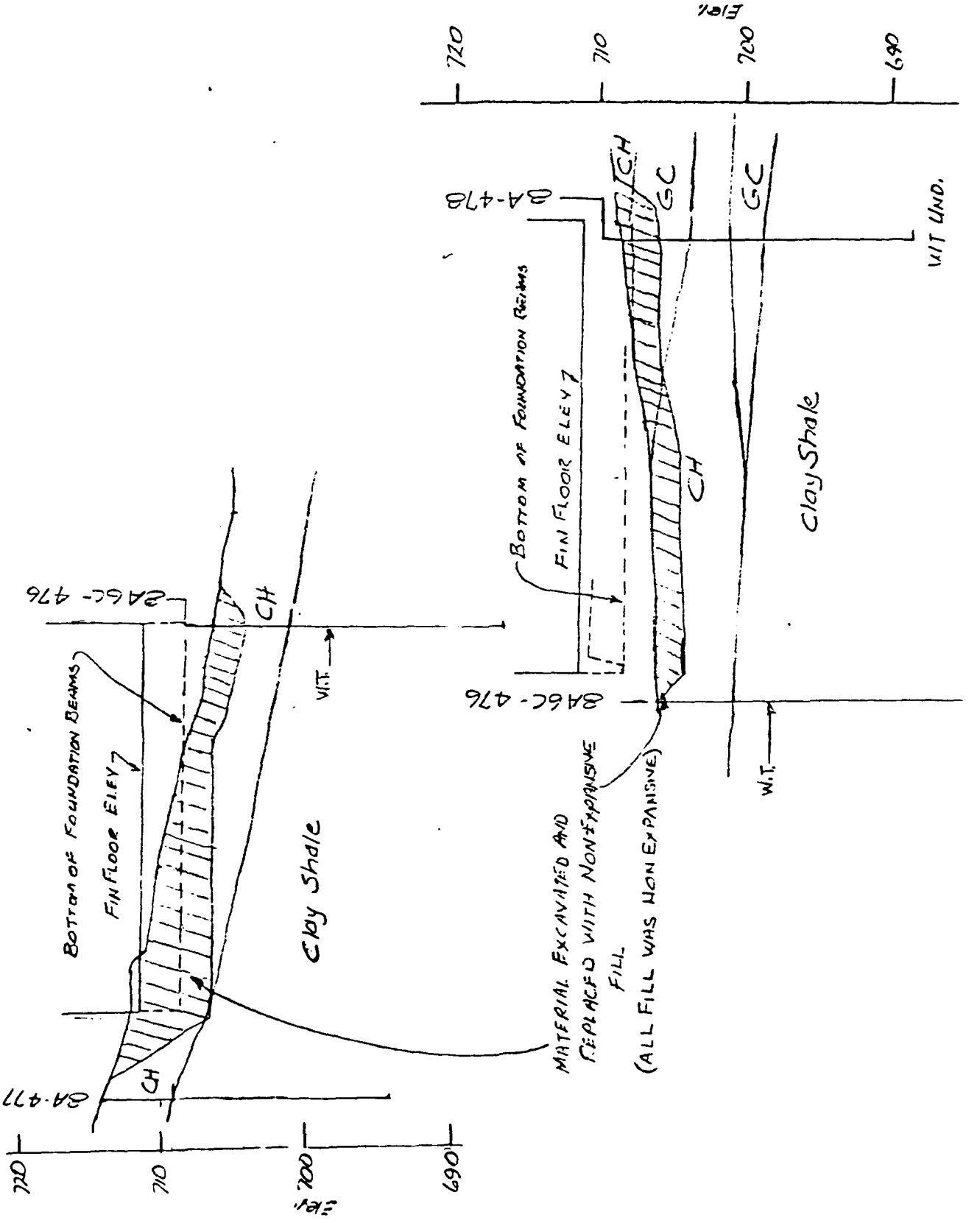

Figure D1. Subsurface profiles, Troop Medical Clinic
Fort Sam Houston

During latter stages of construction of the foundation, it was noticed that the horizontal reinforcing steel in the interior ribs was not being satisfactorily anchored into the perimeter foundation beams. To remedy this mistake, the contractor broke out part of the concrete in the floor and beam system and grouted in additional transverse steel.

Performance

4. General. Performance of the structure to date (November 1983) appears to be satisfactory with the few exceptions listed below.

(1) A small hairline crack has developed in the brick below the window frame in the exterior south wall.

(2) A small crack has appeared in the exterior precast panel of the east wall. The crack is 0.02-inch wide at the bottom and fades out where the smooth concrete meets the exposed aggregate concrete.

(3) A noticeable crack has developed in the precast concrete above the front entrance door. The crack is 0.07 inch wide at the bottom and 0.03 inch wide at the top.

(4) A significant erosion channel has developed adjacent to the foundation at the southeast corner of the building. Tests have indicated that the roof drain at this location is partially blocked and water pouring through the roof scupper has eroded the foundation soils.

(5) Several cracks, generally at the top of door frames, have developed in the south wall of the south corridor.

(6) Roof and window frame leaks were noted in the office in the southeast corner of the building (Room 116).

5. Survey. The performance of the foundation was determined by running a level through 30 points on the floor slab, Figure 31 of PART III. The floor slab shows a typical center lift (heave) mode movement with a slight skew toward the northeast corner of the building. Generally the differential movement of the structure is well within tolerance limits. Typical and "worse case" differential movement between adjacent points are given in Table D1a. All other points show less deflection ratios. According to Skempton and MacDonald (1956), wall panels and sheet rock walls should be able to tolerate differential movements on the order of 1/300. Consequently, it is inferred

Table D1

Differential Displacements Troop Medical Clinic

a. Adjacent points

Survey Points	Differential Settlement
1 - 5	1/400
18 - 24	1/480
21 - 22	1/427
22 - 23	1/458
27 - 25	1/230

b. Three adjacent points

Survey Points	Differential Settlement
26-27-28	1/1400
20-21-22	1/976
21-22-23	1/850
27-28-average 18,19	1/820

that except in the area of survey points 27 - 25, the structure is performing satisfactorily.

6. Woodburn (1979) has developed performance criteria based on the differential movement of three adjacent points. Typical and "worse case" deflections using three adjacent points are shown in Table D1b. According to Woodburn, masonry wall panels and sheet rock walls should be able to tolerate differential movements on the order of 1/800. As shown by the above table, the movement at the southeast corner of the building is approximating the tolerance limit.

Recommendations

7. It is recommended that the roof drains in the southeast corner of the building be repaired to a functional condition. Although it may be only accidental, it is noted that the poorest foundation performance coincides with the malfunctioning roof drain.

8. The progression of cracks in the precast concrete panels should be monitored on a bi-weekly basis. The resident office personnel have placed small dental plaster patches across the crack to make a quick determination of additional movement.

9. Should movement progress to any significant extent, the foundation should be stabilized before the building moves to the extent that the Pest Management Facility has moved. It is considered that some form of intrusion groutng will be used, such as was done for the Night Lighting Vault, Fort Polk, should it become necessary to affect foundation repairs.

APPENDIX E: INFLUENCE OF SOIL MODEL ON MAT PERFORMANCE

Introduction

1. Parametric analyses were completed using plate on semi-infinite elastic program SLAB2 and plate on Winkler foundation program WESLIQID to determine the influence of soil behavior on mat performance. Influence of soil type was determined by a comparison of mat performance calculated by SLAB2 and WESLIQID. Influence of soil stiffness was determined by calculations of bending moments using program SLAB2 for mats subject to imposed heave.

2. Programs SLAB2 and WESLIQID were used to analyze the bending moments and displacements of a 200-ft square, flat concrete mat with a Young's modulus of 432,000 ksf and Poisson's ratio 0.15. The soil Poisson's ratio was assumed 0.3. Symmetrical loads were applied so that only 1/4 of the mat need be modeled by the finite element mesh. This mesh was divided into 100 square elements of equal size of 10 ft on each side.

Influence of Soil Model

3. Bending moments calculated by programs SLAB2 and WESLIQID for similar displacement patterns caused by imposed loads and heaves may be compared to determine influence of the soil model. An analysis of the 200-ft square mat of 12-inch thickness was performed first using SLAB2. Input parameters included a uniform applied pressure $q = 2$ psi and Young's soil modulus $E_s = 400$ ksf. Bending moments and displacements distributed from the center to middle edge calculated by this initial run using program SLAB2 are shown in Figure E1. The coefficient of subgrade reaction for each nodal point of the mesh was subsequently determined by

$$k_{sf} = q/\rho \qquad \text{(E1)}$$

where ρ is the settlement calculated from SLAB2 at each nodal point. Program WESLIQID was then applied using these k_{sf} for the imposed load $q = 2$ psi. Displacements calculated by both programs SLAB2 and WESLIQID for pressure $q = 2$ psi in Figure E1 are essentially idential as expected. The bending moments calculated by these programs differ near the edge where results from SLAB2 indicate larger bending moments than results from WESLIQID.

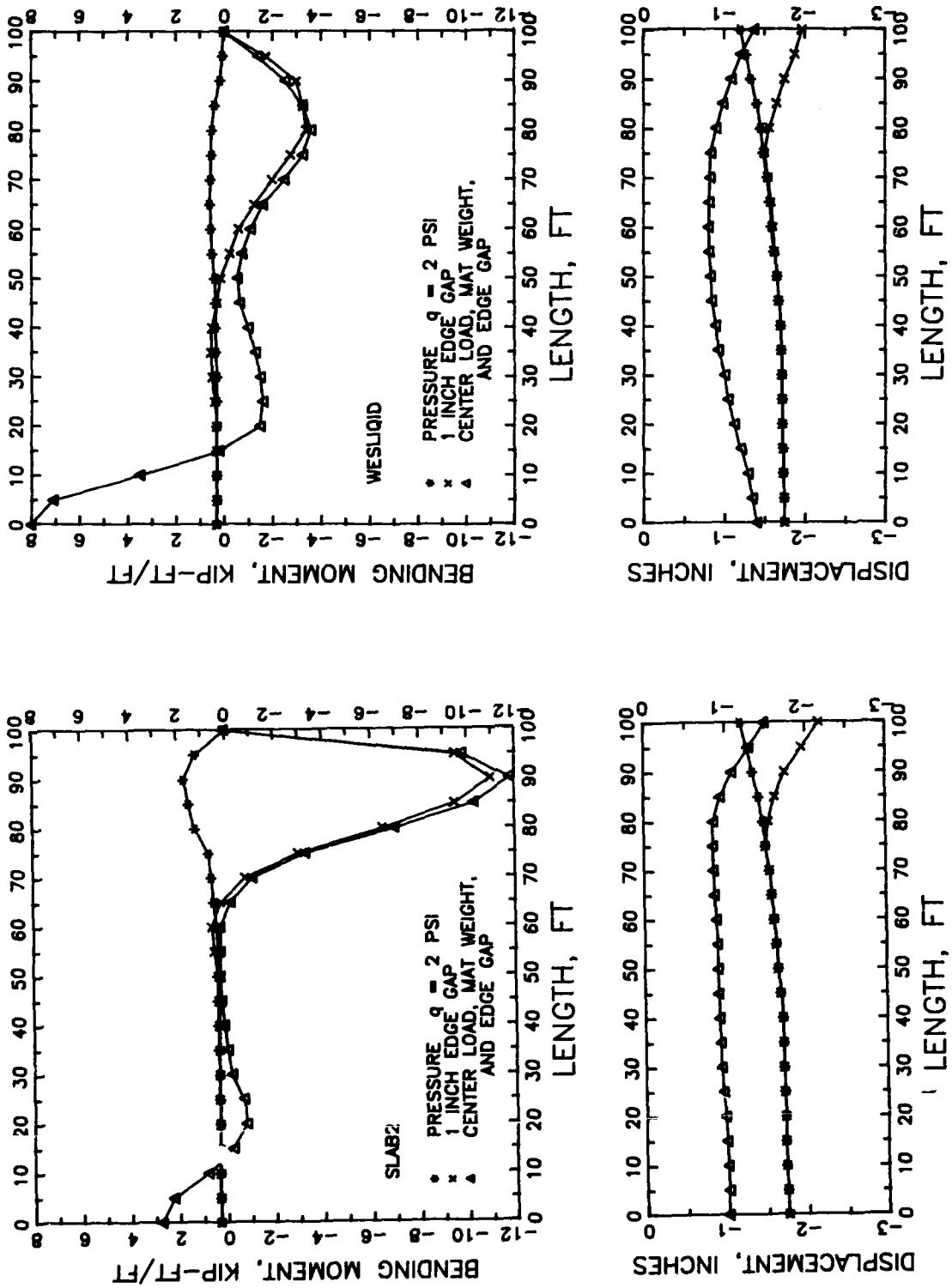

Figure E1. Comparison of results between SLAB2 and WESLIQID

4. Programs SLAB2 and WESLIQID were applied in a second analysis using q = 2 psi and an imposed identical 1 inch edge gap around the perimeter of the mat, Figure E1. Displacements calculated from this second analysis indicate edge-down displacements, but the mat on elastic soil appears more flexible with greater edge down displacement than the mat on Winkler soil. Bending moments are substantially more negative near the edge for the mat on elastic soil of program SLAB2 than the mat on Winkler soil of program WESLIQID.

5. A third analysis imposed a center load of 115,200 pounds on the mat, the weight of the mat, and the same edge gap as the second analysis, Figure E1. Displacements calculated for this third analysis are less than those for the previous two analyses because of the smaller applied loads. The displacement pattern calculated by SLAB2 does not show as much settlement in the center as calculated by WESLIQID. The elastic material shares the load with adjacent soil elements, while the Winkler soil does not. The positive bending moments calculated by WESLIQID are subsequently much larger near the mat center than those calculated by SLAB2.

Influence of Soil Stiffness

6. Program SLAB2 was applied to determine the influence of the stiffness of an elastic soil on the maximum bending moment. An imposed center heave was simulated by applying a 1 inch gap at the mat perimeter. Edge lift was simulated by applying a 0.4 inch gap beneath the mat center. The mat is sufficiently flexible such that the mat is fully supported by the soil. The maximum negative bending moments due to center lift, Figure E2a, occurs approximately 10 ft from the mat perimeter and maximum positive bending moment imposed by edge lift, Figure E2b, occurs at the center. Figure E2 shows that increasing the soil elastic modulus causes significant increases in the magnitude of the maximum bending moments when heave is imposed. If heave is not imposed, an increasing elastic soil modulus tends to decrease bending moments because of improved soil support and reduced settlement and mat distortion.

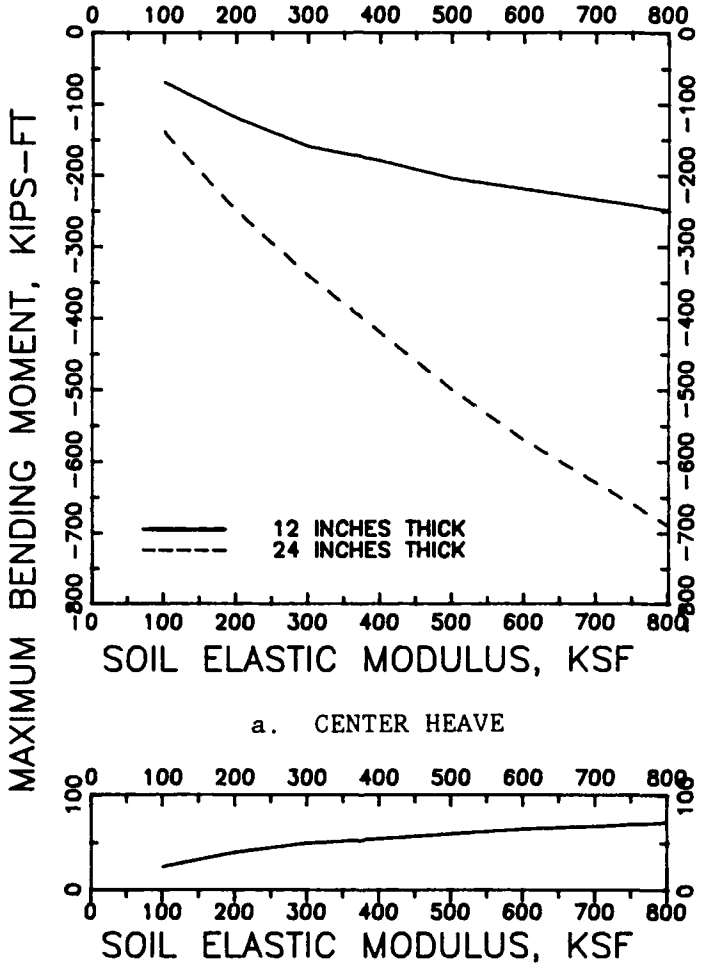

a. CENTER HEAVE

b. EDGE HEAVE, 12 INCHES THICK

Figure E2. Maximum bending moments of a 10-ft wide strip of 200-ft by 200-ft mat 12 or 24 inches thick subject to heave

APPENDIX F

LIGHT TRACK VEHICLE FOUNDATION DESIGN

PROJECT TITLE RRAD BLDG. 333

LIGHT TRACK VEHICLE FOUNDATION DESIGN.

SOIL REPORT PREPARED BY FORT WORTH DISTRICT DATED MARCH 1981 RECOMMENDS RIB MAT FOR LIGHT TRACK VEHICLE, MATERIAL STAGING, & HEAT TREATMENT BLDG'S. THESE MAT TYPE FDN. ARE TO BE DESIGNED ACCORDING TO POST TENSIONING INSTITUTE (PTI) METHOD. BASIC PTI APPROACH ASSUMES THAT ALL STIFFENING BEAMS ARE CARRYING LOADS ABOVE SLAB UNIFORMLY. IN ADDITION, ONLY BEAMS ARE TAKING SHEAR STRESS IN SLAB. HOWEVER, SOIL REPORT SUGGEST THAT ONLY BEAMS UNDER COLUMNS ARE SUBJECTED TO COLUMN LOADS. PSEC HAVE TALKED TO DIFFERENT PEOPLE WHO HAVE USED PTI METHOD BEFORE AND NO CONSISTENT OPINION/AGREEMENT CAN BE REACHED. IT SEEMS THAT NO BUILDING OF THE LIGHT TRACKING VEHICLE SHOP SIZE & COLUMN LOADING HAS EVER BEEN DESIGNED ACCORDING TO PTI METHOD. THE FOLLOWING IS A SUMMARY OF OPINION:

1) CLIFF FREYERMUTH OF PTI (602-265-9158)
- PTI METHOD IS DEVELOPED FOR RESIDENTIAL AND LIGHT INDUSTRIAL BLDG. ONLY. IT DOESN'T APPLY TO HEAVY CONCENTRATED COLUMN LOAD (150K ± IN THIS PROJECT)
- FORMULARS USED IN PTI ASSUMES UNIFORM PERIMETER LOADING
- BEAM DEPTH SHOULD NOT BE MORE THAN 30 IN AND NO TEST HAD EVER BEEN DONE ON 8" THK. SLAB IN THE PAST.

2) BEN BACKA - FORT WORTH DISTRICT REVIEWER
- e_m VALUE (8') PROVIDED APPEARS HIGH, y_m 1.5" SEEMS REASONABLE
- ASSUME ONLY BEAMS ARE TAKING BENDING MOMENT

SYSTEM BLDG. 333 FDN. SLAB/BM

checked 2/16/82

COMPONENT

JOB NO. 9316 DATE 1/11/82

DESIGNER Sea Fan

PSEC FACILITIES SYSTEMS ENGINEERING CORPORATION
LOS ANGELES, CA. RICHLAND, WA DUBLIN, IRELAND

AND THUS SLAB BETWEEN BEAMS DO NOT HAVE TO BE DESIGNED TO TAKE THE CALCULATED BENDING MOMENT; THIS RESULT IN SUBSTANTIAL SAVING IN CONCRETE SLAB THICKNESS & REINFORCING BAR. THIS ASSUMPTION APPEAR TO BE QUESTIONABLE.

- RAN SOME CALCULATION HIMSELF AND ENCOUNTERED SOME DEFLECTION PROBLEM. BEAM MAY HAVE TO BE 54" DEEP. (817-334-3177)

3) GARLAND YOUNG - HEAD OF STRUCTURAL DESIGN GROUP AT FORT WORTH DISTRICT, ALSO A MEMBER OF THE COMMITTEE WHICH PREPARE THIS PTI BOOK.

- AGREE THAT CONCENTRATED COLUMN LOAD SHOULD NOT BE ASSUMED TO BE EVENLY DISTRIBUTED & SUPPORTED BY THE WHOLE SLAB.
- DOES NOT THINK PUTTING A ISOLATION JOINT AROUND COLUMN PIER AND HAVE COLUMN FOOTING UNDER SLAB IS A GOOD SOLUTION. RATIONALE IS THAT IT DESTROY THE RIB MAT CONCEPT. 817-334-2305
- SUGGEST WIDEN BEAM INTERSECTIONS AT COLUMN LOCATIONS TO FORM DIAMOND SHAPED FOOTING.

4) JACK FLETCHER 817-334-2117

FSEC PROPOSE TO DO THE FOLLOWING =

a) WIDEN BEAM INTERSECTIONS TO FORM DIAMOND SHAPED FOOTING TO SUPPORT CONC. COL. LOAD

b) BEAMS WILL BE SIZED TO SUPPORT SLAB DL & FLR. L.L. ONLY.

c) PTI METHOD WILL BE USED TO FIND MOMENT SHEAR & DEFLECTION IN SLAB. NO POST TENSIONING WILL BE USED.

d) SINCE BUILDING IS 300' x 675', INTERIOR

SYSTEM

COMPONENT

Checked 2/16/82

JOB NO. 931 DATE 1/11/82

DESIGNER Sea Fu

SLAB WILL BE SUBJECTED TO VERY SMALL BENDING MOMENT. (SEE FIG. 5.3 PTI BOOK) MAX. MOMENT APPEAR AT A DISTANCE B FROM EDGE OF SLAB. THEREFORE SPACE BEAMS AT 12'-6" AT PERIMETER OF SLAB TO ALLOW T-BEAM ACTION WHILE INTERIOR BEAMS CAN STAY AT 25'-0" O.C. SIMILARLY, THERE WILL BE NO SHEAR PROBLEM IN THE BEAM @ PERIMETER DUE TO CLOSER BEAM SPACING.

P (PERIMETER LOAD) = 8' HIGH x 8" CONC. BLOCK WALL.

e) THE EXIST. 5' ± OF FILL MATERIAL SHALL BE REMOVED AND REPLACED WITH NON-EXPANSIVE FILL MATERIAL.

SYSTEM

COMPONENT

Checked 2/16/82

JOB NO. 9316 DATE 2/8/82

DESIGNER Sean Fan

RIB MAT DESIGN

REF. DESIGN & CONSTRUCTION OF POST-TENSIONED SLABS-ON-GROUND BY PTI.

$q_a = 2000$ PSF
$e_m = 8'$ EDGE LIFT
$= 5'$ CENTER LIFT
$y_m = 1.5''$
$\mu = 0.5$
SLAB THICKNESS = 8"
PERIMETER LOADING
$P = 18' @ 92\#/\square' = 736\#/'$
FLR. LIVE LOAD = $150 \times .5$
$= 75$ PSF
CONC. $f'_c = 3000$ PSI

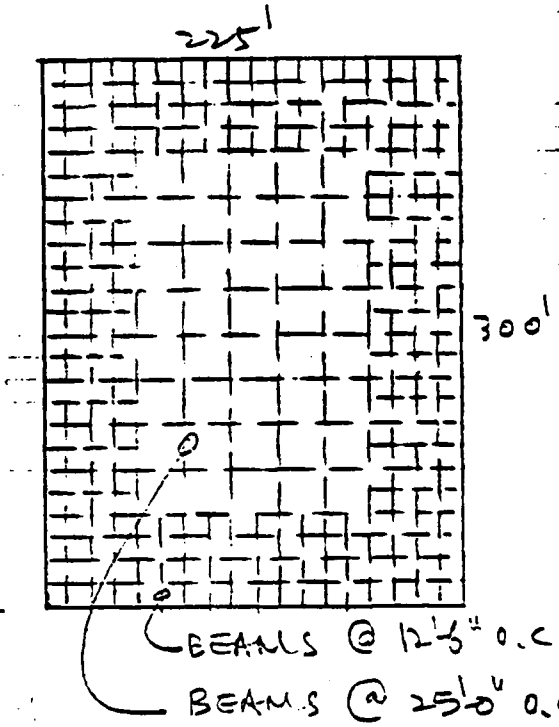

SECTION PROPERTIES (SHORT DIR.)

BEAM DEPTH = 36"
BEAM WIDTH = 15" x 25 = 375"
MOM. OF I = 3332669 IN^4
NEUTRAL AXIS Y = 8.81" FROM TOP OF SLAB

SECTION PROPERTIES (LONG DIR.)

BEAM DEPTH = 36"
BEAM WIDTH = 15" x 19 = 285"
MOM. OF I = 2524567 IN^4
NEUTRAL AXIS Y = 8.86" FROM TOP OF SLAB

SYSTEM
COMPONENT
checked 2/16/82
JOB NO. 9316 DATE 2/9/82
DESIGNER

RIB MAT DESIGN (CONT.)

CHECK SOIL PRESSURE UNDER BEAM

SLAB	$300' \times 225' \times .67' \times .15 = 6784^k$	
BEAM	$9325' \times 2.33' \times 1.25' \times .15 = 4074$	
LESS	$300 \times 1.25 \times 1.25 \times 2.33 \times .15 = (164)$	
PERIMETER LOAD (3 SIDES)	$750 \times 736 = 552$	
LIVE LOAD	$225 \times 300 \times 75 = 5063$	
MISC. PARTITION LOAD ETC.	$= 191$	16500^k

TOTAL BEAM AREA $= 9325 \times 1.25 - 300 \times 1.25 \times 1.25$
$= 11188 \square'$

SOIL PRESSURE $= \frac{16500}{11188} = 1.47$ KSF < 2 KSF

TRIAL SECTION ASSUME $\beta = 15'$

a) CENTER LIFT $6\beta = 90'$

LONG DIRECTION

$\frac{\Delta}{90} = \frac{1}{360}$ $\Delta = 3''$

$$X = \frac{(\gamma_m L)^{.205} (S)^{1.059} (P)^{.523} (\rho_w)^{1.296}}{380\,\Delta} \quad (3a)^*$$

$$= \frac{(1.5 \times 300)^{.205} (12.5)^{1.059} (736)^{.523} (5)^{1.296}}{380 \times 3} = 11.32$$

$$d = X^{.824} = 11.32^{(.824)} = 7.39 \text{ IN} \quad (3c)$$

SHORT DIRECTION

$$X = \frac{(1.5 \times 225)^{.205} (12.5)^{1.059} (736)^{.523} (5)^{1.296}}{380 \times 3}$$

$$= 10.67$$

$$d = 10.67^{(.824)} = 7.04 \text{ IN}$$

* EQ. NUMBER IN PTI REFERENCE

SYSTEM

COMPONENT

Checked 2/16/82

JOB NO. 9311 DATE 2/9/82

DESIGNER

RIB MAT DESIGN (CONT.)

TRIAL SECTION (CONT.)

b) EDGE LIFT

LONG DIRECTION

$\frac{\Delta}{\ell_0} = \frac{1}{1700} \Rightarrow \Delta = .635$

$$X = \frac{(L)^{.35}(S)^{.88}(e_m)^{.74}(y_m)^{.76}}{12\,\Delta\,(\rho)^{.01}} \qquad (4a)$$

$$= \frac{(300)^{.35}(12.5)^{.88}(8)^{.74}(1.5)^{.76}}{12 \times .635\,(736)^{.01}}$$

$= 52.94$

$d = 52.94^{1.176}$

$= 106.5'' \cong 8.87'$ TOO DEEP.

SHORT DIRECTION

$$X = \frac{(225)^{.35}(12.5)^{.88}(8)^{.74}(1.5)^{.76}}{12 \times .635\,(736)^{.01}}$$

$= 47.87$

$d = 47.87^{1.176}$

$= 94.5 \cong 7.88'$ TOO DEEP

TRY 36" DP. x 15" WIDE BM

SYSTEM

COMPONENT

checked ~~STD~~ 2/16/82

JOB NO. 9316 DATE 2/9/82

DESIGNER Sean Fan

RIE MAT DESIGN (CONT.)

CENTER LIFT DESIGN

$M_\ell = A_o[B(e_m)^{1.238} + C]$ (13)

$B = (Y_m - 1)/3 = .17$

$C = [8 - (\frac{P-613}{255})][\frac{4 - Y_m}{3}]$ (15)

$= [8 - (\frac{736-613}{255})][\frac{4-1.5}{3}] = 6.26$

$A_o = \frac{1}{727}[(L)^{.013}(S)^{.306}(d)^{.688}(P)^{.534}(Y_m)^{.193}]$

$= \frac{1}{727}[(300)^{.013}(12.5)^{.306}(36)^{.688}(736)^{.534}(1.5)^{.193}]$

$= 1.39$

$M_\ell = 1.39[.17(5)^{1.238} + 6.26] = 10.43^{1k}/FT.$ ←

$M_s = [\frac{58 + e_m}{60}] M_\ell$ (16)

$= [\frac{58+5}{60}] 10.43^{1k} = 10.95^{1k}/FT.$ ←

$\Delta_o = [\frac{(Y_m L)^{.205}(S)^{1.059}(P)^{.523}(e_m)^{1.296}}{380\ (d)^{1.214}}]$ (27)

= EXPECTED DIFFERENTIAL DEFLECTION

$\Delta_{oL} = [\frac{(1.5 \times 300)^{.205}(12.5)^{1.059}(736)^{.523}(5)^{1.296}}{380\ (36)^{1.214}}] = .44''$ ←

$\Delta_{oS} = .44'' \times (\frac{225}{300})^{.205} = .41''$ ←

$\beta_s = \frac{1}{12}\sqrt[4]{\frac{1.5 \times 10^6 \times 3332669}{4 \times 300 \times 12}} = 11.37$

$\Delta_{S\,ALLOW.} = \frac{12 \times 6 \times 11.37}{360} = 2.27'' > .41''$ ←

SYSTEM

COMPONENT

checked 2/16/82

JOB NO. 9311 DATE 2/9/82

DESIGNER

FSEC FACILITIES SYSTEMS ENGINEERING CORPORATION
LOS ANGELES, CA. RICHLAND, WA DUBLIN, IRELAND

RIB MAT DESIGN (CONT.)

CENTER LIFT DESIGN

$$\beta L = \frac{1}{12}\sqrt[4]{\frac{1.5\times10^6\times2524567}{225\times12\times4}} = 11.4$$

$$\Delta L_{ALLOW} = \frac{12\times6\times11.4}{360} = 2.28'' > .44'' \leftarrow$$

$$V_s = \frac{1}{1350}\left[(L)^{.19}(S)^{.45}(d)^{.20}(P)^{.54}(y_m)^{.04}(e_m)^{.97}\right] \quad (31)$$

$$= \frac{1}{1350}\left[(225)^{.19}(12.5)^{.45}(36)^{.20}(736)^{.54}(1.5)^{.04}(5)^{.97}\right]$$

$$= 2.26 \text{ K/FT.}$$

$$v_s = \frac{2.26\times300\times1000}{25\times15\times36} = 50.2 \text{ PSI} \leftarrow$$

$$V_\ell = \frac{1}{1940}\left[(L)^{.09}(S)^{.71}(d)^{.43}(P)^{.44}(y_m)^{.16}(e_m)^{.93}\right] \quad (32)$$

$$= \frac{1}{1940}\left[(300)^{.09}(12.5)^{.71}(36)^{.43}(736)^{.44}(1.5)^{.16}(5)^{.93}\right]$$

$$= 2.10 \text{ K/FT.}$$

$$v_\ell = \frac{2.1\times225\times1000}{19\times15\times36} = 46.1 \text{ PSI} \leftarrow$$

EDGE LIFT DESIGN

$$M_\ell = \left[\frac{(S)^{.10}(d e_m)^{.78}(y_m)^{.66}}{7.2(L)^{.0065}(P)^{.04}}\right] \quad (17)$$

$$= \left[\frac{(12.5)^{.10}(36\times8)^{.78}(1.5)^{.66}}{7.2(300)^{.0065}(736)^{.04}}\right] = 14.32 \text{ K/FT.} \leftarrow$$

$$M_s = (d)^{.35}\left[\frac{19+e_m}{57.75}\right]M_\ell \quad (18)$$

$$= (36)^{.35}\left[\frac{19+8}{57.75}\right]14.32 = 23.47 \text{ K/FT.} \leftarrow$$

SYSTEM

COMPONENT

Checked 2/16/82

JOB NO. 9315 DATE 2/9/82

DESIGNER

RIB MAT DESIGN (CONT.)

EDGE LIFT DESIGN (CONT.)

$$\Delta_o = \left[\frac{(L)^{.35}(S)^{.88}(e_m)^{.74}(y_m)^{.76}}{15.9\,(d)^{.85}\,(p)^{.01}}\right] \quad (28)$$

$$\Delta_{oL} = \left[\frac{(300)^{.35}(12.5)^{.88}(8)^{.74}(1.5)^{.76}}{15.9\,(36)^{.85}\,(736)^{.01}}\right]$$

$$= 1.21'' \leftarrow$$

$$\Delta_{oS} = 1.21'' \times \left(\frac{225}{300}\right)^{.35} = 1.1'' \leftarrow$$

$\beta_S = 11.37'$ $\beta_L = 11.4'$

$$\Delta_{L\,ALLOW} = \frac{12 \times 6 \times 11.4}{800} = 1.03 < 1.21 \leftarrow$$

$$\Delta_{S\,ALLOW.} = \frac{12 \times 6 \times 11.37}{800} = 1.02 < 1.1 \leftarrow$$

$$V = \left[\frac{(L)^{.07}(d)^{.40}(p)^{.03}(e_m)^{.16}(y_m)^{.67}}{3.0\,(S)^{.015}}\right] \quad (33)$$

$$V_L = \left[\frac{(300)^{.07}(36)^{.40}(736)^{.03}(8)^{.16}(1.5)^{.67}}{3.0\,(12.5)^{.015}}\right] = 4.45^{K/'}$$

$$v_L = \frac{4.45 \times 225 \times 1000}{19 \times 15 \times 36} = 97.6 \text{ psi} \leftarrow$$

$$V_S = 4.45^{K/'} \times \left(\frac{225}{300}\right)^{.07} = 4.36^{K/'}$$

$$v_S = \frac{4.36 \times 1000 \times 300}{25 \times 15 \times 36} = 96.9 \text{ psi} \leftarrow$$

SHEAR @ EDGE OF BEAM = 82.4 psi

$\cong 1.5\sqrt{3000} = 82.2$ psi

= SHEAR STRESS ALLOWED.

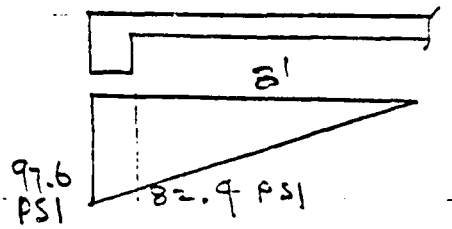

SYSTEM

COMPONENT

checked 2/16/82

JOB NO. 9316 DATE 2/9/82

DESIGNER

SLAB & BEAM REINFORCEMENT DESIGN

SLAB REINF.

$A_s = .002 \times 12'' \times 8'' = .192 \ \square''/\text{FT. OF SLAB}$

USE #4 @ 12" O.C. EW. ←

BOTT. BM REINF. EDGE UFT

$M = 23.47^{\text{IK}}$ $\quad f_c = \frac{2}{3} \times 3000 = 2000 \text{ PSI}$ $\quad f_s = \frac{2}{3} \times 60{,}000 = 40{,}000 \text{ PSI}$ } PER AEIM MANUAL CHAP. VI

TREAT SLAB & BM AS A T-BEAM

BEAM FLANGE

$8'' \times 8'' = 64''$

$\times 2 = 128'' + 1'\text{-}3''$

$= 11'\text{-}11''$

SAY 12'-6" TO MATCH BEAM SPACING.

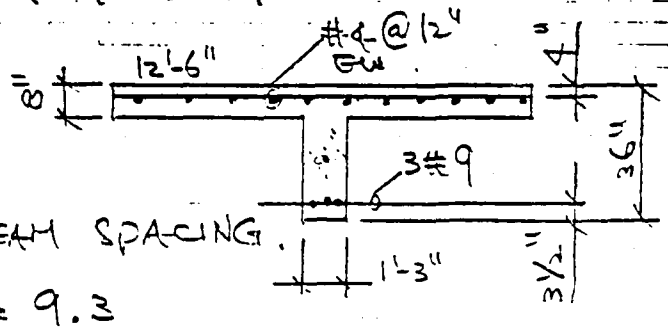

$n = \frac{E_s}{E_c} = \frac{29000{,}000}{57000\sqrt{3000}} = 9.3$

TRY 3 #9 BOTT. STL.

$nA_s = 9.3(3 \times 1.0) = 27.9 \ \square''$

$nA'_s = 2 \times 9.3(12.5 \times .2) = 23.3 \ \square''$

ASSUME N.A. IS WITHIN 8" SLAB

$\frac{(12.5 \times 12)(32.5k)^2}{2} - 23.3(4 - 32.5k) = 27.9(1-k)32.5$

$79218.8k^2 + 1664k - 999.95 = 0 \Rightarrow k = .1024$

$kd = 3.33'' < 8'' \qquad j = 1 - k/3 = .966$

$f_s = \frac{M}{A_s jd} = \frac{23.47 \times 12 \times 12.5}{3 \times .966 \times 32.5} = 37.4 \text{ KSI} < 40 \text{ KSI}$

$f_c = \frac{2M}{kjbd^2} = \frac{2 \times 23.47 \times 12 \times 12.5}{(.1024)(.966)(150)(32.5)^2}$

$= .449 \text{ KSI} < \frac{2}{3} f'_c = 2000 \text{ KSI}$

USE 3#9 @ BOTT. ←

SYSTEM

COMPONENT

checked 2/16/82

JOB NO. 9316 DATE 2/11/82

DESIGNER

SLAB & BEAM REINFORCEMENT DESIGN (CONT.)

TOP BM REINF. CENTER UPT

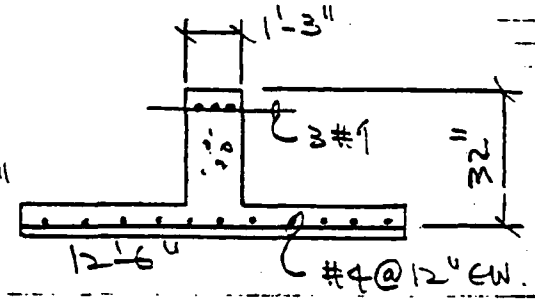

$M = 10.95^{1K}$

$kA_s = 9.3(12.5 \times .2) = 23.25 \square''$

$2kA'_s = 2 \times 9.3 \times (3 \times 1.0) = 55.8 \square''$

$$\frac{15(32k)^2}{2} + 55.8(32k - 3.5) = 23.25(1-k)32$$

$7680k^2 + 2529.6k - 939.3 = 0$

$k = .221 \qquad kd = 7.07''$

$j = 1 - k/3 = 1 - \frac{.221}{3} = .926$

$$f_s = \frac{10.95 \times 12 \times 12.5}{(12.5 \times .2)(.926 \times 32)} = 22.2 \text{ KSI} < 40 \text{ KSI}$$

$$f_c = \frac{2M}{kjbd^2} = \frac{2 \times 10.95 \times 12 \times 12.5}{(.221)(.926)(15)(32)^2}$$

$= 1.045 \text{ KSI} < 2000 \text{ PSI}$ O.K.

USE #4 @ 12" O.C. EW ←

INTERIOR BLDG. SLAB

BEAM SPACING IS 25' WHICH IS TOO WIDE TO ALLOW T-BEAM ACTION. ∴ TREAT SLAB AS BEAM. FROM CHART SHOWN ON PG. F-12, SLAB MOMENT DECREASES TOWARDS CENTER OF SLAB. ASSUME 2^K M.

$$A_s = \frac{2 \times 12}{40 \times 4 \times .87} = .17 < \#4 @ 12'' \text{ EW} \quad \text{O.K.}$$

$$f_c = \frac{2 \times 2 \times 12}{(.39)(.37)(12)(4)^2} = .737 \text{ KSI} < 2 \text{ KSI} \quad \text{O.K.}$$

USE #4 @ 12" O.C. EW. ←

SYSTEM

COMPONENT

checked 2/16/82

JOB NO. 9316 DATE 2/11/82

DESIGNER

RI-AD BLDG. 333 F-12

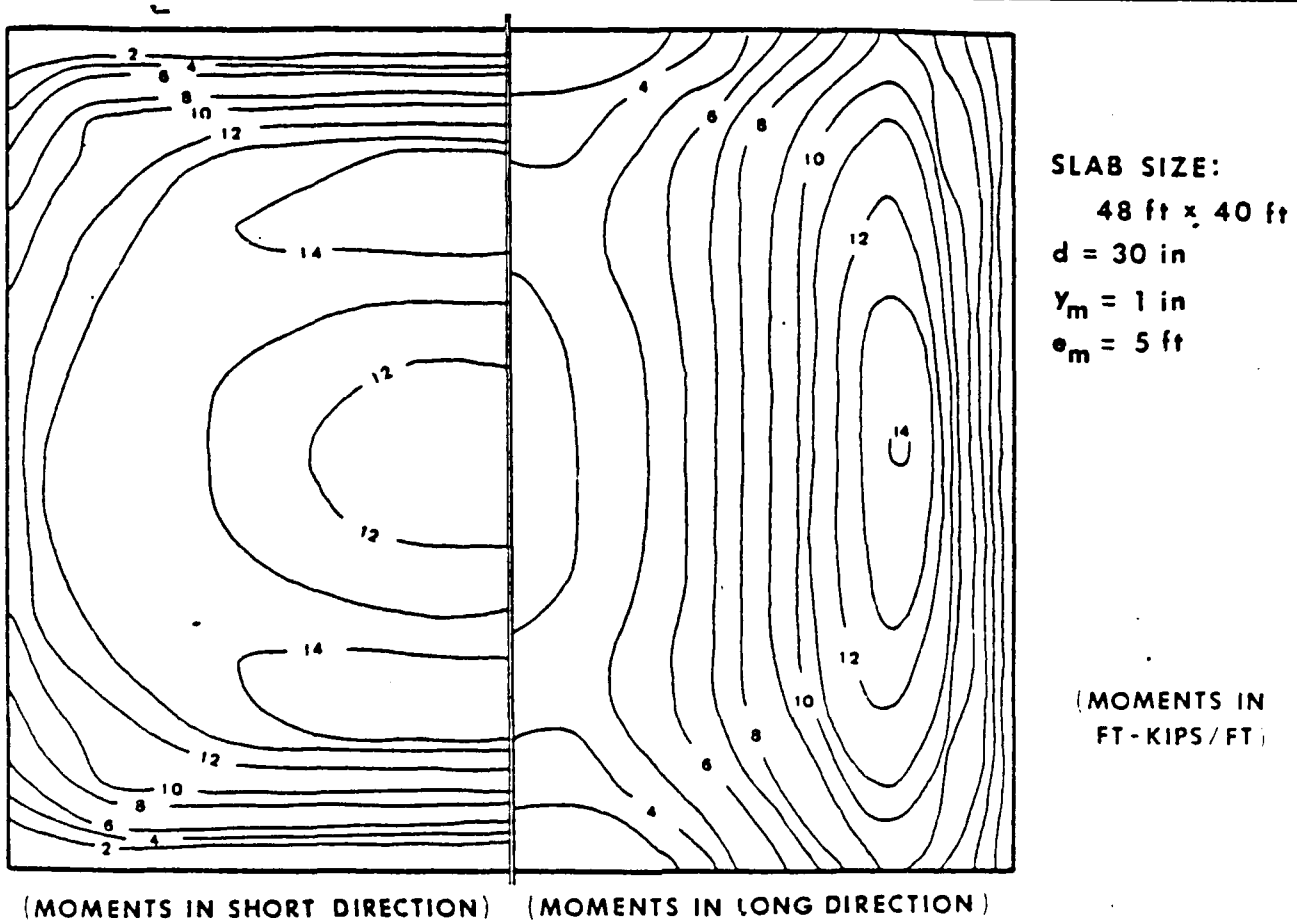

Fig. 5.2 Typical distribution of center lift bending moment over surface of slab (108)

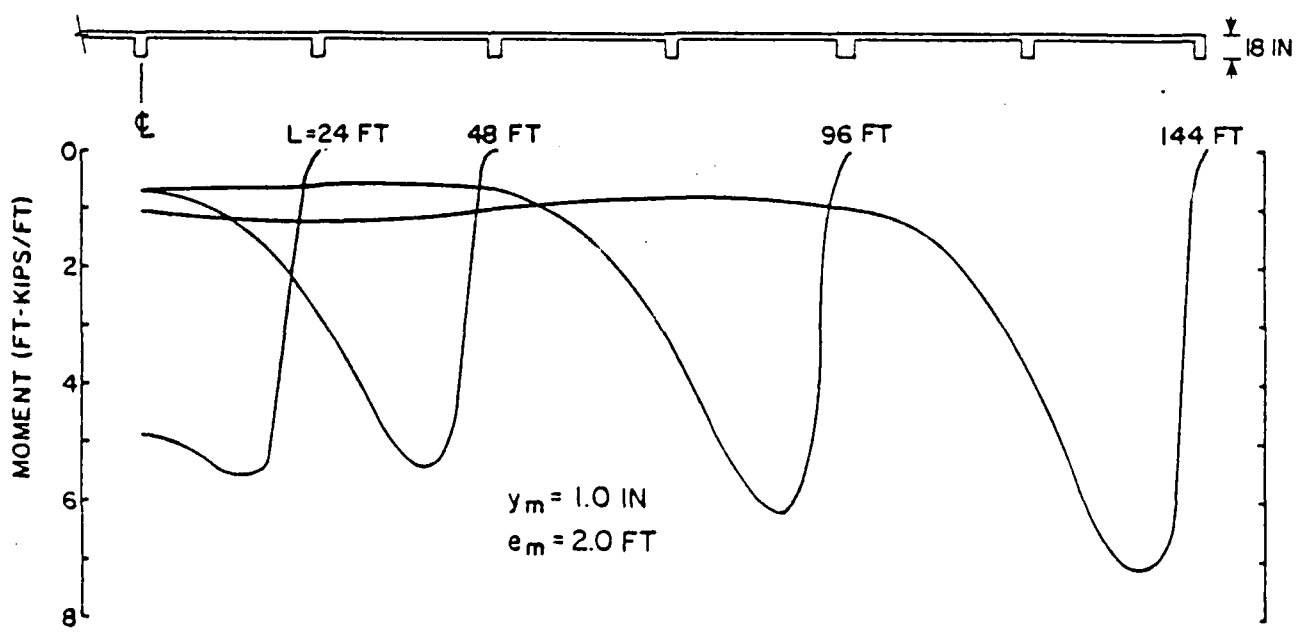

Fig. 5.3 Typical variation of moment along the longitudinal axis as slab length increases (108)

FOOTING DESIGN

FOOTING IS SUBJECTED TO BOTH VERTICAL LOAD & MOMENT. (EXCEPT @ WIND COLUMN WHERE NO MOMENT EXIST) HOWEVER, SINCE ALL FOOTINGS ARE INTEGRAL/MONOLITHIC W/ SLAB AND OVERTURNING IS RESISTED BY TIE BEAMS, THEREFORE, IGNORE MOMENT IN FOOTING DESIGN. WIDEN BEAM INTERSECTIONS @ COLUMN LOCATIONS TO FORM DIAMOND SHAPED FOOTING TO TAKE VERTICAL COLUMN LOADS.

EXTERIOR COLUMN

FROM COLUMN CALC., $P = 129.4^K$

SINCE LOAD INCLUDE TEMPORARY LOADS SUCH AS SNOW LOAD, CRANE LOAD OR ROOF LIVE LOAD, USE ONLY 75% OF 'P' FOR SIZING FOOTING

$$129.4 \times .75 = 97^K$$

$$\text{AREA NEEDED} = \frac{97^K}{2 - .45} = 62.6\ \square'$$

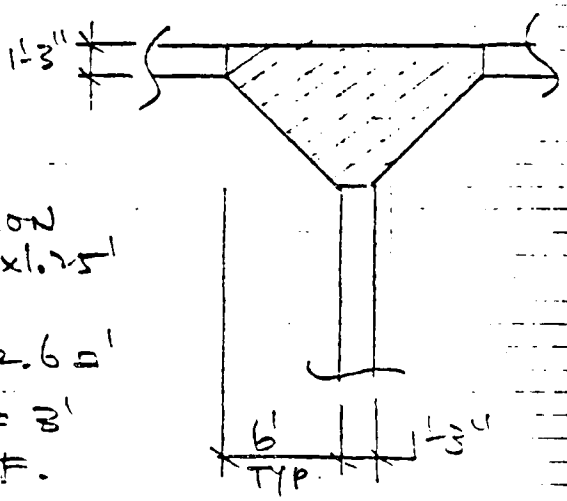

AREA PROVIDED = SHADED PORTION

$= 6' \times 6' + 13.25' \times 1.25' + 6 \times 1.25'$

$= 60.1\ \square' \cong 62.6\ \square'$

SINCE DEPTH OF FOOTING = 3'

∴ PROVIDE NOMINAL REINF. @ BOTT.

USE #5 @ 12" O.C. EW. ←

SYSTEM

COMPONENT

Checked 2/16/82

JOB NO. DATE 2/9/82

DESIGNER

FOOTING DESIGN (CONT.)

EXTERIOR CORNER COL. & EXT. COL. @ EXP. JT.

$P = 63.7^k \times .75 = \frac{47^k}{1.55\ KSF} = 30.3\ \square'$

AREA PROVIDED $= \frac{6 \times 6}{2} + 7.25 \times 1.25 + 6 \times 1.25 = 34.6\ \square' > 30.3\ \square'$ o.k.

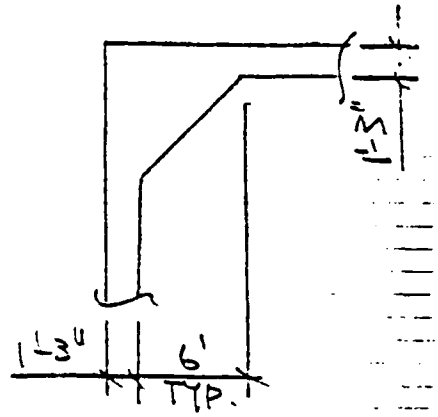

TYP. INTERIOR COL.

$P = 219.2^k \times .75 = \frac{164.4^k}{1.55\ KSF} = 106.1$

AREA PROVIDED $= 6 \times 6 \times 2 + 13.25 \times 1.25 + 12 \times 1.25 = 103.6 \cong 106.1\ \square'$ o.k.

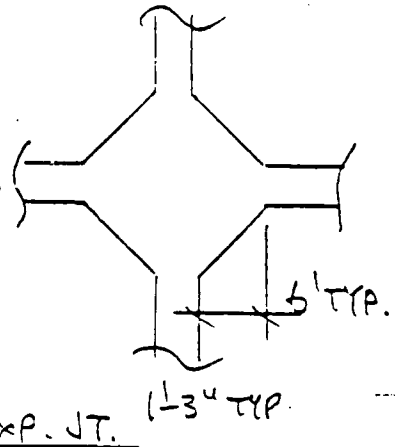

TYP. END WALL COL. & INT. COL. @ EXP. JT.

$P = 109.6^k \times .75 = \frac{82.2}{1.55} = 53\ \square'$

AREA PROVIDED $= 6' \times 6' + 13.25' \times 1.25' + 6' \times 1.25' = 60\ \square' > 53\ \square'$ o.k.

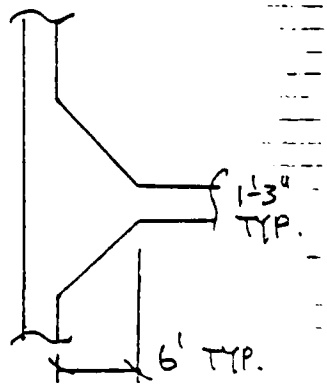

SYSTEM

COMPONENT

checked 2/16/82

JOB NO. 9316 DATE 2/9/82

DESIGNER

Summary

FOUNDATION DESIGN ANALYSIS
RED RIVER ARMY DEPOT MAINTENANCE MODERNIZATION

The following summarizes the foundations report prepared March 1981 by the Foundations and Materials Branch, U. S. Army Engineer District Fort Worth. The original report and additional reference material including boring logs, locations of boring logs and soil samples, and results of laboratory soil tests may be obtained from this district office.

General

1. This project will provide an efficient modernized maintenance facility for the overhaul and dieselization of the light track family of vehicles. The project will consist of three buildings, a Light Track Vehicle Shop (Building 333), a Material Staging and Control Facility (Building 312) and a Heat Treating Facility (Building 328). The Light Track Vehicle Shop Building will be approximately 197,610 square feet in area, Material Staging and Control Facility will be approximately 125,000 square feet, and the Heat Treating Facility will be approximately 500 square feet. At this stage of planning, all structures are thought to be steel frame structures with concrete masonry unit walls.

2. The proposed site is located on the eastern edge of the Red River Army Depot in an area bounded by Texas Avenue on the north, Avenue K on the east, Eigth Street on the south and Avenue G on the west. The site is generlly level; however, some drainage ditches are in the area.

Subsurface Investigations

3. During April and May 1979, 22 borings were drilled in the areas of the three proposed structures. These borings were drilled to determine the subsurface conditions and to obtain samples for testing. Samples of the subsurface materials were obtained with an 8-inch earth auger, a 6-inch Denlison barrel sampler and a 6-inch core barrel sampler. Samples recovered from the borings were sealed in airtight containers and shipped to the laboratories for testing.

4. General Geology. Red River Army Depot lies in the north central portion of Bowie County, Texas, and is situated within the West Gulf Coastal Plains physiographic province. This area is characterized by very gentle topography. The region is underlain by sedimentary deposits of Tertiary Age.

The primary geologic strata are assigned to the Midway and Wilcox groups and dip to the south at a rate slightly steeper than the change in surface elevation. The Midway group has a thickness of approximately 400 feet and consists chiefly of clay shale. The Wilcox is predominantly sandy and silty clay shale. These primary strata are generally masked by a thin soil stratum, consisting of both residual and transported materials. Overburden generally consists of silts and clays with varying amounts of sand.

5. Site Conditions. Boring logs revealed that much of the area has been covered with earth fill materials. The fill materials range in thickness up to approximately 8 feet, and when classified consists of medium to high plasticity clays (CL and CH), clayey sands (SC), clayey sandy gravels (GC), sandy silty clays (ML-CL) and silty sands (SM). Some organic materials are contained within the fill material. In three of the borings, natural overburden soils were encountered at ground surface. From ground surface to depths of 2 to 3 feet below existing ground surface, the natural overburden soils are medium to high plasticity clays (CL and CH). Underlying the top 2 to 3 feet of overburden soils and the fill materials is a medium to high plasticity clay (CL and CH). Thickness of the fill materials and the overburden soils range from 5.1 to 13.0 feet.

6. The primary geologic formation encountered beneath the overburden soils consist of a clay shale tentatively identified as a portion of the Midway group of the Tertiary system. The clay shale is soft (rock classification) and ranges from highly weathered (altered to a clay consistency) immediately beneath the overburden-primary contact to weathered at depths 3 to 4 feet below the overburden-primary contact. The clay shale extended to the total depth investigated, 30 feet below existing ground surface.

7. All borings were allowed to stand open overnight to allow ground water levels to stabilize. Water levels at the time of drilling ranged from 2.8 to 19.5 feet below grade. Average depth to ground water was about 9.5 feet. Based on previous experience in the general area, it is believed that the water table is a perched water table associated with the lower overburden soils.

8. Laboratory Testing. Identification, moisture content, density, unconfined compression, one-point triaxial compression and controlled expansion-consolidation tests were performed on samples of subsurface materials. The compressive strength of the subsurface materials from results of unconfined compression tests and one-point triaxial compression tests ranged from 2.6 to 10.4 ksf. Expansion-consolidation test results from method C of ASTM D 4546 indicate expansive pressures from 0.50 to 2.0 ksf in excess of the overburden pressure, with deeper materials having the larger expansive pressures.

Discussion

9. The proposed site is in an existing level plant area with little topographic relief (except for drainage ditches) across the site. A review of subsurface conditions and laboratory test data revealed three distinct potential founding strata: surface fill material, overburden clay, and primary clay shale. The fill material consists of a conglomerate of discontinuous layers and pockets of loosely compacted clays (CH and CL), sands (SC and SM), and clayey gravels (GC). This stratum does not express the strength to satisfactorily support the proposed structures. The clay overburden likewise does not possess the strength and consolidation characteristics to satisfactorily support the structures. The primary clay shale at a depth of approximately 24 feet below ground surface is capable of supporting the proposed structures. Footings bottomed at the above depth could be sized for an allowable bearing pressure of 10 ksf considering down load only. The disadvantage of using the clay shale as the founding medium is the potential heave of the clay overburden and shale on the pier shaft and heave of the clay shale beneath the footing base. It was computed that deep footings would move upward approximately 3 inches due to swelling of the subsurface materials. This amount of movement, either uniform or differential, is considered to be excessive for the type structure proposed. Assuming the foundation would experience 3 inches of differential movement, the angular distortion would be on the order of 1 to 100, a limit where structural damage would occur.

10. Based on the above engineering studies, it was concluded that the existing soils (overburden and primary) are not satisfactory founding media. The alternatives are to improve the engineering characteristics of the

existing soils or to remove the unsuitable existing soils to a reasonable depth and replace with compacted nonexpansive material. Considering the characteristics of the fill material, in place improvement is considered to be excessively expensive. Removal of this material and replacement with compacted fill is the best solution to the problem. Removal and replacement with compacted fill would provide an excellent stratum on which to support a shallow foundation and on which to support floor slabs. The foundation for the proposed structures can then consist of a ribbed mat slab supported on the compacted nonexpansive fill material.

11. The removal and replacement of the existing fill material does not entirely eliminate the potential for heave at the subject site. The nonexpansive fill, by definition, will not heave. The underlying CH overburden and upper primary soils, however, will experience some volume change. It was determined that the mat slab could experience 1.5 inches vertical movement resulting from heaving of the overburden and upper primary soils. Based on an analysis of existing moisture conditions, it is believed that this amount of expansion could occur within an 8-foot radius. Consequently, the foundation floor system should be stiffened to the extent that the angular distortion of the structures does not exceed 0.0015L (L = distance between adjacent columns).

Recommendations

12. Based on field investigations, laboratory testing and engineering studies, it is recommended that the proposed Light Track Vehicle Shop (Building 333), Material staging and Control Facility (Building 312) and Heat Treating Facility (Building 328) be founded on a reinforced concrete ribbed mat slab. The mat slabs should consist of a monolithic floor slab and beams. The beams should bottom not less than 24 inches below outside finished grade and should be sized in such a manner that an allowable bearing capacity value of 2.0 ksf is not exceeded. Beams and beam intersections should be widened and reinforced at column locations to form footings which will distribute column loads along the beams and over an area such that the above allowable bearing capacity is not exceeded. The load used to size the beams should consist of full dead load plus that portion of the live load that reacts continuously, usually 50 percent.

13. To prepare the subgrade for the three proposed structures, all of existing fill material (approximately 5 feet) should be removed. The excavated materials should then be replaced with nonexpansive fill materials. Nonexpansive fill materials should have a plasticity index equal to or less than 12 and should be compacted to not less than 92 percent maximum density as determined bvy ASTM D 1557. Any additional fill material required to bring the floor slabs up to required grade should also be nonexpansive and compacted to the same density. A polyethylene vapor barrier and a 6-inch capillary water barrier should be placed beneath all floor slabs on grade. The ribbed mat slabs should be designed in accordance with the AEIM, Chapter VI, Structural. Using the PTI method of designing the mat slab, the following design parameters should be used: $q_a = 2.0$ ksf, $e_m = 8.0$ feet, $y_m = 1.5$ inches, and $\mu_s = 0.5$.

APPENDIX G

FIELD TESTS

TABLE OF CONTENTS

	Heading	Page
I.	PRESSUREMETER TESTS	G2
II.	CONE PENETRATION TESTS	G28
III.	PLATE BEARING TESTS	G39
IV.	PIEZOMETRIC DATA	G43
V.	ELEVATION DATA	G44
VI.	EARTH PRESSURE DATA	G47
VII.	STRAIN GAGE DATA	G47

I. PRESSUREMETER TESTS

Briaud Engineers
1805 Laura Lane
College Station, Texas 77840

Purpose and Scope

1. The geotechnical investigation reported herein was undertaken as part of a program to evaluate the settlement of a raft foundation to be constructed at the Red River Army Depot near Texarkana, Texas. In this report, the results of pressuremeter tests performed at the site, Figure G1, to a depth of 33.5 ft below the surface of the fill are presented. A total of 8 tests were performed on November 26, 1983. Also included is a method of estimating an equivalent modulus of deformation of the soil to be used in settlement analysis.

Authorization

2. This work was authorized by Purchase Order No. DACA39-84-M-0073, signed by William M. Landes and Mary S. Parrette on November 7, 1983.

Soil Conditions

3. The soil profile was obtained from the cuttings taken off the hand auger bucket and is shown in Figure G2. The location of the water table was not recorded during the test, but from previus studies it is expected to be 10 ft below ground surface.

Tests

4. The pressuremeter used at the site was a pressuremeter model TEXAM developed at Texas A&M University and sold commercially by Roctest, Inc.; this is a monocell pressuremeter inflated with water which allows to perform preboring or selfboring tests. The probe is 58 mm (2.28 in.) in diameter and has an initial deflated volume of 1050 cc (64.1 $in.^3$). A total of 8 tests were performed in addition to the two calibrations (volume losses and membrane resistance). A hand auger was used at the site and proved to provide a high quality borehole. The first hole drilled (BH 1) was terminated at 5 ft due to the presence of an unexpected concrete pipe. The second hole (BH 2) was

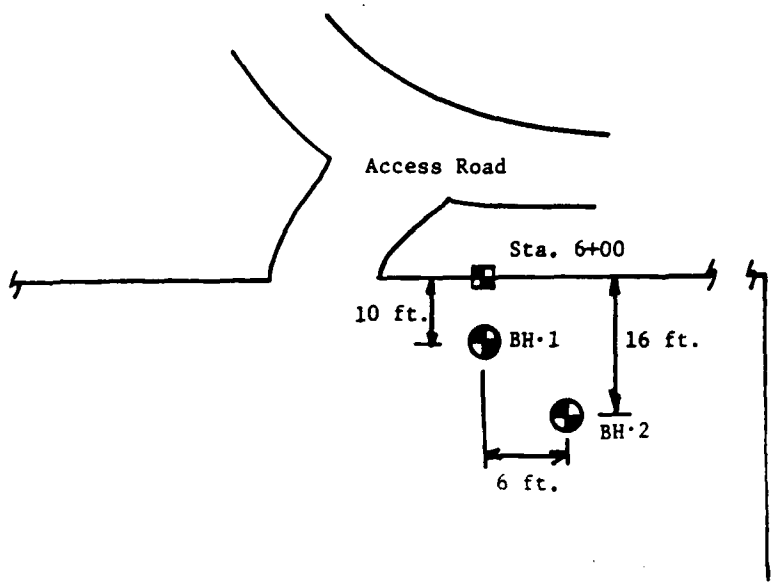

(a) Plan of Site

NOTE: Tests were performed from excavation level but are reported as of top of fill level.

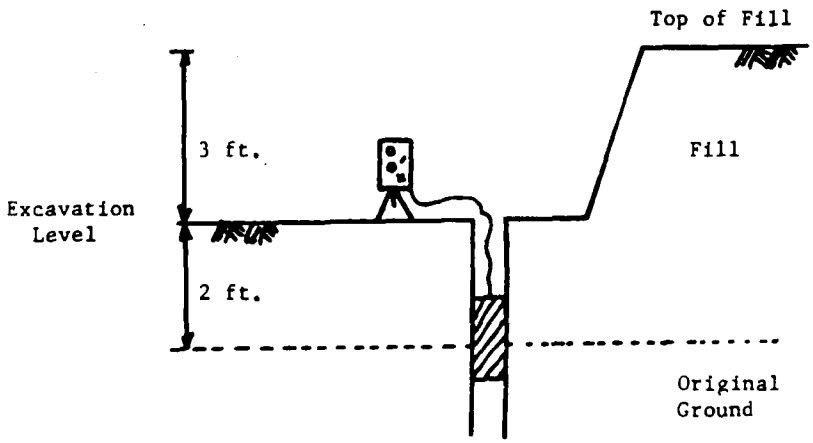

(b) Elevation

Figure G1. Site

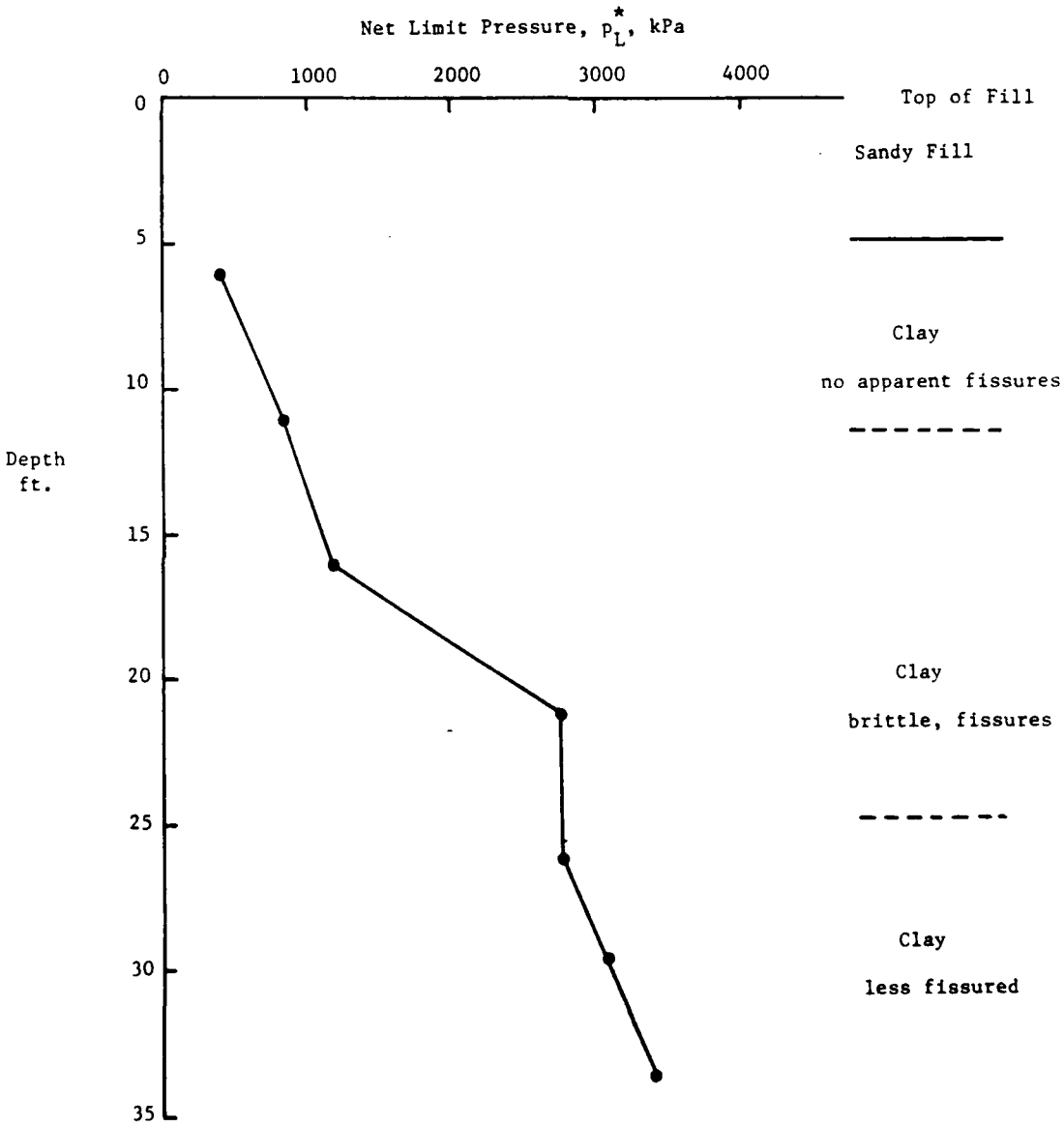

Figure G2. Soil classification and net limit pressure profile

drilled approximately 10 ft from BH•1 and was terminated at the desired depth. Figure G1 shows the location of the boreholes relative to Station 6+00, situated 5 ft away from the expected edge of the foundation.

5. The raw data obtained in the field was corrected for membrane resistance and volume losses in order to obtain the final corrected pressuremeter curves, shown in Figures G3 through G10 as P versus $\Delta R/R_o$ curves. For each test, a first loading modulus E_i, a reload modulus E_r and a net limit pressure p_l^* were calculated. The first loading modulus was obtained from the straight part of the pressuremeter (PMT) curve on the first loading; the reload modulus was obtained from the slope of the unload-reload cycle; the E moduli were calculated from shear G moduli assuming a Poisson's ratio of 0.33 in all cases. The limit pressure was obtained by manual extension of the curve. The results are tabulated, Table G1, and illustrated on Figures G2, G11 and G12.

Coefficient of Earth Pressure at Rest

6. To obtain the total horizontal pressure at rest, P_{OH}, the initial part of the curves, Figures G3 through G10, were plotted as P versus log ($\Delta R/R_o$) to accentuate the curvature. A graphical procedure (similar to the calculation of the preconsolidation pressure P_c (Casagrande 1936)* is used to obtain P_{OH}. This new method is based on the definite analogy between P_c and the consolidation test on one hand and P_{OH} and the preboring pressuremeter test on the other hand (Briaud, Tucker, Felio 1983)*. This calculation for each test is presented in Figures G13 through G17. For some tests, the determination of P_{OH} is impossible and P_{OH} had to be estimated from the other tests. To calculate the coefficient of horizontal pressure at rest, K_o, an evaluation of the vertical stress and pore water pressure is required. The total vertical stress was computed by assuming a total unit weight of 18 kN/m^3 and the pore pressure at the test level was taken as the hydrostatic pressure. The values of the coefficient of earth pressure at rest K_o are given on Table G1. Figure G18 illustrates the P_{OH} profile and Figure G19 shows the K_o profile at the site.

---

*Refer to references at the end of this section, I. PRESSUREMETER TESTS

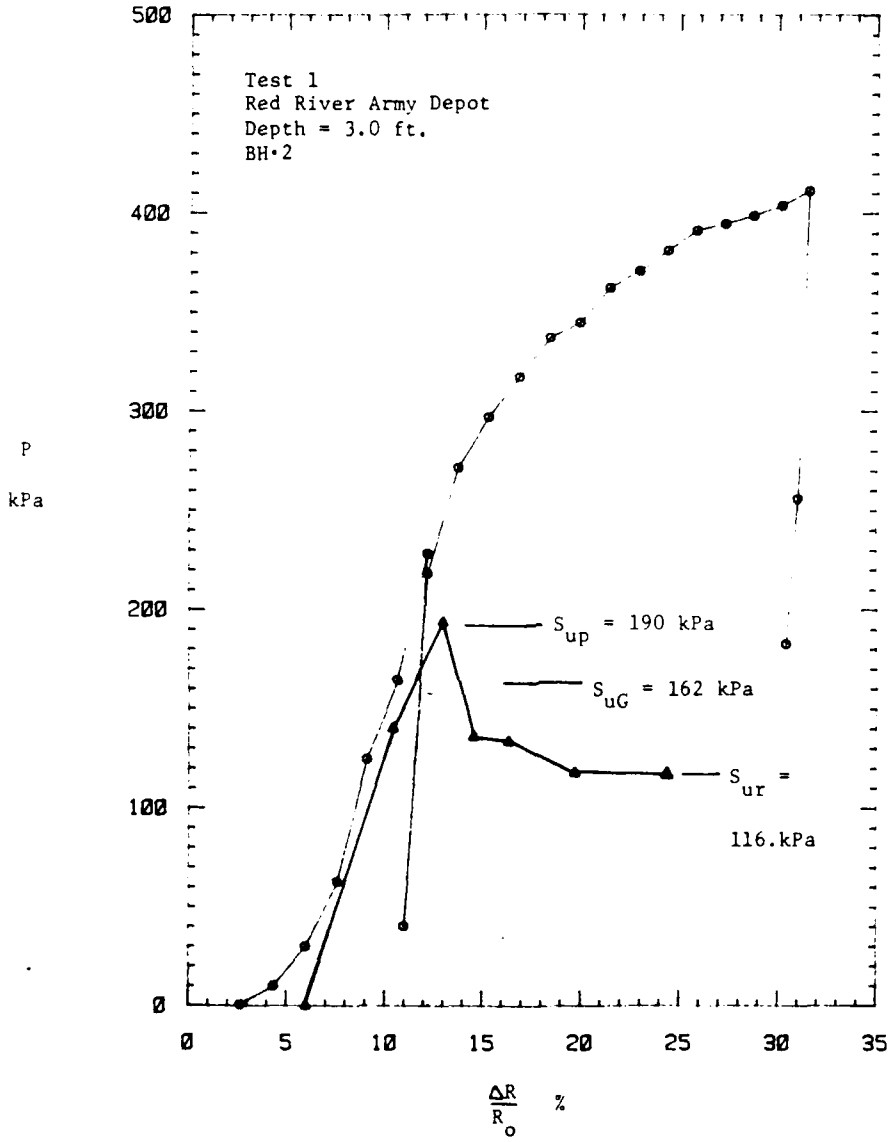

P_1 = 420 kPa

P_{OH} = 18 kPa

E_i = 4943 kPa

E_r = 22469 kPa

Figure G3. Pressuremeter curve for Test 1, depth = 3.0 ft, for hole BH 2

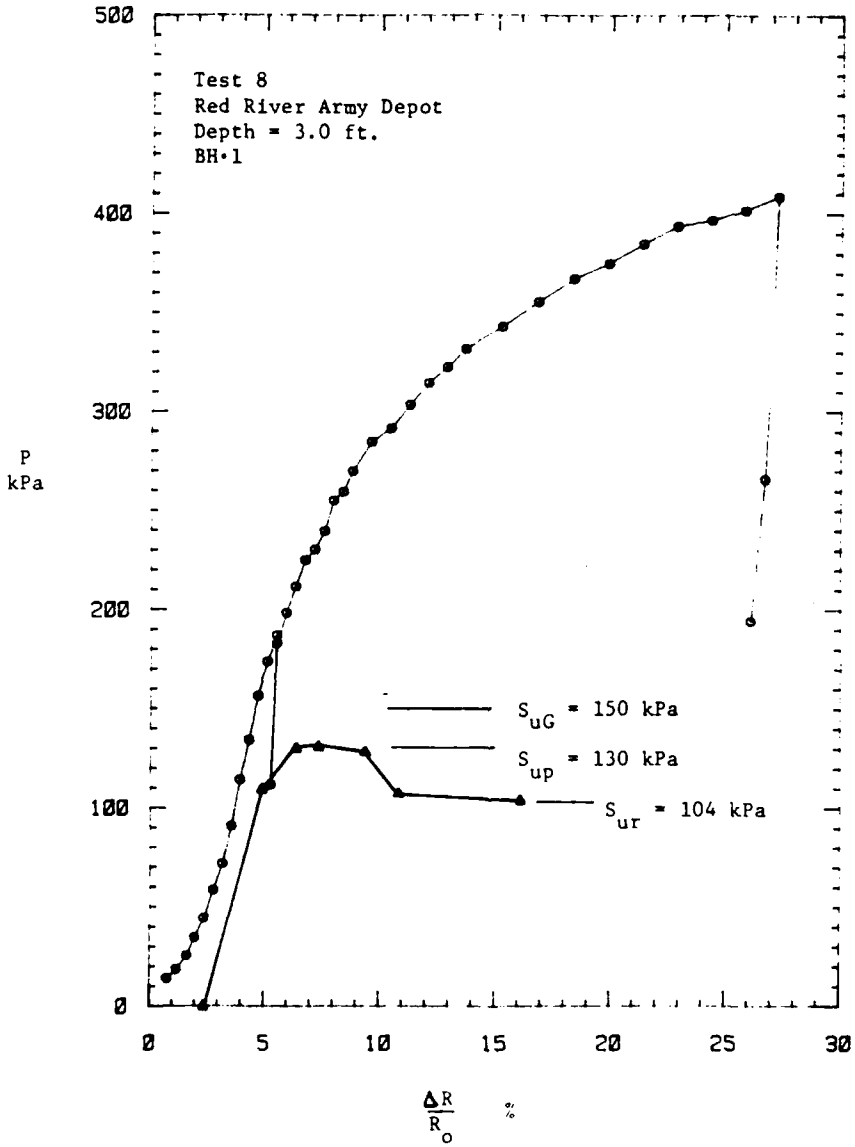

P_1 = 410 kPa

P_{OH} = 28 kPa

E_i = 7684 kPa

E_r = 38866 kPa

Figure G4. Pressuremeter curve for Test 8, depth = 3.0 ft, for hole BH•1

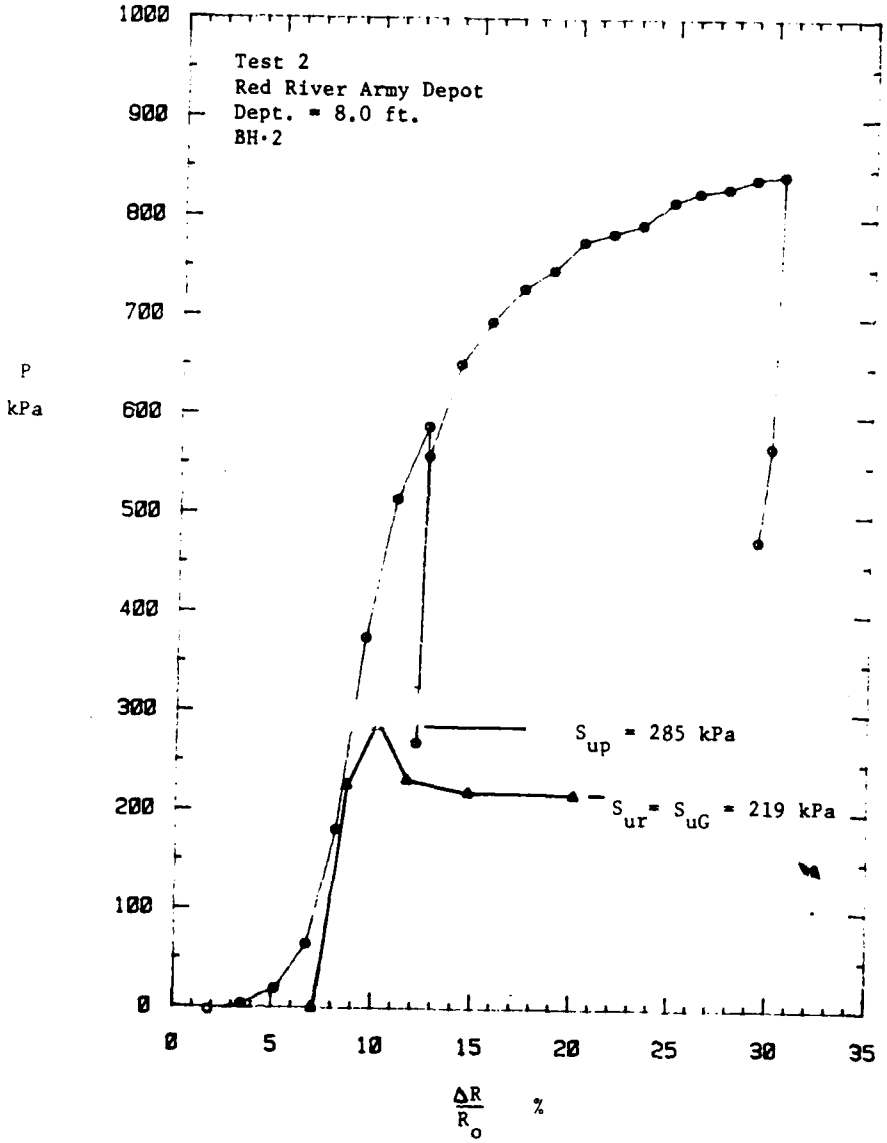

P_L = 850 kPa

P_{OH} = 40 kPa

E_i = 16747 kPa

E_r = 106875 kPa

Figure G5. Pressuremeter curve for Test 2, depth = 8.0 ft, for hole BH 2

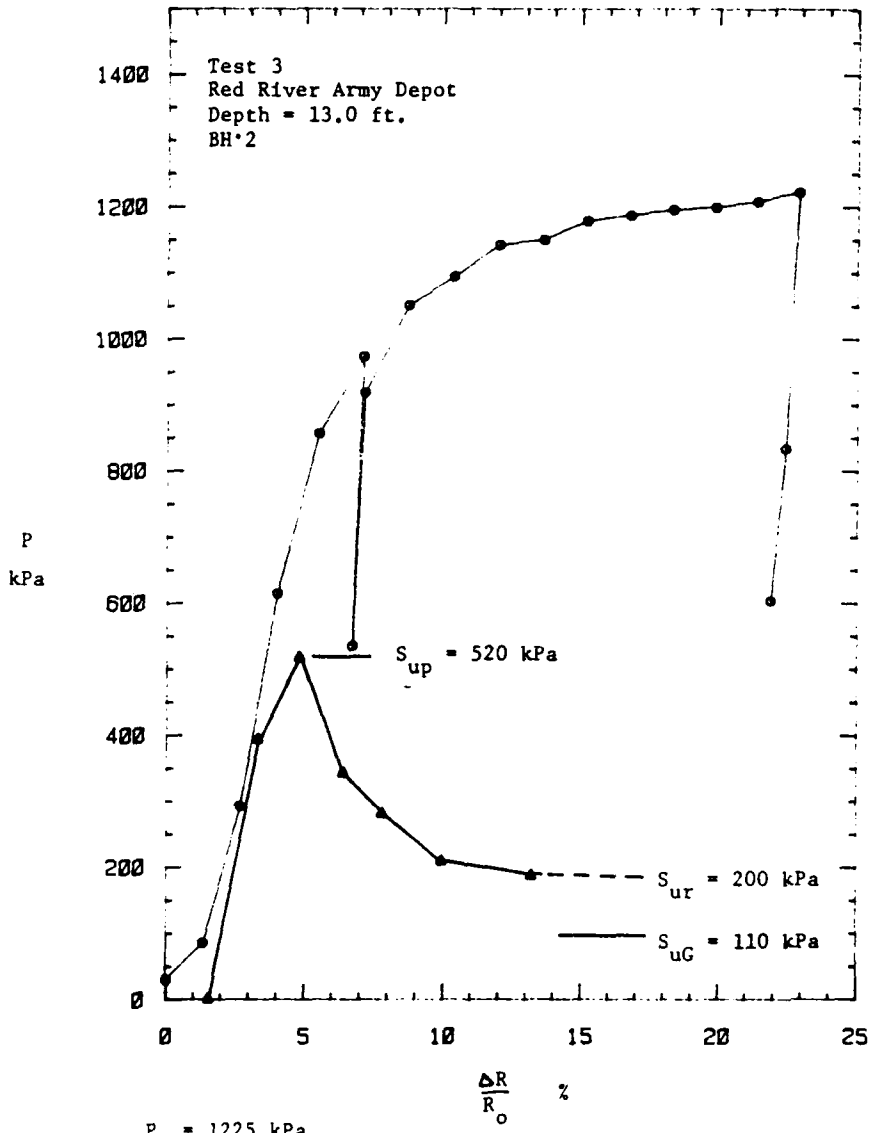

P_L = 1225 kPa

P_{OH} = 60 kPa

E_i = 28092 kPa

E_r = 112350 kPa

Figure G6. Pressuremeter curve for Test 3, depth = 13.0 ft, for hole BH 2

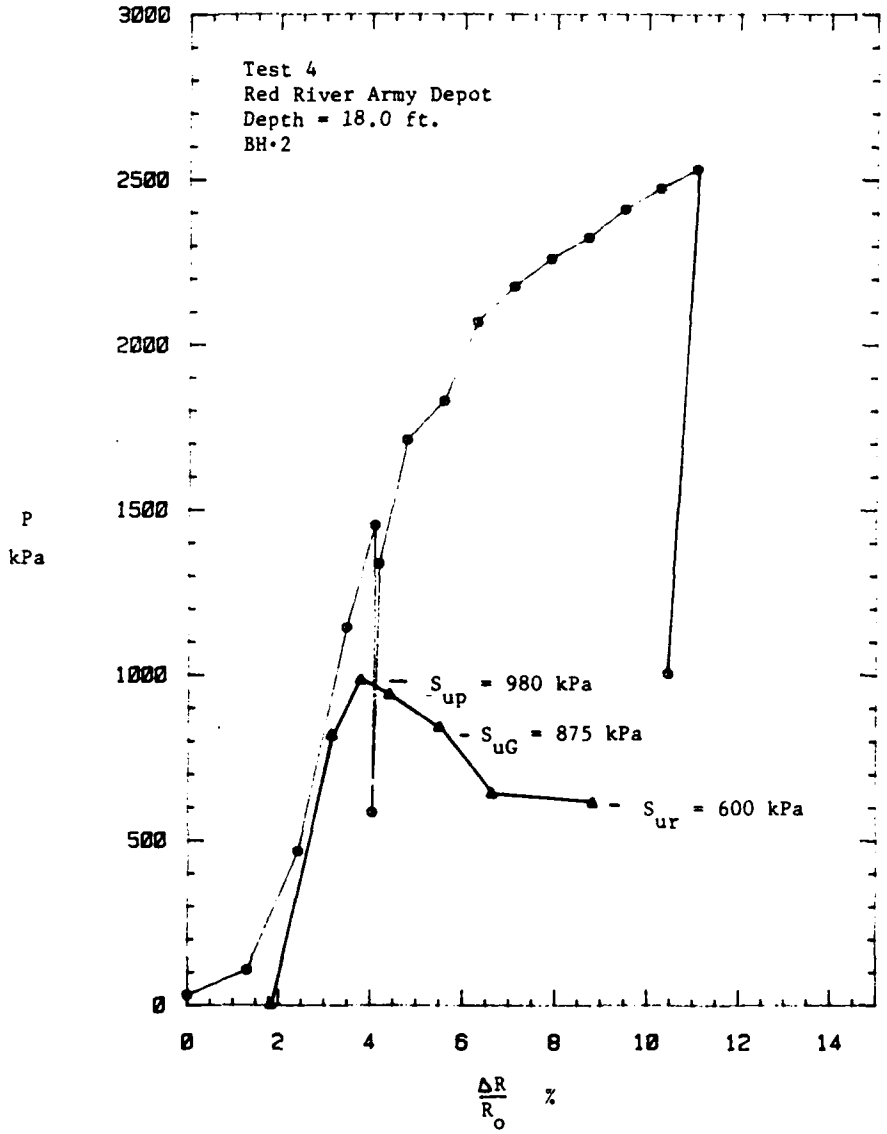

P_L = 2810 kPa

P_{OH} = 110 kPa

E_i = 88381 kPa

E_r = 518700 kPa

Figure G7. Pressuremeter curve for Test 4, depth = 18.0 ft, for hole BH 2

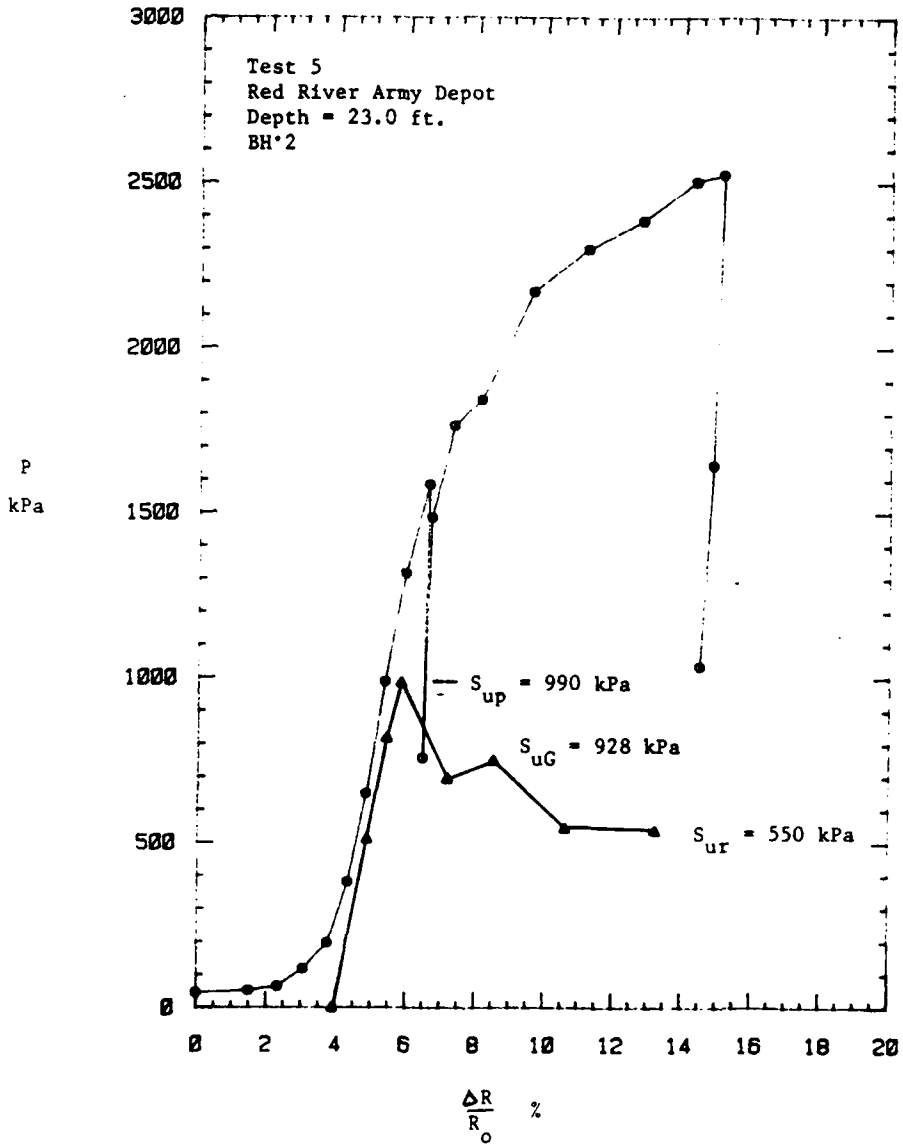

P_L = 2850 kPa

P_{OH} = 90 kPa

E_i = 82225 kPa

E_r = 327180 kPa

Figure G8. Pressuremeter curve for Test 5, depth = 23.0 ft, for hole BH 2

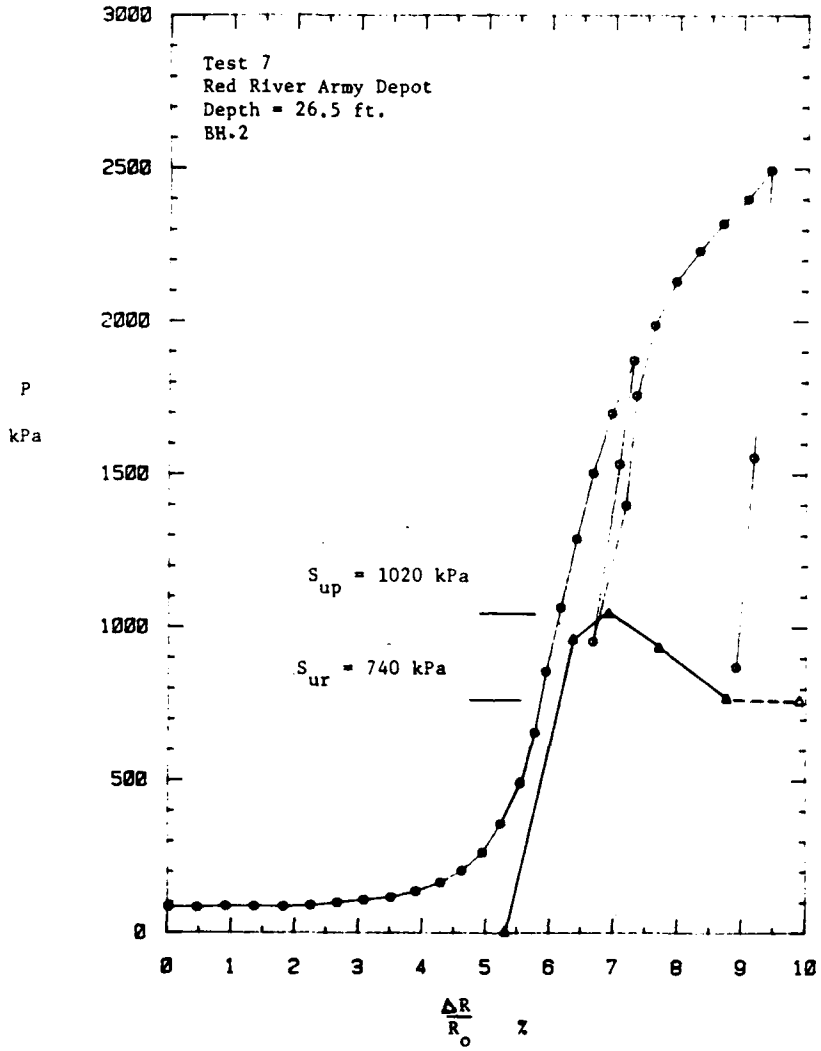

P_L = 3200 kPa

P_{OH} = 135 kPa

E_i = 136690 kPa

E_r = 178270 kPa

Figure G9. Pressuremeter curve for Test 7, depth = 26.5 ft, for hole BH•2

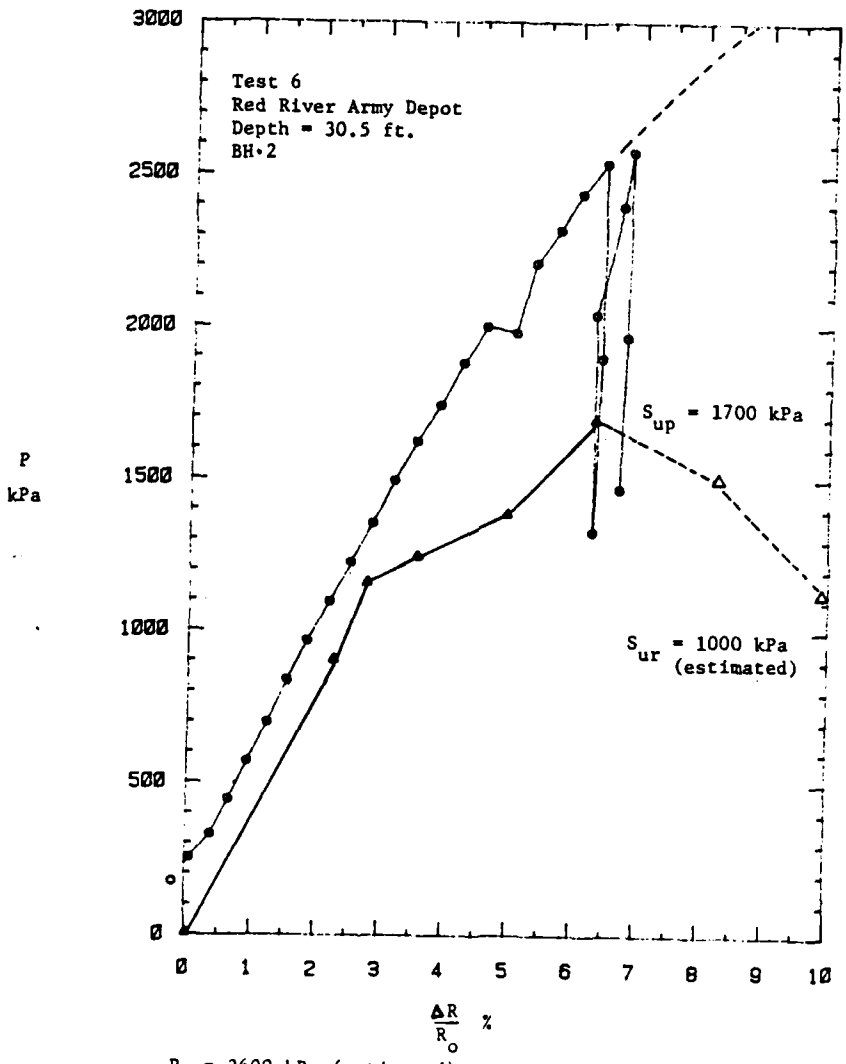

P_L = 3600 kPa (estimated)

P_{OH} = 200 kPa (estimated)

E_i = 56525 kPa

E_r = 796230 kPa

Figure G10. Pressuremeter curve for Test 6, depth = 30.5, for hole BH 2

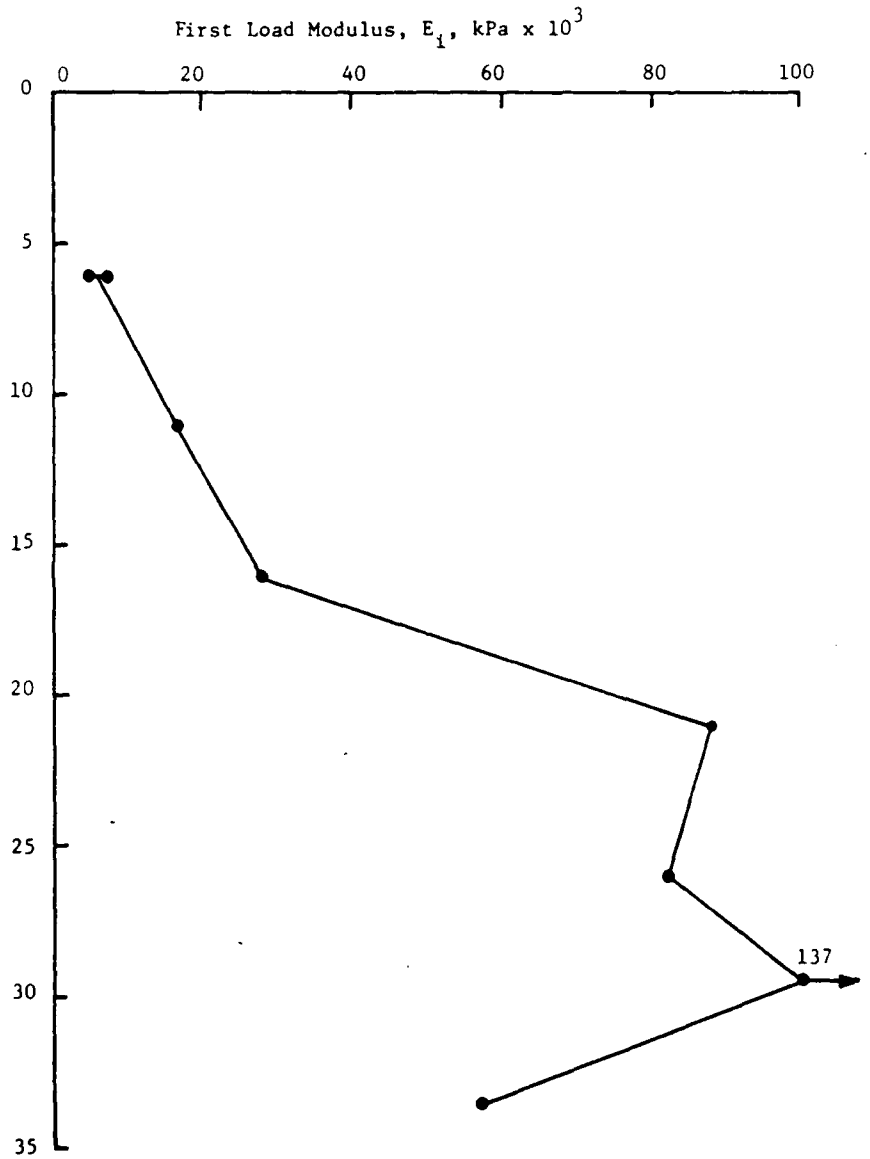

Figure G11. First load modulus profile

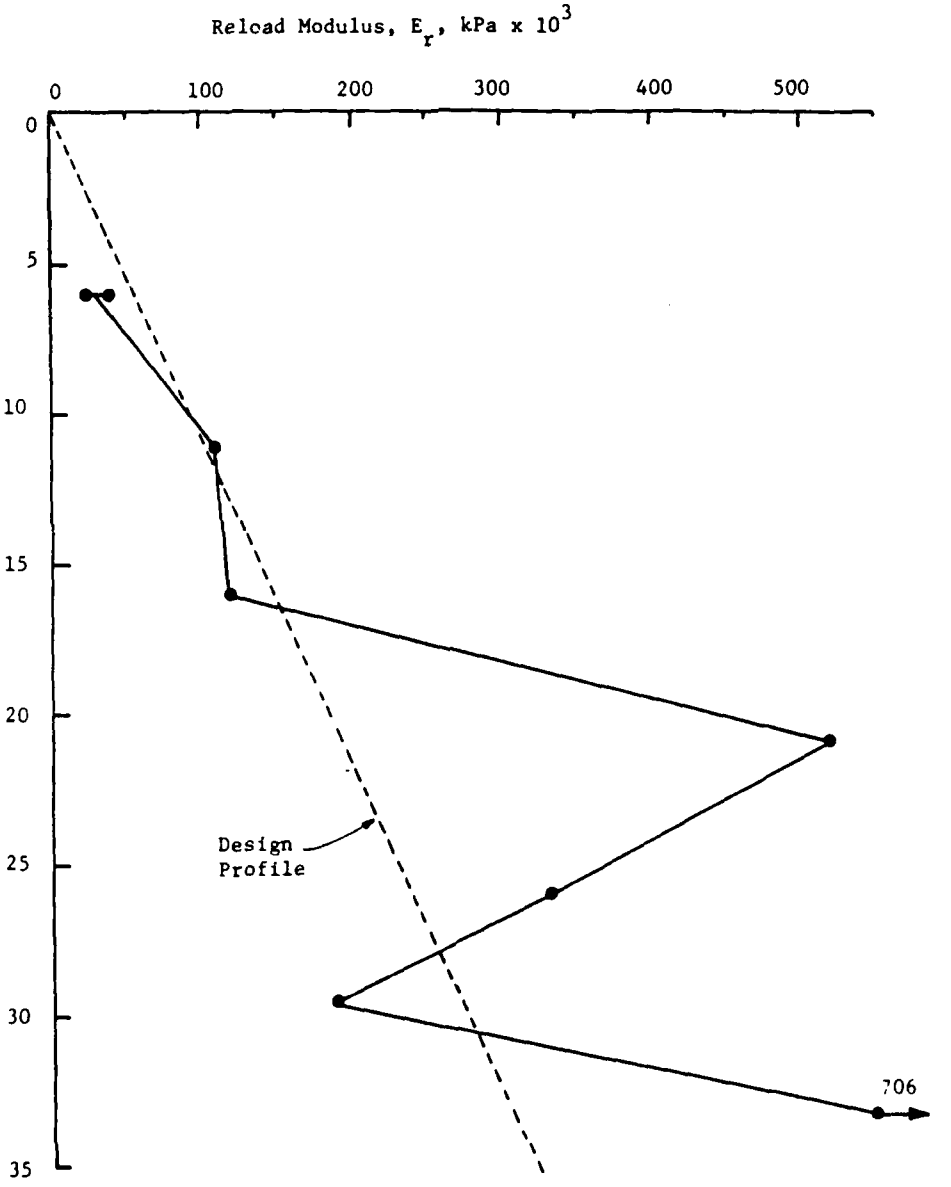

Figure G12. Reload modulus profile

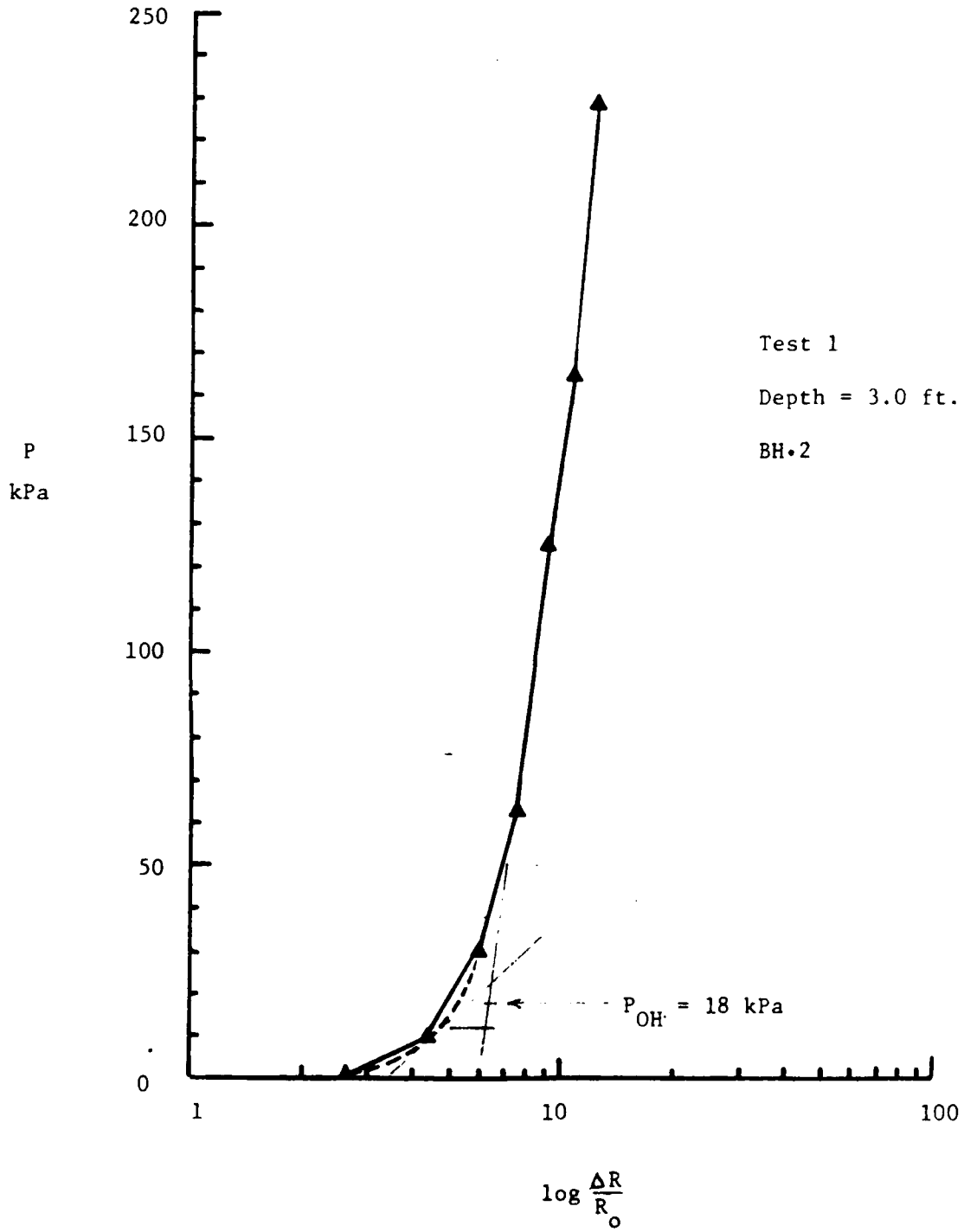

Figure G13. P_{OH} determination for Test 1, depth = 3.0 ft, for hole BH 2

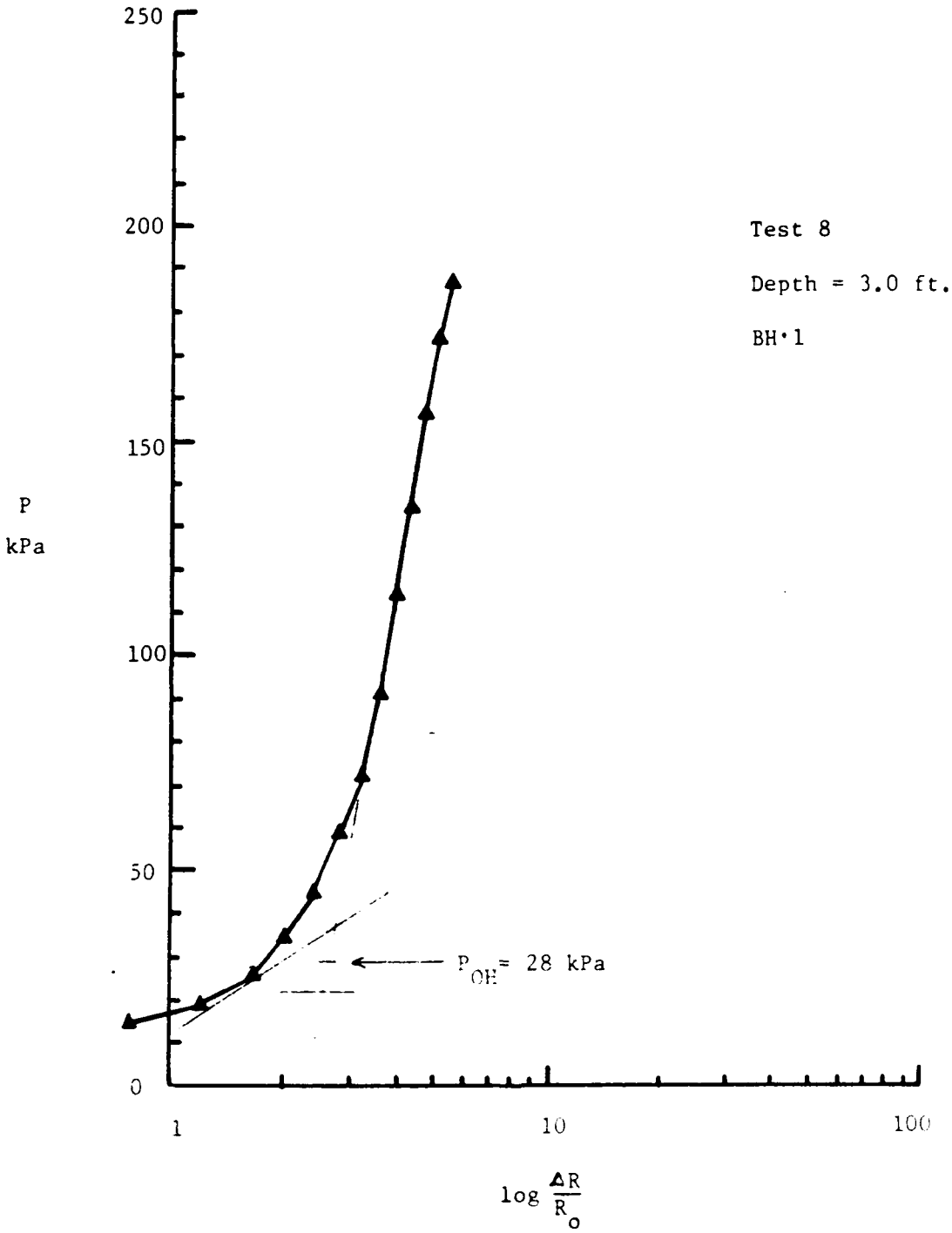

Figure G14. P_{OH} determination for Test 8, depth = 3.0 ft, for hole BH•1

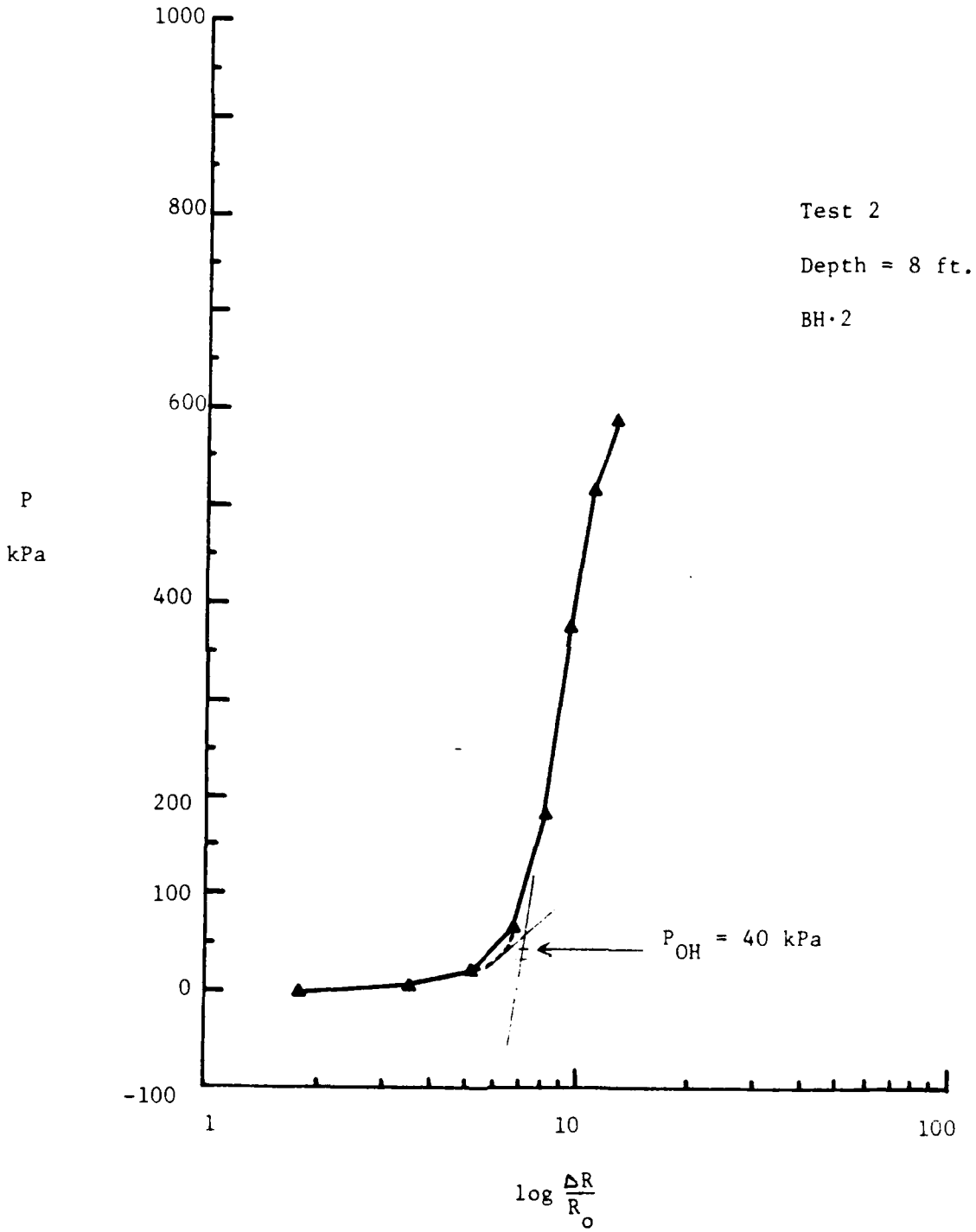

Figure G15. P_{OH} determination for Test 2, depth = 8 ft, for hole BH·2

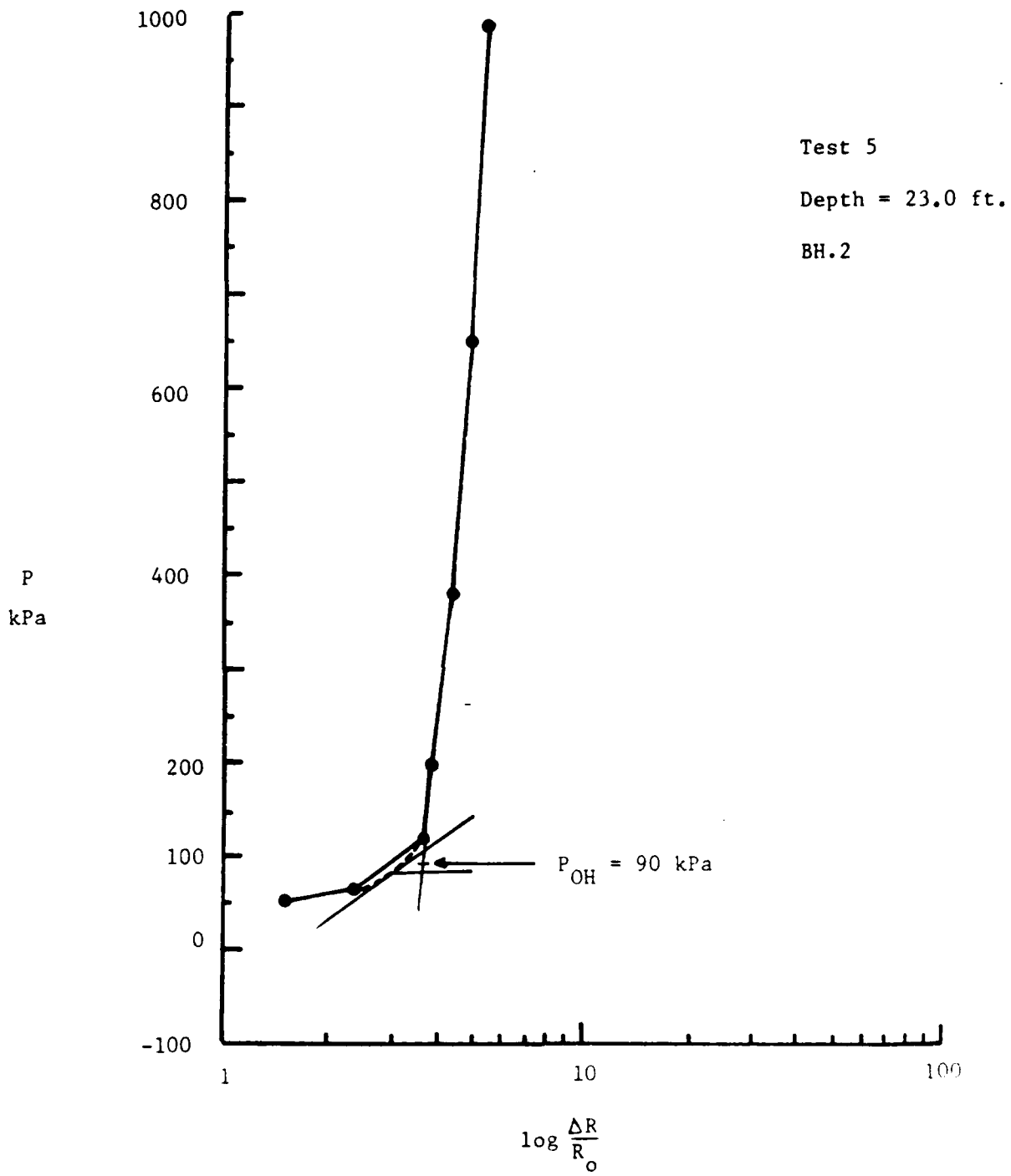

Figure G16. P_{OH} determination for Test 5, depth = 23.0 ft, for hole BH•2

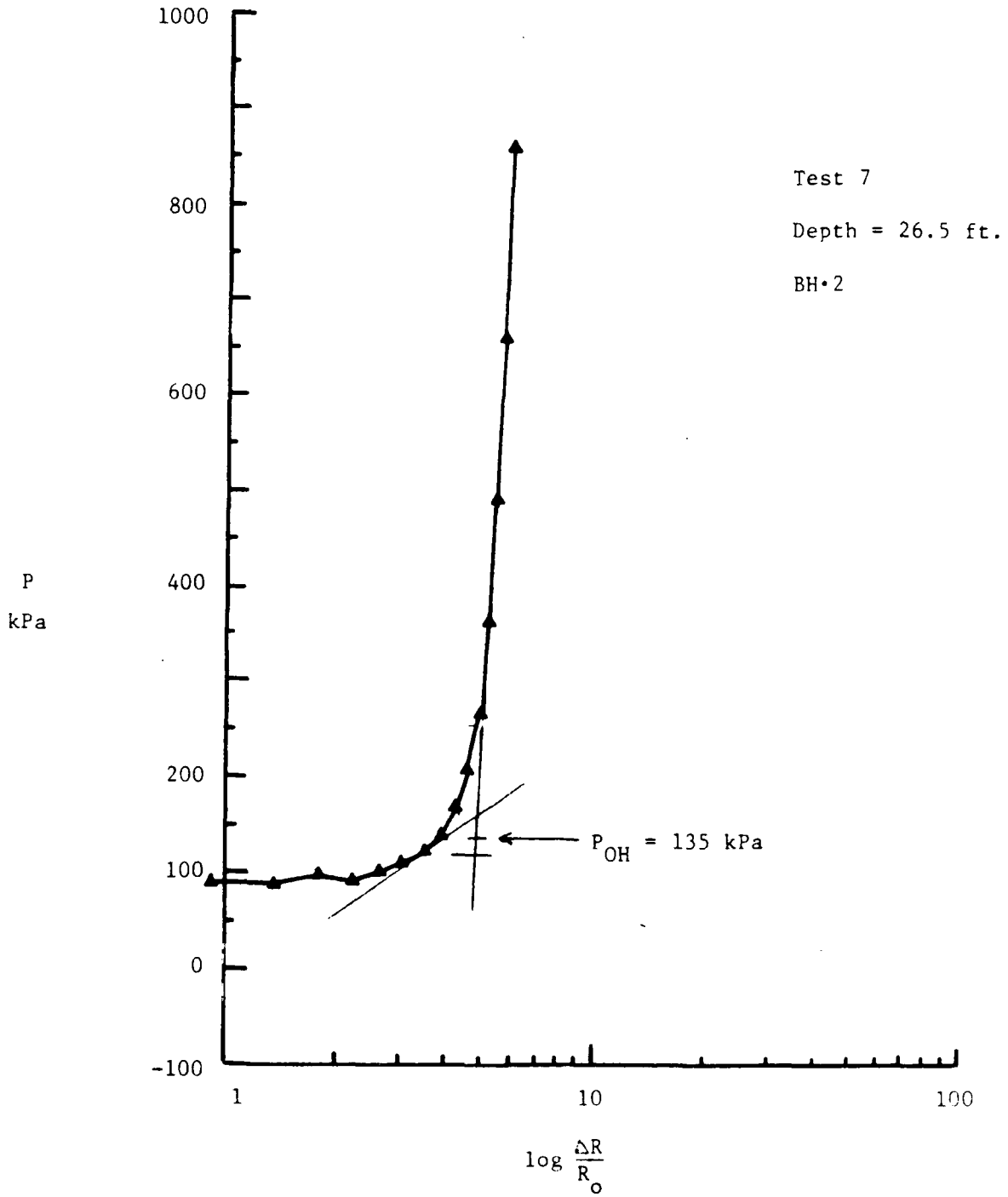

Figure G17. P_{OH} determination for Test 7, depth = 26.5 ft, for hole BH 2

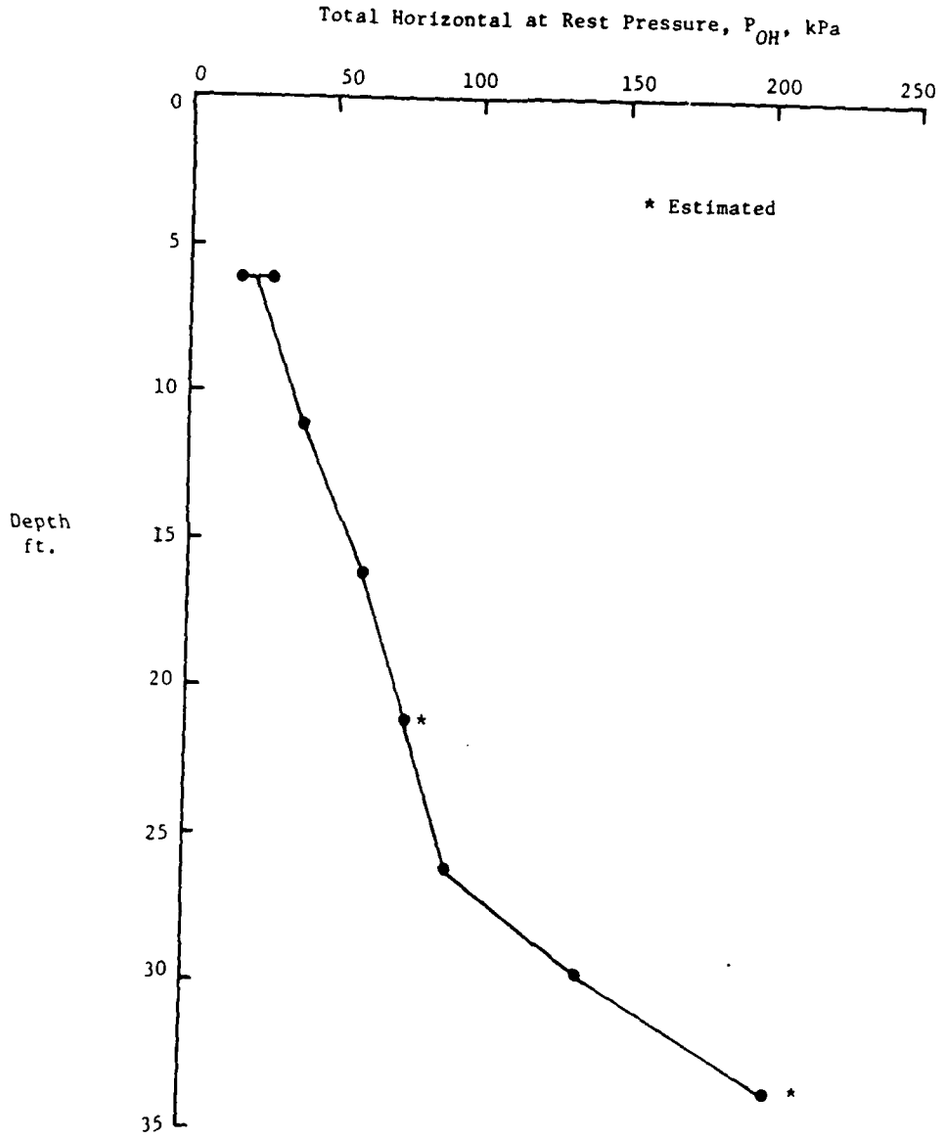

Figure G18. Total horizontal at rest pressure profile

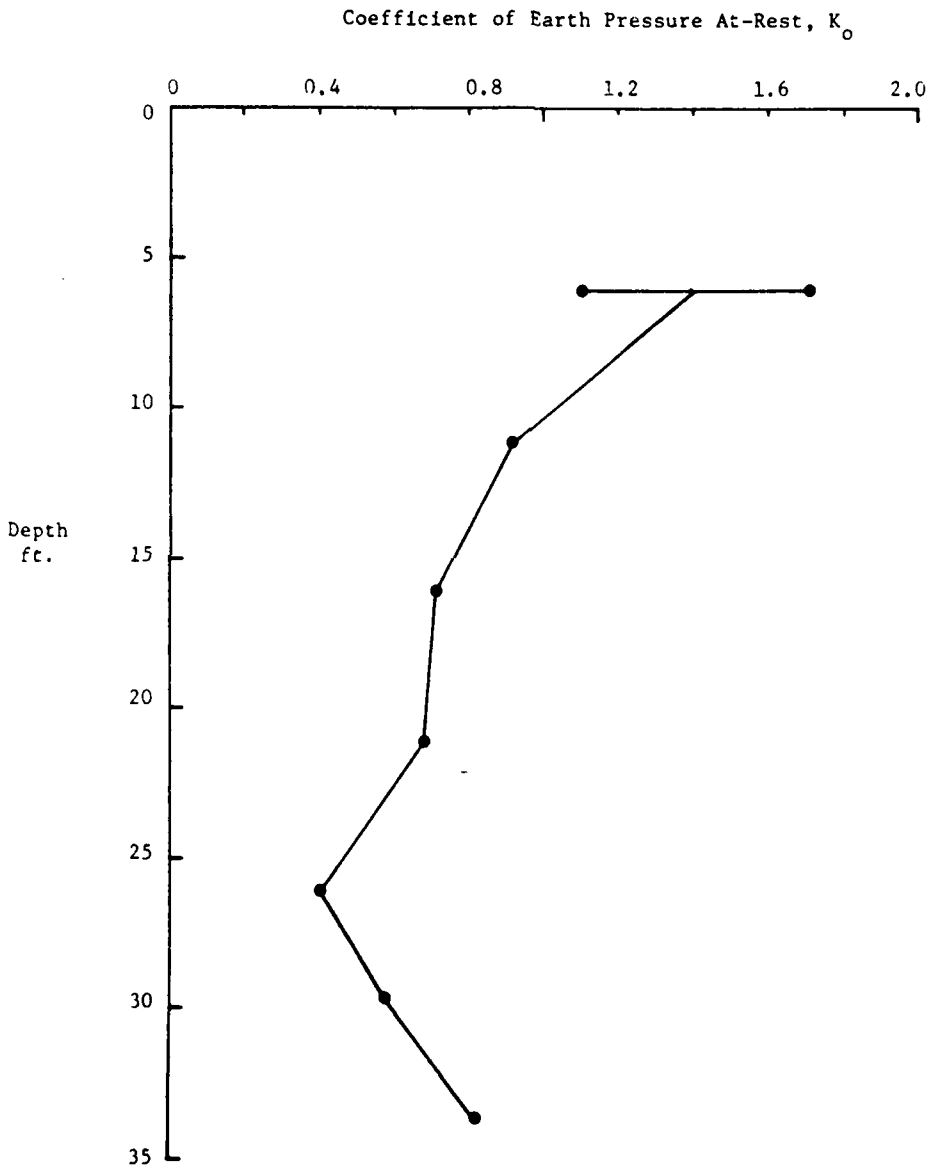

Figure G19. Coefficient of earth pressure at rest profile

Table G1.

Summary of Pressuremeter Test Results

Test	Depth[1] ft	Depth[1] m	P_1, kPa	P_{OH} kPa	P_1^* kPa	Overburden[2] Pressure, kPa	Pore[3] Pressure, kPa	K_o	E_i kPa 100^3	E_r kPa 10^3	Undrained Strength, kPa Peak	Residual	Anderson
1	3.0	0.9	420	28	392	16.5	0.0	1.70	4.94	22.47	190	116	162
8	3.0	0.9	410	18	392	16.5	0.0	1.09	7.68	38.87	130	104	150
2	2.4	0.8	850	40	810	43.9	0.0	0.91	16.75	106.88	285	220	219
3	13.0	4.0	1225	60	1165	71.3	9.1	0.71	28.09	112.35	520	200	110
4	18.0	5.5	2810	75[4]	2735	98.8	24.0	0.68	88.38	518.70	980	600	875[5]
5	23.0	7.0	2850	90	2760	126.2	39.0	0.40	82.23	327.18	990	550	928[5]
7	26.5	8.1	3200	135	3065	145.4	50.0	0.58	136.69	78.22	1020	740	2121[5]
6	30.5	9.3	3600[4]	200[4]	3400	167.3	62.0	0.82	56.53	706.23	1700[4]	1000[4]	——

[1]Measured from excavation level

[2]Assumed soil density = 18 kN/m^3

[3]From water table at 10 ft below excavation surface or 15 ft below top of fill

[4]Estimated

[5]Last portion of the curve is not well defined

Shear Strength Parameters

7. To compute the undrained shear strength, the shear stress versus strain curve is constructed from the PMT curve and the peak and residual strengths are obtained (Baguelin et al, 1978). In addition, the method devised by Gibson and Anderson (1961) was used to calculate the shear strength. For some tests, however, this last method is inaccurate because the strain level in the soil was not sufficient. The shear strength parameters derived from the PMT tests are tabulated in Table G1 and illustrated on Figure G20.

Equivalent Modulus Computations

8. To compute the settlement of the proposed raft foundation 300-ft square, three methods have been used.

9. Briaud Method. This general method was proposed by Briaud (1979). The method consists in assuming a strain influence factor distribution with depth and to weigh the layer moduli according to the corresponding areas under that distribution. According to this method the equivalent reload pressuremeter modulus is 489,000 kPa or 70,894 psi.

10. Gibson Soil Method. This approach is based on the work by Gibson (1967). It assumes a constant Poisson's ratio of 0.5 and a flexible footing uniformly loaded with a pressure q. The shear modulus $G(z)$ is assumed to increase linearly with depth z:

$$G(z) = mz \tag{G1}$$

$$m = \frac{G}{z} = \frac{E}{2(1+\mu)z} \tag{G2}$$

The solution for the vertical displacement at the ground level under the center of the raft exerting a pressure q on such a Gibson soil is (Poulos and David 1974):

$$\rho = \frac{q}{2m} \tag{G3}$$

For this problem the assumed bearing pressure is 100 kPa (2 ksf); the design E_r modulus profile gives $m = 2778$ kPa/ft (Figure G12). The calculated settlement is $\rho = 0.22$ inches.

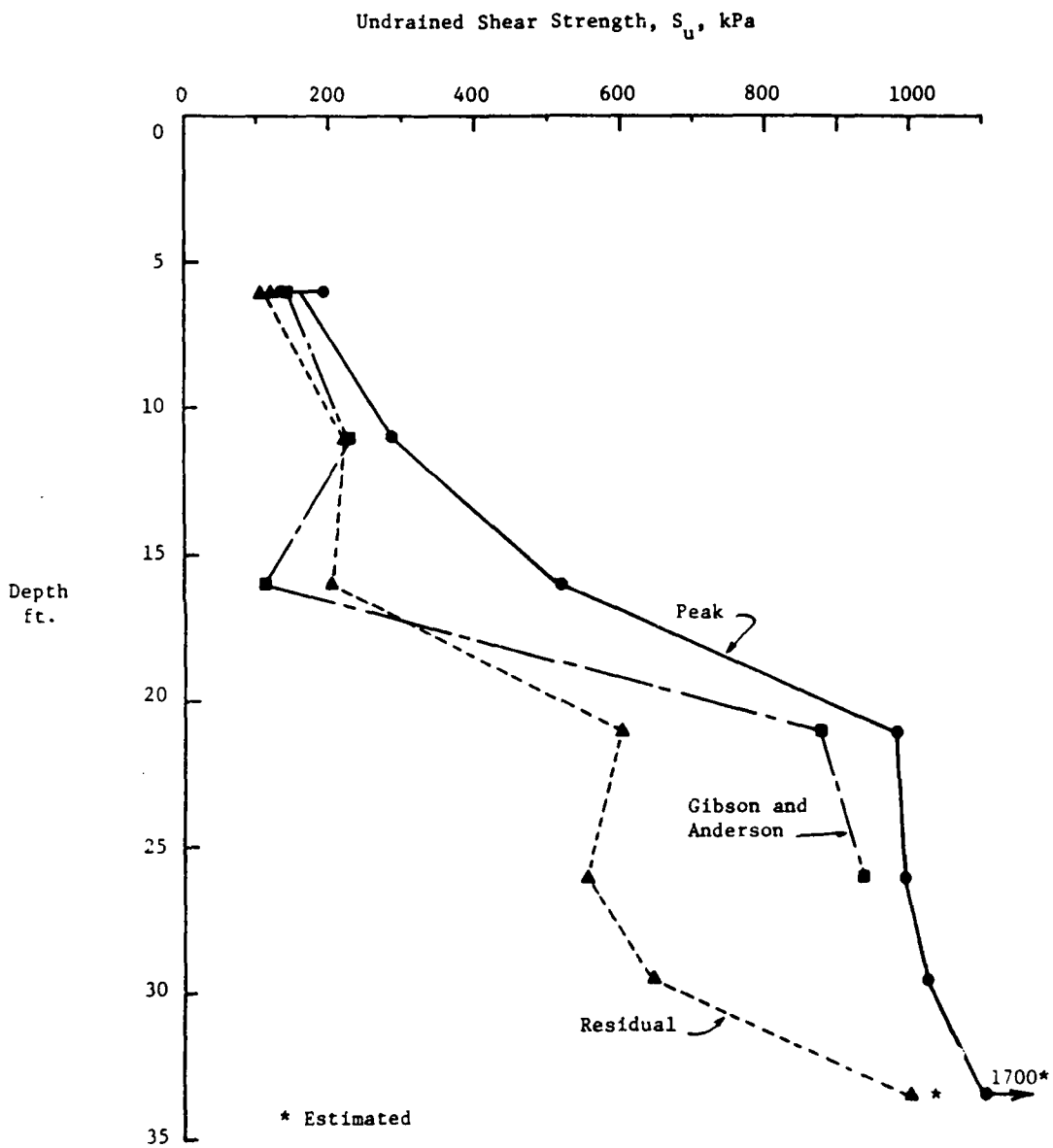

Figure G20. Undrained shear strength profile

11. The previous analysis assumes a linearly increasing modulus with depth. In the case of a homogeneous, semi-infinite half-space, the solution for a circular, flexible, uniformly loaded area of diameter B is

$$\rho = \frac{qB(1 - \mu^2)}{E_s^*}$$

Let $\mu = 0.5$ and equate equation G3 to G4. The equivalent homogeneous modulus E_s^* can be obtained for a linearly increasing modulus profile

$$\frac{3qB}{4E_s^*} = \frac{q}{2m} \tag{G5a}$$

or

$$E_s^* = \frac{3mB}{2} \tag{G5b}$$

In this case:

$$m = 2778 \text{ kPa/ft}$$
$$B = 300 \text{ ft}$$

So that according to this second method the equivalent reload modulus is E_s^* = 1,250,000 kPa or 178,955 psi.

12. Menard Method. This method is described in detail by Briaud et al. (1983). The settlement equation requires the computation of an equivalent initial modulus E_i within a zone of influence 8B deep. The expression for this equivalent modulus is

$$\frac{1}{E_i} = \frac{1}{4} \cdot \left[\frac{1}{E_1} + \frac{1}{0.85E_2} + \frac{1}{E_{3/4/5}} + \frac{1}{2.5E_{6/7/8}} + \frac{1}{2.5E_{9/16}} \right] \tag{G6}$$

where $E_{p/q}$ is the harmonic mean of the moduli of layers p to q. For example,

$$\frac{3}{E_{3/4/5}} = \frac{1}{E_3} + \frac{1}{E_4} + \frac{1}{E_5}$$

Using this method and a linear increase of the initial modulus with depth given by $E_{i(z)} = 500z$ where $E_{i(z)}$ is in kPa and z is in ft, the equivalent initial modulus E_d = 124,000 kPa (17,752 psi). The settlement for

a bearing pressure of 100 kPa (2 ksf) according to Menard method is ρ = 0.54 in. Using this settlement value and Equation G4, the equivalent modulus is E_s^* = 500,000 kPa (71,582 psi).

References

Baguelin, F., Jezequel, J. F., and Shields, D. H. 1978. The Pressuremeter and Foundation Engineering, Trans Tech Publications, Clausthal, Germany

Briaud, J.-L. 1979. "The Pressuremeter: Application to Pavement Design," PhD Dissertation, Civil Engineering Department, University of Ottawa, Canada

Briaud, J.-L., Tucker, L. M., and Felio, G. Y. 1983. "Pressuremeter, Cone Penetrometer and Foundation Design," Short Course Notes, Texas A&M University, College Station, TX

Casagrande, A. 1936. "The Determination of the Preconsolidation Load and Its Practical Significance," Proceedings, First International Conference on Soil Mechanics and Foundation Engineering, Vol 3, Cambridge, MA, pp 60-64

Gibson, R. E. 1967. "Some Results Concerning Displacements and Stresses in a Non-homogeneous Elastic Half-space," Geotechnique, Vol 17, pp 58-67; Also 1968, Vol 18, pp 275-276; 1969, Vol 19, pp 160-161.

Poulos, H. G. and Davis, E. H. 1974. Elastic Solutions for Soil and Rock Mechanics, John Wiley & Sons, pp 193-194.

II. CONE PENETRATION TEST

by

Recep Yilmaz[1] and Rick A. Klopp[2]
FUGRO INTER, INC.
10165 Harwin, Suite 170
Houston, TX 77036

Authorization

13. Authorization to conduct this work was given by Contract/Purchase Order No. DACW39-84-M-3972 dated 8 August 1984.

Location

14. The location was approximately 15 ft to the east of an existing concrete slab and was identified in the field by a representative of the Waterways Experiment Station.

Equipment

15. The CPT sounding was conducted using our Mobile Electronic Cone Penetrometer System unit as described in the enclosed brochure. The system is particularly designed for foundation design and earthwork control applications where reliable, accurate on-site measurements of subsurface properties are required.

16. One of the greater advantages of the cone penetrometer is the speed of operations which permits stratigraphy and engineering properties to be determined quickly and economically. Another important advantage is the continuous penetration record which permits location of thin strata that could easily be missed by conventinal drilling and sampling.

17. The entire system is mounted on a rugged, all-terrain truck which contains 11 system components including strip-chart recorders and data processing equipment. The sounding was conducted using an electronic friction sleeve penetrometer tip. The tip was hydraulically pushed into the ground at a constant rate of 2 cm/sec and a continuous record of tip bearing resistance

---

[1] Senior Staff Engineer

[2] Supervisor, Onshore Operations

and side friction resistance on a sleeve located just above the tip was obtained. Strip-chart records of tip and sleeve friction resistance were continuously plotted and available for immediate evaluation of soil conditions. The data was also stored on magnetic tape for computer processing. An accurate determination of stratigraphy was possible from the evaluation of tip resistance (q), sleeve friction resistance (f_s), and friction ratio (f_r). The latter being the ratio of f_s to q_c, expressed as a percentage, and determined by means of our office-based computer. It is used as the basis for soil classification.

Tests

18. Fugro conducted a single Cone Penetration Test (CPT) sounding to a depth of approximately 12.5 meters. Based upon the friction ratio, the general soil conditions were determined and are presented along with the CPT log on Figure G21. A key to soil classification and symbols used on the CPT log is presented on Figure G22. Due to the friction buildup along the cone rods, the 20-ton thrust capacity of the truck was exceeded at approximately 12.5 meters and the sounding was terminated. The general soil profile consisted of a silty clay to clayey silt strata from about 3 to 12.5 meters and was overlain by a silty fill deposit.

19. Analysis. The methods of interpretation of CPT data depends on whether the soil responds to the cone penetration in a drained or undrained manner. As generally accepted, most soils which classify as silty clay respond to cone penetration in an undrained manner. The measured undrained shear strength of clayey soils in the laboratory depends significantly on the type of test used, the rate of strain, and the orientation of the failure planes. When evaluating the undrained shear strength C_u from cone penetration testing, the following equation is used

$$C_u = \frac{q_c - \gamma z}{N_k} \qquad \text{(G8)}$$

where

q_c = tip resistance, kg/cm^2

γ = total unit weight, kg/cm^3

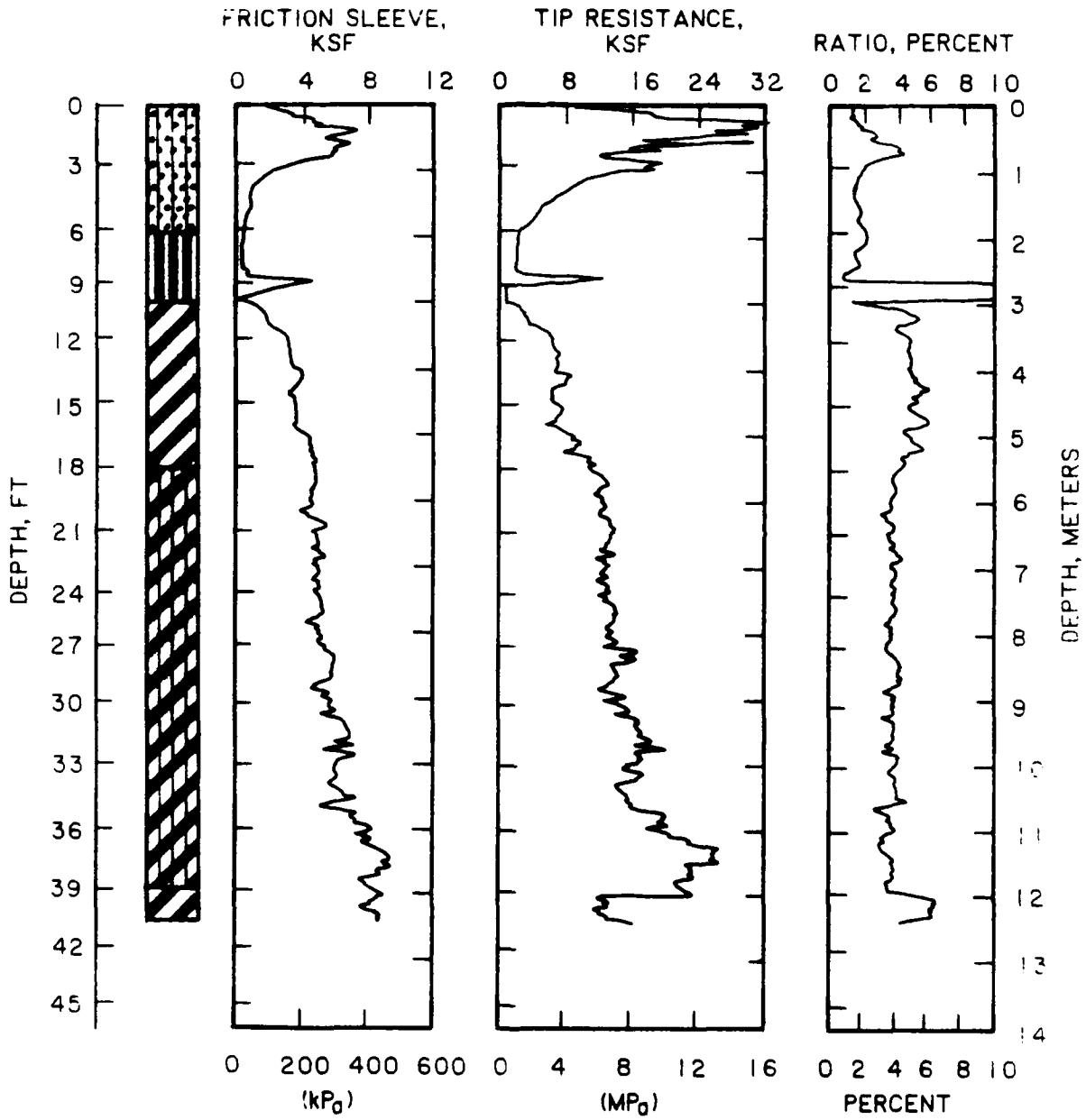

Figure G21. Results of cone penetration test

KEY TO SOIL CLASSIFICATION AND SYMBOLS

SOIL TYPE
(Shown in Symbol Column)

Sand, Silt, Clay

FILL, Sandy, Silty, Clayey

Predominant type shown heavy

SAMPLE TYPE
(Shown in Samples Column)

Undisturbed, Rock Core, Split Spoon, No Recovery

TERMS DESCRIBING CONSISTENCY OR CONDITION

COARSE GRAINED SOILS (Major Portion Retained on No. 200 Sieve)

Includes (1) clean gravels & sand described as fine, medium or coarse, depending on distribution of grain sizes & (2) silty or clayey gravels & sands (3) fine grained low plasticity soils (PI < 10) such as sandy silts. Condition is rated according to relative density, as determined by lab tests or estimated from resistance to sampler penetration.

Descriptive Term	Penetration Resistance*	Relative Density
Loose	0 – 10	0 to 40 %
Medium Dense	10 – 30	40 to 70 %
Dense	30 – 50	70 to 90 %
Very Dense	Over 50	90 to 100 %

**Blows/Ft., 140# hammer, 30" drop*

FINE GRAINED SOILS (Major Portion Passing No. 200 Sieve)

Includes (1) inorganic & organic silts & clays, (2) sandy, gravelly or silty clays, & (3) clayey silts. Consistency is rated according to shearing strength, as indicated by penetrometer readings or by unconfined compression tests for soils with PI ≥ 10

Descriptive Term	Cohesive Shear Strength Tons/Sq. Ft.
Very Soft	Less Than 0.125
Soft	0.125 to 0.25
Firm	0.25 to 0.50
Stiff	0.50 to 1.00
Very Stiff	1.00 to 2.00
Hard	2.00 and Higher

NOTE: SLICKENSIDED AND FISSURED CLAY MAY HAVE LOWER UNCONFINED COMPRESSIVE STRENGTHS THAN SHOWN ABOVE, BECAUSE OF PLANES OF WEAKNESS OR SHRINKAGE CRACKS; CONSISTENCY RATINGS OF SUCH SOILS ARE BASED ON HAND PENETROMETER READINGS

TERMS CHARACTERIZING SOIL STRUCTURE

Parting	paper thin in size
Seam	1/8" – 3" thick
Layer	greater than 3"
Fissured	containing shrinkage cracks, frequently filled with fine sand or silt, usually more or less vertical
Sensitive	pertaining to cohesive soils that are subject to appreciable loss of strength when remolded
Interbedded	composed of alternate layers of different soil types
Laminated	composed of thin layers of varying color and texture
Calcareous	containing appreciable quantities of calcium carbonate
Well Graded	having wide range in grain sizes and substantial amounts of all intermediate particle sizes
Poorly Graded	predominately of one grain size, or having a range of sizes with some intermediate size missing
Flocculated	pertaining to cohesive soils that exhibit a loose knit or flakey structure
Slickensided	having inclined planes of weakness that are slick and glossy in appearance

DEGREE OF SLICKENSIDED DEVELOPMENT

Slightly Slickensided	slickensides present at intervals of 1'-2', soil does not easily break along these planes
Moderately Slickensided	slickensides spaced at intervals of 1'-2', soil breaks easily along these planes
Extremely Slickensided	continuous and interconnected slickensides spaced at intervals of 4"-12", soil breaks along the slickensides into pieces 3"-6" in size
Intensely Slickensided	slickensides spaced at intervals of less than 4", continuous in all directions; soil breaks down along planes into nodules 1/4"-2" in size

FUGRO INTER, INC
Consulting Engineers and Geologists

Figure G22. Key to soil classification and symbols

z = depth, cm

N_k = cone factor for tip

The N_k value equals a Terzaghi-type bearing capacity factor for the cohesive contribution to bearing, but is applied here to the small-diameter, deep foundation case represented by q_c data.

Evaluation of N_k

20. N_k does not possess a constant value, but varies with the stress-strain properties of the soil. In general, the more sensitive the clay, the lower N_k value is obtained. Fugro's experience in clayey soils and data presented by Lunne and Kleven (1981)* shows that for normally consolidated marine clays, N_k falls between 11 and 19 with an average of 15. The estimation of the undrained shear strength in silty soils becomes more difficult and the above equations may not accurately define the strength where cone penetration may cause a partially drained soil response. As an example of the difficulties in a silty soil, consider Figure G23 which shows a plot of $N_k = q_c/C_u$ against undrained shear strength for a Fugro test site. The undrained shear strengths were measured with triaxial undrained unconsolidated (uu) and selfboring pressuremeter (SBP) tests and were representative of normally consolidated marine silty clays.

21. In an effort to obtain an appropriate N_k factor, we have conducted an analysis of CPT data, laboratory results of borings for various geotechnical projects in the Texarkana area, information supplied by the Waterways Experiment Station, and our past experience with similar soils.

22. A determination of the overconsolidation ratio (OCR) by use of the CPT data showed the deposit to be moderately overconsolidated. Values of N_k between 15 and 30 for overconsolidated deposits are suggested by Toolan and Fox (1977). For the soils encountered we have used a lower bound of 25 and an upper bound of 35 for N_k and have plotted this data on Figure G24 along with the recommended mean.

23. From conversations between Lawrence Johnson of the Waterways Experiment Station and Rick Klopp of Fugro, the results from laboratory

---

*Refer to references in this section, II. CONE PENETRATION TEST

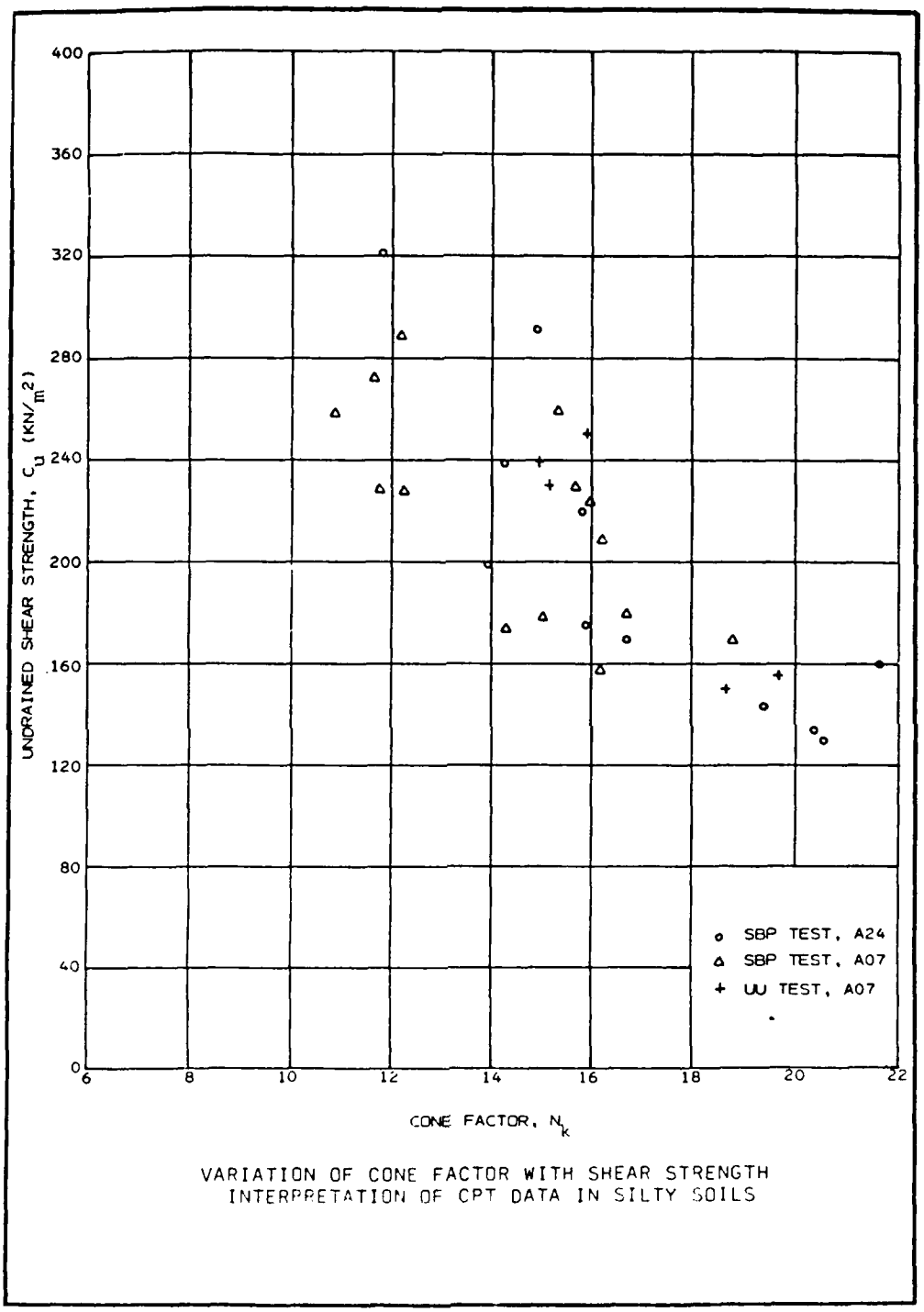

FUGRO INTER, INC.
Consulting Engineers and Geologists

Figure G23. Variation of cone factor with shear strength interpretation of CPT data in silty soils

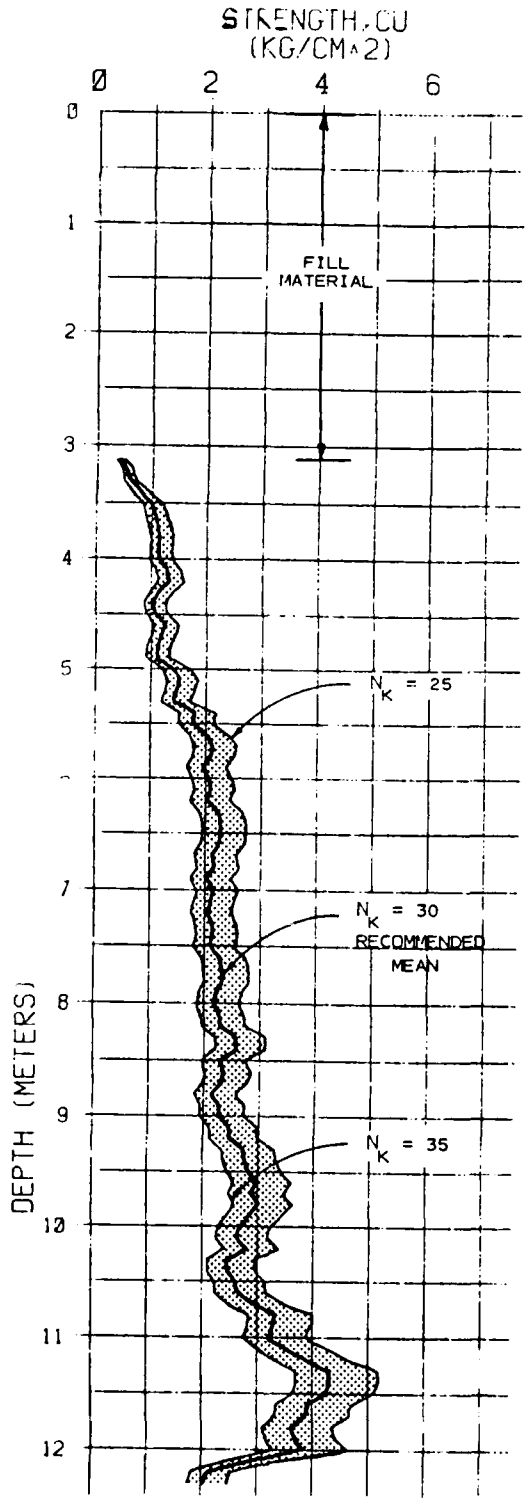

Figure G24. Recommended value for N_k at test site

testing of samples for determination of undrained shear strength conducted by the Waterways Experiment Station show values somewhat lower than our recommended mean. We believe that this may be due to sample disturbance.

Elastic Soil Modulus

24. Based on the above discussion concerning undrained shear strength, and provided that the cone resistance relates to an undrained soil response, the methods for determining Young's Modulus in clays should be relevant. An estimation of undrained Young's Modulus E_u can be made using empirical correlations with the undrained shear strength C_u in the form

$$E_u = \alpha C_u \qquad \text{G9)}$$

where α is a constant that depends on stress or strain level, OCR, sensitivity, and other factors. The choice of the relevant stress or strain level is very important due to the non-linear behavior of soil. Figure G25 presents data that shows the variation of the ratio E_u/C_u with stress level for seven different normally consolidated cohesive soils whose plasticity index PI ranged from 15 to 75. Figure G26 shows the variation of E_u/C_u with OCR at two stress levels for the same soils presented on Figure G25. Based on Waterways Experiment Station supplied laboratory data, soil types numbers 3, 4, and 5 show the best correlation. Using the charts presented on Figure G26 and the OCR of the soil, we estimate that E_u/C_u approximates 200 to 400 and have presented this data with depth on Figure G27. As discussed, the shear stress level is a factor which has great influence on E_u. For example, low values of E_u/C_u would be expected for highly plastic clays with a high shear stress level, and higher values for lightly loaded clays of low plasticity. The actual use of the E_u data also has an effect on the stress level that should be utilized. For example, axial loading on piles yields a lower level of strain than lateral loading and the corresponding value of E_u would change.

25. Silty soils present some difficulties for accurate and reliable inerpretations for classification and for fundamental soil properties based on conventional electric friction cone data. An important factor relates to whether cone penetration evokes a drained or undrained soil response. It is considered that silty soils will respond in an undrained or partially drained

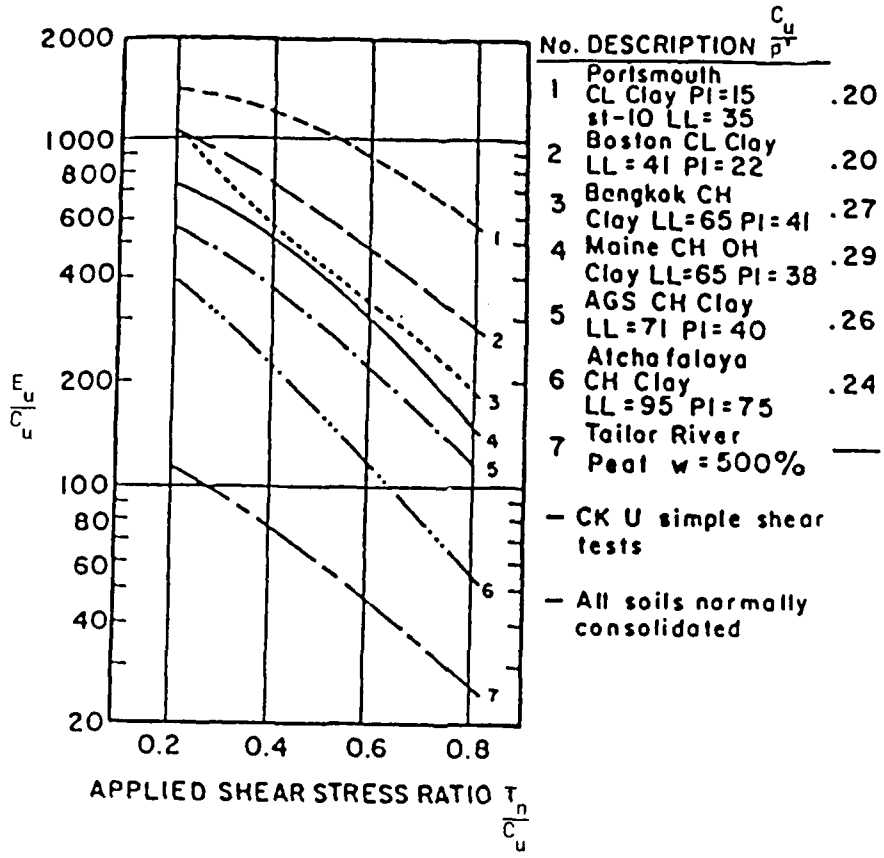

Figure G25. Chart for determination of stiffness ratio interpretation of CPT data in silty soils (after Ladd et al 1977)

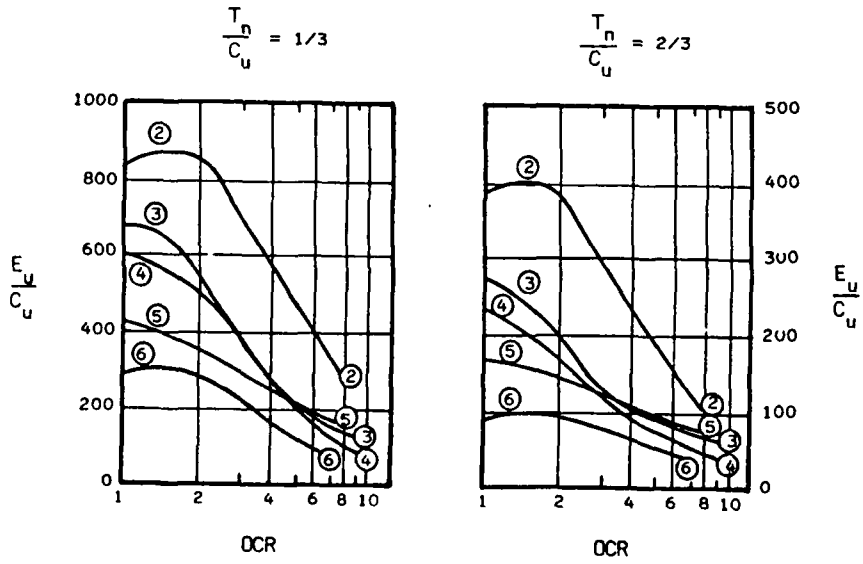

Figure G26. Chart for determination of stiffness ratio with respect to OCR interpretation of CPT data in silty soils (after Ladd et al 1977)

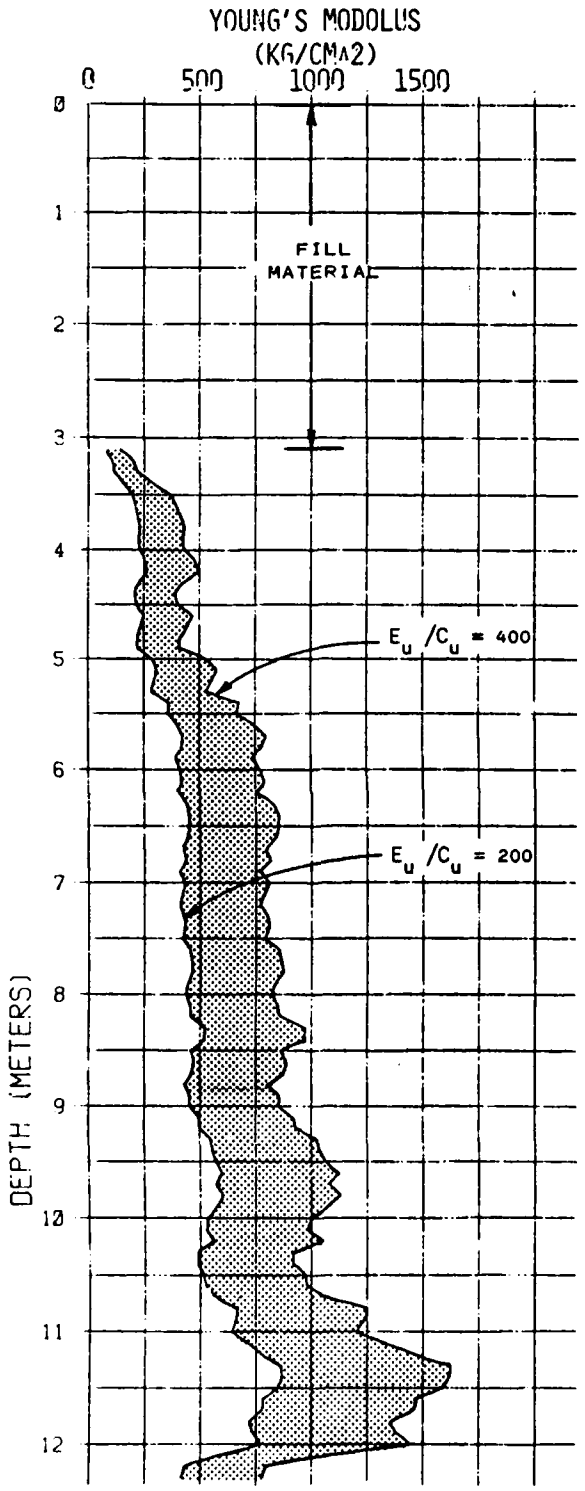

Figure G27. Young's soil modulus with depth

manner. Overconsolidation effects in silty soils also complicates determination of geotechnical properties. Therefore a need for local correlation with laboratory results becomes necessary. Cone penetration testing is useful for determination of the undisturbed values of C_u and E_u although empirical correlations are required.

References

Ladd, C. C., Foott, R., Ishihara, K., Schlosser, F., and Poulos, H. G. 1977. "Stress - Deformation and Strength Characteristics," Proceedings of the Ninth International Conference on Soil Mechanics and Foundation Engineering, Tokyo, Japan, Vol II, pp 421-494

Lunne, T. and Kleven, A. 1981. "Role of CPT in North Sea Foundation Engineering," Symposium on Cone Penetration Testing and Experience, Geotechnical Engineering Division, American Society of Civil Engineers, pp 49-75

Toolan, F. E. and Fox, D. A. 1977. "Geotechnical Planning of Piled Foundations for Offshore Platforms", Proceedings of the Institute of Civil Engineers, Vol 62, Part 1, pp 221-244

III. PLATE LOAD TESTS

by

Department of the Army
Fort Worth District, Corps of Engineers
P. O. Box 17300, Fort Worth, TX 76102

Table G2.
Test Data Summary

Test	Location	Material	Coefficient of Subgrade Reaction Uncorrected, pci	Corrected, pci
PB-1	35 ft E 15 ft N of A-26	Natural Grade, el 365.33 ft	323	280
PB-2	25 ft W 65 ft N of A-26	Compacted Fill, el 365.33 ft	333	290
PB-3	15 ft N of A-26	21 in. below Fill	364	310
PB-4	38 ft E of A-14	Upper Midway Clay Shale, el 358.68 ft	150	150
PB-5	40 ft S 40 ft W of A-19	Compacted Fill, el 365.33 ft	470	385
PB-6	At L-29	Compacted Fill, el 365.33 ft	455	360

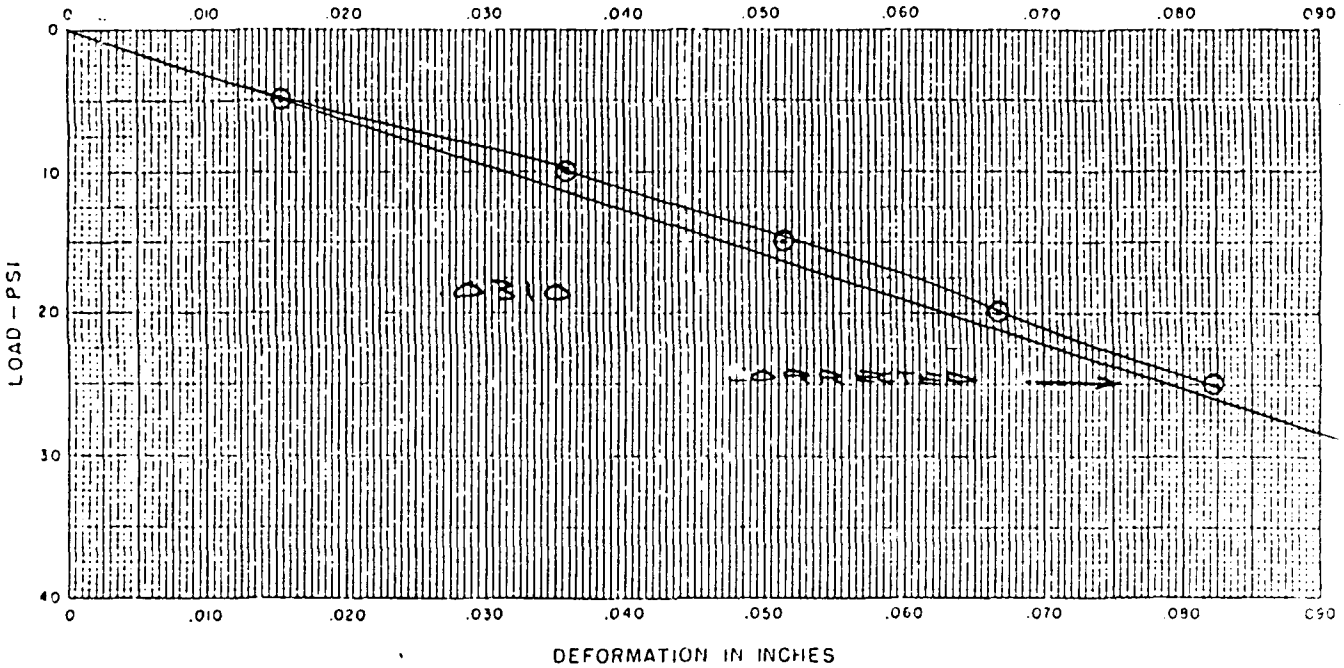

Figure G28. Plate bearing test PB-1

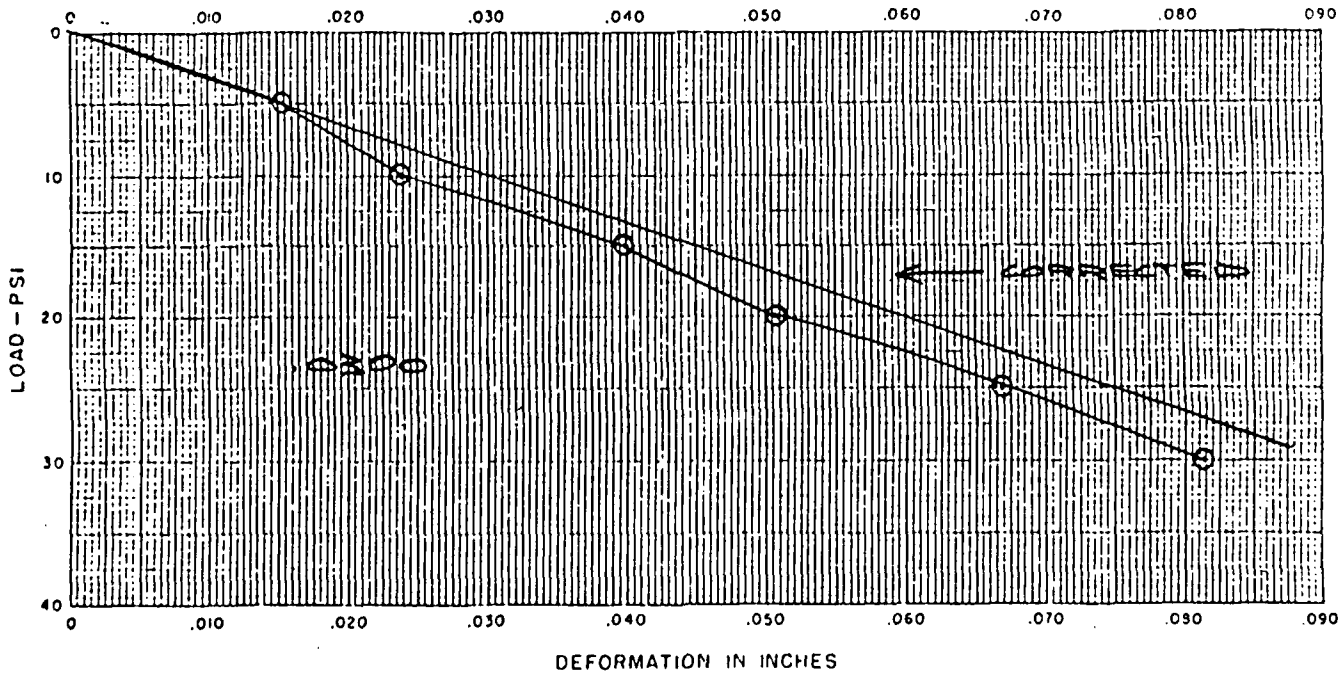

Figure G29. Plate bearing test PB-2

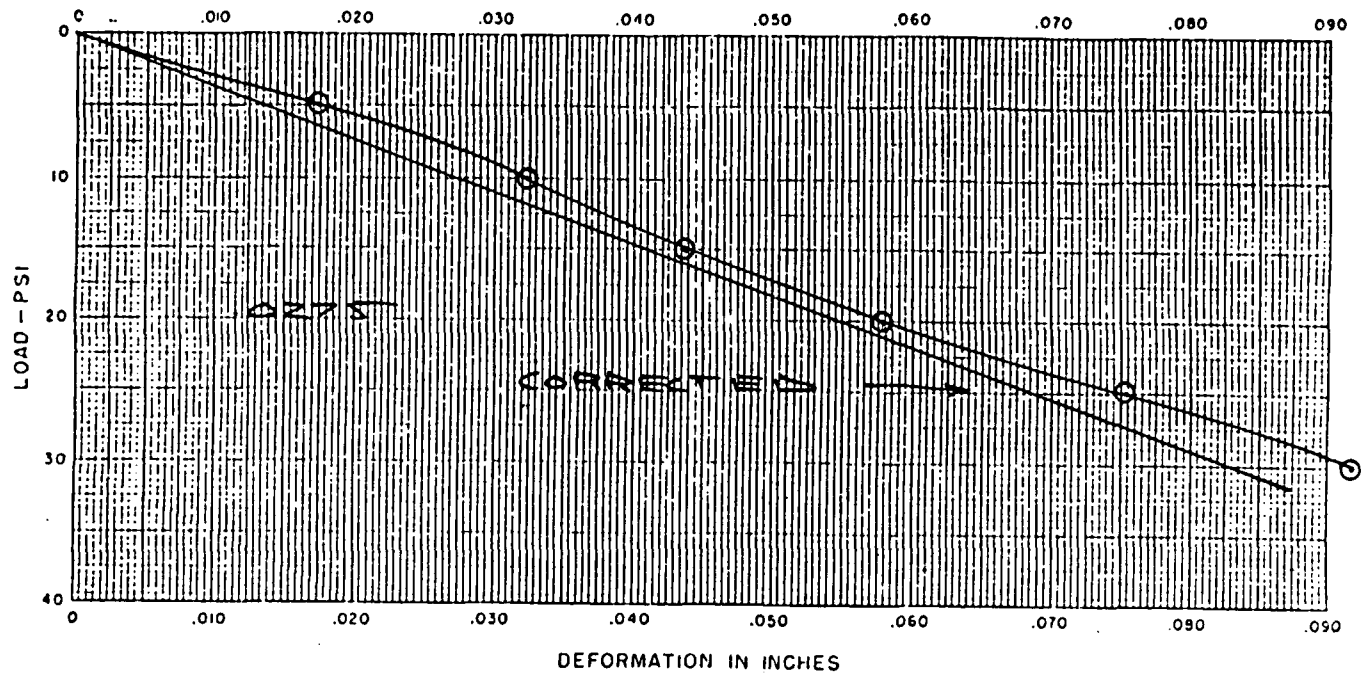

Figure G30. Plate bearing test PB-3

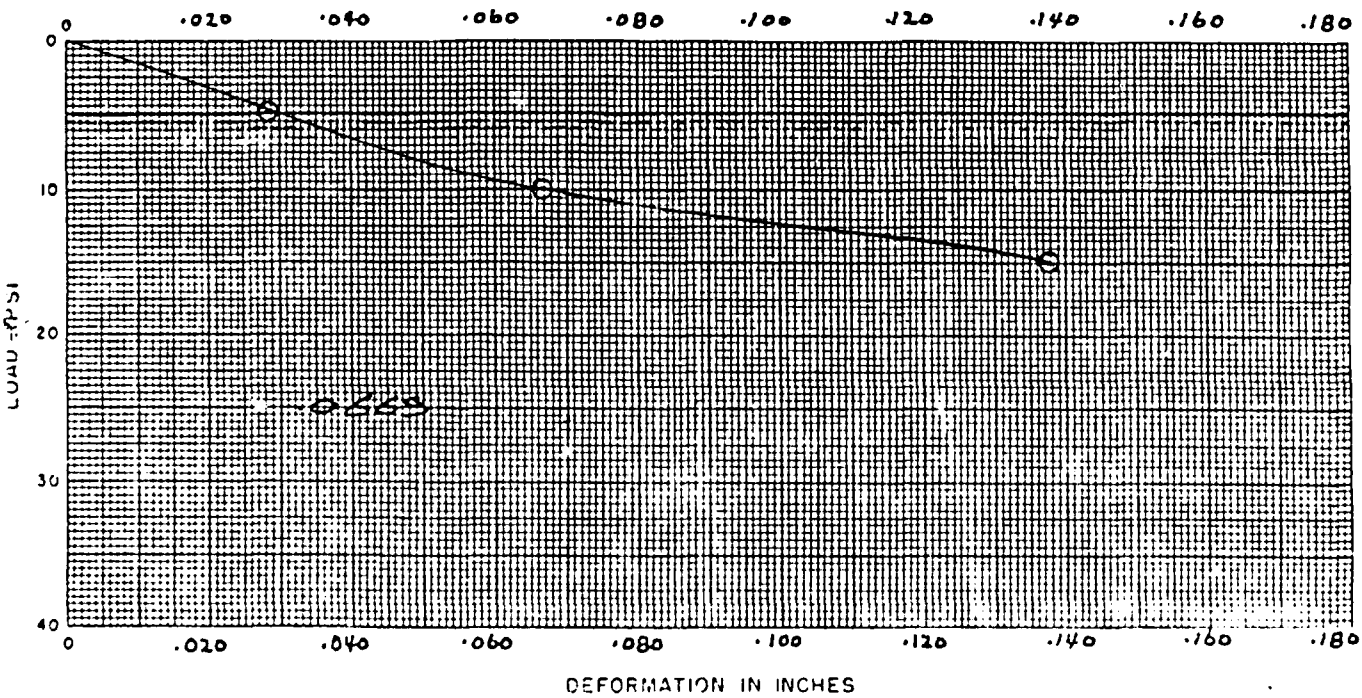

Figure G31. Plate bearing test PB-4

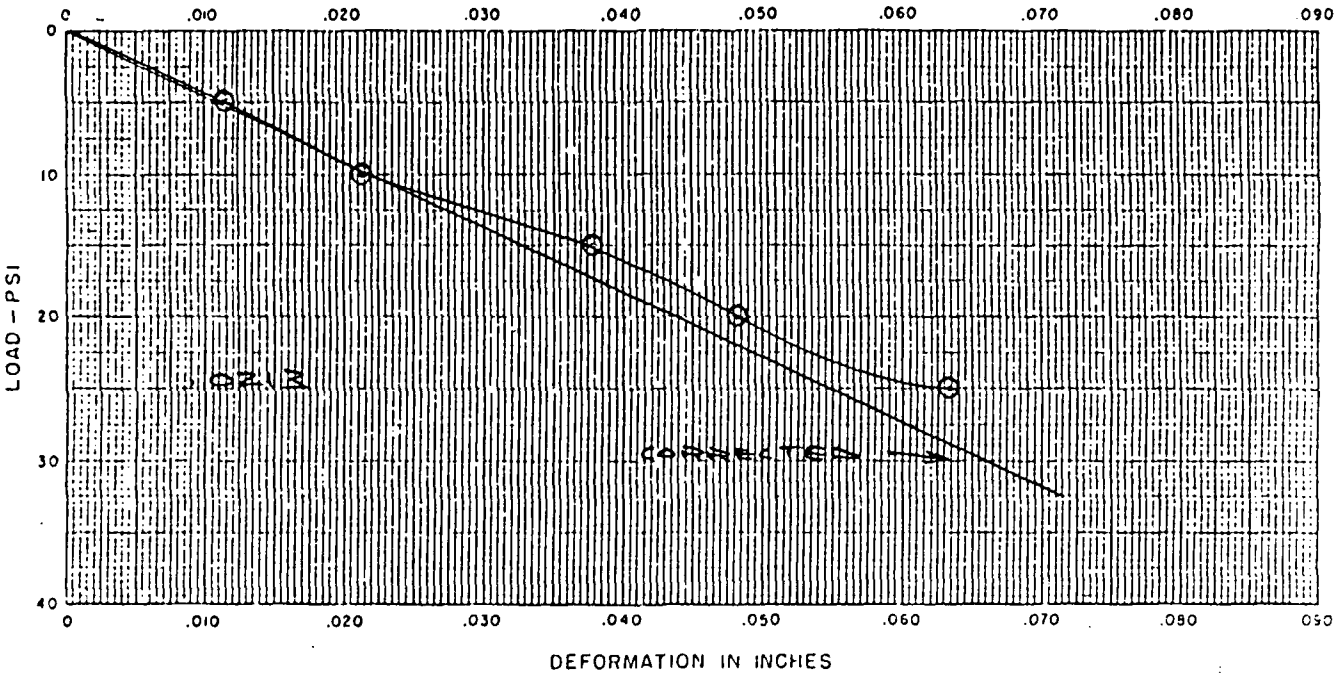

Figure G32. Plate bearing test PB-5

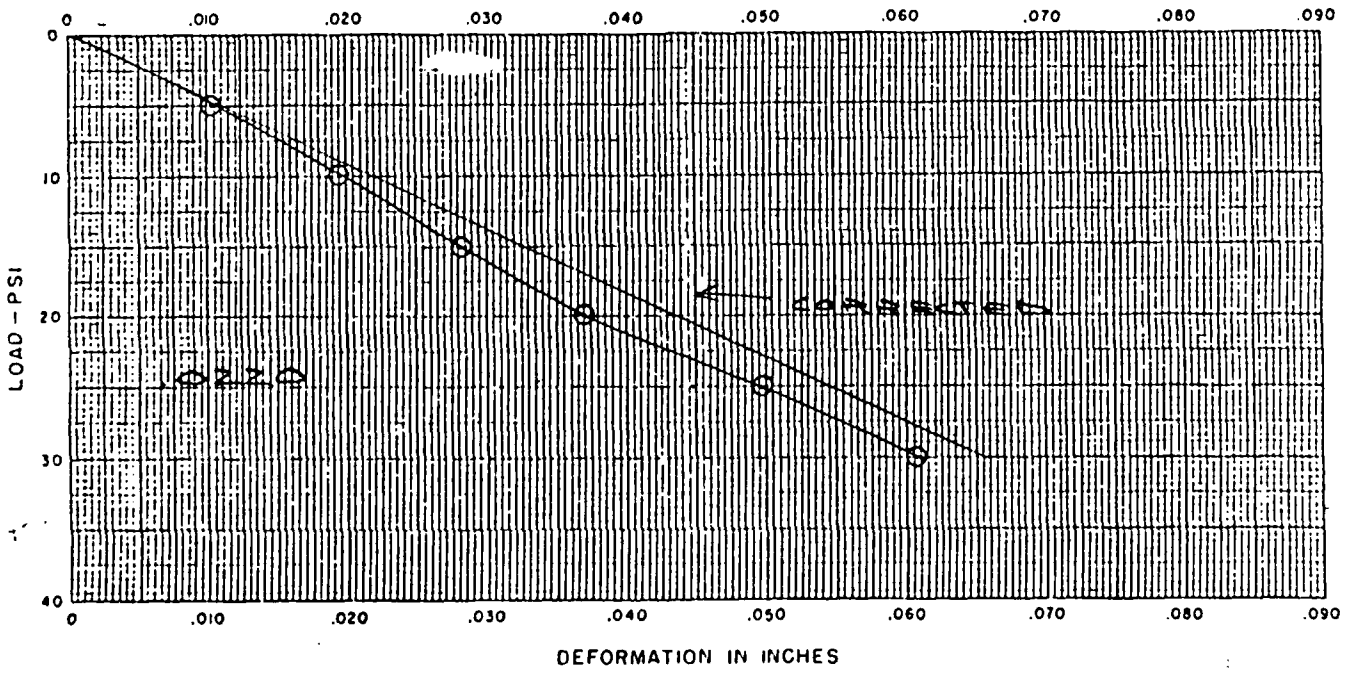

Figure G33. Plate bearing test PB-6

IV. PIEZOMETRIC DATA

a. Permeability From Falling Head Tests

Piezometer	Tip Depth, Ft	Permeability, cm/sec
1	80	10^{-8}
2	50	10^{-8}
3	40	10^{-8}
4	26	10^{-6}
5	8	10^{-5}
6	5	10^{-4}

b. Water Head in Piezometers

Date	Piezometer No. and Head, Ft					
	1	2	3	4	5	6
6/14/85	29.31	29.88	32.94	19.29	6.18	2.76
8/23/85	8.59	19.32	33.88	20.17	5.47	2.02
11/15/85	7.34	20.54	33.71	199.37	2.80	dry
2/13/86	6.32	21.90	32.61	18.21	1.54	dry
6/02/86	0.77	22.01	33.05	19.27	4.27	dry
8/25/86	0.10	24.80	34.04	20.25	5.13	0.53
2/09/87	dry	27.02	33.05	18.85	1.25	dry
5/12/87	dry	28.20	33.28	18.42	3.83	0.30
5/25/88	dry	31.73	33.28	19.42	0.30	0.40

V. ELEVATION DATA

Location	Original el, Ft 9/06/84	Date and Change in Elevation, inches				
		10/31/84	01/28/85	08/28/85	06/05/86	05/12/87
A-1	366.061	-0.108	-0.108	-0.300	-0.384	-0.204
A-2	366.061	-0.048	-0.096	-0.216	-0.372	-0.084
B-1	366.014	-0.108	-0.096	-0.252	-0.348	-0.132
B-2	366.013	-0.036	-0.060	-0.060	-0.228	0.108
D-1	366.062	-0.120	-0.168	-0.216	-0.252	-0.108
D-2	366.055	-0.036	-0.084	-0.084	-0.192	0.036
A-4	366.047	-0.156	-0.276	-0.288	-0.276	-0.264
B-4	366.038	-0.108	-0.216	-0.096	-0.336	-0.060
A-6	366.039	-0.204	-0.228	-0.324	-0.336	-0.312
A-8	366.041	-0.252	-0.312	-0.456	-0.372	-0.480
B-8	366.001	-0.120	-0.036	-0.132	-0.324	-0.132
A-10	366.041	-0.336	-0.360	-0.588	-0.504	-0.540
B-10	366.039	-0.204	-0.180	-0.324	-0.324	-0.276
A-13	366.064	-0.252	-0.252	-0.456	-0.408	-0.420
B-13	366.058	-0.120	-0.072	-0.168	-0.096	-0.096
A-15	366.041	-0.156	-0.132	-0.348	-0.132	-0.276
B-15	366.046	-0.120	-0.132	-0.252	-0.120	-0.192
A-17	366.037	-0.192	-0.084	-0.360	-0.288	-0.360
B-17	366.073	-0.096	-0.012	-0.168	-0.204	-0.132
B-6	366.079	-0.036	-0.084	-0.036	-0.108	0.012
A-19	366.056	-0.132	-0.024	-0.216	-0.192	-0.252
B-19	366.035	-0.084	-0.024	-0.228	-0.132	-0.144
A-21	366.066	-0.252	-0.156	-0.444	-0.240	-0.528
B-21	366.049	-0.156	-0.096	-0.360	-0.348	-0.456
A-23	366.066	-0.120	-0.204	-0.276	-0.132	-0.276
B-23	366.085	-0.084	-0.168	-0.120	0.012	-0.120
A-25	366.070	-0.096	-0.144	-0.192	-0.192	-0.168
B-25	366.037	-0.108	-0.180	-0.108	-0.180	-0.084
A-27	366.055	-0.084	-0.144	-0.192	-0.204	-0.216
B-27	366.058	-0.012	-0.072	-0.036	-0.108	-0.048
A-29	366.076	-0.072	-0.060	-0.156	-0.096	-0.180
B-29	366.065	-0.036	-0.060	-0.072	-0.012	-0.084
A-30	366.078	-0.012	0.048	-0.156	0.060	-0.132
B-30	366.067	0.000	0.048	-0.168	0.000	-0.108
A-26	366.036	-0.012	-0.024	-0.084	-0.096	-0.036
A.5-26	366.012	0.000	-0.036	-0.072	-0.228	-0.036
B-26	366.018	0.036	-0.084	-0.012	-0.120	0.024
B.5-26	366.026	0.024	-0.024	0.012	-0.216	0.060
C-26	366.048	0.048	0.012	0.060	-0.180	0.132
C.5-26	366.026	0.012	0.348	0.024	-0.312	0.012
D-26	366.032	0.000	0.240	-0.036	-0.384	-0.036
D.5-26	366.043	-0.012	0.312	-0.012	-0.504	-0.144
E-26	366.038	0.036	0.288	0.036	-0.288	0.060
E.5-26	366.065	-0.024	0.192	-0.036	-0.324	0.024

Location	Original el, Ft 9/06/84	Date and Change in Elevation, inches				
		10/31/84	01/28/85	08/28/85	06/05/86	05/12/87
F-26	366.056	0.000	0.132	-0.048	-0.288	0.000
F.5-26	366.048	0.048	0.240	-0.060	-0.240	0.012
G-26	366.059	0.012	0.096	-0.096	-0.228	0.144
G.5-26	366.068	0.060	0.180	0.000	-0.144	0.024
H-26	366.074	0.072	0.156	0.060	-0.084	0.108
H.5-26	366.067	0.096	0.228	-0.288	-0.132	0.108
J-26	366.037	0.060	0.084	0.264	-0.252	0.012
J.5-26	366.065	-0.012	0.036	-0.348	-0.468	-0.144
K-26	366.045	-0.024	-0.012	-0.174	-0.516	-0.252
K.5-26	366.089	0.048	0.108	0.000	-0.408	-0.108
L-26	366.092	0.012	0.072	0.048	-0.384	-0.072
L.5-26	366.038	0.048	0.120	0.024	-0.336	-0.084
M-26	366.026	0.024	-0.024	-0.024	-0.408	-0.132
M.5-26	366.015	-0.012	0.012	-0.108	-0.456	-0.288
N-26	366.036	0.012	-0.072	-0.204	-0.540	-0.420
D-10	366.044	-0.156	-0.228	-0.288	-0.492	-0.276
D-13	366.045	-0.120	covered	-0.204	-0.444	-0.204
D-19	366.054	-0.144	-0.168	-0.192	-0.456	-0.276
D-21	366.065	-0.780	-0.804	-1.020	-1.200	-1.152
D-29	366.063	-0.036	-0.048	-0.324	-0.264	-0.252
D-30	366.066	-0.036	0.084	-0.288	-0.204	-0.132
F-1	366.063	-0.048	covered	-0.120	-0.120	0.072
F-2	366.050	-0.276	covered	-0.276	-0.276	-0.012
G-3	366.030	-0.108	-0.084	-0.120	-0.168	0.084
G-5	366.038	-0.120	-0.048	-0.072	-0.336	0.012
G-8	366.031	-0.108	0.036	0.048	-0.300	0.072
H-1	366.052	-0.132	-0.012	tiles on	-0.012	0.048
H-2	366.098	-0.204	-0.096	-0.120	-0.096	0.084
F-10	366.043	-0.024	0.168	0.000	-0.060	0.072
H-10	366.035	-0.012	0.192	0.012	-0.132	0.036
G-13	366.075	-0.132	-0.060	-0.120	-0.384	-0.060
G-15	366.069	-0.156	-0.060	-0.108	-0.312	-0.108
G-17	366.053	-0.132	-0.120	-0.156	-0.204	-0.144
F-21	366.054	-0.948	-0.948	-1.044	-1.044	-1.200
H-21	366.054	-0.720	stack on	-0.924	-1.128	-0.984
G-23	366.074	-0.168	-0.060	-0.096	-0.192	-0.180
F-24	366.077	-0.012	0.060	-0.024	-0.420	-0.060
G-25	366.074	-0.012	-0.060	-0.132	-0.384	-0.168
F-27	366.055	-0.024	0.084	-0.144	-0.156	-0.156
G-27	366.063	-0.012	-0.024	-0.216	-0.324	-0.252
F-29	366.058	0.036	0.060	-0.264	-0.180	-0.168
H-29	366.053	0.012	-0.012	-0.396	-0.252	-0.228
F-30	366.055	0.084	0.096	-0.360	-0.096	-0.120
H-30	366.074	0.012	-0.012	-0.456	-0.264	-0.240
K-1	366.062	-0.168	0.000	-0.144	-0.216	0.084
M-1	366.065	-0.120	-0.036	-0.132	-0.180	0.048

Location	Original el, Ft 9/06/84	Date and Change in Elevation, inches				
		10/31/84	01/28/85	08/28/85	06/05/86	05/12/87
N-1	366.052	-0.144	0.060	-0.048	-0.036	0.168
K-2	366.070	-0.180	-0.084	-0.120	-0.300	0.204
M-2	366.070	-0.156	-0.024	-0.048	-0.156	0.252
N-2	366.082	-0.144	0.072	-0.024	-0.048	0.264
M-4	366.061	-0.168	0.084	0.024	-0.216	0.240
N-4	366.035	-0.168	0.060	-0.012	-0.084	0.180
M-6	366.053	-0.132	0.072	0.036	-0.252	0.228
N-6	366.053	-0.144	0.024	-0.060	-0.324	0.108
M-8	366.051	-0.168	-0.036	0.024	-0.300	-0.132
N-8	366.070	-0.144	0.036	-0.108	-0.408	0.000
K-10	366.052	-0.156	0.000	-0.156	-0.444	-0.144
M-10	366.035	-0.096	0.180	-0.072	-0.204	-0.120
N-10	366.058	-0.120	0.108	-0.168	-0.276	-0.132
K-13	366.065	-0.132	-0.084	-0.192	-0.528	-0.252
M-13	366.088	-0.168	-0.168	covered		
N-13	366.070	-0.156	-0.120	-0.300	-0.456	-0.324
M-15	366.012	-0.192	-0.120	-0.156	-0.540	-0.156
N-15	366.050	-0.168	-0.168	-0.288	-0.648	-0.288
M-17	366.042	-0.132	covered	-0.180	-0.360	-0.192
K-19	366.051	-0.120	-0.192	-0.204	-0.504	-0.240
M-19	366.022	0.000	0.000	-0.036	-0.348	-0.084
N-19	366.008	-0.048	-0.120	-0.204	-0.504	-0.312
K-21	366.026	-0.660	-0.408	-0.912	-1.200	-1.080
M-21	366.002	-0.672	-0.768	-0.948	-1.308	-1.152
N-21	366.043	-0.624	-0.720	-0.924	-1.296	-1.260
M-23	366.041	-0.024	-0.084	-0.180	covered	-0.120
N-23	366.047	-0.108	-0.132	-0.336	-0.648	-0.528
M-25	366.061	-0.012	-0.036	-0.168	-0.564	-0.180
N-25	366.059	-0.132	-0.192	-0.420	-0.816	-0.480
M-27	366.061	-0.012	0.012	-0.084	-0.348	-0.204
N-27	366.051	-0.048	-0.048	-0.192	-0.432	-0.372
K-29	366.042	-0.024	0.024	-0.300	-0.300	-0.216
M-29	366.051	-0.036	-0.024	-0.288	-0.276	-0.288
N-29	366.066	-0.012	0.072	-0.288	-0.288	-0.300
K-30	366.062	-0.036	0.060	-0.336	-0.360	-0.180
M-30	366.062	-0.024	0.108	-0.300	-0.180	-0.240
N-30	366.071	0.000	0.144	-0.240	-0.144	-0.240

VI. EARTH PRESSURE DATA

Cell	M-3	M-5A	M-4	M-5	M-6	M-1	M-7	M-2	M-8	M-9	M-10	M-11	M-12
Distance From A-26, Ft	2	9	17	31	49	62	74	88	99	112	124	138	152
Date	Earth Pressure, psi												
07/26/84	2.86	2.41	1.93	3.22	3.02	3.33	1.49	3.82	3.17	2.83	4.98	3.82	3.11
07/27/84	3.29	3.16	0.00	4.15	1.43	4.44	3.88	0.00	0.00	3.54	1.18	6.47	4.81
08/03/84	0.00	4.21	0.00	6.76	1.75	4.03	1.79	0.76	3.02	3.54	5.11	3.97	2.02
08/17/84	1.00	0.45	0.00	0.31	0.00	0.00	0.00	0.00	0.00	0.00	3.41	0.88	3.88
09/07/84	1.29	0.15	0.00	0.00	0.00	0.00	0.30	0.00	0.00	0.00	2.23	0.44	2.95
11/08/84	2.14	0.90	0.00	0.92	0.00	0.83	1.04	0.15	0.43	0.00	2.23	2.50	4.04
02/12/85	2.00	1.95	1.04	0.00	1.11	4.03	2.09	1.98	1.01	0.28	1.44	2.79	3.42
06/05/85	3.86	2.86	7.26	0.15	0.48	2.22	1.79	1.53	0.86	0.14	1.84	4.85	5.43
08/23/85	3.43	8.12	15.85	0.31	0.00	1.81	2.24	1.22	2.16	0.00	1.31	3.38	5.28
11/15/85	3.57	15.94	21.63	0.00	0.00	2.08	2.09	1.07	1.73	0.00	0.92	3.68	5.43
02/13/86	3.43	19.55	26.52	1.54	0.00	3.89	3.13	2.14	1.58	0.00	0.26	1.76	3.88
06/02/86	3.71	26.92	29.04	0.77	0.00	2.08	2.54	1.83	2.45	0.00	1.44	5.88	7.30
08/25/86	4.00	36.10	28.55	0.92	0.00	1.95	2.69	1.53	2.73	0.00	0.92	7.52	9.02
02/23/87	4.71	42.26	27.26	2.00	0.00	3.47	3.43	2.60	2.88	0.00	1.05	7.65	9.00
05/12/87	4.86	42.71	27.56	2.15	0.79	2.22	3.28	2.60	3.60	0.00	1.97	9.71	10.09
05/25/88	5.43	40.90	25.19	2.92	1.27	2.36	4.18	2.14	4.60	0.42	1.84	7.94	7.92

VI. STRAIN GAGE DATA

Gage	SG-1	SG-2	SG-3	SG-4	SG-5	SG-6	SG-7	SG-8	SG-9	SG-10
Distance From A-26, Ft	141	112	80	38	16	142	112	75	38	16
Date	Strain, Microinches/inch									
07/26/84						- 52	- 91	- 82	- 89	- 68
07/27/84						116	- 57	- 98	- 61	- 78
08/03/84	- 77	-153	- 56	- 91	- 79	158	- 83	- 84	- 25	- 8
08/17/84	- 85	- 97	-127	-112	- 61	378	- 68	- 85	- 22	- 60
09/07/84	- 47	- 83	-105	-109	- 91	321	- 70	- 95	- 30	- 63
11/08/84	60	- 47	-103	-110	- 96	655	- 4	- 93	- 12	- 21
02/12/85	175	- 51	- 98	- 98	- 93	796	39	- 84	- 9	- 26
06/05/85	219	-159	-180	-122	-126	376	- 5	- 86	- 20	- 38
08/23/85	- 2	-277	-226	-121	-155	303	- 5	-102	- 35	- 52
11/15/85	39	-333	-231	-135	-148	469	55	-112	- 15	- 33
02/13/86	110	-308	-235	-146	-155	660	123	-110	- 12	- 26
06/02/86	1	-349	-261	-163	-199	-266	128	-113	- 23	- 34
08/25/86	1	-360	-267	-294	-221	-3149	33	-120	- 53	- 49
02/23/87	2	-367	-288	-193	-260	57	315	-120	- 20	- 24
05/12/87	- 23	-386	-300	-188	-277	- 59	335	- 93	- 26	- 53
05/25/88	- 53	-394	-326	16	-329	-461	- 5	- 60	14	-187

Note: Negative strains refer to tension; positive strains refer to compression